UNIVERSITÀ DELLA CALABRIA

UNIVERSITÀ DELLA CALABRIA

Dipartimento di Farmacia e Scienze della Salute e della Nutrizione

Dottorato di Ricerca in

MEDICINA TRASLAZIONALE

CICLO XXXIII

Estrogen Related Receptor α (ERRα): a new target linking metabolism to Adrenocortical cancer progression

Settore Scientifico Disciplinare BIO/13

Coordinatore: Ch.mo Prof. Sebastiano Andò

Supervisore/Tutor: Ch.mo Prof. Vincenzo Pezzi

Dottoranda: Dott.ssa Marta Claudia Nocito

Index

Abstract

ABSTRACT

I Carcinomi surrenalici (ACC) sono tumori rari e altamente aggressivi, associati a una prognosi infausta per un alto rischio di recidiva e di opzioni terapeutiche limitate [Stojadinovic A. et al., 2002]. Ad oggi sono stati indicati diversi approcci terapeutici, ma la chirurgia rimane il trattamento di prima scelta per la rimozione del tumore primario o delle metastasi isolate [Crucitti F. et. al., 1996]. L'evidenza della presenza di recidive o metastasi in regioni distali in un terzo dei pazienti trattati chirurgicamente fa emergere la necessità di individuare una terapia adiuvante che possa eliminare questo rischio [Donatini G. et. al., 2014]. Ad oggi, il Mitotano rappresenta l'unico farmaco approvato negli USA e in Europa per il trattamento dell'ACC. La chemioterapia è riservata agli stadi avanzati della malattia, con evidenti metastasi resistenti al trattamento con mitotano. L'eziologia del cancro surrenale rimane ancora ignota, ma studi effettuati negli ultimi 10 anni suggeriscono che alcune mutazioni genetiche nella ghiandola surrenale sono alla base della genesi di un tumore maligno. Quella più diffusa interessa il locus (11p15) del fattore di crescita II insulino-simile (IGF-II). Infatti, l'IGF-II è over-espresso nel 90% degli ACCs e determina un effetto mitogenico autocrino attraverso l'attivazione delle vie di segnalazione mediate dal recettore IGF1R [Logie A. et al., 1999] quale la via Ras/MEK/ERK e Pi3K/Akt. È stata inoltre rilevata una upregulation dell'IGFIR nel 90% dei casi [Giordano T.J. et al., 2003]. Studi seguenti hanno evidenziato la presenza nell'ACC di un'overespressione del recettore estrogenico alfa (ER-α). Sirianni e collaboratori hanno meglio definito i pathways innescati in risposta all'attivazione dell'ER-α dimostrando l'esistenza di un cross-talk tra ERα ed IGFIR [Sirianni R. et al., 2012]. Inoltre, più recentemente [Casaburi I. et al., 2015] è stato osservato come nell'ACC via sia una overespressione dell'ERRα e che tale recettore è implicato nella patogenesi di questo tipo di tumore. È riportato che l'ERRα è un recettore nucleare coinvolto nel controllo di funzioni cellulari che riguardano principalmente il metabolismo energetico e la biogenesi mitocondriale [Villena J.A. et al., 2008] e che la diminuzione dell'espressione di ERRα è associata all'inibizione della crescita delle cellule tumorali [Stein R.A. et al., 2008]. Infatti, diversi studi hanno rilevato come ERRα possa rappresentare un marcatore prognostico del tumore al seno, alle ovaie, al colon e alla prostata [Kraus R.J. et al., 2002; Suzuki T. et al., 2004; Cavallini A. et al., 2005; Cheung C.P. et al., 2005]. La downregulation dell'espressione di ERRα potrebbe inibire, infatti,

significativamente la crescita delle cellule tumorali [Wu Q. et al., 2013; Chang C.Y. et al., 2011], mentre la sovraespressione di ERRα è legata ad un esito clinico infausto e conferisce resistenza ai farmaci [Kraus R.J. et al., 2002; Suzuki T. et al., 2004]. Questi dati suggeriscono, quindi, che ERRα rappresenta un nuovo target molecolare per il trattamento del cancro [Stein R.A. et al., 2008]. In uno studio condotto in cellule H295R di tumore adrenocorticale [Casaburi I. et al., 2015], è stato dimostrato che la deplezione di ERRα dopo trattamento con un agonista inverso denominato XCT790, causa la riduzione della massa e della funzione mitocondriale portando all'attivazione di meccanismi che esitano nella morte delle cellule tumorali. Questi risultati confermano che ERRα svolge un ruolo importante nella regolazione della funzione mitocondriale e nella biogenesi mitocondriale nelle cellule di ACC supportando l'ipotesi che può essere considerato come un regolatore "master" della riprogrammazione metabolica nell'ACC. Recentemente è stata dimostrata una correlazione tra uso della curcumina e modulazione dell'espressione dell'ERRα. È stato evidenziato, infatti, come in cellule di osteosarcoma, la curcumina riduce l'espressione genica di ERRα attraverso l'upregolazione del microRNA miR-125. In particolare, è stato osservato come la curcumina promuove l'apoptosi attivando il signalling miR-125/ERRα [Chen P. et al., 2017]. La curcumina, il principale componente dei rizomi essiccati di Curcuma longa, è stata utilizzata come colorante alimentare per secoli nei paesi dell'Asia orientale [Malik M. et al., 2009]. Precedenti studi hanno dimostrato come la curcumina presenta una vasta gamma di attività farmacologiche tra cui quella anti-infiammatoria, anti-diabetica, cardio-protettiva e neuro-protettiva [Aggarwal B.B. et al., 2005]. Inoltre, la curcumina è in grado di promuovere la guarigione di ferite, proteggere dalle lesioni epatiche, dalla formazione di cataratta e dalla tossicità polmonare [Aggarwal B.B. & Harikumar K.B., 2009]. Nel 1995 alcuni ricercatori [Menon L.G. et al., 1995] proposero la possibilità che la curcumina avesse un effetto antitumorale. Da allora, l'attività anticancro della curcumina è stata ampiamente studiata. Prove crescenti suggeriscono che la curcumina può essere utilizzata sia per la prevenzione che per il trattamento in diversi tipi di tumori umani [Anand P. et al., 2008; Ravindran J. et al., 2009; Bar-Sela G. et al., 2010; Quan-Jun Y. et al., 2015]. Negli Stati Uniti, il National Cancer Institute ha classificato la curcumina come agente anticancerogeno e chemo-preventivo di terza generazione [Odot J. et al., 2004]. Sebbene è stato dimostrato in diversi studi come la curcumina svolga un ruolo essenziale nell'inibire la proliferazione e la metastatizzazione delle cellule tumorali [Shishodia S. et

al., 2007; Troselj K.G. & Kujundzic R.N., 2014], i meccanismi molecolari alla base del suo effetto antitumorale rimangono poco conosciuti. Inoltre, sebbene la curcumina abbia numerose attività farmacologiche, il suo utilizzo come agente terapeutico non è stato ancora approvato a causa della sua bassa biodisponibilità [Anand P. et al., 2007]. Tra i fattori che contribuiscono a questo limite possono essere inclusi: bassa solubilità in acqua, scarso assorbimento, bassa distribuzione tissutale, alto tasso di metabolismo, inattività dei prodotti metabolici e/o rapida eliminazione e clearance dall'organismo [Ravindranath V. & Chandrasekhara N., 1980]. Gli effetti farmacologici ottimali richiedono una dose orale maggiore di 0,8 g/die. Pertanto, nel corso degli anni, al fine di migliorare il profilo farmacocinetico della curcumina e l'assorbimento cellulare, sono state sviluppate diverse strategie. Queste includono derivati strutturali della curcumina, preparazione di analoghi e nuovi sistemi di somministrazione di farmaci che potrebbero migliorarne la solubilità e prolungarne il tempo di permanenza nel plasma. Recentemente, diverse ricerche sono state effettuate con lo scopo di formulare "delivery systems" più efficienti come ad esempio l'incapsulazione della curcumina in nanoparticelle polimeriche o in liposomi che però non hanno ottenuto molto successo [Ji H. et al., 2016]. Recentemente è stato messo a punto un sistema alternativo ai tradizionali "delivery systems" denominato "Solid Lipid Nanoparticles" (SLN) che offre diversi vantaggi nel trasporto di farmaci poco solubili. Il sistema SLN conferisce alla molecola bioattiva maggiore stabilità e biocompatibilità e minori problemi di tossicità rispetto ad altri sistemi di trasporto. Le SLN possono essere somministrate sia per via orale che per via parenterale o transdermica. A ciò si associa il vantaggio che le metodiche di preparazione delle SLN sono semplici e di facile esecuzione e necessitano di pochi eccipienti nella formulazione [Rompicharla S.V.K. et al., 2017]. Pertanto, la preparazione di una nuova formulazione utilizzando il sistema SLN potrebbe migliorare notevolmente la stabilità, la biodisponibilità e l'efficacia antitumorale della curcumina.

Alla luce di questi dati di letteratura, lo scopo di questo lavoro di tesi era di indagare il ruolo di ERRα sui cambiamenti metabolici che si verificano in diverse linee cellulari ACC. Abbiamo anche studiato se i cambiamenti cellulari indotti dalla sovraespressione o dall'esaurimento di ERRα sono in grado di supportare o modulare la progressione dell'ACC.

Con la proteomica e l'analizzatore Seahorse XF, che consente l'analisi in tempo reale dei flussi glicolitici e mitocondriali, abbiamo studiato e rilevato un ruolo importante di ERRα nella regolazione dei cambiamenti metabolici nelle cellule ACC. Usando cloni stabili che sovraesprimono (ERR+/+) o con un'espressione del gene ESRRA silenziata (shERR-/-) nelle cellule ACC abbiamo rilevato che la sovraespressione di ERRα conferisce alle cellule ACC una migliore forma fisica mitocondriale mentre le cellule ERR-/- hanno una ridotta basale e massimale frequenza respiratoria e una ridotta capacità di riserva.

Successivamente abbiamo studiato gli effetti della ridotta espressione di ERRα sulle funzioni bioenergetiche di tre linee cellulari ACC utilizzando XCT790. I risultati del test ATP mostrano che XCT790 ha abbassato i livelli di ATP nelle cellule H295R e SW13 sensibili al mitotano, mentre era inefficace nelle cellule MUC1 resistenti al mitotano. Infatti, l'analisi del contributo energetico dei mitocondri e della glicolisi rivela un'estrema plasticità metabolica nelle cellule MUC1 e H295R rispetto alle cellule SW13, che sembrano mostrare un fenotipo glicolitico. La valutazione delle funzioni mitocondriali ha rivelato la capacità di XCT790 di influenzare negativamente la frequenza respiratoria massima in tutte e tre le linee cellulari.

È noto che le alterazioni metaboliche nelle cellule tumorali non sono esclusivamente associate a fenomeni di sopravvivenza e proliferazione ma incidono anche sulla motilità cellulare. I nostri dati hanno rivelato chiaramente un'influenza diretta dell'espressione di ERRα sulla motilità delle H295R. La sovraespressione di ERRα ha aumentato significativamente la migrazione delle cellule H295R e la vimentina del marker EMT mentre la downregulation del recettore metabolico, mediante ablazione genetica o con approcci farmacologici, ha mostrato una riduzione sia della motilità cellulare che dell'espressione della vimentina.

Altri dati importanti provenienti dal nostro studio sono l'impatto di ERRα sulla capacità delle cellule H295R di crescere in condizioni non aderenti come sferoidi 3D, una caratteristica dell'aggressività tumorale che caratterizza le cellule staminali tumorali (TIC). XCT790 è stato in grado di ridurre la formazione e la motilità degli sferoidi 3D non solo nelle cellule SW13 ma anche, e soprattutto, nelle cellule MUC-1 resistenti al mitotano suggerendo, ancora una volta, che il targeting di ERRα potrebbe essere una chemioterapia efficace da considerare per il trattamento del mitotano fenotipo ACC resistente.

Nuovi recenti risultati hanno riportato il colesterolo come un nuovo ligando endogeno di ERRα. I nostri esperimenti confermano il ruolo del colesterolo come attivatore di ERRα che induce la motilità cellulare nelle cellule ACC.

In questa tesi ci siamo anche chiesti se, oltre al colesterolo, esistessero altre molecole naturali in grado di modulare l'espressione e l'attività di ERRα. La nostra ricerca si è concentrata su un prodotto naturale derivato dalla pianta, la curcumina. I nostri risultati hanno mostrato chiaramente che la curcumina, riducendo l'espressione di ERRα, esercitava un effetto inibitorio dipendente dal tempo e dalla dose sulla crescita delle cellule H295R inducendo l'attivazione di eventi apoptotici. Inoltre, il test per ottenere colture di sferoidi 3D ha confermato come la curcumina possa modulare la capacità delle cellule H295R di espandersi, cioè di ridurre la loro capacità di metastatizzare, un atteggiamento strettamente correlato alla transizione epiteliale-mesenchimale (EMT) in cui le cellule epiteliali acquisiscono le caratteristiche delle cellule mesenchimali non polarizzate e migratorie.

Inoltre, in base al ruolo metabolico di ERRα, l'uso della curcumina ha indotto cambiamenti significativi nel profilo bioenergetico delle cellule H295R. In particolare, i valori OCR ed ECAR ed i parametri energetici derivati dall'analisi dei dati di Seahorse e associati alle funzioni mitocondriali e glicolitiche, sono stati tutti ridotti dalla curcumina in modo dose dipendente.

È noto che la limitazione dell'uso terapeutico della curcumina è dovuta principalmente alla sua scarsa biodisponibilità. Pertanto, al fine di migliorare il profilo farmacocinetico e l'assorbimento cellulare della curcumina, abbiamo prodotto SLN di curcumina e abbiamo riscontrato un maggiore effetto inibitorio dose-dipendente sulla proliferazione delle cellule H295R rispetto alla curcumina non modificata. Il trattamento con SLNs-CUR ha una risposta dose-dipendente sulla proliferazione cellulare maggiore rispetto alla curcumina talquale, con un'elevata significatività già alla dose di 10μM alle 24h, fino ad un'inibizione >75% nelle 72h di trattamento. Le cellule sono state anche trattate con il veicolo SLN alle stesse dosi e per 72 ore, per dimostrare che non ha effetti tossici quando somministrato da solo.

In conclusione, in questa tesi è stato dimostrato che ERRα è un fattore regolatore chiave che modula il profilo metabolico e di conseguenza la motilità delle cellule ACC. È stato, inoltre, dimostrato che l'inibizione di questo recettore, da parte di molecole sintetiche o

naturali, può bloccare fortemente non solo la crescita delle cellule ACC resistenti al mitotano, ma anche i processi di transizione delle cellule ACC a fenotipo più aggressivo e invasivo. Per questo motivo, ERRα può essere considerato un nuovo importante target da tenere in considerazione nella progettazione di una nuova strategia terapeutica per combattere la progressione del cancro corticosurrenale.

Il lavoro è oggetto attualmente di due pubblicazioni scientifiche in preparazione:

- DE LUCA A., AVENA P., CHIMENTO A., **NOCITO M. C.**, SCULCO S., LA PADULA D., ZAVAGLIA L., GIULIETTI M., HANTEL C., SIRIANNI R., CASABURI I., PEZZI V. *Estrogen Related receptor alfa (ERRα) a bridge between metabolism and adrenocortical cancer progression.*

- **NOCITO M. C.**, SCULCO S., AVENA P., DE LUCA A., CHIMENTO A., SIRIANNI R., CASABURI I., PEZZI V. *Curcumin targeting ERRα inhibits Adrenocortical carcinoma growth and progression.*

Inoltre, precedentemente, questo lavoro ha contribuito alla realizzazione di una ulteriore pubblicazione e di due REVIEWS:

- TROTTA F., AVENA P., CHIMENTO A., RAGO V., DE LUCA A., SCULCO S., **NOCITO M. C.**, MALIVINDI R., FALLO F., PEZZANI R., PILON C., LASORSA F. M., BARILE S. N., PALMIERI L., LERARIO A. M., PEZZI V., CASABURI I., SIRIANNI R. (2020). *Statins Reduce Intratumor Cholesterol Affecting Adrenocortical Cancer Growth.* Mol Cancer Ther. Sep;19(9):1909-1921. Doi: 10.1158/1535-7163.

- CASABURI I., CHIMENTO A., DE LUCA A., **NOCITO M. C.**, SCULCO S., AVENA P., TROTTA F., RAGO V., SIRIANNI R., PEZZI V. (2018). *Cholesterol as an Endogenous ERRα Agonist: A New Perspective to Cancer Treatment.* Front Endocrinol (Lausanne). Sep 11;9:525. Doi: 10.3389/fendo.2018.00525. eCollection 2018. Review.

- **NOCITO M. C.**, DE LUCA A., PRESTIA F., AVENA P., LA PADULA D., ZAVAGLIA L., SIRIANNI R., CASABURI I., PUOCI F., CHIMENTO A., PEZZI V. (2021). *Antitumoral Activities of Curcumin and Recent Advances to Improve its Oral Bioavability*. Biomedicines. Oct 14;9(10):1476. Doi: 10.3390/biomedicines9101476. Revie

Background

1. Adrenocortical cancers

1.1 Introduction

Tumors that originate from the adrenal cortex can be divided into benign adenomas and malignant adenocarcinomas. They differ from other cancers because the cancer may be associated to an endocrine component [Allolio B. & Fassnacht M., 2006].

Secreting forms are responsible for the onset of endocrine syndromes which vary depending on the type of hormone produced in excess:

- Cushing's syndrome, caused by hypersecretion of cortisol;
- Conn's syndrome, caused by aldosterone hypersecretion;
- hirsutism and virilization, caused by hypersecretion of androgens.

ACC can be asymptomatic or can present with symptoms of hormone excess or complaints referable to the mass [Brennan M.F.,1987; Schulick & Brennan 1999a]. Generally ACC present an immature steroidogenesis and almost all of these tumors exhibit hormonal precursor excess but, approximately, 60% of all ACC patients will present with hormone-related signs and symptoms (so-called "functional tumors") [Schulick & Brennan 1999a; Schulick & Brennan 1999b].

Differential diagnosis between ACA and ACC is of pivotal clinical relevance, as the prognosis and clinical management of benign and malignant ACTs is entirely different. Imaging techniques including computed tomography, magnetic resonance imaging and positron emission tomography with 18F-2-fluoro-2-deoxy-D-glucose (FDG-PET) can be used for assessing malignancy, but none of these techniques are absolutely reliable [Terzolo M. et al., 2011; Morelli V. et al., 2013]. It is very difficult to establish malignancy in small adrenal tumors and to exclude it in large tumors with the available imaging techniques. Currently used guidelines propose to remove adrenal tumors with a diameter of >6 cm, as they are associated with a risk of malignancy >25% [Aron D. et al., 2012]. Some hormonal features (eg, androgen secretion characteristic for malignant tumors) can also be exploited in diagnosis. Most recent data using urinary steroid hormone metabolomics showed characteristic patterns of steroid secretion and metabolism in ACC samples [Arlt W. et al., 2011]. The histological diagnosis of malignancy is also often difficult [Patalano A. et al., 2009] and novel markers of

malignancy are intensively searched for using bioinformatics approaches to establish an early and specific differential diagnosis between ACC and ACA.

1.2 Adrenocortical adenoma

It is a benign neoplastic proliferation of adrenocortical cells almost always associated with clinical, histological and instrumental evidences of hyperfunction.

Dimensions are variable depending on the hormone produced:

- adenoma with hyperaldosteronism is usually unilateral and of yellowish color, around 1.5 cm of size and non-enveloped;
- adenoma with hypercortisolism is unilateral, has dimensions of about 4 cm, is yellow-brown and is encapsulated;
- adenoma with virilization is unilateral, has dimensions of about 5 cm, is red-brown and is encapsulated.

In many patients, adrenal adenomas is asymptomatic, except for begning hormones producing tumors. In case of large tumors, patients may have symptoms due to the compression of other organs, such as feeling of abdominal fullness or localized abdominal pain. More frequent with advancing age, adrenocortical adenomas have a peak between 50 and 70 years and the most affected are women (58%) and the right side.

1.3 Adrenocortical carcinoma

People per year with an increased incidence in the first and fourth-fifth decades of life. By gender, females are the most affected (55-60%) [Else T. et al., 2014]. ACC is burdened by a poor prognosis with a mean 5-year survival rate between 16 and 47%, falling to 5-10% in the advanced stages. The cornerstones in the pathogenesis of ACC are considered to be the genetic alterations of the IGF-2, p53 and β-catenin molecular pathways [Barlaskar F.M. & Hammer G.D., 2007]. Additionally, other genes, such as ZNFR3, identified by a genome-wide study, appear potentially involved in the tumorigenesis of ACC [Assie G. et al., 2014b]. Comparative genomic hybridization (CGH) demonstrated several complex mutations in ACC with chromosomal gains at 4q, 4p16, 5p15, 5q12-13, 9q34, 12q13, 12q24, 19p and losses at 1p, 2q, 11q, 17p, 22p and 22q. Genes within these regions that are potentially involved in neoplastic transformation include fibroblast

growth factor 4 (*FGF4*), cyclin-dependent kinase 4 (*CDK4*), and cyclin E1 (*CCNE1*). A epigenetic study performed on 51 ACCs identified a promoter hypermethylation of the *H19, GOS2, PLAGLI* and *NDRG2* genes [Else T. et al., 2014]. However, it has been recently observed that the dysregulation of some miRNAs, such as the upregulation of miR-483 and the downregulation of miR-195 and miR-335, could play a substantial role in the ACC tumorigenesis [Assie G. et al., 2014a].

When ACC manifests as a condition of steroid hormone excess, the clinical picture is dominated mainly by hypercortisolism and/or hyperandrogenism, whereas symptoms of estrogen hypersecretion such as gynaecomastia and testicular atrophy are pathognomonic in male patients [Fassnacht M. et al., 2011]. DHEA-S represents a possible hormonal marker of ACC, conversely a decreased serum DHEA-S concentration likely indicates an adrenal adenoma [Fassnacht M. et al., 2004]. Mineralocorticoid excess is a rare event, that occurs with severe hypertension and hypokalemia. Notably however, an excess of glucocorticoids could produce a similar effect [Fassnacht M. et al., 2011]. Although few ACC appear non-secreting, they may produce an excessive amount of adrenal precur- mass spectrometry methods revealed that >95% of ACC patients are able to autonomously secrete steroids or steroid precursors [Arlt W. et al., 2011]. Imaging plays a key role in the diagnosis of primary ACC, in the involvement of surrounding tissues and in its spread to distance sites. Either computerized tomography (CT) or magnetic resonance imaging (MRI) exploiting particular features such as Hounsfield unit (HU) values chemical shift imaging, respectively allow adequate diagnostic accuracy to be achieve [Blake M.A. et al., 2006; Terzolo M. et al., 2011] as suggested by an analysis of the German ACC registry showing that the value of 13 HU may be considered as the threshold for benign from malignant adrenal masses [Petersenn S. et al., 2015]. More recently, the fluorine 18 fluorodeoxyglucose (18F-FDG) positron emission tomography (PET) or PET/CT was introduced as a diagnostic tool for ACC [Wong K.K. Et al., 2011]. 11C-metomidate, due to its particular ability to bind 11 β-hydroxylase, has been proposed for the identification of tumors of adrenocortical origin [Hennings J. et al., 2006]. The introduction of [123I]IMTO for single photon emission computed tomography (SPECT) and planar scintigraphy has provided a diagnostic alternative to PET for the discrimination of adrenal masses from non-adrenal tissues [Hahner S. et al., 2013]. The first official TNM classification for ACC was established only in 2004 by the International Union Against Cancer (UICC) and the World Health Organization (WHO).

It was based on the criteria described by MacFarlane [Macfarlane D.A., 1958] and later modified by [Sullivan M. et al., 1978]. A significant improvement in the prognostic assessment was due to the adoption of the ENSAT (European Network for the Study of Adrenal Tumors) ACC staging system, which proposes a careful prognostic differentiation among the stages [Fassnacht M. et al., 2009] (Table I). The use of this system in recent years has greatly improved the diagnostic accuracy and the prediction of survival for stage compared to the criteria previously adopted [Lughezzani G. et al., 2010].

Stage
1. T1, N0, M0
2. T2, N0, M0
3. T1-T2, N1, M0; T3-T4, N0-N1, M0
4. any T, any N, M1

Table I. Staging system for ACC proposed by the European Network for the Study of Adrenal Tumors (ENSAT).

Classification criteria of the tumor stage according to the TNM system: Stage 1: T1, tumor ≤5 cm; N0, no positive lymph nodes; M0, no distant metastases. Stage 2: T2, tumor >5 cm; N0, no positive lymph nodes; M0, no distant metastases. Stage 3: T1, tumor ≤5 cm – T2, tumor >5 cm; N1, positive lymph node(s); M0, no distant metastases; T3, tumor infiltration into surrounding tissue – T4, tumor invasion into adjacent organs or venous tumor thrombus in vena cava or renal vein. N0, no positive lymph nodes – N1, positive lymph node(s). M0, no distant metastases. Stage 4: T1, tumor ≤5 cm – T2, tumor >5 cm; T3, tumor infiltration into surrounding tissue – T4, tumor invasion into adjacent organs or venous tumor thrombus in vena cava or renal vein; N0, no positive lymph nodes – N1, positive lymph node(s). M1, presence of distant metastasis.

1.3.1 Treatment options

ACC is a neoplastic disease with a poor prognosis. Current studies in this field have indicated the need for a multidisciplinary approach in the management of this tumor [Creemers S.G. et al., 2016; Stigliano A. et al., 2016]. Surgery remains the most effective treatment choice for the primary tumor or in for the removal of isolated metastases [Crucitti F. et al., 1996; Else T. et al., 2014]. The experience that at least one-third of patients show loco-regional recurrence or distant metastases even after a radical surgical excision introduced the concept of adjuvant therapy in these patients [Donatini G. et. Al.,

2014]. Despite an extensive surgical resection, the survival rate of these patients is estimated as ~50% after 5 years [Vaughan E.D., 2004]. Although these data support the need for an adjuvant cancer therapy, the therapeutic options in ACC currently remain under debate. At present, mitotane represents the only drug approved in Europe and in the United States for ACC treatment; however, opinions regarding its use in adjuvant settings are still highly discordant [Huang H. & Fojo T., 2008]. Currently, chemotherapy is reserved for those cases of advanced disease with evidence of distant metastases unresponsive to mitotane treatment. Many efforts are directed to the development of targeted therapy in ACC. Several strategies have been developed *in vitro* and some clinical trials have been conducted with small molecules, such as inhibitors of tyrosine kinase receptors or serine/threonine kinase receptors and monoclonal antibodies.

1.3.2 Surgery

Surgery is the only truly effective therapy in the treatment of ACC. A complete surgical resection (R0) is the treatment of choice, avoiding tumor spread that is considered an adverse prognostic factor. The achievement of R0 resection status often requires a radical surgery with a wide dissection of the neighboring organs. It represents a predictor of long-term survival [Icard P. et al., 2001]. The choice of an open approach vs laparoscopic approach is debated. Open adrenalectomy is classically the more secure treatment recommended in patients with localized (stage I-II) and locally advanced (stage III) ACC. Comparative data concerning the two surgical techniques are lacking and originate from retrospective data that involved selection bias [Porpiglia F. et al., 2010; Lombardi C.P. et al.; 2012]. It is likely that laparoscopic surgery might be reserved only for selected cases with masses of small size. However, these statements must be confirmed by prospective trials. Regardless of the surgical option chosen, the surgical team must have proven experience in the oncologic ACC surgery. Although lymphadenectomy has never been considered as a standard procedure in the adrenalectomy, recent studies show that lymph nodes dissection is significantly associated with a reduction of the relapse rate in patients with localized disease [Gaujoux S. & Brennan M.F., 2012; Reibetanz J. et al., 2012]. However, confirmatory data are needed in order to standardize the surgical procedure. The therapeutic option of removing metastases is founded on the observation that their excision is associated with longterm survival [Kemp C.D. et al., 2011; Ripley R.T. et al; 2011] and the consideration that many ACC are metastatic at the onset [Stojadinovic A.

et al., 2002]. Encouraging results from several retrospective studies show that the metastasectomy correlates with an improvement of progression-free and overall survival [Datrice N.M. et al., 2012; Erdogan I. et al., 2013]. Finally, although the objective of debulking surgery is to reduce either the compressive effect exerted by a large size mass, on surrounding organs or the hormonal excess secreted by the tumor, lacking in this surgical approach is an oncological rationale [Crucitti F. et. al., 1996].

1.3.3 Mitotane

Currently, mitotane represents the only therapeutic option approved by the US Food and Drug Administration and European Medicine Executive Agency for the treatment of ACC [Schteingart D.E. et al., 2005]. Mitotane is a derivative of the insecticide dichlorodiphenyldichloroethane (DDT) with adrenolytic and cytotoxic activity toward the fasciculata and reticularis adrenal areas. It inhibits steroidogenic pathways acting mainly at the level of the cholesterol side chain cleavage enzymes CYP11A1 and CYP11B1 [Lin C.W. et al., 2012; Lehmann T.P. et al., 2013]. Mitotane metabolites (o',p-DDA and o',p- DDE, respectively) are the products of a hydroxylation that occurs in the liver and of which o',p-DDA represents the active form [van Slooten H. et al., 1984]. It has indeed been shown, that o',p-DDA measurements reflect the mitotane response in treated patients [Hermsen I.G. et al., 2011]. Drug administration is oral, with the aim of reaching the therapeutic target between 14 and 20 mg/dl [Hermsen I.G. et al., 2011; Kerkhofs T.M. et al.,2013] above which side effects involving the gastrointestinal tract and central nervous system frequently manifest [Fassnacht M. & Allolio B., 2009]. A study showed that blood mitotane concentrations ≥14 mg/l were associated with a prolonged recurrence-free survival (RFS) in patients following macroscopically radical surgery [Terzolo M. et al., 2013]. Furthermore, the measurement of plasma mitotane levels in the management of patients with ACC is mandatory. Different treatment strategies have been proposed to achieve the therapeutic dose even if the high-dose regimen appears to be the most effective for reaching the target concentration more rapidly [Fassnacht M. & Allolio B., 2009]. Mitotane has been shown to be an inducer of hepatic cytochrome CYP3A4 and thus able to interfere with the metabolism of other drugs including chemotherapeutic agents [van Erp N.P. et al., 2011]. This drug property complicates the management of other codition-related treatments, such as antihypertensives, statins, antibiotics and others, that are also being used in ACC patients

[Kroiss M. et al., 2011]. Furthermore, future protocols involving mitotane and antineoplastic drugs in combination should consider this particular drug feature. Several studies regarding mitotane use in the clinical setting of ACC have reported conflicting results. However, the retrospective nature of these studies exposes them to numerous biases, mainly related to the different concentrations used and the lack of mitotane plasma level measurements. In fact, the response rate, as evaluated in series in which mitotane treatment was given without considering plasma concentration and those with patients in whose the drug concentration had been assessed, ranged from 25 to 55% respectively [van Slooten H. et al., 1984; Haak H.R. et al.,1994; Baudin E. et al., 2001; Hermsen I.G. et al., 2011]. An extensive retrospective case-control study performed on two independent cohorts showed significantly improved RFS compared to untreated control patients ($p<0.0001$). Overall survival (OS) was 110 months in the mitotane group vs 52 and 67 months in the control group ($p=0.01$) [Terzolo M. et al., 2007]. These data have allowed the introduction of the concept of using mitotane in the adjuvant therapy of patients affected by ACC. Currently, an international, multicentric, prospective, randomized trial, called ADIUVO, designed to evaluate the effectiveness of mitotane in adjuvant therapy is ongoing. The recent ESMO guidelines recommend adjuvant mitotane treatment in stage III patients with potential residual disease (R1 or Rx resection status) and Ki-67 >10%. For patients in stages I or II, R0 resection and Ki-67 <10%, adjuvant mitotane therapy is not considered mandatory. Mitotane should be administered progressively to reach the dose of 6 g/day over 4-6 days, adjusting the dosage according to the patient's tolerance and the plasma drug level [Berruti A. et al., 2012a].

1.3.4 Chemotherapy

Among the different available treatment protocols for advanced ACC, chemotherapy is offered in combination with mitotane. The rationale of this combination is related to the ability of mitotane to overcome the drug-resistance induced by P-glycoprotein which is widely expressed in ACC [Bates S.E. et al., 1991]. Several chemotherapeutic agents, such as 15iethylsti, cisplatin, doxorubicin, and others have been used alone or in combination with mitotane in the treatment of advanced ACC [Bukowski R.M. et al., 1993; Khan T.S. et al., 2000; Schteingart D.E. et al., 2000; Berruti A. et al., 2005]. Although variable percentages have been reported, the results from these studies demonstrate that cisplatin alone or in combination with etoposide have a higher effectiveness in advanced ACC

[Bukowski R.M. et al., 1993; Bonacci R. et al., 1998; Williamson S.K. et al., 2000]. The First International Randomized Trial in Locally Advanced and Metastatic Adrenocortical Carcinoma Treatment (FIRM-ACT) clearly confirmed the advantage of the regimen of etoposide-doxorubicin-cisplatin (EDP) in combination with mitotane (Berruti *et al* protocol) [Berruti A. et al., 2005] compared to streptozotocin plus mitotane (Khan *et al* protocol) [Khan T.S. et al., 2000] (Table II). In Berruti *et al* study, an overall response rate of 48.6% was achieved [Berruti A. et al., 2005], whereas in the Khan *et al* regimen, the International Consensus Conference on Adrenal Cancer of Ann Arbor recommended the use of these protocols as first-line regimens against metastatic ACC in 2003 [Schteingart D.E. et al., 2000]. Despite the expectations, no significant differences were found in OS (overall survival) (median 14.8 vs 12 months, respectively). Similarly, quality of life and adverse events were comparable in patients receiving the two treatments, thus confirming the poor prognosis of patients with advanced ACC [Fassnacht M. et al., 2012]. Gemcitabine alone or in combination with mitotane demonstrated a good efficacy *in vitro* and its effectiveness was dependent on the sensitivity of the ACC cells to mitotane [Germano A. et al., 2014].

Berruti et al protocol (EDP/ M) (53)	*Every 28 days:*	
	Day 1	40 mg/m2 Doxorubicin
	Day 2	100 mg/m2 Etoposide
	Days 3 and 4	100 mg/m2 Etoposide + 40 mg/m2 cisplatin
Khan et al protocol (Sz/ M) (54)	*Every 21 days:*	
	Days 1-5	1 g Streptozotocin
	Subsequently	2 g Streptozotocin
	Daily	Mitotane with a blood level between 14-20 mg/l

Table II. Regimen protocols in the FIRM-ACT study

1.3.5 Radiotherapy

The effectiveness of radiotherapy in ACC has been extensively debated. A retrospective analysis from the German ACC Registry, demonstrated that adjuvant radiotherapy

resulted in a significantly better 5-year RFS, but did not affect OS and disease-free survival (DFS) [Fassnacht M. et al., 2006]. In a retrospective study from the United States, radiotherapy was reported to decrease the risk of local failure 4.7 times compared with alone [Sabolch A. et al., 2011]. In contrast another retrospective study did not find a difference between adjuvant radiotherapy and surgery alone [Habra M.A. et a., 2013]. Some *in vitro* studies support the potential combination of mitotane and radiotherapy. In fact, these studies reported an inhibitory effect of mitotane in association with ionizing radiations on ACC cell lines [Polat B. et al., 2009; Cerquetti L. et al., 2010]. Considering the current data, radiotherapy is intended for patients with R1 or Rx resection status with a high risk for local recurrence [Polat B. et al., 2009]. However, the potential use of this method alone or in combination with other therapy should be investigated in future prospective clinical trials.

1.3.6 Targeted therapy

The failure of conventional therapies in advanced ACC and recent knowledge regarding the molecular pathways, involving oncosuppressor genes, such as *TP53, CDKN1C, CDKN2A* and *MEN1*, and oncogenes such as *IGF2, CTNNB1* and *RAS* involved in this malignancy have encouraged many efforts in developing new strategies against ACC [Barlaskar F.M. & Hammer G.D., 2007].

- ***Insulin-like growth factor-2 mTOR pathway.*** Overexpression of insulin-like growth factor-2 (IGF-2) is the most important molecular event occurring in >90% of ACCs [Ragazzon B. et al., 2011]. Its hypersecretion induces an uncontrolled activation of the PI3K/Akt/ mTOR pathway by IGF-1R [de Reynies A. et al., 2009]. Preclinical *in vitro* and *in vivo* studies on xenograft models showed that NVP-AEW541, a small molecule inhibitor, and IMC-A12, a human monoclonal antibody, were able to reduce cell proliferation, inhibiting the IGF-2 downstream pathway. The association of both molecules with mitotane 17iethylstilbest inhibited tumor growth [Barlaskar F.M. et al., 2009; Tacon L.J. et al., 2011]. Two phase I studies have demonstrated the effectiveness of figitumumab, a monoclonal anti-IGF-1R antibody and linsitinib (OSI-906), a tyrosine kinase inhibitor binding IGF-1R inducing a clinical response in 57 and 33% of patients, respectively [Haluska P. et al., 2010]. The results of a phase III study to evaluate the

therapeutic potential of OSI-906 were published, which were disappointing [Fassnacht M. et al., 2015]. An association was found between *IGF2* overexpression, mTOR hyper-activation and reduced expression of miR-99a and miR-100 [Doghman M. et al., 2010]. A role of mTOR in normal and adrenal tumors has been demonstrated by several studies [De Martino M.C. et al., 2010; Doghman M. et al., 2010]. And its inhibition by everolimus (RAD-001) leads to cell growth reduction both *in vitro* and *in vivo*, confirming the importance of microRNA regulation of the IGF-2/mTOR 18iethylst cascade [Doghman M. et al., 2010]. Based on these data, a phase I trial tested the effects of temsirolimus (CCI-779), another inhibitor of mTOR in combination with cixutumumab, an anti-IGF-R1 monoclonal antibody, demonstrating a positive effect on tumor growth in 4 of 10 patients treated [Naing A. et al., 2011]. A recent trial from the United States investigating the combination of cixutumumab and mitotane as first line treatment in patients with metastatic ACC reported effectiveness in 8/20 patients enrolled [Lerario A.M. et al., 2014].

- ***Angiogenesis.*** Most solid tumors display marked angiogenesis and substantial data highlight the vascular endothelial growth factor (VEGF) overexpression in ACC (70). Despite expectations for the inhibitors of this pathway, the results of clinical trials have been quite disappointing. A monoclonal VEGF antibody in combination with capecitabine administered in a series of 10 patients affected by advanced ACC did not show any positive results [Wortmann S. et al., 2010]. A partial response with capecitabine at a dose of 200 mg/die has been described only in one case, a 40-year-old patient with chemoresistant ACC [Chacon R. et al., 2005]. Both sorafenib and sunitinib, tyrosine kinase inhibitors able to target VEGF, produced poor results also [Tacon L.J. et al., 2011]. A phase II trial consisting of the administration of sunitinib in 38 patients with unresponsive ACC recorded a progression-free survival ranging from 5.6 to 12.2 months [Kroiss M. et al., 2012]. A phase I trial described a positive response in two patients affected by advanced ACC who received sorafenib in combination with tipifarnib, a farnesyltransferase inhibitor. Moreover, only in a single case report, a regression of metastatic ACC with sorafenib administration has been observed [Butler C. et al., 2010]. Recently, a phase II study investigating the combined effect of sorafenib with metronomic paclitaxel did not show any clinical improvement,

contradicting the obtained *in vitro* results [Berruti A. et al., 2012b]. A partial response to sunitinib in a patients with metastatic ACC, after chemotherapy treatment, has been described [Lee J.O. et al., 2009]. Moreover, Gangadhar *et al* reported a partial response, in a patient with advanced ACC, who received combination treatment with sirolimus, an mTOR inhibitor, and sunitinib [Gangadhar T.C. et al., 2011]. Finally, a role for 19iethylsti-1 in ACC angiogenesis has been hypothesized thus representing a new selective therapeutic target in ACC [Xu Y.Z. et al., 2011].

- ***Tyrosine kinase inhibitors.*** Microarray transcriptome analyses have provided new knowledge regarding the hyperactivated molecular pathways involved in ACC, thereby suggesting new potential target molecules for treatment strategies to address [Assie G. et al., 2010; Ragazzon B. et al., 2011]. Frequently, these targets are represented by growth factors and therefore the therapeutic concept is based on the inhibition of protein kinases involved in signal transduction, often tyrosine kinase receptors [Tacon L.J. et al., 2011]. A clinical study performed on 10 patients with advanced disease treated with erlotinib, an EGFR inhibitor, in combination with gemcitabine demonstrated very limited effectiveness [Quinkler M. et al., 2008]. In a phase II study, treatment with imatinib 19iethyls, a PDGFR inhibitor, was associated with disease progression in 75% of patients with severe side effects [Gross D.J. et al., 2006]. It is likely that the failure of these therapies is related to the low presence of these receptors in ACC. Interestingly, no mutation of the EGFR gene has been detected [Adam P. et al., 2010].
- ***MDR/P-glycoprotein.*** The chemoresistant properties of ACC have been classically related to the overexpression of the multidrug resistance protein MDR-1 (P-glycoprotein, Pgp), a debated drug efflux pump [Bates S.E. et al., 1991]. Even with results from an *in vitro* study suggesting that mitotane enhances doxorubicin activity by interfering with Pgp [Gagliano T. et al., 2014], the exact role of MDR-1 protein in ACC needs to be elucidated. Furthermore, a clinical trial using doxorubicin, vincristine, and etoposide in combination with mitotane failed to demonstrated therapeutic effectiveness [Abraham J. et al., 2002].
- ***PPAR-γ antagonists.*** Thiazolidinediones effects are somewhat different in the oncologic field [Kahn C.R. et al., 2000]. The PPAR-γ receptor is widely expressed in normal and in tumor adrenal tissue. It is involved in the IGF-2/IGF-1R

signaling pathway, by inhibiting Akt activation [Betz M.J. et al., 2005; Ferruzzi P. et al., 2005]. It has been shown that these compounds are able to inhibit cell proliferation in ACC cell models and in xenograft models [Betz M.J. et al., 2005; Ferruzzi P. et al., 2005; Luconi M. et al., 2010; Cerquetti L. et al., 2011]. In particular, it has been shown that rosiglitazone, a thiazolidinediones class member, activating both PPAR-γ-dependent and -independent pathways, led to a growth arrest, cell death and reduction of *VEGF* expression involved in adrenocortical angiogenesis [Betz M.J. et al., 2005; Cerquetti L. et al., 2011].

- ***Wnt/β-catenin pathway.*** The constitutive activation of this pathway is found in 85% of ACC [Tissier F. et al., 2005]. Moreover, nuclear localization of β-catenin represents a worse prognostic factor in ACC [Tissier F. et al., 2005; Gaujoux S. et al., 2011]. Preclinical *in vitro* studies were performed with PKF115-584, a small molecule inhibitor of the T-cell factor (Tcf)/β-catenin complex, on β-catenin-dependent transcription and proliferation processes in H295R ACC cells, that harbored *CTNNB1* gene mutations. As a results, this treatment was able to inhibit cell growth and induce apoptosis in the H295R adrenocortical cell line but not in HeLa, a human epitheliod cervical carcinoma cell line, confirming that the Wnt/β-catenin pathway is an useful target in ACC [Doghman M. et al., 2008]. Another *in vitro* study demonstrated that β-catenin silencing inhibited cell proliferation and induced apoptosis in the H295R cell line [Gaujoux S. et al., 2013].
- ***Steroidogenic factor-1.*** Steroidogenic factor-1 (SF-1) is a nuclear transcription factor involved in the steroidogenic tissue development [Sbiera S. et al., 2010]. It is frequently overexpressed in pediatric ACCs, whereas in the adult population some abnormalities on chromosome 9 have been described. However, a higher nuclear SF-1 expression level has been associated with a worse prognosis in ACC [Sbiera S. et al., 2010] and is positively correlated with advanced ENSAT stages, and a higher mitotic index and Weiss score [Duregon E. et al., 2013]. An increased SF-1 dosage was observed to stimulate proliferation, decrease apoptosis in adrenocortical cells, and induce tumorigenesis in transgenic mice [Doghman M. et al., 2007]. SF-1 silencing affected TGF-β and Wnt/β-catenin signaling, suggesting crosstalk between these pathways in a study performed on the H295R adrenocortical cell line. Moreover, SF-1 knockdown showed a significant

reduction of cell proliferation be interference with S-phase of the cell cycle [Doghman M. et al., 2007; Ehrlund A. et al., 2012]. Two members of the alkyloxyphenol class, AC-45594 and OOP, the synthetic SF-1 inverse agonists have been shown to inhibit proliferation in both H295R and SW13 adrenocortical cell lines through an SF-1 non-selective mechanism. In contrast, SID7969543 (IsoQ A) and the compounds numbered 31 and 32, members of the IsoQ class, induced a selective inhibition of cell proliferation when SF-1 was increased strongly suggesting that the IsoQ molecules targeted SF-1-related genes [Doghman M. et al., 2009].

- ***Gene therapy and immunotherapy.*** The rationale of gene therapy lies in correcting the gene regulation, reactivating oncosuppressor genes and/or inhibiting oncogenes during tumorigenesis. Systemic therapy with antisense oligonucleotides represents an innovative approach for ACC treatment. A construct, composed of the herpes simplex virus thymidine kinase (HSV-TK) gene driven by the CYP11B1 promoter with a P450scc enhancer element, increased the chemosensitivity in a Y1 mouse ACC cell line [Chuman Y. et al., 2000]. Immunotherapy represents another therapeutic approach that relies on the stimulation of the immune system against specific target proteins of neoplastic cells. This approach, using dendritic cells, was effective in stimulating the immune response [Sbiera S. et al., 2008], inducing antigen-specific Th1 immunity in a study performed on two patients with advanced secreting ACC. However, no clinical benefit has been shown [Papewalis C. et al., 2006]. In the cytokine family, interferon-β (INF-β) showed an inhibitory effect *in vitro* on ACC cell lines and primary ACC human cell cultures. Furthermore, when co-administered INF-β, sensitized ACC cells to mitotane [van Koetsveld P.M. et al., 2013]. Recently, a phase I clinical study was conducted with interleukin- 13-*Pseudomonas* exotoxin in patients affected by advanced ACC, exploiting the rationale that the α2 receptor of interleukin 13 (IL13Rα2) is more highly expressed in ACC than in normal adrenal tissue. This study showed a low disease stability rate lasting a few months before the ACCs progressed [Liu-Chittenden Y. et al., 2015]. *miRNA*. Recent biological advances concerning microRNA dysregulation in all cancers including ACC highlights the hypothetical consideration of these small non-coding RNAs as potential target molecules for anti-cancer treatment [Iorio M.V. & Croce C.M.;

2012]. Because miRNAs may function as tumor suppressors, the assumption of replacement miRNA cancer therapy must not disregard the identification of a miRNA deficiency. In a previous analysis of miRNA expression in adrenocortical tumors, miR-7 was the most significantly under-expressed miRNA when compared to normal adrenal tissue [Soon P.S. et al., 2009]. Glover *et al* provided the first demonstration of the effectiveness of the nanoparticle systemic delivery of miR-7 in the reduction of cell growth in both cell lines and in an ACC xenograft model, respectively. Furthermore, they demonstrated that miR-7 functions as a tumor suppressor in ACC leading to the repression of several genes involved in the pathogenesis of ACC, including *RAF-1, mTOR* and *CDK1* [Glover A.R. et al., 2015].

- ***Estrogen pathway.*** Recent advance confirms an estrogenic pathway in normal adrenal tissue and in adrenal tumors. A differential expression of estrogen receptors (ER) α and β has been demonstrated in ACCs [de Cremoux P. et al., 2008]. Moreover, Barzon *et al* showed an increased aromatase activity in ACC, hypothesizing a paracrine estrogenic effect at the tumor level [Barzon L. et al., 2008]. An *in vitro* study demonstrated that hydroxytamoxifen, increasing the pro-apoptotic factor FasL expression, reduced H295R cell proliferation by Erα downregulation and Erβ upregulation, respectively [Montanaro D. et al., 2005]. Erα activation may occur by an 17-β estradiol (E2)-dependent mechanism or alternatively by IGF-II/ IGF1R in a ligand-independent manner, activating proliferative pathways *in vitro*, such as IGF1R/AKT signaling, in H295R cell lines. Furthermore, in the same study, hydroxytamoxifen, an active metabolite of the estrogen antagonist tamoxifen, reduced IGF1R protein levels and cell proliferation induced by E2 and IGF-II both *in vitro* and in an ACC xenograft model [Sirianni R. et al., 2012]. These data indicate a crucial role of the estrogenic pathway in ACC and support the possibility of using antiestrogens in the treatment of ACC. A recent interesting study elucidated the ability of a non-steroidal G-protein-coupled receptor (GPER) agonist to exert a growth inhibitory effect, mediated by activation of the ERK1/2 pathway, both in the H295R cell line and in xenograft ACC [Chimento A. et al., 2015]. Finally, the compound XCT790, an inverse agonist of the transcription factor estrogen-related receptor α (ERRα) [Giguere V. et al., 1988], an orphan member of the nuclear hormone receptor

superfamily with a similar sequence to Erα involved in cellular metabolism and mitochondrial biogenesis [Deblois G. & Giguere V.; 2011], was able to reduce cell growth in both the H295R cell line and in an ACC xenograft model, with impaired mitochondrial functioning leading progressively to cell death recentemente [Casaburi I. et al., 2015].

- ***Metomidate.*** $^{[123I]}$IMTO single-photon emission CT imaging has been recently introduced as a novel tracer for the identification of adrenocortical tumors [Hahner S. et al., 2013]. Treatment options with $^{[131I]}$IMTO depend on the $^{[123I]}$IMTO uptake in the lesion potentially related to ACC [Hahner S. et al., 2013]. A recent experience in 11 patients with advanced ACC receiving ≤20GBq $^{[131I]}$IMTO, showed a low progression-free survival in six responders [Hahner S. et al., 2012].
- ***Interventional radiology.*** Minimally invasive procedures such as radiofrequency thermal ablation (RFA), or transarterial chemoembolization (TACE) represent an alternative to surgery in advanced metastatic malignancies. The same approach was adopted also in the treatment of lesions in the liver, kidney, lymph nodes and lung for stage IV ACC patients [Wood B.J. et al., 2003]. Wood *et al* observed that RFA induced a growth arrest in 8 of 15 lesions after 6 months of follow-up. The procedure was safe and was not associated with any particular side effects [Wood B.J. et al., 2003]. TACE allows the selective infusion of high doses of cytotoxic drugs in the metastatic lesion reducing the systemic toxicity. In a French study, this technique was associated with a median survival of 11 months in 21 patients with liver metastatic disease [Cazejust J. et al., 2010]. These procedures provide palliative benefits, are safe and inexpensive while implying minimal morbidity and a short recovery, however, none of these methods have been supported by a clinical trial.

1.3.7 Conclusion

Despite the enormous progress achieved in the biological knowledge of this tumor, the ACC remains an oncological disease burdened by a high mortality. Surgery is still the first therapeutic option and the only potentially curative treatment. Currently, mitotane is the only drug approved by international pharmaceutical agencies for ACC treatment.

Although mitotane treatment in the adjuvant setting is still debated, the recent ESMO guidelines recommend its use in adjuvant setting after surgery in patients with incomplete resection status. The optimal chemotherapy regimen is considered to be etoposide-doxorubicin-cisplatin (EDP) in combination with mitotane in patients with advanced metastatic disease, although this regimen is burdened by substantial side effects. The current -OMICs approach has permitted the discover of different molecules belonging to pathways potentially involved in the pathogenesis of the ACC. The therapeutic option described in isolated and metastatic ACC are summarized in **Figure 1.1**. Future efforts should be made not only to explore new frontiers but also to investigate innovative therapies in the clinical field. ACC urgently requires new therapeutic strategies. The clinical translation of new research products *in vitro* and in preclinical studies may help improve the standard of care in these patients. Achieving this objective in a rare disease such as ACC will require the carefully selection of the clinical series to be devoted to experimentation and an increasead collaborative network of research centers involved in the study of this malignancy.

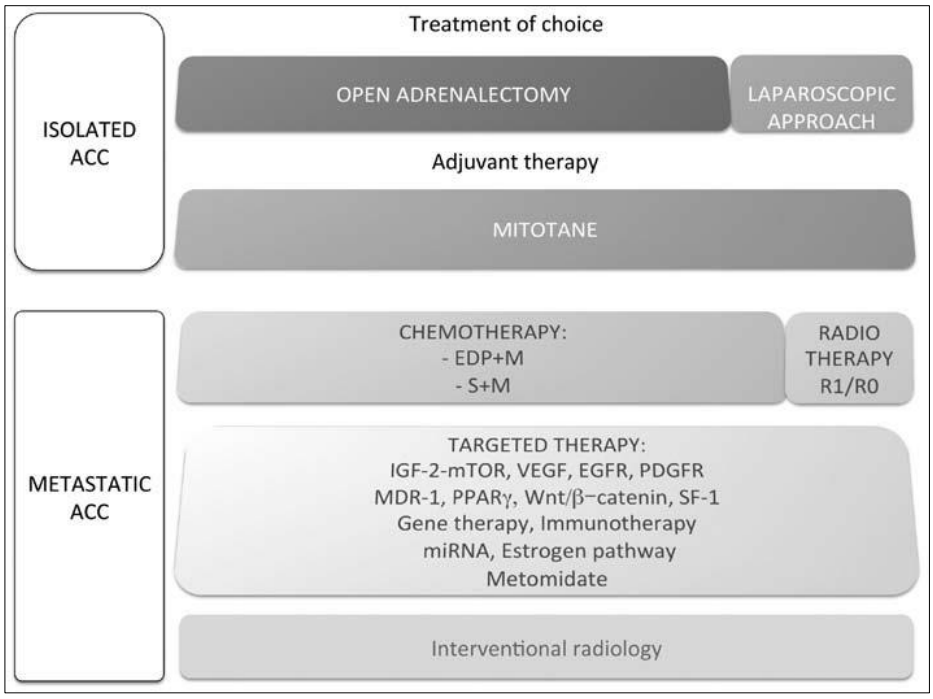

Figure 1.1 Treatment of choice in isolated and metastatic adrenocortical carcinoma (ACC)

1.4 Cancer cell metabolism and ACC

During carcinogenesis and tumor progression, neoplastic cells may reprogram their metabolism, showing a preference for glycolysis pathway for energy production, even in the presence of oxygen, a phenomenon known as the "Warburg effect" **[Figure 1.2].**

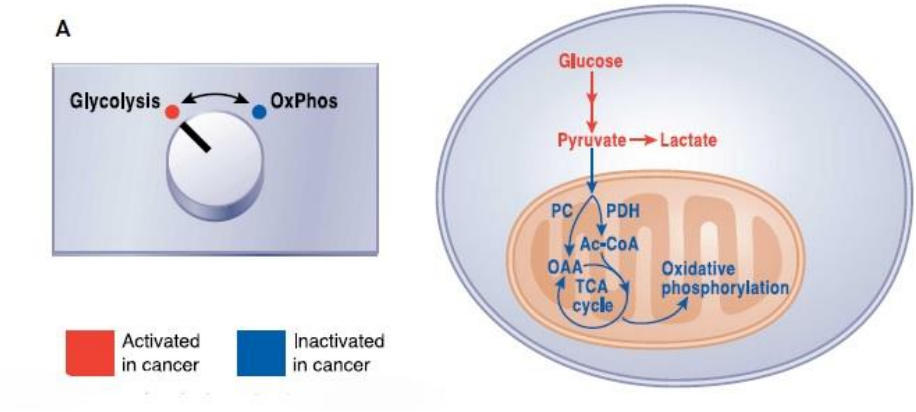

Figure 1.2 Relationship between glycolysis and oxidative phosphorylation in cancer cells. A common view of cancer cell metabolism invokes aswitch from glucose oxidation in normal tissues toward glycolysis and suppressed oxidative phosphorylation (OxPhos) in cancer.

This aerobic glycolysis implies the conversion of pyruvate to lactic acid, leading to a reduction in intracellular pH [Gatenby R.A. & Gillies R.J.; 2004]. To prevent acid-induced apoptosis as well as glycolysis inhibition by accumulation of the end product, cancer cells upregulate proteins related to pH regulation and lactate transport, including the glucose transporter GLUT1, the pH regulator carbonic anhydrase IX (CAIX) [Chiche J. et al., 2010; Tennant D.A. et al., 2010] and monocarboxylate transporters (MCTs) [Chiche J. et al., 2010]. Therefore, many malignancies show a significant increase in the expression of these plasma membrane transporters, with associations with poor patient's prognosis [de Oliveira A.T. et al., 2012; Pinheiro C. et al., 2012; Miranda-Goncalves V. et al., 2013; Pinheiro C. et al., 2014]. The MCT family has 14 members, being isoforms 1, 2 and 4 the most well studied isoforms responsible for the transport of monocarboxylates, including lactate, coupled with a proton across the plasma membrane. As consequence from their substrate affinities, MCT1 and MCT4 mediate monocarboxylate efflux from cells, while MCT2 is involved in monocarboxylate uptake [Halestrap A.P., 2012]. Importantly, these transporters require co-expression with chaperones for proper plasma membrane localization and activity. The main chaperone

of MCT1 and MCT4 is CD147 [Kirk P. et al., 2000; Wilson M.C. et al., 2005], while MCT2 is mainly associated with gp70 [18]. CD44 has also been recently described as a MCT chaperone [Slomiany M.G. et al., 2009]; however CD147 and CD44 expressions do not account for all MCT1/4 positive cases, suggesting that an additional MCT chaperone still remains to be identified [Pinheiro C. et al., 2010].

The metabolic profile of adrenocortical tumors is very little explored [Fenske W. et al., 2009]. However, 18F-fluorodeoxyglucose positron emission tomography (FDG-PET) data suggest that adrenocortical carcinomas show high levels of glucose consumption [Nunes M.L. et al., 2010; Deandreis D. et al., 2011; Bourdeau I. et al., 2013; Takeuchi S. et al., 2014], indicating a possible clinical relevance of the glycolytic metabolism for the management of this neoplasia.

In a recent study was evaluated the prognostic value of metabolism-related key proteins in adrenocortical carcinoma. The immunohistochemical expression of MCT1, MCT2, MCT4, CD147, CD44, GLUT1 and CAIX was evaluated in a series of 154 adult patients with adrenocortical neoplasia and associated with patients' clinicopathological parameters. A significant increase in was found for membranous expression of MCT4, GLUT1 and CAIX in carcinomas, when compared to adenomas. Importantly MCT1, GLUT1 and CAIX expressions were significantly associated with poor prognostic variables, including high nuclear grade, high mitotic index, advanced tumor staging, presence of metastasis, as well as shorter overall and disease free survival. In opposition, MCT2 membranous expression was associated with favorable prognostic parameters. Importantly, cytoplasmic expression of CD147 was identified as an independent predictor of longer overall survival and cytoplasmic expression of CAIX as an independent predictor of longer disease-free survival. They provide evidence for a metabolic reprogramming in adrenocortical malignant tumors towards the hyperglycolytic and acid-resistant phenotype, which was associated with poor prognosis [Pinheiro C. et al., 2015].

The major findings described so far allowed us to establish 2 h predominant expression profiles, the glycolytic and the oxidative phenotypes **[Figure 1.3],** which were associated with the clinicopathological parameters.

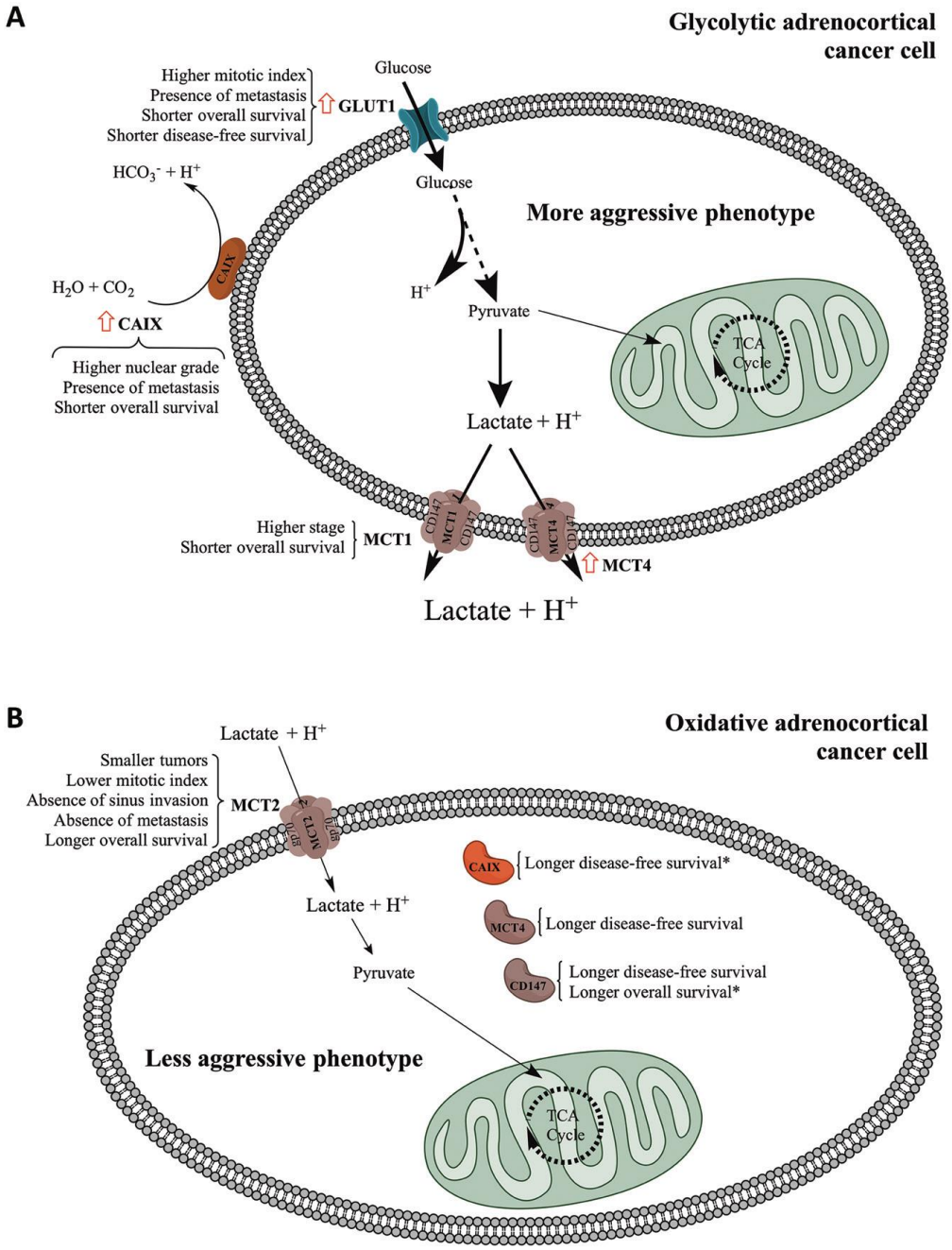

Figure 1.3 Schematic representation of Glycolytic *versus* oxidative phenotype. The schematic representation distinguishes the major findings for plasma membrane and cytoplasmic expression of the different proteins studied. Red arrow: significant increase in expression frequency when comparing adenomas to carcinomas. * Independent predictors of survival as determined by multivariate analysis.

An important conclusion from recent studies, and from a similar study in mice bearing KRAS-driven tumors [Davidson S.M. et al., 2016], is that non–small cell lung tumors demonstrate higher levels of both glycolysis and glucose oxidation relative to adjacent,

benign lung. This finding sharply contrasts with the frequently invoked “switch” from oxidativemetabolism to glycolysis inmalignant tissue, commonly used to explain the Warburg effect **[Figure 1.2].** Rather, the data support a model in which the amplitude of both pathways is increased simultaneously, perhaps through increased substrate delivery and enzyme expression in tumor cells **[Figure 1.4].** It is also significant that human tumors exhibit substantial heterogeneity of metabolic phenotypes, both between tumors and even within distinct regions of the same tumor [Hensley C.T. et al., 2016].

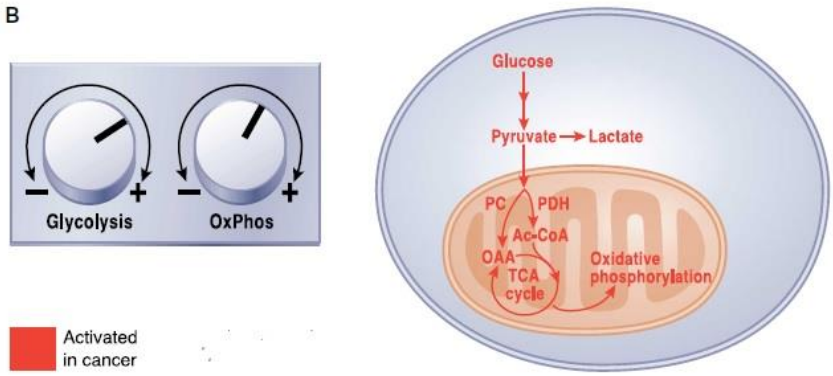

Figure 1.4 Analysis of metabolic activity in intact tumors from humans ankd mice argues against a switch. Rather, tumors appear to enhance both glycolysis and glucose oxidation simultaneously relative to surrounding tissue.

Awareness that the metabolic phenotype of cells within tumours is heterogeneous — and distinct from that of their normal counterparts — is growing **[Figure 1.5].** In general, tumour cells metabolize glucose, lactate, pyruvate, hydroxybutyrate, acetate, glutamine, and fatty acids at much higher rates than their nontumour equivalents; however, the metabolic ecology of tumours is complex because they contain multiple metabolic compartments, which are linked by the transfer of these catabolites. This metabolic variability and flexibility enables tumour cells to generate ATP as an energy source, while maintaining the reduction–oxidation (redox) balance and committing resources to biosynthesis — processes that are essential for cell survival, growth, and proliferation. Importantly, experimental evidence indicates that metabolic coupling between cell

populations with different, complementary metabolic profiles can induce cancer progression [DeBerardinis R.J. & Chandel N.S., 2016].

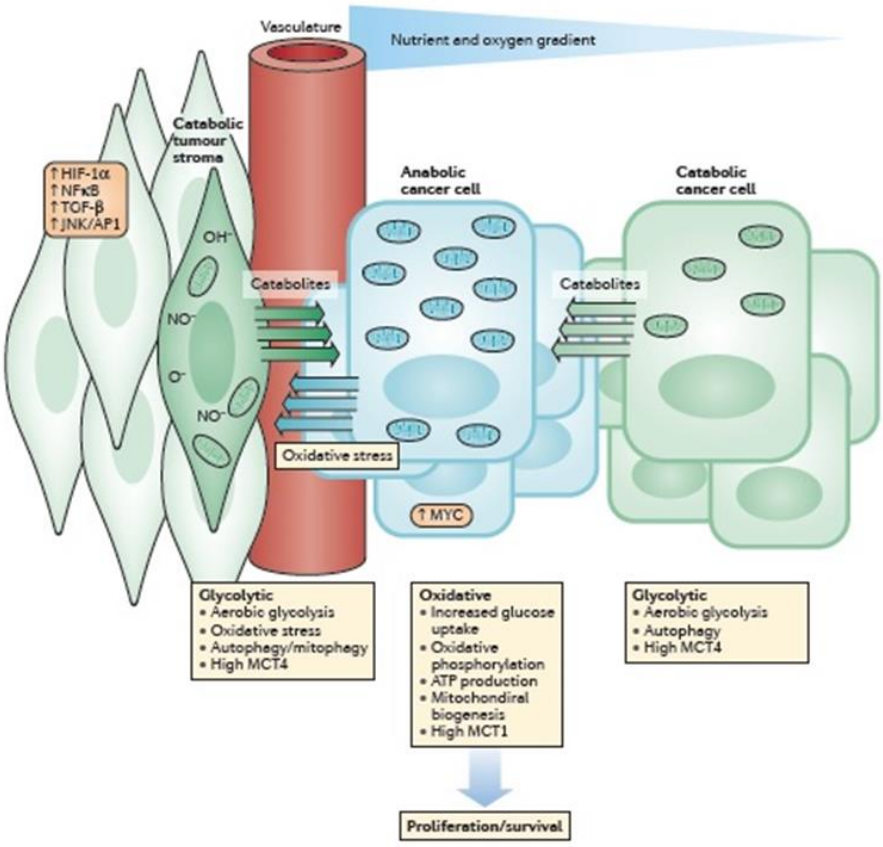

Figure 1.5 Metabolic heterogeneity in tumours. Within tumours, cancer-cell metabolism can vary depending on influences of the tumour microenvironment and the distance to the vasculature. Cancer cells located closer to the blood supply profit from their access to nutrients and oxygen, and generate ATP aerobically via oxidative phosphorylation and upregulate anabolic pathways, supporting rapid proliferation. The oxidative stress caused by these rapidly proliferating cancer cells induces glycolysis and autophagy in the surrounding stromal cells that generates catabolites, such as lactate or ketones, which in turn are taken up by anabolic cancer cells, and used to fuel mitochondrial metabolism and ATP production (reverse Warburg effect). Similarly, low nutrient availability requires that tumour cells located further from the vasculature and in proximity to anabolic tumour-cell populations commit to alternative catabolic metabolic pathways, such as autophagy, allowing greater adaptability to meet their resources and energy needs. ATP, adenosine triphosphate; HIF-1α, hypoxia-inducible factor 1α; JNK/AP1, c-Jun *N*-terminal kinases/activator protein 1; MCT1, monocarboxylate transporter 1; MCT4, monocarboxylate transporter 4; NFκB, nuclear factor κB; TGF-β, transforming growth factor β.

Indeed, mitochondria remain functional and produce intermediates for the biosynthesis of structural precursors in cancer cells with the oxidative phenotype [DeBerardinis R.J. et al., 2008]. However, the glycolytic state prevails in tumor cells and reflects a metabolic

profile known to favor tumor angiogenesis, invasion and migration [Pugh C.W. & Ratcliffe P.J., 2003], events poorly investigated in ACC.

2. The Estrogen-Related Receptor Alpha (ERRα)

2.1 Domain organization of estrogen receptors and estrogen – related receptors

Nuclear steroid receptors comprise five separate domains **[Figure 2.1A].** From the amino-terminus, the hormone-independent transcription activation domain comprises also a nuclear localization signal. It is followed by the DNA-binding domain, which contains a second nuclear localization signal. The DNA-binding domain is separated by a short hinge region from the ligand-binding domain, which is the largest domain and contains a dimerization domain and a transcription repression domain. The second transcription activator domain, which is ligand dependent, is at the carboxy-terminus. There are two estrogen receptors. The first, cloned in 1985 from estrogen-responsive breast cancer cells [Walter P. et al., 1985; Green S. et al., 1986], is expressed in classic estrogen target cells and tissues and is responsible for the standard estrogen responses listed above. It is this receptor that is measured as an important prognostic and predictive biomarker in hormone-dependent breast cancer. The second, which is a 59.2 kDa receptor of 530 amino acids, identified in 1996,56 was called estrogen receptor beta; the former was renamed estrogen receptor alpha at this time to distinguish between the two. Estrogen receptor beta is reported to be expressed more widely than oestrogen receptor alpha and its function is less well understood. Conservation between the two paralogs is variable: low in the domains that interact with transcription activators and in the hinge region, at 25-30%; intermediate in the ligand-binding domain, at 60%; and highest, at 90%, in the DNA-binding domain **[Figure 2.1C].**

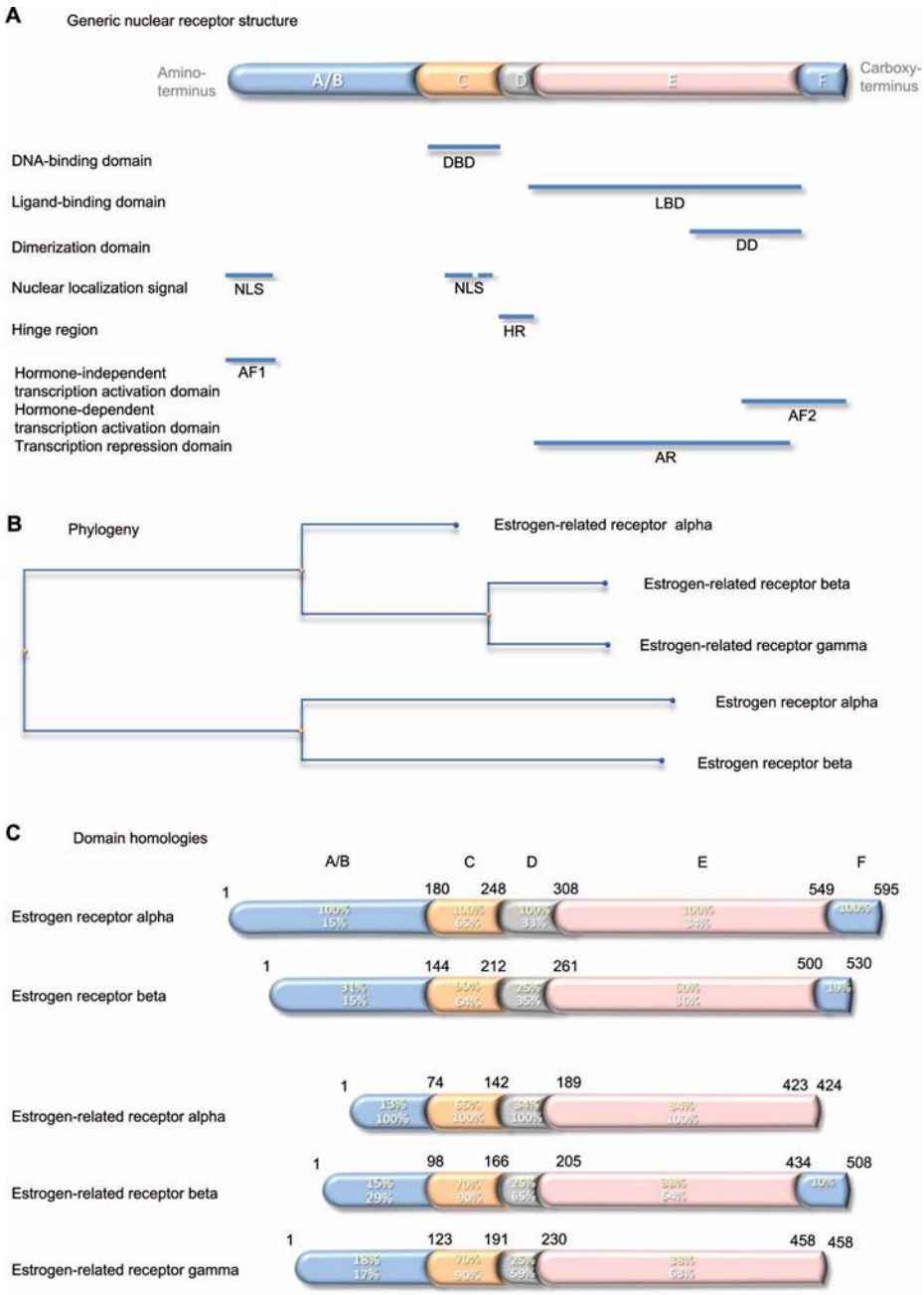

Figure 2.1 Generic nuclear receptor structure, and estrogen receptor family phylogeny and shared homologies.

Notes: Steroid hormone receptors share a conserved five-domain structure (**A**): domain A/B, which is involved in transcription activation and nuclear localization; domain C, which is the DBD; domain D, which serves as a hinge between the DBD and LBD; domain E, which is the LBD, responsible also for dimerization, transcription activation, and transcription repression; and domain F, which contains part of the second transcription activation domain. Phylogenetic analysis indicates that the genes that encode the five estrogen receptor proteins have evolved from a common precursor gene (**B**). The estrogen-related receptor alpha is the most distant. The percentage conservation between the estrogen receptor alpha (yellow

text) and the other four proteins, and between the estrogen-related receptor alpha (white text) and the other four proteins, is shown for each of the five domains (**C**).

Abbreviations: NLS, nuclear localization signal; AF1, hormone-independent transcription activation domain; DBD, DNA-binding domain; HR, hinge region; LBD, ligand-binding domain; DD, dimerization domain; AR, transcription repression domain; AF2, hormone-dependent transcription activation domain.

2.2 Estrogen-related receptor alpha

In 1988, 8 years before discovery of estrogen receptor beta, two other members of the estrogen receptor family were discovered by Giguère et al. [Giguere V. et al., 1988] a 45.5 kDa, 423 amino acid residue protein named estrogen-related receptor alpha; and a 56.2 kDa, 508 amino acid residue protein named estrogen-related receptor beta. Later, the estrogen-related receptor gamma of 51.3 kDa, 458 amino acid residue protein was identified [Schwabe J.W. et al., 1993; Chen F. et al., 1999]. Evolutionarily, estrogen-related receptor beta and gamma are closer to each other than to estrogen-related receptor alpha **[Figure 2.1 B].** Comparison of the primary sequences in the different receptor domains shows relatively strong conservation of around 65% in the DNA-binding domains and less, around 35%, in the ligand-binding domains. Conservation is loweroutwith these domains, and the estrogen-related receptors alpha and gamma lack an F domain **[Figure 2.1 C**]. The estrogen-related receptor alpha interacts with coregulator proteins and binds to specific DNA sequences of its target gene promoters, primarily as a homodimer. The peroxisome proliferator-activated receptor (PPAR) gamma coactivator (PGC)-1 family (PGC-1α, PGC-1β, and PPRC-1) and the p160 SRC proteins interact with this estrogen-related receptor alpha coactivator surface via LXXLL motifs [Xu J. et al., 2009]. The most notable difference between estrogen-related receptors and estrogen receptors is that the former function as aporeceptors when they are not bound to ligand.

2.3 Estrogen receptor family DNA-binding domains

Arguably the domain most central to the specific functions of the estrogen receptor family is the conserved DNA-binding domain that recognizes sequences in the responsive genes and dictates with which genes the receptor will interact. This relatively short sequence of 70 amino acid residues contains two zinc-binding elements. In each, a zinc ion is ligated tetrahedrally by four cysteine residues **[Figure 2.2]**. This class II zinc-binding motif

comprises, from the amino-terminus, a zinc finger, an alpha helix, the second zinc finger, and the second alpha helix. The first alpha helix is the recognition helix that fits into the major groove of the double-stranded DNA. The structure of the estrogen receptor alpha DNA-binding domain in complex with DNA illustrates that the receptor dimer locates primarily on one face of the DNA helix **[Figure 2.2C]** [Schwabe J.W. et al., 1993]. The side chains of the residues make specific contacts with four DNA bases. The three residues responsible for the DNA interface are referred to sometimes as the proximal box. One of these residues, alanine in the estrogen-related receptors, is a glycine in the two estrogen receptors. The second region of intermolecular interaction is responsible for the dimerization interface and is referred to sometimes as the distal box. This region contains uniquely in estrogen-related receptor alpha a single conservative substitution of a serine in place of a threonine.

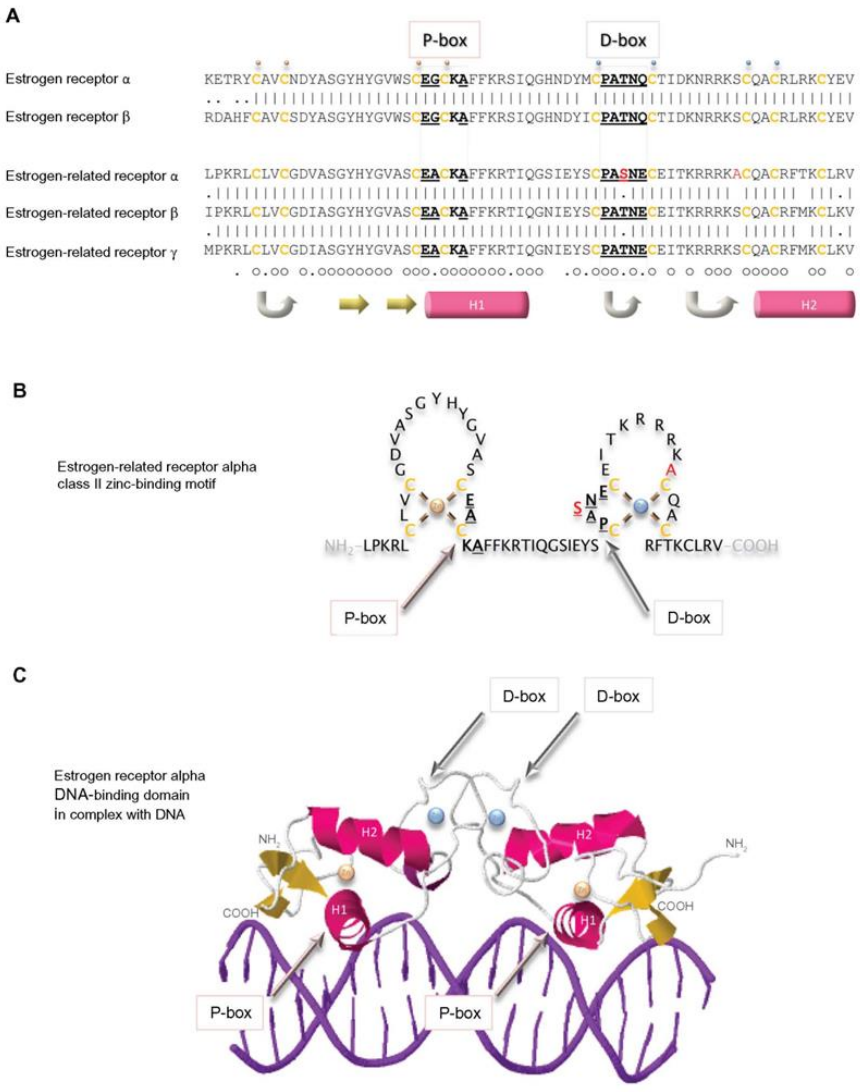

Figure 2.2 DNA-binding domains of the estrogen receptors.

Notes: The primary sequences of the DNA-binding domains of the five estrogen receptors are aligned (**A**). Vertical lines indicate amino acid residues that are identical in estrogen receptor alpha and beta, or in the three estrogen-related receptors, and dots indicate conserved substitution of residues. Residues that are identical in all five proteins are indicated by a small circle, and those that are substituted conservatively by a dot underneath the sequences. Cysteine residues are colored ochre and are in bold. The residues in the proximal box (P-box) that are responsible for interaction with DNA and those in the distal box (D-box) that are involved in the dimerization interface are in bold and are underlined. The two residues that are unique to estrogen-related receptor alpha are colored red. A small gold sphere is above the four cysteine residues that bind tetrahedrally to one zinc ion and a small blue sphere is above the cysteine residues that bind tetrahedrally to the second zinc ion. Regions of secondary structure are indicated below the sequences: turn (gray arrow), beta strand (yellow arrow), and alpha helix (pink cylinder). The estrogen-related receptor alpha DNA-binding class Iizinc-binding motif is illustrated graphically (**B**) and a ribbon representation of the structure of the of the estrogen receptor alpha in complex with DNA is shown (**C**) with the same conventions as in (**A**).

Members of the estrogen receptor family bind to specific conserved DNA recognition sequences in the DNA of their responsive genes **[Figure 2.3]**. Often, but not always, located proximal to the promoters, they may be up to 100 kb from the promoter of the responsive gene. The canonical estrogen response element or ERE 5′-AGGTCA-3′ is followed by three bases of indeterminate sequence and then by the inverse sequence 5′-TGACCT-3′ [Klein-Hitpass L. et al., 1986; Berry M. et al., 1989; May F.E. et al., 1993; May F.E. & Westley B.R.; 1995; Klinge C.M. et al., 2001]. The palindromic nature of the perfect ERE is predictable given the perfect dimeric structure formed by interaction of the two receptor DNA-binding domains **[Fig 2.2C].** Reduction in the length of the palindromic sequence by a base on either side reduces the affinity of the interaction with the receptor dimer. The third base pair of the ERE half-site, G–C, provides binding energy, and the fourth base pair, T–A, makes a positive contact with the receptor. Most EREs identified differ from the canonical sequence by at least one base pair [May F.E. & Westley B.R.; 1995].

The estrogen-related receptor alpha affects the transcription of known estrogen-responsive genes, such as those that encode lactoferrin, osteopontin, thyroid receptor alpha, aromatase (*CYP19*), and TFF1 [May F.E. & Westley B.R.; 1986; Prest S.J. et al., 2002] via interaction with the EREs in these genes [Yang N. et al., 1996; Vanacker J.M. et al., 1998a; Vanacker J.M. et al., 1998b; Yang C. et al., 1998; Lu D. et al., 2001].

Detailed analysis suggests that estrogen-related receptor alpha binds particularly well if the sequence is preceded by 5′-TAA-3′ or 5′-TCA-3′, and it is suggested that the estrogen-related receptor alpha response element (ERRE) is 5′-TA/CA AGGTCA-3′. The presence of a combined ERRE and ERE will ensure regulation of a gene by both receptors. It is noteworthy that the *TFF1* promoter contains an imperfect ERRE and an imperfect ERE **[Figure 2.3].**

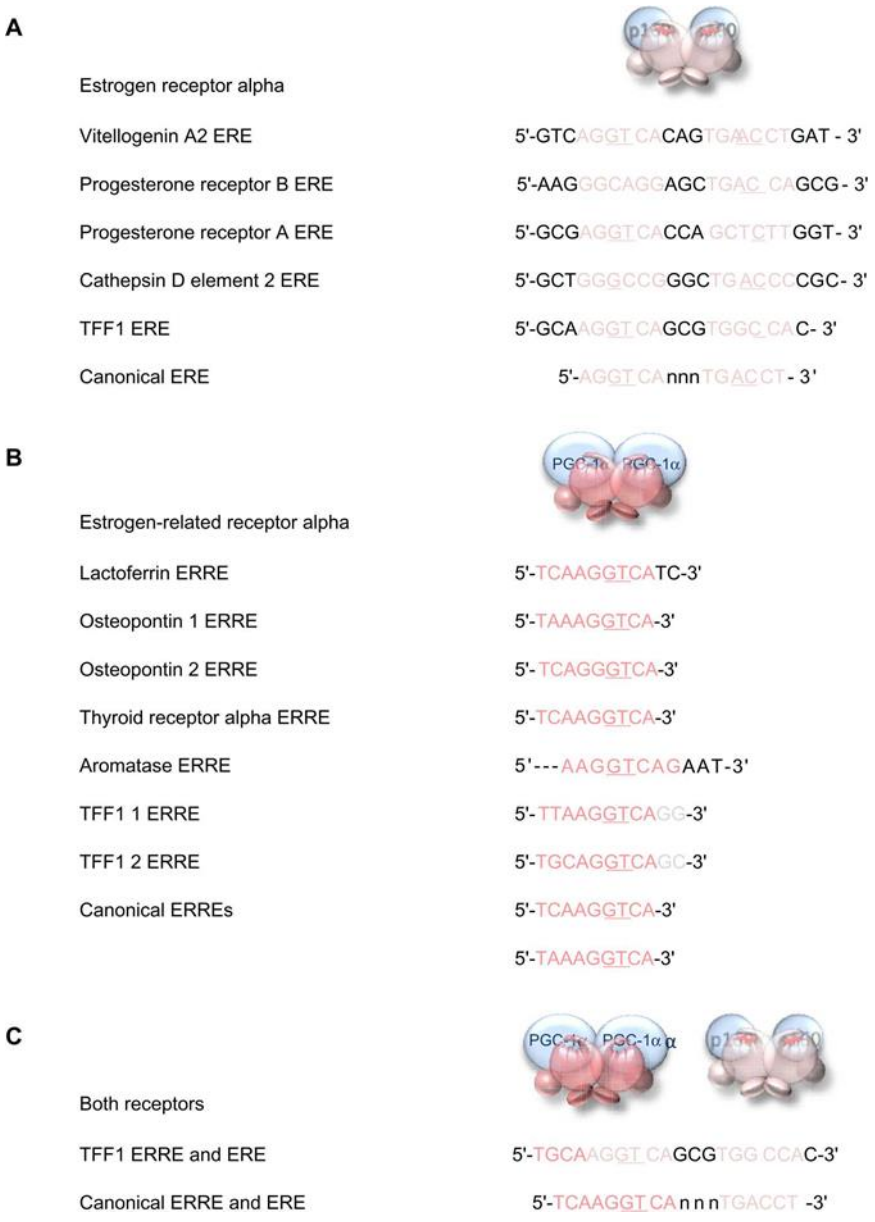

Figure 2.3 DNA response elements recognized by estrogen receptor alpha and estrogen-related receptor alpha

Notes: The sequences of the EREs identified in key estrogen responsive genes are aligned above the consensus perfect palindromic sequence (**A**). The sequences of the ERREs identified in its responsive genes are aligned above the canonical sequence (**B**). The dual ERRE and ERE found in the promoter region of the *TFF1* gene is shown above a perfect combined ERRE and ERE (**C**). The important third and fourth base pairs of the EREor ERRE half-sites that provide binding energy and make positive contact with the receptor, respectively, are underlined when they are the conserved canonical sequence in the response elements.

Abbreviations: ERE, estrogen response element; ERRE, estrogen-related receptor alpha response element.

2.4 Estrogen receptor family ligand-binding domains

The ligand-binding domains of the estrogen receptor family are composed almost entirely of 12 helices, of which eleven are arranged in three antiparallel layers [Brzozowski A.M. et al., 1997]. Helices 5, 6, 9, and 10 comprise the central core layer, which is sandwiched between helices 1–4 on one face and helices 7, 8, and 11 on the other **[Figure 2.4A].** In the estrogen receptors, this wedge-shaped molecular scaffold creates a sizeable hydrophobic cavity at its narrower end into which estrogens slip and interact with high affinity. The remaining secondary structural elements, a small two-stranded antiparallel β-sheet and helix 12, flank the main three-layered motif on either side of the hydrophobic pocket **[Figure 2.4A].** After interaction with estrogens, helix 12 is positioned as a lid over the ligand-binding pocket to secure the ligand in position and posit the hydrophobic side chains of helix 12 toward the steroid **[Figure 2.4B]** [Brzozowski A.M. et al., 1997]. This conformation creates a surface on the receptor that includes the charged residues, Lys362 at the end of helix 3 and Asp538, Glu542, and Asp545 from helix 12, that were identified by mutation analysis to be important for transcription activation **[Figure 2.4A]** [Danielian P.S. et al., 1992]. Subsequent analysis of the structure of the ligand-binding domain of estrogen receptor alpha bound to the synthetic estrogen diethylstilbestrol and a coactivator peptide with an LXXLL motif identified more fully the coactivator recruitment surface [Shiau A.K. et al., 1998]. The interaction surface comprises a hydrophobic cleft formed with residues from helices 3, 4, 5, and 12 and the turn between helices 3 and 4 **[Figure 2.4C]**. Interaction of the amphipathic alpha-helical coactivator peptide buries approximately 1,000 Å2 of the hydrophobic interaction surface. The majority of the residues involved in the interaction are hydrophobic. In addition, the main chain conformation of the coactivator peptide is stabilized by charged capping

interactions at either end of the peptide helix with Lys362 from helix 3 and Glu542 from helix 12 of the receptor **[Figure 2.4C]**.

After interaction of antiestrogens such as the active metabolite of tamoxifen, 4-hydroxytamoxifen, or raloxifene with the ligand-binding domain of estrogen receptor alpha, a portion of the ligand remains outside the ligand-binding pocket **[Figure 2.4A]** [Brzozowski A.M. et al., 1997; Shiau A.K. et al., 1998]. The extruded ligand prevents alignment of helix 12 over the ligand-binding pocket and hence formation of a complete coactivator recruitment surface. Instead, helix 12 is positioned over the hydrophobic cleft between helices 3, 4, and 5, in which position it precludes completely interaction of coactivators with this surface of the receptor. The secondary and tertiary structures of the ligand-binding domains of estrogen-related receptors are extremely similar to those of the estrogen receptors, but subtle differences are proposed to allow them to function as aporeceptors and explain the failure to identify their natural ligands. Notably, in the structure of the estrogen-related aporeceptor alpha, helix 12 is positioned across the ligand-binding domain **[Figure 2.4A]** [Kallen J. et al., 2004]. Thus the four charged residues, Lys244 in helix 3 and Lys412, Glu416, and Glu419 in helix 12, equivalent to those thought originally to be critical for activation of transcription in estrogen receptor alpha, are on the same face of the receptor in the absence of ligand. The crystal structure of estrogen-related receptor alpha includes the coactivator peptide of PGC-1α bound to the receptor coactivator recruitment surface; it is not known if the presence of this peptide facilitates stabilization of the active conformation of estrogen-related receptor alpha in the crystals, or if the structure of the aporeceptor ligand-binding pocket would be more open in the absence of the PGC-1α peptide. The coactivator recruitment surface of estrogen-related receptor alpha formed from helices 3, 4, 5, and 12 is similar to that of estrogen receptor alpha. The PGC-1α peptide is anchored by canonical charge clamp interactions with Lys244 from helix 3 and Glu416 from helix 12, and many of the conserved hydrophobic residues interact with the coactivator peptides in both structures **[Figure 2.4C]** [Shiau A.K. et al., 1998; Kallen J. et al., 2004]. The estrogen-related receptor alpha ligand-binding pocket is delineated by 22 amino acid residues, most of which have hydrophobic side chains. It is occluded by bulky hydrophobic side chains, in particular that of the phenylalanine Phe232 from helix 3, [Kallen J. et al., 2004] which is an alanine in the other four receptors, to create a cavity of only 100 Å3, which is substantially smaller than those of the estrogen receptor alpha (490 Å3) or beta (390 Å3)

[Figure 2.4B]. Removal of this hydrophobic side chain abolishes activity of the aporeceptor. It is proposed that the presence in the ligand-binding pocket of Phe232 and other bulky hydrophobic side chains, notably Phe286 from the small beta sheet, Phe399 from helix 11, and Phe414 from helix 12, recapitulates the interactions provided by hydrophobic steroids in the estrogen receptors and allows the aporeceptor to hold an active conformation able to interact with coactivator proteins [Kallen J. et al., 2004]. Disruption of the interactions between Phe232, Phe286, Phe399, and Phe414 destabilizes the active conformation of the estrogen-related aporeceptor alpha.

Interestingly, estrogen-related receptor alpha retains the charged Glu235 and Arg276, of which the equivalent residues in estrogen receptor alpha form a hydrogen bond network with the hydroxyl group on carbon 3 of the A ring of all three estrogens. Estrogen-related receptor alpha retains also the polar His298 that forms a hydrogen bond with the hydroxyl group on carbon 17 of the D ring of estradiol and estriol. It is suggested, however, that insertion of an estrogen into the ligand-binding pocket of estrogen-related receptor alpha would cause such serious steric clashes, notably with the side chains of Phe232 and Phe399, that even the A ring would not be accommodated **[Figure 2.4B]** [Kallen J. et al., 2004]. The occlusion of the estrogen-related receptor alpha ligand-binding pocket by bulky hydrophobic side chains indicates that the introduction of a molecule with more than four or five carbon atoms would necessitate a conformational change that would displace helix 12 from the coactivator surface [Kallen J. et al., 2004]. The estrogen-related receptor alpha does not bind estrogens or 4-hydroxytamoxifen, but does interact with the synthetic estrogen diethylstilbestrol to prevent the receptor interaction with SRC-1. Antagonist effects of 39iethylstilbestrol on estrogen-related receptor alpha activity have been reported by some but not all authors [Lu D. et al., 2001; Suetsugi M. et al., 2003]. Modeling indicates that diethylstilbestrol would only be accommodated in the estrogen-related receptor alpha ligand-binding pocket if the side chains of Phe232 from helix 3 and Phe399 from helix 11 were to assume different conformations, and if Phe414 was removed from the hydrophobic cavity by displacement of helix 12. That these conformational changes would disrupt the favorable cluster of phenylalanines Phe232, Phe286, Phe399, and Phe414, might indicate that the affinity of 39iethylstilbestrol for estrogen-related receptor alpha would be weak. Substitution of Phe232 with an alanine residue, which is found in the equivalent position in the other four members of the estrogen receptor family, allows 4-hydroxytamoxifen to bind estrogen-related receptor

alpha with a relatively high affinity of 4×10–8 M [Coward P. et al., 2001]. Despite the steric constraints described above, several phytoestrogens: the flavone 6,3′,4′-trihydroxyflavone and the isoflavones genistein, daidzein, and biochanin A, have been reported to be agonists for estrogen-related receptor alpha activity [Suetsugi M. et al., 2003]. Phytoestrogens are produced by plants, have bactericidal and fungicidal activity, and represent the major natural exogenous sources of estrogenic compounds. The results indicate that it is possible for a ligand to interact with estrogen-related receptor alpha to augment its activity.

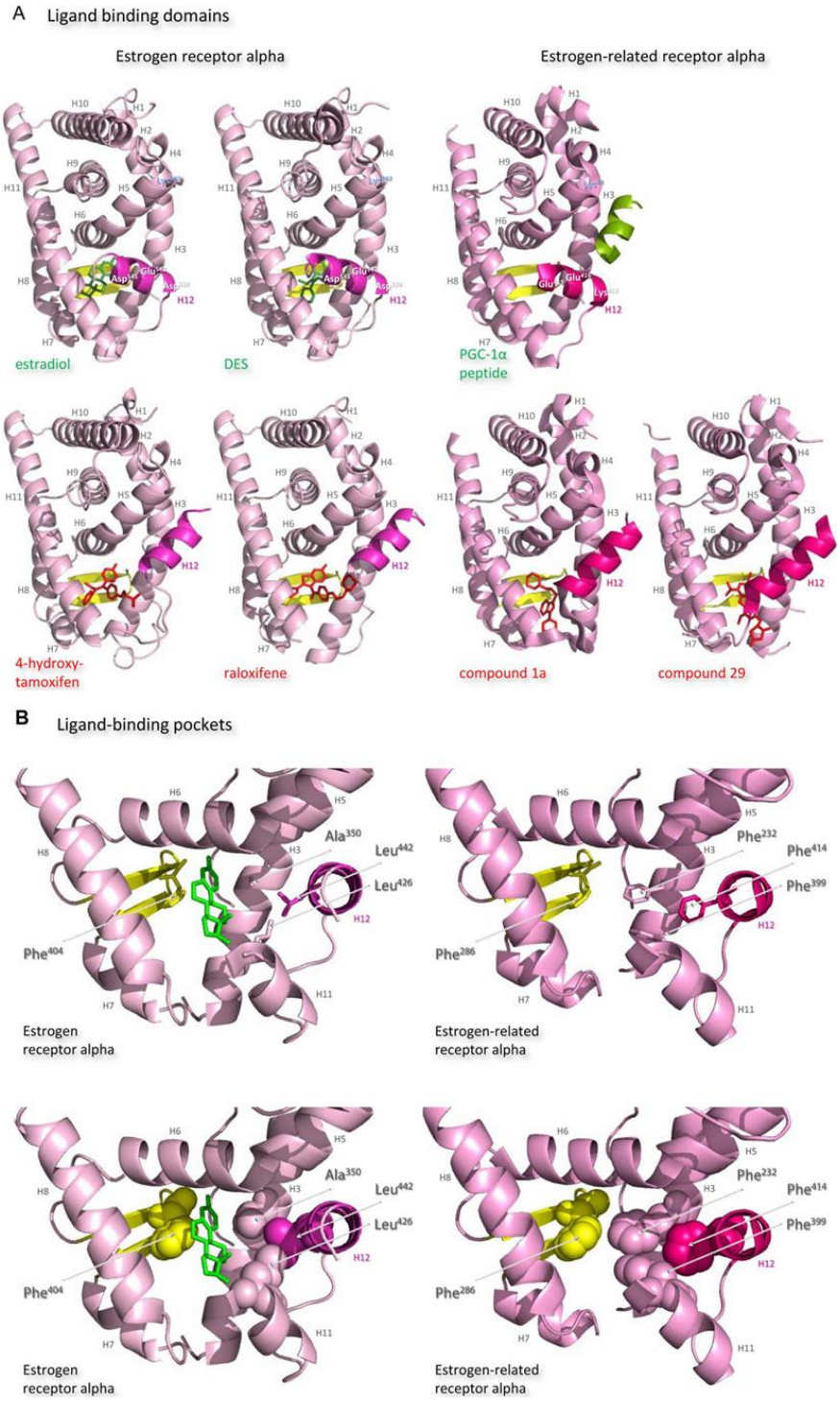
A Ligand binding domains
Estrogen receptor alpha
Estrogen-related receptor alpha
estradiol
DES
PGC-1α peptide
4-hydroxy-tamoxifen
raloxifene
compound 1a
compound 29
B Ligand-binding pockets
Ala350
Leu442
Leu426
Phe404
Phe232
Phe414
Phe399
Phe286
Estrogen receptor alpha
Estrogen-related receptor alpha

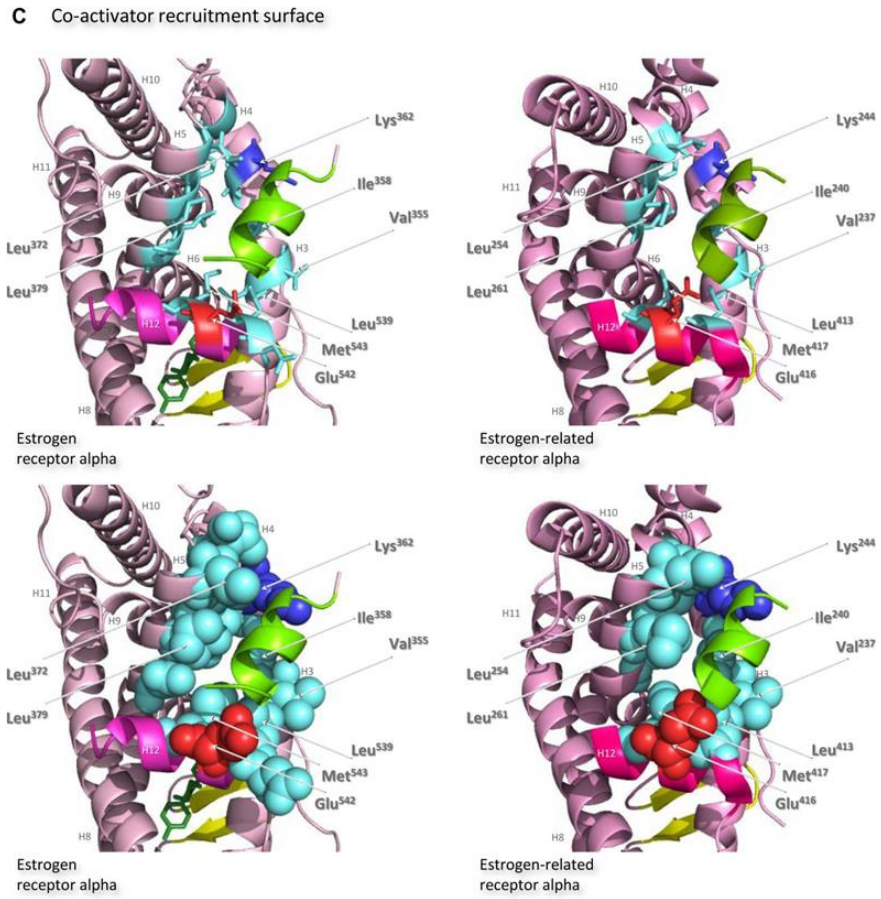

Figure 2.4 Structures of the ligand-binding domains of estrogen receptor alpha and estrogen-related receptor alpha in complex with their ligands

Notes: Ribbon representations of the three-dimensional crystal structures of the ligand-binding domains of estrogen receptor alpha in complex with estradiol (a); DES (b); 4-hydroxy-tamoxifen, a high-affinity metabolite of tamoxifen (c); and raloxifene (d), and of estrogen-related receptor alpha in complex with a PGC-1α peptide €; compound 1a (f); and compound 29 (g) **(A).** Helices 1–11 of estrogen receptor alpha are colored pale pink and those of estrogen-related receptor alpha pink. The 12th helices are colored darker shades of pink and the short antiparallel beta sheets are colored yellow. The ligands, shown in stick view, and coactivator peptides, shown in a ribbon representation, are colored green if they increase activity of the receptor and red if they inhibit its activity. The helices are numbered and the four charged residues proposed initially to be critical for coregulator interaction are labeled. Ribbon representations of the ligand-binding pockets of estrogen receptor alpha in complex with estradiol and of estrogen-related receptor alpha in complex with a PGC-1α peptide are shown with estradiol shown in stick representation **(B).** The molecules are rotated to the right compared to the views shown in (A), with helix 11 to the front and helix 12 to the right of the structures. Much of helix 11 has been removed to allow better visualization of the occupancy of the ligand-binding pockets. The side chains of the four phenylalanine residues, Phe232, Phe286, Phe399, and Phe414, that are orientated towards the ligand-binding pocket of estrogen-related receptor alpha and are thought to contribute to stabilization of its active conformation, and the equivalent residues of estrogen receptor alpha, Ala350, Phe404, Leu426, and Leu442, are indicated and labeled, and their side chains are

shown in stick representation (top) or in space-filling mode (bottom). Helices are numbered and colored as in (A). Ribbon representations of the coactivator recruitment surfaces of estrogen receptor alpha in complex with DES and a GRIP1 peptide, and of estrogen-related receptor alpha in complex with a PGC-1α peptide, are shown **(C).** The molecules are rotated slightly to the left compared to the views shown in (A) to allow better visualization of the hydrophobic cleft formed between helices 3, 4, 5, and 12. The helices are numbered and colored as in (A). The residues involved in the coactivator peptide interaction are shown in stick representation (top) and space-filling representation (bottom). Most have hydrophobic side chains and are colored light blue. The charged Lys and Glu residues that form charged capping interactions at either end of the coactivator peptide are colored blue and red, respectively. Conserved residues that were identified as being involved in interactions with the coactivator peptides in both structures and that are clearly visible in the figure are indicated. All images were created with PyMol Molecular Graphics Software (Schrödinger, Portland, OR, USA).

Abbreviations: DES, diethylstilbestrol; PGC, peroxisome proliferator-activated receptor gamma coactivator.

2.5 Physiological functions of estrogen-related receptor alpha

Discovery of estrogen-related receptor alpha immediately prompted questions of its physiological function: whether it overlapped with that of the estrogen receptor and if the receptor had a role in breast cancer. Estrogen-related receptor alpha is expressed in the later stages of embryonic development and is abundant in heart, skeletal muscle, and the nervous system. The physiological role of estrogen-related receptor alpha, and of estrogen-related receptor gamma, is to act as an energy sensor to control cellular adaptation to energy demand and stress. To this end, estrogen-related receptor alpha is expressed at high levels in tissues with high energy demands, such as muscle and brown adipose tissue. Cells that do not express active estrogen-related receptor alpha cannot produce sufficient energy in times of peak demand.

2.5.1 Role of estrogen-related receptor alpha in metabolism

In adipose tissue, estrogen-related receptor alpha increases the differentiation of mesenchymal stem cells into adipocytes and hence enhances fat deposition. Further, estrogen-related receptor alpha has a role in the regulation of energy metabolism in adipocytes. It increases lipid uptake, fatty acid beta-oxidation, the tricarboxylic acid cycle, oxidative phosphorylation, and mitochondrial biogenesis and function. Effects of estrogen-related receptor alpha on metabolism extend to other tissues with high energy

requirements, notably cardiomyocytes and macrophages [Casaburi I. et al., 2018]. The importance of estrogen-related receptor alpha in metabolic regulation is emphasized by the demonstration that *esrra*-null mice have impaired fat absorption and metabolism and are relatively resistant to fat-induced obesity [Luo J. et al., 2003]. These lean mice are unable to adapt to cold environments and develop cardiac contractile dysfunction. The cardiac hypertrophy induced by stress in *esrra*-null mice is caused by reduced ATP synthesis and reduced phosphocreatine storage [Huss J.M. et al. 2007].

2.5.2 Role of estrogen-related receptor alpha in osteogenesis

Estrogen-related receptor alpha influences the differentiation of myocytes, T-cells, intestinal epithelial cells, and osteoblasts. A report indicated that estrogen-related receptor alpha has a role in bone development and metabolism during embryogenesis [Bonnelye E. et al. 1997]. Its messenger RNA is expressed in murine bone cells during bone formation by endochondral and intramembranous ossification and in primary human osteoblasts. Estrogen-related receptor alpha was found to affect transcription of an osteopontin gene promoter; osteopontin is an important constituent of the mineralized extracellular matrix of bones [Bonnelye E. et al. 1997]. In *essra*-null mice, absence of estrogen-related receptor alpha increased modestly osteoblast differentiation and cancellous bone mineral density, as well as mesenchymal cell differentiation into osteoblasts [Delhon I. et al., 2009]. Further, estrogen-related receptor alpha was shown to decrease differentiation of human mesenchymal stem cells into osteoblasts, osteopontin expression, and mineral deposition, but to increase adipocyte differentiation [Delhon I. et al., 2009]. In a different strain of *essra*-null mice, female bones aged less compared to those of wild-type mice even after estrogen depletion and their marrow mesenchymal stem cells showed greater ability to differentiate into osteoblasts ex vivo [Teyssier C. et al. 2009]. Thus estrogen-related receptor alpha has a pivotal role in determination of mesenchymal stem cell fate and is implicated in inhibition of mineralization by osteoblasts [Bonnelye E. et al. 1997 Delhon I. et al., 2009; Teyssier C. et al. 2009].

2.5.3 Genes induced by estrogen-related receptor alpha

Genomic studies indicate that estrogen-related receptor alpha regulates large numbers of genes involved in energy metabolism. Estrogen-related receptors interact with the promoters of most mitochondrial and cellular genes that encode enzymes involved in the glycolytic pathway, the tricarboxylic acid cycle, and oxidative phosphorylation, and in nucleic acid, amino acid, lipid, and pyruvate synthesis. Estrogen-related receptor alpha is involved in the transcriptional regulation of genes required for mitochondrial biogenesis, the tricarboxylic acid cycle, oxidative phosphorylation, fatty acid oxidation, and lipid metabolism [Puigserver P. et al., 1998; Yoon J.C. et al., 2001; Huss J.M. et al., 2004]. For instance, estrogen-related receptor alpha induces expression of *NRF1*, *GAP*α, and *PPAR*α [Mootha V.K. et al., 2004]. The nuclear receptor coactivators PGC-1α, PGC-1β, and PPRC-1 are implicated in the regulation of these genes and in the autoregulation of the expression of estrogen-related receptor alpha. It has been suggested that the metabolic effects of estrogen-related receptor alpha are controlled by PGC-1α [Huss J.M. et al., 2004]. PGC-1α is expressed at low basal levels but is induced by fasting and other metabolic stresses [Puigserver P. et al., 1998]. PGC-1β, a related coactivator, has similar functions, but its expression may not be regulated as acutely by variations in energy demand [Yoon J.C. et al., 2001] **[Figure 2.5]**.

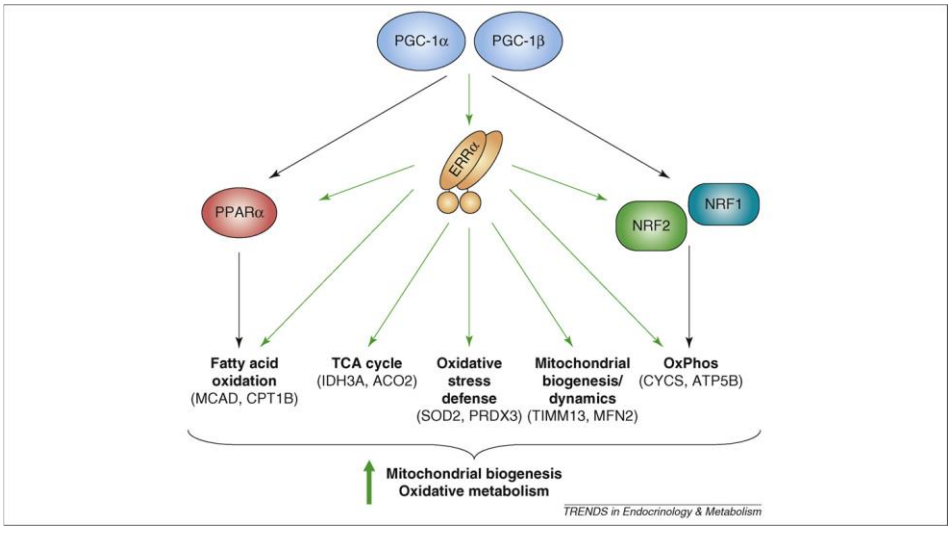

Figure 2.5 ERRa regulates genes important for mitochondrial biogenesis and oxidative metabolism. ERRa acts as a downstream effector of PGC-1a and PGC-1b in the regulation of expression of genes with roles in fatty acid oxidation, the TCA cycle, oxidative stress responses, mitochondrial biogenesis and dynamics, and oxidative phosphorylation (OxPhos). It acts both directly on genes encoding mitochondrial

structural components and enzymes, as well as indirectly by enhancing expression of other transcriptional factors, such as PPARa, NRF1 and NRF2/GABP, that regulate these pathways.

2.5.4 Activation of estrogen-related receptor alpha

If the estrogen-related receptor alpha is fully functional in the absence of ligand, does this mean that it is constitutively active? Current thoughts are that its activity is regulated in two main ways. First, its activation is limited by the intracellular concentrations of its coregulators. Rather than being regulated by interaction with a classic ligand with resultant stabilization of an active receptor conformation, the magnitude of estrogen-related receptor alpha activity is thought to be dependent largely on the presence of transcriptional coactivators of transcription such as PGC-1α, PGC-1β and PPARβ, SRC-3 and PPGC183 [Kressler D. et al., 2002; Lin J. et al., 2002] or corepressors of transcription such as RIP140 and nuclear receptor corepressor 1 (NcoR1) [Castet A. et al., 2006; Perez-Schindler J. et al., 2012]. Whether or not the coactivators induce or stabilize the active conformation of estrogen-related receptor alpha is unknown. Certainly, the coregulators are essential for most estrogen-related receptor alpha activity and have been termed surrogate ligands. Induction of the expression of the coregulators by external metabolic stress activates estrogen-related receptor alpha. Secondly, receptor activity is controlled by posttranslational modification, namely by phosphorylation initiated by the interaction of growth factors such as the IGFs and epidermal growth factors (EGFs) with their cognate receptors and consequent signal transduction. Recruitment of estrogen-related receptor alpha to the *TFF1* promoter and resultant transcription are increased in the presence of EGF, possibly via phosphorylation of the DNA-binding domain [Barry J.B. & Giguere V., 2005]. Activation of HER2 increases the transcriptional activity of estrogen-related receptor alpha by phosphorylation at multiple residues, including in the carboxy-terminus [Ariazi E.A. et al., 2007]. In vitro analyses of the ability of estrogen-related receptor alpha to induce transcription from the *TFF1* gene in breast cancer cells demonstrated that the induction is increased by activation of growth factor receptors including EGF receptor, HER2 and the type I IGF receptor [Chang C.Y. et al., 2011], In addition, phosphorylation-dependent, amino-terminal SUMOylation reduces transcriptional activity of estrogen-related receptor alpha [Tremblay A.M. et al., 2008] and acetylation by p300 coactivator-associated factor

(PCAF) of four lysine resides in its DNA-binding domain modulates its activity [Wilson B.J. et al., 2010].

2.6 ERRα Agonists

The constitutive activity of ERRα does not exclude the existence of a molecule able to modulate its activity enabling the recruitment of cofactors and playing a critical role in the maintenance of energy homeostasis as well as in disease progression. Recently, several synthetic antagonists have been identified [Busch B.B. et al., 2004; Willy P.J. et al., 2004; Chisamore M.J. et al., 2009a]. Moreover, dietary products, including cholesterol, have been reported as potential agonists [Teng C.T. et al., 2014; Teng C.T. et al., 2017]. Suetsugi and collaborators identified agonists through virtual ligand screening on an ERRα ligand binding model based on the crystalline structure of ERRγ-LBD [Suetsugi M. et al., 2003]. Thus, four ligands, increasing the transcriptional activity of ERRα, have been identified: isoflavones (genistein, daidzein, and biochanin A) and a flavone (trihydroxyflavone) [Suetsugi M. et al., 2003]. Later, scientists synthesized the potential molecules able to interact with the ligand-domain, guided by ERRα crystalline structure, but they were not able to demonstrate the activity of the agonists [Hyatt S.M. et al., 2007]. Moreover, Peng and collaborators synthesized a series of pyrid (1,2-a) pyrimidin-4 in order to produce more powerful ERRα agonists and to confirm the ability to induce the receptor transcriptional activity. These compounds have improved glucose and fatty acid uptake from muscle cells [Peng L. et al., 2011] and thus, could have a clinical utility for the treatment of metabolic diseases, including metabolic syndrome and diabetes.

2.7 Cholesterol: The First Endogenous ERRα Agonist

Recently, an important study investigated the binding ability of ERRα with endogenous lipids [Wei W. et al., 2016]. To this aim experiments by using chromatography techniques were performed according to previous approaches validated for the study of PPAR with endogenous lipids from the lipidome. The experimental model used is the mouse brain, selected for the high expression of ERRα. The receptor was expressed, purified, and immobilized onto a resin and then incubated with enriching lipidomes. This experimental approach allowed the identification of a single ion that was significantly enriched by the

beads bound to ERRL-BD and this ion was identified as cholesterol. Furthermore, to check the specificity of the interaction between ERRα and cholesterol, authors used targeted LC-MS method to increase the detection sensitivity for the lower-abundance sterols [McDonald J.G. et al., 2007]. The latter results were in agreement with those from lipidomic experiments. Moreover, in order to verify the specificity of ERRα-LBD-cholesterol interaction, a deeper investigation was performed with a competitive binding assay by using diethylstilbestrol (DES), a synthetic ERRα antagonist, that binds to the lipid-binding pocket of ERRα [Tremblay A.M. et al., 2008]. A further confirmation was obtained by the authors with circular dichroism (CD) spectroscopy tests, where cholesterol, DES and the inverse agonist XCT790, all induced a conformational change in ERRα-LBD, while estradiol did not. These results suggested that Cholesterol-ERRα-LBD binding is more than a simple hydrophobic interaction. In addition, dye-labeled cholesterol derivatives were used and, after fluorescence polarization assay, the results showed that cholesterol binds the ligand-binding pocket of ERRα through its hydroxyl group. These findings indicate that cholesterol could exert a functional control of the ERRα activity [Wei W. et al., 2016].

2.8 Cholesterol and ERRα in Breast, Prostate, and Adrenocortical Cancer

A new potential therapeutic application in a clinical setting controlling cholesterol levels come out from the observations on the role played by ERRa in breast (BC) and prostate (PC) cancers. In BC, high ERRα expression characterizes tumors with poor prognosis [Ariazi E.A. et al., 2002]. Moreover, ERRα mRNA is positively correlated with the oncogene ERBB2 and AIB1 [Surowiak P. et al., 2006] and inversely correlated with that of Erα and progesterone receptor that are good prognostic factors for the anti-hormonal treatment of breast cancer patients. Indeed, depending on the cellular context, ERRα could act promoting or inhibiting transcription [Kraus R.J. et al., 2002]. Findings suggested that in ER-negative BC, ERRα compensates for the loss of Erα in addition to triggering the expression of Erα-independent genes since it recognizes estrogen response element (ERE) as is the case for vascular endothelial growth factor (VEGF) promoting BC metastasis [Stein R.A. et al., 2008; Stein R.A. et al., 2009]. By contrast, in Erpositive BC cells, ERRα negatively controls ERE transcription by interacting with corepressor such as RIP1. Alternatively, ERRα could promote BC cells growth by enhancing circulating estrogen production. In fact, it has been found that ERRα could activate steroid

sulfotransferase (SULT2A1) that works to maintain high level of peripheral dehydroepiandrosteronesulfate (DHEAS), an important metabolite in estrogen synthesis in adrenal tissues. In addition, it has also been evidenced that SULT2A1 inactivates tamoxifen and raloxifene. Thus, high ERRα expression in breast cancer by enhancing SULT2A1 activity could also support breast cancer cell resistance to anti-hormonal therapy [Apak T.I. & Duffel M.W., 2004]. The enhanced expression of ERRα has been found also in prostate cancer (Pca) and Pca cell lines [Cheung C.P. et al., 2005]. A study indicates a positive correlation between ERRα expression and the Gleason jscore while results from a preclinical study showed that ERRα can promote the hypoxic growth adaptation of prostate cancer cells by interacting with HIF-1α. As above explained, ERRα is also expressed in the bone regulating activity of osteoblasts and osteoclasts, that is implicated into the mixed osteolytic and osteoblastic lesions observed in advanced prostate cancer patients [Bonnelye E. & Aubin J.E., 2013]. An increased cholesterol biosynthesis, regulated by sterol regulatory element-binding protein−2 (SREBP-2), is a key player in the initiation and progression of Pca where an enhanced stem cell population was observed [Li X. et al., 2016]. Moreover, aberrant cholesteryl ester accumulation in lipid droplets exacerbates cancer invasiveness and characterize high-grade Pca with PTEN loss and consequently, constitutive PI3K/Akt activation promotes metabolic dysregulation where ERRα/PGC-1α, as already mentioned, play a central role [Deblois G. et al., 2013]. In addition, the cholesterol metabolite, 27-hydroxyl-cholesterol (27-OHC) is now recognized as selective estrogen receptor modulator (SERM) which promotes tumorigenesis in ER-positive BC [Warner M. & Gustafsson J.A.; 2014]. Higher levels of 27-OHC have been reported in Erα-positive breast cancers with respect to normal breast tissue, along with an observed reduction in the 27-OHC metabolizing enzyme such as CYP7B1 [Wu Q. et al., 2013]. Results from in vivo experiments demonstrated that 27-OHC alone is sufficient to support estrogenic activity in ER-dependent breast cancer cells [Wu Q. et al., 2013]. Accordingly, an increased growth and metastasis of ER-positive tumors were observed in a mouse model of breast cancer fed only with a cholesterol-rich diet [Wu Q. et al., 2013]. The function of cholesterol as an ERRα agonist may provide the molecular basis and mechanistic insight into clinical studies suggesting that drugs able to lower cholesterol levels (i.e., statins) can be used to treat or prevent breast and prostate cancer.

Cholesterol could have positive growing effects, over its physiological role, also in the adrenocortical cancer (ACC). The treatment of ACC cell model with XCT-790, to the purpose of reducing ERRa expression, impaired cancer cell growth, both *in vitro* and *in vivo* [Casaburi I. et al., 2015]. These data well correlate with that reporting an increased ERRα expression in ACC compared to normal adrenal and adenoma [Felizola S.J. et al., 2013] underling the involvement of this metabolic receptor in ACC biology.

As previously explained, ERRα transcriptional activity in normal cells is directed to modulate cellular metabolism, supporting the growth of rapidly dividing cells and to control metabolic programs required for cellular energy homeostasis in differentiated cells and to satisfy energy request during cell differentiation. The recent identification of cholesterol as an endogenous ERRα agonist evidenced that this sterol enhances the interaction between ERRα and PGC-1β in osteoclasts, promoting osteoclastogenesis and bone resorption. Similarly, cholesterol promotes ERRα interaction with PGC-1α in myocytes inducing myogenesis and decreasing muscle toxicity. The discovery of this new molecular mechanism has elucidated the genesis of two important phenomena with an unexplained mechanism: the statin-induced muscle toxicity and the bisphosphonate suppression of bone resorption. Moreover, the discovery of cholesterol as an agonist of ERRα demonstrated that this receptor works as a metabolic sensing nuclear receptor distinguishing it from steroid receptors that respond to an acute and steep rise in hormonal levels. Consequently, ERRα is constitutively active because cholesterol is ubiquitous. This new mechanism calls fresh thinking about the role of ERRα in cancer cells keeping in mind the key role played by this receptor as modulator of cancer metabolism. As previously explained, the metabolic alterations of lipids, carbohydrates, and proteins are one of the hallmarks of cancers [Hanahan D. & Weinberg R.A., 2011]. In particular, an increase in the glycolytic rate at the expense of oxidative phosphorylation even in the presence of adequate oxygen concentrations (Warburg effect) [Warburg O., 1956] allows a rapid adaptation of tumor cells to the continuous metabolic changes that, together with the tumor microenvironment, are the driving forces for cancer survival and its evolution. Given the high interconnection between enzymes that regulate the metabolism and the molecular pathways induced by altered oncogenes, research of the key regulators that behave on metabolic adaptations and proliferative, anti-apoptotic, invasive and metastatic responses, could represent elective targets to break down tumors with a single shot. The ERRα could work for this end due to its location at the intersection of dysregulated

metabolism and oncogenic pathways. In several cancer cells, the expression and the activity of ERRα, together with its cofactors (PGC-1 α/β), is further influenced by oncogenic signals (IGF1-/IGF1R pathway, estrogen signaling, Wnt/b-cat/TCF, mTOR pathway) **[Figure 2.6A]** and can thus be re-directed to induce metabolic programs **[Figure 2.6B]** favoring tumor growth and progression. **[Figure 2.6C]**. In this context, an increased level of cholesterol, through the new molecular mechanism, supports all tumor-related processes **[Figure 2.6D]**. Accordingly, high levels of cholesterol are associated with an increased risk of different type of cancers including breast, prostate [Gutierrez-Pajares J.L. et al., 2016] and CRC [Wang C. et al., 2017]. Although epidemiological data on the correlation between cholesterol and cancer are conflicting, the preclinical results positively highlight different molecular aspects revealing how oncogenic growth signaling meet the bioenergetics and biosynthetic demands of rapidly proliferating tumor cells. In fact, altered cholesterol pathway in cancer could be reached through different mechanisms. One of the most important is the constitutive activity of the oncogenic PI3K/AKT/mTOR signaling pathway that enhances intracellular cholesterol levels by: (i) inducing cholesterol synthesis through the activation of the transcription factor SREBP (sterol regulatory element binding proteins); (ii) inducing LDL receptor–mediated cholesterol import; (iii) inhibiting ABCA1-mediated cholesterol export. Moreover, high-energy demanding cancer related process are strictly related to the cross-talk between tumor cells and some key players of the tumor microenvironment (TME), such as macrophages (TAM, tumor-associated macrophage), that in turn, fuels cancer progression through the formation of an inflammatory milieu characterized by the production of different cytokines such as IL-1, IL-6, and IL-8 among others. The latter, as above reported, could be a target of ERRα action **[Figure 2.6E]**. For most solid tumors, infiltration by inflammatory cells such as macrophages is associated with poor prognosis [Illemann M. et al., 2014; Mantovani A. et al., 2017]. The links between inflammation and cholesterol are best exemplified by atherosclerosis, but similar mechanisms may also contribute to other metabolic disorders including cancer. It is noteworthy that cholesterol accumulation in TAM triggers the phenotype switch from M1, antitumorigenic, to M2-like macrophage, protumorigenic [Leitinger N. & Schulman I.G., 2013]. Based on these considerations, the use of therapeutic strategy aimed to reduce cholesterol levels, such as statins **[Figure 2.6F]** or drugs targeting the SREBP metabolic pathways **[Figure 2.6G]**,

could be a promising option to counteract metabolic rewiring in cancer cells where ERRα plays a pivotal role.

In conclusion, identification of cholesterol as an endogenous ERRα agonist has already elucidated the most likely mechanisms underlying the side-effects induced by statins and bisphosphonate, but at the same time, it gives new perspectives to be further investigated in order to explore new therapeutic options for the treatment of ERRα overexpressing tumors. This alternative approach could bring additional benefits to the treatment of tumors that have already adopted successful therapies, but especially for those tumors, such as ACC, which are characterized by a limited or failed therapeutic choice [Casaburi I. et al., 2018].

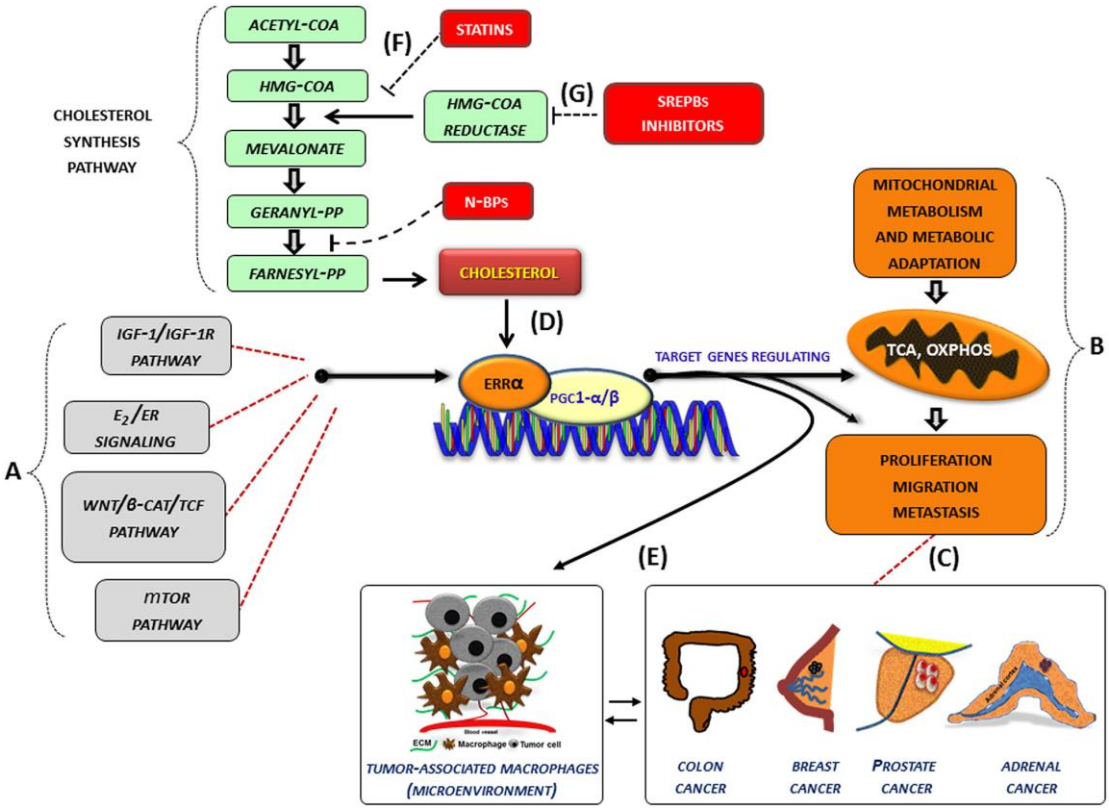

Figure 2.6 Role of cholesterol as modulator of ERRα action in cancer. (A–G) Schematic representation of how cholesterol, as a new ERRα ligand, can contribute to the complex molecular network consisting in the functional cross-talk between oncogenes and oncogenic pathways (IGF-1/IGF-1R, E2/ER, β-catenin/TCF, mTOR) **(A)** that support the overexpression of ERRa. In turn, ERRa, together with its main cofactors (PGC-1a and PGC-1b) and activators, such as cholesterol **(D)**, affects cancer cell metabolism promoting proliferation, migration and, metastasis **(B)** of different tumor phenotypes **(C).** All these bioenergy-consuming functions are strictly related to € the cross-talk between tumor cells and some key

players of the tumor microenvironment, such as macrophages (tumor-associate macrophages). The use of drugs [statins, **(F)**, N-bisphosphonates, N-BPs, SREBPs inhibitors, **(G)**] able to reduce cholesterol levels and ERRa transcriptional activity could widen the therapeutic opportunities for the treatment of different ERRa overexpressing tumors. More details are explained within the text. E2, estradiol; ER, estrogen receptor; IGF-1/IGF-1R, insulin-like growth factor-1/insulin-like growth factor-1 receptor; WNT, Wingless-type MMTV integration site family member; TCF, T-cell factor; TOR, mammalian target of rapamycin; N-BPs, nitrogen-containing bisphosphonates.

2.9 ERRα in invasion, angiogenesis and metastasis

One of the hallmarks of aggressive tumors is their metastatic ability dictated by their invasion and migration potential as well as their capability to establish tumor vascularization. The glycolytic state that prevails in tumor cells reflects a metabolic profile known to favor tumor angiogenesis, invasion and migration [Pugh C.W. & Ratcliffe P.J., 2003]. Since ERRα could contribute to the metabolic reprogramming of cancer cells, it can be envisioned that it also affects metastatic potential of these cells. In normal tissues, decreased expression of ERRα was shown to affect cell migration during zebrafish gastrulation *in vivo* [Bardet P.L. et al., 2005]. It also affects breast cancer cell migration *in vitro*, albeit without affecting proliferation rates [Stein R.A. et al., 2008]. The absence of ERRα is also able to impair tumorigenic potential in aggressive breast cancer cells xenograft in nude mice [Stein R.A. et al., 2008]. These observations are supported by the finding that ERRα and its coactivator PGC-1α bind to the promoter of and regulate the expression of VEGF, an important factor involved in tumor angiogenesis and invasion [Arany Z. et al.; 2008; Stein R.A. et al., 2009]. The PGC-1/ERR axis has also been shown to be a potent inducer of VEGF53 and to promote angiogenesis [Arany Z. et al.; 2008] in muscle. In addition, the kinase suppressor of ras1 (KSR1) is able to regulate ERRα and PGC-1α to promote oncogenic ras-dependent and anchorage-independent growth of cancer cells [Fisher K.W. et al., 2011]. ERRa has also been shown to regulate the expression of HIF in breast cancer cells and to associate with the HIFα/β heterodimer to promote its transcriptional activity on angiogenic and migratory target genes like VEGF [Ao A. et al., 2008]. ERRα is also thought to cooperate HIF to induce the metabolic reprogramming towards the metastatic-promoting glycolytic state in tumor cells [Ao A. et al., 2008]. The PGC-1/ERR axis also regulates the expression of WNT11, a process that involves ERRα in a transcriptional complex with β-catenin [Dwyer M.A. et al., 2010]. Ablation of either ERRα or β-catenin expression decreases the migratory

capacity of cancer cells of various origins, an observation that provides biological significance to this ERRα/β-catenin/WNT11 signaling pathway. In addition, functional genomics has identified ERRα target genes involved in invasion and migration and in promoting tumor vascularization such as FGF and CXCR4 [Deblois G. et al., 2010]. Studies reviewed herein clearly show that modulation of cellular energy metabolism by the PGC-1/ERR transcriptional axis plays a major role in the process of tumorigenesis. In normal cells, the activity of the PGC-1/ERR axis can be used to increase cellular metabolism, to support the growth of rapidly dividing cells, to direct metabolic programs necessary for cell differentiation and to maintain cellular energy homeostasis in differentiated cells. Indeed, the action of the PGC-1/ERR axis can have both proliferative and anti-proliferative outcomes, which are likely dependent on the composition of the PGC-1/ERR complexes present in these cells. In cancer cells, the activity of the PGC-1/ERR axis is further influenced by oncogenic signals and can thus be re-directed to induce metabolic programs favoring or attenuating cell growth and proliferation **[Figure 2.7]** [Deblois G. et al., 2013].

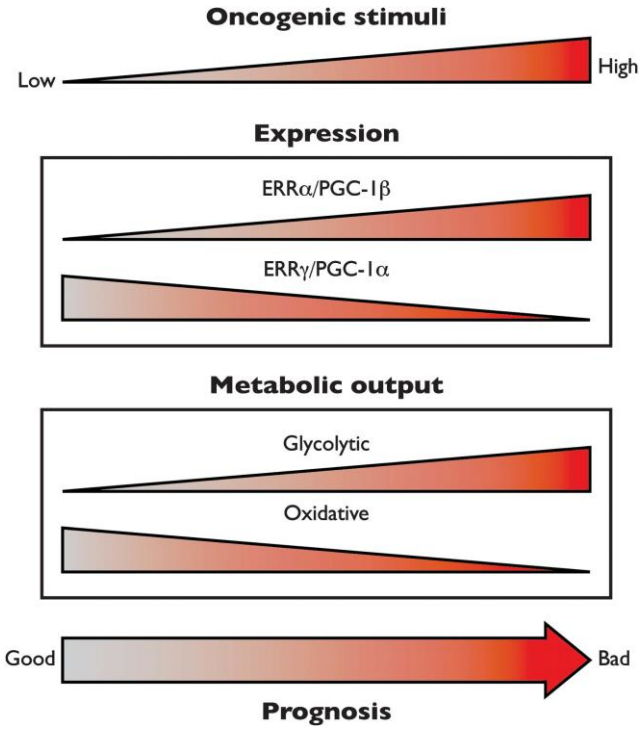

Figure 2.7 Schematic representation of the potential involvement of the PGC-1/ERR axis and its specific components on metabolic output and its consequences on oncogenic progression.

3. Curcumin

3.1 Introduction

Curcuma is one of the largest genera in the Zingiberaceae family which comprises approximately 133 species. It is widely distributed in the tropical regions spanning India to Southern China and Northern Australia [Prasad S. et al., 2011]. The species of greatest interest is *Curcuma longa* L., which is cultivated particularly in India. It consists of an underground root (rhizome) from which, once dried and ground, a powder with a characteristic yellow-orange color is obtained. Curcumin extract is composed of three curcuminoids at different proportions such as curcumin (1, 7-bis (hydroxyl-3-methoxyphenyl)-1,6- heptadiene-3, 5-dione) (curcumin I) (~ 77%), demethoxy curcumin (curcumin II) (17–18%) and bis-demethoxycurcumin (curcumin III) (3–5%) **[Figure 3.1]** [Sandur S.K. et al., 2007]. The volatile fraction is quantitatively important, which mainly contains several terpenic compounds including α-zingiberene, curlone and α-turmerone [Dosoky N.S. et al., 2019]. Among the curcuminoids, the polyphenol curcumin is the most active. In particular it was used to treat infections, in liver and skin disorders, burns, wounds and to counteract inflammatory states [Aggarwal B. et al., 2007]. Moreover, scientific studies shown that curcumin possesses a wide range of pharmacological proprieties, acting as an antimicrobial, antiviral, antifungal, antioxidant, antimalarial, anti-inflammatory, hypoglycemic, antiaging and antitumoral agent [Cianfruglia L. et al., 2019].

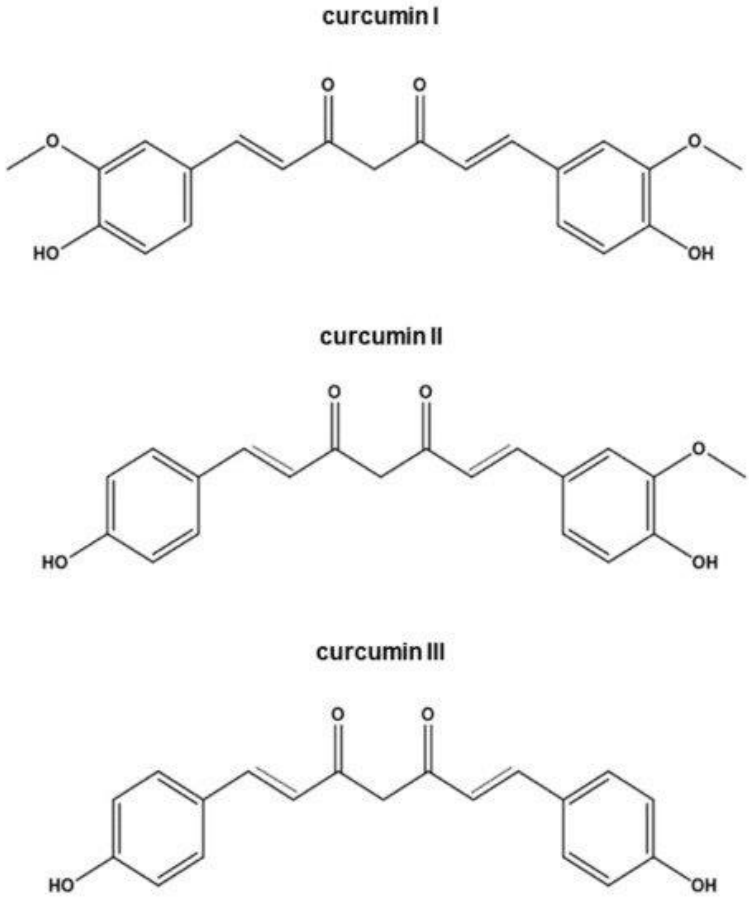

Figure 3.1. Chemical structures of curcumin I, II, III.

3.2 Antioxidant Activity

Antioxidant and anti-inflammatory properties are the two main mechanisms that explain most of the effects of curcumin. Curcumin has been shown to improve systemic markers of oxidative stress [Sahebkar A. et al., 2015]. Some studies show that it can increase serum activities by antioxidants such as superoxide dismutase (SOD). A recent systematic review, a meta-analysis of randomized control data relating to the efficacy of integration with purified curcuminoids on oxidative stress parameters, highlighted a involvement in all the investigated parameters of oxidative stress including the activities of SOD and catalase, as well as serum concentrations of glute peroxidase (GSH) and lipid peroxides [Sahebkar A. et al., 2015]. The effect of curcumin on free radicals comes explained by several mechanisms. It is able to recognize different forms of free radicals, such as reactive oxygen and nitrogen species (ROS and RNS, respectively) [Menon V.P. & Sudheer A.R., 2007]; it can modulate the activity of GSH, catalase and SOD enzymes active in the neutralization of free radicals. Furthermore, it can inhibit ROS-generating

enzymes such as lipoxygenase / cyclooxygenase and xanthine hydrogenase / oxidase [Lin Y.G. et al., 2007]. The hypothesis of oxidative stress in premature aging and age-related disorders highlights the antioxidative beneficial effects of curcumin in prevention and therapy of neurodegenerative diseases [Joseph J.A., 2005]. One of the few studies carried out on humans showed that curcumin, with a dose-dependent mechanism, increases the activity of proteins G in the cell membranes of the central cortex [Cowburn R.F., 2001]. This stimulatory effect was found to be more evident in the healthy elderly rather than in those with Alzheimer's. Curcumin also appears to have an agonist or modulatory action against estrogen receptors in the brain [Jefremov V. et al., 2007] and in the periphery [Zhang A., 1994], which are coupled to protein G [Kelly M.J., 2001]. Given its remarkable lipophilicity, curcumin is able to cross the blood brain barrier and this suggests that the neuroprotective effects could involve the G protein mediated estrogen receptor stimulation. Previous research has shown that relevant oxidative modification of G proteins in neurodegeneration models can initiate or promote neuronal death signals [Nishida M., 2002]. Thus it was shown that the oxidative stimulation of protein G by pro-oxidant agents, oxytocin and hydrogen peroxide, highly expressed during premature aging and in neurodegenerative diseases, could be reduced with curcumin.

3.3 Anti-inflammatory activity

Oxidative stress has been implicated in many chronic diseases and its processes pathological are closely related to those of inflammation, as one can be easily induced by the other. In fact, inflammatory cells are known to release a number of reactive species at the site of inflammation leading to oxidative stress, which demonstrates the relationship between oxidative stress and inflammation [Biswas S.K., 2016]. Curcumin regulates numerous transcription factors, cytokines, protein kinases, molecules of adhesion, redox states and enzymes that are linked to inflammation, inducing its downregulation. It inhibits the expression of various factors, such as interleukin 1β (IL-1β), interleukin 6 (IL-6), necrosis factor α (TNF-α) and cyclin E.

TNFα is the major mediator of inflammation. It is regulated by the activation of some transcription factors, including nuclear factors NF-kB. Therefore, agents that cause the downregulation of NF-kB and its regulatory gene represent a potential target for the

treatment of various diseases: curcumin has been recognized as a powerful blocker of the activation of this nuclear factor.

In both chronic and acute inflammatory disorders, but also in various neoplasms, this transcription factor plays a crucial role in the signal transduction pathway [Barnes P. et al., 1997]. In the inactive state, nuclear factor NF-kB is localized in the cytoplasm: for it to be activated, the latter must migrate from the cytoplasm to the nucleus; migration is regulated by the activation of various kinases and by the phosphorylation and degradation of IkB, that is, the cytoplasmic inhibitor of NF-kB [Jobin C. et al., 1999].

Curcumin action is expressed precisely at this level through the inhibition of the signals that lead to the activation of the nuclear factor such as the inhibition of phosphorylation and IkB degradation induced by TNF.

In another study, curcumin was shown to inhibit TNF-induced activation of NF-kB in human ML-1a myeloid cells [Singh S. & Aggarwal B.B., 1995], but also that induced by other agents such as, for example, hydrogen peroxide.

TNF and hydrogen peroxide are responsible for the production of reactive oxygen intermediates (ROI), an increase in ROI levels can trigger the inflammatory response that is expressed through the activation of the factor itself. Curcumin appears to exert its anti-inflammatory activity by reducing ROI levels in plasma, resulting in indirect inhibition of the activation of the nuclear factor NF-kB [Singh S. & Aggarwal B.B., 1995].

3.4 Hypoglycemic activity

The various inflammatory cytokines and some transcription factors such as NF-kB and NRF2, as well as in inflammatory diseases, are also implicated in various metabolic disorders including diabetes. TNFα and NF-kB activations are related to an increased resistance to insulin [Moller D.E. & Berger J.P. et al., 2003]. In diabetes, curcumin can act by decreasing blood glucose levels and increasing the antioxidant status of pancreatic β cells [Pari P. & Murugan P., 2007]. In fact, some studies have evaluated the correlation existing between the stimulation induced by curcumin on the β cells of the pancreas and the hypoglycemic activity of this molecule, highlighting the ability of curcumin to stimulate the electrical activity in the pancreatic β cells of the rat, through the " activation of the volume-regulated anion channel, causing a depolarization of pancreatic β cells with

consequent release of insulin. Other studies have shown that curcumin reduces macrophage infiltration of adipose tissue, increasing adiponectin production and decreasing nuclear hepatic activity of NF-kB and inflammation markers, thus reducing inflammatory and metabolic changes associated with diabetes [Bharat B. et al., 2009].

3.5 Antitumoral Activities of Curcumin

Several studies indicated that curcumin can prevent and suppress tumor initiation, promotion and progression and can be used to treat cancer by interfering with several signaling pathways [Wang H. et al., 2021; Kunnumakkara A.B., 2017].

This propriety is due to its ability to target critical processes primarily involved in cancer development, such as proliferation, apoptosis and metastasis.

3.5.1 Antiproliferative Effects of Curcumin

Some molecular alterations associated with carcinogenesis occur in signaling pathways regulating cell proliferation [Kotecha R. et al., 2016]. Accumulating data show that curcumin displays in vitro antiproliferative effects on several types of cancer such as breast, colorectal, bladder, brain and gastrointestinal through several mechanisms of action [Song X. et al., 2019]. Generally, the antiproliferative effects of curcumin could be attributed to its ability to regulate cell cycle progression, protein kinases activity and transcription factor expression.

In breast cancer cell lines, curcumin inhibits proliferation by reducing cyclin D1 expression at mRNA and protein levels, consequently decreasing CDK4 activity [Mukhopadhyay A. et al., 2002; Zhou Q.M. et al., 2011]. In MCF-7 breast cancer cells, curcumin caused G1 cell cycle arrest, cyclin E proteosomal degradation, p53 upregulation and an increase in p21 and p27 CDK inhibitor levels [Aggarwal B.B. et al., 2007]. In MCF-7 and MDA-MB-231 breast cancer cells, a G2/M cell cycle arrest by curcumin was also reported. Specifically, following GSK3β upregulation, a loss of nuclear β-catenin produced a downregulation of its downstream target, cyclin D1 [Prasad C.P. et al., 2009]. Additionally, curcumin is a potent inhibitor of NF-kB [Liu, J.L. et al., 2017]. In addition, curcumin was proven to be effective to sensitize MDA-MB-231 and MCF-7 cells to commonly used chemotherapeutic agents paclitaxel, cisplatin and doxorubicin [Zhou Q.

et al., 2015]. In a recent work, it has been shown that curcumin inhibited the growth of MDA-MB-231 and MDA-MB-468 triple-negative breast cancer cells by reducing the expression of histone methyl transferase EZH2 and reactivating that of DLC1 [Zhou X. et al., 2020]. EZH2 is an oncogenic factor commonly upregulated in human cancers [Chase A. & Cross N.C., 2011], while DLC1 is a downregulated tumor suppressor in many malignant tumors [Ren G. & Li G., 2021].

In vitro studies showed that curcumin significantly inhibited colon cancer cell growth modulating multiple molecular targets and distinct signaling pathways [Pricci M. et al., 2020; Calibasi-Kocal G. et al., 2019]. A study performed by Lim et al. demonstrated that in a HCT-116 human colon cancer cell line, curcumin downregulated CDK2 expression, causing G1 phase arrest [Lim T.G. et al., 2014]. Moreover, in the same cell line, curcumin enhanced ROS generation and downregulated the transcription factor E2F4 and its target genes, including cyclin A, p21 and p27 [Kim K.C. et al., 2010]. Another study by Watson et al. investigated curcumin cytotoxicity in HCT-116 and HT29 cell lines, showing a time- and dose-dependent cell proliferation inhibition when p53 was upregulated [Watson J.L. et al., 2010]. Curcumin prevented cell proliferation by cell cycle arrest at the G2/M phase in both HCT116 p53+/+ and p53−/− cells in a concentration-dependent manner and induced senescence accompanied by autophagy [Mosieniak G. et al., 2012]. Recently, Calibasi-Kocal et al. demonstrated antiproliferative, wound healing, anti-invasive and antimigratory effects of curcumin not only on HCT-116 cells, but also on the LoVo metastatic colorectal cancer cell line, confirming its anticancer activity [Calibasi-Kocal G. et al., 2019].

The antitumoral effects of curcumin were also demonstrated in bladder cancer cells. Curcumin's inhibitory effects were observed in T24 [Zhang L. et al., 2018; Shi J. et al., 2017], 5637 [Shi J. et al., 2017] and in RT4 [Zhang L. et al., 2018] human bladder cancer cell lines. In T24 and RT4 cells, a decrease in Trop2, a cell surface receptor that transduces via calcium signals, is required for curcumin-mediated effects including inhibition of cell proliferation and migration, apoptosis and cell cycle arrest. A Trop2 decrease caused a reduction in the expression levels of its downstream target cyclin E1, and an increase in p27 levels [Zhang L. et al., 2018].

Curcumin has been shown to decrease malignant characteristics of glioblastoma cells acting on several targets, including growth factor receptors, kinases, transcriptional

factors and inflammatory cytokines [Walker B.C. & Mittal S., 2020]. In the U87 human glioma cell line, curcumin inhibited proliferation-suppressing cyclin D1 and induced p21 expression. In these cells, curcumin via ERK and JNK signaling induced expression of the transcription factor Egr-1 which, in turn, increased p21 gene expression [Choi B.H. et al., 2008]. In the same cells, curcumin induced G2/M cell cycle arrest and apoptosis by increasing FoxO1 expression [Cheng C. et al., 2016]. In U251 and SNB19 human glioblastoma cells curcumin reduced the expression of Skp2 and upregulated p57 [Wang L. et al., 2015]. Skp2, a component of the ubiquitin proteasome system, is responsible for ubiquitin-mediated degradation of the cell cycle inhibitors p21, p27 and p57 [Wu J. et al., 2020]. Recently, Luo et al. demonstrated that curcumin decreased proliferation of U251 and LN229 human glioblastoma cells via inhibition of HDGF [Luo Q. et al., 2019], an angiogenesis-promoting growth factor commonly upregulated in gliomas. In human glioma cell lines U251 and LN229, HDGF forms a complex with β-catenin promoting tumor growth and metastasis. Curcumin significantly reduced HDGF expression, and consequently its binding to β-catenin [Luo Q. et al., 2019]. Moreover, several studies provided evidence that curcumin potentiated the effects of chemotherapy and radiation therapy while protecting normal tissue, selectively inducing cell death in glioblastoma cancer cells [Fratantonio D. et al., 2019; Seyithanoglu, M.H. et al., 2019].

In gastrointestinal cancer cell lines, curcumin inhibited ODC and increased SMOX activity, two key enzymes in polyamine synthesis and catabolism, respectively. Importantly, elevated levels of polyamines have been associated with several cancers, and altered levels of the rate limiting enzymes in both biosynthesis and catabolism have been observed. The combination of curcumin with ODC inhibitor DFMO significantly potentiated ODC inhibition decreasing AGS gastric adenocarcinoma cell growth [Murray-Stewart T. et al., 2018]. Evidence regarding curcumin's potential in gastric cancer prevention has been accumulating. Curcumin induced cell-cycle arrest at the G1 phase by downregulating cyclin D1 expression in BGC823, SGC7901, MKN1 and MGC803 gastric cancer cells by inhibiting EGF/PAK1/NF-kB pathway [Cai X.Z. et al., 2009]. Moreover, curcumin exerted antiproliferative effects by inhibiting the Wnt/β-catenin signaling pathway. In SNU1, SNU-5 and AGS human gastric cancer cells, curcumin caused a reduction in Wnt3a, LRP6, phospho-LRP6, β-catenin, phospho-β-catenin, c-Myc and survivin [Zheng R. et al., 2017]. The antiproliferative effects of curcumin were also demonstrated in SGC-7901 and BGC-823 gastric cancer cells by

activating p53/p21 and inhibiting PI3K signaling pathways [Fu H. et al., 2018]. In another work, SGC7901 gastric cancer cell proliferation was reduced after curcumin treatment via c-Myc/long non-coding RNA (lncRNA) H19 downregulation and p53 upregulation [Liu G. et al., 2016]. Studies reported that H19, an oncogenic lncRNA [Ghafouri-Fard S. et al., 2020], is abnormally upregulated in gastric cancer and contributes to cellular proliferation by directly inactivating p53 [Yang F. et al., 2012]. Furthermore, the oncogene c-Myc was shown to directly induce H19 expression by binding to the H19 promoter, and thereby promoting proliferation of gastric cancer cells [Yoshimura H. et al., 2018]. A recent investigation defined curcumin effects on microRNAs expression related to gastric cancer cell proliferation [Sun C. et al., 2019]. In SGC-7901 cells, curcumin inhibited cell cycle progression and induced apoptosis by upregulating miR-34a, which decreased CDK4 and cyclin D1 protein expression. The same effects were obtained by transfecting the cells with specific miR-34a agomir [Sun C. et al., 2019]. In BGC-823 and SGC7901 gastric cancer cells, curcumin inhibited cell proliferation and increased cell death by upregulating miR-33b which, in turn, decreased expression of the apoptosis inhibitor XIAP by targeting its 3′ UTR [Sun Q. et al., 2016].

Mounting evidence indicates that curcumin affects several molecular pathways involved in melanoma pathogenesis, making it a promising therapeutic agent to be used against this type of cancer [Nabavi S.M. et al., 2018]. This phytochemical compound was able to arrest cell cycle at the G2/M phase by inhibiting NF-kB and iNOS activity in human melanoma A375 and MeWo cells [Zheng M. et al., 2004]. Another study postulated that curcumin's effect on cell cycle arrest at the G2/M phase was dependent on PDE inhibition, an enzyme that catalyzed cAMP and/or cGMP hydrolysis. Specifically, curcumin decreased cell proliferation and cell cycle progression by inhibiting PDE1A, cyclin A, UHRF1 and DNMT1 expression while increasing that of p21 and p27 in B16F10 murine melanoma cells [Abusnina A. et al., 2011]. Another report showed that curcumin caused cell cycle arrest at the G2/M phase, and induced autophagy by downregulating Akt/mTOR axis in human melanoma A375 and C8161 cell lines [Zhao G. et al., 2016]. Curcumin antiproliferative effects were also observed in other three melanoma cell lines (C32, G-361, and WM 266-4), all of which are characterized by B-Raf mutations. In these cells, curcumin antitumor effects were associated with the suppression of NF-kB and IKK activity but were independent from the inhibition of B-Raf/MEK/ERK and Akt pathways [Siwak D.R. et al., 2005].

3.5.2 Pro-Apoptotic Effects of Curcumin

In addition to antiproliferative properties, curcumin shows extensive therapeutic potential as an apoptotic inducer through several mechanisms demonstrated in different cancer cell models. In MCF-7 breast cancer cells, a sub-cytotoxic dose of curcumin induced apoptotic cell death through an increase in histone H3 acetylation and glutathionylation which, in turn, promoted the transcriptional activation of different proapoptotic genes [Cianfruglia L. et al., 2019]. Several reports indicated that, in breast cancer cells, curcumin induced apoptosis via p53-dependent and -independent pathways [Talib W.H. et al., 2018; Bae Y.H. et al., 2013]. Patel et al. demonstrated that, in MCF-7 cells, curcumin enhanced p53 expression and activated Parp-1-mediated apoptotic pathways [Patel P.B. et al., 2015]. The p53-independent effects of curcumin were observed in cancer cells lacking a functional p53 protein such as MDA-MB-231. In these cells, curcumin induced ROS generation which altered mitochondrial membrane permeability, reduced intracellular GSH levels, increased Bax/Bcl-2 ratio and cleaved-caspase 3 expression [Moghtaderi H. et al., 2017]. In MDA-MB-231 cells, curcumin inhibited NF-kB p65, triggering apoptosis [Chiu T.L. & Su C.C., 2009]. Moreover, in the same cell line, curcumin was able to mediate apoptotic cell death through FAS inhibition [Fan H. et al., 2016].

The apoptotic effects of curcumin were evident in melanoma. In A375 cells, curcumin promoted tumor cell apoptosis by inhibiting the JAK-2/STAT-3 signaling pathway and downregulating Bcl-2 [Zhang Y.P. et al., 2015]. Moreover, the ability of curcumin to induce apoptosis was demonstrated in four human melanoma cell lines (PMWK, Sk-mel-2, Sk-mel-28, and Mewo) with mutant p53 through the activation of FAS/caspase 8 pathway [Bush J.A. et al., 2001]. Curcumin-dependent apoptosis was also observed in HEY ovarian cancer cells where p53 knockdown or p53 inhibition did not prevent curcumin's inhibitory effect. In these cells, apoptosis occurred through the activation of p38 MAPK, the inhibition of pro-survival Akt signaling, along with a decreased expression of Bcl-2 and survivin [Watson J.L. et al., 2010]. Additionally, in the multiple myeloma RPMI 8226 cell line, curcumin upregulated p53 and Bax protein levels and downregulated MDM2, a known p53 inhibitor [Li W. et al., 2015].

In colorectal cancer cells, curcumin triggered the apoptotic process via the subsequent modulation of various target molecules [Pricci M. et al., 2020]. In HT-29 colon cancer

cells, curcumin-induced apoptosis was related to a decreased COX2 expression and AKT phosphorylation along with an increased activation of AMPK signaling [Lee Y.K. et al., 2009]. Moreover, this polyphenol promoted apoptosis in HCT116, HT29, and SW620 colorectal cancer cell lines by suppressing constitutive and inducible NF-kB activity and NF-kB-regulated gene products such as Bcl-2, Bcl-xL, IAP-2, COX2 and cyclin D1 [Sandur S.K. et al., 2009]. Additionally, Narayan et al. showed that curcumin inhibited the Wnt/β-catenin pathway by inducing the caspase 3-mediated cleavage of beta-catenin, E-cadherin and APC, leading to loss of cell–cell adhesion and apoptosis in HCT-116 colon cancer cells [Narayan S., 2004]. It has been reported that curcumin can activate extrinsic apoptotic pathway, upregulating DR5 protein in HCT-116 and HT-29 colon cancer cells [Jung E.M. et al., 2005]. Furthermore, curcumin triggered Fas-mediated caspase 8 activation in HT-29 cells [Cao A. et al., 2013]. In these cells, treatment with curcumin caused a mithocondrial [Ca^{2+}] increase, cytochrome c release from mitochondria to cytosol, mithocondrial membrane potential reduction, Bax increase and Bcl-2 as well as caspase 3 and 7 activation [Cao A. et al., 2013]. Curcumin-induced Bcl-2 downregulation and Bax upregulation in both HCT-116 [Moragoda L. et al., 2001] and COLO-205 colon cancer cells [Su C.C. et al., 2006].

Caspase 3/7 activity was investigated by Shi et al. in bladder cancer cells. The authors demonstrated the ability of curcumin to induce apoptosis through a caspase-dependent mechanism in two human urinary bladder carcinoma cells [Shi J. et al., 2017]. The same apoptotic mechanism was also observed in other cancer types such as glioblastoma [Klinger N.V. et al., 2016]. A similar feature also occurs in human osteosarcoma (HOS) cells, where curcumin caused cell cycle arrest determining apoptosis, as demonstrated by caspase 3 and PARP-1 cleavage [Lee D.S. et al., 2009]. Recently, it was observed that curcumin inhibited ODC activity and polyamine biosynthesis in AGS gastric adenocarcinoma cells. In this type of cell, curcumin caused an increase in ROS levels responsible for DNA damage and, thus, apoptosis [Murray-Stewart T. et al., 2018].

The pro-apoptotic effects of curcumin are also mediated by the modulation of miRNAs in several cancer cells. Curcumin reduced Bcl-2 expression by upregulating miR-15a and miR-16 in MCF-7 cells [Yang J. et al.; 2010] and promoted apoptosis through the miR-186 signaling pathway in human lung adenocarcinoma cells [Zhang, J. et al., 2010]. Recently, in RT4 schwannoma cells, Sohn et al. demonstrated that curcumin enhanced

the expression of apoptotic protein Bax and decreased Bcl-2, as well as determined caspase 3/9 activation. All of these events were related to curcumin-mediated miRNA 344a-3p upregulation [Sohn E.J. et al., 2018].

3.5.3 Antimetastatic Effects of Curcumin

In addition to the antiproliferative and apoptotic effects, curcumin acts as an antimetastatic agent [Kim M.J. et al., 2020; Calibasi-Kocal G. et al., 2019].

The metastatic cascade starts with the loss of cell-to-cell and cell-to-substrate adhesion, a feature of the EMT process, which allows the acquisition of a mobile phenotype, the dissociation of cells from primary tumor and the spread to distant tissues and organs [Gao D. et al., 2018].

The effects of curcumin on genes involved in EMT was evaluated in breast cancer cells. It was demonstrated that curcumin decreased the gene transcription and protein expression of Axl, Slug, CD24 and RhoA, which regulate EMT and, consequently, migration and invasion of MCF-10F and MDA-MB-231 breast cancer cells. Curcumin elicited these effects through the upregulation of miR-34a, which acts as a tumor suppressor gene in both cell lines [Gallardo M. et al. 2020]. The antimetastatic effects of curcumin occur through the modulation of several signaling pathways, including NF-kB. NF-kB/p65 transcriptionally regulates TWIST1, SLUG and SIP1 which, in turn, repress E-cadherin while activating the mesenchymal markers N-cadherin and MMP11, resulting in EMT progression [Pires B.R. et al., 2017]. In MCF-7 cells, curcumin was able to inhibit uPA production by preventing NF-kB activation [Zong H. et al., 2012]. Through the same mechanism, curcumin downregulated CXCL1 and 2, two inflammatory cytokines involved in MDA-MB-231 breast cancer cells migration [Bachmeier B.E. et al., 2008]. A critical event in tumor cell invasion and metastasis is the degradation of the extracellular matrix by MMPs, enzymes that degrade a range of extracellular matrix proteins, allowing cancer cells to migrate and invade [Irani S., 2019]. Curcumin was able to inhibit LPA-activated invasion by attenuating the RhoA/ROCK/MMPs pathway in MCF-7 cells [Sun K. et al., 2016]. Similarly, in SO-Rb50 and Y79 human retinoblastoma cell lines, curcumin reduced migration and invasion by decreasing MMP2, RhoA, ROCK1 and vimentin expression. The authors provided evidence that, in these cells, curcumin's antitumor activity requires miR-99a upregulation and JAK/STAT3 pathway inhibition

[Li Y. et al., 2018]. MMP's decrease after curcumin treatment was also observed in T24 and 5637 human bladder cancer cell lines [Shi J. et al., 2017]. Additionally, in T24 and RT4 bladder cancer cells, curcumin's antimetastatic mechanism included a Trop2 decrease [Zhang L. et al., 2018], a gene also involved in tumor aggressiveness and metastasis formation [Zaman S. et al., 2019]. In prostate cancer cells, curcumin treatment suppressed EGF, heregulin-stimulated PC-3 and androgen-induced LNCaP cell invasion. Particularly, curcumin significantly reduced MMP9 activity and downregulated cellular matriptase, a membrane-anchored serine protease involved in tumor formation and invasion [Cheng T.S. et al., 2013]. Recently, in an HCT-116 human colorectal carcinoma cell line, it has been demonstrated that the expression of proteins related to cell migration, including MMP9 and claudin-3, was downregulated by increasing doses of curcumin [Xiang L. et al., 2008]. These data were confirmed by an independent group using the same cell line in addition to LoVo human metastatic colon cancer cells, establishing curcumin anti-invasive and antimigratory properties [Calibasi-Kocal G. et al., 2019]. Furthermore, in human melanoma A375 cells, curcumin decreased MMP2 and MMP9 expression while increasing TIMP-2, a tissue inhibitor of metalloproteinases [Zhang Y.P. et al., 2015]. Activation of melanoma cell migration and invasion by OPN was also counteracted by curcumin. Specifically, curcumin was able to downregulate pro-MMP2 activation by preventing OPN-mediated NF-kB nuclear translocation [Philip S. & Kundu G.C., 2003]. The ability of curcumin to interfere with NFk-B pathway was also evident in Hela cervical cancer cells, where it was also demonstrated an effect on Wnt/β-catenin signaling, two pathways involved in proliferation and invasion of cervical cancer [Ghasemi F. et al., 2019]. It has been shown that STAT3 activation is associated with metastasis formation in several tumors [Jin W., 2020]. In SCLC cells curcumin inhibited cell migration, invasion and angiogenesis by inhibiting JAK/STAT3 signaling activated in response to IL-6. As a consequence, curcumin downregulated the expression of ICAM, VEGF, MMP2 and MMP7 STAT3-regulated genes involved in tumor invasion [Yang C.L. et al., 2012]. Curcumin inhibited the JAK/STAT3 signaling pathway also in SKOV3 human ovarian cancer cells, causing a decrease in fascin, an actin-binding protein involved in cell adhesion, migration, and invasion [Kim M.J. et al., 2020]. Curcumin is able to prevent invasion by inhibiting AKT, mTOR and P70S6K phosphorylation, as demonstrated in human melanoma A375 and C8161 cells [Zhao G. et al., 2016] and TC1889 human thymic carcinoma cells [Han Z. et al., 2020]. Additionally, it has been

demonstrated that curcumin reduced cell invasion and migration in NSCLC A549 cells by increasing miR-206, which further suppressed PI3K/AKT/mTOR pathway activation [Wang N. et al, 2020]. The observation that curcumin inhibited NEDD4-mediated signaling in SNB19 and A1207 glioma cells, thus interfering with cell motility, is very interesting [Wang X. et al, 2017]. NEDD4 is a E3-ubiquitin ligase involved in the degradation of CNrasGEFs, guanine nucleotide exchange factors (GEFs), that serve as RAS activators, thus, promoting glioma cell migration and invasion [Zhang H. et al, 2013].

3.6 ERRα and Curcumin

In the United States, the National Cancer Institute has classified curcumin as the third generation of anti-cancer and chemo-preventive agents [Odot J. et al., 2004]. Curcumin in a study on osteosarcoma cells inhibited their growth and metastasis, the mechanisms are not fully elucidated. To understand the molecular alterations of curcumin-mediated growth inhibition, total RNA was extracted from vehicle or curcumin-treated U2OS cells and gene expression profiling was performed by sequential RNA analysis. It was found that curcumin treatment led to a significant downregulation of a number of genes compared to the control. These downregulated genes include ERRα and its target genes [Deblois G. et al., 2009]: ATPase, Caþþ transporting, ubiquitous (ATP2A3), oxoglutarate dehydrogenase-like (OGD), ATP synthetase, Hþ transport, fo mitochondrial complex, C1 subunit (subunit 9) (ATP5G1), erb-b2 receptor tyrosine kinase 2 (ERBB2), ERRa (ESRRA), enolase 3 (beta, muscle) (ENO3), NADH dehydrogenase (ubiquinone) 1 alpha sub-complex, 11, 14.7kDa (NDUFA11), pyruvate dehydrogenase kinase, isoenzyme 3 (PDK3), lactate dehydrogenase A (LDHA) and phosphoenolpyruvate carboxyl kinase 2 (mitochondrial) (PCK2). These downregulated genes were validated by quantitative PCR analysis of RNA samples extracted from additional curcumin-treated U2OS cells. In order to confirm that curcumin is capable of blocking the expression of the ERRα protein, western blot was performed. Treatment of U2OS cells with curcumin dramatically reduced the level of the ERRα protein. These data provided evidence that curcumin targets the ERRα signaling pathway in osteosarcoma [Chen P. et al., 2017]. In this study it was hypothesized that the inhibitory effect of curcumin on U2OS cells could be enhanced by ERRα siRNA. As expected, ERRα silencing sensitized osteosarcoma cells to curcumin-induced cell death. Combined administration of curcumin and ERRα siRNA

induced a significant inhibition of U2OS cell growth and of excess cleaved caspase-7 and cleaved PARP. These results demonstrated that ERRα overexpression in osteosarcoma cells confers resistance to curcumin treatment. In the study, Chen P. and collaborators tested the effect of miR-125a, as it directly regulates the expression of the ERRα gene through the binding sites at the ERRα 30 UTR site [Ji H.L. et al., 2014]. Furthermore, it was found that miR-125a in a dose of 50 nM effectively decreased the expression of ERRα while the downregulation of the level of miR-125a with the inhibitor of miR-125b induced an increase in ERRα expression. From the RNA-seq gene expression profile, curcumin increased miR-125 levels and thus this suggests that curcumin inhibited ERRα gene expression by up-regulation of miR-125a expression.

3.7 Bioavailability of Curcumin and Therapeutic Promises

Although the beneficial effects of curcumin are known, it has not yet been approved as a therapeutic agent due to its low bioavailability [Anand P. et al., 2007]. Among factors contributing to this limit, the following can be included: low water solubility, poor absorption, low tissue distribution, high rate of metabolism, inactivity of metabolic products and/or rapid elimination and clearance from the body [Ravindranath V. & Chandrasekhara N., 1980]. Curcumin undergoes extensive phase I and II biotransformation [Pan M.H. et al., 1999]. The primary site of metabolism for curcumin is the liver, together with the intestine and gut microbiota; curcumin double bonds are reduced in enterocytes and hepatocytes by a reductase to produce dihydrocurcumin, tetrahydrocurcumin, hexa-hydrocurcumin and octahydrocurcumin. Phase II metabolism that occurs in the intestinal and hepatic cytosol is quite active on both curcumin and its phase I metabolites, especially through conjugation reaction with glucuronic acid and sulfate at the phenolic site catalyzed by UGTs and SULTs enzymes, respectively [Pan M.H. et al., 1999].

Over the years, in order to improve curcumin pharmacokinetic profile and cellular uptake, several strategies have been developed. These include curcumin structural derivatives, analogues preparation and novel drug delivery systems that could enhance its solubility and extend its plasma residence time.

3.8 Curcumin Structural Derivatives and Analogues

Structural modifications on the curcumin chemical backbone led to curcumin derivatives and analogues [Tomeh M.A. et al., 2019; Li W. et al., 2019; He Y. et al., 2018; Basile V. et al., 2009; Sribalan R. et al., 2015]. The derivatives category includes all those compounds that maintain the basic structure of pharmacophore and, specifically, the two phenolic rings and the α, β-unsaturated dichetonic bridge which are the portions responsible for the molecule pharmacological activities **[Figure 3.2]** [Bayomi S.M. et al., 2013]. Curcumin derivatives are generally synthesized by modification of the hydroxyl group of the phenol ring, which can be acylated, alkylated, glycosylated and aminoacylated **[Figure 3.2A]**. Studies on the kinetic stability of synthetic curcumin derivatives showed that glycosylation of the pharmacophore aromatic ring improves the water solubility of the compound, which increases its kinetic stability and leads to a better therapeutic response. In the II phase of curcumin metabolism, conjugation reactions take place on the hydroxyl groups (4-OH) attached to the phenyl rings of curcumin respectively [Pan M.H. et al., 1999].

Thus, curcumin stability can be increased by masking the 4-OH groups, thereby extending the active molecule retention time in the body. Benzyl rings are also crucial for inhibiting tumor growth; their modification with hydrophobic substituents such as CH3 groups have been linked with an enhancement of the curcumin derivatives antitumor activity [Xu G. et al., 2012]. O-methoxy substitution was found to be more effective in suppressing the NF-kB activity, although this modification simultaneously affected curcumin lipophilicity [Sandur S.K. et al., 2007]. Methoxy groups could be demethylated to hydroxyl groups. The reactive chain methylene group, responsible for conformational flexibility, is important for its antitumor/anticancer activity but not for redox regulatory or apoptotic activities. This group could be acylated, alkylated or substituted with an arylidene group (Ar-CH), thereby introducing substituents on the C7 chain [Zhao C. et al., 2013]. The hydrogenation reaction of double bonds and carbonyl groups on the C7 chain allows the simplest derivatives to be obtained **[Figure 3.2B]**, such as DHC, THC, HHC and OHC [Bayomi S.M. et al., 2013]. A comparative study on curcumin and its derivatives demonstrated greater antioxidant activity for several hydrogenated curcumin derivatives compared to the original compound [Somparn P. et al., 2007]. Tetrahydrocurcumin, a non-electrophilic curcumin derivative, showed greater

antioxidant activity than DHC and unmodified curcumin, although it failed to suppress STAT3 signaling pathway and to induce apoptosis [Anand P. et al., 2008]. This is evidence that the electrophilic nature of curcumin is essential for STAT3 signaling pathway inhibition. Other curcumin derivatives also include those obtained by exploiting the reactivity of the central β-diketone with hydrazine **[Figure 3.2C]**. Such heterocyclizations reactions lead to a masking and stiffening of the central 1,3-diketone 1,3-ketoenol system [Reddy A.R. et al., 2013] and, after evaluation of the antioxidant activity of these compounds, it is possible to assert that several of these azoles are better antioxidants than curcumin [Sherin D.R. & Rajasekharan K.N., 2015]. Oxidation and cleavage are further possible modifications to the β-diketone functional group, all suitably operated to improve the characteristics of the original pharmacophore **[Figure 3.2C]**. Additionally, it is possible to adopt another approach which may help to increase the curcumin bioavailability, such as the formation of metal complexes, or coordination compounds, which are adducts formed by the reaction of Lewis acids and bases [Wanninger S. et al., 2015]. Metal complexes are generally obtained by reacting curcumin, which exploits the chelating capacity of the β-diketone group with a metal salt. The metals most used for this purpose are Boron, Copper, Iron, Gallium, Manganese, Palladium, Vanadium, Zinc and Magnesium. By complexing curcumin with metal ions, such as Zn^{2+}, Cu^{2+}, Mg^{2+}, an increase in water/glycerol solubility (1:1) and fair stability to light and heat were observed [Tomeh M.A. et al., 2019; Wanninger S. et al., 2015].

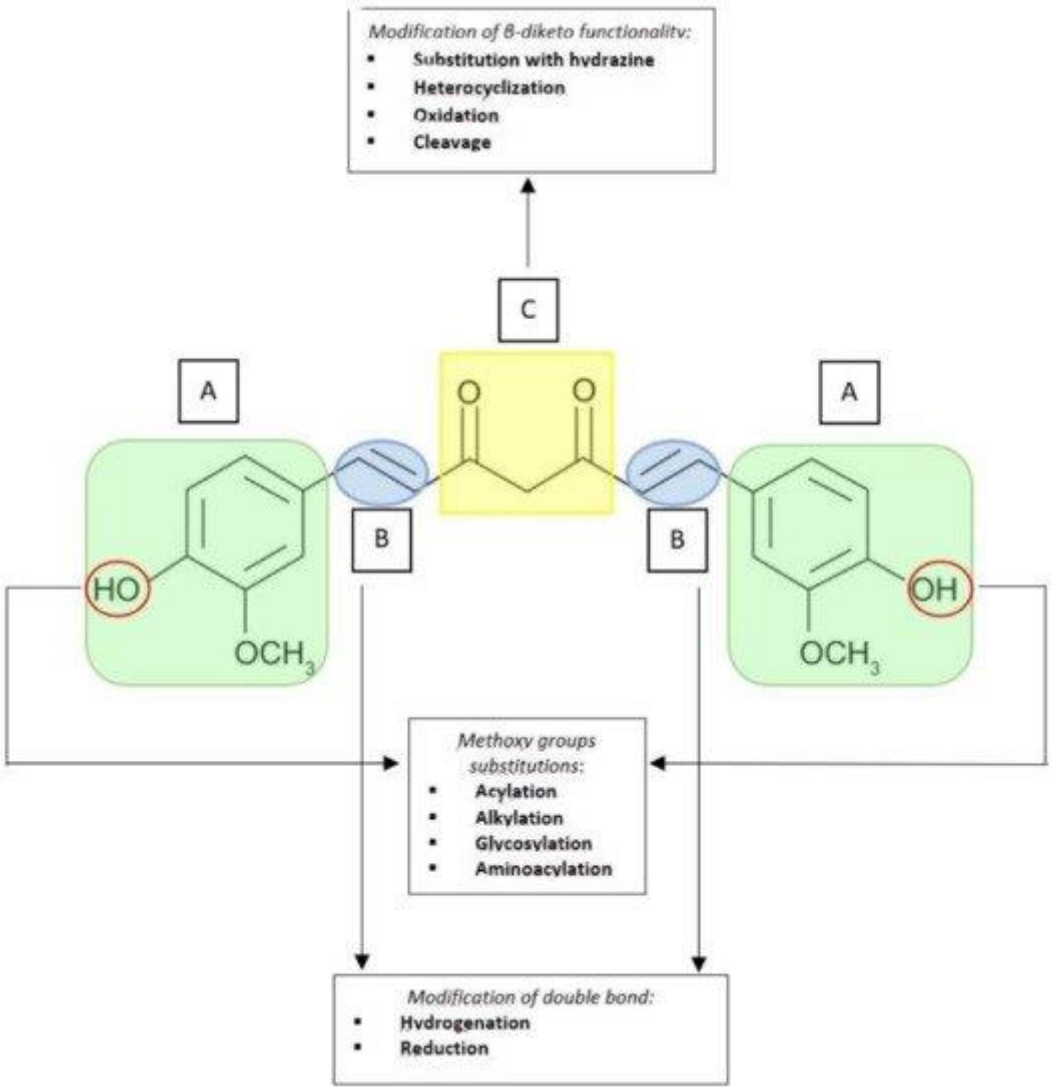

Figure 3.2 General chemical structure of curcumin derivatives. Curcumin chemical structure include two aromatic rings (**A**) linked to a β-dichetonic group (**C**) through a double bond (**B**).

Numerous curcumin analogues have been synthesized and tested to study their interaction with known biological targets and improve the pharmacological profile of this natural product [He Y. et al., 2018; Paulraj F. et al., 2019]. Some curcumin analogues are not obtained starting from the original molecule, but they are synthesized following a condensation reaction between aryl-aldehydes and acetylacetone; through this biosynthetic route, many curcumin analogues have been obtained. The use of acetylacetone derivatives, bearing substituents on the central carbon, leads to analogues with alkyl substituents on the central carbon of the C7 chain [Yerdelen K.O. et al., 2015]. Another strategy concerns the modification of the carbon atom number that makes up the

central C7 chain [Yerdelen K.O. et al., 2015]. A greater antitumor activity than curcumin has been observed with the use of a variety of newly synthesized DAP curcumin analogues. These compounds, which possess two aromatic rings (aryl groups) joined by five carbon atoms, were able to suppress cancer growth through modulation of several factors such as NF-kB, MAPK, STAT, AKT-PTEN [Paulraj F. et al., 2019]. DAPs anticancer effects in different cancer cell lines were summarized by Paulraj and co-workers [Paulraj F. et al., 2019].

A particular scientific interest has been shown towards the EF24 analogue, which displayed a better antitumor activity, a lower toxicity in normal cells, a marked increase in bioavailability and a lower metabolic rate compared to the natural compound [Li W. et al., 2019; He Y. et al., 2018]. In vivo studies have shown that, while dietary curcumin is poorly absorbed through the intestinal tract and therefore does not have a therapeutic effect at low doses, on the contrary, EF24 has greater oral bioavailability in mice [Reid J.M. et al., 2014], explaining, to some extent, its improved in vivo activity compared to curcumin. Several studies indicated that EF24 reduces cancer cell growth by inducing cell cycle arrest followed by caspase-mediated apoptosis [Selvendiran K. Et al., 2007; He G. et al., 2016]. These actions occur by modulating multiple pathways that determining the inhibition of NF-kB [Kasinski A.L. et al., 2008] and HIF-1α activity [Thomas S.L. et al., 2008] and regulating reactive oxygen species (ROS) [He G. et al., 2016; Tan X. et al., 2010]. NF-kB signaling suppression has been found to be a fundamental aspect for its anticancer activity, since NF-kB is a transcription factor involved in the regulation of genes that monitor cell proliferation, differentiation, cell cycle control and metastasis [Yu H. et al., 2020]. According to a discovery by Yin et al. [Yin D.L. et al., 2016], EF24 is able to inhibit the catalytic activity of the IKK protein complex, which blocks the phosphorylation of IkB and causes its degradation while preventing the nuclear translocation of the p65 subunit. EF24 conferred radiation-induced cell death mainly by inhibiting radiation-induced NF-kB signaling in MCF-7 cells [Aravindan S. et al., 2013]. Similar effects were also observed in human neuroblastoma cells [Aravindan S. et al., 2013]. EF24 also regulates HIF-1α expression, which is closely associated with the outcome of chemotherapy in cancer treatment. EF24 overcomes sorafenib resistance through VHL tumor suppressor-dependent HIF-1α degradation and NF-kB inactivation in hepatocellular carcinoma cells [Liang Y. et al., 2013]. Another notable EF24 antitumor mechanism is ROS production regulation. Tan et al. showed that EF24 inhibited ROS

generation and activated ARE-dependent gene transcription in platinum-sensitive (IGROV1) and platinum-resistant (SK-OV-3) human ovarian cancer cells [Tan X. Et al., 2010]. On the contrary, the ability of EF24 to increase ROS production and then induce apoptosis in cancer cells via a redox-dependent mechanism was found in breast MDA-MB-231, prostate DU-145 [Adams B.K. et al., 2005], gastric SGC-7901 and BGC-823 [Zou P. et al., 2016], and colon HCT-116 and SW-620 human cancer cells [He G. et al., 2016], suggesting that the EF24 role in ROS induction may be cell type dependent. EF24 ability to interfere with the targeted inhibition of antiapoptotic proteins belonging to the Bcl-2 family is being exploited in clinical settings for the treatment of age-related diseases. Although this mechanism has not been fully elucidated, the function of EF24 and other curcumin analogues as senolytic agents is well demonstrated, as they are able to selectively kill the senescent cells (cells that are no longer able to replicate) that accumulate in various organs and tissues as a result of the progress of the damage that occurs with aging. EF24 exerts its senolytic effect by inducing apoptotic death in target cells via proteasome-mediated downregulation from Bcl-2 family proteins, which represents a protection factor for senescent cells, as they are resistant to the induction of apoptosis as a result of the expression of these proteins [Li W. et al., 2019].

Selvendiran et al. [Selvendiran K. et al., 2011] demonstrated the ability of curcumin analog HO-3867 to reduce in vitro and in vivo ovarian cancer growth. In particular, this compound enhanced the therapeutic potential of cisplatin in A2780R drug-resistant ovarian cancer cells. The results confirmed that the co-administration of HO-3867 with cisplatin resulted in greater inhibitory effects than cisplatin alone, with cell cycle arrest and apoptotic mechanism being significantly induced by targeting the STAT3 pathway in both in vitro cells and in vivo xenograft tumors [Selvendiran K. et al., 2011].

A recent study investigated the antitumor properties of MS13, another diarylpentanoid curcumin analog, on primary (SW480) and metastatic (SW620) human colon cancer cells [Ismail N.I. et al., 2020]. MS13 was more cytotoxic in a dose-dependent manner and had a higher growth inhibitory effect towards SW480 and SW620 cells compared to curcumin. Several factors may explain its increased cytotoxicity activity; these include removal of β-diketone, the reduction in the electron donation capacity of OH at position 4′ [Liang G. et al., 2009] or the 3′,4′-dimethoxy or 3′-methoxy-4′-hydroxy substituents on the phenyl rings [Lin L. et al., 2006].

Recently, Shen et al. [Shen H. et al., 2021] tested the efficacy of the B14 analog in MCF-7 and MDA-MB-2310 breast cancer cells. The results indicated that B14 was more potent than curcumin in inhibiting cell viability, colony formation, migration and invasion. Particularly, this analog, functioning simultaneously in multiple pathways, displayed a selective antitumor activity on MCF-7 and MDA-MB-231 cells, but not on MCF-10A breast epithelial cells. Furthermore, in tumor-bearing mice, analog B14 significantly reduced tumor growth and inhibited cell proliferation and angiogenesis. Additionally, pharmacokinetic tests revealed that B14 was more stable and bioavailable than curcumin in vivo [Shen H. et al., 2021].

3.9 Curcumin Delivery Systems

As already stated, despite curcumin's remarkable beneficial biological effects, it showed low water solubility in acid and neutral conditions, chemical instability in neutral and alkaline environments, and rapid enzymatic metabolism, which limit its bioavailability. Curcumin bioavailability can be enhanced by:

- Delaying metabolism through its entrapment within the hydrophobic phases that isolate it from aqueous phase or cell membranes enzymes;
- Improving its bioaccessibility through an increase in the quantity that is solubilized inside the mixed micelles present in the small intestine; this can be achieved by inserting surfactants, phospholipids, fatty acids or monoglycerides into the curcumin-loaded carrier particles;
- Promoting its absorption by loading curcumin into particles carrier that contain substances able to increase epithelium cell membranes permeability or block efflux transporters [Zheng B. et al., 2020]. Therefore, in order to ameliorate curcumin's pharmacokinetic characteristics, various methodological approaches have been attempted, such as polymeric approaches, magnetic approaches, solid lipid nanoparticles, liposomes, phytosomes, micelles, β-cyclodextrins and solid dispersions [Nocito M.C. et al., 2021] **[Figure 3.3].**

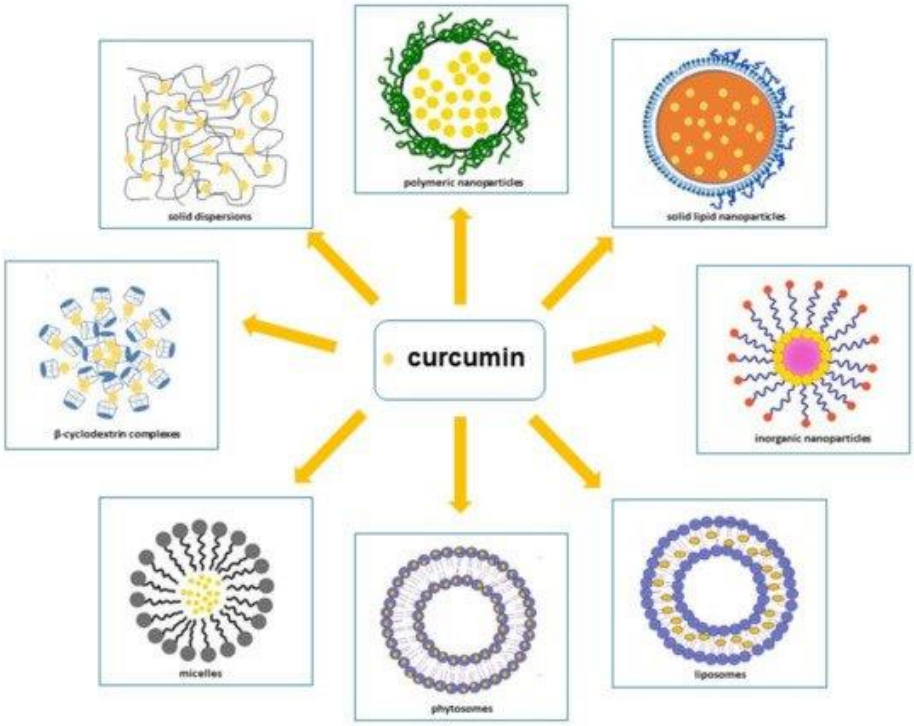

Figure 3.3 Principal delivery systems to enhance curcumin oral bioavailability. In the figure the polymeric nanoparticles, inorganic nanoparticles and micelles images were adapted from Praditya et al. [Praditya D. et al., 2019]; the phytosomes and liposomes images were adapted from Yang et al. [Yang S. et al., 2020]; the solid lipid na-noparticles image was adapted from Li et al. [Li R. et al., 2010]; the β cyclodextrin complexes image was adapted from Yallapu et al. [Yallapu M.M. et al., 2010].

Specifically, in this thesis we wanted to experiment the pharmacological action of curcumin as a component of a new nutraceutical formulation that uses the SLN system and that can be used as an adjuvant in preventing the progression of adrenocortical carcinoma.

3.9.1 Solid Lipid Nanoparticles

Solid lipid nanoparticles (SLNs) are colloidal lipid carriers of size between 50 and 1000 nm and composed by biodegradable physiological lipids [Manjunath K. et al., 2005]. Unlike liposomes, they are rigid particles used both for hydrophobic drugs loading and for their controlled and targeted delivery to the reticuloendothelial system. SLNs possess the advantages of high drug load capacity, good stability, excellent biocompatibility and increased bioavailability [Mukherjee S. et al., 2009]. In SLN preparation, lipids are used with a low melting point and solids at room or body temperature and surfactants through various methods including HPH [Jenning V. et al., 2002]. Among the solid lipids used in

SLN preparation there are monostearin, glyceryl monostearate, precyrene ATO 5 (mono, di, triglycerides of C16-C18 fatty acids), compritol ATO 888, stearic acid and glyceryl trioleate which can improve the curcumin chemical stability [Manjunath K. et al., 2005]. Surfactants such as poloxamer 188, Tween 80 and DDAB, are able to reduce interfacial tension between lipid hydrophobic surface and aqueous environment by acting as surface stabilizers [Manjunath K. et al., 2005]. Several studies have evaluated not only curcumin SLNs physico-chemical properties, stability, bioenhancement, bioavailability, but also cellular uptake in vitro and antitumor efficacy in vitro and in vivo [Baek J.S. et al., 2017; Guorgui J. et al., 2018; Gota V.S. et al., 2010; Ban C. et al., 2020]. Curcumin SLNs using tristearin and PEGylated surfactants have recently been prepared. The study showed that SLN-loaded curcumin with long PEGylates showed increased absorption and long-term stability after oral administration in rats. Furthermore, the bioavailability of curcumin was also 12 times higher in SLNs formulated with long PEGylates than in those formulated with shorter PEGylates [Ban C. et al., 2020]. In another study, it has been demonstrated that the presence of sodium caseinate (NaCas) and sodium caseinate-lactose (NaCas-Lac) conjugates as bioemulsifiers to stabilize curcumin SLNs provided a steric hindrance, allowing dispersibility and greater curcumin stability at pH acid. In addition, this formulation displayed a better antioxidant activity compared to that of free curcumin [Huang S. et al., 2020]. However, the SLNs use as oral delivery system is limited by drug burst release from SLNs in acid environment. In order to inhibit curcumin rapid release in acid conditions and improve curcumin bioavailability, Baek et al. prepared curcumin SLNs coated with N-carboxymethyl chitosan [Baek J.S. et al., 2017]. The results showed that this formulation showed a prolonged release in simulated intestinal fluid and greater absorption and oral bioavailability compared to free curcumin. Furthermore, curcumin exhibited a strong cytotoxicity compared to curcumin solution in MCF-7 breast cancer cells [Baek J.S. et al., 2017]. Using glyceryl monostearate and poloxamer 188 surfactant were developed curcumin SLNs and evaluated its efficiency in MDA-MB-231 breast cancer cells [Bhatt H. et al., 2018]. The results confirmed that curcumin was stably encapsulated in the lipid matrix and its solubility and release were improved compared to the free curcumin solution. Moreover, curcumin SLNs exhibited higher cellular uptake and higher cytotoxicity by apoptosis induction compared to the free drug [Bhatt H. et al., 2018]. Guorgui et al. demonstrated that plasma levels of curcumin encapsulated in SLNs and in d-α-Tocopheryl polyethylene glycol 1000 succinate-stabilized curcumin (TPGS-

CUR) increased when administrated in mice [Guorgui J. et al., 2018]. Additionally, these formulations reduced growth of Hodgkin's lymphoma xenograft models by 50.5% and 43.0%, respectively, compared to free curcumin [Guorgui J. et al., 2018]. Similarly, inhibitory effects were observed in Hodgkin lymphoma L-540 cells, as proven by curcumin SLNs ability to reduce the expression of XIAP and Mcl-1, proteins involved in cell proliferation and apoptosis, and of cytokines IL-6 and TNF-α as well as to enhance the growth inhibitory effect of bleomycin, doxorubicin and vinblastine chemotherapeutic drugs [Guorgui J. et al., 2018].

3.10 Clinical Trials with Curcumin

In recent decades, several clinical studies have been performed to evaluate the effect of curcumin in cancer patients. Depending on the tumor type, curcumin can act by causing a decrease in the patients symptoms or, in other cases, it can lead to an improvement in tumor markers and vital parameters [Salehi B. et al., 2019]. Currently, 71 clinical studies reported in cancer patients treated with curcumin alone or in combination with other compounds were listed in the United States National Library of Medicine *(clinicaltrials.gov)*. Pharmacologically, curcumin is shown to be well-tolerated and relatively safe to use in patients. The clinical trials conducted, thus far, have reported relatively no toxicity [Gupta S.C. et al., 2013]. Phase I clinical trial conducted by Cheng et al. showed that oral administration of 8 g/day of curcumin for 3 months is non-toxic to patients with high-risk or pre-malignant lesions [Cheng A.L. et al., 2001].

A phase II trial of curcumin conducted in twenty-five patients with advanced pancreatic cancer showed that oral curcumin was tolerated without toxicity at doses of 8 g/d for up to 18 months [Dhillon N. et al., 2008]. Particularly, it has been observed that two of them showed clinical biological activity; one patient reported having a stable disease for up to 18 months and another had a marked tumor regression along with an increase in the serum levels of cytokines (IL-6, IL-8, IL-10, and IL-1 receptor antagonists) [Dhillon N. et al., 2008]. Additionally, curcumin downregulated expression of the NF-kB, COX-2, and phosphorylated signal transducer and activator of transcription 3 in peripheral blood mononuclear cells from patients [Dhillon N. et al., 2008]. In another phase II pilot study, a combination of docetaxel, prednisone and curcumin was well-tolerated in patients with castration-resistant prostate cancer [Mahammedi H. et al., 2016]. Dützmann et al.

investigated the intratumoral concentrations and clinical tolerance of micellar curcuminoids composed by 57.4 mg curcumin, 11.2 mg demethoxycurcumin, and 1.4 mg bis-demethoxycurcumin administrated three times day for 4 days in glioblastoma patients [Dutzmann S. et al., 2016]. The results revealed that oral administration of this formulation generated quantifiable concentrations of total curcuminoids in glioblastomas with likely effects on intratumoral energy metabolism [Dutzmann S. et al., 2016]. Furthermore, in patients with orbital pseudotumors, head and neck squamous carcinoma, breast, lung and prostate cancers, curcumin application demonstrated beneficial effects with reductions in tumors volume and tumor markers [Salehi B. et al., 2019]. Another study carried out on 11 volunteer patients with osteosarcoma aimed to quantitatively evaluate curcumin levels in the bloodstream following the intake of SLNs; this study highlighted an improvement in the bioavailability of this polyphenol, when compared with the results obtained on subjects who received unformulated curcuminoids extract [Gota V.S. et al., 201]. However, further studies are needed to evaluate both the long-term tolerability after chronic administration and the relationship between plasma curcumin levels and disease markers. In a phase I clinical trial, an oral formulation of curcumin was evaluated in fifteen patients with advanced colorectal cancer refractory to standard chemotherapies. The results showed an absence of toxicity with curcumin, while 2 of the 15 patients showed stable disease after 2 months of curcumin treatment [Sharma R.A. et al., 2004]. Carroll et al., in a phase II clinical study conducted on patients with colon cancer lesions, demonstrated that curcumin administration for 30 days determined a significant 40% reduction in aberrant crypt foci (ACF) [Carroll R.E. et al., 2011]. These data suggested curcumin use as a cancer prevention agent. However, although curcumin in cancer patients has often improved life quality and reduced tumor markers, it is also true that curcumin has sometimes shown limited effect in some patients with disease advanced stage. Preclinical studies conducted so far confirmed the important role of curcumin and, in particular, the benefits that its synthetic derivatives or nanoformulations could bring to human health. New efforts are needed to confirm the efficacy of curcumin-based products for the treatment of human diseases and to ensure that the products are non-toxic once introduced into the body. Several ongoing clinical trials should provide a deeper understanding of curcumin-based formulation efficacy and mechanism of action against human diseases.

3.11 Conclusions

Curcumin is one of the most promising clinical compounds of the last few decades. Its therapeutic benefits have been demonstrated in various chronic diseases and, above all, in various cancers. Precisely in the antitumor field, curcumin is able to modulate the action of growth factors, cytokines, transcription factors and genes that regulate cell proliferation, apoptosis and the metastatic process. Some of curcumin's multiple pharmacological activities have been used experimentally and clinically in both humans and animals. Notable among these are the antioxidant, anti-inflammatory and anticarcinogenic properties, which all seem related. It is encouraging that curcumin is of low toxicity. Most of the data supporting the antitumour activity of curcumin was obtained in vitro. Unfortunately, the challenges of low solubility and rapid elimination and then poor bioavailability, have delayed its adoption as a therapeutic agent. These efforts have led to the development of several curcumin formulations that have been systematically prepared to improve the absorption, water solubility, distribution and, hence, the bioavailability of curcumin. These methods have been promising with respect to preclinical and clinical efficacy and involve the use of both synthetic derivatives and analogues of curcumin as well as formulations of nanoparticles, liposomes, phytosomes, micelles and natural adjuvants such as piperine. All of these approaches generated a significant improvement in the bioavailability, absorption and retention time of curcumin, along with increased delivery to target tissues, as widely reported. However, further investigations are needed to fulfil the significant promise they currently hold and reveal new perspectives for the further enhancement of the therapeutic capacity of this interesting natural molecule. Specifically, in this thesis we wanted to experiment the pharmacological action of curcumin as a component of a new nutraceutical formulation that uses the SLN system. SLN-CUR formulation obtained was used to test its efficacy on the expression of ERRα and as a potential inhibitor of the growth and progression of adrenocortical carcinoma.

Materials and Methods

4. Materials and Methods

4.1 Cell culture and tissues

Adrenocortical cancer cells used for experiments were H295R, SW13, MUC1. H295R and SW13 cells were obtained from the American Type Culture Collection (ATCC, Rockville, MD). H295R cultured in DMEM/F12 (Dulbecco's modified Eagle's Medium/Nutrient Mixture- F12 Ham) supplemented with 1% ITS Liquid Media Supplement, 5% fetal bovine serum (FBS), 2.5% nu-serum, 1% glutamine, 1% penicillin/streptomycin (complete medium) while SW13 cells maintained in DMEM/F12 supplemented with 10% FBS, 1% glutamine, 1% penicillin/streptomycin. MUC-1 cells were obtained from Constanze Hantel (University of Zurich – Switzerland) and cultured in Advanced DMEM/F12 Medium containing 10% FBS and 1% penicillin/streptomycin. The wild type H295R cells and the cell deriving from H295R cell lines in which the ERRα gene has been stably silenced (sh ERRα # 1, sh ERRα # 2, sh ERRα # 3, sh ERRα # 5, sh ERRα # 6, sh ERRα # 7, sh ERRα # 8), were grown in complete medium with puromicyn. All cell lines were cultured at 37°C in 5% CO2 in a humidified atmosphere. DMEM/F12 and supplements were from Sigma-Aldrich, Milano, Italy while Advanced DMEM/F12 Medium and ITS were Gibco-Thermo Fisher Scientific, Monza, Italy.

4.2 Western blot analysis

Whole cell lysate was prepared in RIPA buffer (50 mM Tris-HCl, 150 mM NaCl, 1% NP-40, 0.5% sodium deoxycholate, 2 mM sodium fluoride, 2 mM EDTA, 0.1% SDS and a mixture of protease inhibitors) or in ice-cold lysis buffer (10 mM Tris-HCl pH 8, 150 mM NaCl, 1% Triton X-100, 60 mM octylglucoside). Western blot analysis was performed using equal quantity of protein. Protein concentration was determined by Bradford method (Sigma- Aldrich) and equal amounts were subjected to Western blot analysis. Samples were analyzed by 11% SDS-PAGE and blotted into a nitrocellulose membrane. Blots were incubated overnight at 4°C with anti-ERRα polyclonal antibody (from Abcam, Cambridge, UK), anti-Vimentin, anti-Cyclin D1, anti-Cyclin E, anti-Cyclin, anti-Cyclin CDK4, anti-Parp1 and anti-BCL-XL (from Santa Cruz Biotechnology, Santa Cruz CA, USA). GAPDH antibody (from Santa Cruz Biotechnology, Santa Cruz CA, USA) were used as internal control. All antibodies were

incubated with appropriate horseradish peroxidase conjugated secondary antibodies for 1 h at room temperature. The immunoreactive products were detected by the ECL Western blotting detection system (Amersham Pharmacia Biotech, Piscataway, NJ).

4.3 Stable transfection

The H295R cells were grown in a complete, antibiotic-free medium in 6-well multiwells to reach a confluence of approximately 60%. After 48 h cells were transfected following the protocol indicated by the Santa Cruz. For this purpose two solutions were prepared: A.140 µl of transfection medium with addition of 10 µl of Plasmid Transfection Reagent, B. 130 µl of transfection medium with addition of 20 µl corresponding to 2 µg of plasmid DNA (respectively sh-ERRα and sh-control). The two solutions were incubated 5 minutes at room temperature, then they were combined and the mixture was incubated 30 minutes at room temperature. After the incubation time, the A / B mixture was added to the cells in culture. The cells were then incubated for 24 hours in a humidified incubator at 37 ° C and 5% CO2. After this period the transfection solution was removed and the normal growth medium was added. For the production of stable clones, 72 hours after transfection, the cells were selected by adding puromycin (Sigma Aldrich) in a concentration of 10 µg/ml. Cells resistant to antibiotics have formed clones that have been isolated and amplified. After about three weeks the concentration of puromycin was decreased to 1µg/ml.

4.4 Colony formation assay

This test allows an agent's ability to inhibit cell growth to be evaluated in vitro. The reduction in the number of colonies can derive both from the block of proliferation and from the induction of cell death. Clonal efficiency, or the ability to form colonies, is a parameter capable of measuring even partial damage to the complex enzyme structure that the cell needs to replicate. Specifically, wild type MUC1 cells were plated in complete medium and allowed to attach. Once attached cells were untreated and treated with different XCT790 doses (1, 5, 10 µM) for 24 h. After 24h all MUC1 cells, untreated and pretreated, were trypsinized, counted, replated in 12- well plates and allowed to grow for 14 days. The colonies formed were fixed for 15 minutes with paraformaldehyde (Sigma Aldrich) and then stained with blue of comaxies (Sigma Aldrich) for 10 minutes.

The medium was changed and surviving cells were allowed to grow colonies of ≥50 cells for 2 weeks, washed, fixed, and stained with Comassie Brilliant Blue, and counted. The quantitative analysis of the number of colonies (>50 cells) was performed by counting the colored colonies with Olympus CKX53 Inverted Microscope and was indicated as a colony formation ratio, expressed as a percentage of the untreated control.

4.5 Wound-Healing Assay

The wound-healing assay is simple, inexpensive and one of the earliest developed methods to study directional cell migration in vitro. This method mimics cell migration during wound healing in vivo. The basic steps involve creating a "wound" in a cell monolayer, capturing the images at the beginning and at regular intervals during cell migration to close the wound, and comparing the images to quantify the migration rate of the cells.

4.6 Boyden chamber assay

The Boyden chamber assay is based on a chamber of two medium-filled compartments separated by a microporous membrane. The transwell inserts (8 μm pore size, 24- well plate, Corning Costar, Cambridge, MA) were used to evaluate cell migration ability. Wild type, sh control and sh ERRα clones H295R cells were placed in the upper compartment and are allowed to migrate through the pores of the membrane into the lower compartment. Wild type MUC1 cells, instead, were plated in complete medium and allowed to attach. Once attached cells were untreated and treated with different doses of XCT790 (1, 5, 10 μM), Mitotane (2.5, 25, 40 μM) and Simvastatin (2.5, 5, 10 μM) for 18 h. After this time all MUC1 cells, untreated and pretreated, were trypsinized, counted, replated in the transwell inserts. Cells were incubated at 37 ° C with 5% CO2 for 24h. Cells migrated to the lower surface of the filter were fixed and stained with a Comassie Brilliant Blue solution for 5 minutes. The number of cells that have migrated to the lower side of the membrane was determined by ImageJ.

4.7 Cell viability assay

Cell viability was measured using colorimetric 3-(4,5-dimethylthiazol-2-yl)-2,5-diphenyltetrazolium bromide (MTT) assay (Sigma-Aldrich), which measures

mitochondrial activity in viable cells. Specifically, the cells were plated in a 48-well plate and, after 48 h, were treated with increasing XCT790 doses (1, 5, 10μM) for 24, 48, 72, 96h and curcumin doses (5, 10, 20, 40, 80μM) for 24, 48, 72h. After treatment, fresh MTT, resuspended in phosphate buffered saline (PBS), was added to each well (final concentration 0.33 mg/ml) and the plate was incubated at 37 °C for 2 h in a humidified 5% CO2 incubator. After incubation, media were removed, and formazan crystals were dissolved in 200 μL of DMSO (Sigma-Aldrich) for few min with gentle agitation. Each experiment was performed with six replicates and the optical density was measured at 570 nm with a spectrophotometer (Synergy H1 plate reader, BioTek Instruments, Inc., Winooski, VT, USA). Experiments were repeated three times.

4.8 RNA extraction, reverse transcription and real time PCR

Total RNA was extracted with PureLink™ RNA Mini Kit (Invitrogen, Carlsbad, CA). One microgram of total RNA was reverse transcribed in a final volume of 50 μl using the ImProm-II Reverse transcription system kit (Promega Italia S.r.l., Milano, Italy); cDNA was diluted 1:3 in nuclease-free water and used for RT-PCR. Quantitative PCR was performed using:

- Vimentin-specific primers:
  Forward 5'-CCTTGAACGCAAAGTGGAATC-3',
  Reverse 5'- GACATGCTGTTCCTGAATCTGAG-3';
- ERRα-specific primers:
  Forward 5'-CTGGTGGTTGAGCCTGAGAAG-3'
  Reverse 5'- ACCACAATCTCTCGGTCAAAGAG-3';
- Cyclin D1-specific primers:
  Forward 5'-CACGCGCAGACCTTCC -3'
  Reverse 5'-ATGGAGGCGGATTGGAA -3'
- Cyclin E-specific primers:
  Forward 5'-CAGTATCCCCAGCAATCTTTATACA -3',
  Reverse 5'-AATTCAAGGCAGTCAACATCCA -3';
- Bcl-XL-specific primers:
  Forward 5'- AACGGCGGCTGGGATAC-3',
  Reverse 5'- GCTCTCGGCTGCTGCATT-3'.

PCR reactions were performed in the iCycler iQ Detection System (Bio- Rad Laboratories S.r.l., Milano, Italia) using 0.1 μmol/L of each primer, in a total volume of 30 μl reaction mixture following the manufacturer's recommendations. SYBR Green Universal PCR Master Mix (Bio-Rad) was used for gene amplification. Each sample was normalized to its 18s content. The relative gene expression levels were normalized to a calibrator (Basal, untreated H295R cells). Final results were expressed as n-fold differences in gene expression relative to 18s and calibrator, calculated using the ΔΔCt method as previously published [Chimento A. et al., 2015].

4.9 Spheroids culture

A single cell suspension was prepared using enzymatic (1x Trypsin-EDTA, Sigma Aldrich), and manual disaggregation (25 gauge needle) (Shaw et al. 2012). Cells were plated at a density of 500 cells/cm^2 in spherois medium (DMEM-F12/ B27/ EGF (20ng/ml)/ Pen-Strep) in non-adherent conditions, in culture dishes coated with (2-hydroxyethylmethacrylate) (poly-HEMA, Sigma). Cells were grown for 5 days and maintained in a humidified incubator at 37°C at an atmospheric pressure in 5% (v/v) carbon dioxide/air. After 5 days for culture, spheres >50 μm were counted using an eye piece graticule, and the percentage of cells plated which formed spheres was calculated and is referred to as percentage spheroids formation, and was normalized to one (1 = 100% TSFE, tumor-spheres formation efficiency) [De Luca A. et al., 2015].

4.10 Seahorse XFe96 metabolic flux analysis

4.10.1 Mitochondrial Stress Analysis

Real-time oxygen consumption rates (OCR) determined using the Seahorse Extracellular Flux (XF96) analyzer (Seahorse Bioscience, MA, USA). Adrenocortical cancer cells (H295R, SW13, MUC1) were seeded into XF96-well cell culture plates (Seahorse Bioscience, MA, USA) and incubated overnight at 37°C in a 5% CO2 humidified atmosphere. After 48h, cells were treated with XCT790 (1-5-10 μM) or Simvastatin (2,5-5-10 μM) for 16h. H295R were treated also with curcumin (5-10 μM). At the end of treatment, cells were washed in warm XF assay media supplemented with 10mM glucose, 1mM Pyruvate, 2mM L-glutamine and adjusted at pH 7.4. Cells were then maintained for 1h in 175 μL/well of XF assay media at 37°C, in a non-CO_2 incubator. During the cell

incubation time, 25 µL of a solution of XF assay media containing 10µM oligomycin, 9µM FCCP, 10µM rotenone, 10µM antimycin A were loaded into the injection ports of the XFe-96 sensor cartridge. Data set was analyzed by XFe-96 software and GraphPad Prism software, using one-way ANOVA and Student's t-test calculations. All experiments were performed in quadruplicate at least three times.

4.10.2 Glycolytic Stress Analysis

The extracellular acidification rate in real time (ECAR) was determined using the Seahorse Extracellular Flux Analyzer (XF96, Seahorse Bioscience, MA, USA). Adrenocortical cancer cells (H295R, SW13, MUC1) were seeded into XF96-well cell culture plates (Seahorse Bioscience, MA, USA), and incubated overnight at 37°C in a 5% CO2 humidified atmosphere. After 48h, cells were treated with XCT790 (1-5-10 µM) or Simvastatin (2,5-5-10 µM) for 16h. H295R were treated also with curcumin (5-10 µM). At the end of treatment, cells were washed in a specific buffer (XF medium, pH 7.4) for the determination of metabolic flows added with 2 mM of L-glutamine. The cells were then maintained for 1 hour in 175 µl of XF medium at 37 ° C, in an incubator without CO_2. During the incubation time, 25 µl of a XF buffer solution containing glucose (10 mM) oligomycin (1µM), 2-deoxy-D-glucose (50 mM), were placed in specific housings of the analyzer (injection ports). The various ECAR measurements obtained were normalized taking into account the protein concentration within the individual wells.

4.10.3 Agilent Seahorse XF Real-Time ATP Rate Assay

The XF Real-Time ATP Rate Assay was determined using the Seahorse Extracellular Flux Analyzer (XF96, Seahorse Bioscience, MA, USA). Adrenocortical cancer cells (H295R, SW13, MUC1) were seeded into XF96-well cell culture plates (Seahorse Bioscience, MA, USA) and incubated overnight at 37°C in a 5% CO2 humidified atmosphere. After 48h, cells were treated with XCT790 (1-5-10 µM) for 16h. At the end of treatment, cells were washed in warm XF assay media supplemented with 10mM glucose, 1mM Pyruvate, 2mM L-glutamine and adjusted at pH 7.4. Cells were then maintained for 1h in 175 µL/well of XF assay media at 37°C, in a non-CO2 incubator. During the cell incubation time, 25 µL of a solution of XF assay media containing 15 µM oligomycin, 5 µM rotenone,/antimycin A, were loaded into the injection ports of the XFe-

96 sensor cartridge. Data set was analyzed by XFe-96 software and GraphPad Prism software, using one-way ANOVA and Student's t-test calculations. All experiments were performed in quadruplicate at least three times.

4.11 Determination of DNA fragmentation: TUNEL (Terminal deoxynucleotidyl transferase mediated dUTP nick-end labeling) assay

A distinctive feature of the late apoptosis process is the DNA fragmentation that generates a multitude of double-strand breaks - DSBs, making the 3-hydroxy groups accessible. This feature constitutes a valid starting point for apoptosis identification methods such as TUNEL (Terminal deoxynucleotidyl transferase dUTP Nick End Labeling). This technique allows to detect fragmented DNA by labeling the terminal residue of nucleic acids. The DeadEnd ™ Fluorometric TUNEL System (Promega) kit was used to reveal DNA fragmentation after 48h treatment with curcumin, following the manufacturer's instructions. Specifically the cells are cultured on slides for 48h, treated with curcumin (40 μM) in complete medium for 48h; then they were washed with PBS (Phospate buffered saline) and fixed in 4% paraformaldehyde for 25 minutes at room temperature. The cells were then washed with PBS and permeabilized with 0.2% Triton X-100 in PBS for 5 minutes. After two washes with deionized water, they were incubated with the TdT enzyme (terminal deoxynucleotidyl transferase) and with EdUTP (5-Ethynyl-2'-deoxyuridine 5'-triphosphate) 60 minutes at 37 ° C. After one hour the reaction was stopped with the specific NaCl and sodium citrate solution of the kit and after three washes with PBS the cells were stained with a solution of Dapi (4 ', 6-diamidine-2-phenylindole) in order to to analyze nuclear morphology. The cells were observed with a fluorescence microscope with a 200x objective.

4.12 Comet assay

To measure DNA damage, H295R cells were plated in growth medium for 48 h in 6-well plates and then treated with vehicle alone and with curcumin 10 μm for 24 h. Glass slides were coated in 1% agarose and left at 4 °C overnight. After 24h of treatment, cells were trypsinized and a mixture of 100 μL of cells and 100 μL of 1% agarose was added rapidly on previously prepared slides. Covered with coverslips and allowed to solidify for 10 min at 4°C. Then slides were incubated with lysis buffer (2.5 M NaCl, 0.1 M EDTA, 10 mM

Trizma, 200 mM NaOH, 0.5% Triton X-100, 10% DMSO, pH 10) at 4 °C for 30 min in the dark. After 30 min, coverslips were gently removed and slides were reincubated with lysis buffer at 4°C for other 30 min. Then, remove lysis buffer and incubate slides in alkaline buffer (300 mM NaOH, 1 mM EDTA, pH > 13) at room temperature for 20 min to allow the DNA to unwind. Electrophoresis was performed at room temperature in ice-cold alkaline electrophoresis buffer for 1 h at 40 V. After electrophoresis, wash slides three times with neutralization buffer containing trizma at pH 7.5 for 5 minutes each. Then, cells were fixed in 70% ethanol for 10 min, stained with 60 µL of DAPI solution (0.2 µg × mL−1) and then covered with coverslips. Slides were visualized using a 20× objective on a fluorescent microscope (Fluoview FV300 confocal laser scanning microscope, Olympus Corporation). All chemicals were from Sigma/Merck (Darmstadt, Germany).

4.13 Proteomic analysis

H295R cells, cultured in complete medium for 24h, were treated with XCT790 (10µM) in serum free-medium (SFM) for the next 24h while a cell plate was left in SFM and treated with DMSO (0.01%) as control. At the end of the experiment, the cells were lysed in a lysis buffer (Urea 8M in 100mM Tris pH8.0). Lysis was followed by two sonication cycles for a maximum time per cycle of 2 minutes. Samples were analyzed at the Congentech institute in Milan. 50µg for each sample were digested with Lys-C and trypsin, desalted C18 and injected into technical replicate in Data Dependent Acquisition (DDA) using a Q-ex-HF spectrometer, with a gradient setting equal to 75 minutes. Data were submitted to Maxquant for Label Free quantitative analysis against a Human database and statistic was performed with Perseus. Finally, the Anova statistical analysis was performed on three samples and then the t-tests ($p < 0.05$) in pairs. The post-analytical phase made use of the software available on the net called Panther and associated with the Gene-Onthology database.

4.14 Preparation of Curcumin Solid Lipid Nanoparticles (SLNs-CUR)

Curcumin and Phosphatidylcholine in a predetermined ratio (1:20 w/w) were dissolved in volatile organic solvent (Dichloromethane), while a water-soluble stabilizer (Kolliphor

P188) and a polymer (PolyVinyl Alcohol) were dissolved in water. In order to form the nanoemulsion, both phases were combined and agitated by vigorous stirring at 40 °C. After 1 hour, the unincorporated curcumin particles were removed by centrifugation at 1500 rpm, while surnatant was frozen and then freeze-dried. Encapsulation efficiency was estimating by evaluating drug in prepared formulation after dissolving in Methanol. All drug estimations were done using calibration curve through UV spectrophotometer.

4.15 Statistics

All experiments were performed at least three times. Data were expressed as mean values ± standard deviation (SD), statistical significance between control and treated samples and between H295R wild type, sh control H295R and sh ERRα # clones H295R, were analyzed using GraphPad Prism 5.0 (GraphPad Software, Inc.; La Jolla, CA, USA) software. Control and treated groups, and also H295R wild type, sh control H295R and sh ERRα # clones H295R, were compared using the analysis of variance (ANOVA). A comparison of individual treatments was also performed, using Student's t test. Significance was defined as $p < 0.05$.m.

Aim of the study

5. Aim of the study and main results achieved

Aim of this thesis was to investigate the role of ERRα on metabolic changes that occurs in different ACC cell lines. We also investigated if cellular changes induced by overexpression or depletion of ERRα are able to support or modulate ACC progression.

By proteomic and the Seahorse XF analyser, which allows the real-time analysis of glycolytic and mitochondrial flows, we investigated and revealed an important role of ERRα in regulating metabolic changes in ACC cells. Using stable clones overexpressing (ERR+/+) or with a silenced (shERR-/-) ESRRA gene expression in ACC cells we revealed that ERRα overexpression gives to ACC cells a better mitochondrial fitness while ERR-/- cells have a reduced basal and maximal respiration rates as well as the spare capacity.

We next investigated the effects of reduced ERRα expression on the bioenergetic functions of three ACC cell lines by using XCT790. Results from the ATP assay show that XCT790 lowered ATP levels in mitotane sensible H295R and SW13 cells, while was ineffective in mitotane-resistant MUC1 cells. Indeed, the analysis of the energetic contribution of mitochondria and glycolysis reveals an extreme metabolic plasticity in MUC1 cells and H295R compared to SW13 cells, which appear to exhibit a glycolytic phenotype. The evaluation of mitochondrial functions revealed the ability of XCT790 to negatively affect the maximal respiration rate in all three-cell lines.

It is well known that metabolic alterations in cancer cells are not exclusively associated with survival and proliferation phenomena but also affect cell motility. Our data revealed clearly a direct influence of ERRα expression on H295R motility. ERRα overexpression significantly increased H295R cell migration and EMT marker vimentin while downregulation of the metabolic receptor, by either genetic ablation or with pharmacological approaches showed a reduction of both cell motility and vimentin expression.

Other important data coming from our study is the impact of ERRα on the ability of H295R cells to grow in non-adherent conditions as 3D-spheroids, a feature of tumor aggressiveness that characterizes tumor-initiating stem-like cells (TICs). XCT790 was able to reduce 3D-spheroids formation and motility not only in SW13 cells but also, and above all, in mitotane-resistant MUC-1cells suggesting, once again, that targeting ERRα

could be an effective chemotherapy to consider for the treatment of mitotane-resistant ACC phenotype.

New recent findings reported cholesterol as a new endogenous ligand of ERRα. Our experiments confirm the role of cholesterol as an activator of ERRα inducing cell motility in ACC cells.

In this thesis, we also wondered if, in addition to cholesterol, there were other natural molecules able to modulate the expression and activity of ERRα. Our research focused on a natural product derived from plant, curcumin. Our results clearly showed that curcumin, while reducing the expression of ERRα, exerted a time- and dose-dependent inhibitory effect on H295R cell growth by inducing the activation of apoptotic events. Furthermore, the assay for obtaining cultures of 3D spheroids confirmed how curcumin could modulate the ability of H295R cells to expand, i.e. to reduce their ability to metastasize, an attitude closely related to the epithelial-mesenchymal transition (EMT) in which epithelial cells acquire the characteristics of non-polarized and migrating mesenchymal cells.

Moreover, according to the metabolic role of ERRα, the use of curcumin induced significant changes to the bioenergetics profile of H295R cells. Specifically, OCR and ECAR values and the energetic parameters derived from Seahorse data analysis and associated with mitochondrial and glycolytic functions, were all reduced by curcumin in a dose dependent manner.

It is known that the limitation of the therapeutic use of curcumin is mainly due to its poor bioavailability. Therefore, in order to improve the pharmacokinetic profile and cellular absorption of curcumin, we produced curcumin SLNs and we found a greater dose-dependent inhibitory effects on H295R cell proliferation compared to unmodified curcumin. Treatment with SLNs-CUR has a greater dose-dependent response on cell proliferation compared to tal qual curcumin, with a high significance already at the dose of 10μM at 24h, up to an inhibition> 75% in the 72h of treatment. Cells were also treated with the SLN vehicle at the same doses and for 72h, to demonstrate that it has no toxic effect when administered alone.

In conclusion, in this thesis it has been shown that ERRα is a key regulator factor modulating metabolic profile and consequently motility of ACC cells. It has be also

evidenced that the inhibition of this receptor, by synthetic or natural molecules, can strongly block not only the growth of mitotane-resistant ACC cells, but also the processes of transition of ACC cells to more aggressive and invasive phenotype. For this reason, ERRα can be considered a new important target to take in consideration in design new therapeutic strategy to fight the Adrenocortical cancer progression.

Results

6. Results

6.1 Proteomic analysis of H295R cells: effects of XCT790 on cell metabolism

To identify differentially regulated proteins upon ERRα inhibitor, H295R cells were exposed for 24h to either vehicle or XCT790 (10 μM), and cell lysates were subject to label free quantitative proteomics. Differential expression analysis, between untreated and XCT790-treated cells, showed significant changes for a large amount of proteins. Specifically, the analysis revealed significant modulation of 1447 genes including 757 upregulated and 690 down-regulated genes. Using the Kyoto Encyclopedia of Genes and Genomes (KEGG) pathway database we identified that these proteins fall within several pathways with significant relative abundance ($p<0.05$). As shown in **Figure 6.1** most pathways related to cell metabolism were down-regulated by XCT790. Starting from these data we next investigated metabolic functions of the available ACC cell models in response to ERRα manipulation.

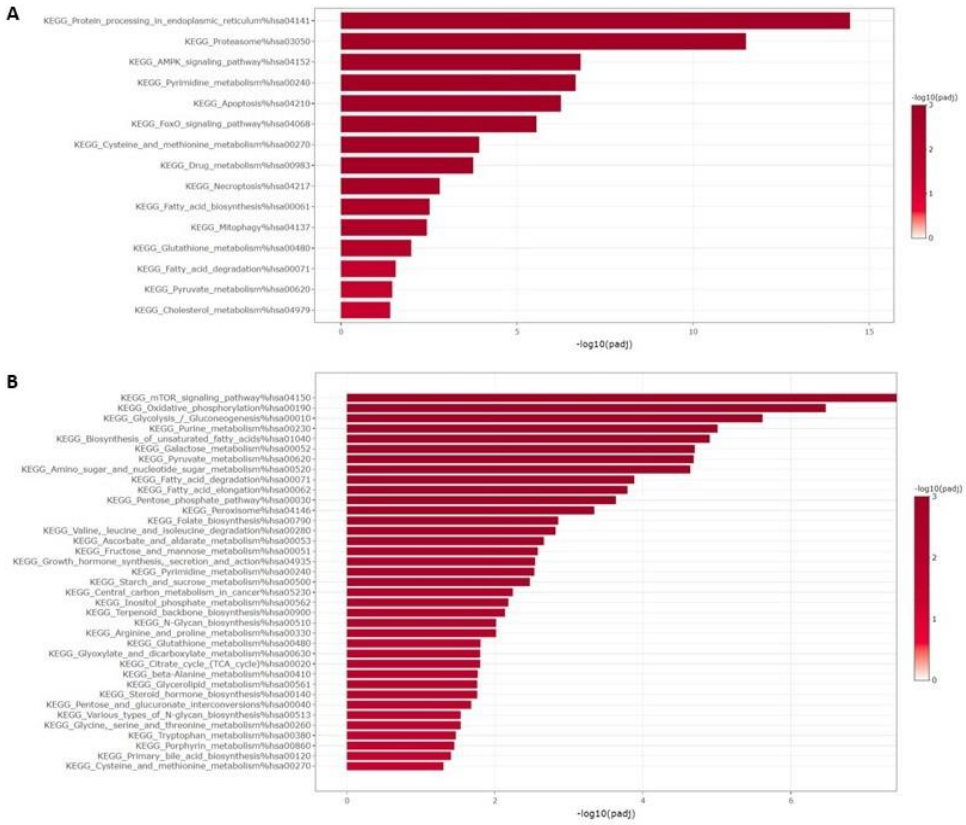

Figure 6.1 Functional enrichment analysis of differentially expressed proteins (A: up-regulated; B: down-regulated proteins) between untreated and XCT790-treated cells. For this analysis, we used KEGG database and selected metabolism-related pathways. Only significant enriched pathways are reported (FDR-adjusted p-value, padj<0.05, i.e. -log10(padj)>1.3)

6.2 Role of ERRα in metabolic functions of different ACC cell lines

We analyzed the metabolic changes in ACC cells related to different expression levels of ERRα using over-expressing (ERR+/+) or silenced (shERR-/-) H295R cells. H295R transfected with an empty vector (shCTR) was used as control. Seahorse XF96 Flux Analyzer (Agilent) has been used to profile oxidative phosphorylation as well as glycolysis and ATP production. The ATP Real-Time rate assay quantifies simultaneously the rate of ATP production from glycolysis and mitochondria. Data analysis revealed that H295R, shCTR, shERR-/- and wild type H295R (WT) cells showed the same amount of ATP content. By contrast, H295R ERR+ cells displayed a better performance in terms of ATP levels **[Figure 6.2A].** Moreover, in H295R and shCTR cells, glycolysis and OXPHOS contributed equally in the production of ATP **[Figure 6.2B]** while ERRα silenced or overexpressing cells showed an opposite trend. Specifically, ERR+/+ cells are characterized by an oxidative profile while the glycolytic rate is enhanced in ERR-/- cells **[Figure 6.2B].** A deeper analysis by using Mito Stress assay **[Figure 6.2C]** revealed that OCR levels are increased in ERR+ cells compared to shCTR and ERR-/- cells. The most interesting aspect obtained following the inhibition of the main energy flows is that ERRα overexpression gives to H295R cells a better mitochondrial fitness in terms of basal **[Figure 6.2D]**, maximal respiration rates **[Figure 6.2E]** and spare capacity **[Figure 6.3A]**. In ERR-/- cells, a small but significant reduction in the maximal respiration (Fig 2E) is observed, while spare capacity reduction **[Figure 6.3A]** and basal respiration not coupled to ATP production (proton leak) significantly increased **[Figure 6.3B].**

Glycolytic functions were detected by monitoring the extracellular acidification rate (ECAR) after a sequential injection of glucose, oligomycin, and 2-deoxy-D-glucose (2-DG) that allowed us to evaluate different glycolytic function parameters **[Figure 6.2F].** Glycolysis **[Figure 6.2G]** and glycolytic capacity **[Figure 6.2H]** were both increased in ERR-/- and ERR+/+ cells compared to shCTR cells while the glycolytic reserve **[Figure 6.3C]** was increased in ERR-/- and reduced in ERR+/+ cells.

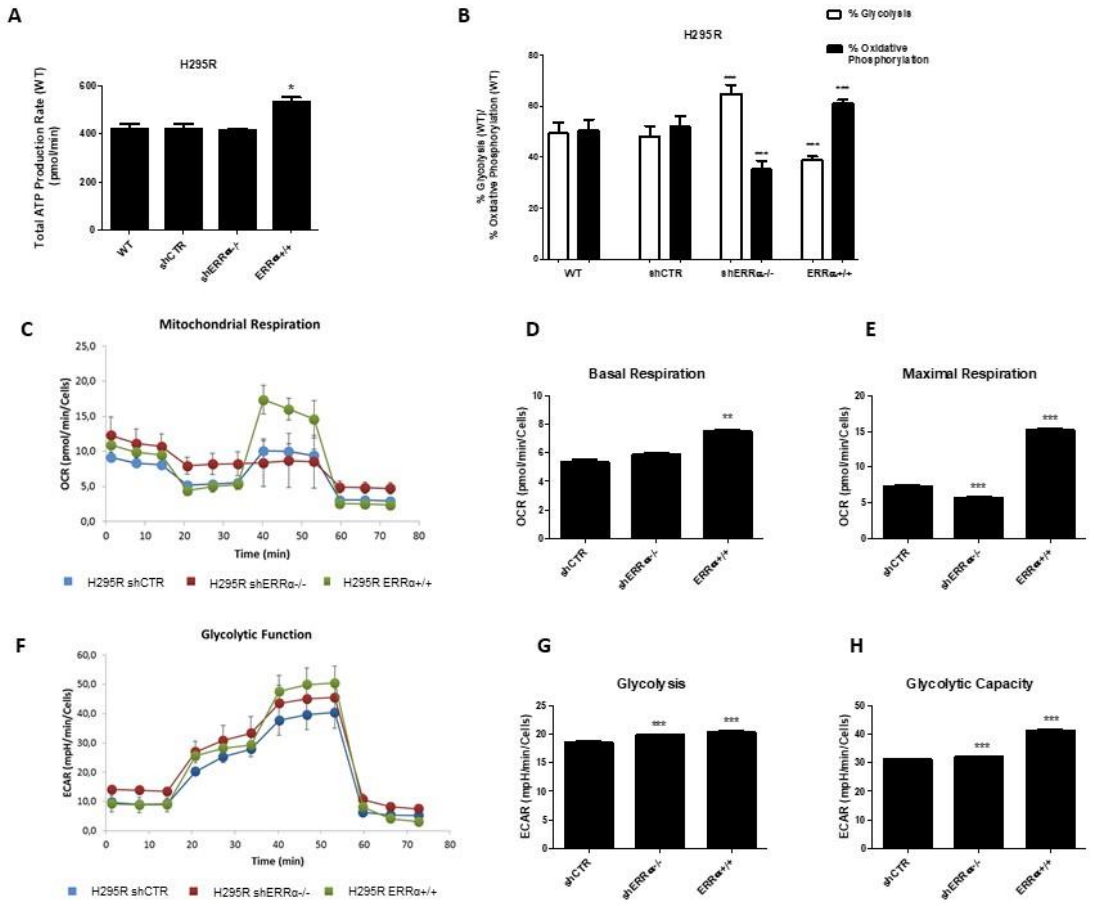

Figure 6.2 The metabolic profiles of H295R WT, shCTR, shERRα-/- and shERRα+/+ cells monolayers was assessed using the Seahorse XF-e96 analyzer following Agilent Seahorse XF Real-Time ATP Rate Assay. The Real-Time ATP Rate Assay was performed in DMEM, pH 7.4, supplemented with 10 mM glucose, 1 mM pyruvate and 2mM glutamine. Oligomycin (2 µg/mL final), and rotenone/antimycin A (2 µM final) were acutely added via the injector port. (**A**) is a representative image of Total ATP Production Rate (WT) (pmol/min). **(B)** is a representative image of real-time measurement of % Glycolysis (WT)/% Oxidative Phosphorylation (WT) after the sequential addition of the specific inhibitors.

Cell mito stress test profile of H295R WT, shCTRL, shERRα-/- and , shERRα+/+ cells monolayers was assessed using the Seahorse XF-e96 analyzer following the MITO Stress TEST. The H295R cells were grown in a monolayer for 18 hours. The MITO Stress TEST was performed in DMEM supplemented with 10 mM glucose, 1 mM pyruvate and 2mM glutamine. (OCR) after the sequential addition of the specific inhibitors. Oligomycin (2 µg/mL final), FCCP (800 nM final), and rotenone/antimycin A (1 and 2 µM final, respectively) were acutely added via the injector port. **(C)** Real-time oxygen consumption (OCR) rates were assessed using Seahorse XF96. The linear graph shows the same time course, but with three different injections to evaluate the oxygen consumption rate: 1-before the injection of oligomycin, 2- after the injection of carbonyl cyanide- (triphoromethoxy) phenylhydazone (FCCP) , 3- after the injection of rotenone antimicin. **(D)** Basal respiration. **(E)** Maximal respiration.

Cell glyco stress test profile of H295R WT, shCTRL, shERRα-/- and , shERRα+/+ cells monolayers was assessed using the Seahorse XF-e96 analyzer following the GLYCO Stress TEST. The H295R cells were

grown in a monolayer for 18 hours. The GLYCO Stress TEST was performed in DMEM supplemented with 2mM glutamine. (ECAR) after the sequential addition of the specific inhibitors. Glucose (10 mM final), Oligomycin (1 µM final), and 2-DG (50 mM final) were acutely added via the injector port. **(F)** Real-time extracellular acidification (ECAR) rates were assessed by Seahorse XF96. The linear graph shows the same time course, but with three different injections to evaluate the extracellular acidification rate: 1-before the glucose injection, 2-after the injection of carbonyl oligomycin, 3-after the injection of 2-deoxy -D-glucose. **(G)** Glycolysis. **(H)** Glycolytic capacity. (*P<0.05; **P<0,01; ***P<0.001).

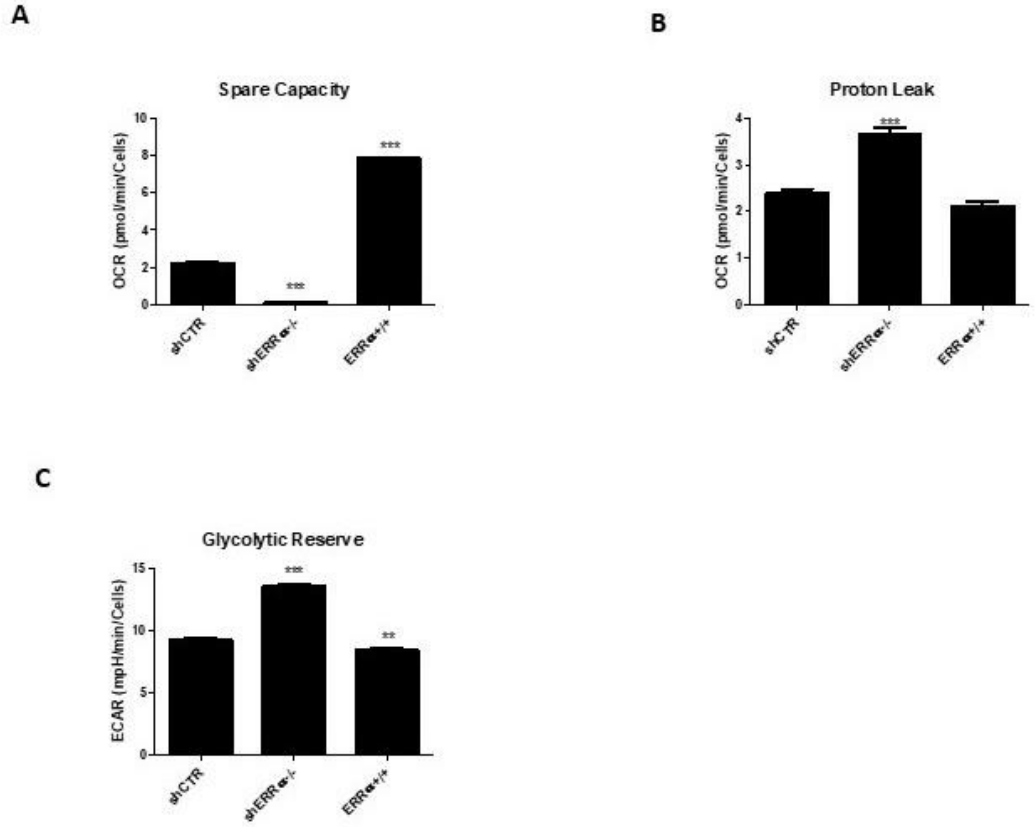

Figure 6.3 Cell mito stress test profile of H295R, shCTRL, ERRα-/- and , ERRα+/+ cells monolayers was assessed using the Seahorse XF-e96 analyzer following the MITO Stress TEST. The H295R cells were grown in a monolayer for 18 hours. The MITO Stress TEST was performed in DMEM supplemented with 10 mM glucose, 1 mM pyruvate and 2mM glutamine. (OCR) after the sequential addition of the specific inhibitors. Oligomycin (2 µg/mL final), FCCP (800 nM final), and rotenone/antimycin A (1 and 2 µM final, respectively) were acutely added via the injector port. Real-time oxygen consumption (OCR) rates were assessed using Seahorse XF96. The linear graph shows the same time course, but with three different injections to evaluate the oxygen consumption rate: 1-before the injection of oligomycin, 2- after the injection of carbonyl cyanide- (triphoromethoxy) phenylhydazone (FCCP) , 3- after the injection of rotenone antimicin. **(A)** Proton Leak, **(B)** Spare Capacity.

Cell glyco stress test profile of H295R, shCTRL, shERRα-/- and, shERRα+/+ cells monolayers was assessed using the Seahorse XF-e96 analyzer following the GLYCO Stress TEST. The H295R cells were grown in a monolayer for 18 hours. The GLYCO Stress TEST was performed in DMEM supplemented with 2mM glutamine. (ECAR) after the sequential addition of the specific inhibitors. Glucose (10 mM

final), Oligomycin (1 µM final), and 2-DG (50 mM final) were acutely added via the injector port. Real-time extracellular acidification (ECAR) rates were assessed by Seahorse XF96. The linear graph shows the same time course, but with three different injections to evaluate the extracellular acidification rate: 1-before the glucose injection, 2-after the injection of carbonyl oligomycin, 3-after the injection of 2-deoxy -D-glucose**. (C)** Glycolytic Reserve. (*P<0.05; **P<0,01; ***P<0.001).

We next investigated the effects of reduced ERRα expression on the bioenergetic functions of H295R cells by using XCT790. Results from the ATP assay show that XCT790 lowered ATP levels but significant effects are achieved only with the highest dose **[Figure 6.4A]**. In particular, doses higher than 1µm reduced the contribution of OXPHOS and increased the amount of ATP derived from glycolysis **[Figure 6.4B]**.
The evaluation of mitochondrial functions upon XCT790 treatment revealed that basal respiration rate decreased in H295R cells treated with 10µM **[Figure 6.4D]**. The maximal respiration rate **[Figure 6.4E]** and spare capacity **[Figure 6.5A]** were dose-dependently decreased by XCT790, while the trend of OCR levels associated with the proton leak is similar to those of basal respiration **[Figure 6.5B]**. Glycolytic flux analysis **[Figure 6.4F]** revealed that glycolysis increased **[Figure 6.4G]** with the highest dose of XCT790 while the glycolytic capacity **[Figure 6.4H]** and reserve **[Figure 6.5C]** were dose-dependently affected.

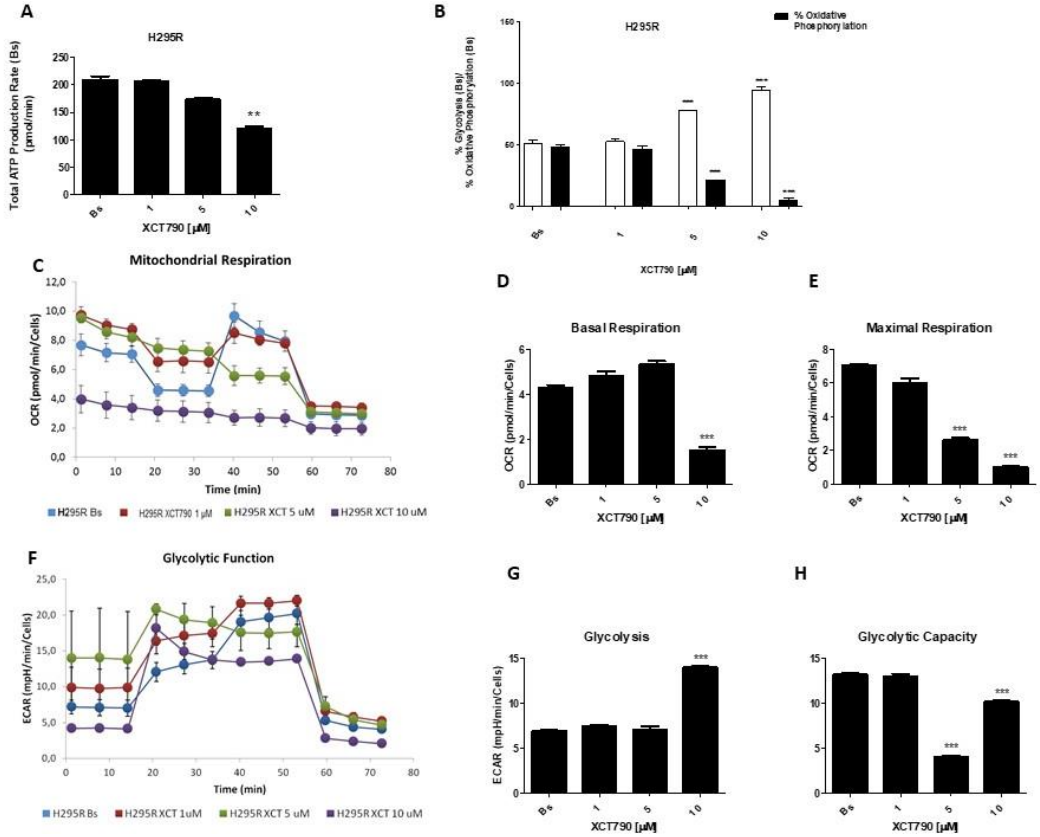

Figure 6.4 The metabolic profiles of H295R cells monolayers was assessed using the Seahorse XF-e96 analyzer following Agilent Seahorse XF Real-Time ATP Rate Assay, after treatment with 1, 5, 10 μM XCT790, for 18h. The Real-Time ATP Rate Assay was performed in DMEM, pH 7.4, supplemented with 10 mM glucose, 1 mM pyruvate and 2mM glutamine. Oligomycin (2 μg/mL final), and rotenone/antimycin A (2 μM final) were acutely added via the injector port. (**A)** is a representative image of Total ATP Production Rate (WT) (pmol/min). **(B)** is a representative image of real-time measurement of % Glycolysis (WT)/% Oxidative Phosphorylation (WT) after the sequential addition of the specific inhibitors.

Cell mito stress test profile of H295R cells monolayers was assessed using the Seahorse XF-e96 analyzer following the MITO Stress TEST. The H295R cells grown in a monolayer were treated with XCT790 (1, 5 and 10 μM) for 18 hours. The MITO Stress TEST was performed in DMEM supplemented with 10 mM glucose, 1 mM pyruvate and 2mM glutamine. (OCR) after the sequential addition of the specific inhibitors. Oligomycin (1.5 μM final), FCCP (0.5 μM final), and rotenone/antimycin A (0.5 μM final, respectively) were acutely added via the injector port. **(C)** Real-time oxygen consumption (OCR) rates were assessed using Seahorse XF96. The linear graph shows the same time course, but with three different injections to evaluate the oxygen consumption rate: 1-before the injection of oligomycin, 2- after the injection of carbonyl cyanide- (triphoromethoxy) phenylhydazone (FCCP) , 3- after the injection of rotenone antimicin. **(D)** Basal respiration. **(E)** Maximal respiration.

Cell glyco stress test profile of H295R cells monolayers was assessed using the Seahorse XF-e96 analyzer following the GLYCO Stress TEST. The H295R cells grown in a monolayer were treated with XCT790 (1, 5 and 10 μM) for 18 hours The GLYCO Stress TEST was performed in DMEM supplemented with 2mM glutamine. (ECAR) after the sequential addition of the specific inhibitors. Glucose (10 mM final), Oligomycin (1 μM final), and 2-DG (50 mM final) were acutely added via the injector port. **(F)** Real-time extracellular acidification (ECAR) rates were assessed by Seahorse XF96. The linear graph shows the same time course, but with three different injections to evaluate the extracellular acidification rate: 1-before the glucose injection, 2-after the injection of carbonyl oligomycin, 3-after the injection of 2-deoxy -D-glucose. **(G)** Glycolysis. **(H)** Glycolytic capacity. (*P<0.05; **P<0,01; ***P<0.001).

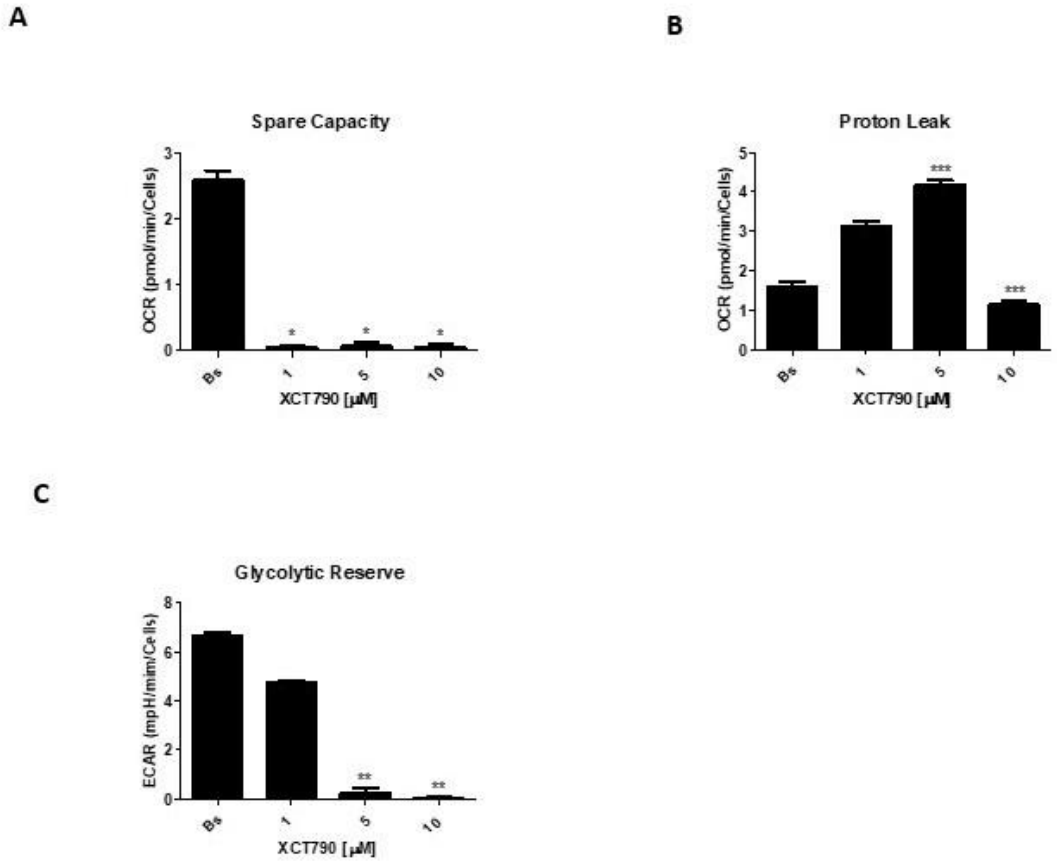

Figure 6.5 Cell mito stress test profile of H295R cells monolayers was assessed using the Seahorse XF-e96 analyzer following the MITO Stress TEST. The H295R cells grown in a monolayer were treated with XCT790 (1, 5 and 10 µM) for 18 hours. The MITO Stress TEST was performed in DMEM supplemented with 10 mM glucose, 1 mM pyruvate and 2mM glutamine. (OCR) after the sequential addition of the specific inhibitors. Oligomycin (2 µg/mL final), FCCP (800 nM final), and rotenone/antimycin A (1 and 2 µM final, respectively) were acutely added via the injector port. Real-time oxygen consumption (OCR) rates were assessed using Seahorse XF96. The linear graph shows the same time course, but with three different injections to evaluate the oxygen consumption rate: 1-before the injection of oligomycin, 2- after the injection of carbonyl cyanide- (triphoromethoxy) phenylhydazone (FCCP) , 3- after the injection of rotenone antimicin. **(A)** Spare Capacity, **(B)** Proton Leak.

Cell glyco stress test profile of H295R cells monolayers was assessed using the Seahorse XF-e96 analyzer following the GLYCO Stress TEST. The H295R cells grown in a monolayer were treated with XCT790 (1, 5 and 10 µM) for 18 hours . The GLYCO Stress TEST was performed in DMEM supplemented with 2mM glutamine. (ECAR) after the sequential addition of the specific inhibitors. Glucose (10 mM final), Oligomycin (1 µM final), and 2-DG (50 mM final) were acutely added via the injector port. Real-time extracellular acidification (ECAR) rates were assessed by Seahorse XF96. The linear graph shows the same time course, but with three different injections to evaluate the extracellular acidification rate: 1-before the glucose injection, 2-after the injection of carbonyl oligomycin, 3-after the injection of 2-deoxy -D-glucose**.** **(C)** Glycolytic Reserve. (*P<0.05; **P<0,01; ***P<0.001).

Dose-dependent effects of XCT790 were also observed in SW13 cells where drug decreased OCR and ECAR values associated with all parameters related to ATP content **[Figure 6.6A-B]**, mitochondrial metabolism **[Figure 6.6C-E** and **Figure 6.7A-B]** and glycolysis **[Figure 6.6F-H** and **Figure 6.7C]**.

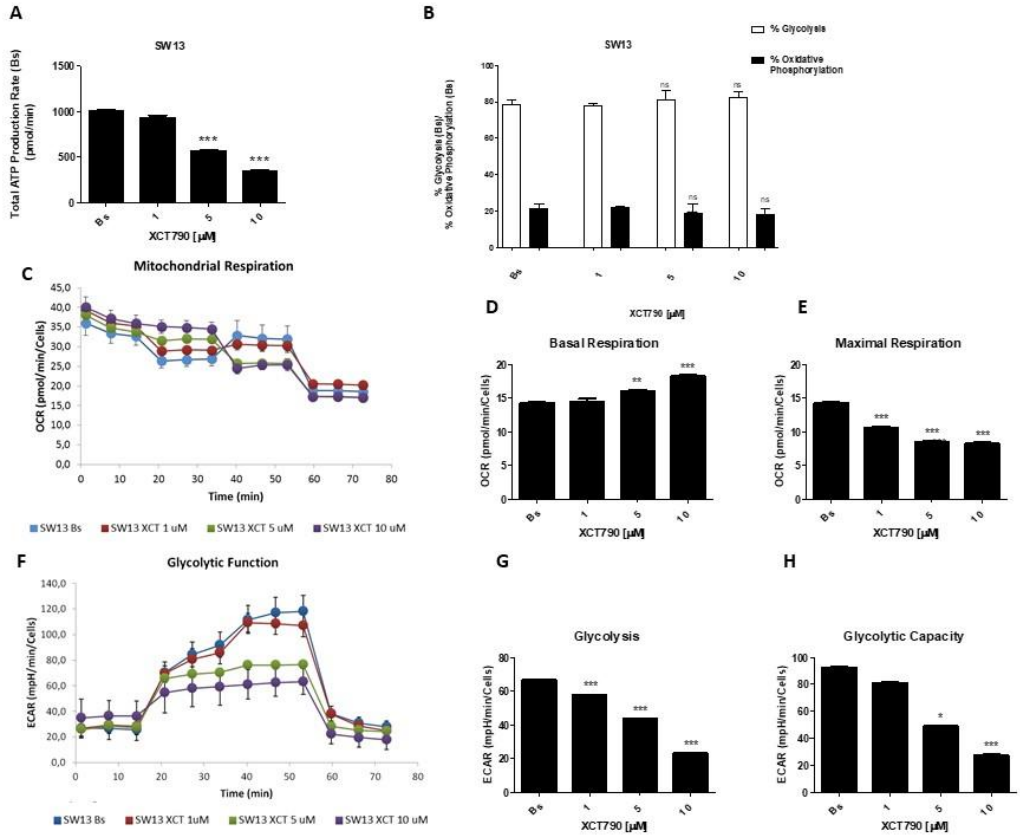

Figure 6.6 The metabolic profiles of SW13 cells monolayers was assessed using the Seahorse XF-e96 analyzer following Agilent Seahorse XF Real-Time ATP Rate Assay, after treatment with 1, 5, 10 µM XCT790, for 18h. The Real-Time ATP Rate Assay was performed in DMEM, pH 7.4, supplemented with 10 mM glucose, 1 mM pyruvate and 2mM glutamine. Oligomycin (2 µg/mL final), and rotenone/antimycin A (2 µM final) were acutely added via the injector port. (**A**) is a representative image of Total ATP Production Rate (WT) (pmol/min). **(B)** is a representative image of real-time measurement of % Glycolysis (WT)/% Oxidative Phosphorylation (WT) after the sequential addition of the specific inhibitors.

Cell mito stress test profile of SW13 cells monolayers was assessed using the Seahorse XF-e96 analyzer following the MITO Stress TEST. The SW!3 cells grown in a monolayer were treated with XCT790 (1, 5 and 10 µM) for 18 hours. The MITO Stress TEST was performed in DMEM supplemented with 10 mM glucose, 1 mM pyruvate and 2mM glutamine. (OCR) after the sequential addition of the specific inhibitors. Oligomycin (1.5 µM final), FCCP (0.5 µM final), and rotenone/antimycin A (0.5 µM final, respectively) were acutely added via the injector port. **(C)** Real-time oxygen consumption (OCR) rates were assessed using Seahorse XF96. The linear graph shows the same time course, but with three different injections to

evaluate the oxygen consumption rate: 1-before the injection of oligomycin, 2- after the injection of carbonyl cyanide- (triphoromethoxy) phenylhydazone (FCCP) , 3- after the injection of rotenone antimicin. **(D)** Basal respiration. **(E)** Maximal respiration.

Cell glyco stress test profile of SW13 cells monolayers was assessed using the Seahorse XF-e96 analyzer following the GLYCO Stress TEST. The SW13 cells grown in a monolayer were treated with XCT790 (1, 5 and 10 µM) for 18 hours The GLYCO Stress TEST was performed in DMEM supplemented with 2mM glutamine. (ECAR) after the sequential addition of the specific inhibitors. Glucose (10 mM final), Oligomycin (1 µM final), and 2-DG (50 mM final) were acutely added via the injector port. **(F)** Real-time extracellular acidification (ECAR) rates were assessed by Seahorse XF96. The linear graph shows the same time course, but with three different injections to evaluate the extracellular acidification rate: 1-before the glucose injection, 2-after the injection of carbonyl oligomycin, 3-after the injection of 2-deoxy -D-glucose. **(G)** Glycolysis. **(H)** Glycolytic capacity. (*P<0.05; **P<0,01; ***P<0.001).

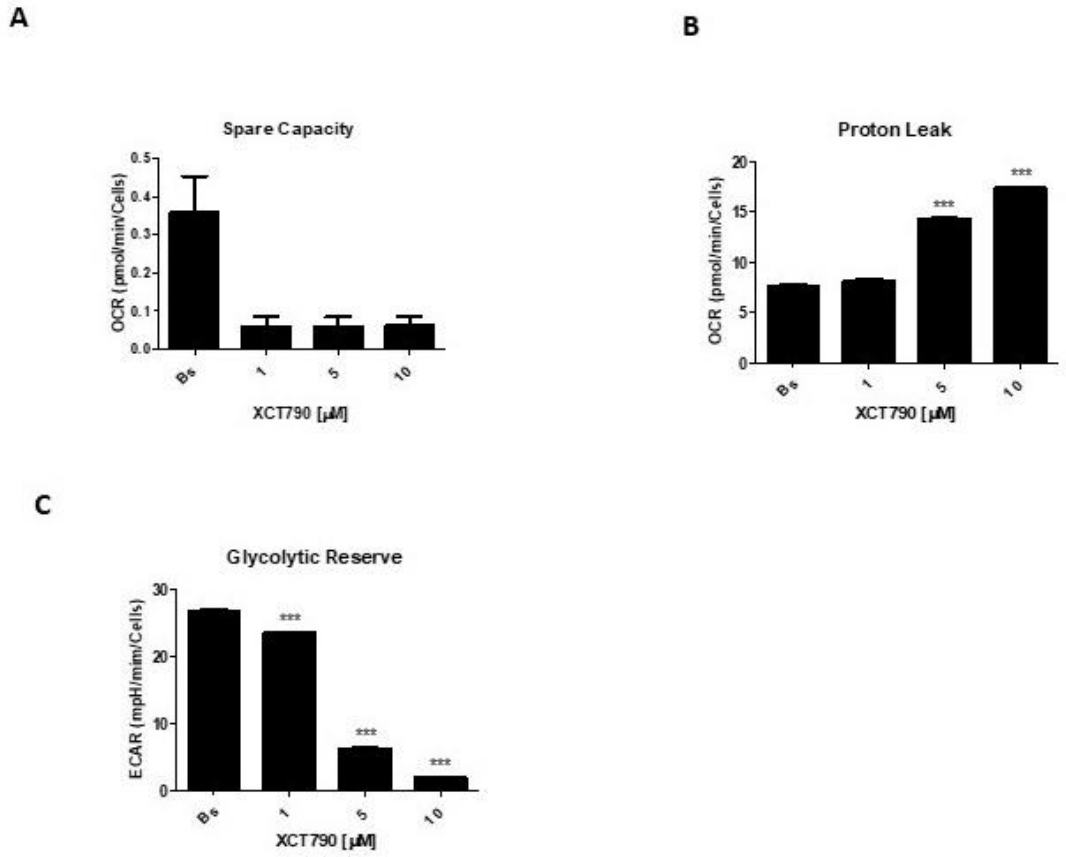

Figure 6.7 Cell mito stress test profile of SW13 cells monolayers was assessed using the Seahorse XF-e96 analyzer following the MITO Stress TEST. The SW13 cells grown in a monolayer were treated with XCT790 (1, 5 and 10 µM) for 18 hours. The MITO Stress TEST was performed in DMEM supplemented with 10 mM glucose, 1 mM pyruvate and 2mM glutamine. (OCR) after the sequential addition of the specific inhibitors. Oligomycin (2 µg/mL final), FCCP (800 nM final), and rotenone/antimycin A (1 and 2 µM final, respectively) were acutely added via the injector port. Real-time oxygen consumption (OCR) rates were assessed using Seahorse XF96. The linear graph shows the same time course, but with three different injections to evaluate the oxygen consumption rate: 1-before the injection of oligomycin, 2- after

the injection of carbonyl cyanide- (triphoromethoxy) phenylhydazone (FCCP) , 3- after the injection of rotenone antimicin. . **(A)** Spare Capacity, **(B)** Proton Leak.

Cell glyco stress test profile of SW13 cells monolayers was assessed using the Seahorse XF-e96 analyzer following the GLYCO Stress TEST. The SW13 cells grown in a monolayer were treated with XCT790 (1, 5 and 10 μM) for 18 hours . The GLYCO Stress TEST was performed in DMEM supplemented with 2mM glutamine. (ECAR) after the sequential addition of the specific inhibitors. Glucose (10 mM final), Oligomycin (1 μM final), and 2-DG (50 mM final) were acutely added via the injector port. Real-time extracellular acidification (ECAR) rates were assessed by Seahorse XF96. The linear graph shows the same time course, but with three different injections to evaluate the extracellular acidification rate: 1-before the glucose injection, 2-after the injection of carbonyl oligomycin, 3-after the injection of 2-deoxy -D-glucose**. (C)** Glycolytic Reserve. (*P<0.05; **P<0,01; ***P<0.001).

The metabolic profile of mitotane-resistant MUC1 cells showed that total ATP content was unaffected by XCT790 **[Figure 6.8A]** but the highest dose of XCT790 caused a shift from a balanced energy state to an increased glycolytic function **[Figure 6.8B]**. Accordingly, XCT790 treatment reduced maximal respiration **[Figure 6.8E]** and spare capacity **[Figure 6.9A]** while enhanced the proton leak **[Figure 6.9B]**. Moreover, the glycolysis and all glycolytic function parameters were only modestly affected **[Figure 6.8F-H** and **Figure 6.9C]**.

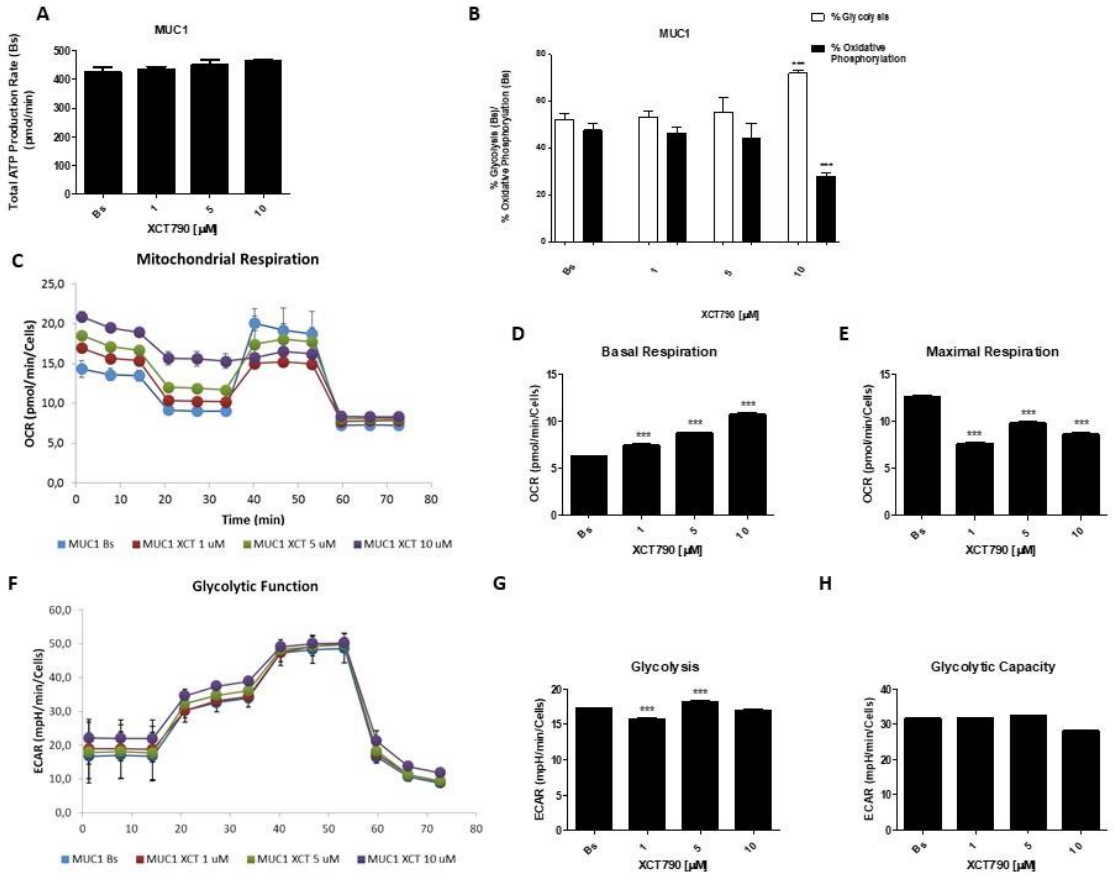

Figure 6.8 The metabolic profiles of MUC1 cells monolayers was assessed using the Seahorse XF-e96 analyzer following Agilent Seahorse XF Real-Time ATP Rate Assay, after treatment with 1, 5, 10 μM XCT790, for 18h. The Real-Time ATP Rate Assay was performed in DMEM, pH 7.4, supplemented with 10 mM glucose, 1 mM pyruvate and 2mM glutamine. Oligomycin (2 μg/mL final), and rotenone/antimycin A (2 μM final) were acutely added via the injector port. **(A)** is a representative image of Total ATP Production Rate (WT) (pmol/min). **(B)** is a representative image of real-time measurement of % Glycolysis (WT)/% Oxidative Phosphorylation (WT) after the sequential addition of the specific inhibitors.

Cell mito stress test profile of MUC1 cells monolayers was assessed using the Seahorse XF-e96 analyzer following the MITO Stress TEST. **(C)** The MUC1 cells grown in a monolayer were treated with XCT790 (1, 5 and 10 μM) for 18 hours. The MITO Stress TEST was performed in DMEM supplemented with 10 mM glucose, 1 mM pyruvate and 2mM glutamine. (OCR) after the sequential addition of the specific inhibitors. Oligomycin (1.5 μM final), FCCP (0.5 μM final), and rotenone/antimycin A (0.5 μM final, respectively) were acutely added via the injector port. **(D)** Real-time oxygen consumption (OCR) rates were assessed using Seahorse XF96. The linear graph shows the same time course, but with three different injections to evaluate the oxygen consumption rate: 1-before the injection of oligomycin, 2- after the injection of carbonyl cyanide- (triphoromethoxy) phenylhydazone (FCCP) , 3- after the injection of rotenone antimicin. **(B)** Basal respiration. **(E)** Maximal respiration.

Cell glyco stress test profile of MUC1 cells monolayers was assessed using the Seahorse XF-e96 analyzer following the GLYCO Stress TEST. The MUC1 cells grown in a monolayer were treated with XCT790 (1, 5 and 10 μM) for 18 hours The GLYCO Stress TEST was performed in DMEM supplemented with 2mM glutamine. (ECAR) after the sequential addition of the specific inhibitors. Glucose (10 mM final), Oligomycin (1 μM final), and 2-DG (50 mM final) were acutely added via the injector port. **(F)** Real-time extracellular acidification (ECAR) rates were assessed by Seahorse XF96. The linear graph shows the same time course, but with three different injections to evaluate the extracellular acidification rate: 1-before the glucose injection, 2-after the injection of carbonyl oligomycin, 3-after the injection of 2-deoxy -D-glucose. **(G)** Glycolysis. **(H)** Glycolytic capacity. (*P<0.05; **P<0,01; ***P<0.001).

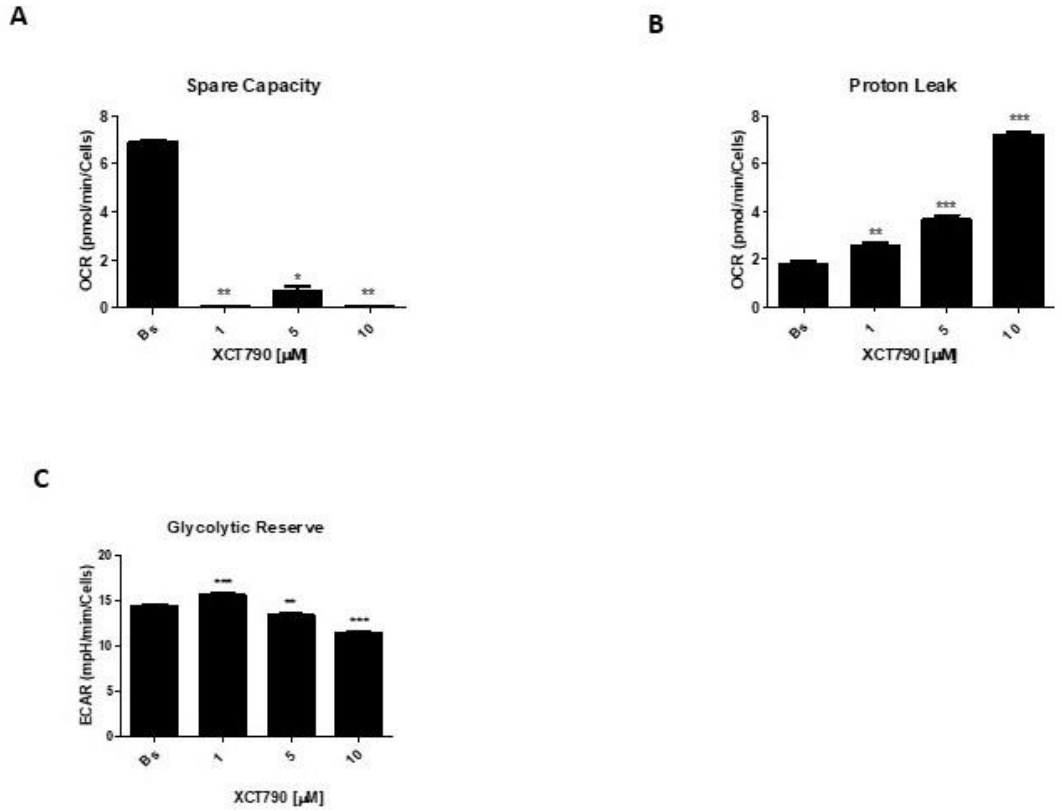

Figure 6.9 Cell mito stress test profile of MUC1 cells monolayers was assessed using the Seahorse XF-e96 analyzer following the MITO Stress TEST. The MUC1 cells grown in a monolayer were treated with XCT790 (1, 5 and 10 µM) for 18 hours. The MITO Stress TEST was performed in DMEM supplemented with 10 mM glucose, 1 mM pyruvate and 2mM glutamine. (OCR) after the sequential addition of the specific inhibitors. Oligomycin (2 µg/mL final), FCCP (800 nM final), and rotenone/antimycin A (1 and 2 µM final, respectively) were acutely added via the injector port. Real-time oxygen consumption (OCR) rates were assessed using Seahorse XF96. The linear graph shows the same time course, but with three different injections to evaluate the oxygen consumption rate: 1-before the injection of oligomycin, 2- after the injection of carbonyl cyanide- (triphoromethoxy) phenylhydazone (FCCP) , 3- after the injection of rotenone antimicin. **(A)** Spare Capacity, **(B)** Proton Leak.

Cell glyco stress test profile of MUC1 cells monolayers was assessed using the Seahorse XF-e96 analyzer following the GLYCO Stress TEST. The MUC1 cells grown in a monolayer were treated with XCT790 (1, 5 and 10 µM) for 18 hours . The GLYCO Stress TEST was performed in DMEM supplemented with 2mM glutamine. (ECAR) after the sequential addition of the specific inhibitors. Glucose (10 mM final), Oligomycin (1 µM final), and 2-DG (50 mM final) were acutely added via the injector port. Real-time extracellular acidification (ECAR) rates were assessed by Seahorse XF96. The linear graph shows the same time course, but with three different injections to evaluate the extracellular acidification rate: 1-before the glucose injection, 2-after the injection of carbonyl oligomycin, 3-after the injection of 2-deoxy -D-glucose**.** **(C)** Glycolytic Reserve. (*P<0.05; **P<0,01; ***P<0.001).

6.3 Effects of ERRα modulation on ACC cell motility

We first investigated the effects of increased doses of XCT-790 on H295R cell motility. Our results show that treatment of H295R cells with XCT790 for 18 hours (a time shorter than what required to cause cell death) decreased H295R migration in a dose dependent manner as evidenced by scratch **[Figure 6.10A]** and Boyden chambers **[Figure 6.10B]**.

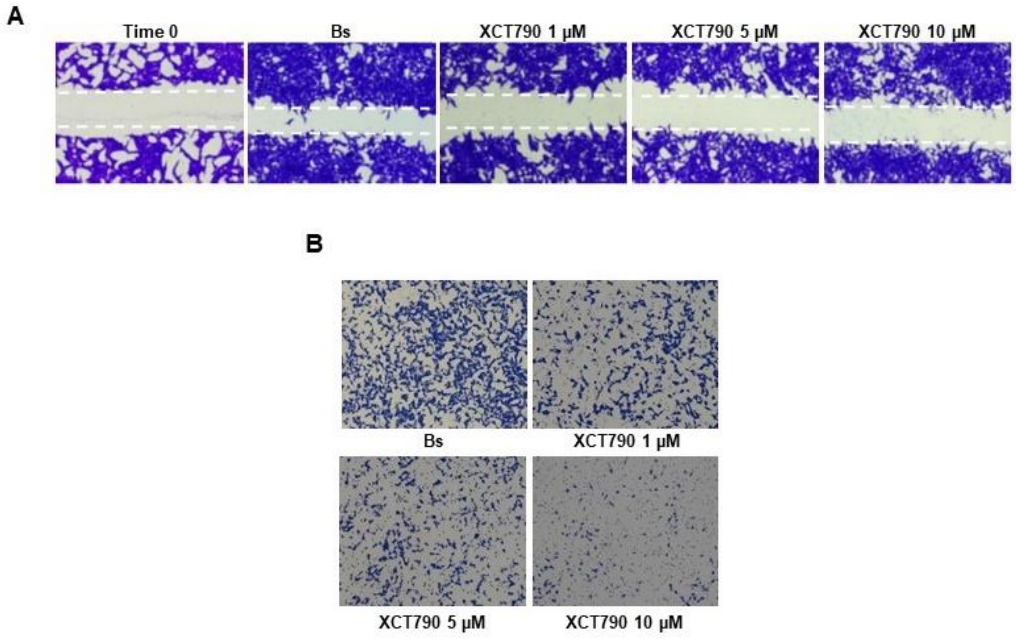

Figure 6.10 XCT790 inhibits H295R invasion and migration. (A, B) H295R cells were treated with vehicle (Bs) or XCT790 (1, 5, 10 µM) for 18 h and wound healing **(A)** and transwell migration **(B)** assays were performed. Images are from a representative experiment. **(A)** Cells were grown in 12- well plates until about 80- 90% confluency was reached and then a 10- µL pipette tip was used to create a scratch/wound with clear edges across the width of a well. Cells motility was observed under a microscope. **(B)** In the transwell migration assay, XCT790 was added in the upper lower compartment. After treatment, migrated cells to the lower surfaces of the membranes were observed under a microscope and then counted. Right graph represents the mean ± SE of three independent experiments of migrated cells number expressed setting untreated cells as 100% (Bs) (*$P \leq 0.05$ vs bs).

We next investigated the motility of H295R cell clones. By scratch assay we observed that ERRα overexpression significantly increased H295R cell migration while cells with a reduced expression levels of ERRα (shERR-/-) showed a decreased cell motility **[Figure 6.11A]**. Similar results were obtained using Boyden chambers assays **[Figure**

6.11B].

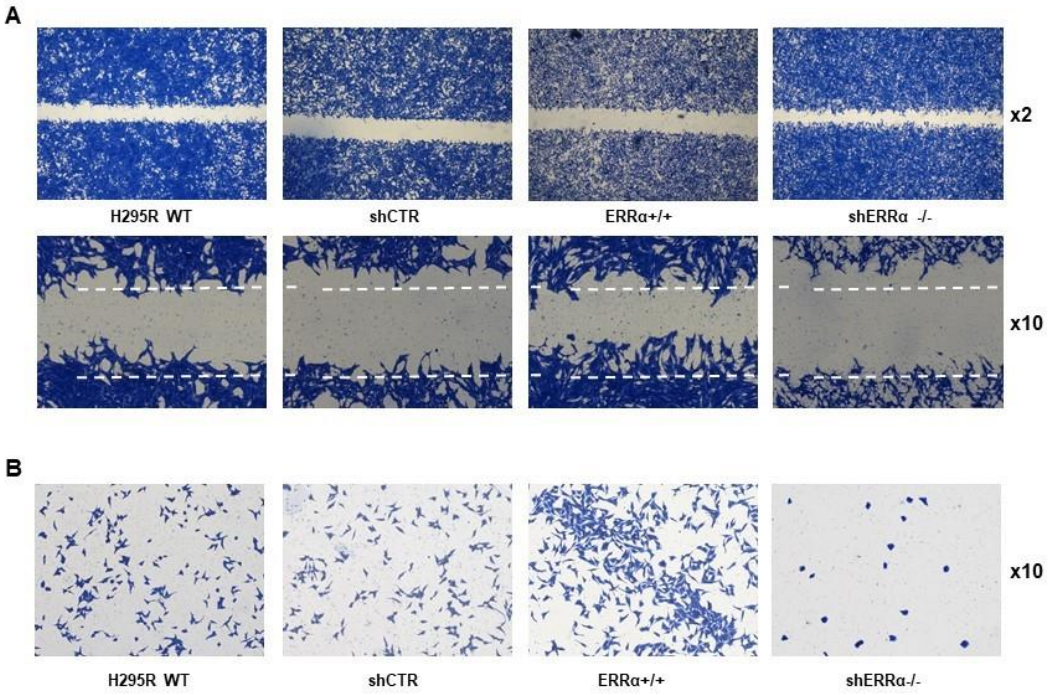

Figure 6.11 ERRα overexpression is involved in H295R motility and migration. H295R wild type (H295R WT), H295R clones *knock in* (ERRαα+/+) or *knock out* (shERRα-/-) for ERRα gene and H295R stably transfected with control plasmid (H295R shCTR) were used in wound healing (24h) **(A)** and transwell migration (18h) **(B)** assays. **(A)** Cells were grown in 12- well plates until about 80- 90% confluency was reached and then a 10- μL pipette tip was used to create a scratch/wound with clear edges across the width of a well. Cells motility was observed under a microscope. **(B)** Migrated cells to the lower surfaces of the membranes were observed under a microscope. Images are from a representative experiment x2 (A) or x10 (A and B).

Transient Ectopic expression of ERRα in H295R cells increased Vimentin, a known EMT marker **[Figure 6.12B]**, whose expression was reduced by XCT790 in both basal **[Figure 6.12A]** and ERRα overexpressing cells **[Figure 6.12B]**. These results were also confirmed in H295R cell clones where the expression levels of vimentin were increased in shERRα +/+ cells, and reduced in shERRα-/- **[Figure 6.12C]**.

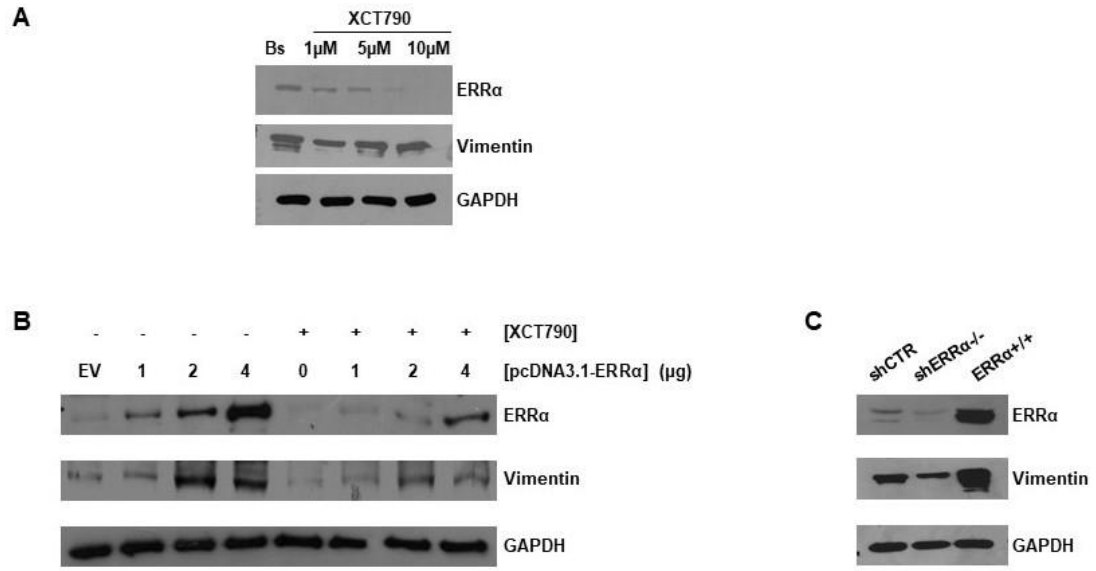

Figure 6.12 ERRα modulates H295R EMT markers expression. (A) Cells were untreated (Bs) or treated with XCT790 (1, 5, 10 μM) for 24 h. Total proteins were analyzed by WB using antibodies against ERRα and Vimentin. GAPDH was used as loading control. (B) H295R were transfected with an empty vector (EV) or an expression plasmid for ERRα (pcDNA3.1-ERRα) for 48h. After transfection cells were treated for 24h with XCT790 (10 μM). Total proteins were analyzed by WB using antibodies against ERRα and Vimentin. GAPDH was used as loading control. (C) Total proteins from H295R clones knock in (ERRα+/+) or knock out (shERRα-/-) for ERRα gene and H295R stably transfected with control plasmid (H295R shCTR) were analyzed by WB using antibodies against ERRα and Vimentin. GAPDH was used as loading control. Blots are representative of three independent experiments with similar results.

These data well correlated with the observation that transient ERRα overexpression in H295R enhanced cell growth in adherent-independent conditions, allowing the formation and increasing the number of 3D-spheroids **[Figure 6.13A]**. By contrast, XCT790 treatment reduced the ability of H295R cells to grow in non-adherent conditions preventing spheroids formation **[Figure 6.13B]**. These data were further confirmed in H295R clones. ShERRα -/- cells have a lower efficiency to growth as spheroids compared to shCTR or wild type cells, while shERRα +/+ cells easily formed spheroids **[Figure 6.13C]**. Since spheroids are composed by the most aggressive cell type among the heterogeneous cancer cells, we enriched spheroids by dissociating and reseeding the same cells for 5 weeks in non-adherent condition before testing them ($H295R^{Sph-5}$) for motility assays. Migration ability of these cells was higher than adherent cells **[Figure 6.13D]** and showed an enhanced expression of vimentin compared to H295R cells grown in adherent

condition **[Figure 6.13E]**.

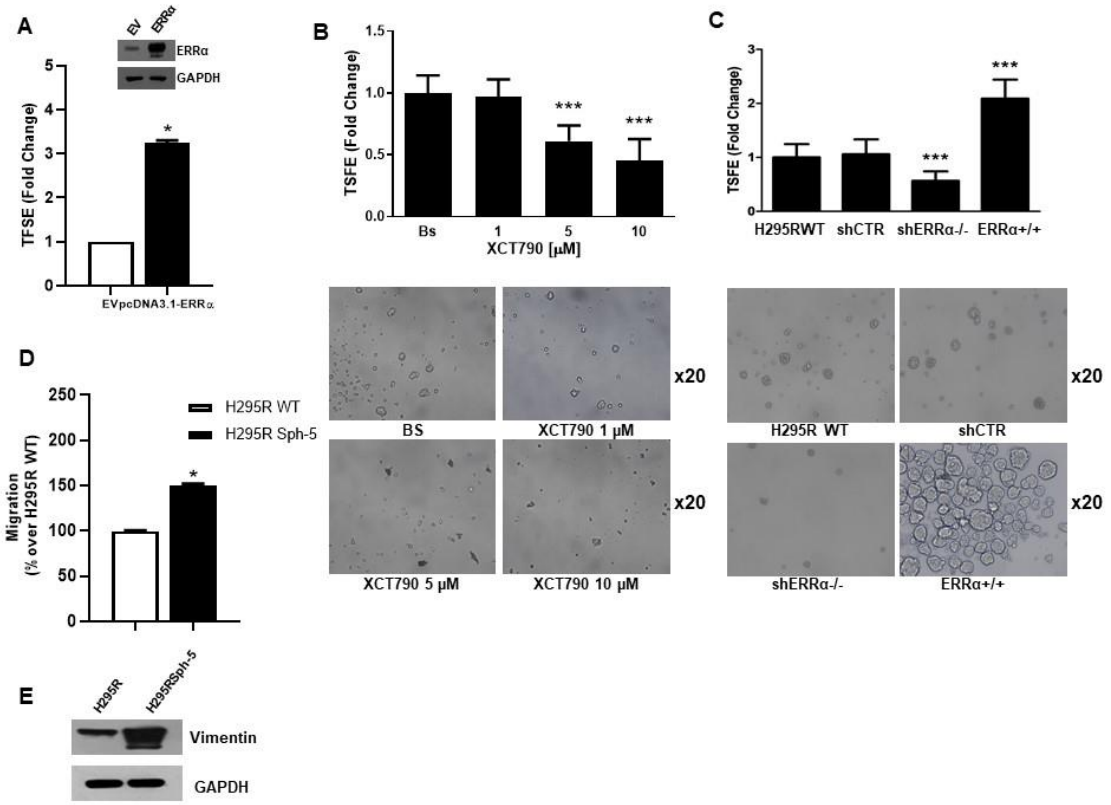

Figure 6.13 ERRα overexpression is involved in H295R 3D-spheroids formation. (A) H295R cells were transfected with an empty vector (EV) or an expression plasmid for ERRα (pcDNA3.1-ERRα) for 48h and then grown as 3D-spheroids for 5 days. Spheroids were counted under the microscope and results were expressed as fold induction over control ±SD (TSFE, tumor spheroids formation efficiency); *p <0.05. insert. **(A)** WB for ERRα in H295R transfected with an empty vector (EV) or an expression plasmid for ERRα at the time of spheroid counts. **(B)** H295R cells were untreated (Bs) or treated with XCT790 (1, 5, 10 μM) for 24 h. Tumour spheres formation efficiency (TSFE) was evaluated 5 days later (***P < 0.05 vs shCTR). Images below graph are from a representative experiment (x20). **(C)** H295R wild type (H295R WT), H295R clones *knock in* (ERR+/+) or *knock out* (shERR-/-) for ERRα gene and H295R stably transfected with control plasmid (H295R shCTR) were used to evaluate 3D-spheroids formation. Tumour spheres formation efficiency (TSFE) was evaluated 5 days later (***P < 0.05 vs shCTR) after plating. Images below graph are from a representative experiment (x20). **(D)** H295R spheroids (H295RSph-5) were allowed to grow for 5 days and then trypsinized and reseeded weekly in spheroid media for 5 weeks. Boyden chamber motility assay was performed by filling the lower chamber with 10% FBS to attract cells. 5×10^5 cells/well, cells were re-suspended in DMEM-F12 containing 0,5% FBS and carefully transferred into the upper chambers. The Boyden chamber was incubated at 37°C with 5% CO_2 for 24 h. At the end of the experiment, cells were removed from upper side of the membrane using a cotton swab, whereas the cells that migrated to the lower wells were fixed and stained in a Coomassie Blue solution for 5 min. Migrated cells were randomly photographed and counted with ImageJ. *p <0.05 versus H295R cells. **(E)** H295R cells and H295R grown as spheroids for 5 weeks (H295RSph-5), were analyzed by WB using

antibody against Vimentin. GAPDH was used as loading control. Blots are representative of three independent experiments with similar results.

Then H295R^{Sph-5} represent a useful experimental model of a more aggressive ACC phenotype.

We also investigated the effects of XCT790 using SW13 and MUC1 cells a different ACC cell model, derived from a small cell carcinoma in the adrenal cortex of a 55-year-old female. Although this cell line was taken from a surgically removed adrenal, SW13 cells do not produce steroids and it is unclear whether the cell line was derived from a primary cancer arising from the adrenal cortex or is a metastatic foci within the adrenal cortex. In SW13 cells we observed that XCT790 was able to decrease ERRα protein expression **[Figure 6.14A]**, cell viability **[Figure 6.14B]**, cell motility **[Figure 6.14C]** and spheroid formation efficiency **[Figure 6.14D].** We next investigated the effects of XCT790 on adrenocortical cancer cell model (MUC-1) isolated from a mitotane- and chemo-resistant tumor.

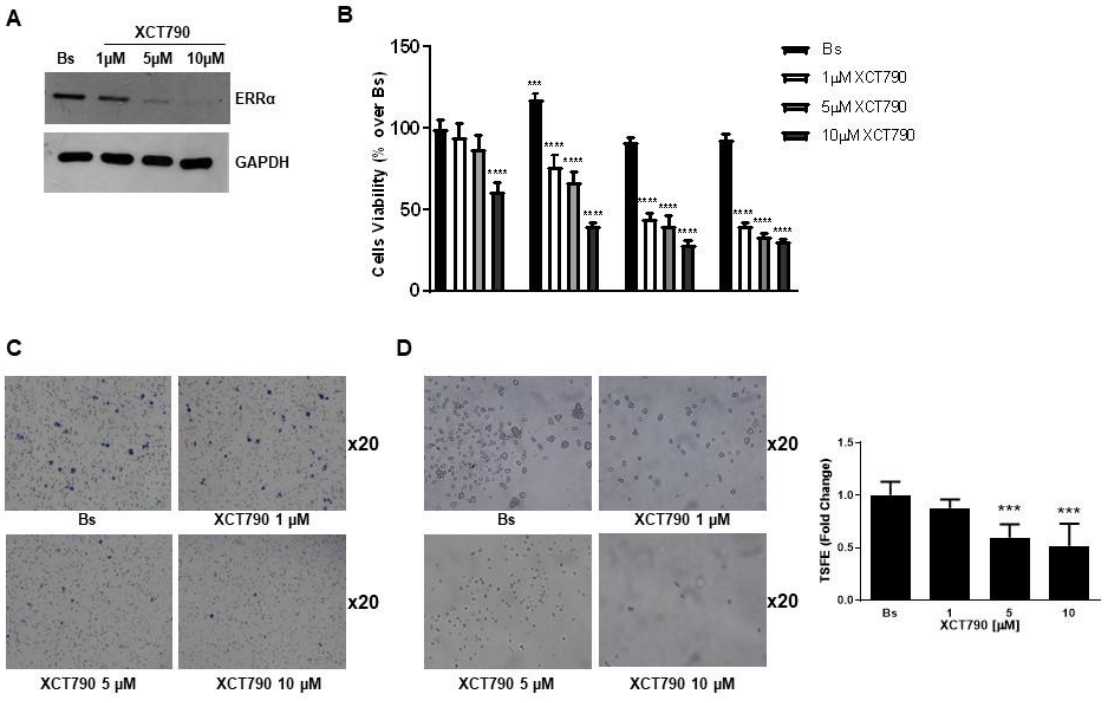

Figure 6.14 XCT790 decrease ERRα protein expression, cell viability and motility in SW13 cells. SW13 cells were untreated (Bs) or treated with XCT790 (1, 5, 10 μM) for 24 (A) or 18 (C) hours or different times (24, 48, 72, 96h) (B). (A) Total proteins were analyzed by WB using antibodies against ERRα. Blots are from one experiment representative of three with similar results. GAPDH was used as loading control. (B) Cell viability was evaluated by MTT assay (***P < 0.006 vs Bs, ****P < 0.0001 vs Bs). (C)

In the transwell migration assay, XCT790 was added in the upper compartment. After treatment, migrated cells to the lower surfaces of the membranes were observed under a microscope and then counted (x20). (D) SW13 cells were untreated (Bs) or treated with XCT790 (1, 5, 10 μM) for 24 h. Tumour spheres formation efficiency (TSFE) was evaluated 5 days later (***P < 0.05 vs Bs). Images right graph are from a representative experiment (x20).

Compared to H295R and SW13 cells, in MUC-1 cells the drug was less effective in reducing ERRα protein expression **[Figure 6.15A]**, colony formation **[Figure 6.15B]**, motility **[Figure 6.15C]** and spheroid formation efficiency **[Figure 6.15E]**. It is worth to note that a sub-therapeutic (25 μM) and the therapeutic dose (40 μM) of mitotane (1,1-dichloro-2-(ochlorophenyl)-2-(p-chloro-phenyl)-ethane or o,p69 DDD), an inhibitor of steroid synthesis with adrenolytic activity, were tested in parallel experiments **[Figure 6.15D]** confirming MUC-1 as mitotane-resistant cells to the only specific ACC drug currently used in clinic. Our results indicate that XCT790 could be considered an effective chemotherapy also in the treatment of mitotane-resistant ACC phenotype.

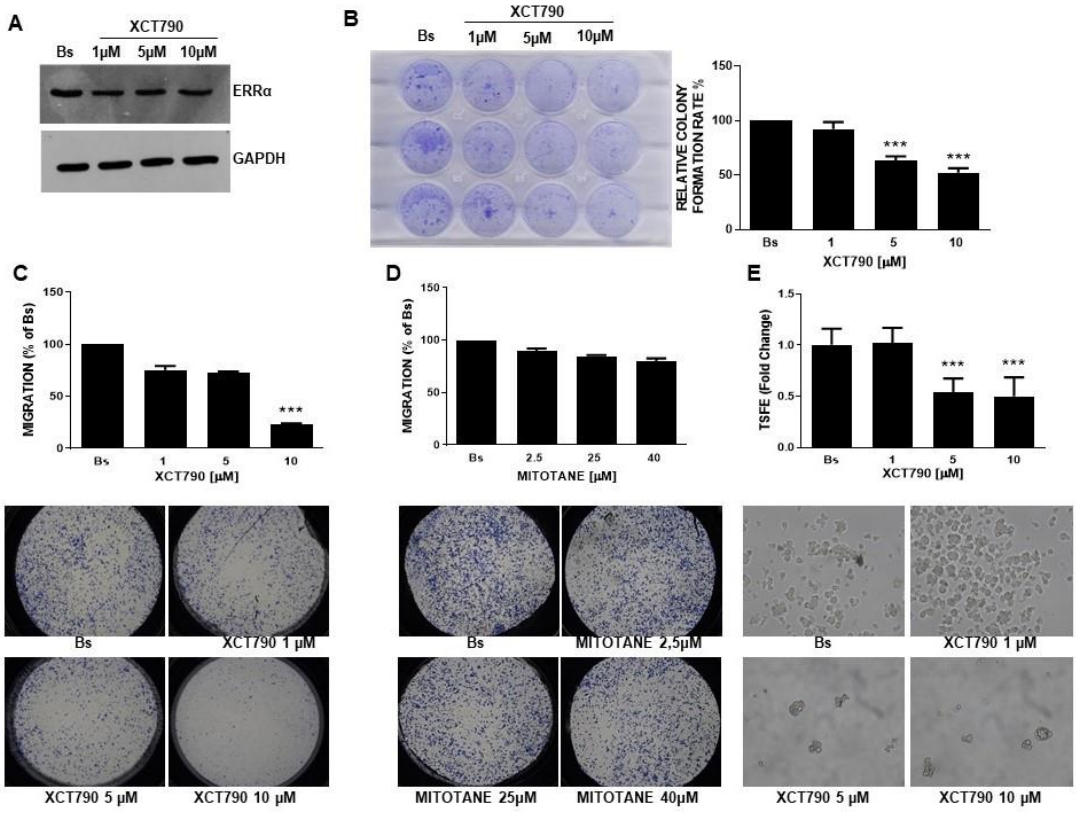

Figure 6.15 Effects of XCT790 treatment on ERRα expression and colony formation in MUC1 cells. **(A)** Cells were untreated (Bs) or treated with XCT790 (1, 5, 10 μM) for 24 h. Total proteins were analyzed by WB using antibodies against ERRα. GAPDH was used as loading control. Blots are from one experiment representative of three with similar results. **(B)** MUC1 cells were seeded in 12- well plates and

allowed to grow out in the absence or presence different XCT790 (1, 5, 10 μM) doses for 14 days. Colonies were stained with 0.05% Coomassie Blue in methanol/water/acetic acid (45:45:10, v/v). Colony number (relative colony formation rate) was assessed using Image J (NIH) and normalized to untreated cells (Bs). **(C)** MUC1 cells were seeded in the Boyden insert and solvent or mitotane (2.5, 25, 40 μM) were added in the well; the cells were allowed to migrate across the membrane for 18 hours. At the end of the experiment, migrated cells were stained with Coomassie Brilliant Blue solution for 10 minutes and counted under an inverted microscope (Olympus CKX53) (x2). **(D)** Right graph represents the mean ± SE of three independent experiments of migrated cells number expressed setting untreated cells as 100% (Bs). MUC1 cells were untreated (Bs) or treated with XCT790 (1, 5, 10 μM) for 24 h. Tumour spheres formation efficiency (TSFE) was evaluated 5 days later (***P < 0.05 vs Bs). Images right graph are from a representative experiment (x20).

6.4 Cholesterol as potential ERRa modulator in ACC

Recently, cholesterol has been recognized as a natural ERRα ligand. Importantly, the authors also demonstrated that cholesterol-induced modulations of the metabolic pathways in breast cancer are mediated via ERRα [Ghanbari F. et al., 2021]

To verify a similar functional interaction between ERRα and cholesterol in ACC, we cultivated H295R wild type or ERRα modified H295R cells in medium containing lipoprotein-free serum. Results from Boyden chambers and scratch assays confirmed that, in FBS containing medium, ERR-/- cells have a reduced migratory ability compared to shCTR cells while ERR+/+ cells migrated more rapidly. The absence of cholesterol negatively affected motility in all tested cell **[Figure 6.16A** and **Figure 6.16B]**. Furthermore, cholesterol depletion reduces ERRα transcription levels in silenced and over-expressing cells without affecting shCTR. In addition, data related to vimentin expression showed a similar trend obtained with motility assays but the only significant reduction in EMT marker expression was obtained in shCTR cells **[Figure 6.16C]**. These data indicate that cholesterol-ERRα complex is able to influence processes underlying motility, but the presence of other ligands or cofactors cannot be excluded. These observations opens a new interesting field of investigation.

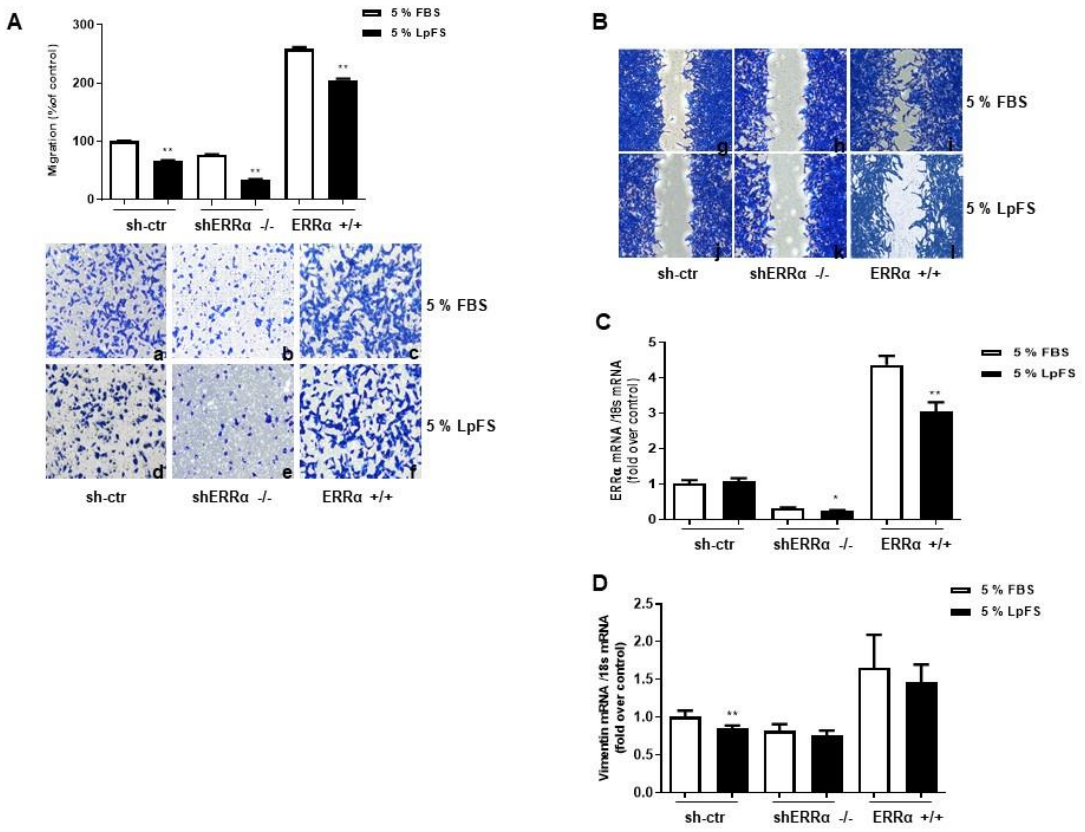

Figure 6.16 ERRα expression and cholesterol serum levels affect H295R cells proliferation and migration. (A) H295R cell clones with expression of the receptor stably silenced (shERRα -/-), over-expressed (ERRα +/+) and unchanged (sh-ctr) were plated in boyden chambers for 18h. Migrated cells to the lower surfaces of the membranes were fixed, stained and observed under a microscope and then counted. Images are from a representative experiment. Histograms represent the mean ± SE of three independent experiments of migrated cell numbers expressed as % over sh-ctr. H295R cell clones were plated in six well plate and allowed to grow to confluency (B). The cells monolayer was submitted to a scratch wound, hence cells were washed with PBS and the medium was replaced to the cells. Pictures of the scratch closure were taken 24h after injury. Stained cells were observed under a microscope. Images are representative of an experiment. mRNA was extracted from H295R cell clones and analyzed by real time RT-PCR. Gene expression in each sample was normalized to 18S rRNA content (C-D). Final results are expressed as n-fold differences of gene expression relative to calibrator chosen to be sh-ctr.

The data collected so far show that ERRα depletion after treatment with XCT790 causes a reduction in mitochondrial mass and function leading to the activation of mechanisms that result in the death of cancer cells. These results confirm that ERRα plays an important role in the regulation of mitochondrial function and in mitochondrial biogenesis in ACC cells, supporting the hypothesis that it can be considered as the "master" regulator of metabolic reprogramming in ACC.

Recently, has been demonstrated a correlation between use of curcumin and modulation of ERRα expression. Curcumin, in other in vitro experimental models, reduces the gene and protein expression of ERRα [Chen P. et al., 2017] and exerts inhibitory effects on the growth of different tumor cell lines [Shishodia S. et al., 2007; Troselj K.G. & Kujundzic R.N., 2014]. However, the effects of the administration of this nutraceutical in adrenocortical cancer have not been evaluated to date. For this reason, in the second phase of our study we wanted to verify the effects of the administration of curcumin on the expression of ERRα in parallel with those on the proliferation of H295R cells.

6.5 Effects of curcumin on ERRα expression and on the viability of H295R cells

It is known that curcumin, in other experimental models in vitro, reduces gene and protein ERRα expression [Chen P. et al., 2017] and exerts inhibitory effects on the growth of different tumor cell lines [Shishodia S. et al., 2007; Troselj K.G. & Kujundzic R.N., 2014]. However, the effects of its administration in adrenocortical cancer have not been evaluated to date. For this reason, in the first phase of my study we verified the effects of curcumin administration on ERRα expression in parallel with those on H295R cells proliferation. As can be seen in **Figure 6.17** using increasing doses of curcumin, the mRNA levels **[Figure 6.17A]** and protein **[Figure 6.17B]** are significantly down-regulated starting from the dose of 40 μM. In order to verify if these effects were also correlated with a decrease in cell proliferation, we treated H295R cells with the same doses of curcumin used for different times (24, 48 and 72 h), observing a time dependent inhibitory effect of cell viability measured by MTT assay **[Figure 6.17C]** already starting from 24h of treatment and with a significant inhibition at a dose of 20 μM.

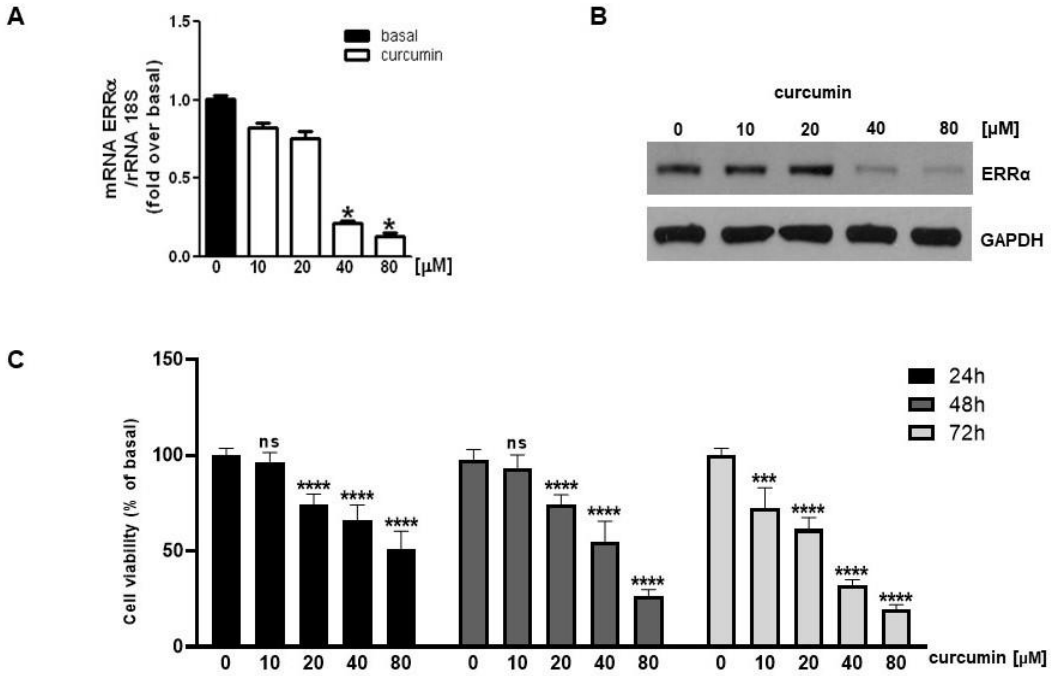

Figure 6.17 Effects of curcumin on ERRα expression and on the viability of H295R cells. The cells were maintained for 48h in complete medium and were subsequently untreated (basal) or treated for 12h (A, B) with increasing doses of curcumin (10, 20, 40, 80 μM). **A)** Real-time PCR was used to analyze the mRNA levels of the ERRα gene. The columns represent the mean of the values from three separate RNA samples; the bars, the standard deviation (SD). Each sample was normalized with respect to its own 18S rRNA content. * P <0.05 compared with baseline. **B)** Western blot analysis of ERRα was performed on 40 μg of proteins. The GAPDH was used as a loading control. The blots are representative of three independent experiments with similar results. **C)** The cells were maintained in complete medium for 48h and subsequently treated in complete medium at the times indicated with the vehicle (0) or increasing doses of curcumin (10-20-40-80 μM). Proliferation was evaluated by MTT assay as indicated in the chapter of Materials and Methods. The results are expressed as the mean ± SD of three independent experiments each performed in triplicate (*, P <0.05 compared with the control (0)).

6.6 Effect of curcumin treatment on mRNA and protein expression of cyclin / CDK in H295R cells

Cell proliferation is regulated by the cell cycle, which in turn is governed by the activation of cyclin / CDK (cyclin dependent kinase) protein complexes, the formation of which is necessary for normal progression through the various phases of the cycle [John P. et al., 2001]. In order to clarify if the effects of the use of curcumin on the growth of H295R

cells were associated with a cell cycle arrest, we investigated the expression of regulatory markers of the G1 / S passage of the cell cycle, such as cyclin D1 (CD1) and cyclin E (CDE) and their related partners, type 4 (CDK4) and type 2 (CDK2) dependent cyclin kinases, respectively. It is evident that treatment with the 40 μM dose of curcumin decreases mRNA expression of both cyclin D1 **[Figure 6.18A]** and cyclin E **[Figure 6.18B]** (after 12 hours of treatment) as well as **[Figure 6.18A,B]** protein expression **[Figure 6.18C]** after 24h of treatment.

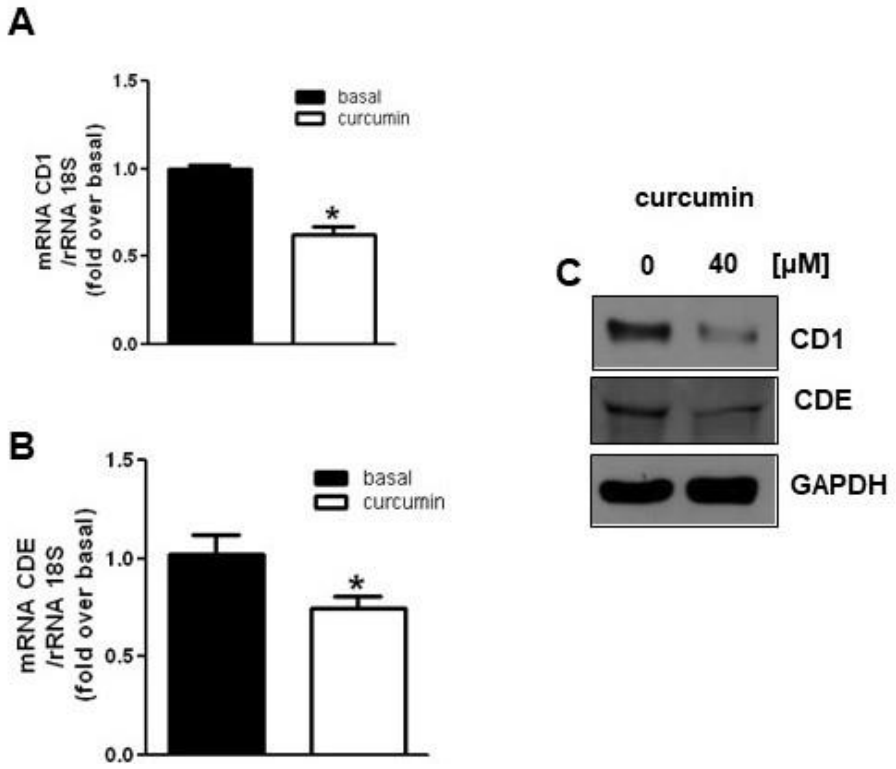

Figure 6.18 Effect of curcumin treatment on mRNA and protein expression of cyclin D1 and cyclin E in H295R cells. A, B) The cells were kept for 48h in complete medium and were subsequently untreated (basal) or treated for 12h (A, C) with curcumin (40 μM). Real-time PCR was used to analyze CD1 and CDE gene mRNA levels. The columns represent the mean of the values from three separate RNA samples; the bars, the standard deviation (SD). Each sample was normalized with respect to its own 18S rRNA content. * P <0.05 compared with baseline. **C)** Western blot analysis of CD1 and CDE was performed on 40 μg of proteins. The GAPDH was used as a loading control. The blots are representative of three independent experiments with similar results.

Furthermore, it is evident that the use of curcumin also decreases the protein expression levels of kinases associated with the related cyclins, (CDK4 and CDK2) **[Figure 6.19]**,

suggesting a cell block in the G1 / S phase.

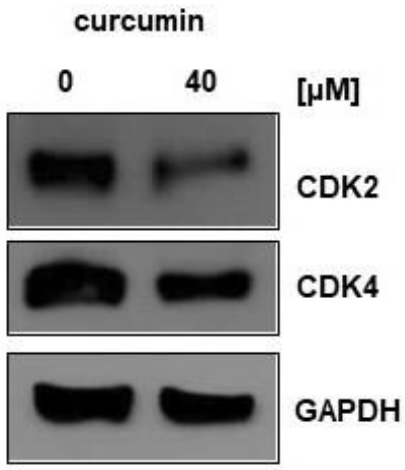

Figure 6.19 Effect of curcumin treatment on the protein expression of type 2 (CDK2) and 4 (CDK4) cyclin-dependent kinases in H295R cells. The cells were kept for 48h in complete medium and were subsequently untreated (basal) or treated for 24h with curcumin (40 µM). Western blot analysis of CD1 and CDE was performed on 40 µg of proteins. The GAPDH was used as a loading control. The blots are representative of three independent experiments with similar results.

6.7 Curcumin induces apoptosis in H295R cells

At this point, we wanted to verify if the reduction in cell proliferation was associated with molecular events of programmed cell death. To identify the death pathway that curcumin determines in H295R cells, we performed two different assays to evaluate DNA damage, the main characteristic of the late apoptotic process. To measure single and double-strand DNA breaks at the cellular level, COMET assay is an efficient experiment **[Figure 6.20].**

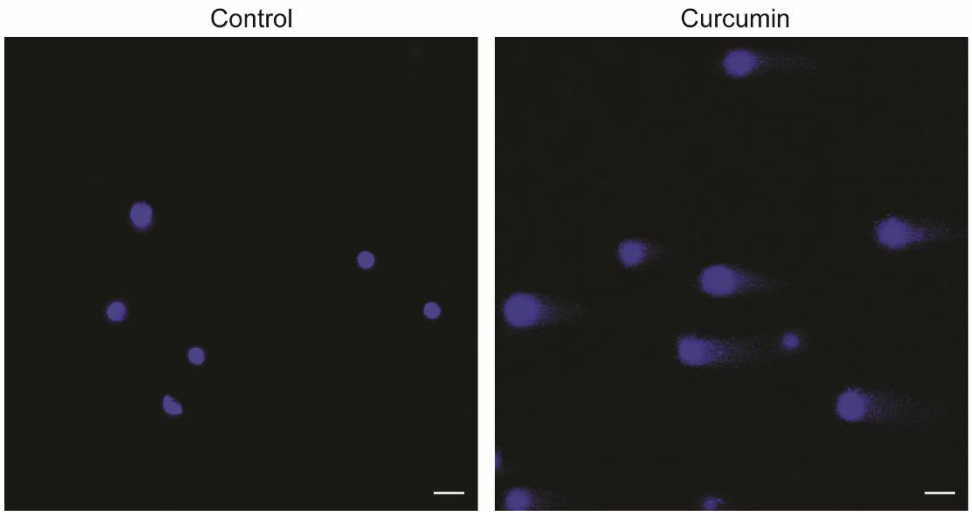

Figure 6.20 Comet assay in H295R cells. The cells were kept untreated (basal) and treated with curcumin (40 μM) for 24 h; after treatment cell were trypsinized and a mixture of cells and agarose was added on slides and was subjected to electrophoresis. Then, cells were fixed in 70% ethanol and processed for COMET assay. Counterstained nuclei were interpreted with Dapi. The fluorescent signal was observed under a fluorescence microscope (magnification 20x). The images are representative of an experiment repeated twice.

Instead, to evaluate DNA fragmentation we used TUNEL assay. **Figure 6.21** shows how in cells treated with the most effective dose of curcumin there is an increase in the fluorescence of fragmented DNA **[Figure 6.21A]**. It is reported by various literature data that during the apoptotic process the activation of caspases occurs [Thorburn A., 2004], specific proteases responsible in turn for the cleavage of a set of proteins including PARP-1 (poly- (ADP) ribose polymerase), an enzyme involved in the DNA repair process and in the maintenance of genomic stability [Wilson M.R., 1998]. After 24 h, treatment with curcumin revealed the cleavage of PARP-1, as can be seen from the presence of its 89 KDa form **[Figure 6.21B]**.

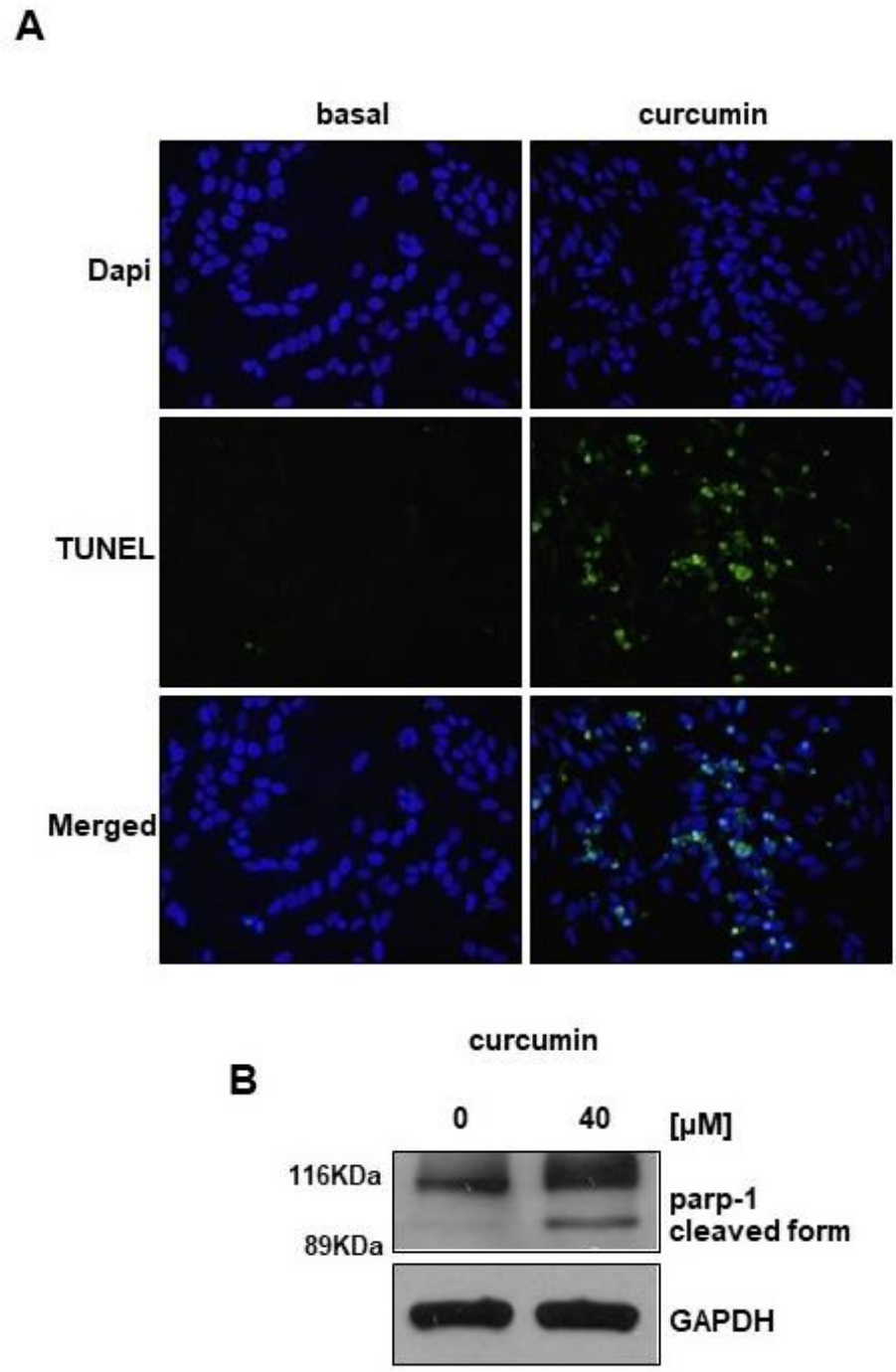

Figure 6.21 Curcumin induces apoptosis in H295R cells. A) The cells were kept untreated (basal) and treated with curcumin (40 μM) for 48 h; after treatment they were fixed with paraformaldehyde and processed for TUNEL staining. Counterstained nuclei were interpreted with Dapi. The fluorescent signal was observed under a fluorescence microscope (magnification 200x). The images are representative of an experiment repeated twice. **B)** The cells were kept untreated (basal) and treated with curcumin (40 μM) for 24h; Western blot analysis of parp-1 was performed on 40 μg of proteins. The GAPDH was used as a loading control. The blots are representative of three independent experiments with similar results.

The activation and regulation of the apoptotic process can be triggered both by extrinsic signals, that is, coming from outside the cell, and intrinsic and require the involvement of proteins that belong to the Bcl-2 family. This protein family includes both proapoptotic members such as Bax, Bid, Bak and antiapoptotic members such as Bcl2, Bclxl [Cory S. and Adams J.M., 2002]. Since these members play a crucial role in the regulation of the apoptotic pathway, we evaluated the changes in the gene and protein expression levels of an antiapototic marker such as Bcl-xL, belonging to the Bcl-2 family, both by real time PCR and western blot analysis. which is known to be a target of transcriptional regulation by ERRα. As can be seen in **Figure 6.22**, treatment with curcumin decreases the expression of Bcl-xL both at the transcriptoma level **[Figure 6.22A]** and at the protein level **[Figure 6.22B].**

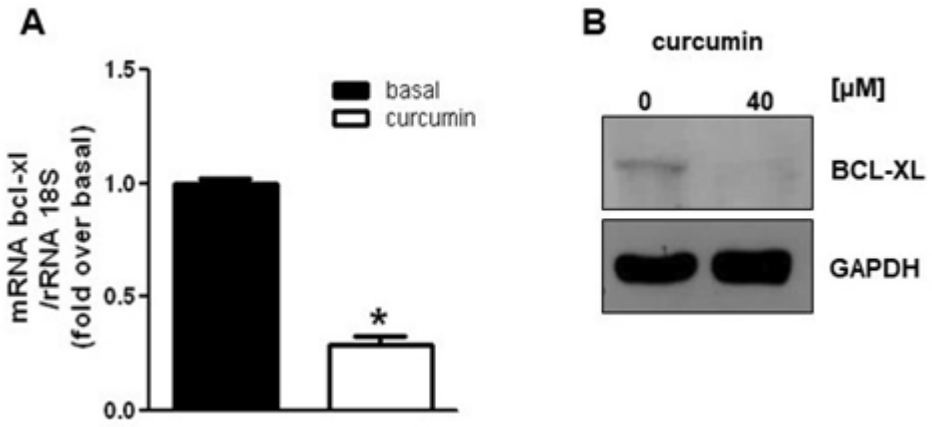

Figure 6.22 Effect of curcumin treatment on the expression of Bcl-xL in H295R cells. A) The cells were kept for 48h in complete medium and were subsequently untreated (basal) or treated for 12h with curcumin (40 μM). Real-time PCR was used to analyze the mRNA levels of the Bcl-xL gene. The columns represent the mean of the values from three separate RNA samples; the bars, the standard deviation (SD). Each sample was normalized with respect to its own 18S rRNA content. * $P < 0.05$ compared with baseline. **B)** The cells were maintained for 48h in complete medium and were subsequently untreated (0) or treated for 24h with curcumin (40 μM). Western blot analysis of Bcl-xL was performed on 40 μg of proteins. The GAPDH was used as a loading control. The blots are representative of three independent experiments with similar results.

6.8 Effect of curcumin treatment on metastatic potential

Furthermore, in order to evaluate whether curcumin could exert any effect on the ability of H295R cells to expand, that is, on their metastatic potential, the assay for obtaining cultures of 3D spheroids was carried out. The metastatic potential in cancer cells is closely correlated with the epithelium-mesenchymal transition (EMT), a process in which, following a chronic stimulus, epithelial cells with basal-apical polarity lose their phenotype and acquire the characteristics of the cells non-polarized and migrating mesenchymal cells [Onder T.T. et. al., 2008]. Recently, this process is considered to be the basis of the development and evolution of tumors. In a recent work the involvement of ERRα in the induction of EMT in osteosarcoma cells was demonstrated [Chen Y. et al., 2017] and in another study [De Luca A. et al., 2015] it was demonstrated how mitochondrial biogenesis is required for anchorage-independent survival and spread of tumor initiating stem-like cells (TICs) into breast cancer cells. TICs are characterized by the ability to survive and expand in the form of clones as tumor-spheres when placed in non-adherent conditions, called 3D-spheroids, which are more dependent on mitochondrial growth than a population of tumor cells. For this reason, the 3D-spheroids could represent a valid experimental model to investigate the role of ERRα and, in general, of cellular metabolism also in the metastatic potential of adrenal tumor.

As can be seen in **Figure 6.23**, curcumin prevents the formation of spheroids of H295R cells in a percentage equal to about 70% **[Figure 6.23A,B]**, which suggests that it would inhibit not only growth but also the progression of any relapses of the tumor.

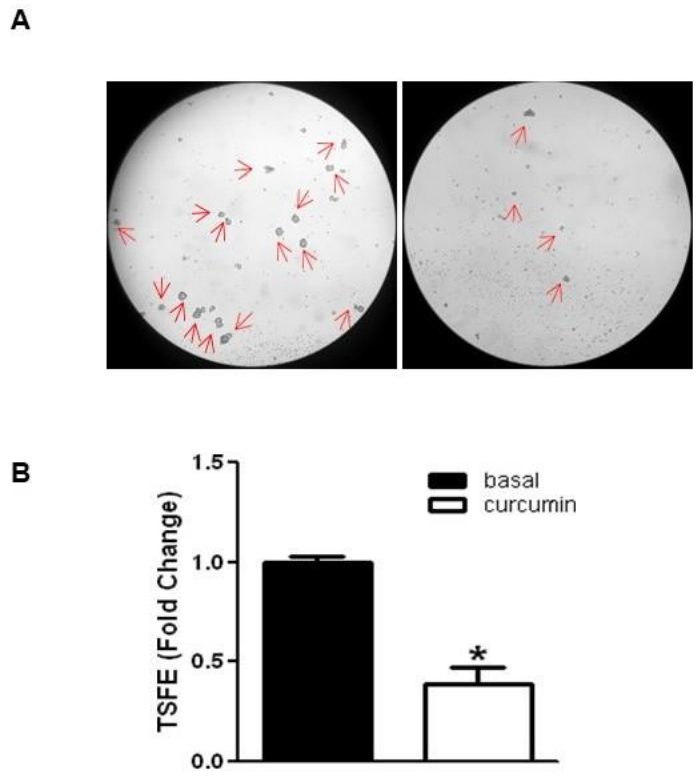

Figure 6.23 Effect of curcumin treatment on the formation of spheroids in H295R cells. H295R cells were seeded at low density (5000 cells / mL) in six-well multiwells, then treated with 40μM of curcumin. After 5 days the spheroids> 50 microns formed were observed under the optical microscope to one degree (200x) photographed **(A)** and counted. **B)** The tumor spheroid formation efficiency (TSFE) is expressed as the fold change of the treated cells compared to the untreated ones (control). The graph is representative of two independent experiments with similar results. * P <0.05 compared with basal (basal).

6.9 Metabolic effects of Curcumin in H295R

We determined the effects of curcumin on mitochondrial respiration (OXPHOS) in H295R cells by using the seahorse 96XF Extracellular Flux Analyzer. Specifically, cells were treated with vehicle or curcumin (5 and 10 μM) for 16 hours and the oxygen consumption rate (OCR) was evaluated after a sequential inhibition of the main mitochondrial energy flows. As shown in **Figure 6.24**, curcumin treatment reduced the intact cell OCR, indicating a dose-dependent reduction of OXPHOS in H295R cells. Furthermore, we assessed specific mitochondrial functions, in particular, Spare capacity **[Figure 6.24E].** Curcumin significantly reduced basal respiration **[Figure 6.24B]** which represents the basal mitochondrial OXPHOS activity. Furthermore, in the presence of FCCP, the uncoupler agent, OCR was dramatically increased, while this change was

blocked by ETC inhibitors, rotenone and antimycin A, inhibiting electron transfer through complex I and complex III. As well, curcumin markedly reduced maximal respiration **[Figure 6.24C]** in a dose dependent manner. Integrated mitochondrial electron transfer chain, which drives the H+ pump, powers ATP Synthase to catalyze generation of ATP. In H295R cells, we found that curcumin dose-dependently reduced ATP production **[Figure 6.24D]** while all doses of curcumin significantly reduced the Spare capacity **[Figure 6.24E]** and increased Proton leak respiration **[Figure 6.24F].** These data clearly indicated that curcumin suppressed mitochondrial respiration, resulting in reduced ATP supplement.

A

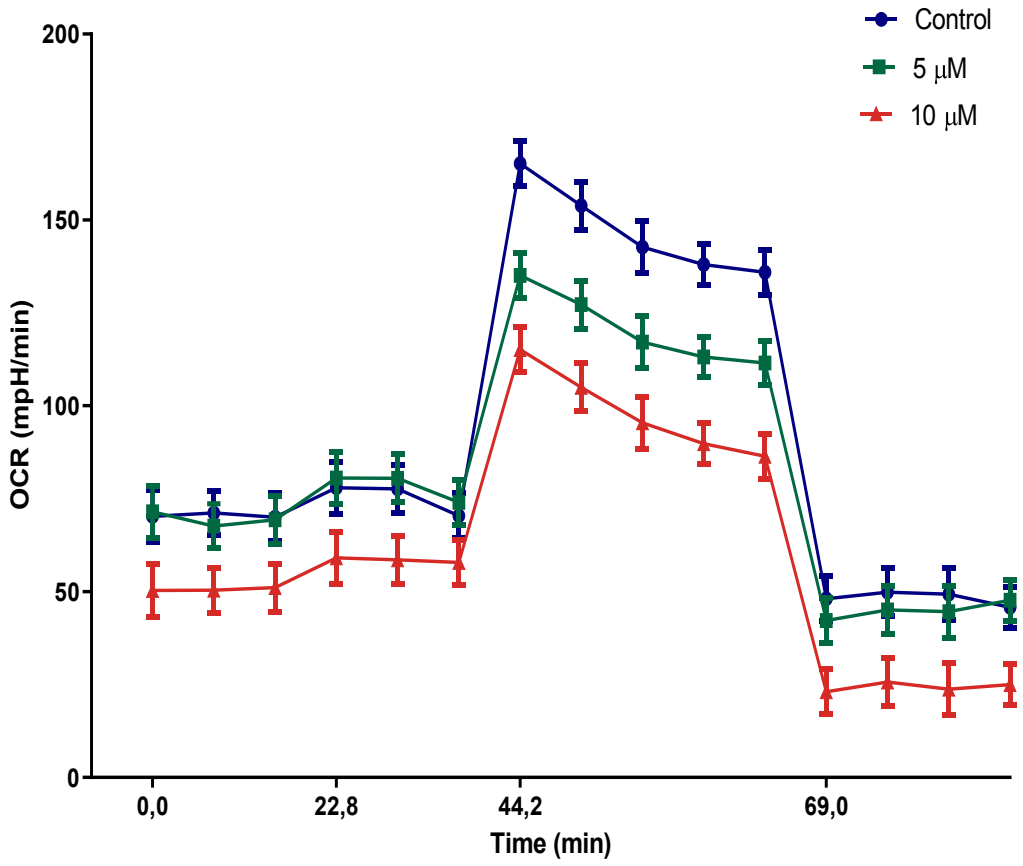

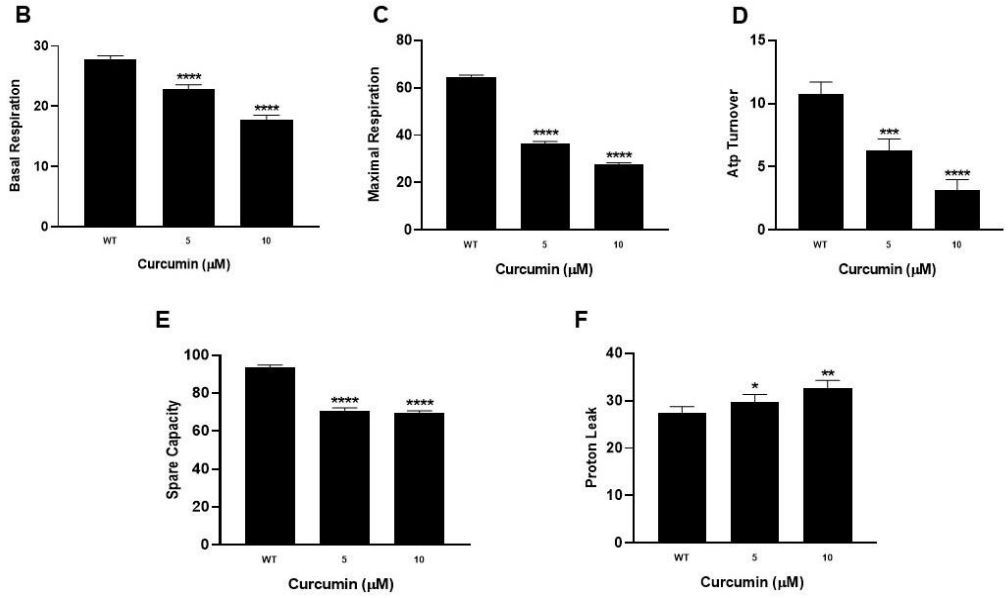

Figure 6.24 Curcumin reduces the oxidative metabolism of H295R cells. Monolayer grown H295R cells were treated with curcumin (5 and 10 μM) for 16 hours. Real-time oxygen consumption (OCR) rates were assessed using the Seahorse XF96. **A-** The line graph shows the same time course, but with three different injections to assess the rate of oxygen consumption: 1-before oligomycin injection, 2- after carbonyl cyanide injection- (trifuoromethoxy) phenylhydrazone (FCCP), 3- after the injection of rotenone \ antimycin. **B-** Basal respiration. **C-** Maximal respiration. **D-** ATP turnover. **E-** Spare capacity. **F-** Proton leak.

6.10 Effects on the rate of extracellular acidification induced by treatment with curcumin

The effects induced by curcumin treatment on glycolytic functions of H295R cells were evaluated by measuring the extracellular acidification rate (ECAR) from the generation of protons during conversion of glucose to lactate in glycolysis. ECAR was measured sequentially at basal level, with glucose and in the presence of ATP synthase inhibitor (Oligomycin) and glycolysis inhibitor (2DG) with XF96 Seahorse extracellular flux analyzer and Glycolysis Stress Assay. Specifically, ECAR was evaluated in intact cells incubated with vehicle or curcumin (5 and 10 μM) for 16 hours. Results clearly indicated a dose-dependent effect of curcumin on ECAR **[Figure 6.25A].** To further understand the role of curcumin in regulating aerobic glycolysis, we analyzed changes related to glycolytic capacity **[Figure 6.25B]** and glycolytic reserve **[Figure 6.25C]** that

were both negatively affected by the treatments.

Taken together, our findings suggest that curcumin is able to interfere with cellular bioenergetics.

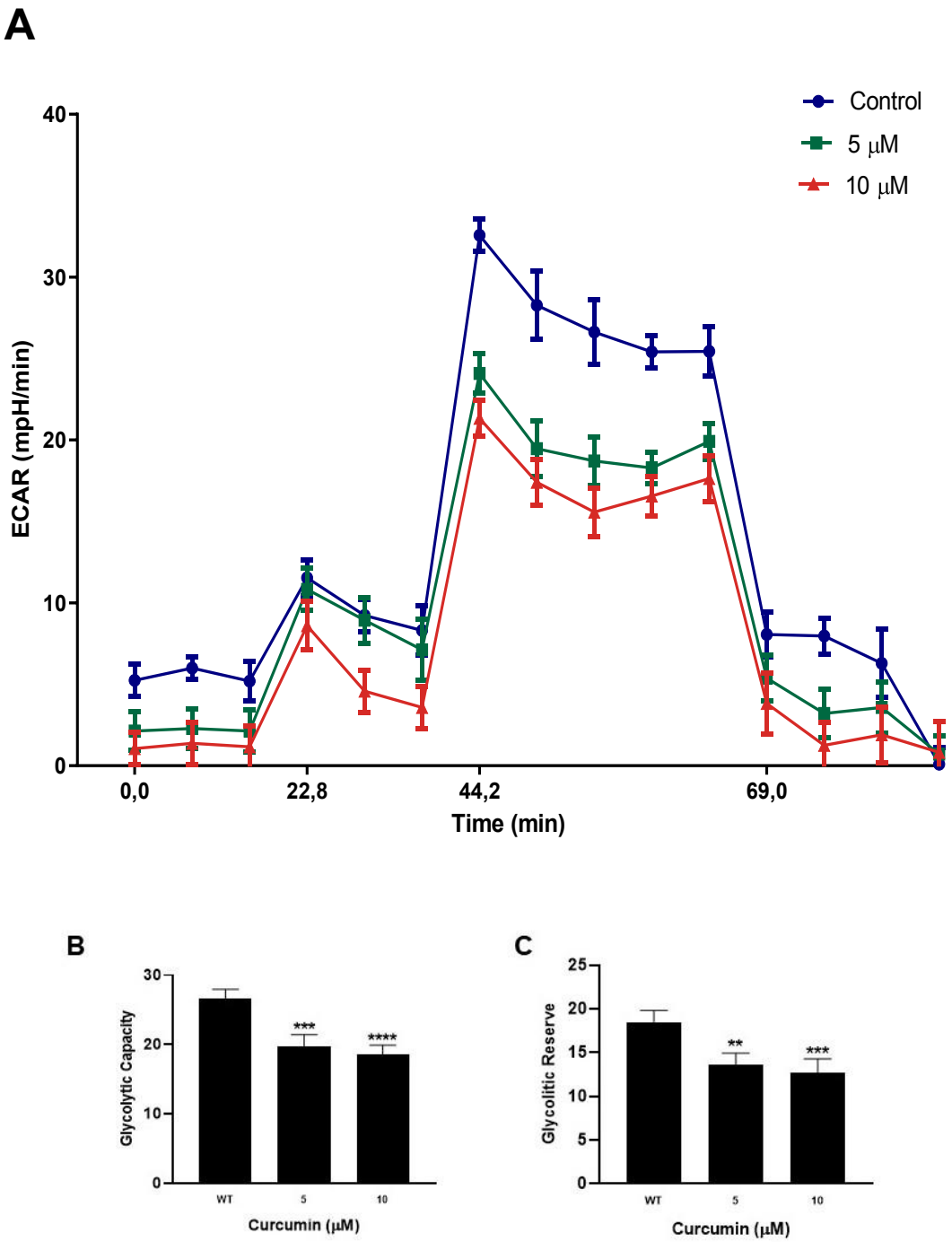

Figure 6.25 Curcumin reduces the glycolytic metabolism of H295R cells. Monolayer grown H295R cells were treated with curcumin (5 and 10 μM) for 16 hours. Real-time extracellular acidification (ECAR) rates were evaluated by Seahorse XF96. **A-** The linear graph shows the same time course, but

with three different injections to assess the extracellular acidification rate: 1-before glucose injection, 2-after carbonyl oligomycin injection, 3-after 2-deoxy injection -D-glucose. **B-** Glycolytic capacity. **C-** Glycolytic reserve.

The results presented so far highlight the efficacy of curcumin treatment which is able to decrease the viability of H295R adrenocortical carcinoma cells in a time and dose dependent manner and through the modulation of ERRα expression exhibits antiproliferative and pro-apoptotic effects. Furthermore, the assay for obtaining cultures of 3D spheroids confirmed that curcumin is also able to modulate the motility of H295R cells and therefore to reduce their metastatic capacity. However, although the beneficial effects of curcumin are known, it has not yet been approved as a therapeutic agent due to its low bioavailability. Therefore, in order to improve the pharmacokinetic profile of curcumin and cellular absorption, in collaboration with Chemistry and Pharmaceutical Technologies Laboratory of the University of Calabria, we have produced curcumin SLNs (SLN-CUR) and we tested its effectiveness on cell proliferation.

We treated H295R cells with the same doses of curcumin and curcumin SLN for different times (24, 48 and 72 h).

As shown in **Figure 6.26**, treatment with SLNs-CUR has a greater dose-dependent response on cell proliferation compared to talqual curcumin **[Figure 6.26A],** with a high significance already at the dose of 10μM at 24h, up to an inhibition > 75% in the 72h of treatment. Furthermore, the cells were also treated with the SLN vehicle at the same doses and for 72h, to demonstrate that it has no toxic effect when administered alone **[Figure 6.26C].**

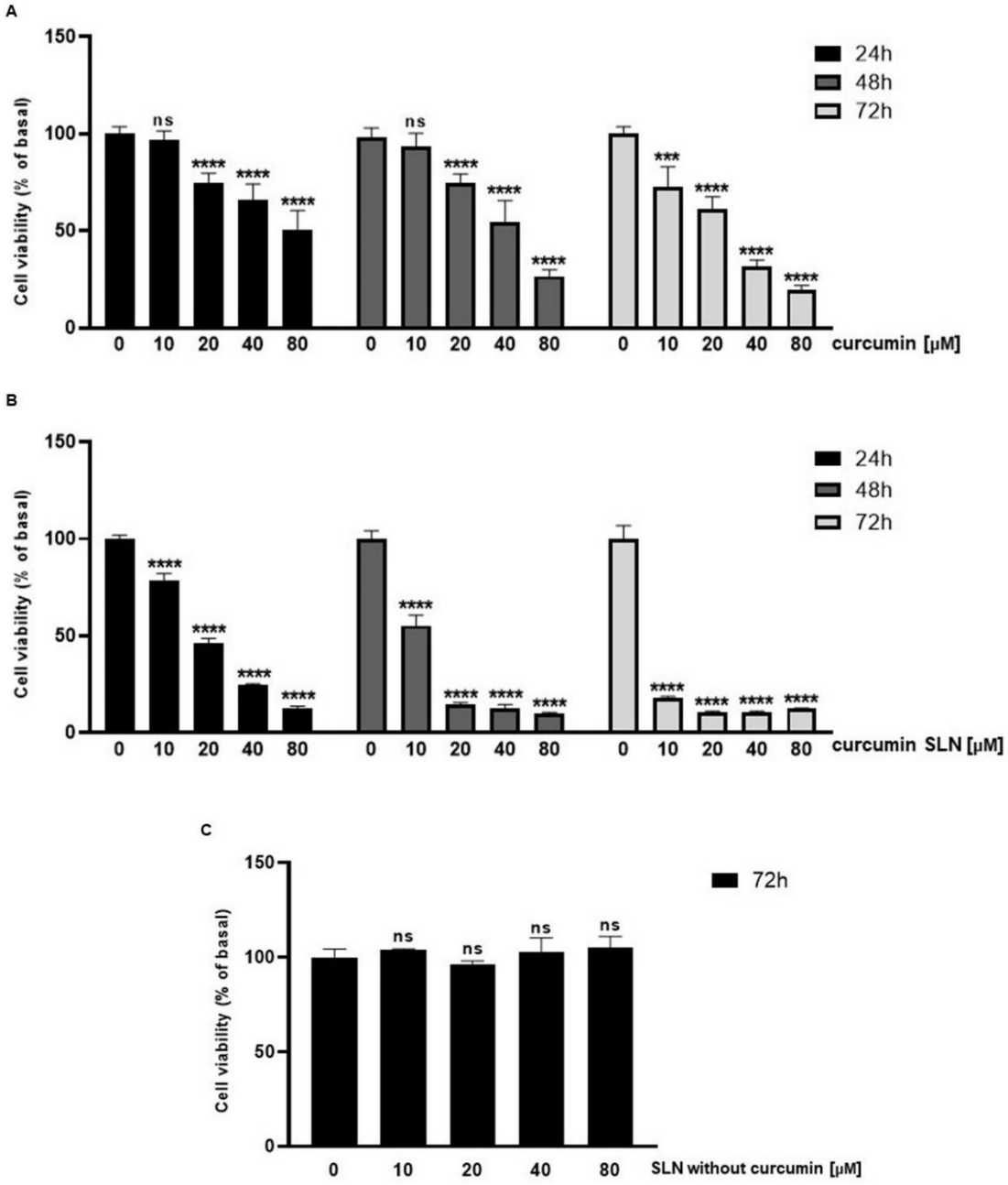

Figure 6.26 Effects of SLNs curcumin on the viability of H295R cells. The cells were maintained for 48h in complete medium and were subsequently untreated (basal) or treated for 24, 48, 72 with increasing doses of talqual curcumin **(A)** and SLNs curcumin **(B)** (10, 20, 40, 80 μM). The cells were also treated with the SLN vehicle at the same doses and for 72h **(C).** Proliferation was evaluated by MTT assay as indicated in the chapter of Materials and Methods. The results are expressed as the mean ± SD of three independent experiments each performed in triplicate (*, P <0.05 compared with the control (0)).

Discussion

7. Discussion

The biology of adrenocortical cancer is characterized by an extremely complex molecular heterogeneity and limited therapeutic options [Else T. et al., 2014; De Martino M.C. et al., 2013]. Genomics studies on ACC confirmed the presence of a large number of molecular events together with common feature including mutation of TP53, β-catenin gene overexpression, IGFII/IGFIR/PI3K/AKT/mTOR cascade activation [Pollak M., 2008]. These observations together with negative results coming from monotheraphy targeting these pathways in ACC patients, confirm that ACC pathogenesis is a multi-molecular event. Genetic modifications and molecular pathways alterations have as a common purpose the survival and proliferation of the transformed phenotype. It is currently accepted that these changes are associated with a concurrent adaptation and reprogramming of cellular metabolism [Cantor J.R. & Sabatini D.M., 2012]. ERRα is a common downstream target of multiple pathways and a key factor in controlling the expression and activity of various bioenergetics processes. Previous study from our laboratory [Casaburi I. et al., 2015] demonstrated that ERRα protein depletion by its inverse agonist, XCT790, caused in ACC cells a reduction of mitochondrial mass and function leading to cell death. Accordingly, *in vivo* experiments by using H295R cells as xenograft model confirmed that pharmacological inhibition of ERRα strongly inhibited ACC cell growth without exerting any toxic effects. These results are in agreement with previous *in vivo* studies performed in breast [Chisamore M.J. et al., 2009], endometrial [Kokabu T. et al., 2019] and leukemia [Michalek R.D. et al., 2011] tumor cells suggesting that ERRα depletion may be a treatment specific for high energy demanding cells such as tumor cells.

In the current study, we focused our interest on the role of ERRα on metabolic changes that occurs in differenht ACC cell lines. We also investigated if cellular changes induced by overexpression or depletion of ERRα are able to support or modulate ACC progression.

In the first part of the study, we performed a proteomic analysis to delineate the differential expression between untreated and XCT790-treated H295R cells. The inverse agonist of ERRα was able to significant changes for a large amount of proteins. In particular, Gene Ontology (GO) function and Kyoto Encyclopedia of Genes and Genomes (KEGG 2021) pathway enrichment analyses identified overrepresented GO terms, the

majority of which are composed of genes involved in cell metabolism (*Glycolysis/Gluconeogenesis, Pentose phosphate pathway, Oxidative phosphorylation, Pyruvate metabolism, Fatty acid elongation and degradation, Protein processing in endoplasmic reticulum,*" along with others) and downregulated by XCT790. By contrast, genes upregulated by the treatment belong to pathways involved in the *cell cycle*, *apoptosis* and *protein degradation*. Similar results were observed in studies conducted on breast cancers [De Luca A. et al., 2015]. According to the metabolic role of ERRα, several of these genes have been shown to be physiologically relevant ERRα targets [Deblois G. et al., 2009] and involved in tumor biology as documented by the active research in this field [Song C.S. & Chatterjee B., 2021; Zhong Y. et al., 2021; Manna S. et al., 2016; Park S. et al., 2019].

The data obtained with the proteomic analysis were implemented through the functional study on ACC cellular metabolism using the Seahorse XF analyser, which allows the real-time analysis of glycolytic and mitochondrial flows. We selected stable clones overexpressing (ERR+/+) or with a silenced (shERR-/-) ESRRA gene expression in H295R cells in order to dissect the impact of ERRα in ACC metabolism. As expected, H295R overexpressing ERRα cells displayed higher ATP content compare to ERR-/- and shcontrol cells. Specifically, ERR+/+ cells are characterized by an oxidative profile while the glycolytic rate is enhanced in ERR-/- cells. Since ERRα target genes belong to both glycolytic and mitochondrial pathways, the ability of ERR-/- cells to compensate for a reduced mitochondrial function by increasing the glycolytic contribution to ATP generation, implies the involvement of different factors and/or alternative activated pathways. Indeed, the glycolytic assay test revealed that although the glycolytic capacity increased both in ERR-/- and ERR+/+ cells, the glycolytic reserve increased in ERR-/- while is reduced in ERR+/+ cells. This last observation suggest that while alternative metabolic pathways are activated in response to ERRα depletion, the ERRα overexpression considerably increases oxidative metabolic pathway together with a greater mitochondrial coupling efficiency (data not shown) to the expense of reserve capacity. Accordingly, the seahorse analysis suggested that ERRα overexpression gives to H295R cells a better mitochondrial fitness while ERR-/- cells have a reduced basal and maximal respiration rates as well as the spare capacity. Moreover, given the role of ERRα as a master regulator of cell metabolism mainly associated with mitochondria [Audet-

Walsh É. & Giguére V., 2015], it is not surprising to have a significant increase in the proton leak parameter as indicative of defective mitochondria in these cells.

We next investigated the effects of reduced ERRα expression on the bioenergetic functions of three ACC cells by using XCT790. Results from the ATP assay show that XCT790 lowered ATP levels in mitotane sensible H295R and SW13 cells, while was ineffective in mitotane-resistant MUC1 cells. Indeed, the analysis of the energetic contribution of mitochondria and glycolysis reveals an extreme metabolic plasticity in MUC1 cells and H295R compared to SW13 cells, which appear to exhibit a glycolytic phenotype. The evaluation of mitochondrial functions revealed the ability of XCT790 to negatively affect the maximal respiration rate in all three-cell lines. In addition, spare respiratory capacity was dose-dependently impaired in all cell models, indicating an affective ability of the cells to cope with sudden increased need for ATP. The mitochondrial spare capacity is as an important aspect of the mitochondrial function. When cells are subjected to stress, energy demand increases, with more ATP required maintaining cellular functions. A cell with a larger spare respiratory capacity can produce more ATP and overcome more stress, which indicates that this is an estimative of the cell's ability to cope with large increases in ATP turnover. Consequently, exposure to XCT790 can adversely affect the ability of cells to cope with other stresses. This observation pave the rode for further studies on the potential additive effects of combined therapies in drug-resistant ACC phenotype. Indeed, in our cell models the increased glycolytic activity, that is more efficient in MUC1 cells compared to the other two cell lines, seems to be the manly adaptive metabolic stress response under XCT790 treatments.

It is well known that metabolic alterations in cancer cells are not exclusively associated with survival and proliferation phenomena but also affect cell motility, a process with a high energy need and a new field of intense investigations [Bergers G. & Fendt S.M., 2021]. In addition, although many highly migratory and metastatic tumor cells are metabolically associated with the glycolytic phenotype, the contribution of the mitochondria becomes significant in many others [Zanotelli M.R. et al., 2021].

ERRα, has an enormous impact on tumor progression since as transcriptional factor drives the expression of many gene involved in invasion, angiogenesis and metastasis in several tumors [Casaburi I. et al., 2018]. Accordingly, the absence of ERRα is able to impair tumorigenic potential in aggressive xenografted breast cancer cells and ERRα/PGC-1α

complex binds to the promoter of VEGF regulating its expression, promoting tumor angiogenesis and invasion. ERRα knockdown attenuated the migration and invasion in endometrial cancer cells [Sladek R. et al., 1997], gastric cancer [Zhong Y. et al., 2021], non-small cell lung cancers [Mukherjee T.K. et al., 2021] and bladder cancer [Ye X. et al., 2019].

It is therefore evident that ERRα plays a dual role, as an important metabolic adaptive regulator and as a transcriptional modulator of genes involved in different energy-intensive process promoting tumor progression such as EMT. Accordingly, in ovarian cancer cell lines, the active constituent of cordyceps, cordycepin, downregulated ERRa and mitochondrial activity avoiding EMT and migration [Liu G. et al., 2018].

Our data revealed clearly a direct influence of ERRa expression on H295R motility. ERRα overexpression significantly increased H295R cell migration and EMT marker vimentin while downregulation of the metabolic receptor, by either genetic ablation or with pharmacological approaches showed a reduction of both cell motility and vimentin expression.

Other important data coming from our study is the impact of ERRα on the ability of H295R cells to grow in non-adherent conditions as 3D-spheroids, a feature of tumor aggressiveness that characterizes tumor-initiating stem-like cells (TICs). TICS are a small sub-population of tumor cells that are resistant to most anti-cancer therapies and share many features with stem cells [De Luca A. et al., 2015]. Interestingly, long serial 3D-spheroid culture ($H295R^{Sph-5}$) obtained after 5 weeks showed enhanced motility and vimentin expression compared to H295R cells grown in adherent condition. Further studies are underway to define which metabolic changes are associated with this more aggressive phenotype. In this setting, XCT790 was able to reduce 3D-spheroids formation and motility not only in SW13 cells but also, and above all, in mitotane-resistant MUC-1cells suggesting, once again, that targeting ERRα could be an effective chemotherapy to consider for the treatment of mitotane-resistant ACC phenotype.

ERRs have been considered as orphan receptors since no endogenous ligands have been found for a long-time. New recent findings reported cholesterol as a new endogenous ligand of ERRα [Casaburi I. et al., 2018], able to (i) promote the recruitment of PGC-1s to ERRα, (ii) increase ERRα gene expression and protein content (autoregulatory positive loop), (iii) increase the transcriptional activity of the ERRα/PGC1α complex on target genes [Wei W. et al., 2016; Ghanbari F. et al., 2020]. In this new setting, cholesterol as a

modulator of the metabolic gatekeeper complex, becomes relevant in high cholesterol demanding tissue, such as the adrenal gland.

Our experiments confirm the role of cholesterol as an activator of ERRα inducing cell motility in ACC cells. In fact, motility assays performed with lipoprotein-deprived serum, thus without cholesterol, were negatively affected in H295R cells. In addition, the absence of cholesterol slightly reduced the ERRα and vimentin gene expression suggesting the involvement of different cofactors to be explored with further studies.

In this study, we also wondered if, in addition to cholesterol, there were other natural molecules able to modulate the expression and activity of ERRα. Our research focused on a natural product derived from plant, curcumin. Indeed, natural compounds garner considerable attention from the scientific community mainly due to their ability to check and prevent the onset and progress of cancer. They are primarily used due to their nontoxic nature and the fewer side effects they cause compared to chemotherapeutic drugs. Furthermore, such natural products perform even better when given as an adjuvant along with traditional chemotherapeutic drugs, thereby enhancing the potential of chemotherapeutics and simultaneously reducing their undesired side effects. Curcumin, a naturally occurring polyphenol compound found in the plant Curcuma longa, is used as an Indian spice. It regulates not only the various pathways of the immune system, cell cycle checkpoints, apoptosis, and antioxidant response but also numerous intracellular targets, including pathways and protein molecules controlling tumor progression. In a recent preclinical study, it was demonstrated that curcumin was able to reduce cancer cell growth and induce cell death by apoptosis in osteosarcoma cells. The authors proved that inhibitory effects were associated with a significant reduction of ERRα expression [Chen P. et al., 2017]. Similarly, our results clearly showed that curcumin, while reducing the expression of ERRα, exerted a time- and dose-dependent inhibitory effect on H295R cell growth by inducing the activation of apoptotic events. It is known that cell proliferation is controlled by the cell cycle, which in turn is governed by the activation of the cyclin / CDK protein complexes (cyclin dependent kinases) whose formation is necessary for normal progression through the various phases of the cycle (John PC , et al., 2001). A dysregulated cell cycle due to overexpression of cyclins and CDKs or to inactivation of the tumor suppressor p53 or the CDK inhibitor p21waf1 / cip1 (p21) is a characteristic of tumor cells (Hartwell, L. H, and. Kastan M . B, 1994). Any agent that negatively regulates the expression of cyclins or CDKs will cause a cell cycle arrest that can occur both in the

G1 / S or G2 / M phase, an irreversible event that will eventually lead to cell apoptosis. In this thesis we have highlighted how curcumin treatment down-regulates cyclin D1 and cyclin E both at the mRNA and protein level in parallel with a decrease in the protein expression of cyclin-dependent kinases type 4 (CDK4) and type 2 (CDK2), suggesting that these cells do not exceed the check point of the G1 / S phase, thus determining a block at this level, responsible for the initiation of the apoptotic process.

It is now clear how apoptosis can occur both through an extrinsic (Kim R, et al., 2006) and intrinsic (Fadeel B and Orrenius S, 2005) mechanism. In the latter, the Bcl-2 family of proteins plays a central role (Cory S and Adams J M., 2002) comprising both pro-apoptotic proteins such as Bax, Bad, Bak, Bid and antiapoptotic Bcl-2, Bcl-xL which modulate the executing phase of the cellular death pathway.

During the apoptotic process, DNA fragmentation and the cleavage/activation of caspases occur (Thorburn A, 2004), specific proteases responsible in turn for the cleavage of a set of proteins including PARP-1 (poly- (ADP) ribose polymerase), an enzyme involved in the DNA repair process and in maintaining genomic stability (Wilson MR, 1998). In this thesis, H295R cells, following treatment with curcumin, responded with a reduction in Bcl-xL gene and protein levels, with an inactivation/cleavage of the PARP-1 protein and with DNA damage as confirmed by the assay COMET and the assay TUNEL.

Furthermore, the assay for obtaining cultures of 3D spheroids confirmed how curcumin could modulate the ability of H295R cells to expand, i.e. to reduce their ability to metastasize, an attitude closely related to the epithelial-mesenchymal transition (EMT) in which epithelial cells acquire the characteristics of non-polarized and migrating mesenchymal cells (Onder TT, et al., 2008). Recently, an involvement of ERRα has been demonstrated in this process, considered at the basis of the development and evolution of tumors (Chen Y, et al., 2017).

Furthermore, according to the metabolic role of ERRα, the use of curcumin induced significant changes to the bioenergetics profile of H295R cells. Specifically, OCR and ECAR values and the energetic parameters derived from Seahorse data analysis and associated with mitochondrial and glycolytic functions, were all reduced by curcumin in a dose dependent manner. In particular, according to the above described apoptotic effects induced by the flavonoid, we observed an increase in the proton leak values as consequence of the collapse of mitochondrial potential that is a feature of intrinsic

apoptotic mechanism activated by curcumin in several cancer models [Yu C. et al., 2021]. This death mechanism is most likely responsible for curcumin's inhibitory effects on the growth and formation of spheroids, an experimental model representing a more aggressive tumor phenotype than adhesion-growing cells.

Despite the observed effects in ACC cells, together with the enormous amount of data in the literature, highlighting the efficient antitumor activity of this flavonoid, it is known that the limitation of the therapeutic use of curcumin is mainly due to its poor bioavailability. Therefore, in order to improve the pharmacokinetic profile and cellular absorption of curcumin, in collaboration with Chemistry and Pharmaceutical Technologies Laboratory (University of Calabria), we produced curcumin SLNs and we found a greater dose-dependent inhibitory effects on H295R cell proliferation compared to unmodified curcumin.

Treatment with SLNs-CUR has a greater dose-dependent response on cell proliferation compared to tal qual curcumin, with a high significance already at the dose of 10μM at 24h, up to an inhibition> 75% in the 72h of treatment. Cells were also treated with the SLN vehicle at the same doses and for 72h, to demonstrate that it has no toxic effect when administered alone.

In conclusion, in this thesis it has been shown that ERRα is a key regulator factor modulating metabolic profile and consequently motility of ACC cells. It has be also evidenced that the inhibition of this receptor, by synthetic or natural molecules, can strongly block not only the growth of mitotane-resistant ACC cells, but also the processes of transition of ACC cells to more aggressive and invasive phenotype. For this reason, ERRα can be considered a new important target to take in consideration in design new therapeutic strategy to fight the Adrenocortical cancer progression.

References

8. REFERENCES

- **Abraham J.,** Bakke S, Rutt A, Meadows B, Merino M, Alexander R, Schrump D, Bartlett D, Choyke P, Robey R et al. 2002. A phase II trial of combination chemotherapy and surgical resection for the treatment of metastatic adrenocortical carcinoma: continuous infusion doxorubicin, vincristine, and etoposide with daily mitotane as a P-glycoprotein antagonist. Cancer 94(9): 2333-2343.
- **Adam P.,** Hahner S, Hartmann M, Heinrich B, Quinkler M, Willenberg HS, Saeger W, Sbiera S, Schmull S, Voelker HU et al. 2010. Epidermal growth factor receptor in adrenocortical tumors: analysis of gene sequence, protein expression and correlation with clinical outcome. Modern pathology : an official journal of the United States and Canadian Academy of Pathology, Inc 23(12): 1596-1604.
- **Adams B.K**., Cai J., Armstrong J., Herold M.; Lu Y.J.; Sun A.; Snyder J.P.; Liotta D.C.; Jones D.P.; Shoji M. EF24, a novel synthetic curcumin analog, induces apoptosis in cancer cells via a redox-dependent mechanism. Anti-Cancer Drugs 2005, 16, 263–275.
- **Aggarwal B.**, Kumar A, Aggarwal M, Shishodia S. Curcumin derived from turmeric (Curcuma longa): a spice for all seasons. In: Bagchi D, Preuss H, eds. Phytopharmaceuticals in Cancer Chemoprevention. Boca Raton, Fla: CRC Press; 349- 387, 2005.
- **Aggarwal B.B., & Harikumar, K.B.** (2009). Potential therapeutic effects of curcumin, the anti-inflammatory agent, against neurodegenerative, cardiovascular, pulmonary, metabolic, autoimmune and neoplastic diseases. The international journal of biochemistry & cell biology, 41(1), 40-59.
- **Aggarwal B.B.,** Banerjee, S.; Bharadwaj, U.; Sung, B.; Shishodia, S.; Sethi, G. Curcumin induces the degradation of cyclin E expression through ubiquitin-dependent pathway and up-regulates cyclin-dependent kinase inhibitors p21 and p27 in multiple human tumor cell lines. Biochem. Pharmacol. 2007, 73, 1024–1032
- **Allolio B., Fassnacht M.** 2006. Clinical review: Adrenocortical carcinoma: clinical update. The Journal of clinical endocrinology and metabolism 91(6): 2027-2037.

- **Anand P.,** Sundaram C, Jhurani S, Kunnumakkara AB, Aggarwal BB. 2008. Curcumin and cancer: An "old-age" disease with an "age-old" solution. Cancer Lett 267: 133– 164.
- **Anand P.,** Thomas, S.G.; Kunnumakkara, A.B.; Sundaram, C.; Harikumar, K.B.; Sung, B.; Tharakan, S.T.; Misra, K.; Priyadarsini, I.K.; Rajasekharan, K.N.; et al. Biological activities of curcumin and its analogues (Congeners) made by man and Mother Nature. Biochem. Pharmacol. 2008, 76, 1590–1611.
- **Ao A.,** Wang H, Kamarajugadda S, Lu J. 2008. Involvement of estrogen-related receptors in transcriptional response to hypoxia and growth of solid tumors. Proceedings of the National Academy of Sciences of the United States of America 105(22): 7821-7826.
- **Apak T.I., Duffel M.W.** 2004. Interactions of the stereoisomers of alpha-hydroxytamoxifen with human hydroxysteroid sulfotransferase SULT2A1 and rat hydroxysteroid sulfotransferase STa. Drug metabolism and disposition: the biological fate of chemicals 32(12): 1501-1508.
- **Arany Z.,** Foo SY, Ma Y, Ruas JL, Bommi-Reddy A, Girnun G, Cooper M, Laznik D, Chinsomboon J, Rangwala SM et al. 2008. HIF-independent regulation of VEGF and angiogenesis by the transcriptional coactivator PGC-1alpha. Nature 451(7181): 1008-1012.
- **Aravindan S.,** Natarajan, M.; Awasthi, V.; Herman, T.S.; Aravindan, N. Novel synthetic monoketone transmute radiation-triggered NFkappaB-dependent TNFalpha cross-signaling feedback maintained NFkappaB and favors neuroblastoma regression. PLoS ONE 2013, 8, e72464.
- **Aravindan S.,** Natarajan, M.; Herman, T.S.; Awasthi, V.; Aravindan, N. Molecular basis of 'hypoxic' breast cancer cell radio-sensitization: Phytochemicals converge on radiation induced Rel signaling. Radiat. Oncol 2013, 8, 46.
- **Ariazi E.A.,** Clark G.M, Mertz J.E. 2002. Estrogen-related receptor alpha and estrogen-related receptor gamma associate with unfavorable and favorable biomarkers, respectively, in human breast cancer. Cancer research 62(22): 6510-6518.

- **Ariazi E.A.,** Kraus R.J, Farrell M.L, Jordan V.C, Mertz J.E. 2007. Estrogen-related receptor alpha1 transcriptional activities are regulated in part via the ErbB2/HER2 signaling pathway. Molecular cancer research : MCR 5(1): 71-85.
- **Arlt W.,** Biehl M, Taylor AE, Hahner S, Libe R, Hughes BA, Schneider P, Smith DJ, Stiekema H, Krone N et al. 2011. Urine steroid metabolomics as a biomarker tool for detecting malignancy in adrenal tumors. The Journal of clinical endocrinology and metabolism 96(12): 3775-3784.
- **Aron D.,** Terzolo M, Cawood TJ. 2012. Adrenal incidentalomas. Best practice & research Clinical endocrinology & metabolism 26(1): 69-82.
- **Assie G.,** Guillaud-Bataille M, Ragazzon B, Bertagna X, Bertherat J, Clauser E. 2010. The pathophysiology, diagnosis and prognosis of adrenocortical tumors revisited by transcriptome analyses. Trends in endocrinology and metabolism: TEM 21(5): 325-334.
- **Assie G.,** Jouinot A, Bertherat J. 2014a. The 'omics' of adrenocortical tumours for personalized medicine. Nature reviews Endocrinology 10(4): 215-228.
- **Assie G.,** Letouze E, Fassnacht M, Jouinot A, Luscap W, Barreau O, Omeiri H, Rodriguez S, Perlemoine K, Rene-Corail F et al. 2014b. Integrated genomic characterization of adrenocortical carcinoma. Nature genetics 46(6): 607-612
- **Audet-Walsh É., & Giguére V.** (2015). The multiple universes of estrogen-related receptor α and γ in metabolic control and related diseases. Acta Pharmacologica Sinica, 36(1), 51-61.
- **Baek J.S.,** Cho, C.W. Surface modification of solid lipid nanoparticles for oral delivery of curcumin: Improvement of bioavailability through enhanced cellular uptake, and lymphatic uptake. Eur. J. Pharm. Biopharm. 2017, 117, 132–140.
- **Ban C.,** Jo, M.; Park, Y.H.; Kim, J.H.; Han, J.Y.; Lee, K.W.; Kweon, D.H.; Choi, Y.J. Enhancing the oral bioavailability of curcumin using solid lipid nanoparticles. Food Chem. 2020, 302, 125328.
- **Bardet P.L.,** Schubert M, Horard B, Holland L.Z, Laudet V, Holland N.D, Vanacker J.M. 2005. Expression of estrogen-receptor related receptors in amphioxus and zebrafish: implications for the evolution of posterior brain segmentation at the invertebrate-to-vertebrate transition. Evolution & development 7(3): 223-233.

- **Barlaskar F.M., Hammer G.D.** 2007. The molecular genetics of adrenocortical carcinoma. Reviews in endocrine & metabolic disorders 8(4): 343-348.
- **Barlaskar F.M.,** Spalding A.C, Heaton J.H, Kuick R, Kim A.C, Thomas D.G, Giordano T.J, Ben-Josef E, Hammer G.D. 2009. Preclinical targeting of the type I insulin-like growth factor receptor in adrenocortical carcinoma. The Journal of clinical endocrinology and metabolism 94(1): 204-212.
- **Barnes P.,** Karin, M. Nuclear factor-kappa B. A pivotal transcription factor in chronic inflammatory diseases. N. Engl. J. Med. 336, 1066-1071,1997.
- **Barry J.B. & Giguere V**. 2005. Epidermal growth factor-induced signaling in breast cancer cells results in selective target gene activation by orphan nuclear receptor estrogen-related receptor alpha. Cancer research 65(14): 6120-6129.
- **Bar-Sela G.,** Epelbaum R, Schaffer M. 2010. Curcumin as an anti-cancer agent: Review of the gap between basic and clinical applications. Curr Med Chem 17: 190– 197.
- **Barzon L.,** Masi G, Pacenti M, Trevisan M, Fallo F, Remo A, Martignoni G, Montanaro D, Pezzi V, Palu G. 2008. Expression of aromatase and estrogen receptors in human adrenocortical tumors. Virchows Archiv : an international journal of pathology 452(2): 181-191.
- **Basile V.,** Ferrari, E.; Lazzari, S.; Belluti, S.; Pignedoli, F.; Imbriano, C. Curcumin derivatives: Molecular basis of their anti-cancer activity. Biochem. Pharmacol. 2009, 78, 1305–1315.
- **Bates S.E.,** Shieh C.Y, Mickley L.A, Dichek H.L, Gazdar A, Loriaux D.L, Fojo A.T. 1991. Mitotane enhances cytotoxicity of chemotherapy in cell lines expressing a multidrug resistance gene (mdr-1/P-glycoprotein) which is also expressed by adrenocortical carcinomas. The Journal of clinical endocrinology and metabolism 73(1): 18-29.
- **Baudin E.,** Pellegriti G, Bonnay M, Penfornis A, Laplanche A, Vassal G, Schlumberger M. 2001. Impact of monitoring plasma 1,1-dichlorodiphenildichloroethane (o,p'DDD) levels on the treatment of patients with adrenocortical carcinoma. Cancer 92(6): 1385-1392.
- **Bayomi S.M.,** El-Kashef, H.A.; El-Ashmawy, M.B.; Nasr, M.N.A.; El-Sherbeny, M.A.; Badria, F.A.; Abou-Zeid, L.A.; Ghaly, M.A.; Abdel-Aziz, N.I. Synthesis

and biological evaluation of new curcumin derivatives as antioxidant and antitumor agents. Med. Chem. Res. 2013, 22, 1147–1162.

- **Bergers G. & Fendt S.M.** (2021). The metabolism of cancer cells during metastasis. Nature Reviews Cancer, 21(3), 162-180.
- **Berruti A.,** Baudin E, Gelderblom H, Haak HR, Porpiglia F, Fassnacht M, Pentheroudakis G, Group EGW. 2012a. Adrenal cancer: ESMO Clinical Practice Guidelines for diagnosis, treatment and follow-up. Annals of oncology : official journal of the European Society
- **Berruti A.,** Sperone P, Ferrero A, Germano A, Ardito A, Priola AM, De Francia S, Volante M, Daffara F, Generali D et al. 2012b. Phase II study of weekly paclitaxel and sorafenib as second/third-line therapy in patients with adrenocortical carcinoma. European journal of endocrinology 166(3): 451-458.
- **Berruti A.,** Terzolo M, Sperone P, Pia A, Della Casa S, Gross DJ, Carnaghi C, Casali P, Porpiglia F, Mantero F et al. 2005. Etoposide, doxorubicin and cisplatin plus mitotane in the treatment of advanced adrenocortical carcinoma: a large prospective phase II trial. Endocrine-related cancer 12(3): 657-666.
- **Berry M.,** Nunez A.M, Chambon P. 1989. Estrogen-responsive element of the human pS2 gene is an imperfectly palindromic sequence. Proceedings of the National Academy of Sciences of the United States of America 86(4): 1218-1222.
- **Betz M.J.,** Shapiro I, Fassnacht M, Hahner S, Reincke M, Beuschlein F, German, Austrian Adrenal N. 2005. Peroxisome proliferator-activated receptor-gamma agonists suppress adrenocortical tumor cell proliferation and induce differentiation. The Journal of clinical endocrinology and metabolism 90(7): 3886-3896.
- **Bharat B.,** Aggarwal B.B, Kuzhuvelil B. Harikumar. Potential therapeutic effects of curcumin, the anti-inflammatory agent, against neurodegenerative, cardiovascular, pulmonary, metabolic, autoimmune and neoplastic disease. The International Journal of Biochemistry & Cell Biology 41, 40-51, 2009.
- **Bhatt H.,** Rompicharla, S.V.K.; Komanduri, N.; Aashma, S.; Paradkar, S.; Ghosh, B.; Biswas, S. Development of curcumin-loaded solid lipid nanoparticles utilizing glyceryl monostearate as single lipid using QbD approach: Characterization and evaluation of anticancer activity against human breast cancer cell line. Curr. Drug Deliv. 2018, 15, 1271–1283.

- **Biswas S.K.** Does the Interdependence between Oxidative Stress and Inflammation Explain the Antioxidant Paradox? Oxid. Med. Cell. Longev. 2016, 5698931, 2016.
- **Blake M.A.,** Kalra M.K, Sweeney A.T, Lucey B.C, Maher M.M, Sahani D.V, Halpern E.F, Mueller P.R, Hahn P.F, Boland G.W. 2006. Distinguishing benign from malignant adrenal masses: multi-detector row CT protocol with 10-minute delay. Radiology 238(2): 578-585.
- **Bonacci R.,** Gigliotti A, Baudin E, Wion-Barbot N, Emy P, Bonnay M, Cailleux AF, Nakib I, Schlumberger M, Reseau C. 1998. Cytotoxic therapy with etoposide and cisplatin in advanced adrenocortical carcinoma. British journal of cancer 78(4): 546-549.
- **Bonnelye E. & Aubin J.E.** 2013. An energetic orphan in an endocrine tissue: a revised perspective of the function of estrogen receptor-related receptor alpha in bone and cartilage. Journal of bone and mineral research : the official journal of the American Society for Bone and Mineral Research 28(2): 225-233.
- **Bonnelye E.,** Vanacker JM, Dittmar T, Begue A, Desbiens X, Denhardt DT, Aubin JE, Laudet V, Fournier B. 1997. The ERR-1 orphan receptor is a transcriptional activator expressed during bone development. Molecular endocrinology 11(7): 905-916.
- **Bourdeau I.,** MacKenzie-Feder J, Lacroix A. 2013. Recent advances in adrenocortical carcinoma in adults. Current opinion in endocrinology, diabetes, and obesity 20(3): 192-197.
- **Brennan M.F.** 1987. Adrenocortical carcinoma. CA: a cancer journal for clinicians 37(6): 348-365.
- **Brzozowski A.M.,** Pike AC, Dauter Z, Hubbard R.E, Bonn T, Engstrom O, Ohman L, Greene G.L, Gustafsson J.A, Carlquist M. 1997. Molecular basis of agonism and antagonism in the oestrogen receptor. Nature 389(6652): 753-758.
- **Bukowski R.M.,** Wolfe M, Levine H.S, Crawford D.E, Stephens R.L, Gaynor E, Harker W.G. 1993. Phase II trial of mitotane and cisplatin in patients with adrenal carcinoma: a Southwest Oncology Group study. Journal of clinical oncology : official journal of the American Society of Clinical Oncology 11(1): 161-165.
- **Busch B.B.,** Stevens W.C, Jr., Martin R, Ordentlich P, Zhou S, Sapp D.W, Horlick R.A, Mohan R. 2004. Identification of a selective inverse agonist for the

orphan nuclear receptor estrogen-related receptor alpha. Journal of medicinal chemistry 47(23): 5593-5596.

- **Butler C.,** Butler W.M, Rizvi A.A. 2010. Sustained remission with the kinase inhibitor sorafenib in stage IV metastatic adrenocortical carcinoma. Endocrine practice : official journal of the American College of Endocrinology and the American Association of Clinical Endocrinologists 16(3): 441-445.
- **Calibasi-Kocal G.,** Pakdemirli, A.; Bayrak, S.; Ozupek, N.M.; Sever, T.; Basbinar, Y.; Ellidokuz, H.; Yigitbasi, T. Curcumin effects on cell proliferation, angiogenesis and metastasis in colorectal cancer. J. BUON Off. J. Balk. Union Oncol. 2019, 24, 1482–1487.
- **Cantor J.R. & Sabatini D.M**. (2012). Cancer cell metabolism: one hallmark, many faces. Cancer discovery, 2(10), 881-898.
- **Carroll R.E.,** Benya, R.V.; Turgeon, D.K.; Vareed, S.; Neuman, M.; Rodriguez, L.; Kakarala, M.; Carpenter, P.M.; McLaren, Meyskens, F.L., Jr.; et al. Phase IIa clinical trial of curcumin for the prevention of colorectal neoplasia. Cancer Prev. Res. 2011, 4, 354–364.
- **Casaburi I.,** Avena P, De Luca A et al. Estrogen related receptor alpha (ERRαlpha) a promising target for the therapy of adrenocortical carcinoma (ACC). Oncotarget. 25135- 48, 2015.
- **Casaburi I.,** Chimento A, De Luca A, Nocito M, Sculco S, Avena P, Trotta F, Rago V, Sirianni R, Pezzi V. 2018. Cholesterol as an Endogenous ERRα Agonist: A New Perspective to Cancer Treatment. Frontiers in endocrinology 9: 525.
- **Castet A.,** Herledan A, Bonnet S, Jalaguier S, Vanacker JM, Cavailles V. 2006. Receptor-interacting protein 140 differentially regulates estrogen receptor-related receptor transactivation depending on target genes. Molecular endocrinology 20(5): 1035-1047.
- **Cavallini A.,** Notarnicola M, Giannini R, Montemurro S, Lorusso D, Visconti A, Minervini F, Caruso MG. 2005. Oestrogen receptor-related receptor alpha (ERR[alpha]) and oestrogen receptors (ER[alpha] and ER[beta]) exhibit different gene expression in human colorectal tumour progression. Eur J Cancer 41: 1487–1494.
- **Cazejust J.,** De Baere T, Auperin A, Deschamps F, Hechelhammer L, Abdel-Rehim M, Schlumberger M, Leboulleux S, Baudin E. 2010. Transcatheter arterial

chemoembolization for liver metastases in patients with adrenocortical carcinoma. Journal of vascular and interventional radiology: JVIR 21(10): 1527-1532.

- **Cerquetti L.,** Sampaoli C, Amendola D, Bucci B, Misiti S, Raza G, De Paula U, Marchese R, Brunetti E, Toscano V et al. 2010. Mitotane sensitizes adrenocortical cancer cells to ionizing radiations by involvement of the cyclin B1/CDK complex in G2 arrest and mismatch repair enzymes modulation. International journal of oncology 37(2): 493-501.
- **Chacon R.,** Tossen G, Loria FS, Chacon M. 2005. CASE 2. Response in a patient with metastatic adrenal cortical carcinoma with thalidomide. Journal of clinical oncology : official journal of the American Society of Clinical Oncology 23(7): 1579-1580.
- **Chang C.Y.,** Kazmin D, Jasper J.S, Kunder R, Zuercher W.J, McDonnell D.P. 2011. The metabolic regulator ERRalpha, a downstream target of HER2/IGF-1R, as a therapeutic target in breast cancer. Cancer cell 20(4): 500-510.
- **Chase A. & Cross N.C.** Aberrations of EZH2 in cancer. Clin. Cancer Res. 2011, 17, 2613–2618.
- **Chen F.,** Zhang Q, McDonald T, Davidoff MJ, Bailey W, Bai C, Liu Q, Caskey CT. 1999. Identification of two hERR2-related novel nuclear receptors utilizing bioinformatics and inverse PCR. Gene 228(1-2): 101-109.
- **Chen Y.,** Zhang K, Li Y, He Q. Estrogen-related receptor α participates transforming growth factor-β (TGF-β) induced epithelial-mesenchymal transition of osteosarcoma cells. Cell Adh Migr. 11(4):338-346, 2017.
- **Chen P.,** Wang, H., Yang, F., Chen, H., He, W., & Wang, J. (2017). Curcumin promotes osteosarcoma cell death by activating miR- 125a/ERRα signal pathway. Journal of cellular biochemistry, 118(1), 74-81.
- **Cheng A.L.,** Hsu, C.H.; Lin, J.K.; Hsu, M.M.; Ho, Y.F.; Shen, T.S.; Ko, J.Y.; Lin, J.T.; Lin, B.R.; Ming-Shiang, W.; et al. Phase I clinical trial of curcumin, a chemopreventive agent, in patients with high-risk or pre-malignant lesions. Anticancer Res. 2001, 21, 2895–2900.
- **Cheng C.,** Jiao, J.T.; Qian, Y.; Guo, X.Y.; Huang, J.; Dai, M.C.; Zhang, L.; Ding, X.P.; Zong, D.; Shao, J.F. Curcumin induces G2/M arrest and triggers apoptosis

via FoxO1 signaling in U87 human glioma cells. Mol. Med. Rep. 2016, 13, 3763–3770.

- **Cheung C.P.,** Yu S, Wong K.B, Chan L.W, Lai F.M, Wang X, Suetsugi M, Chen S, Chan F.L. 2005. Expression and functional study of estrogen receptor-related receptors in human prostatic cells and tissues. The Journal of clinical endocrinology and metabolism 90(3): 1830-1844.
- **Chiche J.,** Brahimi-Horn M.C, Pouyssegur J. 2010. Tumour hypoxia induces a metabolic shift causing acidosis: a common feature in cancer. Journal of cellular and molecular medicine 14(4): 771-794.
- **Chimento A.,** Sirianni R, Casaburi I, Zolea F, Rizza P, Avena P, Malivindi R, De Luca A, Campana C, Martire E et al. 2015. GPER agonist G-1 decreases adrenocortical carcinoma (ACC) cell growth in vitro and in vivo. Oncotarget 6(22): 19190-19203.
- **Chisamore M.J.,** Cunningham M.E, Flores O, Wilkinson H.A, Chen J.D. 2009a. Characterization of a novel small molecule subtype specific estrogen-related receptor alpha antagonist in MCF-7 breast cancer cells. PloS one 4(5): e5624.
- **Chisamore, M.J.,** Wilkinson, H. A., Flores, O., & Chen, J. D. (2009). Estrogen-related receptor-α antagonist inhibits both estrogen receptor–positive and estrogen receptor–negative breast tumor growth in mouse xenografts. Molecular cancer therapeutics, 8(3), 672-681.
- **Choi B.H.,** Kim, C.G.; Bae, Y.S.; Lim, Y.; Lee, Y.H.; Shin, S.Y. P21(Waf1/Cip1) expression by curcumin in U-87MG human glioma cells: Role of early growth response-1 expression. Cancer Res. 2008, 68, 1369–1377.
- **Chuman Y.,** Zhan Z, Fojo T. 2000. Construction of gene therapy vectors targeting adrenocortical cells: enhancement of activity and specificity with agents modulating the cyclic adenosine 3',5'-monophosphate pathway. The Journal of clinical endocrinology and metabolism 85(1): 253-262.
- **Cianfruglia L.,** Minnelli, C.; Laudadio, E.; Scire, A.; Armeni, T. Side effects of curcumin: Epigenetic and antiproliferative implications for normal dermal fibroblast and breast cancer cells. Antioxidants 2019, 8, 382.
- **Cory S. & Adams J.M.** The Bcl2 family: regulators of the cellular life-or-death switch. Nat Rev Cancer; 2(9):647-56, 2002.

- **Coward P.,** Lee D, Hull MV, Lehmann JM. 2001. 4-Hydroxytamoxifen binds to and deactivates the estrogen-related receptor gamma. Proceedings of the National Academy of Sciences of the United States of America 98(15): 8880-8884.
- **Cowburn R.F.** Receptor-G-protein signalling in Alzheimer's disease. Biochem. Soc. Symp, 67: 163-175, 2001.
- **Creemers S.G.,** Hofland L.J., Korpershoek E, Franssen G.J., van Kemenade F.J., de Herder W.W., Feelders R.A. 2016. Future directions in the diagnosis and medical treatment of adrenocortical carcinoma. Endocrine-related cancer 23(1): R43-69.
- **Crucitti F.,** Bellantone R, Ferrante A, Boscherini M, Crucitti P. 1996. The Italian Registry for Adrenal Cortical Carcinoma: analysis of a multiinstitutional series of 129 patients. The ACC Italian Registry Study Group. Surgery 119(2): 161-170.
- **Danielian P.S.,** White R, Lees J.A., Parker M.G. 1992. Identification of a conserved region required for hormone dependent transcriptional activation by steroid hormone receptors. The EMBO journal 11(3): 1025-1033.
- **Datrice N.M.,** Langan R.C., Ripley R.T., Kemp C.D., Steinberg S.M., Wood B.J., Libutti S.K., Fojo T, Schrump D.S., Avital I. 2012. Operative management for recurrent and metastatic adrenocortical carcinoma. Journal of surgical oncology 105(7): 709-713.
- **Davidson S.M.,** Papagiannakopoulos T, Olenchock B.A, Heyman J.E, Keibler M.A, Luengo A, Bauer M.R, Jha A.K, O'Brien J.P, Pierce K.A et al. 2016. Environment Impacts the Metabolic Dependencies of Ras-Driven Non-Small Cell Lung Cancer. Cell metabolism 23(3): 517-528.
- **de Cremoux P.,** Rosenberg D, Goussard J, Bremont-Weil C, Tissier F, Tran-Perennou C, Groussin L, Bertagna X, Bertherat J, Raffin-Sanson ML. 2008. Expression of progesterone and estradiol receptors in normal adrenal cortex, adrenocortical tumors, and primary pigmented nodular adrenocortical disease. Endocrine-related cancer 15(2): 465-474.
- **De Luca A.,** Fiorillo, M., Peiris-Pagès, M., Ozsvari, B., Smith, D.L., Sanchez-Alvarez, R., ... & Sotgia, F. (2015). Mitochondrial biogenesis is required for the anchorage-independent survival and propagation of stem-like cancer cells. Oncotarget, 6(17), 14777.

- **De Martino M.C.,** van Koetsveld P.M, Pivonello R, Hofland L.J. 2010. Role of the mTOR pathway in normal and tumoral adrenal cells. Neuroendocrinology 92 Suppl 1: 28-34.
- **De Martino, M.C.,** Al Ghuzlan, A., Aubert, S., Assié, G., Scoazec, J. Y., Leboulleux, S., ... & Baudin, E. (2013). Molecular screening for a personalized treatment approach in advanced adrenocortical cancer. The Journal of Clinical Endocrinology & Metabolism, 98(10), 4080-4088.
- **de Oliveira A.T.,** Pinheiro C, Longatto-Filho A, Brito M.J, Martinho O, Matos D, Carvalho A.L, Vazquez V.L, Silva T.B, Scapulatempo C. et al. 2012. Co-expression of monocarboxylate transporter 1 (MCT1) and its chaperone (CD147) is associated with low survival in patients with gastrointestinal stromal tumors (GISTs). Journal of bioenergetics and biomembranes 44(1): 171-178.
- **de Reynies A.,** Assie G, Rickman D.S, Tissier F, Groussin L, Rene-Corail F, Dousset B, Bertagna X, Clauser E, Bertherat J. 2009. Gene expression profiling reveals a new classification of adrenocortical tumors and identifies molecular predictors of malignancy and survival. Journal of clinical oncology : official journal of the American Society of Clinical Oncology 27(7): 1108-1115.
- **Deandreis D.,** Leboulleux S, Caramella C, Schlumberger M, Baudin E. 2011. FDG PET in the management of patients with adrenal masses and adrenocortical carcinoma. Hormones & cancer 2(6): 354-362.
- **DeBerardinis R.J. & Chandel N.S.** 2016. Fundamentals of cancer metabolism. Science advances 2(5): e1600200.
- **DeBerardinis R.J.,** Lum J.J, Hatzivassiliou G, Thompson C.B. 2008. The biology of cancer: metabolic reprogramming fuels cell growth and proliferation. Cell metabolism 7(1): 11-20.
- **Deblois G.,** Chahrour G, Perry M.C, Sylvain-Drolet G, Muller W.J, Giguere V. 2010. Transcriptional control of the ERBB2 amplicon by ERRalpha and PGC-1beta promotes mammary gland tumorigenesis. Cancer research 70(24): 10277-10287.
- **Deblois G. & Giguere V.** 2011. Functional and physiological genomics of estrogen-related receptors (ERRs) in health and disease. Biochimica et biophysica acta 1812(8): 1032-1040.

- **Deblois G.,** Hall J.A, Perry M-C, Laganiere J, Ghahremani M, Park M, Hallett M, Giguere V. Genome-wide identification of direct target genes implicates estrogen-related receptor a as a determinant of breast cancer heterogeneity. Cancer Res 69:6149–6157, 2009.
- **Deblois G.,** St-Pierre J, Giguere V. 2013. The PGC-1/ERR signaling axis in cancer. Oncogene 32(30): 3483-3490.
- **Delhon I.,** Gutzwiller S, Morvan F, Rangwala S, Wyder L, Evans G, Studer A, Kneissel M, Fournier B. 2009. Absence of estrogen receptor-related-alpha increases osteoblastic differentiation and cancellous bone mineral density. Endocrinology 150(10): 4463-4472.
- **Dhillon N.,** Aggarwal, B.B.; Newman, R.A.; Wolff, R.A.; Kunnumakkara, A.B.; Abbruzzese, J.L.; Ng, C.S.; Badmaev, V.; Kurzrock, R. Phase II trial of curcumin in patients with advanced pancreatic cancer. Clin. Cancer Res. 2008, 14, 4491–4499.
- **Doghman M.,** Cazareth J, Douguet D, Madoux F, Hodder P, Lalli E. 2009. Inhibition of adrenocortical carcinoma cell proliferation by steroidogenic factor-1 inverse agonists. The Journal of clinical endocrinology and metabolism 94(6): 2178-2183.
- **Doghman M.,** Cazareth J, Lalli E. 2008. The T cell factor/beta-catenin antagonist PKF115-584 inhibits proliferation of adrenocortical carcinoma cells. The Journal of clinical endocrinology and metabolism 93(8): 3222-3225.
- **Doghman M.,** El Wakil A, Cardinaud B, Thomas E, Wang J, Zhao W, Peralta-Del Valle MH, Figueiredo BC, Zambetti GP, Lalli E. 2010. Regulation of insulin-like growth factor-mammalian target of rapamycin signaling by microRNA in childhood adrenocortical tumors. Cancer research 70(11): 4666-4675.
- **Doghman M.,** Karpova T, Rodrigues GA, Arhatte M, De Moura J, Cavalli LR, Virolle V, Barbry P, Zambetti GP, Figueiredo BC et al. 2007. Increased steroidogenic factor-1 dosage triggers adrenocortical cell proliferation and cancer. Molecular endocrinology 21(12): 2968-2987.
- **Donatini G.,** Caiazzo R, Do Cao C, Aubert S, Zerrweck C, El-Kathib Z, Gauthier T, Leteurtre E, Wemeau JL, Vantyghem MC et al. 2014. Long-term survival after adrenalectomy for stage I/II adrenocortical carcinoma (ACC): a retrospective

comparative cohort study of laparoscopic versus open approach. Annals of surgical oncology 21(1): 284-291.

- **Dosoky N.S.,** Satyal, P.; Setzer, W.N. Variations in the volatile compositions of Curcuma species. Foods 2019, 8, 53.
- **Duregon E.,** Volante M, Giorcelli J, Terzolo M, Lalli E, Papotti M. 2013. Diagnostic and prognostic role of steroidogenic factor 1 in adrenocortical carcinoma: a validation study focusing on clinical and pathologic correlates. Human pathology 44(5): 822-828.
- **Dutzmann S.,** Schiborr C., Kocher A., Pilatus U., Hattingen E., Weissenberger J., Gessler F., Quick-Weller J., Franz K., Seifert V. et al. Intratumoral concentrations and effects of orally administered micellar curcuminoids in glioblastoma patients. Nutr. Cancer 2016, 68, 943–948.
- **Dwyer M.A.,** Joseph J.D., Wade H.E., Eaton M.L., Kunder R.S., Kazmin D, Chang C.Y., McDonnell D.P. 2010. WNT11 expression is induced by estrogen-related receptor alpha and beta-catenin and acts in an autocrine manner to increase cancer cell migration. Cancer research 70(22): 9298-9308.
- **Ehrlund A.,** Jonsson P., Vedin L.L, Williams C, Gustafsson J.A, Treuter E. 2012. Knockdown of SF-1 and RNF31 affects components of steroidogenesis, TGFbeta, and Wnt/beta-catenin signaling in adrenocortical carcinoma cells. PloS one 7(3): e32080.
- **Else T.,** Kim A.C, Sabolch A, Raymond V.M, Kandathil A, Caoili E.M, Jolly S, Miller B.S, Giordano T.J, Hammer G.D. 2014. Adrenocortical carcinoma. Endocrine reviews 35(2): 282-326.
- **Erdogan I.,** Deutschbein T, Jurowich C, Kroiss M, Ronchi C, Quinkler M, Waldmann J, Willenberg HS, Beuschlein F, Fottner C et al. 2013. The role of surgery in the management of recurrent adrenocortical carcinoma. The Journal of clinical endocrinology and metabolism 98(1): 181-191.
- **Fassnacht M. & Allolio B**. 2009. Clinical management of adrenocortical carcinoma. Best practice & research Clinical endocrinology & metabolism 23(2): 273-289.
- **Fassnacht M.,** Berruti A, Baudin E, Demeure M.J, Gilbert J, Haak H, Kroiss M, Quinn D.I, Hesseltine E, Ronchi C.L. et al. 2015. Linsitinib (OSI-906) versus

placebo for patients with locally advanced or metastatic adrenocortical carcinoma: a double-blind, randomised, phase 3 study. The Lancet Oncology 16(4): 426-435.

- **Fassnacht M.,** Hahner S, Polat B, Koschker A.C, Kenn W, Flentje M, Allolio B. 2006. Efficacy of adjuvant radiotherapy of the tumor bed on local recurrence of adrenocortical carcinoma. The Journal of clinical endocrinology and metabolism 91(11): 4501-4504.
- **Fassnacht M.,** Johanssen S, Quinkler M, Bucsky P, Willenberg H.S, Beuschlein F, Terzolo M, Mueller H.H, Hahner S, Allolio B et al. 2009. Limited prognostic value of the 2004 International Union Against Cancer staging classification for adrenocortical carcinoma: proposal for a Revised TNM Classification. Cancer 115(2): 243-250.
- **Fassnacht M.,** Kenn W, Allolio B. 2004. Adrenal tumors: how to establish malignancy ? Journal of endocrinological investigation 27(4): 387-399.
- **Fassnacht M.,** Libe R, Kroiss M, Allolio B. 2011. Adrenocortical carcinoma: a clinician's update. Nature reviews Endocrinology 7(6): 323-335.
- **Fassnacht M.,** Terzolo M, Allolio B, Baudin E, Haak H, Berruti A, Welin S, Schade-Brittinger C, Lacroix A, Jarzab B. et al. 2012. Combination chemotherapy in advanced adrenocortical carcinoma. The New England journal of medicine 366(23): 2189-2197.
- **Felizola S.J.,** Nakamura Y., Hui X.G., Satoh F., Morimoto R., McNamara K.M., Midorikawa S., Suzuki S., Rainey W.E., Sasano H. 2013. Estrogen-related receptor alpha in normal adrenal cortex and adrenocortical tumors: involvement in development and oncogenesis. Molecular and cellular endocrinology 365(2): 207-211.
- **Fenske W.,** Volker H.U, Adam P, Hahner S, Johanssen S, Wortmann S, Schmidt M, Morcos M, Muller-Hermelink H.K, Allolio B. et al. 2009. Glucose transporter GLUT1 expression is an stage-independent predictor of clinical outcome in adrenocortical carcinoma. Endocrine-related cancer 16(3): 919-928.
- **Ferruzzi P.,** Ceni E, Tarocchi M, Grappone C, Milani S, Galli A, Fiorelli G, Serio M, Mannelli M. 2005. Thiazolidinediones inhibit growth and invasiveness of the human adrenocortical cancer cell line H295R. The Journal of clinical endocrinology and metabolism 90(3): 1332-1339.

- **Fisher K.W.,** Das B, Kortum R.L, Chaika O.V, Lewis R.E. 2011. Kinase suppressor of ras 1 (KSR1) regulates PGC1alpha and estrogen-related receptor alpha to promote oncogenic Ras-dependent anchorage-independent growth. Molecular and cellular biology 31(12): 2453-2461.
- **Gagliano T.,** Gentilin E, Benfini K, Di Pasquale C, Tassinari M, Falletta S, Feo C, Tagliati F, Uberti E.D, Zatelli M.C. 2014. Mitotane enhances doxorubicin cytotoxic activity by inhibiting P-gp in human adrenocortical carcinoma cells. Endocrine 47(3): 943-951.
- **Gangadhar T.C.,** Cohen E.E, Wu K, Janisch L, Geary D, Kocherginsky M, House L.K, Ramirez J, Undevia S.D, Maitland M.L et al. 2011. Two drug interaction studies of sirolimus in combination with sorafenib or sunitinib in patients with advanced malignancies. Clinical cancer research : an official journal of the American Association for Cancer Research 17(7): 1956-1963.
- **Gatenby R.A. & Gillies R.J.** 2004. Why do cancers have high aerobic glycolysis? Nature reviews Cancer 4(11): 891-899.
- **Gaujoux S.,** Brennan MF. 2012. Recommendation for standardized surgical management of primary adrenocortical carcinoma. Surgery 152(1): 123-132.
- **Gaujoux S.,** Grabar S, Fassnacht M, Ragazzon B, Launay P, Libe R, Chokri I, Audebourg A, Royer B, Sbiera S et al. 2011. beta-catenin activation is associated with specific clinical and pathologic characteristics and a poor outcome in adrenocortical carcinoma. Clinical cancer research : an official journal of the American Association for Cancer Research 17(2): 328-336.
- **Gaujoux S.,** Hantel C, Launay P, Bonnet S, Perlemoine K, Lefevre L, Guillaud-Bataille M, Beuschlein F, Tissier F, Bertherat J. et al. 2013. Silencing mutated beta-catenin inhibits cell proliferation and stimulates apoptosis in the adrenocortical cancer cell line H295R. PloS one 8(2): e55743.
- **Germano A.,** Rapa I, Volante M, Lo Buono N, Carturan S, Berruti A, Terzolo M, Papotti M. 2014. Cytotoxic activity of gemcitabine, alone or in combination with mitotane, in adrenocortical carcinoma cell lines. Molecular and cellular endocrinology 382(1): 1-7.
- **Ghanbari F.,** Fortier A.M., Park M. & Philip, A. (2021). Cholesterol-Induced Metabolic Reprogramming in Breast Cancer Cells Is Mediated via the ERRα Pathway. Cancers, 13(11), 2605.

- **Ghanbari F.,** Mader S., Philip A. Cholesterol as an Endogenous Ligand of ERRalpha Promotes ERRalpha-Mediated Cellular Proliferation and Metabolic Target Gene Expression in Breast Cancer Cells. Cells 2020.
- **Giguere V.,** Yang N, Segui P, Evans R.M. 1988. Identification of a new class of steroid hormone receptors. Nature 331(6151): 91-94.
- **Giordano T.J.,** Thomas D.G, Kuick R, Lizyness M, Misek D.E, Smith A.L, Sanders D, Aljundi R.T, Gauger P.G, Thompson N.W, Taylor J.M, Hanash S.M: Distinct transcriptional profiles of adrenocortical tumors uncovered by DNA microarray analysis. Am J Pathol 162:521–31, 2003.
- **Glover A.R.,** Zhao J.T., Gill A.J., Weiss J., Mugridge N., Kim E., Feeney A.L., Ip J.C., Reid G., Clarke S. et al. 2015. MicroRNA-7 as a tumor suppressor and novel therapeutic for adrenocortical carcinoma. Oncotarget 6(34): 36675-36688.
- **Gota V.S.,** Maru G.B., Soni T.G., Gandhi T.R., Kochar N., Agarwal M.G. Safety and pharmacokinetics of a solid lipid curcumin particle formulation in osteosarcoma patients and healthy volunteers. J. Agric. Food Chem. 2010, 58, 2095–2099.
- **Green S.,** Walter P, Greene G, Krust A, Goffin C, Jensen E, Scrace G, Waterfield M, Chambon P. 1986. Cloning of the human oestrogen receptor cDNA. Journal of steroid biochemistry 24(1): 77-83.
- **Gross D.J.,** Munter G, Bitan M, Siegal T, Gabizon A, Weitzen R, Merimsky O, Ackerstein A, Salmon A, Sella A. et al. 2006. The role of imatinib mesylate (Glivec) for treatment of patients with malignant endocrine tumors positive for c-kit or PDGF-R. Endocrine-related cancer 13(2): 535-540.
- **Guorgui J.,** Wang R., Mattheolabakis G., Mackenzie G.G. Curcumin formulated in solid lipid nanoparticles has enhanced efficacy in Hodgkin's lymphoma in mice. Arch. Biochem. Biophys. 2018, 648, 12–19.
- **Gupta S.C.,** Patchva S., Aggarwal B.B. Therapeutic roles of curcumin: Lessons learned from clinical trials. AAPS J. 2013, 15, 195–218.
- **Gutierrez-Pajares J.L.,** Ben Hassen C, Chevalier S, Frank PG. 2016. SR-BI: Linking Cholesterol and Lipoprotein Metabolism with Breast and Prostate Cancer. Frontiers in pharmacology 7: 338.
- **Haak H.R.,** Hermans J, van de Velde C.J, Lentjes E.G, Goslings B.M, Fleuren G.J, Krans H.M. 1994. Optimal treatment of adrenocortical carcinoma with

mitotane: results in a consecutive series of 96 patients. British journal of cancer 69(5): 947-951.

- **Habra M.A.,** Ejaz S, Feng L, Das P, Deniz F, Grubbs E.G, Phan A, Waguespack S.G, Ayala-Ramirez M, Jimenez C. et al. 2013. A retrospective cohort analysis of the efficacy of adjuvant radiotherapy after primary surgical resection in patients with adrenocortical carcinoma. The Journal of clinical endocrinology and metabolism 98(1): 192-197.
- **Hahner S.,** Kreissl M.C, Fassnacht M, Haenscheid H, Bock S, Verburg F.A, Knoedler P, Lang K, Reiners C, Buck A.K. et al. 2013. Functional characterization of adrenal lesions using [123I]IMTO-SPECT/CT. The Journal of clinical endocrinology and metabolism 98(4): 1508-1518.
- **Hahner S.,** Kreissl M.C, Fassnacht M, Haenscheid H, Knoedler P, Lang K, Buck A.K, Reiners C, Allolio B, Schirbel A. 2012. [131I]iodometomidate for targeted radionuclide therapy of advanced adrenocortical carcinoma. The Journal of clinical endocrinology and metabolism 97(3): 914-922.
- **Halestrap A.P.** 2012. The monocarboxylate transporter family--Structure and functional characterization. IUBMB life 64(1): 1-9.
- **Haluska P.,** Worden F, Olmos D, Yin D, Schteingart D, Batzel GN, Paccagnella ML, de Bono JS, Gualberto A, Hammer GD. 2010. Safety, tolerability, and pharmacokinetics of the anti-IGF-1R monoclonal antibody figitumumab in patients with refractory adrenocortical carcinoma. Cancer chemotherapy and pharmacology 65(4): 765-773.
- **Han Z.,** Zhang J., Zhang K., Zhao Y. Curcumin inhibits cell viability, migration, and invasion of thymic carcinoma cells via downregulation of microRNA-27a. Phytother. Res. PTR 2020, 34, 1629–1637.
- **Hanahan D.,** Weinberg RA. 2011. Hallmarks of cancer: the next generation. Cell 144(5): 646-674.
- **He G.,** Feng C., Vinothkumar R., Chen W., Dai X., Chen X., Ye Q., Qiu C., Zhou H., Wang Y. et al. Curcumin analog EF24 induces apoptosis via ROS-dependent mitochondrial dysfunction in human colorectal cancer cells. Cancer Chemother. Pharmacol. 2016, 78, 1151–1161.
- **He Y.,** Li W., Hu G., Sun H., Kong Q. Bioactivities of EF24, a novel curcumin analog: A review. Front. Oncol. 2018, 8, 614.

- **Hennings J.,** Lindhe O, Bergstrom M, Langstrom B, Sundin A, Hellman P. 2006. [11C]metomidate positron emission tomography of adrenocortical tumors in correlation with histopathological findings. The Journal of clinical endocrinology and metabolism 91(4): 1410-1414.
- **Hensley C.T.,** Faubert B, Yuan Q, Lev-Cohain N, Jin E, Kim J, Jiang L, Ko B, Skelton R, Loudat L. et al. 2016. Metabolic Heterogeneity in Human Lung Tumors. Cell 164(4): 681-694.
- **Hermsen I.G.,** Fassnacht M, Terzolo M, Houterman S, den Hartigh J, Leboulleux S, Daffara F, Berruti A, Chadarevian R, Schlumberger M. et al. 2011. Plasma concentrations of o,p'DDD, o,p'DDA, and o,p'DDE as predictors of tumor response to mitotane in adrenocortical carcinoma: results of a retrospective ENS@T multicenter study. The Journal of clinical endocrinology and metabolism 96(6): 1844-1851.
- **Huang H. & Fojo T.** 2008. Adjuvant mitotane for adrenocortical cancer--a recurring controversy. The Journal of clinical endocrinology and metabolism 93(10): 3730-3732.
- **Huang S.,** He J., Cao L., Lin H., Zhang W., Zhong Q. Improved physicochemical properties of curcumin-loaded solid lipid nanoparticles stabilized by sodium caseinate-lactose Maillard conjugate. J. Agric. Food Chem. 2020, 68, 7072–7081.
- **Huss J.M.,** Imahashi K., Dufour C.R., Weinheimer C.J., Courtois M., Kovacs A., Giguere V., Murphy E., Kelly D.P. 2007. The nuclear receptor ERRalpha is required for the bioenergetic and functional adaptation to cardiac pressure overload. Cell metabolism 6(1): 25-37.
- **Huss J.M.,** Torra I.P., Staels B., Giguere V., Kelly D.P. 2004. Estrogen-related receptor alpha directs peroxisome proliferator-activated receptor alpha signaling in the transcriptional control of energy metabolism in cardiac and skeletal muscle. Molecular and cellular biology 24(20): 9079-9091.
- **Hyatt S.M.,** Lockamy E.L., Stein R.A., McDonnell D.P., Miller A.B., Orband-Miller L.A., Willson T.M., Zuercher W.J. 2007. On the intractability of estrogen-related receptor alpha as a target for activation by small molecules. Journal of medicinal chemistry 50(26): 6722-6724.
- **Icard P.,** Goudet P, Charpenay C, Andreassian B, Carnaille B, Chapuis Y, Cougard P, Henry J.F, Proye C. 2001. Adrenocortical carcinomas: surgical trends

and results of a 253-patient series from the French Association of Endocrine Surgeons study group. World journal of surgery 25(7): 891-897.

- **Illemann M.,** Laerum O.D, Hasselby J.P, Thurison T, Hoyer-Hansen G, Nielsen H.J, Danish Study Group on Early Detection of Colorectal C, Christensen I.J. 2014. Urokinase-type plasminogen activator receptor (uPAR) on tumor-associated macrophages is a marker of poor prognosis in colorectal cancer. Cancer medicine 3(4): 855-864.
- **Iorio M.V. & Croce C.M.** 2012. MicroRNA dysregulation in cancer: diagnostics, monitoring and therapeutics. A comprehensive review. EMBO molecular medicine 4(3): 143-159.
- **Ismail N.I.,** Othman I., Abas F., Lajis N.H., Naidu R. The curcumin analogue, MS13 (1,5-Bis(4-hydroxy-3- methoxyphenyl)-1,4-pentadiene-3-one), inhibits cell proliferation and induces apoptosis in primary and metastatic human colon cancer cells. Molecules 2020, 25, 3798.
- **Jefremov V.,** Zilmer M, Zilmer K., Bogdanovic N, Karelson E. Antioxidative effects of plant polyfenols: from protection of G protein signalling to prevention of age- related pathologies. Ann. N.Y. Acad. Sci. 1095, 449-457, 2007.
- **Jenning V.,** Lippacher A., Gohla S.H. Medium scale production of solid lipid nanoparticles (SLN) by high pressure homogenization. J. Microencapsul. 2002, 19, 1–10.
- **Ji H.L.,** Song C.C., Li Y.F., He J.J., Li Y.L., Zheng X.L., & Yang G.S. (2014). miR-125a inhibits porcine preadipocytes differentiation by targeting ERRα. Molecular and cellular biochemistry, 395(1), 155-165.
- **Ji H.,** Tang J., Li M., Ren J., Zheng N., & Wu L. (2016). Curcumin-loaded solid lipid nanoparticles with Brij78 and TPGS improved in vivo oral bioavailability and in situ intestinal absorption of curcumin. Drug Delivery, 23(2), 459-470.
- **Jin W**. Role of JAK/STAT3 signaling in the regulation of metastasis, the transition of cancer stem cells, and chemoresistance of cancer by epithelial-mesenchymal transition. Cells 2020, 9, 217.
- **Jobin C.,** Bradham C.A., Russo M.P., Juma B., Narula A.S., Brenner D.A., Sartor R.B. Curcumin blocks cytokine- mediated NF-kappa B activation and proinflammatory gene expression by inhibiting factor I-kappa B kinase activity. J. Immunol. 163, 3474-3483, 1999.

- **John P.,** Mews M., Moore R. Cyclin/Cdk complexes: their involvement in cell cycle progression and mitotic division. Protoplasma, 216: 119-142, 2001.
- **Joseph J.A.** Reversing the deleterious effects of aging on neuronal communication and behaviour: beneficial properties of fruit polyfenolic compounds. Am. J. Clin, 81 (Suppl.): 313S-316S, 2005.
- **Kahn C.R.,** Chen L., Cohen S.E. 2000. Unraveling the mechanism of action of thiazolidinediones. The Journal of clinical investigation 106(11): 1305-1307.
- **Kallen J.,** Schlaeppi J.M., Bitsch F, Filipuzzi I, Schilb A, Riou V, Graham A, Strauss A, Geiser M, Fournier B. 2004. Evidence for ligand-independent transcriptional activation of the human estrogen-related receptor alpha (ERRalpha): crystal structure of ERRalpha ligand binding domain in complex with peroxisome proliferator-activated receptor coactivator-1alpha. The Journal of biological chemistry 279(47): 49330-49337.
- **Kasinski A.L.,** Du Y.; Thomas S.L.; Zhao J.; Sun S.Y.; Khuri F.R.; Wang C.Y.; Shoji M.; Sun A.; Snyder J.P.; et al. Inhibition of IkappaB kinase-nuclear factor-kappaB signaling pathway by 3,5-bis(2-flurobenzylidene)piperidin-4-one (EF24), a novel monoketone analog of curcumin. Mol. Pharmacol. 2008, 74, 654–661.
- **Kelly M.J.** Rapid actions of plasma membrane estrogen receptors. Trends Endocrinol. Metab, 12: 152-156, 2001.
- **Kemp C.D.,** Ripley R.T., Mathur A., Steinberg S.M., Nguyen D.M., Fojo T., Schrump D.S. 2011. Pulmonary resection for metastatic adrenocortical carcinoma: the National Cancer Institute experience. The Annals of thoracic surgery 92(4): 1195-1200.
- **Kerkhofs T.M.,** Baudin E., Terzolo M., Allolio B., Chadarevian R., Mueller H.H., Skogseid B., Leboulleux S., Mantero F., Haak H.R. et al. 2013. Comparison of two mitotane starting dose regimens in patients with advanced adrenocortical carcinoma. The Journal of clinical endocrinology and metabolism 98(12): 4759-4767.
- **Khan T.S.,** Imam H., Juhlin C., Skogseid B., Grondal S., Tibblin S., Wilander E., Oberg K., Eriksson B. 2000. Streptozocin and o,p'DDD in the treatment of adrenocortical cancer patients: long-term survival in its adjuvant use. Annals of oncology : official journal of the European Society for Medical Oncology 11(10): 1281-1287.

- **Kim K.C. & Lee C.** Curcumin induces downregulation of E2F4 expression and apoptotic cell death in HCT116 human colon cancer cells; Involvement of reactive oxygen species. Korean J. Physiol. Pharmacol. Off. J. Korean Physiol. Soc. Korean Soc. Pharmacol. 2010, 14, 391–397.
- **Kim M.J.,** Park K.S., Kim K.T., Gil E.Y. The inhibitory effect of curcumin via fascin suppression through JAK/STAT3 pathway on metastasis and recurrence of ovary cancer cells. BMC Women's Health 2020, 20, 256.
- **Kirk P.,** Wilson M.C, Heddle C, Brown M.H, Barclay A.N, Halestrap A.P. 2000. CD147 is tightly associated with lactate transporters MCT1 and MCT4 and facilitates their cell surface expression. The EMBO journal 19(15): 3896-3904.
- **Klein-Hitpass L.,** Schorpp M, Wagner U, Ryffel G.U. 1986. An estrogen-responsive element derived from the 5' flanking region of the Xenopus vitellogenin A2 gene functions in transfected human cells. Cell 46(7): 1053-1061.
- **Klinge C.M.,** Jernigan S.C., Smith S.L., Tyulmenkov V.V., Kulakosky P.C. 2001. Estrogen response element sequence impacts the conformation and transcriptional activity of estrogen receptor alpha. Molecular and cellular endocrinology 174(1-2): 151-166.
- **Kokabu T.,** Mori T., Matsushima H., Yoriki K., Kataoka H., Tarumi Y. & Kitawaki J. (2019). Antitumor effect of XCT790, an ERRα inverse agonist, on ERα-negative endometrial cancer cells. Cellular Oncology, 42(2), 223-235.
- **Kotecha R.,** Takami A., Espinoza J.L. Dietary phytochemicals and cancer chemoprevention: A review of the clinical evidence. Oncotarget 2016, 7, 52517–52529.
- **Kraus R.J.,** Ariazi E.A., Farrell M.L., Mertz J.E. 2002. Estrogen-related receptor alpha 1 actively antagonizes estrogen receptor-regulated transcription in MCF-7 mammary cells. The Journal of biological chemistry 277(27): 24826-24834.
- **Kressler D.,** Schreiber S.N., Knutti D., Kralli A. 2002. The PGC-1-related protein PERC is a selective coactivator of estrogen receptor alpha. The Journal of biological chemistry 277(16): 13918-13925.
- **Kroiss M.,** Quinkler M, Johanssen S, van Erp N.P, Lankheet N, Pollinger A, Laubner K, Strasburger C.J, Hahner S, Muller H.H. et al. 2012. Sunitinib in refractory adrenocortical carcinoma: a phase II, single-arm, open-label trial. The Journal of clinical endocrinology and metabolism 97(10): 3495-3503.

- **Kroiss M.,** Quinkler M, Lutz W.K, Allolio B, Fassnacht M. 2011. Drug interactions with mitotane by induction of CYP3A4 metabolism in the clinical management of adrenocortical carcinoma. Clinical endocrinology 75(5): 585-591.
- **Kunnumakkara A.B.,** Bordoloi D., Harsha C., Banik K., Gupta S.C.; Aggarwal B.B. Curcumin mediates anticancer effects by modulating multiple cell signaling pathways. Clin. Sci. 2017, 131, 1781–1799.
- **Lee J.O.,** Lee K.W., Kim C.J., Kim Y.J., Lee H.E., Kim H., Kim J.H., Bang S.M., Kim J.S., Lee J.S. 2009. Metastatic adrenocortical carcinoma treated with sunitinib: a case report. Japanese journal of clinical oncology 39(3): 183-185.
- **Lehmann T.P.,** Wrzesinski T, Jagodzinski P.P. 2013. The effect of mitotane on viability, steroidogenesis and gene expression in NCIH295R adrenocortical cells. Molecular medicine reports 7(3): 893-900.
- **Leitinger N. & Schulman I.G.** 2013. Phenotypic polarization of macrophages in atherosclerosis. Arteriosclerosis, thrombosis, and vascular biology 33(6): 1120-1126.
- **Lerario A.M.,** Worden F.P., Ramm C.A., Hesseltine E.A., Stadler W.M., Else T., Shah M.H., Agamah E., Rao K., Hammer G.D. 2014. The combination of insulin-like growth factor receptor 1 (IGF1R) antibody cixutumumab and mitotane as a first-line therapy for patients with recurrent/metastatic adrenocortical carcinoma: a multi-institutional NCI-sponsored trial. Hormones & cancer 5(4): 232-239.
- **Li X.,** Wu J.B, Li Q, Shigemura K, Chung L.W, Huang W.C. 2016. SREBP-2 promotes stem cell-like properties and metastasis by transcriptional activation of c-Myc in prostate cancer. Oncotarget 7(11): 12869-12884.
- **Li R.,** Lim S.J., Choi H.G., Lee M.K. Solid lipid nanoparticles as drug delivery system for water-insoluble drugs. J. Pharm. Investig. 2010, 40, 63–73.
- **Li W.,** He Y.; Zhang R.; Zheng G.; Zhou D. The curcumin analog EF24 is a novel senolytic agent. Aging 2019, 11, 771–782.
- **Liang G.,** Shao L., Wang Y., Zhao C., Chu Y., Xiao J., Zhao Y., Li X., Yang S. Exploration and synthesis of curcumin analogues with improved structural stability both in vitro and in vivo as cytotoxic agents. Bioorg. Med. Chem. 2009, 17, 2623–2631.
- **Liang Y.,** Zheng T.; Song R.; Wang J.; Yin D.; Wang L.; Liu H.; Tian L.; Fang X.; Meng X. et al. Hypoxia-mediated sorafenib resistance can be overcome by

EF24 through Von Hippel-Lindau tumor suppressor-dependent HIF-1alpha inhibition in hepatocellular carcinoma. Hepatology 2013, 57, 1847–1857.

- **Lim T.G.,** Lee S.Y.; Huang Z.; Lim D.Y.; Chen H.; Jung S.K.; Bode A.M.; Lee K.W.; Dong Z. Curcumin suppresses proliferation of colon cancer cells by targeting CDK2. Cancer Prev. Res. 2014, 7, 466–474.
- **Lin C.W.,** Chang Y.H., Pu H.F. 2012. Mitotane exhibits dual effects on steroidogenic enzymes gene transcription under basal and cAMP-stimulating microenvironments in NCI-H295 cells. Toxicology 298(1-3): 14-23.
- **Lin J.,** Puigserver P., Donovan J., Tarr P., Spiegelman B.M. 2002. Peroxisome proliferator-activated receptor gamma coactivator 1beta (PGC-1beta), a novel PGC-1-related transcription coactivator associated with host cell factor. The Journal of biological chemistry 277(3): 1645-1648.
- **Lin L.,** Shi Q.; Nyarko A.K.; Bastow K.F.; Wu C.C.; Su C.Y.; Shih C.C.; Lee K.H. Antitumor agents. 250. Design and synthesis of new curcumin analogues as potential anti-prostate cancer agents. J. Med. Chem. 2006, 49, 3963–3972.
- **Lin Y.G.,** Kunnumakkara A.B., Nair A., Merritt W.M., Han L.Y., Armaiz-Pena G.N., Kamat A.A., Spannuth W.A., Gershenson D.M., Lutgendorf S.K. et al. Curcumin inhibits tumor growth and angiogenesis in ovarian carcinoma by targeting the nuclear factor-κB pathway. Clin. Cancer Res, 13, 3423–3430, 2007.
- **Liu G.,** Sun, P., Dong, B., & Sehouli, J. (2018). Key regulator of cellular metabolism, estrogen-related receptor α, a new therapeutic target in endocrine-related gynecological tumor. Cancer Management and Research, 10, 6887.
- **Liu J.L.,** Pan Y.Y.; Chen O.; Luan Y.; Xue X.; Zhao J.J.; Liu L.; Jia H.Y. Curcumin inhibits MCF-7 cells by modulating the NF-kappaB signaling pathway. Oncol. Lett. 2017, 14, 5581–5584.
- **Liu-Chittenden Y.,** Jain M, Kumar P, Patel D, Aufforth R, Neychev V, Sadowski S, Gara S.K, Joshi B.H, Cottle-Delisle C. et al. 2015. Phase I trial of systemic intravenous infusion of interleukin-13-Pseudomonas exotoxin in patients with metastatic adrenocortical carcinoma. Cancer medicine 4(7): 1060-1068.
- **Logie A.,** Boulle N, GastonV, Perin L, Boudou P, Le Bouc Y, Gicquel C. Autocrine role of IGF-II in proliferation of human adrenocortical carcinoma NCI H295R cell line. J Mol Endocrinol, 23:23-32, 1999.

- **Lombardi C.P.,** Raffaelli M., De Crea C., Boniardi M., De Toma G., Marzano L.A., Miccoli P., Minni F., Morino M., Pelizzo M.R. et al. 2012. Open versus endoscopic adrenalectomy in the treatment of localized (stage I/II) adrenocortical carcinoma: results of a multiinstitutional Italian survey. Surgery 152(6): 1158-1164.
- **Lu D.,** Kiriyama Y., Lee K.Y., Giguere V. 2001. Transcriptional regulation of the estrogen-inducible pS2 breast cancer marker gene by the ERR family of orphan nuclear receptors. Cancer research 61(18): 6755-6761.
- **Luconi M.,** Mangoni M., Gelmini S., Poli G., Nesi G., Francalanci M., Pratesi N., Cantini G., Lombardi A., Pepi M. et al. 2010. Rosiglitazone impairs proliferation of human adrenocortical cancer: preclinical study in a xenograft mouse model. Endocrine-related cancer 17(1): 169-177.
- **Lughezzani G.,** Sun M., Perrotte P., Jeldres C., Alasker A., Isbarn H., Budaus L., Shariat S.F., Guazzoni G., Montorsi F. et al. 2010. The European Network for the Study of Adrenal Tumors staging system is prognostically superior to the international union against cancer-staging system: a North American validation. European journal of cancer 46(4): 713-719.
- **Luo J.,** Sladek R, Carrier J, Bader JA, Richard D, Giguere V. 2003. Reduced fat mass in mice lacking orphan nuclear receptor estrogen-related receptor alpha. Molecular and cellular biology 23(22): 7947-7956.
- **Macfarlane D.A.** 1958. Cancer of the adrenal cortex; the natural history, prognosis and treatment in a study of fifty-five cases. Annals of the Royal College of Surgeons of England 23(3): 155-186.
- **Mahammedi H.,** Planchat E., Pouget M.; Durando X.; Cure H.; Guy L.; Van-Praagh I.; Savareux L.; Atger M.; Bayet-Robert M. et al. The new combination docetaxel, prednisone and curcumin in patients with castration-resistant prostate cancer: A pilot phase II study. Oncology 2016, 90, 69–78.
- **Malik M.,** Mendoza M., Payson M., Catherino W.H. 2009. Curcumin, a nutritional supplement with antineoplastic activity, enhances leiomyoma cell apoptosis and decreases fibronectin expression. Fertil Steril 91: 2177– 2184.
- **Manjunath K.,** Reddy J.S., Venkateswarlu V. Solid lipid nanoparticles as drug delivery systems. Methods Find. Exp. Clin. Pharmacol. 2005, 27, 127–144.

- **Manna S.,** Bostner J., Sun Y., Miller L.D., Alayev A., Schwartz N.S., ... & Holz M.K. (2016). ERRα is a marker of tamoxifen response and survival in triple-negative breast cancer. Clinical Cancer Research, 22(6), 1421-1431.
- **Mantovani A.,** Marchesi F, Malesci A, Laghi L, Allavena P. 2017. Tumour-associated macrophages as treatment targets in oncology. Nature reviews Clinical oncology 14(7): 399-416.
- **May F.E.,** Smith D.J., Westley B.R. 1993. The human cathepsin D-encoding gene is transcribed from an estrogen-regulated and a constitutive start point. Gene 134(2): 277-282.
- **May F.E. & Westley B.R.** 1986. Cloning of estrogen-regulated messenger RNA sequences from human breast cancer cells. Cancer research 46(12 Pt 1): 6034-6040.
- **May F.E. & Westley B.R.** 1988. Identification and characterization of estrogen-regulated RNAs in human breast cancer cells. The Journal of biological chemistry 263(26): 12901-12908.
- **May F.E. & Westley B.R.** 1995. Estrogen regulated messenger RNAs in human breast cancer cells. Biomedicine & pharmacotherapy = Biomedecine & pharmacotherapie 49(9): 400-414.
- **McDonald J.G.,** Thompson B.M., McCrum E.C., Russell D.W. 2007. Extraction and analysis of sterols in biological matrices by high performance liquid chromatography electrospray ionization mass spectrometry. Methods in enzymology 432: 145-170.
- **Menon V.P. & Sudheer A.R.** Antioxidant and anti-inflammatory properties of curcumin. Adv. Exp. Med. Biol. 595, 105–125, 2007.
- **Menon L.G.,** Kuttan R.. & Kuttan G. (1995). Inhibition of lung metastasis in mice induced by B16F10 melanoma cells by polyphenolic compounds. Cancer letters, 95(1-2), 221-225.
- **Michalek R.D.,** Gerriets V.A., Nichols A.G., Inoue M., Kazmin D., Chang C.Y., ... & Rathmell J.C. (2011). Estrogen-related receptor-α is a metabolic regulator of effector T-cell activation and differentiation. Proceedings of the National Academy of Sciences, 108(45), 18348-18353.
- **Miranda-Goncalves V.,** Honavar M, Pinheiro C, Martinho O, Pires M.M, Pinheiro C, Cordeiro M, Bebiano G, Costa P, Palmeirim I. et al. 2013.

Monocarboxylate transporters (MCTs) in gliomas: expression and exploitation as therapeutic targets. Neuro-oncology 15(2): 172-188.

- **Moller D.E. & Berger J.P.** Role of PPARs in the regulation of obesity-related insulin sensitivity and inflammation. International Journal of Obesity, 27(3), S17-S21, 2003.
- **Montanaro D.,** Maggiolini M, Recchia AG, Sirianni R, Aquila S, Barzon L, Fallo F, Ando S, Pezzi V. 2005. Antiestrogens upregulate estrogen receptor beta expression and inhibit adrenocortical H295R cell proliferation. Journal of molecular endocrinology 35(2): 245-256.
- **Mootha V.K.,** Handschin C., Arlow D, Xie X, St Pierre J, Sihag S, Yang W, Altshuler D, Puigserver P, Patterson N. et al. 2004. Erralpha and Gabpa/b specify PGC-1alpha-dependent oxidative phosphorylation gene expression that is altered in diabetic muscle. Proceedings of the National Academy of Sciences of the United States of America 101(17): 6570-6575.
- **Morelli V.,** Palmieri S, Salcuni AS, Eller-Vainicher C, Cairoli E, Zhukouskaya V, Scillitani A, Beck-Peccoz P, Chiodini I. 2013. Bilateral and unilateral adrenal incidentalomas: biochemical and clinical characteristics. European journal of endocrinology 168(2): 235-241.
- **Mosieniak G.,** Adamowicz M.; Alster O.; Jaskowiak H.; Szczepankiewicz A.A.; Wilczynski G.M.; Ciechomska I.A.; Sikora E. Curcumin induces permanent growth arrest of human colon cancer cells: Link between senescence and autophagy. Mech. Ageing Dev. 2012, 133, 444–455.
- **Mukherjee S.,** Ray S., Thakur R.S. Solid lipid nanoparticles: A modern formulation approach in drug delivery system. Indian J. Pharm. Sci. 2009, 71, 349–358.
- **Mukherjee T.K.,** Malik P. & Hoidal J.R. (2021). The emerging role of estrogen related receptorα in complications of non- small cell lung cancers. Oncology Letters, 21(4), 1-1.
- **Mukhopadhyay A.,** Banerjee S., Stafford L.J.; Xia C.; Liu M.; Aggarwal B.B. Curcumin-induced suppression of cell proliferation correlates with down-regulation of cyclin D1 expression and CDK4-mediated retinoblastoma protein phosphorylation. Oncogene 2002, 21, 8852–8861.

- **Naing A.,** Kurzrock R, Burger A, Gupta S, Lei X, Busaidy N, Hong D, Chen H.X, Doyle L.A, Heilbrun L.K. et al. 2011. Phase I trial of cixutumumab combined with temsirolimus in patients with advanced cancer. Clinical cancer research: an official journal of the American Association for Cancer Research 17(18): 6052-6060.
- **Nishida M.** Activation mechanism of Gi and G0 by reactive oxygen species. J. Biol. Chem, 277: 9036-9042, 2002.
- **Nocito M.C.,** De Luca A., Prestia F., Avena P., La Padula D., Zavaglia L., Sirianni R., Casaburi I., Puoci F., Chimento A., Pezzi V. (2021). Antitumoral Activities of Curcumin and Recent Advances to ImProve Its Oral Bioavailability. Biomedicines, 9(10), 1476.
- **Nunes M.L.,** Rault A., Teynie J, Valli N, Guyot M, Gaye D, Belleannee G, Tabarin A. 2010. 18F-FDG PET for the identification of adrenocortical carcinomas among indeterminate adrenal tumors at computed tomography scanning. World journal of surgery 34(7): 1506-1510.
- **Odot J.,** Albert P, Carlier A, Tarpin M, Devy J, Madoulet C. In vitro and in vivo anti- tumoral effect of curcumin against melanoma cells. Int J Cancer 111:381–387, 2004.
- **Onder T.T.,** Gupta P.B., Mani S.A., Yang J., Lander E.S., Weinberg R.A. Cancer Res. 68(10):3645-54, 2008.
- **Pan M.H.,** Huang T.M., Lin J.K. Biotransformation of curcumin through reduction and glucuronidation in mice. Drug Metab. Dispos. 1999, 27, 486–494.
- **Papewalis C.,** Fassnacht M, Willenberg H.S, Domberg J, Fenk R, Rohr U.P, Schinner S, Bornstein S.R, Scherbaum W.A, Schott M. 2006. Dendritic cells as potential adjuvant for immunotherapy in adrenocortical carcinoma. Clinical endocrinology 65(2): 215-222.
- **Pari P. & Murugan P.** Influence of tetrahydrocurcumin on hepatic and renal functional markers and protein levels in experimental type 2 diabetic rats, 2007.
- **Park S.,** Safi R., Liu X., Baldi R., Liu W., Liu J., ... & McDonnell D.P. (2019). Inhibition of ERRα prevents mitochondrial pyruvate uptake exposing NADPH-generating pathways as targetable vulnerabilities in breast cancer. Cell reports, 27(12), 3587-3601.

- **Patalano A.,** Brancato V., Mantero F. 2009. Adrenocortical cancer treatment. Hormone research 71 Suppl 1: 99-104.
- **Paulraj F.,** Abas F.; Lajis N.H.; Othman I.; Naidu R. Molecular pathways modulated by curcumin analogue, diarylpentanoids in cancer. Biomolecules 2019, 9, 270.
- **Peng L.,** Gao X, Duan L, Ren X, Wu D, Ding K. 2011. Identification of pyrido[1,2-alpha]pyrimidine-4-ones as new molecules improving the transcriptional functions of estrogen-related receptor alpha. Journal of medicinal chemistry 54(21): 7729-7733.
- **Perez-Schindler J.,** Summermatter S, Salatino S, Zorzato F, Beer M, Balwierz PJ, van Nimwegen E, Feige JN, Auwerx J, Handschin C. 2012. The corepressor NCoR1 antagonizes PGC-1alpha and estrogen-related receptor alpha in the regulation of skeletal muscle function and oxidative metabolism. Molecular and cellular biology 32(24): 4913-4924.
- **Petersenn S.,** Richter PA, Broemel T, Ritter CO, Deutschbein T, Beil FU, Allolio B, Fassnacht M, German ACCSG. 2015. Computed tomography criteria for discrimination of adrenal adenomas and adrenocortical carcinomas: analysis of the German ACC registry. European journal of endocrinology 172(4): 415-422.
- **Philip S. & Kundu G.C.** Osteopontin induces nuclear factor kappa B-mediated promatrix metalloproteinase-2 activation through I kappa B alpha /IKK signaling pathways, and curcumin (diferulolylmethane) down-regulates these pathways. J. Biol. Chem. 2003, 278, 14487–14497.
- Pinheiro C, Granja S, Longatto-Filho A, Faria AM, Fragoso MC, Lovisolo SM, Lerario AM, Almeida MQ, Baltazar F, Zerbini MC. 2015. Metabolic reprogramming: a new relevant pathway in adult adrenocortical tumors. Oncotarget 6(42): 44403-44421.
- **Pinheiro C.,** Longatto-Filho A, Azevedo-Silva J, Casal M, Schmitt F.C, Baltazar F. 2012. Role of monocarboxylate transporters in human cancers: state of the art. Journal of bioenergetics and biomembranes 44(1): 127-139.
- **Pinheiro C.,** Penna V, Morais-Santos F, Abrahao-Machado L.F, Ribeiro G, Curcelli E.C, Olivieri M.V, Morini S, Valenca I, Ribeiro D. et al. 2014. Characterization of monocarboxylate transporters (MCTs) expression in soft

tissue sarcomas: distinct prognostic impact of MCT1 sub-cellular localization. Journal of translational medicine 12: 118.

- **Pinheiro C.,** Reis R.M, Ricardo S, Longatto-Filho A, Schmitt F, Baltazar F. 2010. Expression of monocarboxylate transporters 1, 2, and 4 in human tumours and their association with CD147 and CD44. Journal of biomedicine & biotechnology 2010: 427694.
- **Polat B.,** Fassnacht M, Pfreundner L, Guckenberger M, Bratengeier K, Johanssen S, Kenn W, Hahner S, Allolio B, Flentje M. 2009. Radiotherapy in adrenocortical carcinoma. Cancer 115(13): 2816-2823.
- **Pollak M.** (2008). Insulin and insulin-like growth factor signalling in neoplasia. Nature Reviews Cancer, 8(12), 915-928.
- **Porpiglia F.,** Fiori C, Daffara F, Zaggia B, Bollito E, Volante M, Berruti A, Terzolo M. 2010. Retrospective evaluation of the outcome of open versus laparoscopic adrenalectomy for stage I and II adrenocortical cancer. European urology 57(5): 873-878.
- **Praditya D.,** Kirchhoff L., Bruning J., Rachmawati H., Steinmann J., Steinmann E. Anti-infective Properties of the Golden Spice Curcumin. Front. Microbiol. 2019, 10, 912.
- **Prasad C.P.,** Rath, G.; Mathur, S.; Bhatnagar, D.; Ralhan, R. Potent growth suppressive activity of curcumin in human breast cancer cells: Modulation of Wnt/beta-catenin signaling. Chem. Biol. Interact. 2009, 181, 263–271
- **Prasad S. & Aggarwal B.B.** Turmeric, the golden spice: From traditional medicine to modern medicine. In Herbal Medicine: Biomolecular and Clinical Aspects; Benzie, I.F.F., Wachtel-Galor, S., Eds.; CRC Press: Boca Raton, FL, USA, 2011.
- **Prest S.J.,** May F.E, Westley B.R. 2002. The estrogen-regulated protein, TFF1, stimulates migration of human breast cancer cells. FASEB journal : official publication of the Federation of American Societies for Experimental Biology 16(6): 592-594.
- **Pricci M.,** Girardi B.; Giorgio, F.; Losurdo, G.; Ierardi, E.; Di Leo, A. Curcumin and colorectal cancer: From basic to clinical evidences. Int. J. Mol. Sci. 2020, 21, 2364.

- **Pugh C.W. & Ratcliffe P.J.** 2003. Regulation of angiogenesis by hypoxia: role of the HIF system. Nature medicine 9(6): 677-684.
- **Puigserver P.,** Wu Z, Park C.W, Graves R, Wright M, Spiegelman B.M. 1998. A cold-inducible coactivator of nuclear receptors linked to adaptive thermogenesis. Cell 92(6): 829-839.
- **Quan-Jun Y.,** Jun B, Li-Li W, Yong-Long H, Bin L, Qi Y, Yan L, Cheng G, Gen-Jin Y. 2015. NMR-based metabolomics reveals distinct pathways mediated by curcumin in cachexia mice bearing CT26 tumor. RSC Adv 5: 11766– 11775.
- **Quinkler M.,** Hahner S, Wortmann S, Johanssen S, Adam P, Ritter C, Strasburger C, Allolio B, Fassnacht M. 2008. Treatment of advanced adrenocortical carcinoma with erlotinib plus gemcitabine. The Journal of clinical endocrinology and metabolism 93(6): 2057-2062.
- **Ragazzon B.,** Assie G, Bertherat J. 2011. Transcriptome analysis of adrenocortical cancers: from molecular classification to the identification of new treatments. Endocrine-related cancer 18(2): R15-27.
- **Ravindran J.,** Prasad S., Aggarwal B.B. 2009. Curcumin and cancer cells: How many ways can curry kill tumor cells selectively? AAPS J 11: 495– 510.
- **Ravindranath V. & Chandrasekhara N.** (1980). Absorption and tissue distribution of curcumin in rats. Toxicology, 16(3), 259-265.
- **Reddy A.R.,** Dinesh P.; Prabhakar A.S.; Umasankar K.; Shireesha B.; Raju M.B. A comprehensive review on SAR of curcumin. Mini Rev. Med. Chem. 2013, 13, 1769–1777.
- **Reibetanz J.,** Jurowich C, Erdogan I, Nies C, Rayes N, Dralle H, Behrend M, Allolio B, Fassnacht M, German ACCsg. 2012. Impact of lymphadenectomy on the oncologic outcome of patients with adrenocortical carcinoma. Annals of surgery 255(2): 363-369.
- **Reid J.M.,** Buhrow S.A.; Gilbert J.A.; Jia L.; Shoji M.; Snyder J.P.; Ames M.M. Mouse pharmacokinetics and metabolism of the curcumin analog, 4-piperidinone,3,5-bis[(2-fluorophenyl)methylene]-acetate(3E,5E) (EF-24; NSC 716993). Cancer Chemother. Pharmacol. 2014, 73, 1137–1146.
- **Ren G. & Li G**. Tumor suppressor gene DLC1: Its modifications, interactive molecules, and potential prospects for clinical cancer application. Int. J. Biol. Macromol. 2021, 182, 264–275

- **Ripley R.T.,** Kemp C.D., Davis J.L., Langan R.C., Royal R.E., Libutti S.K., Steinberg S.M., Wood B.J., Kammula U.S., Fojo T. et al. 2011. Liver resection and ablation for metastatic adrenocortical carcinoma. Annals of surgical oncology 18(7): 1972-1979.
- **Rompicharla S.V.K.,** Bhatt H., Shah A., Komanduri N., Vijayasarathy D., Ghosh B. & Biswas S. (2017). Formulation optimization, characterization, and evaluation of in vitro cytotoxic potential of curcumin loaded solid lipid nanoparticles for improved anticancer activity. Chemistry and physics of lipids, 208, 10-18.
- **Sabolch A.,** Feng M, Griffith K, Hammer G, Doherty G, Ben-Josef E. 2011. Adjuvant and definitive radiotherapy for adrenocortical carcinoma. International journal of radiation oncology, biology, physics 80(5): 1477-1484.
- **Sahebkar A.,** Serbanc M.C., Ursoniuc S., Banach M. Effect of curcuminoids on oxidative stress: A systematic review and meta-analysis of randomized controlled trials. J. Funct. Foods 18, 898–909, 2015.
- **Salehi B.,** Stojanovic-Radic Z., Matejic J.; Sharifi-Rad M.; Anil Kumar N.V.; Martins N.; Sharifi-Rad J. The therapeutic potential of curcumin: A review of clinical trials. Eur. J. Med. Chem. 2019, 163, 527–545.
- **Sandur S.K.,** Pandey M.K.; Sung B.; Ahn K.S.; Murakami A.; Sethi G.; Limtrakul P.; Badmaev V.; Aggarwal B.B. Curcumin, demethoxycurcumin, bisdemethoxycurcumin, tetrahydrocurcumin and turmerones differentially regulate anti-inflammatory and anti-proliferative responses through a ROS-independent mechanism. Carcinogenesis 2007, 28, 1765–1773.
- **Sbiera S.,** Schmull S, Assie G, Voelker H.U, Kraus L, Beyer M, Ragazzon B, Beuschlein F, Willenberg H.S, Hahner S. et al. 2010. High diagnostic and prognostic value of steroidogenic factor-1 expression in adrenal tumors. The Journal of clinical endocrinology and metabolism 95(10): E161-171.
- **Sbiera S.,** Wortmann S, Fassnacht M. 2008. Dendritic cell based immunotherapy--a promising therapeutic approach for endocrine malignancies. Hormone and metabolic research = Hormon- und Stoffwechselforschung = Hormones et metabolisme 40(2): 89-98.
- **Schteingart D.E.,** Doherty G.M, Gauger P.G, Giordano T.J, Hammer G.D, Korobkin M, Worden F.P. 2005. Management of patients with adrenal cancer:

recommendations of an international consensus conference. Endocrine-related cancer 12(3): 667-680.

- **Schteingart D.E.** 2000. Conventional and novel strategies in the treatment of adrenocortical cancer. Brazilian journal of medical and biological research = Revista brasileira de pesquisas medicas e biologicas 33(10): 1197-1200.
- **Schulick R.D. & Brennan M.F.** 1999a. Adrenocortical carcinoma. World journal of urology 17(1): 26-34.
- **Schulick R.D & Brennan M.F.** 1999b. Long-term survival after complete resection and repeat resection in patients with adrenocortical carcinoma. Annals of surgical oncology 6(8): 719-726.
- **Schwabe J.W.,** Chapman L, Finch JT, Rhodes D. 1993. The crystal structure of the estrogen receptor DNA-binding domain bound to DNA: how receptors discriminate between their response elements. Cell 75(3): 567-578.
- **Selvendiran K.,** Ahmed S.; Dayton A.; Kuppusamy M.L.; Rivera B.K.; Kalai T.; Hideg K.; Kuppusamy P. HO-3867, a curcumin analog, sensitizes cisplatin-resistant ovarian carcinoma, leading to therapeutic synergy through STAT3 inhibition. Cancer Biol. Ther. 2011, 12, 837–845.
- **Selvendiran K.,** Tong, L.; Vishwanath, S.; Bratasz, A.; Trigg, N.J.; Kutala, V.K.; Hideg, K.; Kuppusamy, P. EF24 induces G2/M arrest and apoptosis in cisplatin-resistant human ovarian cancer cells by increasing PTEN expression. J. Biol. Chem. 2007, 282, 28609–28618.
- **Sharma R.A.,** Euden S.A.; Platton S.L.; Cooke D.N.; Shafayat A.; Hewitt H.R.; Marczylo T.H.; Morgan B.; Hemingway D.; Plummer S.M. et al. Phase I clinical trial of oral curcumin: Biomarkers of systemic activity and compliance. Clin. Cancer Res. Off. J. Am. Assoc. Cancer Res. 2004, 10, 6847–6854.
- **Shen H.,** Shen J.; Pan H.; Xu L.; Sheng H.; Liu B.; Yao M. Curcumin analog B14 has high bioavailability and enhances the effect of anti-breast cancer cells in vitro and in vivo. Cancer Sci. 2021, 112, 815–827
- **Sherin D.R. & Rajasekharan K.N.** Mechanochemical synthesis and antioxidant activity of curcumin-templated azoles. Arch. Pharm. 2015, 348, 908–914.
- **Shi J.,** Zhang X., Shi T., Li H. Antitumor effects of curcumin in human bladder cancer in vitro. Oncol. Lett. 2017, 14, 1157–1161.

- **Shiau A.K.,** Barstad D, Loria P.M, Cheng L, Kushner P.J, Agard D.A, Greene G.L. 1998. The structural basis of estrogen receptor/coactivator recognition and the antagonism of this interaction by tamoxifen. Cell 95(7): 927-937.
- **Shishodia S.,** Chaturvedi M.M., Aggarwal B.B. 2007. Role of curcumin in cancer therapy. Curr Probl Cancer 31: 243– 305.
- **Singh S. & Aggarwal B.B.** Activation of transcription factor Nf-kB is suppressed by curcumin (diferuoilmethane). J. Biol. Chem. 270, 24995-25000, 1995.
- **Sirianni R.,** Zolea F, Chimento A, Ruggiero C, Cerquetti L, Fallo F, Pilon C, Arnaldi G, Carpinelli G, Stigliano A. et al. 2012. Targeting estrogen receptor-alpha reduces adrenocortical cancer (ACC) cell growth in vitro and in vivo: potential therapeutic role of selective estrogen receptor modulators (SERMs) for ACC treatment. The Journal of clinical endocrinology and metabolism 97(12): E2238-2250.
- **Sladek R.,** Bader J.A. & Giguere V. (1997). The orphan nuclear receptor estrogen-related receptor alpha is a transcriptional regulator of the human medium-chain acyl coenzyme A dehydrogenase gene. Molecular and cellular biology, 17(9), 5400-5409.
- **Slomiany M.G.,** Grass G.D., Robertson A.D., Yang X.Y., Maria B.L., Beeson C., Toole B.P. 2009. Hyaluronan, CD44, and emmprin regulate lactate efflux and membrane localization of monocarboxylate transporters in human breast carcinoma cells. Cancer research 69(4): 1293-1301.
- **Somparn P.,** Phisalaphong C., Nakornchai S., Unchern S., Morales N.P. Comparative antioxidant activities of curcumin and its demethoxy and hydrogenated derivatives. Biol. Pharm. Bull. 2007, 30, 74–78.
- **Song C.S. & Chatterjee B.** (2021). Prostate Cancer Stimulation by a Novel Liver X Receptor (LXRa)-Estrogen Related Receptor (ERRa) Axis. Journal of the Endocrine Society, 5 (Suppl 1), A1030.
- **Song X.,** Zhang M., Dai E., Luo Y. Molecular targets of curcumin in breast cancer (Review). Mol. Med. Rep. 2019, 19, 23–29.
- **Soon P.S.,** Tacon L.J., Gill A.J., Bambach C.P., Sywak M.S., Campbell P.R., Yeh M.W., Wong S.G., Clifton-Bligh R.J., Robinson B.G. et al. 2009. miR-195 and miR-483-5p Identified as Predictors of Poor Prognosis in Adrenocortical Cancer.

Clinical cancer research : an official journal of the American Association for Cancer Research 15(24): 7684-7692.

- **Sribalan R.,** Kirubavathi M., Banuppriya G., Padmini V. Synthesis and biological evaluation of new symmetric curcumin derivatives. Bioorg. Med. Chem. Lett. 2015, 25, 4282–4286.
- **Stein R.A.,** Chang C.Y, Kazmin D.A, Way J, Schroeder T, Wergin M, Dewhirst M.W, McDonnell D.P. 2008. Estrogen-related receptor alpha is critical for the growth of estrogen receptor-negative breast cancer. Cancer research 68(21): 8805-8812.
- **Stein R.A.,** Gaillard S, McDonnell D.P. 2009. Estrogen-related receptor alpha induces the expression of vascular endothelial growth factor in breast cancer cells. The Journal of steroid biochemistry and molecular biology 114(1-2): 106-112.
- **Stigliano A.,** Chiodini I, Giordano R, Faggiano A, Canu L, Della Casa S, Loli P, Luconi M, Mantero F, Terzolo M. 2016. Management of adrenocortical carcinoma: a consensus statement of the Italian Society of Endocrinology (SIE). Journal of endocrinological investigation 39(1): 103-121.
- **Stojadinovic A.,** Ghossein R.A, Hoos A, Nissan A, Marshall D, Dudas M, Cordon-Cardo C, Jaques D.P, Brennan M.F. 2002. Adrenocortical carcinoma: clinical, morphologic, and molecular characterization. Journal of clinical oncology : official journal of the American Society of Clinical Oncology 20(4): 941-950.
- **Suetsugi M.,** Su L, Karlsberg K, Yuan Y.C, Chen S. 2003. Flavone and isoflavone phytoestrogens are agonists of estrogen-related receptors. Molecular cancer research : MCR 1(13): 981-991.
- **Sullivan M.,** Boileau M, Hodges C.V. 1978. Adrenal cortical carcinoma. The Journal of urology 120(6): 660-665.
- **Surowiak P.,** Materna V, Gyorffy B, Matkowski R, Wojnar A, Maciejczyk A, Paluchowski P, Dziegiel P, Pudelko M, Kornafel J. et al. 2006. Multivariate analysis of oestrogen receptor alpha, pS2, metallothionein and CD24 expression in invasive breast cancers. British journal of cancer 95(3): 339-346.
- **Suzuki T.,** Miki Y, Moriya T, Shimada N, Ishida T, Hirakawa H, Ohuchi N, Sasano H. 2004. Estrogen-related receptor alpha in human breast carcinoma as a potent prognostic factor. Cancer research 64(13): 4670-4676.

- **Tacon L.J.,** Prichard R.S., Soon P.S, Robinson B.G., Clifton-Bligh R.J., Sidhu S.B. 2011. Current and emerging therapies for advanced adrenocortical carcinoma. The oncologist 16(1): 36-48.
- **Takeuchi S.,** Balachandran A, Habra M.A, Phan A.T, Bassett R.L, Macapinlac H.A, Chuang H.H. 2014. Impact of (1)(8)F-FDG PET/CT on the management of adrenocortical carcinoma: analysis of 106 patients. European journal of nuclear medicine and molecular imaging 41(11): 2066-2073.
- **Tan X.,** Sidell N., Mancini A., Huang R.P., Shenming W.; Horowitz I.R.; Liotta D.C.; Taylor R.N.; Wieser F. Multiple anticancer activities of EF24, a novel curcumin analog, on human ovarian carcinoma cells. Reprod. Sci. 2010, 17, 931–940.
- **Teng C.T.,** Hsieh J.H, Zhao J, Huang R, Xia M, Martin N, Gao X, Dixon D, Auerbach S.S, Witt K.L. et al. 2017. Development of Novel Cell Lines for High-Throughput Screening to Detect Estrogen-Related Receptor Alpha Modulators. SLAS discovery : advancing life sciences R & D 22(6): 720-731.
- **Teng C.T.,** Beames B, Alex Merrick B, Martin N, Romeo C, Jetten A.M. 2014. Development of a stable cell line with an intact PGC-1alpha/ERRalpha axis for screening environmental chemicals. Biochemical and biophysical research communications 444(2): 177-181.
- **Tennant D.A.,** Duran R.V., Gottlieb E. 2010. Targeting metabolic transformation for cancer therapy. Nature reviews Cancer 10(4): 267-277.
- **Terzolo M.,** Angeli A, Fassnacht M, Daffara F, Tauchmanova L, Conton P.A, Rossetto R, Buci L, Sperone P, Grossrubatscher E. et al. 2007. Adjuvant mitotane treatment for adrenocortical carcinoma. The New England journal of medicine 356(23): 2372-2380.
- **Terzolo M.,** Baudin A.E, Ardito A, Kroiss M, Leboulleux S, Daffara F, Perotti P, Feelders R.A, deVries J.H, Zaggia B. et al. 2013. Mitotane levels predict the outcome of patients with adrenocortical carcinoma treated adjuvantly following radical resection. European journal of endocrinology 169(3): 263-270.
- **Terzolo M.,** Stigliano A, Chiodini I, Loli P, Furlani L, Arnaldi G, Reimondo G, Pia A, Toscano V, Zini M. et al. 2011. AME position statement on adrenal incidentaloma. European journal of endocrinology 164(6): 851-870.

- Teyssier C., Gallet M, Rabier B, Monfoulet L, Dine J, Macari C, Espallergues J, Horard B, Giguere V, Cohen-Solal M et al. 2009. Absence of ERRalpha in female mice confers resistance to bone loss induced by age or estrogen-deficiency. PloS one 4(11): e7942.
- **Thomas S.L.,** Zhong D.; Zhou W.; Malik S.; Liotta D.; Snyder J.P.; Hamel E.; Giannakakou P. EF24, a novel curcumin analog, disrupts the microtubule cytoskeleton and inhibits HIF-1. Cell Cycle 2008, 7, 2409–2417.
- **Thorburn A.** Death receptor-induced cell killing. Cell Signal; 16: 139–44, 2004.
- **Tissier F.,** Cavard C, Groussin L, Perlemoine K, Fumey G, Hagnere AM, Rene-Corail F, Jullian E, Gicquel C, Bertagna X et al. 2005. Mutations of beta-catenin in adrenocortical tumors: activation of the Wnt signaling pathway is a frequent event in both benign and malignant adrenocortical tumors. Cancer research 65(17): 7622-7627.
- **Tomeh M.A.,** Hadianamrei R., Zhao, X. A review of curcumin and its derivatives as anticancer agents. Int. J. Mol. Sci. 2019, 20, 1033.
- **Tremblay A.M.,** Wilson B.J., Yang X.J., Giguere V. 2008. Phosphorylation-dependent sumoylation regulates estrogen-related receptor-alpha and -gamma transcriptional activity through a synergy control motif. Molecular endocrinology 22(3): 570-584.
- **Troselj K.G. & Kujundzic R.N**. 2014. Curcumin in combined cancer therapy. Curr Pharm Des 20: 6682– 6696
- van Erp NP, Guchelaar HJ, Ploeger BA, Romijn JA, Hartigh J, Gelderblom H. 2011. Mitotane has a strong and a durable inducing effect on CYP3A4 activity. European journal of endocrinology 164(4): 621-626.
- **van Koetsveld P.M.,** Vitale G., Feelders R.A., Waaijers M., Sprij-Mooij D.M., de Krijger R.R., Speel E.J., Hofland J., Lamberts S.W., de Herder W.W. et al. 2013. Interferon-beta is a potent inhibitor of cell growth and cortisol production in vitro and sensitizes human adrenocortical carcinoma cells to mitotane. Endocrine-related cancer 20(3): 443-454.
- **van Slooten H.,** Moolenaar A.J., van Seters A.P., Smeenk D. 1984. The treatment of adrenocortical carcinoma with o,p'-DDD: prognostic implications of serum level monitoring. European journal of cancer & clinical oncology 20(1): 47-53.

- **Vanacker J.M.,** Bonnelye E, Delmarre C, Laudet V. 1998a. Activation of the thyroid hormone receptor alpha gene promoter by the orphan nuclear receptor ERR alpha. Oncogene 17(19): 2429-2435.
- **Vanacker J.M.,** Delmarre C, Guo X, Laudet V. 1998b. Activation of the osteopontin promoter by the orphan nuclear receptor estrogen receptor related alpha. Cell growth & differentiation : the molecular biology journal of the American Association for Cancer Research 9(12): 1007-1014.
- **Vaughan E.D., Jr.** 2004. Diseases of the adrenal gland. The Medical clinics of North America 88(2): 443-466.
- **Villena J.A. & Kralli A**. ERRα: a metabolic function for the oldest orphan. Trends Endocrinol Metab. 19(8): 269- 276, 2008.
- **Walker B.C. & Mittal S**. Antitumor activity of curcumin in glioblastoma. Int. J. Mol. Sci. 2020, 21, 9435.
- **Walter P.,** Green S., Greene G, Krust A, Bornert JM, Jeltsch JM, Staub A, Jensen E, Scrace G, Waterfield M. et al. 1985. Cloning of the human estrogen receptor cDNA. Proceedings of the National Academy of Sciences of the United States of America 82(23): 7889-7893.
- **Wang C.,** Li P, Xuan J, Zhu C, Liu J, Shan L, Du Q, Ren Y, Ye J. 2017. Cholesterol Enhances Colorectal Cancer Progression via ROS Elevation and MAPK Signaling Pathway Activation. Cellular physiology and biochemistry: international journal of experimental cellular physiology, biochemistry, and pharmacology 42(2): 729-742.
- **Wang H.,** Zhang K.; Liu J.; Yang J.; Tian Y.; Yang C.; Li Y.; Shao M.; Su W.; Song N. Curcumin regulates cancer progression: Focus on ncRNAs and molecular signaling pathways. Front. Oncol. 2021, 11, 660712.
- **Wang L.,** Ye X., Cai X., Su J., Ma R., Yin X., Zhou X., Li H., Wang Z. Curcumin suppresses cell growth and invasion and induces apoptosis by down-regulation of Skp2 pathway in glioma cells. Oncotarget 2015, 6, 18027–18037.
- **Wang N.,** Feng T., Liu X., Liu Q. Curcumin inhibits migration and invasion of non-small cell lung cancer cells through up-regulation of miR-206 and suppression of PI3K/AKT/mTOR signaling pathway. Acta Pharm. 2020, 70, 399–409.

- **Wang X.,** Deng J.; Yuan J.; Tang X.; Wang Y.; Chen H.; Liu Y.; Zhou L. Curcumin exerts its tumor suppressive function via inhibition of NEDD4 oncoprotein in glioma cancer cells. Int. J. Oncol. 2017, 51, 467–477.
- **Wanninger S.,** Lorenz V., Subhan A., Edelmann F.T. Metal complexes of curcumin–synthetic strategies, structures and medicinal applications. Chem. Soc. Rev. 2015, 44, 4986–5002.
- **Warburg O.** 1956. On the origin of cancer cells. Science 123(3191): 309-314.
- **Warner M. & Gustafsson J.A.** 2014. On estrogen, cholesterol metabolism, and breast cancer. The New England journal of medicine 370(6): 572-573.
- **Watson J.L.,** Hill R.; Yaffe P.B.; Greenshields A.; Walsh M.; Lee P.W.; Giacomantonio C.A.; Hoskin, D.W. Curcumin causes superoxide anion production and p53-independent apoptosis in human colon cancer cells. Cancer Lett. 2010, 297, 1–8.
- **Wei W.,** Schwaid A.G, Wang X, Wang X, Chen S, Chu Q, Saghatelian A, Wan Y. 2016. Ligand Activation of ERRalpha by Cholesterol Mediates Statin and Bisphosphonate Effects. Cell metabolism 23(3): 479-491.
- **Williamson S.K.,** Lew D, Miller G.J, Balcerzak S.P, Baker L.H, Crawford E.D. 2000. Phase II evaluation of cisplatin and etoposide followed by mitotane at disease progression in patients with locally advanced or metastatic adrenocortical carcinoma: a Southwest Oncology Group Study. Cancer 88(5): 1159-1165.
- **Willy P.J.,** Murray I.R, Qian J, Busch B.B, Stevens W.C, Jr., Martin R, Mohan R, Zhou S, Ordentlich P, Wei P et al. 2004. Regulation of PPARgamma coactivator 1alpha (PGC-1alpha) signaling by an estrogen-related receptor alpha (ERRalpha) ligand. Proceedings of the National Academy of Sciences of the United States of America 101(24): 8912-8917.
- **Wilson B.J.,** Tremblay A.M, Deblois G, Sylvain-Drolet G, Giguere V. 2010. An acetylation switch modulates the transcriptional activity of estrogen-related receptor alpha. Molecular endocrinology 24(7): 1349-1358.
- **Wilson M.C.,** Meredith D, Fox J.E, Manoharan C, Davies A.J, Halestrap A.P. 2005. Basigin (CD147) is the target for organomercurial inhibition of monocarboxylate transporter isoforms 1 and 4: the ancillary protein for the insensitive MCT2 is EMBIGIN (gp70). The Journal of biological chemistry 280(29): 27213-27221.

- **Wilson M.R.** Apoptosis: unmasking the executioner. Cell Death Differ. 646-652, 1998.
- **Wong K.K.,** Arabi M, Zerizer I, Al-Nahhas A, Rubello D, Gross M.D. 2011. Role of positron emission tomography/computed tomography in adrenal and neuroendocrine tumors: fluorodeoxyglucose and nonfluorodeoxyglucose tracers. Nuclear medicine communications 32(9): 764-781.
- **Wood B.J.,** Abraham J, Hvizda J.L, Alexander H.R, Fojo T. 2003. Radiofrequency ablation of adrenal tumors and adrenocortical carcinoma metastases. Cancer 97(3): 554-560.
- **Wortmann S.,** Quinkler M, Ritter C, Kroiss M, Johanssen S, Hahner S, Allolio B, Fassnacht M. 2010. Bevacizumab plus capecitabine as a salvage therapy in advanced adrenocortical carcinoma. European journal of endocrinology 162(2): 349-356.
- **Wu Q.,** Ishikawa T, Sirianni R, Tang H, McDonald J.G, Yuhanna I.S, Thompson B, Girard L, Mineo C, Brekken R.A et al. 2013. 27-Hydroxycholesterol promotes cell-autonomous, ER-positive breast cancer growth. Cell reports 5(3): 637-645.
- **Xiang L.,** He B., Liu Q., Hu D., Liao W., Li R., Peng X., Wang Q., Zhao G. Antitumor effects of curcumin on the proliferation, migration and apoptosis of human colorectal carcinoma HCT116 cells. Oncol. Rep. 2020, 44, 1997–2008.
- **Xu J.,** Wu R.C, O'Malley B.W. 2009. Normal and cancer-related functions of the p160 steroid receptor co-activator (SRC) family. Nature reviews Cancer 9(9): 615-630.
- **Xu Y.Z.,** Zhu Y, Shen Z.J, Sheng J.Y, He H.C, Ma G, Qi Y.C, Zhao J.P, Wu Y.X, Rui W.B et al. 2011. Significance of heparanase-1 and vascular endothelial growth factor in adrenocortical carcinoma angiogenesis: potential for therapy. Endocrine 40(3): 445-451.
- **Xu G.,** Chu Y., Jiang N., Yang J., Li F. The three dimensional quantitative structure activity relationships (3D-QSAR) and docking studies of curcumin derivatives as androgen receptor antagonists. Int. J. Mol. Sci. 2012, 13, 6138–6155.
- **Yallapu M.M.,** Jaggi M., Chauhan S.C. beta-Cyclodextrin-curcumin self-assembly enhances curcumin delivery in prostate cancer cells. Colloids Surf. B Biointerfaces 2010, 79, 113–125

- **Yang C.,** Zhou D., Chen S. 1998. Modulation of aromatase expression in the breast tissue by ERR alpha-1 orphan receptor. Cancer research 58(24): 5695-5700.
- **Yang N.,** Shigeta H, Shi H, Teng C.T. 1996. Estrogen-related receptor, hERR1, modulates estrogen receptor-mediated response of human lactoferrin gene promoter. The Journal of biological chemistry 271(10): 5795-5804.
- **Yang C.L.,** Liu Y.Y., Ma Y.G., Xue Y.X., Liu D.G., Ren Y., Liu X.B., Li Y., Li Z. Curcumin blocks small cell lung cancer cells migration, invasion, angiogenesis, cell cycle and neoplasia through Janus kinase-STAT3 signalling pathway. PLoS ONE 2012, 7, e37960.
- **Yang S.,** Liu L., Han J., Tang Y. Encapsulating plant ingredients for dermocosmetic application: An updated review of delivery systems and characterization techniques. Int. J. Cosmet. Sci. 2020, 42, 16–28.
- **Ye X.,** Guo J., Zhang H., Meng Q., Ma Y., Lin R., ... & Cheng J. (2019). The enhanced expression of estrogen- related receptor α in human bladder cancer tissues and the effects of estrogen- related receptor α knockdown on bladder cancer cells. Journal of cellular biochemistry, 120(8), 13841-13852.
- **Yerdelen K.O.,** Gul H.I., Sakagami H., Umemura N., Sukuroglu M. Synthesis and cytotoxic activities of a curcumin analogue and its bis-mannich derivatives. Lett. Drug Des. Discov. 2015, 12, 643–649.
- **Yin D.L.,** Liang Y.J., Zheng T.S., Song R.P., Wang J.B., Sun B.S., Pan S.H., Qu L.D., Liu J.R., Jiang H.C. et al. EF24 inhibits tumor growth and metastasis via suppressing NF-kappaB dependent pathways in human cholangiocarcinoma. Sci. Rep. 2016, 6, 32167
- **Yoon J.C.,** Puigserver P., Chen G., Donovan J., Wu Z., Rhee J., Adelmant G., Stafford J., Kahn C.R, Granner D.K. et al. 2001. Control of hepatic gluconeogenesis through the transcriptional coactivator PGC-1. Nature 413(6852): 131-138.
- **Yu C.,** Yang B. & Najafi M. (2021). Targeting of cancer cell death mechanisms by curcumin: Implications to cancer therapy. Basic & clinical pharmacology & toxicology, 129(6), 397-415.

- **Yu H.,** Lin L., Zhang Z., Zhang H., Hu H. Targeting NF-kappaB pathway for the therapy of diseases: Mechanism and clinical study. Signal Transduct. Target. Ther. 2020, 5, 209.
- **Zanotelli M.R.,** Zhang J. & Reinhart-King C.A. (2021). Mechanoresponsive metabolism in cancer cell migration and metastasis. Cell Metabolism, 33(7), 1307-13
- **Zhang A.** A rapid and simple method for measuring the susceptibility of low-density- lipoprotein and very-low-density- lipoprotein to copper catalyzed oxidation. Clin. Chim. Acta, 227: 159-173, 1994.
- **Zhang H.,** Nie W.; Zhang X.; Zhang G.; Li Z.; Wu H.; Shi Q.; Chen Y.; Ding Z.; Zhou X. et al. NEDD4-1 regulates migration and invasion of glioma cells through CNrasGEF ubiquitination in vitro. PLoS ONE 2013, 8, e82789.
- **Zhang L.,** Yang G.; Zhang R.; Dong L.; Chen H.; Bo J.; Xue W.; Huang Y. Curcumin inhibits cell proliferation and motility via suppression of TROP2 in bladder cancer cells. Int. J. Oncol. 2018, 53, 515–526.
- **Zhang Y.P.,** Li Y.Q., Lv Y.T., Wang J.M. Effect of curcumin on the proliferation, apoptosis, migration, and invasion of human melanoma A375 cells. Genet. Mol. Res. 2015, 14, 1056–1067
- **Zhao C.,** Liu Z., Liang G. Promising curcumin-based drug design: Mono-carbonyl analogues of curcumin (MACs). Curr. Pharm. Des. 2013, 19, 2114–2135.
- **Zhao G.,** Han X.; Zheng S.; Li Z.; Sha Y.; Ni J.; Sun Z.; Qiao S.; Song Z. Curcumin induces autophagy, inhibits proliferation and invasion by downregulating AKT/mTOR signaling pathway in human melanoma cells. Oncol. Rep. 2016, 35, 1065–1074.
- **Zheng B. & McClements D.J.** Formulation of more efficacious curcumin delivery systems using colloid science: Enhanced solubility, stability, and bioavailability. Molecules 2020, 25, 2791.
- **Zhong Y.,** He K., Shi L., Chen L., Zhou B., Ma R., ... & Lu J. (2021). Down-regulation of estrogen-related receptor alpha (ERRα) inhibits gastric cancer cell migration and invasion in vitro and in vivo. Aging (Albany NY), 13(4), 5845.

- **Zhou Q.,** Ye M., Lu Y.; Zhang H.; Chen Q.; Huang S.; Su S. Curcumin improves the tumoricidal effect of mitomycin C by suppressing ABCG2 expression in stem cell-like breast cancer cells. PLoS ONE 2015, 10, e0136694.
- **Zhou Q.M.,** Wang X.F., Liu X.J., Zhang H., Lu Y.Y., Su S.B. Curcumin enhanced antiproliferative effect of mitomycin C in human breast cancer MCF-7 cells in vitro and in vivo. Acta Pharmacol. Sin. 2011, 32, 1402–1410.
- **Zhou X.,** Jiao D., Dou M., Zhang W.. Lv L., Chen J., Li L., Wang L., Han X. Curcumin inhibits the growth of triple-negative breast cancer cells by silencing EZH2 and restoring DLC1 expression. J. Cell. Mol. Med. 2020, 24, 10648–10662.
- **Zou P.,** Xia Y., Chen W., Chen X.; Ying S.; Feng Z.; Chen T.; Ye Q.; Wang Z.; Qiu C. et al. EF24 induces ROS-mediated apoptosis via targeting thioredoxin reductase 1 in gastric cancer cells. Oncotarget 2016, 7, 18050–18064.

Scientific Publications

SCIENTIFIC PUBLICATIONS

- Casaburi I., De Luca A., **Nocito M.C.** Sculco S., Avena P., Chimento A., Trotta F., Sirianni R., Pezzi V. Cholesterol as an endogenous ERRα agonist: a new perspective to cancer treatment. Frontiers in Endocrinology, 2018.

- Trotta, F., Avena, P., Chimento, A., Rago, V., De Luca, A., Sculco, S. **Nocito, M.C.,** Malivindi, R., Fallo, F., Pezzani, R., Pilon, C., Lasorsa, F.M., Barile, S.N., Palmieri, L., Lerario, A.M., Pezzi, V., Casaburi. I., Sirianni, R. (2020). Statins reduce intratumor cholesterol affecting adrenocortical cancer growth. Molecular Cancer Therapeutics, 19(9), 1909-1921.

- **Nocito M.C.,** Saraithong P., Newman E. A., Thomas I. H., Rainey W. E., Lerario A. M., Heider A., Else T. SUN-931 Characterization of an Ovarian Steroid Cell Tumor in a VHL Patient. J Endocr Soc., 2020 (Abstract)

- Chimento A., De Luca A., **Nocito M.C.,** Avena P., La Padula D., Zavaglia L., Pezzi V. Role of GPER-Mediated Signaling in Testicular Functions and Tumorigenesis. Cells., 2020

- Chimento A., De Luca A., **Nocito M.C.,** Sculco S., Avena P., La Padula D., Zavaglia L., Sirianni R., Casaburi I., Pezzi V. SIRT1 is involved in adrenocortical cancer growth and motility. J Cell Mol Med., 2021

- **Nocito M.C.,** De Luca A., Prestia F., Avena P., La Padula D., Zavaglia L., Sirianni R., Casaburi I., Puoci F., Chimento A., Pezzi V. Antitumoral Activities of Curcumin and Recent Advances to ImProve Its Oral Bioavailability. Biomedicines, 2021

- Avena P., Casaburi I., Zavaglia L., **Nocito M.C.,** La Padula D., Rago V., Dong J., Thomas P., Mineo C., Sirianni R. 27-Hydroxycholesterol binds GPER and induces progression of Estrogen Receptor-Negative Breast Cancer. Cancers, 2022.

frontiers in Endocrinology

REVIEW
published: 11 September 2018
doi: 10.3389/fendo.2018.00525

Cholesterol as an Endogenous ERRα Agonist: A New Perspective to Cancer Treatment

Ivan Casaburi†, Adele Chimento†, Arianna De Luca, Marta Nocito, Sara Sculco, Paola Avena, Francesca Trotta, Vittoria Rago, Rosa Sirianni‡ and Vincenzo Pezzi‡*

Department of Pharmacy and Health and Nutritional Science, University of Calabria, Cosenza, Italy

OPEN ACCESS

Edited by:
Antimo Migliaccio, Università degli Studi Della Campania "Luigi Vanvitelli" Naples, Italy

Reviewed by:
Didier Picard, Université de Genève, Switzerland
Roberta Malaguarnera, Università Degli Studi Magna Græcia di Catanzaro, Italy

***Correspondence:**
Vincenzo Pezzi
v.pezzi@unical.it

†These authors share co-first authorship

‡These authors share co-last authorship

Specialty section:
This article was submitted to Cancer Endocrinology, a section of the journal Frontiers in Endocrinology

Received: *08 June 2018*
Accepted: *21 August 2018*
Published: *11 September 2018*

Citation:
Casaburi I, Chimento A, De Luca A, Nocito M, Sculco S, Avena P, Trotta F, Rago V, Sirianni R and Pezzi V (2018) Cholesterol as an Endogenous ERRα Agonist: A New Perspective to Cancer Treatment. Front. Endocrinol. 9:525. doi: 10.3389/fendo.2018.00525

The estrogen-related receptors (ERRs) are important members of nuclear receptors which contain three isoforms (α, β, and γ). ERRα is the best-characterized isoform expressed mainly in high-energy demanding tissues where it preferentially works in association with the peroxisome proliferator-activated receptor-γ co-activator 1α (PGC-1α) and PGC-1β. ERRα together with its cofactors modulates cellular metabolism, supports the growth of rapidly dividing cells, directs metabolic programs required for cell differentiation and maintains cellular energy homeostasis in differentiated cells. In cancer cells, the functional association between ERRα and PGC-1s is further influenced by oncogenic signals and induces metabolic programs favoring cell growth and proliferation as well as tumor progression. Recently, cholesterol has been identified as a natural ERRα ligand using a combined biochemical strategy. This new finding highlighted some important physiological aspects related to the use of cholesterol-lowering drugs such as statins and bisphosphonates. Even more meaningful is the link between increased cholesterol levels and certain cancer phenotypes characterized by an overexpressed ERRα such as mammary, prostatic, and colorectal cancers, where the metabolic adaptation affects many cancer processes. Moreover, high-energy demanding cancer-related processes are strictly related to the cross-talk between tumor cells and some key players of tumor microenvironment, such as tumor-associated macrophage that fuels cancer progression. Some evidence suggests that high cholesterol content and ERRα activity favor the inflammatory environment by the production of different cytokines. In this review, starting from the most recent observations on the physiological role of the new signaling activated by the natural ligand of ERRα, we propose a new hypothesis on the suitability to control cholesterol levels as a chance in modulating ERRα activity in those tumors in which its expression and activity are increased.

Keywords: ERRα, cholesterol, cancer metabolism, breast and prostate cancer, colonrectal cancer, adrenocortical carcinoma (ACC), IL-8

GENERAL CONCEPT

Nuclear receptors (NRs) are a large family of transcription factors that are activated by different signal molecules such as steroids, thyroid hormones, vitamins, retinoic acid, oxysterols, and many other metabolites (1).

A distinct subset of the NRs still remains "orphans" (ONRs) waiting for a defined endogenous ligand. Once activated, NRs together with a multitude of co-factors, drive transcription of genes that control cell proliferation, development, reproduction, and different metabolic phenomena upon which those processes are strictly dependent.

A proper functional control of energy pathways within the cells is supported by the coordination of several transcription factors, including NRs, and associated co-factors. Many members of NR superfamily are involved in these processes since they can activate a specific gene expression network in response to hormonal, nutrient, and metabolite signals coming from distinct physiological (or pathological) conditions (2).

ERRs Structure

The estrogen-related receptors (ERRs) are important members of the ONRs family, deeply involved in the control of energy homeostasis. The ERR subfamily comprises three isoforms, namely ERRα (NR3B1), ERRβ (NR3B2), and ERRγ (NR3B3).

ERRα (45.5kDa, 423a.a.) and β (56.2kDa, 508a.a.) were first identified by screening human male gonad cDNA library with a probe synthesized based on the DNA-binding domain sequence of estrogen receptor alpha (ERα) and ERRα cDNA as a probe, respectively (3). The discovery of the third member, ERRγ (51.3kDa, 45a.a.), was made 10 years later by a different methodological approach (4, 5). In addition, several splice variants of human ERRs have been identified although their physiological role is still to be discovered (6). Despite their name and sequence homology with ERs, they do not bind natural estrogens. Moreover, although the existence of functional crosstalk between ERRs and ERs cannot be ruled out, especially in breast cancer pathology, a deeper investigation revealed that ERRs, particularly ERRα, and ERα have a distinct genomic signature and functions (7).

As members of the nuclear receptor superfamily, ERRs are characterized by a conserved structural and functional organization consisting of:

- A N–terminal region (A/B domain) that contains a ligand-independent transcriptional activation function domain (AF-1). The AF-1 domain of all three ERR isoforms contains conserved motifs that allow the control of the transcriptional activity by post-translational modification such as phosphorylation and sumoylation. In particular, phosphorylation-dependent sumoylation of ERRα within the NH-terminal domain of ERRα and ERRγ negatively affects their transcriptional activity without altering DNA binding with cofactors (8). This mechanism becomes particularly important considering the absence of a specific/natural ligand and the constitutively active conformation of this class of receptors that make their functions dependent on the presence of coactivators and corepressor proteins (see below);
- A central C domain, also known as DNA binding domain or DBD, a sequence shared by almost all three ERR members. DBD allows the recognition of DNA sites through the TNAAGGTCA sequence also known as ERR responsive elements or ERREs. In the DBD there are two digitally shaped helical structures, called "zinc fingers," in which a zinc ion is coordinated with 4 cysteines. The P-box (proximal box), placed in the first helical structure, enables the recognition of a specific DNA sequence, while the D-box (distal box), placed in the second structure, is involved in the dimerization process on the DNA sequences. Indeed, ERRs can interact with an ERRE sequence as a monomer, homodimer or as a heterodimer consisting of two distinct ERR isoforms (9–11);
- A region linking C to Ligand Binding Domain (LBD);
- A ligand binding domain or LBD, which adopts a transcriptionally active conformation in the absence of any ligand (12);
- A less conserved C-terminal F region, which is present only in some nuclear receptors, including the ERs.

The sequence analysis of all three receptor isoforms reveals a different sequence homology in their domains: all three members show a high sequence identity in their DBD (93–98%); regarding the LBD, ERRα, and ERRβ are less related (57%) while that of ERRβ and ERRγ are closer (73% sequence identity). The latter domain exhibits a 63% sequence identity between ERRα and ERRγ; high level of sequence identity in the A/B domain (60%) characterizes ERRβ and ERRγ (13).

According to their discovery, ERR isoforms are more strongly related to estrogen receptors (ERα and β) than to any other member of the NR superfamily. In particular, the analysis of each individual domain reveals that the DBDs of ERRα and ERα are 70% homologues, but their LBD is only 36% similar, explaining the reasons for the absence of ERRα response to ER ligands (12).

ERRα: Function, Regulation, and Activity

ERRα discovery determined straightaway questions about its physiological function: ERRα plays a role in embryonic development and its expression level is high in the heart, skeletal muscles, and nervous system. The main physiological role of ERRα is to act as energy sensor to control cellular adaptation to energy demands and to respond to various metabolic stress conditions. Therefore, ERRα is present in high-demand energy tissues, such as muscles and brown adipose tissue. Cells that do not express an activated ERRα cannot produce enough energy at peak demand moments.

In adipose tissue, ERRα promotes the differentiation of mesenchymal stem cells into adipocytes where it regulates energy metabolism. In fact, ERRα increases lipid absorption, β-oxidation, tricarboxylic acid cycle, oxidative phosphorylation, and mitochondrial biogenesis and functions. These metabolic effects are clearly noticeable in all those tissues with high-energy demand including cardiomyocytes and cells of the immune system like macrophages. The prominent role of ERRα in metabolic regulation is underlined by the demonstration

that ERRα gene knockout (ERRα-KO) mice have altered fat absorption and metabolism and are resistant to fat-induced obesity (14). Moreover, these mice are not able to adapt to the cold environment and develop cardiac contraction dysfunction. Stress-induced cardiac hypertrophy in ERRα-KO mice is caused by poor ATP synthesis and reduced phosphocreatine deposition (15).

ERRα influences the differentiation of myocytes, T cells, intestinal epithelial cells and osteoblasts. A study showed that ERRα plays a key role in bone development and metabolism during embryogenesis (16). Its mRNA is expressed in murine bone cells during bone formation by endochondral and intramembranous ossification as well as in primary human osteoblasts. ERRα influences the transcription of the gene coding for osteopontin an essential constituent of the mineralized extracellular bone matrix. In the ERRα-KO mice, the loss of ERRα gene expression modestly increased osteoblastic differentiation and spongy bone mineral density, as well as the differentiation of mesenchymal cells into osteoblasts (17).

The constitutive activity of ERRα is structurally related to the presence of a phenylalanine residue (Phe^{328} on helix H3) within its LBD which maintains a conformational arrangement suitable for the interaction with different cofactors (18). ERRα transcriptional activity is dependent on the presence of co-regulatory proteins, which are differentially expressed in various cells and tissues. ERRα preferentially works in association with the peroxisome proliferator-activated receptor-γ receptor (PPARγ) co-activator-1α (PGC-1α) and PGC-1β (18). The functional interaction between ERRα and PGC-1s is highly specific and it is essential for full ERRα receptor activity in most cells. Moreover, ERRα together with PGC-1s integrates many intracellular signals arising from extrinsic/intrinsic metabolic stresses, as well as from growth factors (18).

The activity of ERRα has been examined by the study on the transcriptional co-activators PGC-1α and PGC-1β, which integrate the signals on nutritional and energetic status and drive expression of genes that control mitochondrial biogenesis, oxidative metabolism, and gluconeogenesis.

The ability of the co-activator PGC-1α to favor the activation of target genes is based on its recruitment at the level of gene-specific regulatory sites through physical interactions with NRs and other transcription factors. Regarding the NRs, the amphipathic propellers of PGC-1α bind the hydrophobic region of LBD domain while PGC-1α has a surface that interacts specifically with ERRα. Moreover, ERRα is a powerful transcriptional activator when PGC-1α or PGC-1β are introduced into the system. The tight dependency between ERRα and PGC-1s as the result of the high affinity between ERRα and PGC-1s, suggests that ERRα activity is mainly controlled by the interactions with PGC-1α and β. In addition, PGC-1s are also able to modulate ERRα gene expression (19). Consistent with the ability of PGC-1 co-activators to induce ERRα expression, ERRα mRNA levels are higher in tissues with elevated levels of PGC-1α and β (19).

Given the predominant role of PGC-1s/ERRα transcriptional complex in controlling cellular metabolism, its involvement in the process of tumorigenesis is evident, considering that metabolic adaptations is an hallmark of cancer cells (20). Nevertheless, there are still many aspects to be clarified. In normal cells, the activity of the PGC-1s/ERRα axis is directed to increase cellular metabolism, to support the growth of rapidly dividing cells, to control metabolic programs during cell differentiation and to preserve energy homeostasis once differentiated (13). In cancer cells, the PGC-1s/ERRα complex is a direct target of oncogenic signals that affect metabolic programs in order to favor or attenuate cell growth and proliferation (18). Moreover, PGC-1α-mediated mitochondrial biogenesis and respiration in cancer cells is functionally related to metastatic dissemination (21). Accordingly, PGC-1α gene suppression, by disabling mitochondrial biogenesis and oxidative phosphorylation, decreases the rate of metastasis (21). These findings are also supported by the observations that:

- ERRα together with its coactivator PGC-1α binds to the promoter and regulates the expression of vascular endothelial growth factor (VEGF), a master regulator of tumor invasion and angiogenesis (22, 23);
- ERRα is able to regulate the expression of HIF (hypoxia-inducible factor) in breast cancer cells and to associate with the HIFα/β heterodimer to promote its transcriptional activity on genes involved in angiogenesis and cell migration (23, 24).
- ERRα cooperates with HIF to induce the cancer metabolic reprogramming toward the metastatic-promoting glycolytic state (25).
- ERRα, together with its coactivator PGC-1α, regulates the expression of WNT11, a mechanism involving ERRα in a transcriptional complex with β-catenin (26). In fact, ablation of either ERRα or β-catenin expression decreases the migratory ability of different types of cancer cells. In addition, functional genomic studies have identified further ERRα target genes playing an important role in the process of invasion, migration and tumor vascularization (27).

All these observations highlight the pivotal role of ERRα in many (altered) processes that characterize tumors especially those signaling driving tumor progression and aggressiveness.

ERRα Agonists

The constitutive activity of ERRα does not exclude the existence of a molecule able to modulate its activity enabling the recruitment of cofactors and playing a critical role in the maintenance of energy homeostasis as well as in disease progression. Recently, several synthetic antagonists have been identified (28–30). Moreover, dietary products, including cholesterol, have been reported as potential agonists (31, 32). Suetsugi and collaborators identified agonists through virtual ligand screening on an ERRα ligand binding model based on the crystalline structure of ERRγ-LBD (33). Thus, four ligands, increasing the transcriptional activity of ERRα, have been identified: isoflavones (genistein, daidzein, and biochanin A) and a flavone (trihydroxyflavone) (33). Later, scientists synthesized the potential molecules able to interact with the ligand-domain, guided by ERRα crystalline structure, but they were not able to demonstrate the activity of the agonists (34). Moreover, Peng and collaborators synthesized a series of pyrid (1,2-α) pyrimidin-4 in

order to produce more powerful ERRα agonists and to confirm the ability to induce the receptor transcriptional activity (35). These compounds have improved glucose and fatty acid uptake from muscle cells (35) and thus, could have a clinical utility for the treatment of metabolic diseases, including metabolic syndrome and diabetes.

Cholesterol: The First Endogenous ERRα Agonist

Recently, an important study investigated the binding ability of ERRα with endogenous lipids (36). To this aim experiments by using chromatography techniques were performed according to previous approaches validated for the study of PPAR with endogenous lipids from the lipidome. The experimental model used is the mouse brain, selected for the high expression of ERRα. The receptor was expressed, purified, and immobilized onto a resin and then incubated with enriching lipidomes. This experimental approach allowed the identification of a single ion that was significantly enriched by the beads bound to ERR-LBD and this ion was identified as cholesterol. Furthermore, to check the specificity of the interaction between ERRα and cholesterol, authors used targeted LC-MS method to increase the detection sensitivity for the lower-abundance sterols (37). The latter results were in agreement with those from lipidomic experiments. Moreover, in order to verify the specificity of ERRα-LBD-cholesterol interaction, a deeper investigation was performed with a competitive binding assay by using diethylstilbestrol (DES), a synthetic ERRα antagonist, that binds to the lipid-binding pocket of ERRα (38). A further confirmation was obtained by the authors with circular dichroism (CD) spectroscopy tests, where cholesterol, DES and the inverse agonist XCT790, all induced a conformational change in ERRα-LBD, while estradiol did not. These results suggested that Cholesterol-ERRα-LBD binding is more than a simple hydrophobic interaction. In addition, dye-labeled cholesterol derivatives were used and, after fluorescence polarization assay, the results showed that cholesterol binds the ligand-binding pocket of ERRα through its hydroxyl group. These findings indicate that cholesterol could exert a functional control of the ERRα activity (36).

Cholesterol Regulates ERRα Transcriptional Activity

The demonstration that cholesterol impacts ERRα activity comes from the investigation during the osteocalciogenesis process. It has been revealed that ERRα-KO mice have a decreased bone resorption and high bone mass indicating that ERRα is able to promote osteoclast differentiation and activity. The suppression of the osteoclast functions was achieved by the use of statins and nitrogen-containing bisphosphonates, two drugs able to inhibit cholesterol biosynthesis, by blocking the HMG-CoA reductase and farnesyl diphosphate synthase (FPPS), respectively (39, 40). Interestingly, in the absence of ERRα, osteoclast differentiation was neither enhanced by cholesterol nor suppressed by statins. In addition, pharmacological inhibition with XCT790 prevented the effects of cholesterol on parental osteoclasts differentiation. All this data strongly supported the ability of cholesterol to promote osteoclastogenesis acting as an ERRα agonist, whereas statins and bisphosphonates suppressed osteoclastogenesis by reducing cholesterol bioavailability.

Moreover, a further demonstration of the ability of cholesterol to modulate the transcriptional activity of ERRα comes out from conventional transactivation assays by using luciferase as the reporter gene. Indeed, the authors decided to modulate cholesterol abundance in the culture medium. To realize this goal, intracellular sterol levels were reduced by: (i) using lipid-free serum, (ii) adding cholesterol bound to hydroxypropyl cyclodextrin, and (iii) adding the hydrophobic statin, lovastatin.

Cyclodextrin and statin, used as a single agent or as combined treatment, were able to reduce ERRα transactivation. Moreover, the addition of exogenous cholesterol to the samples treated with statins and/or cyclodextrin restored the transcriptional activity of the receptor. This data indicated that cholesterol or a downstream sterol, but not a precursor of the cholesterol pathway, affected ERRα activity. An interesting aspect from the results of the research study by Wei et al. (36), is the need for the presence of cofactors to make ERRα functional, even in the presence of an endogenous ligand. In fact, experiments performed with a silenced PGC-1α gene, revealed that luciferase expression was no longer detectable upon cholesterol treatment even in the presence of ectopic ERRα. These results clearly indicate that cholesterol, and most likely other sterols, affects ERRα function in a PGC-1α-dependent fashion. The authors demonstrated also that ERRα is able to recruit PGC-1α and PGC-1β upon cholesterol addition, but upon cholesterol depletion, PGC-1 coactivators are dissociated from ERRα. Specifically, cholesterol enhances the interaction between ERRα and PGC-1β in osteoclast promoting osteoclastogenesis and bone resorption, while promotes ERRα interaction with PGC-1α in myocytes inducing myogenesis and decreasing statins-induced muscle toxicity.

Cholesterol-Lowering Drugs Use and Outcome of Cancer Patients

Many experimental evidence strongly suggest that the inhibition of the mevalonate pathway using statin or bisphosphonate drugs has an impact on oncogenic processes such as cell proliferation, tumor progression, and metastatic potential (41). Statins are inhibitors of HMG-CoA reductase, that block the mevalonate pathway progression limiting the accumulation of the final products such as cholesterol, dolichol, isoprenoids, ubiquinone, and isopentenyladenine (42, 43).

Effects of statins on the outcome of patients affected by different types of cancer, including breast (44, 45), prostate (46–48), ovarian (49), lymphoma (50), renal cell carcinoma (51), and colorectal (52, 53) cancer have been examined in the last years. Some of these studies suggests that statins use is associated with longer survival, while others report no benefits. A recent meta-analysis showed that the average effect of statin use is beneficial for overall survival and cancer-specific survival (54). In particular, the study specified that colorectal, prostate, and

breast cancers, the three largest cancer-type subgroups, showed a benefit from statins use (54). Interestingly, these three tumors are characterized by high expression of ERRα that, depending on the particular tumor phenotype, is associated with tumor progression and/or worst prognosis (55, 56).

Statins may exert their anticancer effect through several molecular mechanisms: via lowering protein prenylation, reducing tumor cell proliferation and migration, inhibiting rat sarcoma (Ras) signaling, inducing apoptosis through inhibition of Akt phosphorylation and consequently mammalian target of rapamycin (mTOR) down-regulation and other pleiotropic effects on cellular level (57, 58).

Bisphosphonates, especially nitrogen-containing bisphosphonates (N-BPs), are widely used to preserve bone health in patients with cancer thank to their ability to negatively regulate osteoclast-mediated bone resorption that is closely associated with metastasis in different cancer types (59). N-BPs work by interfering with two enzymes belonging to the mevalonate pathway called farnesyl pyrophosphate synthase (FPPS) and geranylgeranyl pyrophosphate synthase (GGPPS). The inhibition of mevalonate pathway by N-BPs results in the accumulation of isopentenyl pyrophosphate (IPP), which is then converted to a cytotoxic ATP analog called ApppI. This last event together with the N-BPs-induced inhibition of protein prenylation causes osteoclast dysfunction and reduced bone resorption. Similarly to studies on statins, epidemiological data projecting bisphosphonates as antitumor agents are still controversial. Although further studies are needed to better elucidate the antitumor effects of bisphosphonates, the general concept that is drawn from current available data (60) is that bisphosphonates reduce cancer metastatic lesions in non-solid as well as in solid tumors. Indeed, in addition to their clinical use to preserve bone tissue, emerging *in vitro* and clinical studies suggest that N-BSs have direct effects on cancer cells including induction of apoptosis, inhibition of proliferation, adhesion, invasion and angiogenesis (60). Synergism with chemotherapeutics and enhancement of immune surveillance expand the pleiotropic effects exerted by N-BPs in oncology.

A new regulator of cholesterol metabolism is represented by protein convertase subtilisin/kexin type 9 (PCSK9) (61) an enzyme produced by hepatocytes and secreted into the plasma to bind to the LDL receptor resulting in lysosomal degradation of the receptor. Consequently, PCSK9 reduces the expression of LDL receptors on the cell membrane thereby decreasing the clearance of LDL-cholesterol. PCSK9 inhibitors (monoclonal-antibodies) have become very useful in statin intolerant patients or when statin therapy is unable to reduce LDL (61).

PCSK9 is mostly expressed in the liver (62), which is one of the most common sites for metastasis, thus the ability of PCSK9 and cholesterol to favor a pro-metastatic environment was investigated. Clinical studies are very poor (63, 64), while the majority of the results comes from preclinical experimental models: the PCSK9-KO mice and melanoma cells (65). In the presence of a reduced expression of PCSK9, the number of hepatic metastases was significantly lower. By contrast, PCSK9-KO and wild-type mice fed with a high cholesterol diet showed an increased number of liver metastasis, suggesting a prominent role of cholesterol in tumor-microenvironment interaction. The results obtained on melanoma cells can be extended to other types of cancer.

The identification of cholesterol as ERRα agonist adds a new anticancer mechanism for statins and nitrogen-containing bisphosphonates that could be further investigated to widen the potential therapeutic alternatives in cancers where ERRα is overexpressed. By contrast, the reduction of LDL-R by PCSK9 inhibitors may result in an increased intracellular content of cholesterol within tumor cells that could sustain ERRα activation. Thus, the use of PCSK9 inhibitors in oncology needs further investigations before the preclinical results can be translated into a clinical setting.

ERRα, Cholesterol, and Inflammatory Markers

Cholesterol has been shown to inhibit the expression of chemokines, such as CXCL9 and CXCL10, in macrophages (66) while statins and bisphosphonates enhance CXCL9 and CXCL10 gene expression in wild-type (WT) but not in ERRα-KO macrophages. A similar mechanism was observed for other inflammatory markers such as IL-1β and MMP9. These data suggest that chemokine-suppressive effects of cholesterol in macrophages is dependent on ERRα, revealing an anti-inflammatory role for the NR in a cholesterol-rich environment.

However, a deeper analysis should be performed on the role of cholesterol as the modulator of inflammatory markers produced by macrophages. In fact, an interesting paper (67) reported an induction of IL-8 (CXCL8) in response to cholesterol loading in macrophages foam cells, one of the hallmarks of atherosclerosis (68–70). It has been observed that cholesterol loading, in addition to affecting its own uptake, induces several effects in macrophages including the alteration of the cellular metabolism (71, 72), the increase of phospholipids synthesis (73), the increase of apolipoprotein E synthesis and secretion (74), and the enhancement of lipoprotein and apoprotein internalization and degradation (75). All these phenomena contribute to different phases in the progression of atherosclerosis.

In the paper by Wang et al. (67), macrophages were incubated with or without acetylated LDL (acLDL) in the presence or in the absence of an acyl-CoA:cholesterol-acyltransferase (ACAT) inhibitor before evaluating changes in chemokines mRNA content, growth factors, interleukins, and adhesion molecules. Among these genes, a significative increase in mRNA level was observed only for IL-8. Specifically, cholesterol intake by macrophages through scavenger receptor-mediated endocytosis of acLDL enhanced IL-8 expression both at transcriptional and post-transcriptional level.

These observations arouse some deductions concerning the potential positive effect of cholesterol on the expression of the cytokine IL-8, known to be associated with proliferation, angiogenesis, migration, and chemosensitivity of many cancer cells (76). In fact, IL-8 expression has been detected in numerous cancer types, but its value as a cancer biomarker has been poorly investigated, even though it could be relevant for a good

number of malignant diseases such as thyroid cancers where IL-8 represents the most deeply investigated chemokine in thyroid tumor microenvironment (77).

For these reasons, we can speculate that cholesterol trough ERRα-dependent signaling regulates production of inflammatory markers in cancer cells as well as in macrophages within tumor microenvironment. Therefore, it seems necessary to delve into this last aspect because ERRα could represent a relevant therapeutic target since this receptor is a key functional factor shared by several oncogenic signals belonging to both tumor cells and microenvironment.

ERRα, IL-8, and Colorectal Cancer

Starting from the evidence that ERRα is overexpressed in colorectal (CRC) tumor tissues and cell lines, it was demonstrated that ERRα promotes *in vitro* proliferation and migration (78). Moreover, a close correlation between ERRα protein level and activity and the production of IL-8 in CRC has been found (78). Moreover, chemical inhibition of ERRα activity by treating different CRC cell lines with its inverse agonist, XCT-790, significantly decreased the IL-8 mRNA content, without affecting the expression of other chemokines. These results were further confirmed by ERRα specific silencing experiments. On the other hand, IL-8 expression was upregulated in all CRC cell models characterized by ERRα overexpression.

The same authors, investigating the mechanism by which ERRα regulates the expression of IL-8 in CRC cells revealed that XCT-790 treatment or ERRα gene silencing decreased the promoter activity of IL-8. Moreover, the observation that XCT-790 increased IL-8 mRNA degradation, demonstrated that ERRα regulated IL-8 gene transcription and mRNA stability. Importantly, IL-8 gene silencing suppressed CRC cells proliferation and migration similarly to XCT-790, while a pre-treatment with recombinant IL-8 can rescue the inhibitory effects exerted by XCT-790 on cell proliferation and migration. These results clearly suggest that ERRα activity is directly involved in IL-8-induced CRC cells growth and motility.

Several findings indicate that ERRα activity in CRC could be induced by an excess of cholesterol in the tumor microenvironment. In fact, epidemiologic studies indicate that CRC risk is directly associated with a higher consumption of animal fats and inversely correlated with a diet rich in fruits and vegetables (79, 80). Animal fats diet is also associated with an increased risk of developing chronic intestinal inflammation (81). In fact, an excess of intake in fats of animal origin induces the production of oxidized molecules responsible for lipid oxidation processes able to generate different toxic products for the intestinal epithelial barrier function and the production of pro-inflammatory molecules. All these factors contribute to developing a cancer-prone microenvironment.

The existence of a direct correlation between the levels of cholesterol and the production of IL-8 in the macrophage suggests some interesting hypotheses that could represent the rational basis for further studies: (a) the agonistic action of cholesterol on ERRα in CRC cells could favor the recruitment of co-regulators involved in the enhancement of IL-8 gene expression; (b) a similar mechanism could occur also in macrophages leading the way for new hypotheses on ERRα involvement in the regulation of the inflammatory process within the tumor microenvironment.

Cholesterol and ERRα in Breast, Prostate, and Adrenocortical Cancer

A new potential therapeutic application in a clinical setting controlling cholesterol levels come out from the observations on the role played by ERRα in breast (BC) and prostate (PC) cancers. In BC, high ERRα expression characterizes tumors with poor prognosis (81). Moreover, ERRα mRNA is positively correlated with the oncogene ERBB2 and AIB1 (82) and inversely correlated with that of ERα and progesterone receptor that are good prognostic factors for the anti-hormonal treatment of breast cancer patients. Indeed, depending on the cellular context, ERRα could act promoting or inhibiting transcription (83). Findings suggested that in ER-negative BC, ERRα compensates for the loss of ERα in addition to triggering the expression of ERα-independent genes since it recognizes estrogen response element (ERE) as is the case for vascular endothelial growth factor (VEGF) promoting BC metastasis (23, 24). By contrast, in ER-positive BC cells, ERRα negatively controls ERE transcription by interacting with corepressor such as RIP1. Alternatively, ERRα could promote BC cells growth by enhancing circulating estrogen production. In fact, it has been found that ERRα could activate steroid sulfotransferase (SULT2A1) that works to maintain high level of peripheral dehydroepiandrosteronesulfate (DHEAS), an important metabolite in estrogen synthesis in adrenal tissues. In addition, it has also been evidenced that SULT2A1 inactivates tamoxifen and raloxifene (84). Thus, high ERRα expression in breast cancer by enhancing SULT2A1 activity could also support breast cancer cell resistance to anti-hormonal therapy (84).

The enhanced expression of ERRα has been found also in prostate cancer (PCa) and PCa cell lines (85). A study indicates a positive correlation between ERRα expression and the Gleason score while results from a preclinical study showed that ERRα can promote the hypoxic growth adaptation of prostate cancer cells by interacting with HIF-1α. As above explained, ERRα is also expressed in the bone regulating activity of osteoblasts and osteoclasts, that is implicated into the mixed osteolytic and osteoblastic lesions observed in advanced prostate cancer patients (86).

An increased cholesterol biosynthesis, regulated by sterol regulatory element-binding protein−2 (SREBP-2), is a key player in the initiation and progression of PCa where an enhanced stem cell population was observed (87). Moreover, aberrant cholesteryl ester accumulation in lipid droplets exacerbates cancer invasiveness and characterize high-grade PCa with PTEN loss and consequently, constitutive PI3K/Akt activation promotes metabolic dysregulation where ERRα/PGC-1α, as already mentioned, play a central role (18). In addition, the cholesterol metabolite, 27-hydroxyl-cholesterol (27-OHC) is now recognized as selective estrogen receptor modulator (SERM) which promotes tumorigenesis in ER-positive BC (88). Higher levels of 27-OHC have been reported in ERα-positive breast cancers with respect to normal breast tissue, along with an

observed reduction in the 27-OHC metabolizing enzyme such as CYP7B1 (89). Results from *in vivo* experiments demonstrated that 27-OHC alone is sufficient to support estrogenic activity in ER-dependent breast cancer cells (89). Accordingly, an increased growth and metastasis of ER-positive tumors were observed in a mouse model of breast cancer fed only with a cholesterol-rich diet (89). The function of cholesterol as an ERRα agonist may provide the molecular basis and mechanistic insight into clinical studies suggesting that drugs able to lower cholesterol levels (i.e., statins) can be used to treat or prevent breast and prostate cancer.

A different tumor phenotype where cholesterol could have positive growing effects, over its physiological role, is the adrenocortical cancer (ACC). ACC is a very rare and aggressive disease with very limited therapeutic options (90). The pathogenesis of ACC involves the integration of molecular signals and the interplay of different downstream pathways (i.e., IGFII/IGF1R, β-catenin, Wnt, ERα) (91). Our published results indicate that treatment of ACC cell model with XCT-790, to the purpose of reducing ERRα expression, impaired cancer cell growth, both *in vitro* and *in vivo* (92). Our data well correlate with that reporting an increased ERRα expression in ACC compared to normal adrenal and adenoma (93) underling the involvement of this metabolic receptor in ACC biology. Indeed, our unpublished results revealed that treatment of H295R cells with statins caused a significant reduction in cell growth and motility. Although these data are still preliminary, they suggest that cholesterol may affect various biological processes in ACC through the modulation of ERRα activity. Therefore, cholesterol lowering-drug could extend the therapeutic opportunity to fight this rare tumor.

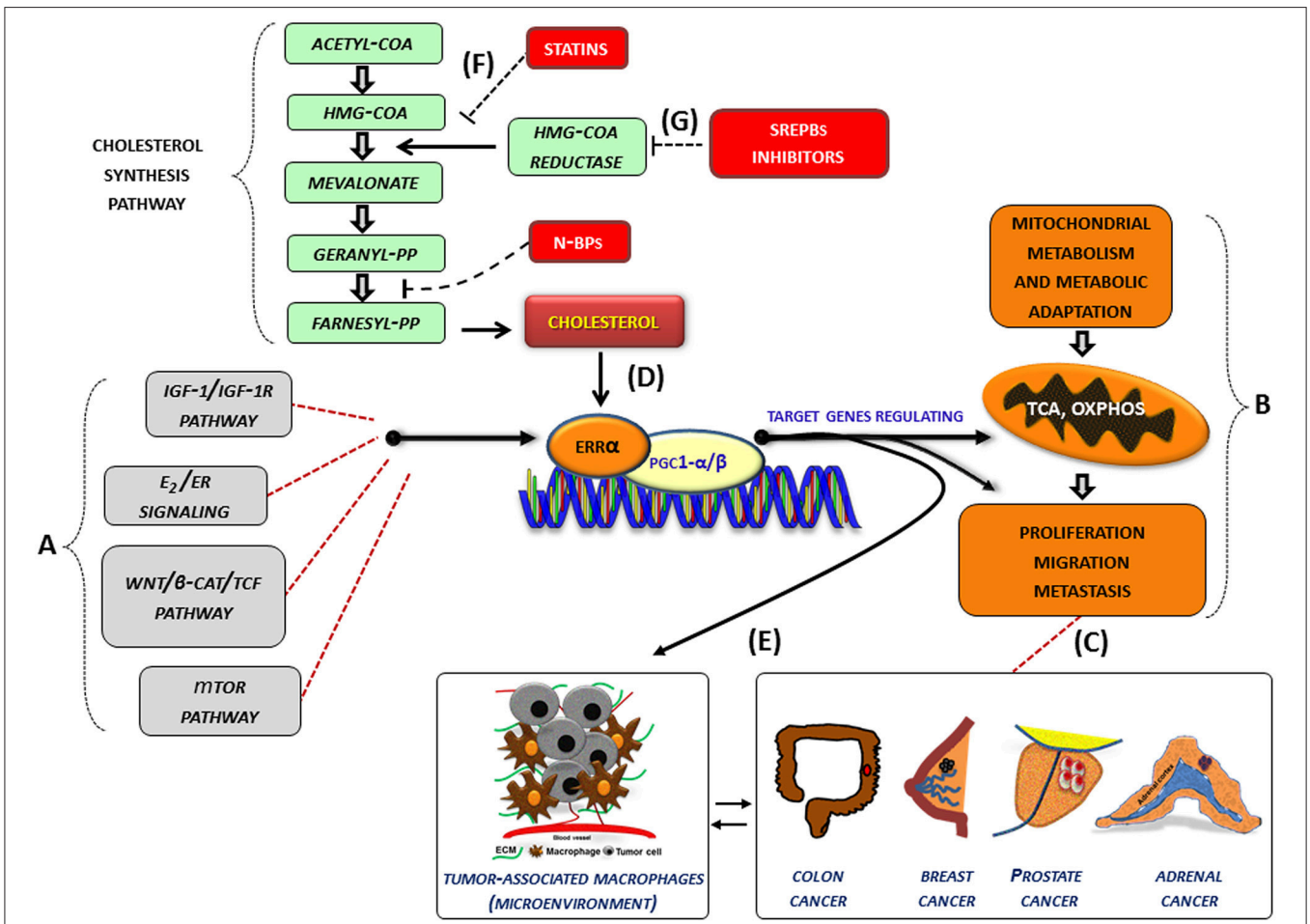

FIGURE 1 | Role of cholesterol as modulator of ERRα action in cancer. **(A–G)** Schematic representation of how cholesterol, as a new ERRα ligand, can contribute to the complex molecular network consisting in the functional cross-talk between oncogenes and oncogenic pathways (IGF-1/IGF-1R, E2/ER, β-catenin/TCF, mTOR) **(A)** that support the overexpression of ERRα. In turn, ERRα, together with its main cofactors (PGC-1α and PGC-1β) and activators, such as cholesterol **(D)**, affects cancer cell metabolism promoting proliferation, migration and, metastasis **(B)** of different tumor phenotypes **(C)**. All these bioenergy-consuming functions are strictly related to **(E)** the cross-talk between tumor cells and some key players of the tumor microenvironment, such as macrophages (tumor-associate macrophages). The use of drugs [statins, **(F)**, N-bisphosphonates, N-BPs, SREBPs inhibitors, **(G)**] able to reduce cholesterol levels and ERRα transcriptional activity could widen the therapeutic opportunities for the treatment of different ERRα overexpressing tumors. More details are explained within the text. E2, estradiol; ER, estrogen receptor; IGF-1/IGF-1R, insulin-like growth factor-1/insulin-like growth factor-1 receptor; WNT, Wingless-type MMTV integration site family member; TCF, T-cell factor; TOR, mammalian target of rapamycin; N-BPs, nitrogen-containing bisphosphonates.

CONCLUSION

The ERRα transcriptional activity in normal cells is directed to modulate cellular metabolism, supporting the growth of rapidly dividing cells and to control metabolic programs required for cellular energy homeostasis in differentiated cells and to satisfy energy request during cell differentiation. The recent identification of cholesterol as an endogenous ERRα agonist evidenced that this sterol enhances the interaction between ERRα and PGC-1β in osteoclasts, promoting osteoclastogenesis and bone resorption. Similarly, cholesterol promotes ERRα interaction with PGC-1α in myocytes inducing myogenesis and decreasing muscle toxicity. The discovery of this new molecular mechanism has elucidated the genesis of two important phenomena with an unexplained mechanism: the statin-induced muscle toxicity and the bisphosphonate suppression of bone resorption.

Moreover, the discovery of cholesterol as an agonist of ERRα demonstrated that this receptor works as a metabolic-sensing nuclear receptor distinguishing it from steroid receptors that respond to an acute and steep rise in hormonal levels. Consequently, ERRα is constitutively active because cholesterol is ubiquitous.

This new mechanism calls fresh thinking about the role of ERRα in cancer cells keeping in mind the key role played by this receptor as modulator of cancer metabolism.

It is well known that the metabolic alterations of lipids, carbohydrates, and proteins are one of the hallmarks of cancers (20). In particular, an increase in the glycolytic rate at the expense of oxidative phosphorylation even in the presence of adequate oxygen concentrations (Warburg effect) (94) allows a rapid adaptation of tumor cells to the continuous metabolic changes that, together with the tumor microenvironment, are the driving forces for cancer survival and its evolution. Given the high interconnection between enzymes that regulate the metabolism and the molecular pathways induced by altered oncogenes, research of the key regulators that behave on metabolic adaptations and proliferative, anti-apoptotic, invasive and metastatic responses, could represent elective targets to break down tumors with a single shot. The ERRα could work for this end due to its location at the intersection of dysregulated metabolism and oncogenic pathways.

In several cancer cells, the expression and the activity of ERRα, together with its cofactors (PGC-1 α/β), is further influenced by oncogenic signals (IGF1-/IGF1R pathway, estrogen signaling, Wnt/β-cat/TCF, mTOR pathway) (**Figure 1A**) and can thus be re-directed to induce metabolic programs (**Figure 1B**) favoring tumor growth and progression. (**Figure 1C**). In this context, an increased level of cholesterol, through the new molecular mechanism, supports all tumor-related processes. (**Figure 1D**). Accordingly, high levels of cholesterol are associated with an increased risk of different type of cancers including breast, prostate (95) and CRC (96).

Although epidemiological data on the correlation between cholesterol and cancer are conflicting, the preclinical results positively highlight different molecular aspects revealing how oncogenic growth signaling meet the bioenergetics and biosynthetic demands of rapidly proliferating tumor cells. In fact, altered cholesterol pathway in cancer could be reached through different mechanisms. One of the most important is the constitutive activity of the oncogenic PI3K/AKT/mTOR signaling pathway that enhances intracellular cholesterol levels by: (i) inducing cholesterol synthesis through the activation of the transcription factor SREBP (sterol regulatory element binding proteins); (ii) inducing LDL receptor–mediated cholesterol import; (iii) inhibiting ABCA1-mediated cholesterol export. Moreover, high-energy demanding cancer related process are strictly related to the cross-talk between tumor cells and some key players of the tumor microenvironment (TME), such as macrophages (TAM, tumor-associated macrophage), that in turn, fuels cancer progression through the formation of an inflammatory milieu characterized by the production of different cytokines such as IL-1, IL-6, and IL-8 among others. The latter, as above reported, could be a target of ERRα action (**Figure 1E**). For most solid tumors, infiltration by inflammatory cells such as macrophages is associated with poor prognosis (97, 98).

The links between inflammation and cholesterol are best exemplified by atherosclerosis, but similar mechanisms may also contribute to other metabolic disorders including cancer. It is noteworthy that cholesterol accumulation in TAM triggers the phenotype switch from M1, antitumorigenic, to M2-like macrophage, protumorigenic (99, 100).

Based on these considerations, the use of therapeutic strategy aimed to reduce cholesterol levels, such as statins (**Figure 1F**) or drugs targeting the SREBP metabolic pathways (**Figure 1G**), could be a promising option to counteract metabolic rewiring in cancer cells where ERRα plays a pivotal role.

In conclusion, identification of cholesterol as an endogenous ERRα agonist has already elucidated the most likely mechanisms underlying the side-effects induced by statins and bisphosphonate, but at the same time, it gives new perspectives to be further investigated in order to explore new therapeutic options for the treatment of ERRα overexpressing tumors. This alternative approach could bring additional benefits to the treatment of tumors that have already adopted successful therapies, but especially for those tumors, such as ACC, which are characterized by a limited or failed therapeutic choice.

AUTHOR CONTRIBUTIONS

IC, AC: literature revision and drafting of the article. ADL, MN, SS, PA, FT, and VR: drafting of the article. RS, VP: critical revision of the article and final approval.

ACKNOWLEDGMENTS

The authors thank the AIRC (Associazione Italiana per la Ricerca sul Cancro, IG2017: Id 20122, PI VP and IG15230, PI RS) for support of their research.

REFERENCES

1. Dhiman VK, Bolt MJ, White KP. Nuclear receptors in cancer - uncovering new and evolving roles through genomic analysis. *Nat Rev Genet.* (2018) 19:160–74. doi: 10.1038/nrg.2017.102
2. Schulman IG. Nuclear receptors as drug targets for metabolic disease. *Adv Drug Deliv Rev.* (2010) 162:307–15. doi: 10.1016/j.addr.2010.07.002
3. Giguere V, Yang N, Segui P, Evans RM. Identification of a new class of steroid hormone receptors. *Nature* (1988) 331:91–4.
4. Hong H, Yang L, Stallcup MR. Hormone-independent transcriptional activation and coactivator binding by novel orphan nuclear receptor ERR3. *J Biol Chem.* (1999) 274:22618–26. doi: 10.1074/jbc.274.32.22618
5. Eudy JD, Yao S, Weston MD, Ma-Edmonds M, Talmadge CB, Cheng JJ, et al. Isolation of a gene encoding a novel member of the nuclear receptor superfamily from the critical region of Usher syndrome type IIa at 1q41. *Genomics* (1998) 50:382–4. doi: 10.1006/geno.1998.5345
6. Tremblay AM, Giguere V. The NR3B subgroup: an ovERRview. *Nucl Recept Signal.* (2007) 5:e009. doi: 10.1621/nrs.05009
7. Tiraby C, Hazen BC, Gantner ML, Kralli A. Estrogen-related receptor gamma promotes mesenchymal-to-epithelial transition and suppresses breast tumor growth. *Cancer Res.* (2011) 71:2518–28. doi: 10.1158/0008-5472.CAN-10-1315
8. Tremblay AM, Wilson BJ, Yang XJ, Giguere V. Phosphorylation-dependent sumoylation regulates estrogen-related receptor-alpha and -gamma transcriptional activity through a synergy control motif. *Molecul Endocrinol.* (2008) 22:570–84. doi: 10.1210/me.2007-0357
9. Gearhart MD, Holmbeck SM, Evans RM, Dyson HJ, Wright PE. Monomeric complex of human orphan estrogen related receptor-2 with DNA: a pseudo-dimer interface mediates extended half-site recognition. *J Molecul Biol.* (2003) 327:819–32. doi: 10.1016/S0022-2836(03)00183-9
10. Giguere V. Transcriptional control of energy homeostasis by the estrogen-related receptors. *Endocr Rev.* (2008) 29:677–96. doi: 10.1210/er.2008-0017
11. Huppunen J, Aarnisalo P. Dimerization modulates the activity of the orphan nuclear receptor ERRgamma. *Biochem Biophys Res Commun.* (2004) 314:964–70. doi: 10.1016/j.bbrc.2003.12.194
12. Kallen J, Schlaeppi JM, Bitsch F, Filipuzzi I, Schilb A, Riou V,et al. Evidence for ligand-independent transcriptional activation of the human estrogen-related receptor alpha (ERRalpha): crystal structure of ERRalpha ligand binding domain in complex with peroxisome proliferator-activated receptor coactivator-1alpha. *J Biol Chem.* (2004) 279:49330–7. doi: 10.1074/jbc.M407999200
13. Huss JM, Garbacz WG, Xie W. Constitutive activities of estrogen-related receptors: transcriptional regulation of metabolism by the ERR pathways in health and disease. *Biochimica et Biophysica Acta* (2015) 1852:1912–27. doi: 10.1016/j.bbadis.2015.06.016
14. Luo J, Sladek R, Carrier J, Bader JA, Richard D, Giguere V. Reduced fat mass in mice lacking orphan nuclear receptor estrogen-related receptor alpha. *Molecul Cell Biol.* (2003) 23:7947–56. doi: 10.1128/MCB.23.22.7947-7956.2003
15. Huss JM, Imahashi K, Dufour CR, Weinheimer CJ, Courtois M, Kovacs A, et al. The nuclear receptor ERRalpha is required for the bioenergetic and functional adaptation to cardiac pressure overload. *Cell Metabol.* (2007) 6:25–37. doi: 10.1016/j.cmet.2007.06.005
16. Bonnelye E, Vanacker JM, Dittmar T, Begue A, Desbiens X, Denhardt DT., et al. The ERR-1 orphan receptor is a transcriptional activator expressed during bone development. *Molecul Endocrinol.* (1997) 11:905–16. doi: 10.1210/mend.11.7.9948
17. Delhon I, Gutzwiller S, Morvan F, Rangwala S, Wyder L, Evans G, et al. Absence of estrogen receptor-related-alpha increases osteoblastic differentiation and cancellous bone mineral density. *Endocrinology* (2009) 150:4463–72. doi: 10.1210/en.2009-0121
18. Deblois G, St-Pierre J, Giguere V. The PGC-1/ERR signaling axis in cancer. *Oncogene* (2013) 32:3483–90. doi: 10.1038/onc.2012.529
19. Villena JA, Kralli A. ERRalpha: a metabolic function for the oldest orphan. Trends in endocrinology and metabolism. *Trends Endocrinol Metab.* (2008) 19:269–76. doi: 10.1016/j.tem.2008.07.005
20. Hanahan D, Weinberg RA. Hallmarks of cancer: the next generation. *Cell* (2011) 144:646–74. doi: 10.1016/j.cell.2011.02.013
21. LeBleu VS, O'Connell JT, Gonzalez Herrera KN, Wikman H, Pantel K, Haigis MC, et al. PGC-1alpha mediates mitochondrial biogenesis and oxidative phosphorylation in cancer cells to promote metastasis. *Nat Cell Biol.* (2014) 16:992–1003. doi: 10.1038/ncb3039
22. Arany Z, Foo SY, Ma Y, Ruas JL, Bommi-Reddy A, Girnun G, et al. HIF-independent regulation of VEGF and angiogenesis by the transcriptional coactivator PGC-1alpha. *Nature* (2008) 1451:8–12. doi: 10.1038/nature06613
23. Stein RA, Gaillard S, McDonnell DP. Estrogen-related receptor alpha induces the expression of vascular endothelial growth factor in breast cancer cells. *J Steroid Biochem Molecul Biol.* (2009) 114:106–12. doi: 10.1016/j.jsbmb.2009.02.010
24. Stein RA, Chang CY, Kazmin DA, Way J, Schroeder T, Wergin M, et al. Estrogen-related receptor alpha is critical for the growth of estrogen receptor-negative breast cancer. *Cancer Res.* (2008) 68:8805–12. doi: 10.1158/0008-5472.CAN-08-1594
25. Ao A, Wang H, Kamarajugadda S, Lu J. Involvement of estrogen-related receptors in transcriptional response to hypoxia and growth of solid tumors. *Proc Natl Acad Sci USA.* (2008) 105:7821–6. doi: 10.1073/pnas.0711677105
26. Dwyer MA, Joseph JD, Wade HE, Eaton ML, Kunder RS, Kazmin D, et al. WNT11 expression is induced by estrogen-related receptor alpha and beta-catenin and acts in an autocrine manner to increase cancer cell migration. *Cancer Res.* (2010) 70:9298–308. doi: 10.1158/0008-5472.CAN-10-0226
27. Deblois G, Giguere V. Functional and physiological genomics of estrogen-related receptors (ERRs) in health and disease. *Biochimica et Biophysica Acta* (2011) 1812:1032–40. doi: 10.1016/j.bbadis.2010.12.009
28. Busch BB, Stevens WC Jr, Martin R, Ordentlich P, Zhou S, Sapp DW, et al. Identification of a selective inverse agonist for the orphan nuclear receptor estrogen-related receptor alpha. *J Med Chem.* (2004) 47:5593–6. doi: 10.1021/jm049334f
29. Chisamore MJ, Cunningham ME, Flores O, Wilkinson HA, Chen JD. Characterization of a novel small molecule subtype specific estrogen-related receptor alpha antagonist in MCF-7 breast cancer cells. *PLoS ONE* (2009) 4:e5624. doi: 10.1371/journal.pone.0005624
30. Willy PJ, Murray IR, Qian J, Busch BB, Stevens WC Jr, Martin R, et al. Regulation of PPARgamma coactivator 1alpha (PGC-1alpha) signaling by an estrogen-related receptor alpha (ERRalpha) ligand. *Proc Natl Acad Sci USA.* (2004) 101:8912–7. doi: 10.1073/pnas.0401420101
31. Teng CT, Beames B, Alex Merrick B, Martin N, Romeo C, Jetten AM. Development of a stable cell line with an intact PGC-1alpha/ERRalpha axis for screening environmental chemicals. *Biochem biophys Res Commun.* (2014) 444:177–81. doi: 10.1016/j.bbrc.2014.01.033
32. Teng CT, Hsieh JH, Zhao J, Huang R, Xia M, Martin N, et al. Development of novel cell lines for high-throughput screening to detect estrogen-related receptor alpha modulators. *SLAS Discov.* (2017) 22:720–31. doi: 10.1177/2472555216689772
33. Suetsugi M, Su L, Karlsberg K, Yuan YC, Chen S. Flavone and isoflavone phytoestrogens are agonists of estrogen-related receptors. *Molecul Cancer Res.* (2003) 1:981–91.
34. Hyatt SM, Lockamy EL, Stein RA, McDonnell DP, Miller AB, Orband-Miller LA. et al. On the intractability of estrogen-related receptor alpha as a target for activation by small molecules. *J Med Chem.* (2007) 50:6722–4. doi: 10.1021/jm7012387
35. Peng L, Gao X, Duan L, Ren X, Wu D, Ding K. Identification of pyrido[1,2-alpha]pyrimidine-4-ones as new molecules improving the transcriptional functions of estrogen-related receptor alpha. *J Med Chem.* (2011) 54:7729–33. doi: 10.1021/jm200976s
36. Wei W, Schwaid AG, Wang X, Wang X, Chen S, Chu Q, et al. Ligand activation of ERRalpha by cholesterol mediates statin and bisphosphonate effects. *Cell Metabol.* (2016) 23:479–91. doi: 10.1016/j.cmet.2015.12.010
37. McDonald JG, Thompson BM, McCrum EC, Russell DW. Extraction and analysis of sterols in biological matrices by high performance liquid chromatography electrospray ionization mass spectrometry. *Method Enzymol.* (2007) 432:145–70. doi: 10.1016/S0076-6879(07)32006-5
38. Tremblay GB, Kunath T, Bergeron D, Lapointe L, Champigny C, Bader JA, et al. Diethylstilbestrol regulates trophoblast stem cell differentiation as a ligand of orphan nuclear receptor ERR beta. *Gene Dev.* (2001) 15:833–8. doi: 10.1101/gad.873401

39. Russell RG. Bisphosphonates: the first 40 years. *Bone* (2011) 49:2–19. doi: 10.1016/j.bone.2011.04.022
40. Toledano JE, Partridge NC. Statins: not just for cholesterol? *Trends Endocrinol Metabol.* (2000) 11:255–6. doi: 10.1016/S1043-2760(00)00295-2
41. Cruz PM, Mo H, McConathy WJ, Sabnis N, Lacko AG. The role of cholesterol metabolism and cholesterol transport in carcinogenesis: a review of scientific findings, relevant to future cancer therapeutics. *Front Pharmacol.* (2013) 4:119. doi: 10.3389/fphar.2013.00119
42. Clendening JW, Pandyra A, Boutros PC, El Ghamrasni S, Khosravi F, Trentin GA, et al. Dysregulation of the mevalonate pathway promotes transformation. *Proc Natl Acad Sci USA*. (2010) 107:15051–6. doi: 10.1073/pnas.0910258107
43. Thurnher M, Nussbaumer O, Gruenbacher G. Novel aspects of mevalonate pathway inhibitors as antitumor agents. *Clin Cancer Res.* (2012) 18:3524–31. doi: 10.1158/1078-0432.CCR-12-0489
44. Cardwell CR, Hicks BM, Hughes C, Murray LJ. Statin use after diagnosis of breast cancer and survival: a population-based cohort study. *Epidemiology* (2015) 26:68–78. doi: 10.1097/EDE.0000000000000189
45. Desai P, Lehman A, Chlebowski RT, Kwan ML, Arun M, Manson, JE, et al. Statins and breast cancer stage and mortality in the Women's Health Initiative. *Cancer Causes Control* (2015) 26:529–39. doi: 10.1007/s10552-015-0530-7
46. Yu O, Eberg M, Benayoun S, Aprikian A, Batist G, Suissa S, et al. Use of statins and the risk of death in patients with prostate cancer. *J Clin Oncol.* (2014) 32:5–11. doi: 10.1200/JCO.2013.49.4757
47. Geybels MS, Wright JL, Holt SK, Kolb S, Feng Z, Stanford JL. Statin use in relation to prostate cancer outcomes in a population-based patient cohort study. *Prostate* (2013) 73:1214–22. doi: 10.1002/pros.22671
48. Caon J, Paquette M, Hamm J, Pickles T. Does statin or ASA affect survival when prostate cancer is treated with external beam radiation therapy? *Prostate Cancer* (2014) 2014:184297. doi: 10.1155/2014/184297
49. Habis M, Wroblewski K, Bradaric M, Ismail N, Yamada SD, Litchfield L, et al. Statin therapy is associated with improved survival in patients with non-serous-papillary epithelial ovarian cancer: a retrospective cohort analysis. *PLoS ONE* (2014) 9:e104521. doi: 10.1371/journal.pone.0104521
50. Nowakowski, GS, Maurer MJ, Habermann TM, Ansell SM, Macon WR, Ristow KM, et al. Statin use and prognosis in patients with diffuse large B-cell lymphoma and follicular lymphoma in the rituximab era. *J Clin Oncol.* (2010) 28:412–7. doi: 10.1200/JCO.2009.23.4245
51. Viers BR, Houston Thompson R, Psutka SP, Lohse CM, Cheville JC, Leibovich BC, et al. The association of statin therapy with clinicopathologic outcomes and survival among patients with localized renal cell carcinoma undergoing nephrectomy. *Urol Oncol.* (2015) 33:388 e11–8. doi: 10.1016/j.urolonc.2015.01.009
52. Cardwell CR, Hicks BM, Hughes C, Murray LJ. Statin use after colorectal cancer diagnosis and survival: a population-based cohort study. *J Clin Oncol.* (2014) 32:3177–83. doi: 10.1200/JCO.2013.54.4569
53. Shao YY, Hsu CH, Yeh KH, Chen HM, Yeh YC, Lai CL, et al. Statin use is associated with improved prognosis of colorectal Cancer in Taiwan. *Clin Colorectal Cancer* (2015) 14:177–84 e4. doi: 10.1016/j.clcc.2015.02.003
54. Zhong S, Zhang X, Chen L, Ma T, Tang J, Zhao J. Statin use and mortality in cancer patients: Systematic review and meta-analysis of observational studies. *Cancer Treat Rev.* (2015) 41:554–67. doi: 10.1016/j.ctrv.2015.04.005
55. Misawa A, Inoue S. Estrogen-related receptors in breast cancer and prostate cancer. *Front Endocrinol* (2015) 6:83. doi: 10.3389/fendo.2015.00083
56. Bernatchez G, Giroux V, Lassalle T, Carpentier AC, Rivard N, Carrier JC. ERRalpha metabolic nuclear receptor controls growth of colon cancer cells. *Carcinogenesis* (2013) 34:2253-61. doi: 10.1093/carcin/bgt180
57. Matusewicz L, Meissner J, Toporkiewicz M, Sikorski AF. The effect of statins on cancer cells–review. *Tumour Biol.* (2015) 36:4889–904. doi: 10.1007/s13277-015-3551-7
58. Zaleska M, Mozenska O, Bil J. Statins use and cancer: an update. *Future Oncol.* (2018) 14:1497–509. doi: 10.2217/fon-2017-0543
59. Maurizi A, Rucci N. The osteoclast in bone metastasis: player and target. *Cancers* (2018) 10:E218. doi: 10.3390/cancers10070218.
60. Van Acker HH, Anguille S, Willemen Y, Smits EL, Van Tendeloo VF. Bisphosphonates for cancer treatment: mechanisms of action and lessons from clinical trials. *Pharmacol Therapeut.* (2016) 158:24–40. doi: 10.1016/j.pharmthera.2015.11.008
61. Liu ZP, Wang Y. PCSK9 inhibitors: novel therapeutic strategies for lowering LDL-cholesterol. *Mini Rev Med Chem.* (2018) 18:1. doi: 10.2174/1389557518666180423111442
62. Seidah NG, Benjannet S, Wickham L, Marcinkiewicz J, Jasmin SB, Stifani S, et al. The secretory proprotein convertase neural apoptosis-regulated convertase 1 (NARC-1): liver regeneration and neuronal differentiation. *Proc Natl Acad Sci USA*. (2003) 100:928–33. doi: 10.1073/pnas.0335507100
63. Benn M, Tybjaerg-Hansen A, Stender S, Frikke-Schmidt R, Nordestgaard BG. Low-density lipoprotein cholesterol and the risk of cancer: a mendelian randomization study. *J Natl Cancer Inst*. (2011) 103:508–19. doi: 10.1093/jnci/djr008
64. Folsom AR, Peacock JM, Boerwinkle E. Sequence variation in proprotein convertase subtilisin/kexin type 9 serine protease gene, low LDL cholesterol, and cancer incidence. *Cancer Epidemiol Biomark Prev*. (2007) 16:2455–8. doi: 10.1158/1055-9965.EPI-07-0502
65. Seidah NG. Proprotein convertase subtilisin kexin 9 (PCSK9) inhibitors in the treatment of hypercholesterolemia and other pathologies. *Curr Pharm Design* (2013) 19:3161–72. doi: 10.2174/1381612811319990313
66. Spann NJ, Garmire LX, McDonald JG, Myers DS, Milne SB, Shibata N, et al. Regulated accumulation of desmosterol integrates macrophage lipid metabolism and inflammatory responses. *Cell* (2012) 151:138–52. doi: 10.1016/j.cell.2012.06.054
67. Wang N, Tabas I, Winchester R, Ravalli S, Rabbani LE, Tall A. Interleukin 8 is induced by cholesterol loading of macrophages and expressed by macrophage foam cells in human atheroma. *J Biol Chem.* (1996) 271:8837–42. doi: 10.1074/jbc.271.15.8837
68. Schaffner T, Taylor K, Bartucci EJ, Fischer-Dzoga K, Beeson JH, Glagov S, et al. Arterial foam cells with distinctive immunomorphologic and histochemical features of macrophages. *Am J Pathol.* (1980) 100:57–80.
69. Klurfeld DM. Identification of foam cells in human atherosclerotic lesions as macrophages using monoclonal antibodies. *Arch Pathol Lab Med.* (1985) 109:445–9.
70. Faggiotto A, Ross R. Studies of hypercholesterolemia in the nonhuman primate. II. Fatty streak conversion to fibrous plaque. *Arteriosclerosis* (1984) 4:341–56.
71. Brown MS, Goldstein JL. A receptor-mediated pathway for cholesterol homeostasis. *Science* (1986) 232:34–47.
72. Brown MS, Goldstein JL. Lipoprotein metabolism in the macrophage: implications for cholesterol deposition in atherosclerosis. *Annu Rev Biochem.* (1983) 52:223–61.
73. Shiratori Y, Okwu AK, Tabas I. Free cholesterol loading of macrophages stimulates phosphatidylcholine biosynthesis and up-regulation of CTP: phosphocholine cytidylyltransferase. *J Biol Chem.* (1994) 269:11337–48.
74. Kayden HJ, Maschio F, Traber MG. The secretion of apolipoprotein E by human monocyte-derived macrophages. *Arch Biochem Biophys*. (1985) 239:388–95. doi: 10.1016/0003-9861(85)90704-0
75. Bottalico LA, Keesler GA, Fless GM, Tabas I. Cholesterol loading of macrophages leads to marked enhancement of native lipoprotein(a) and apoprotein(a) internalization and degradation. *J Biol Chem.* (1993) 268:8569–73.
76. Waugh DJ, Wilson C. The interleukin-8 pathway in cancer. *Clin Cancer Res.* (2008) 14:6735–41. doi: 10.1158/1078-0432.CCR-07-4843
77. Rotondi M, Coperchini F, Latrofa F, Chiovato L. Role of chemokines in thyroid cancer microenvironment: is CXCL8 the main player? *Front Endocrinol.* (2018) 9:314. doi: 10.3389/fendo.2018.00314
78. Ding S, Tang Z, Jiang Y, Huang H, Luo P, Qing B, et al. IL-8 Is involved in estrogen-related receptor alpha-regulated proliferation and migration of colorectal cancer cells. *Digest Diseas Sci.* (2017) 62:3438–46. doi: 10.1007/s10620-017-4779-4
79. Rossin D, Calfapietra S, Sottero B, Poli G, Biasi F. HNE and cholesterol oxidation products in colorectal inflammation and carcinogenesis. *Free Radic Biol Med.* (2017) 111:186–95. doi: 10.1016/j.freeradbiomed.2017.01.017
80. Lewis JD, Abreu MT. Diet as a trigger or therapy for inflammatory bowel diseases. *Gastroenterology* (2017) 152:398–414 e6. doi: 10.1053/j.gastro.2016.10.019

81. Ariazi EA, Clark GM, Mertz JE. Estrogen-related receptor alpha and estrogen-related receptor gamma associate with unfavorable and favorable biomarkers, respectively, in human breast cancer. *Cancer Res.* (2002) 62:6510-8.
82. Surowiak P, Materna V, Gyorffy B, Matkowski R, Wojnar A, Maciejczyk A, et al. Multivariate analysis of oestrogen receptor alpha, pS2, metallothionein and CD24 expression in invasive breast cancers. *Br J Cancer* (2006) 95:339–46. doi: 10.1038/sj.bjc.6603254
83. Kraus RJ, Ariazi EA, Farrell ML, Mertz JE. Estrogen-related receptor alpha 1 actively antagonizes estrogen receptor-regulated transcription in MCF-7 mammary cells. *J Biol Chem.* (2002) 277:24826–34. doi: 10.1074/jbc.M202952200
84. Apak TI, Duffel MW. Interactions of the stereoisomers of alpha-hydroxytamoxifen with human hydroxysteroid sulfotransferase SULT2A1 and rat hydroxysteroid sulfotransferase STa. *Drug Metabol Dispos.* (2004) 32:1501–8. doi: 10.1124/dmd.104.000919
85. Cheung CP, Yu S, Wong KB, Chan LW, Lai FM, Wang X, et al. Expression and functional study of estrogen receptor-related receptors in human prostatic cells and tissues. *J Clin Endocrinol Metabol.* (2005) 90:1830–44. doi: 10.1210/jc.2004-1421
86. Bonnelye E, Aubin JE. An energetic orphan in an endocrine tissue: a revised perspective of the function of estrogen receptor-related receptor alpha in bone and cartilage. *J Bone Miner Res.* (2013) 28:225–33. doi: 10.1002/jbmr.1836
87. Li X, Wu JB, Li Q, Shigemura K, Chung LW, Huang,WC. SREBP-2 promotes stem cell-like properties and metastasis by transcriptional activation of c-Myc in prostate cancer. *Oncotarget* (2016) 7:12869–84. doi: 10.18632/oncotarget.7331
88. Warner M, Gustafsson JA. On estrogen, cholesterol metabolism, and breast cancer. *N Engl J Med.* (2014) 370:572–3. doi: 10.1056/NEJMcibr1315176
89. Wu Q, Ishikawa T, Sirianni R, Tang H, McDonald JG, Yuhanna IS, et al. 27-Hydroxycholesterol promotes cell-autonomous, ER-positive breast cancer growth. *Cell Rep.* (2013) 5:637–45. doi: 10.1016/j.celrep.2013.10.006
90. Glover AR, Ip JC, Zhao JT, Soon PS, Robinson BG, Sidhu SB. Current management options for recurrent adrenocortical carcinoma. *OncoTarget Ther.* (2013) 6:635–43. doi: 10.2147/OTT.S34956
91. Sirianni R, Zolea F, Chimento A, Ruggiero C, Cerquetti L, Fallo F, et al. Targeting estrogen receptor-alpha reduces adrenocortical cancer (ACC) cell growth *in vitro* and *in vivo*: potential therapeutic role of selective estrogen receptor modulators (SERMs) for ACC treatment. *J Clin Endocrinol Metabol.* (2012) 97:E2238–50. doi: 10.1210/jc.2012-2374
92. Casaburi I, Avena P, De Luca A, Chimento A, Sirianni R, Malivindi R, et al. Estrogen related receptor alpha (ERRalpha) a promising target for the therapy of adrenocortical carcinoma (ACC). *Oncotarget* (2015) 6:25135–48. doi: 10.18632/oncotarget.4722
93. Felizola SJ, Nakamura Y, Hui XG, Satoh F, Morimoto R, Midorikawa S, et al. Estrogen-related receptor alpha in normal adrenal cortex and adrenocortical tumors: involvement in development and oncogenesis. *Molecul Cell Endocrinol.* (2013) 365:207–11. doi: 10.1016/j.mce.2012.10.020
94. Warburg O. On the origin of cancer cells. *Science* (1956) 123:309–14.
95. Gutierrez-Pajares JL, Ben Hassen C, Chevalier S, Frank PG. SR-BI: linking cholesterol and lipoprotein metabolism with breast and prostate cancer. *Front Pharmacol.* (2016) 7:338. doi: 10.3389/fphar.2016.00338
96. Wang C, Li P, Xuan J, Zhu C, Liu J, Shan L, et al. Cholesterol enhances colorectal cancer progression via ROS elevation and MAPK signaling pathway activation. *Cell Physiol Biochem.* (2017) 42:729–42. doi: 10.1159/000477890
97. Mantovani A, Marchesi F, Malesci A, Laghi L, Allavena P. Tumour-associated macrophages as treatment targets in oncology. *Nat Rev Clin Oncol.* (2017) 14:399–416. doi: 10.1038/nrclinonc.2016.217
98. Illemann M, Laerum OD, Hasselby JP, Thurison T, Hoyer-Hansen G, Nielsen HJ, et al. Urokinase-type plasminogen activator receptor (uPAR) on tumor-associated macrophages is a marker of poor prognosis in colorectal cancer. *Cancer Med.* (2014) 3:855–64. doi: 10.1002/cam4.242
99. Leitinger N, Schulman IG. Phenotypic polarization of macrophages in atherosclerosis. *Arterioscler Thromb Vascul Biol.* (2013) 33:1120–6. doi: 10.1161/ATVBAHA.112.300173
100. Rhee I. Diverse macrophages polarization in tumor microenvironment. *Arch Pharmacal Res.* (2016) 139:1588–96. doi: 10.1007/s12272-016-0820-y

Conflict of Interest Statement: The authors declare that the research was conducted in the absence of any commercial or financial relationships that could be construed as a potential conflict of interest.

Statins Reduce Intratumor Cholesterol Affecting Adrenocortical Cancer Growth

Francesca Trotta[1], Paola Avena[1], Adele Chimento[1], Vittoria Rago[1], Arianna De Luca[1], Sara Sculco[1], Marta C. Nocito[1], Rocco Malivindi[1], Francesco Fallo[2], Raffaele Pezzani[2], Catia Pilon[2], Francesco M. Lasorsa[3], Simona N. Barile[3], Luigi Palmieri[3], Antonio M. Lerario[4], Vincenzo Pezzi[1], Ivan Casaburi[1], and Rosa Sirianni[1]

ABSTRACT

Mitotane causes hypercholesterolemia in patients with adrenocortical carcinoma (ACC). We suppose that cholesterol increases within the tumor and can be used to activate proliferative pathways. In this study, we used statins to decrease intratumor cholesterol and investigated the effects on ACC growth related to estrogen receptor α (ERα) action at the nuclear and mitochondrial levels. We first used microarray to investigate mitotane effect on genes involved in cholesterol homeostasis and evaluated their relationship with patients' survival in ACC TCGA. We then blocked cholesterol synthesis with simvastatin and determined the effects on H295R cell proliferation, estradiol production, and ERα activity *in vitro* and in xenograft tumors. We found that mitotane increases intratumor cholesterol content and expression of genes involved in cholesterol homeostasis, among them *INSIG*, whose expression affects patients' survival. Treatment of H295R cells with simvastatin to block cholesterol synthesis decreased cellular cholesterol content, and this affected cell viability. Simvastatin reduced estradiol production and decreased nuclear and mitochondrial ERα function. A mitochondrial target of ERα, the respiratory complex IV (COXIV), was reduced after simvastatin treatment, which profoundly affected mitochondrial respiration activating apoptosis. Additionally, simvastatin reduced tumor volume and weight of grafted H295R cells, intratumor cholesterol content, Ki-67 and ERα, COXIV expression and activity and increase terminal deoxynucleotidyl transferase dUTP nick end labeling–positive cells. Collectively, these data demonstrate that a reduction in intratumor cholesterol content prevents estradiol production and inhibits mitochondrial respiratory chain–inducing apoptosis in ACC cells. Inhibition of mitochondrial respiration by simvastatin represents a novel strategy to counteract ACC growth.

Introduction

Adrenocortical carcinoma (ACC) is a rare but aggressive cancer with a very poor prognosis. At present, the only valuable option for ACC therapy is an early prognosis followed by surgical resection of the tumor. Mitotane (1,1-dichloro-2-(ochlorophenyl)-2-(p-chlorophenyl)-ethane or o,p-DDD), an inhibitor of steroid synthesis with adrenolytic activity, alone or combined with cytotoxic drugs such as etoposide, doxorubicin, and platinum agents, is the only specific treatment for ACC (1). Overall survival rate at 5 years is 16% to 38%, but in the case of metastatic disease (stage IV), survival rate at 5 years drops to less than 10% (2). Because mitotane treatment has a relatively low response rate and carries significant systemic toxicity, better treatment methods are critically needed for more effective targeting and inhibition of ACC.

Mitotane works by inhibiting cytochrome P450s involved in steroid synthesis and by inhibiting SOAT1, an enzyme involved in cholesterol esterification, leading to an increase in free cholesterol toxic to the cell. Mitotane serum concentrations above 14 mg/L are required for its therapeutic effects (3). However, even with administration of high doses, effective mitotane serum concentrations are achieved in only half of patients and are never reached in others (4). Doses below 14 mg/L are less effective in inhibiting SOAT1, but still able to induce 3-hydroxy-3-methylglutaryl-coenzyme A reductase (HMGCR) activity in the liver (5), favoring an increase in serum cholesterol levels, a side effect that patients with ACC experience during mitotane treatment (6). Possibly, the increase in serum cholesterol will allow the adrenal tumor to have a higher uptake. Alternatively, a direct effect of mitotane on adrenal HMGCR, affecting *de novo* synthesis, cannot be excluded, because the adrenal can synthesize cholesterol in the endoplasmic reticulum (7). Both uptake or *de novo* synthesis will increase cholesterol availability within the tumor cells, favoring activation of proliferative mechanisms.

Our previous studies have demonstrated that ACC is characterized by aromatase overexpression (8), and insulin-like growth factor II (resulting overexpressed in 90% of ACCs and activating an autocrine mitogenic effect) can induce aromatase transcription (9). Then, it is possible that in patients with ACC, despite normal circulating estrogen levels, a higher local estrogen production can occur, allowing estrogens, through estrogen receptor α (ERα), to foster ACC progression.

[1]Department of Pharmacy, Health and Nutritional Sciences, University of Calabria, Arcavacata di Rende, Cosenza, Italy. [2]Department of Medical and Surgical Sciences, University of Padua, Padua, Italy. [3]Department of Biosciences, Biotechnologies and Biopharmaceutics, University of Bari, and CNR Institute of Biomembranes, Bioenergetics and Molecular Biotechnologies, Bari, Italy. [4]Departments of Molecular and Integrative Physiology and Internal Medicine, University of Michigan, Medical School, Ann Arbor, Michigan.

Note: Supplementary data for this article are available at Molecular Cancer Therapeutics Online (http://mct.aacrjournals.org/).

F. Trotta, P. Avena, and A. Chimento contributed equally to this article.

I. Casaburi and R. Sirianni contributed equally as the co-senior authors of this article.

Corresponding Authors: Rosa Sirianni, University of Calabria, Edificio Polifunzionale, Arcavacata di Rende (CS), Cosenza 87036, Italy. Phone: 39-0984-493182; Fax: 39-0984-493157; E-mail: rosa.sirianni@unical.it and Vincenzo Pezzi, Phone: 39-0984-493148; Fax: 39-0984-493157; E-mail: v.pezzi@unical.it

Mol Cancer Ther 2020;19:1909–21

doi: 10.1158/1535-7163.MCT-19-1063

A study performed on 152 patients with ACC showed that increased intra-abdominal fat is associated with tumor worsening and decreased survival (10). The rise in fat deposition observed in mitotane-treated patients can also be responsible for increased estradiol production, because the adipose tissue has high aromatase expression, which can convert steroid precursors into estrogens (11). Importantly, it has been recently suggested that adipose tissue may contain the steroidogenic machinery necessary for the initiation of *de novo* steroid biosynthesis from cholesterol (12). The increase in cholesterol and body fat is also responsible for lowering hematic mitotane concentration, because the drug is a lipophilic compound and accumulates into circulating lipoprotein fractions and high-lipid–containing tissues (13).

A drug capable of reducing cholesterol synthesis both at hepatic and intratumor levels would be effective in preventing ACC growth. In this study, we propose statins, drugs that target HMGCR, largely used to reduce hypercholesterolemia as a valid treatment for ACC. By reducing cholesterol synthesis within the tumor cells, statins could be a reliable mean to prevent estrogen production and then action through ERα in ACC.

Materials and Methods

Detailed experimental information is provided in the Supplementary Experimental Procedures.

Cell cultures and tissue

H295R, SW13, and Y1 cells were purchased from the ATCC. H295R cells were cultured as previously described (14). SW13 cells were maintained in DMEM/F-12 with 10% FBS. Y1 cells were maintained in DMEM/F-12 with 2.5% FBS and 15% horse serum. Cell monolayers were subcultured into 6-well plates for protein and RNA extraction (4×10^6 cells/plate) and 12 multiwell for colony formation assay (1×10^3 cells/well) and grown for 14 days. Cells were treated with statins or mitotane (Sigma) in DMEM/F-12 containing 10% FBS.

Fresh-frozen samples of adrenocortical tumors, removed at surgery, were collected at the hospital-based Divisions of the University of Padua (Italy). Tissue samples were obtained with the approval of local ethics committees and written-informed consent from patients. Studies were conducted in accordance with the Declaration of Helsinki guidelines as revised in 1983 and approved by the institutional review board of the University of Padua. Diagnosis of malignancy was performed according to the histopathologic criteria proposed by Weiss and colleagues (15) and the modification proposed by Aubert and colleagues (16). Patients included in the mitotane-treated group received the drug for at least 4 months at the dose of 4 to 6 g/day.

MTT assay

The effect of simvastatin on cell viability was measured using 3-[4,5-dimethylthiazol-2-yl]-2,5-diphenyltetrazoliumbromide (MTT) assay as previously described (17). Briefly, cells were cultured in complete medium in 48-well plates (1×10^4 cells/well) for 48 hours and then treated in 10% FBS medium for 24, 48, or 72 hours. Fresh MTT (Sigma), resuspended in PBS, was then added to each well (final concentration 0.33 mg/mL). After 2-hour incubation, cells were lysed with 200 μL of DMSO, and optical density was measured at 570 nm in a multiplate reader (Synergy H1, BioTek, Agilent).

Intracellular cholesterol extraction and colorimetric cholesterol assay

Cholesterol was measured using a colorimetric cholesterol assay kit (Cell Biolabs). Intracellular cholesterol was extracted from cells using a mixture of chloroform, isopropanol, and NP-40 (7: 11: 0.1). The same mix was added to tumor samples of known weight, and lysed using stainless steel beads in the Bullet Blender Tissue Homogenizer (Next Advance, Inc.). Purified water was then added to lysed samples, and upon centrifugation, the organic, bottom phase was taken and dried by vacuum centrifugation. The resulting lipid pellet was resuspended in 200 μL of 1X cholesterol assay buffer. Then, 50 μL of sample was processed according to the manufacturer's instruction.

ELISA for estradiol

The H295R cells were kept in complete medium for 48 hours in multiwells of 12 (1×10^5 cells/well) and treated in DMEM F-12 enriched with 5% DCC-FBS (FBS treated with Dextran coated in order to repair steroids) with increasing doses of simvastatin (2.5, 5, and 10 μmol/L). After 48 hours of treatment, the contents of 17β-estradiol (E2) were measured by means of ELISA (NovaTec) following the manufacturer's instruction.

Spheroids culture

A single-cell suspension was prepared using enzymatic (1X Trypsin-EDTA, Sigma Aldrich, #T3924) and manual disaggregation (25-gauge needle; ref. 18). Cells were plated at a density of 500 cells/cm^2 in spheroids medium [DMEM-F12/B27/EGF (20 ng/mL)/Pen-Strep] in nonadherent conditions, in culture dishes coated with (2-hydroxyethylmethacrylate; poly-HEMA, Sigma, #P3932). Cells were grown for 5 days and maintained in a humidified incubator at 37°C at an atmospheric pressure in 5% (v/v) carbon dioxide/air. After 5 days of culture, spheres >50 μm were counted using an eye piece graticule, and the percentage of cells plated which formed spheres was calculated and is referred to as percentage spheroids formation, and was normalized to one (1 = 100% TSFE, tumor-spheres formation efficiency). Cells were directly seeded on low-attachment plates in the presence of treatments.

Colony formation

The NCI-H295R cells were plated in 12-well plates (1×10^3) and allowed to attach. Treatment commenced for 24 hours with drug alone. Untreated or simvastatin-treated cells were controls. The medium was changed, and surviving cells were allowed to grow colonies of ≥50 cells for 2 weeks, washed, fixed, stained with Coomassie blue, and counted. Total colony numbers were normalized to untreated controls.

Protein extraction and Western blotting

H295R cells were cultured in complete medium for 48 hours in 100 mm plates (2×10^6 cells) before being treated in complete medium with simvastatin for 48 hours and then used for cytosolic and mitochondrial protein extraction. The extracts were then analyzed by Western blotting (WB).

Total proteins were prepared using RIPA buffer. Equal amounts of proteins were subjected to WB analysis. Blots were incubated overnight at 4°C with primary antibodies. Membranes were incubated with horseradish peroxidase (HRP)–conjugated secondary antibodies (Amersham), and immunoreactive bands were visualized with the ECL (Amersham).

Xenograft experiments

All animal procedures approved by the Ethics Research Committee University animals from Calabria (protocol no. 1077/2016-PR from the Ministry of Health to Dr. Sirianni) were performed in female Foxn1nu mice (Harlen Envigo) mice. Following H295R xenograft establishment, mice received 4 mg/kg/d of simvastatin in the water for

24 days, and tumors were harvested and weighed. The water with the treatment has been replaced every week. The dose was chosen to equal the therapeutic dose used for patients of 20 mg/d (based on the equivalence of body surface area; ref. 19).

Immunohistochemistry

IHC experiments were performed using 8-mm-thick paraffin-embedded sections of H295R xenograft tumors from mice treated with vehicle or simvastatin. Slides were deparaffinized and dehydrated and incubated overnight at 4°C with Aromatase (MBL International Corporation, MCA2077S, 1:50), COXIV (Abcam, ab14744, 1:200), Ki-67 (DAKO, M7240, 1:100), CCNE (Bethyl, IHC-00341, 1:100), ERα (Santa Cruz Biotechnology, sc-8002, 1:50), and TOM20 (Santa Cruz Biotechnology, sc-17764, 1:100) primary antibodies. Then, a horse biotinylated anti-mouse/rabbit IgG was applied for 1 hour at room temperature (RT), to form the avidin biotin HRP complex (Vector Laboratories). Immunoreactivity was visualized by DAB (Vector Laboratories). For ERα detection, FITC-conjugated secondary antibodies (Santa Cruz Biotechnology) were used for 1 hour at RT. Fluorescent images were collected on Olympus fluorescent microscope.

Oil red O staining

H295R cells (1×10^6) were plated on glass coverslips for 48 hours and then treated for 48 hours with simvastatin (10 μmol/L). The cells were washed with cold PBS and fixed with 4% paraformaldehyde for 30 minutes at RT. Then, the cells were stained with 0.5% Oil Red O (Sigma-Aldrich) solution for 20 minutes at RT and counterstained with hematoxylin for 2 minutes, followed by PBS washes and microscopic evaluation.

Cytochrome C oxidase/complex IV activity

Cryostat sections (8 μm) were prepared and stored at −80°C until use. For the cytochrome C oxidase (COX) activity staining, frozen sections were brought to RT, washed for 5 minutes with 25 mmol/L sodium phosphate buffer, pH 7.4, and then incubated for 0.5, 1, or 2 hours at 37°C with the COX incubation mixture. The COX solution consisted of 10 mg Cytochrome C (cat# C7752, Sigma-Aldrich), 10 mg 3,3′-diaminobenzidine tetrahydrochloride hydrate (cat# D5637, Sigma-Aldrich), and 2 mg catalase (cat# C1345, Sigma-Aldrich) dissolved in 10 mL of 25 mmol/L sodium phosphate buffer. The solution was filtered after preparation, and the pH was adjusted to 7.2 to 7.4 with 1 N NaOH.

HMGCR activity assay

The HMGCR activity in H295R lysates was measured with HMGCR Activity Assay Kit (CS1090, Sigma) according to the manufacturer's instructions. The assay is based on the spectrophotometric measurement of the decrease in absorbance at 340 nm, which represents the oxidation of NADPH by the catalytic subunit of HMGCR in the presence of the substrate HMG-CoA. Cells were lysed in RIPA buffer containing protease inhibitors. Two microliters of cell lysate were used to measure HMGCR activity. One unit converts 1.0 μmol of NADPH to NADP+ per 1 minute at 37°C. The unit-specific activity is defined as μmol/min/mg protein (units/mg P).

Detection of apoptosis by terminal deoxynucleotidyl transferase dUTP nick end labeling assay

The induction of apoptosis was assessed by the terminal deoxynucleotidyl transferase dUTP nick end labeling (TUNEL) assay, a method that evaluates the fragmentation of DNA. The click-it TUNEL Alexa Fluor Imaging Assay kit (Invitrogen) was used following the manufacturer's instructions. Sections of vehicle- and simvastatin-treated tumors from paraffin-embedded H295R xenografts were cut to a thickness of 5 μm, deparaffinized, dehydrated, and then used for the assay.

Seahorse XFe96 metabolic flux analysis

Real-time oxygen consumption rates (OCR) for H295R cells treated with simvastatin or vehicle (control) were determined using the Seahorse Extracellular Flux (XF96) analyzer (Seahorse Bioscience). H295R cells were maintained in DMEM supplemented with 10% FBS, 2 mmol/L GlutaMAX, and 1% Pen/Strep. Note that 7×10^4 cells were seeded per well into XF96-well cell culture plates (Seahorse Bioscience) and incubated overnight at 37°C in a 5% CO_2 humidified atmosphere. After 24 hours, cells were treated with simvastatin (2.5, 5, and 10 μmol/L) for 48 hours. At the end of treatment, cells were processed as previously published (20).

Microarray

H295R cells (1×10^5) were plated on 60-mm dishes for 48 hours and then treated for 24 hours with Mitotane (25 μmol/L). RNA was extracted using PureLink RNA Mini Kit (Thermo Fisher). The quality of total RNA was first assessed using an Agilent Bioanalyzer 2100 (Agilent Technologies). Biotin-labeled cDNA targets were synthesized starting from 150 ng of total RNA. Double-stranded cDNA synthesis and related cRNA were performed with GeneChip WT Plus Kit (Affymetrix). The same Kit was used to synthesize the sense strand cDNA before to be fragmented and labeled. All steps of the labeling protocol were performed as suggested by Affymetrix, starting from 5.5 μg of ssDNA. Hybridization was performed using the GeneChip Hybridization, Wash, and Stain Kit. A single GeneChip Clariom S was then hybridized with each biotin-labeled sense target. GeneChip arrays were scanned using an Affymetrix GeneChip Scanner 3000 7G using default parameters. Affymetrix GeneChip Command Console software (AGCC) was used to acquire GeneChip images and generate . DAT and CEL files, which were used for subsequent analysis with proprietary software.

RNA extraction, reverse transcription, and real-time PCR

Following total RNA extraction, 1 μg of total RNA was reverse transcribed and then used for PCR reactions performed in the iCycler iQ Detection System (Bio-Rad Laboratories S.r.l.). Final results were expressed as n-fold differences in gene expression relative to 18S and calibrator, calculated using the ΔΔCt method as previously shown (14).

Patients' data analysis

Gene expression and survival data were obtained using two independent cohorts of adrenocortical tumors as follows: Expression Cohort included 33 ACC, 22 adrenocortical adenoma (ACA), and 10 normal adrenal (NC; GEO dataset GSE33371) and The Cancer Genome Atlas cohort included 78 ACC (https://portal.gdc.cancer.gov/legacy-archive).

Statistical analysis

All experiments were performed at least 3 times. Data were expressed as mean values + standard error, and statistical significance between control and treated samples was analyzed using GraphPad Prism 5.0 (GraphPad Software, Inc.) software. Control and treated groups were compared using *t* test or the ANOVA. Significance was defined as $P < 0.05$. Microarray data analysis was performed using Partek Genomics Suite software (PGS), version 6.6 (6.16.0812 for

Mac). Affymetrix CEL-files were extracted, normalized, and summarized using RMA algorithm (CEL file imported by Partek on Wed Feb 21 10:25:17 2018; Probes to Import: Interrogating Probes; Probe filtering: skip; Algorithm: RMA; Background Correction: RMA Background Correction; Normalization: Quantile Normalization; Log Probes using Base: 2; Probeset Summarization: Median Polish; refs. 21–23). Genes differentially expressed were identified using a *t* test.

Results

Mitotane increases intratumor cholesterol content by affecting expression of genes involved in the regulation of cholesterol homeostasis

Here, we wanted to determine if mitotane can also increase cholesterol content in the tumor. As it can be seen in **Fig. 1A**, cholesterol is increased in ACC from patients treated with mitotane compared with tumors from patients with ACC that underwent surgery prior to any treatment. A key enzyme in cholesterol synthesis is HMGCoA reductase (HMGCR). We conducted a retrospective analysis of publicly available microarray data from cohorts of patients with ACC. Expression levels of *HMGCR* are higher in ACC when compared with the NC (**Fig. 1B**). However, its expression does not affect patients' survival (**Fig. 1C**). We evaluated HMGCR protein expression and activity in H295R cells after 2 and 14 days of mitotane treatment. Mitotane increases the enzyme activity (**Fig. 1D**) as previously demonstrated in hepatocytes (**Fig. 1D**).

We also used H295R cells treated with mitotane for 24 hours to perform gene expression microarray analysis. Using a cutoff of 1.5 in fold change and a P value ≤ 0.05, we identified 344 transcripts regulated by mitotane. Importantly, an enrichment analysis for the categories of Gene Ontology (GO) indicated that the drug preferentially increases expression of genes involved in metabolism, and more specifically, we looked into cholesterol metabolism (**Fig. 1E**). Among the genes present in this GO group, we further investigated sterol regulatory element-binding protein 1 (*SREBP1*) and insulin-induced gene 1 (*INSIG1*) encoding for proteins working as cholesterol sensors, and ATP-binding cassette subfamily G member 1 (*ABCG1*), encoding for a protein that mediates cholesterol efflux from the cells to ApoA1 (apolipoprotein A1), a component of HDL. Results from microarray were confirmed by real-time PCR using short-term (24 hours) and long-term (2 and 3 weeks) mitotane-treated H295R cells. As observed in microarray data, *SREBP1, INSIG1*, and *ABCG1* expression was decreased after 24-hour treatment (**Fig. 1F**, **I**, and **L**). On the long-term treatment, expression of SREBP1 was maintained at low level (**Fig. 1G**). Survival data for this factor show that when its expression is low, patients have a trend to a worse outcome, even if not significant (**Fig. 1H**). For INSIG1 and ABCG1, we found that long-term treatment with mitotane did not produce a decrease in gene expression, but mRNA levels were kept similar to those seen in untreated samples (**Fig. 1J** and **M**). The higher expression of these genes maintained in the presence of increased cholesterol amounts (caused by mitotane) indicates loss of cell ability to sense cholesterol levels. Importantly, survival data for *INSIG1* indicate that higher expression is associated with worse survival (**Fig. 1K**). A similar trend in the association was observed for *ABCG1*, even if there was not a significant difference between the two groups (**Fig. 1N**).

A decrease in ACC intracellular cholesterol positively associates with decreased tumor growth *in vitro* and *in vivo*

The use of simvastatin was able to reduce H295R cell viability in a time- and dose-dependent manner (**Fig. 2A**). Importantly, the decreased cell viability was rescued by addition of mevalonate, the product of HMGCoA reductase activity (**Fig. 2B**). These effects were reproduced by fluvastatin and rosuvastatin (Supplementary Fig. S1A). In addition, we used two additional cell lines, SW13 and Y1, and found that all tested statins produced effects similar to those observed in H295R cells (Supplementary Fig. S1B and S1C). In the clonogenic assay, simvastatin-treated cells formed significantly less colonies when compared with vehicle-treated cells, illustrating the tumor-suppressor function of this drug (**Fig. 2C**). When H295R cells were grown as spheroids in the presence of simvastatin, we observed a substantial dose-dependent decrease in sphere numbers (**Fig. 2D**). To evaluate if intratumor cholesterol depletion could reduce ACC growth *in vivo*, xenografts were generated by implanting H295R cells in the flank of athymic nude mice. When tumors reached an average of 200 mm^3, mice were administered vehicle versus simvastatin at 4 mg/kg/day for 24 days, and tumors were measured twice a week. Tumor growth of the statin-treated group was significantly smaller than the vehicle-treated group (**Fig. 2E**). Tumor volume at the end of the experiment was 60% smaller in animals receiving simvastatin (**Fig. 2E**), and tumor weight was decreased by 58% (**Fig. 2F**). In parallel with the decline in tumor size with simvastatin, there was a decrease in Ki-67 staining (**Fig. 2G**; Supplementary Fig. S2A).

Decreased cholesterol availability in ACC impairs estradiol production

After 48-hour treatment, simvastatin at the dose of 10 μmol/L caused a 33% reduction in intracellular cholesterol (**Fig. 3A**). We also evaluated cholesterol content in of H295R xenografts. By adjusting to tissue weight, we found a concentration of 9 ng/mg of tissue, whereas statin decreased this amount to 6.3 ng/mg of tissue (**Fig. 3B**). In addition, frozen sections from tumors were stained for lipids using Oil Red O, and less red stain is observed in treated tumors, indicative of a reduced amount of lipid deposition (**Fig. 3B**; Supplementary Fig. S2B). Thus, intratumor cholesterol has an important cell-autonomous role in ACC growth and in parallel statins lessens ACC tumor development. Treatment of H295R cells for 48 hours with increasing concentrations of simvastatin decreased E2 production in a dose-dependent manner, as demonstrated by ELISA of H295R culture media, with 10 μmol/L producing a 50% decrease in E2 content (**Fig. 3C**). When we evaluated aromatase (*CYP19*) gene expression, we did not find any change in mRNA, neither *in vitro* (**Fig. 3D**) nor *in vivo* (**Fig. 3G**), indicating that simvastatin does not affect transcriptional regulation of this gene. In fact, expression of steroidogenic factor 1 (SF-1) did not change after simvastatin treatment (**Fig. 3E**). However, WB analysis indicated a decrease in aromatase protein content following statin treatment of H295R (**Fig. 3F**), data that were confirmed by IHC on xenografts tumors (**Fig. 3H**; Supplementary Fig. S2C). In addition, the presence of mevalonate was able to overcome the inhibition on aromatase expression seen in the presence of simvastatin (Supplementary Fig. S3A).

Decreased E2 availability in ACC impairs ERα function

ERα has a role in regulating transcription of mitochondrial genes involved in cellular respiration (24). We evaluated both nuclear and mitochondrial ERα activities after simvastatin treatment. Expression of ERα was decreased by simvastatin *in vitro* (**Fig. 4A**; Supplementary Fig. S4A and S4B) and *in vivo* (**Fig. 4B**; Supplementary Fig. S2D), and a similar effect was observed on cyclin E, a known target of ERα, both *in vitro* and *in vivo* (**Fig. 4C** and **D**; Supplementary Fig. S2E). In addition, the presence of mevalonate was able to overcome the

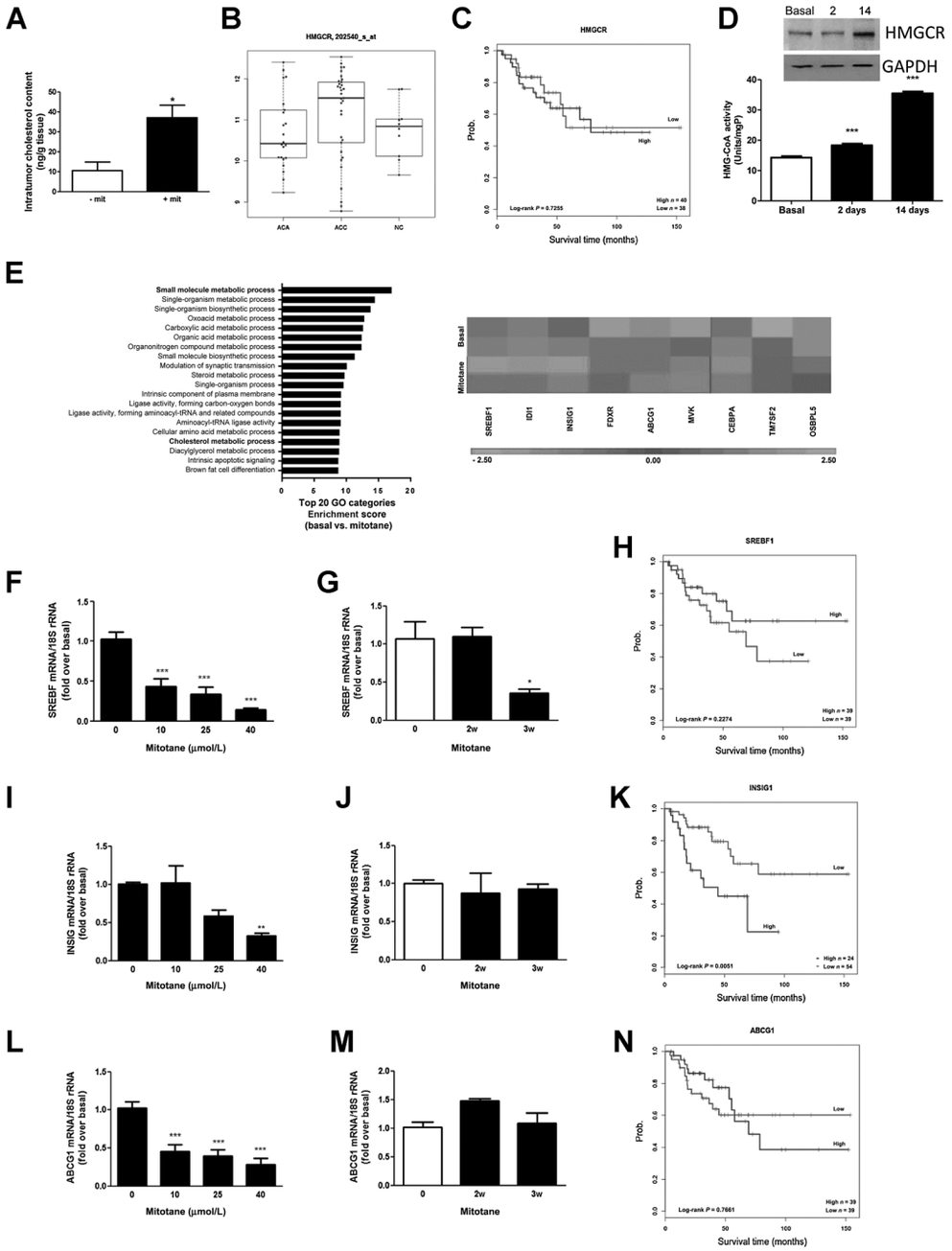

Figure 1.

Mitotane changes the expression of genes involved in cholesterol homeostasis in ACC and negatively affects patients' survival. **A,** Cholesterol was extracted from human ACC samples and its content (ng/mg tissue) measured by colorimetric assay (− Mitotane, $n = 5$, + Mitotane, $n = 7$; *, $P < 0.03$). **B,** Box plot graph for HMGCR gene expression in ACA, ACC, and NC human samples. ACC-ACA: P value = 0.08, ACA-NC: P value = 0.26, ACC-NC: P value = 0.26. Statistical significance was calculated using *limma*. **C,** Survival time in patients with ACC according to *HMGCR* gene expression. **D,** HMGCR expression and activity were evaluated in H295R cells untreated (basal) or treated for 2 and 14 days with mitotane (10 μmol/L). **E,** RNA from H295R cells left untreated (basal) or treated for 24 hours with mitotane (25 μmol/L) was processed for microarray analysis. Enrichment analysis for the categories GO and heat map from microarray data with the most highly upregulated (red) and downregulated (blue) genes involved in the cholesterol biosynthesis pathway. **F** and **G, I** and **J, L** and **M,** mRNA expression of *SRBP1* (**F** and **G**), *INSIG1* (**I** and **J**), and *ABCG1* (**L** and **M**) in H295R cells. The mRNA was extracted and analyzed by QPCR from cells left untreated (0) or treated for 24 hours with Mitotane (10–25–40 μmol/L; **F**, **I**, and **L**) and from cells untreated (0) or treated for different weeks (2 or 3 weeks, w) with Mitotane (10 μmol/L; **G**, **J**, and **M**). Each sample was normalized to 18S rRNA content. Final results are expressed as n-fold differences of gene expression relative to calibrator. Data represent the mean ±SD of values from at least three separate RNA samples (*, $P < 0.05$ and ***, $P < 0.001$ versus calibrator). **H**, **K**, and **N,** Survival time in patients with ACC according to the expression of *SREBP1* (**H**), *INSIG1* (**K**), and *ABCG1* (**N**) genes. Statistical significance was calculated using t test (**A–C**, **H**, **K**, and **N**) or one-way ANOVA followed by a Tukey *post-hoc* multiple comparison test (**D**, **F** and **G**, **I** and **J**, and **L** and **M**). $P < 0.05$ was considered significant.

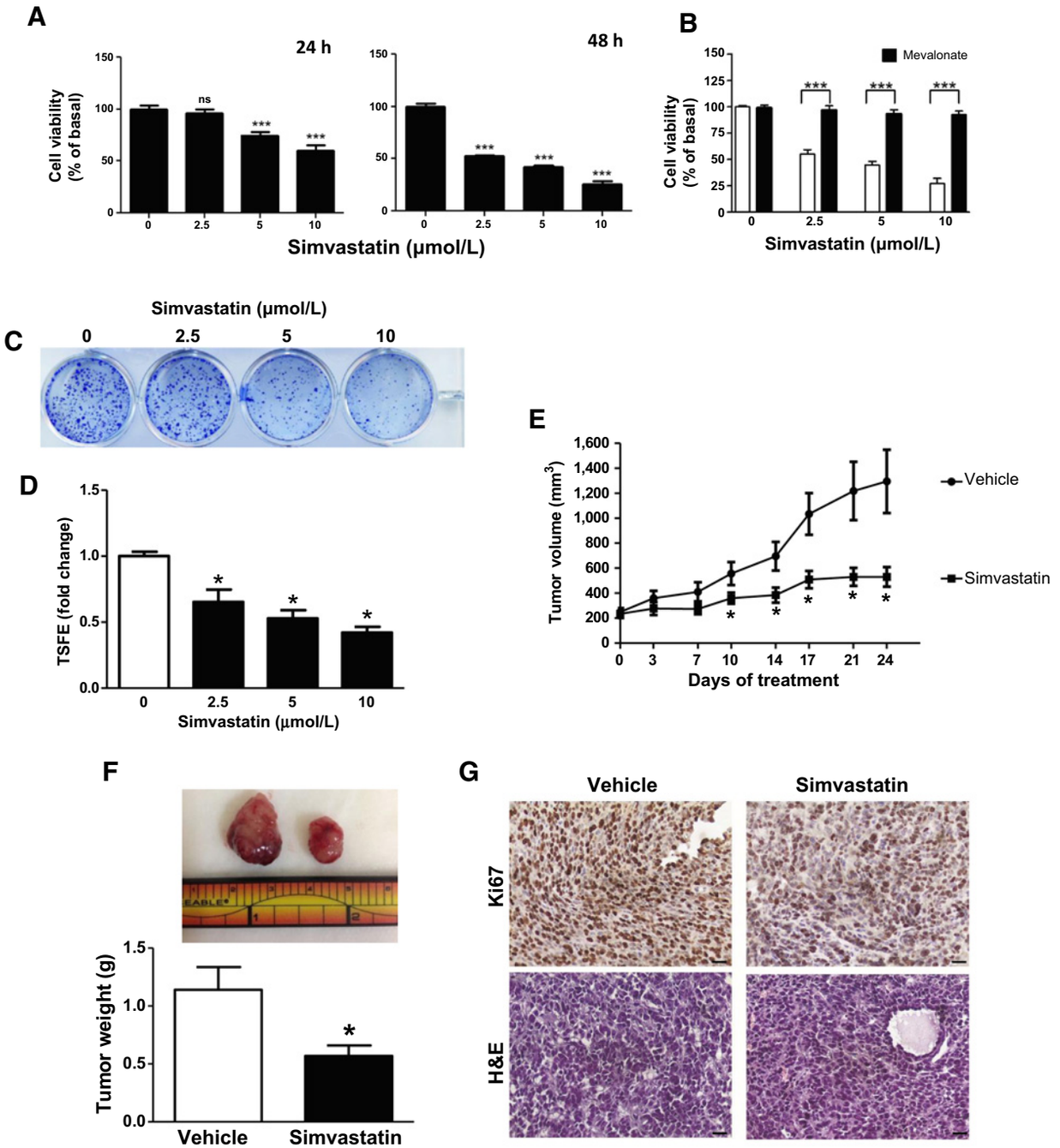

Figure 2.

Simvastatin reduces H295R cell growth, *in vitro* and *in vivo*. **A,** H295R cells were left untreated (0) or treated with increasing doses (2.5, 5, and 10 μmol/L) of simvastatin for 24 and 48 hours. **B,** H295R cells were left untreated (0) or treated with increasing doses (2.5, 5, and 10 μmol/L) of simvastatin with or without mevalonate (100 μmol/L) for 48 hours. **A** and **B,** Cell viability was evaluated by MTT assay (*, $P < 0.05$ and ***, $P < 0.001$ vs. 0). **C,** Representative image of colony formation assay performed on H295R cells (1,000 cells/well) plated for 2 weeks in the presence of simvastatin (2.5, 5, and 10 μmol/L). **D,** H295R cells were plated on low-attachment plates and then left untreated (0) or treated with Simvastatin (2.5, 5, and 10 μmol/L), and TSFE was evaluated 5 days later (*, $P < 0.05$ vs. untreated cells). **E,** H295R cells were injected subcutaneously in the flank region of nude mice, and the resulting tumors were grown to an average of 200 mm^3 21 days after inoculation and then treated with vehicle ($n = 8$) or simvastatin ($n = 7$; 4 mg/kg/day) for 24 days. Values represent the mean ±SE of measured tumor volume over time (*, $P < 0.05$ vs. control). **F,** Representative tumors and final tumor weights, and values are mean ±SEM (*, $P < 0.05$ vs. vehicle). **G,** Ki67 IHC and hematoxylin and eosin (H&E) staining of H295R xenografts (magnification, ×20; scale bar, 25 μm). Statistical significance was calculated using *t* test (**F**) or one-way ANOVA followed by a Tukey *post-hoc* multiple comparison test (**A**, **B**, **D**, and **E**). $P < 0.05$ was considered significant.

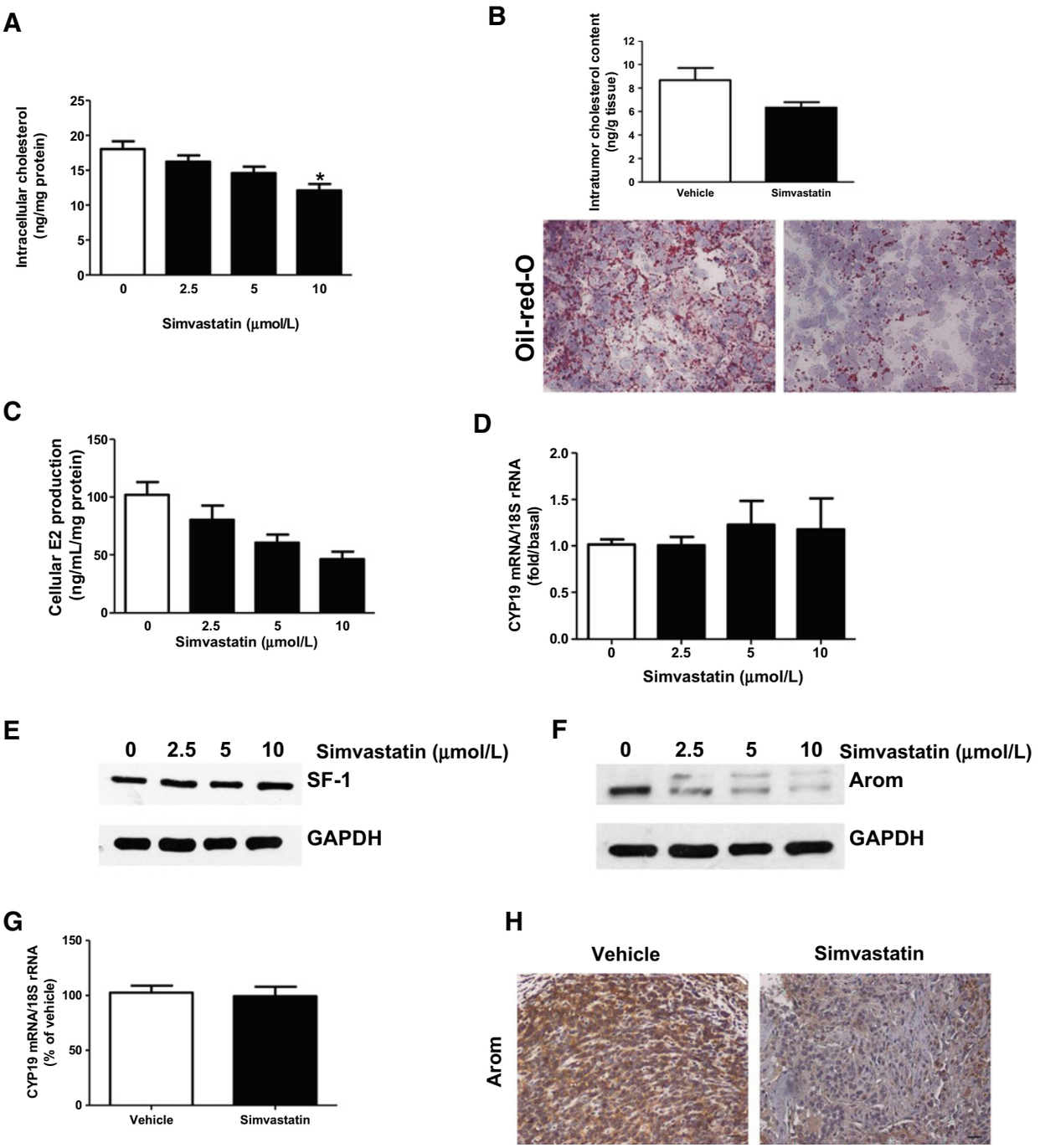

Figure 3.

Simvastatin decreases cholesterol and aromatase content in ACC. **A,** H295R cells were left untreated (0) or treated for 48 hours with simvastatin (2.5, 5, and 10 μmol/L) in growth medium containing 10% lipoprotein-free serum. Cholesterol was extracted and measured by colorimetric assay (*, $P < 0.05$ vs. untreated cells). **B,** (bar graph) Cholesterol content in H295R xenografts samples (*, $P < 0.05$ vs. vehicle; $n = 8$ vehicle; $n = 7$ Simvastatin). **B,** (photograph) Frozen sections of H295R xenografts from vehicle- or simvastatin-treated mice were used for lipids droplets staining by Oil Red O (magnification, ×40; scale bar, 12.5 μm). **C,** H295R cells were treated for 48 hours with the indicated doses of simvastatin added to 5% DCC-FBS, and estradiol (E2) release in the culture medium was measured by ELISA. Values represent the mean ± SE (*, $P < 0.05$ vs. untreated cells). **D–F,** H295R cells untreated (0) or treated for 24 hours with simvastatin (2.5, 5, and 10 μmol/L) were analyzed for *CYP19* gene expression normalized to 18S rRNA by real-time PCR (**D**), and for SF-1 (**E**) or Aromatase (Arom, **F**) protein content by WB. GAPDH was used as a loading control. Blots are from first representative experiment out of at least three performed. **G,** *CYP19* expression in H295R xenografts' samples from vehicle- or simvastatin-treated mice by real-time PCR ($n = 8$ vehicle; $n = 7$ Simvastatin). **H,** IHC staining of Aromatase in untreated or simvastatin-treated H295R xenograft samples (magnification, ×20; scale bar, 25 μmol/L). Statistical significance was calculated using *t* test (**B** and **G**) or one-way ANOVA followed by a Tukey *post-hoc* multiple comparison test (**A**, **C**, and **D**). $P < 0.05$ was considered significant.

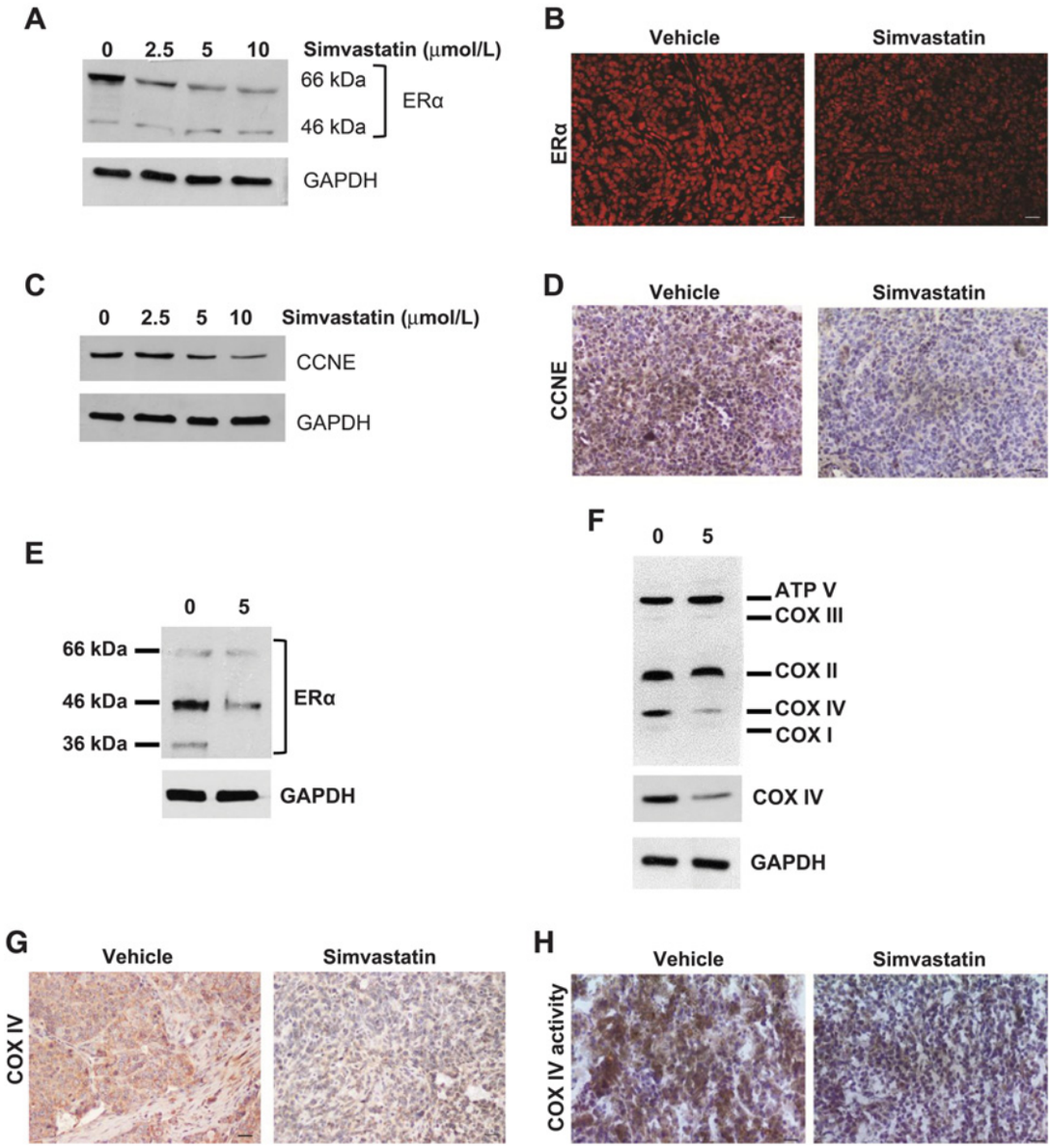

Figure 4.

Simvastatin reduces nuclear and mitochondrial ERα activity. **A** and **C,** WB analysis of ERα (**A**) and Cyclin E (**C**) was performed on equal amounts of total protein extracts from H295R cells left untreated (0) or treated with Simvastatin (2.5, 5, and 10 μmol/L) for 48 hours. GAPDH was used as a loading control. Blots are representative of three independent experiments with similar results. **B** and **D,** Immunofluorescence analysis of ERα expression (**B**) and IHC staining of Cyclin E (**D**) on H295R xenograft tumor samples obtained from vehicle- or simvastatin-treated mice (magnification, ×20; scale bar, 25 μmol/L). **E** and **F,** H295R cells untreated (0) or treated with simvastatin (5 μmol/L) were used for mitochondrial protein extraction. ERα (**E**) and OXPHOS (**F**) protein expression was analyzed by WB. GAPDH was used as a loading control. Blots are representative of three independent experiments with similar results. **G** and **H,** Immunostaining (**G**) and activity (**H**) of COXIV were evaluated on H295R xenograft samples obtained from vehicle- or simvastatin-treated mice (magnification, ×20; scale bar, 25 μm).

inhibition on ERα expression seen in the presence of simvastatin (Supplementary Fig. S3A).

These effects are opposite to those elicited by E2, which instead increased cyclin E expression (Supplementary Fig. S3B). Mitochondrial protein fraction was used for WB analysis of ERα, and we observed that simvastatin-treated samples had a lower content of the nuclear receptor (**Fig. 4E**). WB analysis of all the components of the respiratory chain (COX I to IV plus ATP synthase) can be performed using a mix of five different antibodies (OX-PHOS). With this approach, we identified a decreased expression of COXIV (**Fig. 4F**; Supplementary Fig. S4A and S4B), a known target of ERα. On the contrary, E2 treatment increased COXIV expression and is able to prevent statin-inhibitory effect (Supplementary Fig. S3C). Data were also confirmed on statin-treated xenografts where we observed a reduced COXIV expression (**Fig. 4G**; Supplementary Fig. S2F) and activity (**Fig. 4H**; Supplementary Fig. S2G) compared with vehicle-

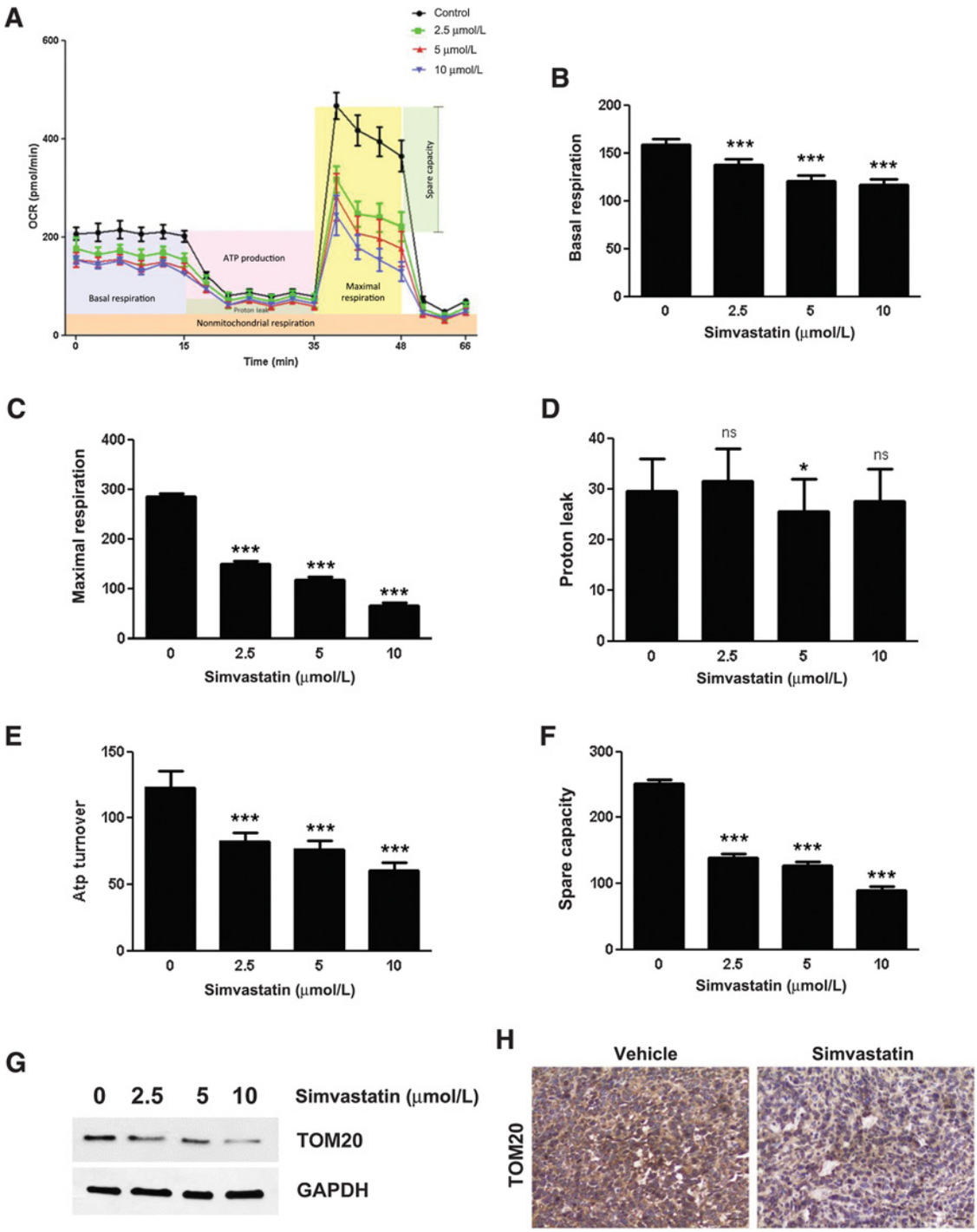

Figure 5.

Simvastatin reduces mitochondrial functions. **A–F,** Mitochondrial respiration described as OCR levels was detected in H295R cells left untreated or treated with Simvastatin (2.5, 5, and 10 μmol/L) for 16 hours by Seahorse XFe96 analyzer. **A,** The linear graph shows time course measurements but with three different injections to evaluate the OCR (1) after the oligomycin injection, (2) after the injection of carbonyl cyanide-(trifuoromethoxy)phenylhydrazone (FCCP), and (3) after the injection of rotenone/antimycin. **B–F,** The histograms are derived from the obtained measurements: (**B**) basal respiration, (**C**) maximal respiration, (**D**) proton leak, (**E**) ATP turnover, and (**F**) spare capacity (*, $P < 0.05$ and ***, $P < 0.001$ simvastatin vs. untreated cells). **G,** Mitochondrial extracts from H295R cells treated for 48 hours were analyzed for TOM20 protein expression by WB. **H,** TOM20 protein expression was evaluated by IHC on H295R xenograft samples obtained from vehicle- or simvastatin-treated mice (magnification, ×20; scale bar, 25 μm).

treated xenografts. We monitored cellular OCR and demonstrated that simvastatin is able to reduce oxygen consumption in a dose-dependent manner (**Fig. 5A**). Statin exposure profoundly affected the oxidative metabolism of H295R cells. Indeed, 16 hours of treatment induced a clear dose-dependent decrease of the basal (**Fig. 5B**) and maximal respiration (**Fig. 5C**) as well as ATP turnover (**Fig. 5E**) and spare capacity (**Fig. 5F**). No effect was observed on proton leak (**Fig. 5D**). We also used immunoblotting to monitor the abundance of a known reliable marker of mitochondrial mass, TOM20, in response to simvastatin treatment. We found that treated H295R cells displayed a reduced expression of TOM20, *in vitro* and *in vivo* (**Fig. 5G** and **H**; Supplementary Fig. S2H).

Decreased cholesterol availability in ACC activates an apoptotic pathway

BAK expression and PARP-1 cleavage were increased in H295R cells treated for 48 hours with simvastatin, indicating activation of apoptosis (**Fig. 6A**; Supplementary Fig. S4C and S4D), further confirmed by TUNEL assay (**Fig. 6B**). Similarly, evaluation of apoptosis on H295R xenografts sections revealed an increase of TUNEL-positive cells under simvastatin treatment (**Fig. 6C**). Because Bak gene is under c-Jun transcriptional control (25), we evaluated c-Jun protein levels after simvastatin treatment. After 48 hours, we observed increased levels of c-Jun and its phosphorylation status, as well as increased levels of pERK1/2, whose sustained activation is associated with apoptosis (26). Addition of mevalonate prevented activation of these kinases in response to simvastatin (**Fig. 6D**; Supplementary Fig. S4C and S4D). Specific inhibitors for ERK1/2 and JNK abrogated Jun and ERK1/2 activation/phosphorylation preventing apoptosis, as indicated by the loss of PARP1 cleavage. These data indicate ERK1/2 and JNK as part of simvastatin-induced apoptotic mechanism (**Fig. 6E**). Similarly to simvastatin, fluvastatin and rosuvastatin inhibited estrogen signaling and activated apoptosis in H295R cells (Supplementary Fig. S4E and S4F).

Discussion

Mitotane represents the first-line therapy for patients with ACC. However, mitotane alone or combined with chemotherapy shows limited efficacy on advanced disease. In addition, mitotane has high toxicity and several side effects including hypercholesterolemia (6, 27). Data from almost 40 years ago report the ability of mitotane to increase liver HMGCR activity *in vitro* and *in vivo* (5). Because the adrenal synthesizes cholesterol *de novo*, mitotane could have a direct effect on adrenal cholesterol synthesis. Having higher cholesterol bioavailability, tumor cells can foster their own growth. To support our hypothesis, we first demonstrate an increase in intratumor cholesterol in patients with ACC treated with mitotane compared with untreated patients. Using previously published microarray data publically available (28), we demonstrated the presence of increased HMGCR expression in ACC samples, which, however, was not associated with decreased survival rate. Increased intratumor cholesterol following mitotane treatment could be due to an increased activity of HMGCR rather than to an increased expression, with the former influencing survival more than the latter. Microarray analysis of mitotane-treated H295R cells helped us in identifying genes involved in cholesterol metabolism and modulated by the drug. Among them, we validated *INSIG1, SREBP1*, and *ABCG1*. *INSIG1* encodes for a protein that retains a chaperone protein (SCAP) in the endoplasmic reticulum, and SCAP is necessary for delivery of SREBP1 to the Golgi, where SREBP1 becomes active. SREBP1 increases transcription of cholesterol-synthesizing genes such as *HMGCR* (29).

Short-term mitotane decreases *INSIG1* and *SREBP1* expression, whereas long-term mitotane maintains low *SREBP1* but high *INSIG1* expression. When looking at survival data of patients with ACC, high *INSIG1* is associated with a shorter survival. *ABCG1* belongs to the family of ATP binding cassette and mediates cholesterol efflux (30). Its expression is decreased by short-term mitotane treatment, but this effect is lost after prolonged treatment, favoring cholesterol accumulation. Because mitotane has a prevalent accumulation in adipose tissue, the circulating levels are often reduced (13, 31), and the therapeutic concentrations of mitotane (between 14 and 20 μg/mL, 40 and 60 μmol/L) are not always reached in patients. Importantly, lower doses (10 and 25 μmol/L) produce effects that are different from what were seen using 40 μmol/L. This raises a question, could cells, in the presence of lower doses of mitotane, escape the normal control of cholesterol homeostasis? Can the increase in cholesterol be responsible for long-term adjustment to mitotane?

Several reports propose a promising role for statins in cancer treatment (32). Here, we demonstrate that simvastatin can reduce intratumor cholesterol synthesis. Based on MTT assay, IC_{50} for simvastatin was calculated to be 10 μmol/L. Since 1 μmol/L simvastatin in the media corresponds to the dose of 0.4586 mg/kg of body weight, we decided to treat mice with 4 mg/kg/day. This dose is equivalent to a human dose of 20 mg/d based on body surface area equivalency. This dose was effective in producing more that 60% decrease in tumor growth. Importantly, this dose decreased intratumor cholesterol content, supporting our hypothesis that a reduction in intratumor cholesterol can decrease ACC growth. Interest for statins is not new for the therapy of ACC; however, it has been considered in association with mitotane to reduce hypercholesterolemia (6, 33). Our data instead suggest the possibility of using lipophilic statins without mitotane but eventually with cytotoxic drugs. Simvastatin, which appears to be the most effective among the tested drugs, should not be combined with mitotane, which is a known inducer of *CYP3A4*, a member of the cytochrome P450 family involved in simvastatin metabolism. A recent case study evaluated management of hypercholesterolemia induced by mitotane treatment. The use of statins, coadministred with mitotane, was uneffective in lowering cholesterol and LDL-c level. Importantly, the patient had two local recurrences within a 7-year period; however, the course of ACC in this patient's case has been better than average. These data support our hypothesis that cholesterol can be implicated in ACC progression.

Cholesterol in tumor adrenal cells is used for steroid synthesis, and a decrease in its availability would affect estradiol production. Our previous study demonstrated that E2 increases tumor growth, and Tamoxifen, which blocks ERα activity, prevents its effects (9). With this information as background, we wanted to investigate if the reduced E2 production, seen after simvastatin treatment, could interfere with ERα function. We first observed a reduction in CCNE, a known nuclear target of ERα. In addition, we investigated if the expression of mitochondrial targets of ERα could be influenced by simvastatin. To support a role for ERα in the mitochondria of tumor adrenal, we show that E2 treatment increases the amount of COXIV levels and prevents simvastatin-inhibitory effect.

In addition, direct effect of statins was reported on mitochondrial function, consequent to a deficiency of complex I (34). The novelty of our data is the involvement of ERα/complex IV in statin-mediated apoptosis. The reduction in COXIV alters the functioning of mitochondrial respiration, changing the mitochondrial potential ultimately

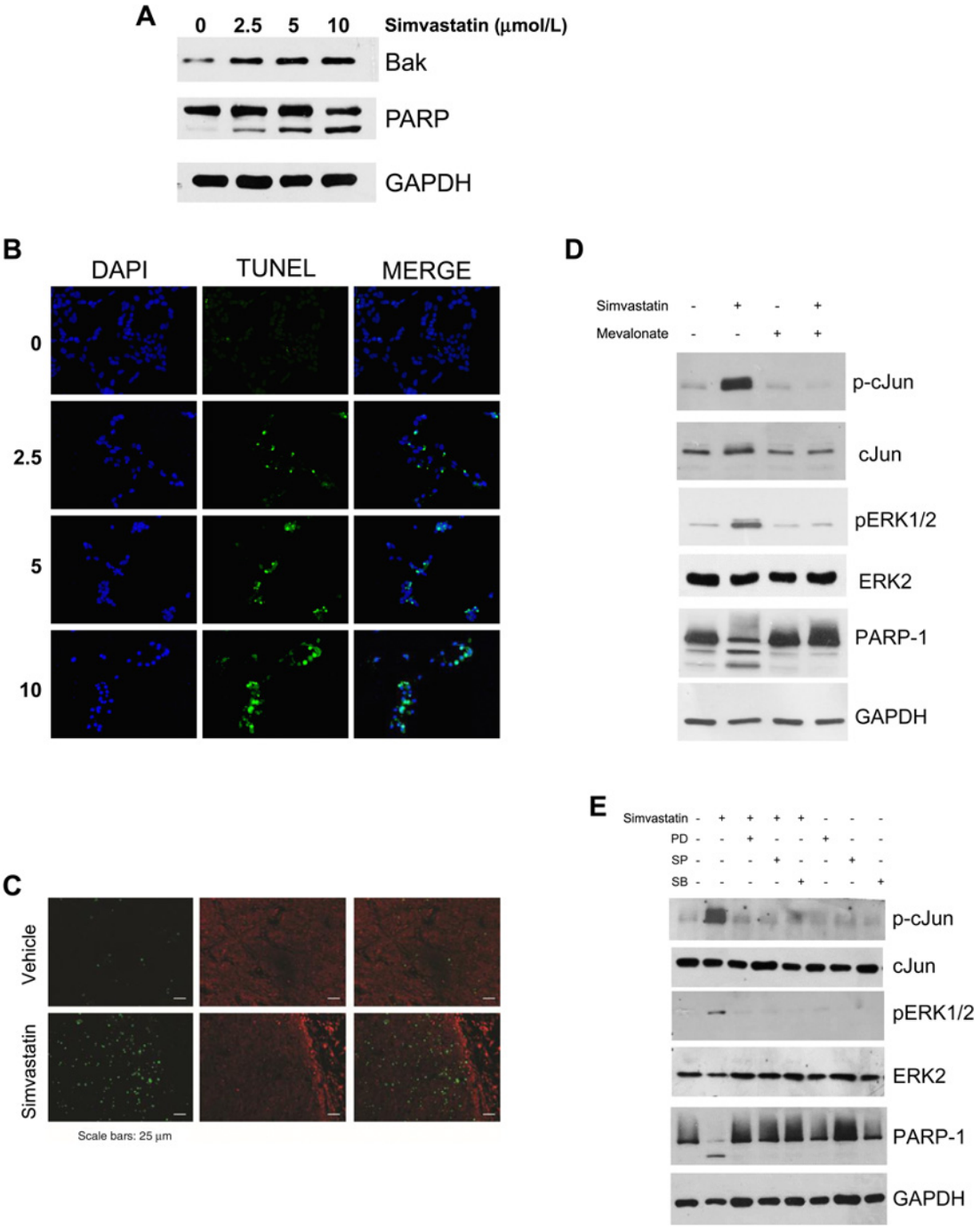

Figure 6.

In vitro and *in vivo* activation of apoptosis by simvastatin in ACC. **A,** Cells were left untreated (0) or treated with simvastatin (2.5, 5, and 10 μmol/L) for 48 hours. WB analyses of Bak and PARP-1 were performed on equal amounts of total protein extracts. GAPDH was used as a loading control. Blots are representative of three independent experiments with similar results. **B,** TUNEL assay was performed on cells treated as described in **A**. DAPI was used as nuclear counterstain. Fluorescent signal was observed under a fluorescent microscope. Images are from a representative experiment. **C,** TUNEL staining was performed on frozen sections of H295R xenograft samples obtained from vehicle- or simvastatin-treated mice (scale bar, 25 μm). **D,** WB analyses for p-cJun, c-Jun, pERK1/2, ERK2, and PARP-1 were performed on total protein extracted from cells treated for 48 hours with simvastatin (5 μmol/L), mevalonate (100 μmol/L), or their combination. **E,** WB analyses for p-cJun, Jun, pERK1/2, ERK2, and PARP-1 were performed on total protein extracted from cells treated for 48 hours with simvastatin (5 μmol/L) alone or combined with PD98059 (10 μmol/L), SP600125 (10 μmol/L), and SB203580 (10 μmol/L). GAPDH was used as a loading control.

leading to organelle damage. High COXIV activity within the tumor occurs in a significant subset of patients with high-grade gliomas and is an independent predictor of poor outcome (35). Importantly, it has been postulated that COXIV activity may be required for the anchorage-independent growth of lung cancer cells (36). In general, mitochondria appear to be an appealing target for the treatment of cancer (37). Effects on COXIV negatively influence mitochondrial function as demonstrated by reduced OCR. We have previously demonstrated that a reduced cell growth is observed in breast cancer cells treated with XCT790, a drug that targets ERRα, a master regulator of cell metabolism. ERRα inhibition reduces OCR and prevents tumor growth (20). We have also used XCT790 to block ERRα in ACC and demonstrated its efficacy in reducing tumor growth (38), further establishing that impairing mitochondrial function reduces ACC growth. It has been shown that mitotane significantly impairs mitochondrial respiratory chain function by selectively inhibiting enzymatic complex IV activity. However, as a consequence of respiratory chain inhibition, mitotane causes a compensatory increase of mitochondrial biogenesis (39). Differently from mitotane, simvastatin reduces TOM20, a marker of mitochondrial mass. Reduced mitochondrial function after treatment with simvastatin causes cell death by apoptosis, the same type of cell death that is observed in H295R and SW13 cells in response to mitotane. This apoptotic mechanism requires activation of c-Jun and sustained ERK1/2 phosphorylation. Farnesyl pyrophosphate or geranylgeranyl pyrophosphate are products of mevalonate that can be anchored onto intracellular proteins through prenylation, thereby ensuring the relocalization of the target proteins in the cell membranes (40–42). Ras is a prenylated protein upstream of ERK1/2 activation. The observation that ERK1/2 phosphorylation is maintained in the presence of simvastatin evidences that its phosphorylation is independent of Ras and potentially involves different pathways. We found that ERK phosphorylation is prevented by addition of p38 and JNK inhibitors, implicating these kinases in the observed sustained ERK activation. Jun expression and activation are increased by treatment with simvastatin and are reversed by addition of mevalonate, which also prevents PARP-1 cleavage, confirming that the apoptotic mechanism is dependent on cholesterol depletion.

Collectively, our data support the hypothesis of using statins for the treatment of ACC. Further preclinical studies are warranted to establish effects on tumor growth when used in combination with chemotherapy. However, their use in therapy as cholesterol-lowering drugs will easily translate preclinical studies into a clinical trial.

Disclosure of Potential Conflicts of Interest

No potential conflicts of interest were disclosed.

Authors' Contributions

Conception and design: V. Pezzi, I. Casaburi, R. Sirianni
Development of methodology: F. Trotta, P. Avena, A. Chimento, V. Rago, A. De Luca, S. Sculco, M.C. Nocito, F.M. Lasorsa, S.N. Barile, L. Palmieri, R. Sirianni
Acquisition of data (provided animals, acquired and managed patients, provided facilities, etc.): F. Trotta, R. Malivindi, R. Pezzani, R. Sirianni
Analysis and interpretation of data (e.g., statistical analysis, biostatistics, computational analysis): F. Fallo, C. Pilon, F.M. Lasorsa, S.N. Barile, L. Palmieri, A.M. Lerario, I. Casaburi, R. Sirianni
Writing, review, and/or revision of the manuscript: P. Avena, A. Chimento, I. Casaburi, R. Sirianni
Administrative, technical, or material support (i.e., reporting or organizing data, constructing databases): F. Trotta, A. De Luca
Study supervision: V. Pezzi, I. Casaburi, R. Sirianni

Acknowledgments

This work was supported by Associazione Italiana per la Ricerca sul Cancro (AIRC) grant IG15230 to Dr. R. Sirianni and IG20122 to Dr. V. Pezzi. Drs. F. Trotta and P. Avena were supported by a fellowship from AIRC.

The costs of publication of this article were defrayed in part by the payment of page charges. This article must therefore be hereby marked *advertisement* in accordance with 18 U.S.C. Section 1734 solely to indicate this fact.

Received November 13, 2019; revised March 8, 2020; accepted June 11, 2020; published first June 16, 2020.

References

1. Kirschner LS. The next generation of therapies for adrenocortical cancers. Trends Endocrinol Metab 2012;23:343–50.
2. Fassnacht M, Johanssen S, Quinkler M, Bucsky P, Willenberg HS, Beuschlein F, et al. Limited prognostic value of the 2004 international union against cancer staging classification for adrenocortical carcinoma: proposal for a revised TNM classification. Cancer 2009;115:243–50.
3. Hermsen IG, Fassnacht M, Terzolo M, Houterman S, den Hartigh J, Leboulleux S, et al. Plasma concentrations of o,p'DDD, o,p'DDA, and o,p'DDE as predictors of tumor response to mitotane in adrenocortical carcinoma: results of a retrospective ENS@T multicenter study. J Clin Endocrinol Metab 2011;96:1844–51.
4. Kerkhofs TM, Baudin E, Terzolo M, Allolio B, Chadarevian R, Mueller HH, et al. Comparison of two mitotane starting dose regimens in patients with advanced adrenocortical carcinoma. J Clin Endocrinol Metab 2013;98:4759–67.
5. Stacpoole PW, Varnado CE, Island DP. Stimulation of rat liver 3-hydroxy-3-methylglutaryl-coenzyme A reductase activity by o,p'-DDD. Biochem Pharmacol 1982;31:857–60.
6. Maher VM, Trainer PJ, Scoppola A, Anderson JV, Thompson GR, Besser GM. Possible mechanism and treatment of o,p'DDD-induced hypercholesterolaemia. Q J Med 1992;84:671–9.
7. Miller WL. Steroidogenesis: unanswered questions. Trends Endocrinol Metab 2017;28:771–93.
8. Barzon L, Masi G, Pacenti M, Trevisan M, Fallo F, Remo A, et al. Expression of aromatase and estrogen receptors in human adrenocortical tumors. Virchows Arch 2008;452:181–91.
9. Sirianni R, Zolea F, Chimento A, Ruggiero C, Cerquetti L, Fallo F, et al. Targeting estrogen receptor-alpha reduces adrenocortical cancer (ACC) cell growth in vitro and in vivo: potential therapeutic role of selective estrogen receptor modulators (SERMs) for ACC treatment. J Clin Endocrinol Metab 2012;97:E2238–50.
10. Miller BS, Ignatoski KM, Daignault S, Lindland C, Doherty M, Gauger PG, et al. Worsening central sarcopenia and increasing intra-abdominal fat correlate with decreased survival in patients with adrenocortical carcinoma. World J Surg 2012;36:1509–16.
11. Simpson ER. Sources of estrogen and their importance. J Steroid Biochem Mol Biol 2003;86:225–30.
12. Li J, Papadopoulos V, Vihma V. Steroid biosynthesis in adipose tissue. Steroids 2015;103:89–104.
13. Hescot S, Seck A, Guerin M, Cockenpot F, Huby T, Broutin S, et al. Lipoprotein-free mitotane exerts high cytotoxic activity in adrenocortical carcinoma. J Clin Endocrinol Metab 2015;100:2890–8.
14. Chimento A, Sirianni R, Casaburi I, Zolea F, Rizza P, Avena P, et al. GPER agonist G-1 decreases adrenocortical carcinoma (ACC) cell growth in vitro and in vivo. Oncotarget 2015;6:19190–203.
15. Weiss LM, Medeiros LJ, Vickery AL Jr. Pathologic features of prognostic significance in adrenocortical carcinoma. Am J Surg Pathol 1989;13:202–6.
16. Aubert S, Wacrenier A, Leroy X, Devos P, Carnaille B, Proye C, et al. Weiss system revisited: a clinicopathologic and immunohistochemical study of 49 adrenocortical tumors. Am J Surg Pathol 2002;26:1612–9.

17. De Luca A, Avena P, Sirianni R, Chimento A, Fallo F, Pilon C, et al. Role of scaffold protein proline-, glutamic acid-, and leucine-rich protein 1 (PELP1) in the modulation of adrenocortical cancer cell growth. Cells 2017;6:42.
18. Shaw FL, Harrison H, Spence K, Ablett MP, Simões BM, Farnie G, et al. A detailed mammosphere assay protocol for the quantification of breast stem cell activity. J Mammary Gland Biol Neoplasia 2012;17:111–7.
19. Reagan-Shaw S, Nihal M, Ahmad N. Dose translation from animal to human studies revisited. FASEB J 2008;22:659–61.
20. De Luca A, Fiorillo M, Peiris-Pages M, Ozsvari B, Smith DL, Sanchez-Alvarez R, et al. Mitochondrial biogenesis is required for the anchorage-independent survival and propagation of stem-like cancer cells. Oncotarget 2015;6:14777–95.
21. Bolstad BM, Irizarry RA, Astrand M, Speed TP. A comparison of normalization methods for high density oligonucleotide array data based on variance and bias. Bioinformatics 2003;19:185–93.
22. Irizarry RA, Bolstad BM, Collin F, Cope LM, Hobbs B, Speed TP. Summaries of Affymetrix GeneChip probe level data. Nucleic Acids Res 2003;31:e15.
23. Wu ZJ, Irizarry RA, Gentleman R, Martinez-Murillo F, Spencer F. A model-based background adjustment for oligonucleotide expression arrays. J Am Statist Assoc 2004;99:909–17.
24. Chen JQ, Cammarata PR, Baines CP, Yager JD. Regulation of mitochondrial respiratory chain biogenesis by estrogens/estrogen receptors and physiological, pathological and pharmacological implications. Biochim Biophys Acta 2009; 1793:1540–70.
25. Jin HO, Park IC, An S, Lee HC, Woo SH, Hong YJ, et al. Up-regulation of Bak and Bim via JNK downstream pathway in the response to nitric oxide in human glioblastoma cells. J Cell Physiol 2006;206:477–86.
26. Cagnol S, Chambard JC. ERK and cell death: mechanisms of ERK-induced cell death–apoptosis, autophagy and senescence. FEBS J 2010;277:2–21.
27. Daffara F, De Francia S, Reimondo G, Zaggia B, Aroasio E, Porpiglia F, et al. Prospective evaluation of mitotane toxicity in adrenocortical cancer patients treated adjuvantly. Endocr Relat Cancer 2008;15:1043–53.
28. Barlaskar FM, Spalding AC, Heaton JH, Kuick R, Kim AC, Thomas DG, et al. Preclinical targeting of the type I insulin-like growth factor receptor in adrenocortical carcinoma. J Clin Endocrinol Metab 2009;94:204–12.
29. Weber LW, Boll M, Stampfl A. Maintaining cholesterol homeostasis: sterol regulatory element-binding proteins. World J Gastroenterol 2004;10:3081–7.
30. Yvan-Charvet L, Wang N, Tall AR. Role of HDL, ABCA1, and ABCG1 transporters in cholesterol efflux and immune responses. Arterioscler Thromb Vasc Biol 2010;30:139–43.
31. van Slooten H, Moolenaar AJ, van Seters AP, Smeenk D. The treatment of adrenocortical carcinoma with o,p'-DDD: prognostic implications of serum level monitoring. Eur J Cancer Clin Oncol 1984;20:47–53.
32. Zhong S, Zhang X, Chen L, Ma T, Tang J, Zhao J. Statin use and mortality in cancer patients: systematic review and meta-analysis of observational studies. Cancer Treat Rev 2015;41:554–67.
33. Tsakiridou ED, Liberopoulos E, Giotaki Z, Tigas S. Proprotein convertase subtilisin-kexin type 9 (PCSK9) inhibitor use in the management of resistant hypercholesterolemia induced by mitotane treatment for adrenocortical cancer. J Clin Lipidol 2018;12:826–9.
34. Sirvent P, Bordenave S, Vermaelen M, Roels B, Vassort G, Mercier J, et al. Simvastatin induces impairment in skeletal muscle while heart is protected. Biochem Biophys Res Commun 2005;338:1426–34.
35. Griguer CE, Cantor AB, Fathallah-Shaykh HM, Gillespie GY, Gordon AS, Markert JM, et al. Prognostic relevance of cytochrome C oxidase in primary glioblastoma multiforme. PLoS One 2013;8:e61035.
36. Telang S, Nelson KK, Siow DL, Yalcin A, Thornburg JM, Imbert-Fernandez Y, et al. Cytochrome c oxidase is activated by the oncoprotein Ras and is required for A549 lung adenocarcinoma growth. Mol Cancer 2012;11:60.
37. Ralph SJ, Neuzil J. Mitochondria as targets for cancer therapy. Mol Nutr Food Res 2009;53:9–28.
38. Casaburi I, Avena P, De Luca A, Chimento A, Sirianni R, Malivindi R, et al. Estrogen related receptor alpha (ERRalpha) a promising target for the therapy of adrenocortical carcinoma (ACC). Oncotarget 2015;6: 25135–48.
39. Hescot S, Slama A, Lombes A, Paci A, Remy H, Leboulleux S, et al. Mitotane alters mitochondrial respiratory chain activity by inducing cytochrome c oxidase defect in human adrenocortical cells. Endocr Relat Cancer 2013;20: 371–81.
40. Nishida S, Matsuoka H, Tsubaki M, Tanimori Y, Yanae M, Fujii Y, et al. Mevastatin induces apoptosis in HL60 cells dependently on decrease in phosphorylated ERK. Mol Cell Biochem 2005;269:109–14.
41. Yanae M, Tsubaki M, Satou T, Itoh T, Imano M, Yamazoe Y, et al. Statin-induced apoptosis via the suppression of ERK1/2 and Akt activation by inhibition of the geranylgeranyl-pyrophosphate biosynthesis in glioblastoma. J Exp Clin Cancer Res 2011;30:74.
42. Wu J, Wong WW, Khosravi F, Minden MD, Penn LZ. Blocking the Raf/MEK/ERK pathway sensitizes acute myelogenous leukemia cells to lovastatin-induced apoptosis. Cancer Res 2004;64:6461–8.

Case Report: This is a retrospective analysis of four cases of Insulinoma diagnosed between
Sep 2016 and Mar 2019. All the patients were males and aged 36, 22, 63 and 15 years respectively. Baseline characteristics, duration to diagnosis of Insulinoma, diagnosis and treatment
given before definitive diagnosis and post-surgery outcomes were analyzed. All the four patients had relatively long latency to diagnosis despite frequent, spontaneous hypoglycemic
episodes, longest being ten years. The patients had a neurological and/or psychiatric diagnosis prior to definitive diagnosis. The symptoms improved with consumption of food. One of the
four patients was on antipsychotics for episodic abnormal behavior before the diagnosis of
Insulinoma. Two of them were on anti-epileptic medications for seizures. All the insulinomas
were localized with CECT without requirement for additional localization techniques. All our
patients responded well to surgical resection of the tumor. All insulinomas were benign grade
1 tumors. Acanthosis nigricans regressed in all the patients post-surgery. In addition, all the
patients had significant weight loss post-surgery. Two of the four patients developed diabetes
mellitus and were on insulin therapy.
Conclusion: A strong index of suspicion of Insulinoma is warranted while dealing with patients
presenting with seizure disorders, behavioral abnormalities and neurological symptoms because the spectrum of symptoms is wide and non-specific. Seeking diagnosis is of utmost importance because of implications on treatment and prognosis.
Reference:
Valente LG, Antwi K, Nicolas GP, Wild D, Christ E. Clinical presentation of 54 patients with endogenous hyperinsulinaemic hypoglycaemia: a neurological chameleon (observational study).
Swiss Med Wkly. 2018 Nov 18;148:w14682.

Tumor Biology

ENDOCRINE NEOPLASIA CASE REPORTS II

Autonomous Cortisol Secretion Coexisting with Pancreatic Neuroendocrine Tumor: A Rare Presentation

Fernanda Faro, MD[1], Gabriela Karman, MD[1], Nathalia Dal-Prá, MD[1], Jéssica Loureiro, MD[1], Cecilia Kauffman Rutenberg Feder, MD[2], Augusto Cezar Santomauro, MD[3], Jose Viana Lima, Physician[4], Bruna Mascarenhas, MD[1], Ana Teresa Santomauro, MD[1], Adriano Namo Cury, MD, PHD[5].
[1]A Beneficência Portuguesa de São Paulo, Sao Paulo, Brazil, [2]Irmandade da Santa Casa de Sao Paulo, SO PAULO, Brazil, [3]Hospital das Clinicas - University Sao Paulo, Sao Paulo, Brazil, [4]Santa Casa de Sao Paulo, Sao Paulo, Brazil, [5]Faculdade de Cincias Mdicas da Santa Casa de SP, Sao Paulo-SP, Brazil.

MON-921

Introduction: neuroendocrine tumors (NET) are a very rare and heterogeneous group of malignancies that can be associated with adrenocortical tumors in approximately 20% of the cases, mostly bilateral and non-functioning. Autonomous cortisol secretion occurs in less than 10% of adrenal incidentalomas and the coexistence of pancreatic neuroendocrine neoplasms and autonomous cortisol secretion is not well-described.
Clinical case: a 54-year-old man with previous history of systemic hypertension and type 2 diabetes mellitus, presented with left hypochondrium pain in the last 18 months, associated with abdominal distension, constipation and nausea. Physical examination without abnormalities. Abdominal tomography demonstrated dilatated pancreatic duct and a solid heterogeneous nodule in left adrenal, measuring about 2.7 cm. Ecoendoscopy revealed a heterogeneous, hypoechoic and oval nodular lesion, located at the transition of pancreatic head and uncinate process, measuring 1.5x1.1cm. Biopsy was performed, showing a pattern of neuroendocrine neoplasia, with chromogranin and synaptophysin +, Ki67 1%. Gallium-68 dotatate PET revealed two pancreatic nodular formations, one in proximal neck/body (1.5 cm) and the other in pancreatic tail (1 cm), presenting SUV of 20.4 and 21, respectively. Adrenal nodule presented minimal increase in radiopharmaceutical concentration. To exclude the hypothesis of metastasis, PET FDG was performed, showing physiological uptake in adrenal nodule. Pituitary MRI had no abnormalities.
Chromogranin A and gastrin values were normal. Pheochromocytoma and primary hyperaldosteronism were excluded. Hypercortisolism investigation presented the following results: 23h salivary cortisol 167ng/dl (NR < 100), 24-hour free urinary cortisol 42.1 mcg/24h (NR 4.2-60), post-1mg and 2mg dexamethasone serum cortisol of 10.8 mcg/dl and 3.8 respectively (serum dexamethasone levels of 193 and 780 ng/dl; NR > 130), ACTH 13 and 11 pg/ml.
By these results, coexistence of non-functioning pancreatic neuroendocrine tumor and autonomous cortisol secretion was confirmed. A total pancreatectomy with partial gastrectomy and bileodigestive anastomosis was performed. Pathological anatomical evidence demonstrated a well-differentiated neuroendocrine tumor (NET G1) and immunohistochemistry analyses showed positive chromogranine A, synaptophysine, Ki67 1% and negative ACTH. Clinical follow-up of the adrenal adenoma was preferred.
Conclusion: although most adrenocortical tumors associated with NET are nonfunctional, hypercortisolism should be considered. Adrenal metastasis and ectopic ACTH secretion are differential diagnosis. Clinical follow-up is an option when patient is asymptomatic and comorbidities are well-controlled.

Tumor Biology

ENDOCRINE NEOPLASIA CASE REPORTS I

Characterization of an Ovarian Steroid Cell Tumor in a VHL Patient

Marta Claudia Nocito, PhD Student, Prakaimuk Saraithong, PhD, Erika A. Newman, MD, Inas H. Thomas, MD, William E. Rainey, MS PHD, Antonio M. Lerario, MD, Amer Heider, MD, Tobias Else, MD.
University of Michigan, Ann Arbor, MI, USA.

SUN-931

Most ovarian steroid cell tumors arise sporadically. However, they can also be observed as a rare manifestation of von Hippel Lindau disease. Here, we present a clinical, pathological and molecular characterization of a steroid cell tumor in a VHL patient. A 14 year old girl with molecularly confirmed diagnosis of VHL developed hirsutism and amenorrhea. Initial clinical hormonal evaluation was notable for elevated 17-OHP of 406ng/dl, androstenedione 275ng/dl, and testosterone 102ng/dl. In order to exclude congenital adrenal hyperplasia as a common cause of hirsutism in adolescents, ACTH stimulation was performed, but no increase in 17-OHP was observed. Anti Muellerian hormone, inhibin (INH) A and INH B were normal. Imaging revealed a bilobed 6cm left adnexal mass. The mass was resected en bloc via a left oophorectomy. Pathological evaluation showed multinodular steroid cell tumor with clear cytoplasm and delicate vascular meshwork. Immunoprofiling demonstrated positivity for inhibin and calretinin; while renal cell carcinoma markers were negative. All laboratory values normalized post-surgery. In addition to clinical measurements pre- and post-surgery, steroid profiles were evaluated by LC-MS/MS. Quantitative RT-PCR analysis showed robust tumor expression of enzymes facilitating the production of androgens, but not estrogens. Further preliminary analysis by exome sequencing confirmed the known germline pathogenic variant in VHL, but no additional obvious somatic driver mutations were identified. Interestingly, the NGS analysis of different specimens from the same tumor revealed multiple different single base pair variants in the VHL gene as a second hit. In summary, hirsutism in VHL patients should raise the suspicion for unusual ovarian tumors. In contrary to the usual theory of a monoclonal expansion after loss of the wt VHL allele, this tumor appeared to be oligoclonal as evidenced by different somatic VHL mutations. This could be either explained by initial parallel occurrence of several clones or that the VHL second hit is not an initial event, but the mutation instead supports tumor expansion following initial steps of tumorigenesis.

Reproductive Endocrinology

SEX, GENDER, AND HORMONES

11-oxygenated C19 Steroids in Normal Weight, Overweight, and Hyperandrogenic Girls

Christine Michele Burt Solorzano, MD[1], Su Hee Kim, MD[1], Jessica A. Lundgren, MD[1], Angela Elizabeth Taylor, PhD[2], Christopher Rolland McCartney, MD[3], Wiebke Arlt, MD DSc FRCP FMedSci[2], John C. Marshall, MD,PhD[4].

[1]University of Virginia, Charlottesville, VA, USA, [2]University of Birmingham, Birmingham, United Kingdom, [3]University of Virginia School of Medicine, Charlottesville, VA, USA, [4]University of Virginia Health System, Charlottesville, VA, USA.

OR27-07

Hyperandrogenism (HA) often begins during puberty and may be a forerunner to polycystic ovary syndrome (PCOS). PCOS women have elevated 11-oxygenated androgens (O'Reilly MW et al, JCEM 2017), but the contribution of these androgens to HA in peri-pubertal girls is unknown. To address this uncertainty, we assessed classical and 11-oxygenated steroid levels at baseline and in response to both ACTH and recombinant human chorionic gonadotropin (r-hCG) administration in peri-pubertal girls. Girls (n=35) were studied in the mid-follicular phase (as relevant): age 13.1±3.1 (7.3-18.8) y (mean ± SD [range]); BMIz 1.1±1.1 (-1.08 to +2.65); Tanner breast 3.8±1.4 (1-5); bone age 14.1±3.1 (7.3-18) y. Of pre-menarcheal (PRE) girls, 4 were normal weight (NW, BMI% 5-84) and 7 overweight (OW, BMI% ≥ 85). Of post-menarcheal (POST) girls, 10 were NW, 6 OW, and 8 HA (3 NW, 5 OW). Blood was drawn at baseline (8 am, no meds); post-ACTH (60 m after 250 mcg IV, 10 h after dexamethasone [DEX, 1 mg PO]); and post-r-hCG (24 h after 50 mcg IV, 10 h after second dose DEX). Serum concentrations of classic (dehydroepiandrosterone [DHEA], androstenedione [A4], testosterone [T], dihydrotestosterone [DHT]) and 11-oxygenated androgens (11OHA4, 11KA4, 11OHT, and 11KT) were measured by liquid chromatography-tandem mass spectrometry. Wilcoxon Rank Sum and simple Spearman correlations were used for comparisons. Unless stated otherwise, $p \leq 0.05$ for all results reported below. At baseline, 11KT was 3-fold higher than T in PRE girls (1.2±0.6 vs. 0.4±0.2 nmol/L), while they did not differ in non-HA POST girls (1.4±0.6 vs. 1.1±0.5 nmol/L). The ratio of A4/T was 6.6±2.7 and 6.0±1.6 in PRE and non-HA POST girls, respectively, while 11KA4/11KT was 3.8±1.8 and 3.7±2.9, respectively; this suggests more efficient activation of 11-oxygenated androgens. Compared to NW POST girls, OW POST girls had higher T at baseline (1.9±0.9 vs. 1.2±0.8 nmol/L) and higher A4 post-ACTH (10.0±4.3 vs. 6.6±1.5 nmol/L). Compared to non-HA POST girls, HA girls had higher T at baseline (2.2±1.1 vs. 1.1±0.5 nmol/L) and higher DHEA, A4, and T post-r-hCG (DHEA: 8.8±2.7 vs. 5.6±2.2; A4: 11.3±4.1 vs. 7.3±2.8; T: 3.4±2.9 vs. 1.2±0.6 nmol/L). 11-oxygenated androgens were not elevated in OW or HA girls. In the entire cohort, HA status correlated with DHEA, A4, and T (r=0.40, 0.54, 0.63), while hirsutism correlated with A4 and T (r=0.47, 0.57). No androgen correlated with BMIz, but T correlated with fasting insulin and HOMA-IR (r=0.37, 0.38). The ratio of classic (DHEA, A4, T) to 11-oxygenated (11OHA4, 11KA4, 11OHT, 11KT) androgens trended higher in non-HA POST girls vs. PRE girls (58%:42% vs. 44%:56%, p=0.056). From early to late puberty, there appears to be a shift away from the 11-oxygenated pathway. Most androgens in HA girls derive from the classic androgen pathway. The mechanisms of the later switch to 11-oxygenated androgen pathway predominance in adult PCOS remain to be elucidated.

Neuroendocrinology and Pituitary

CASE REPORTS IN UNUSUAL PATHOLOGIES IN THE PITUITARY II

Axenfeld Rieger Syndrome: An Uncommon Cause of Growth Hormone Deficiency

Alberto Javier Grana Santini, MD[1], Nicolle M. Canales Ramos, MD[1], Nydia I. Burgos Ortega, MD[1], Wilnelia Medina Torres, MD[2], Janet Colón Castellano, MD[3],

Loida Alejandra Gonzalez-Rodriguez, MD[4], Milliette Alvarado, MD[4], Margarita Ramirez, MD[4].

[1]University Of Puerto Rico Department of endocrinology, San Juan, PR, USA, [2]VA Caribbean Healthcare System, San Juan, PR, USA, [3]Univ of Puerto Rico, Juana Diaz, PR, USA, [4]University of Puerto Rico, San Juan, PR, USA.

cells

MDPI

Review

Role of GPER-Mediated Signaling in Testicular Functions and Tumorigenesis

Adele Chimento *, Arianna De Luca, Marta Claudia Nocito, Paola Avena, Davide La Padula, Lucia Zavaglia and Vincenzo Pezzi *

Department of Pharmacy, Health and Nutritional Sciences, 87036 Arcavacata di Rende Cosenza, Italy; ariannadl@hotmail.it (A.D.L.); nocitomarta90@tiscali.it (M.C.N.); paox1982@hotmail.it (P.A.); davidelapadula@live.it (D.L.P.); luciazavaglia@hotmail.it (L.Z.)

* Correspondence: adele.chimento@unical.it (A.C.); v.pezzi@unical.it (V.P.); Tel.: +39-0984-493184 (A.C.); +39-0984-493148 (V.P.)

Received: 6 August 2020; Accepted: 15 September 2020; Published: 17 September 2020

Abstract: Estrogen signaling plays important roles in testicular functions and tumorigenesis. Fifteen years ago, it was discovered that a member of the G protein-coupled receptor family, GPR30, which binds also with high affinity to estradiol and is responsible, in part, for the rapid non-genomic actions of estrogens. GPR30, renamed as GPER, was detected in several tissues including germ cells (spermatogonia, spermatocytes, spermatids) and somatic cells (Sertoli and Leydig cells). In our previous review published in 2014, we summarized studies that evidenced a role of GPER signaling in mediating estrogen action during spermatogenesis and testis development. In addition, we evidenced that GPER seems to be involved in modulating estrogen-dependent testicular cancer cell growth; however, the effects on cell survival and proliferation depend on specific cell type. In this review, we update the knowledge obtained in the last years on GPER roles in regulating physiological functions of testicular cells and its involvement in neoplastic transformation of both germ and somatic cells. In particular, we will focus our attention on crosstalk among GPER signaling, classical estrogen receptors and other nuclear receptors involved in testis physiology regulation.

Keywords: GPER; testis; germ cells; Leydig cells; Sertoli cells; telocytes; testis physiology; testicular cancer

1. Introduction

The mammalian testis is divided into two compartments, the seminiferous tubules including germ cells in various development stages (spermatogonia, spermatocytes, spermatids, spermatozoa) supported by Sertoli cells and the interstitial tissue consisting of loose connective tissue, blood and lymphatic vessels, Leydig cells, fibroblasts, macrophages, leukocytes, and telocytes [1,2]. Testis physiological function consists of spermatogenesis, a process leading to gametes formation occuring in seminiferous tubules regulated by autocrine/paracrine factors, and steroidogenesis that occurs in Leydig cells [3]. Normal male reproductive development and function are controlled by a complex endocrine regulation in which a proper balance between androgens and estrogens plays a pivotal role [4,5].

Cellular response to estrogens is mediated through interaction with nuclear ERs α and β, which activates genomic and non-genomic signaling [6–11]. In the genomic pathway, the estrogens/ERs complex, binding ERE either directly or indirectly via transcription factors, modulates gene expression in many tissues, including those of the male reproductive tract [7,12,13]. In addition to the classical model of signal transduction, non-genomic mechanisms have been identified for estrogens and provide that their biological effects do not only arise from direct or indirect interaction of ERs with

DNA [8–10]. It has also been reported that ERs and their splicing variants are localized to plasma membrane-mediating non-genomic signaling [10,14–16]. Moreover, several studies revealed that estrogens act also through GPER [17,18]. GPER, originally described as orphan receptor GPR30, is a member of GPCR cell-membrane proteins superfamily, which have a binding domain inside the plasma membrane and endoplasmic reticulum [17].

Estradiol binds to GPER with a high affinity while estrone and estriol have very low binding affinities [17,19]. Furthermore, several environmental estrogens bind to GPER and activate the downstream signaling pathways, such as BPA, genistein, and nonylphenol [20]. A synthetic specific ligand of GPER, G1 [21], together with G15, a specific antagonist, are used as a target tool to evaluate the GPER function in different cells and disease models [22]. GPER is able to mediate both genomic and non-genomic response with its ligands in both normal and cancer cells [23–27]. Particularly, GPER activation determines multiple intracellular events such as EGFR transactivation leading to rapid ERK1/2 activation, PLC and PI3K phosphorylation, AC stimulation, and intracellular calcium mobilization [17,23,25,26,28,29].

It has been well established that GPER is expressed in testicular cells where it regulates specific functions [30–33], but it can also be involved in pathological processes, such as cancer [27,34], including estrogen-dependent testicular tumors [35]. In our previous review [35], we pointed out a role of GPER in mediating estrogen action during spermatogenesis and testis development. In addition, we evidenced that GPER seems to be involved in modulating estrogen-dependent testicular cancer cell growth; however, the effects on cell survival and proliferation depend on specific cell type.

There is a controversy whether GPER acts as an autonomous estrogen receptor or whether GPER interacts with nuclear estrogen receptor signaling pathways in response to estrogens or whether it co-operates with other receptors [36]. Studies performed on knockout mice and cultured cells suggest that GPER can act as an autonomous receptor and can also interact with nuclear estrogen receptors. However, the degree to which GPER acts autonomously likely depends on cell type, differentiation status and pathology [i.e., whether the cell is quiescent, proliferative or cancerous] [36]. The more severe testicular phenotype of ArKO mice, compared ERKO mice, supports the hypothesis that an alternative receptor [that could be GPER] and alternative pathways could be involved in mediating estrogen effects on spermatogenesis. Thus, the generation of a triple KO [ESRs and GPER] would be useful to highlight the cross-talk and functional redundancy between the three different receptors as well as between genomic and non-genomic effects exerted by estrogens in the modulation of spermatogenesis and testicular tumorigenesis [35].

In this review, we update the knowledge obtained in the last years on GPER roles in regulating physiological functions of testicular cells and its involvement in neoplastic transformation of both germ and somatic cells. In particular, we will focus our attention on crosstalk among GPER signaling, classical estrogen receptors and other nuclear receptors involved in the testis physiology regulation.

2. GPER Role in Testicular Interstitial Compartment

Testicular interstitial compartment, located between seminiferous tubules, is delimited from them by a layer of peritubular-myoid cells. Multiple interactions between all testicular cell types and mediated by paracrine factors, influence either cellular growth, differentiation or death [37]. Several studies have investigated GPER role in this intricate network, regulating testicular functions. In this section, we will summarize the results obtained in studies focused on GPER role in Leydig cells and in telocytes (Figure 1).

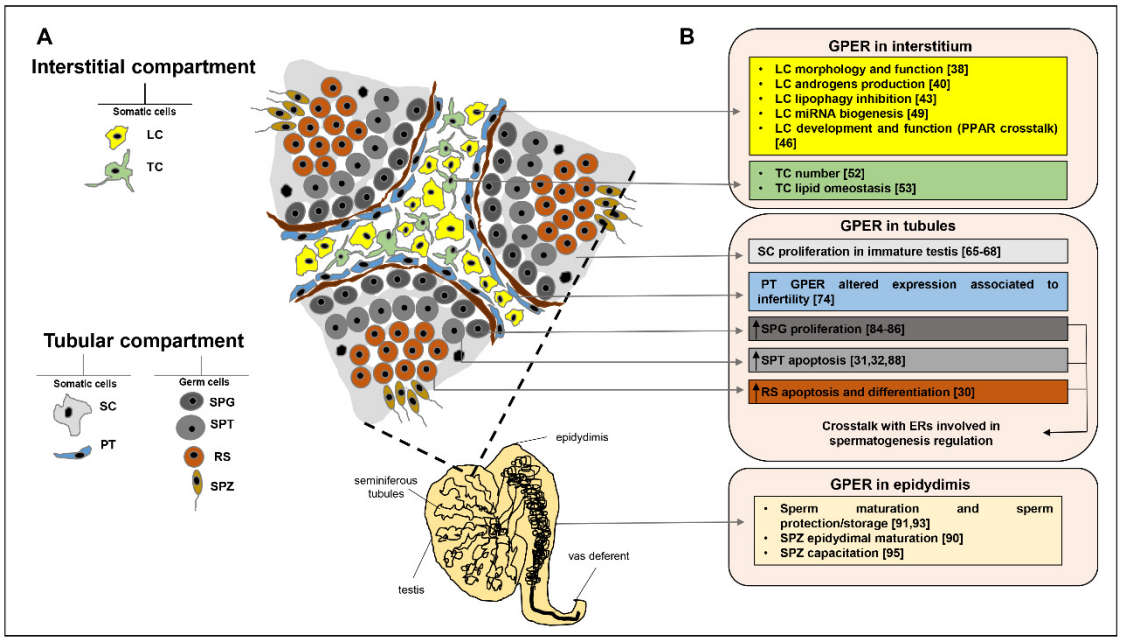

Figure 1. GPER role in testicular interstitial and tubular compartment and in epididymis. In this figure are summarized the knowledge of GPER role (**B**) in testicular interstitial and tubular compartments (**A**) and in epididymis. The drawing represents a cross section of seminiferous tubules, surrounding interstitium and several testicular cell types (**A**). LC: Leydig cells; TC: telocytes; SC: Sertoli cells; PT: peritubular cells; SPG: spermatogonia; SPT: spermatocytes; RS: round spermatids; SPZ: spermatozoa.

2.1. GPER in Leydig Cells

Interstitial Leydig cells are responsible for testis steroidogenesis [1]. Kotula-Balak and colleagues described for the first time that GPER is able to influence Leydig cell morphology and function [38]. In this study, effects of GPER antagonist G15 were evaluated on both C57BL/6 mice at different ages (immature, mature and aged) and on mouse MA-10 Leydig tumor cell line. The authors demonstrated that after G15 treatment, no effect on immature testis was observed, while an overgrowth of interstitial tissue was found in both mature and aged testes. Alterations in the structure and distribution of various Leydig cell organelles after GPER blockage respect to control, were also observed. Immunohistochemical analysis revealed the presence of more lipid droplets in immature Leydig cells, large mitochondria and numerous lipid droplets in the mature ones, and concentric structure of endoplasmic reticulum between normal-looking and normal-distributed mitochondria in aged cells. Moreover, the use of G15 determined a marked decrease in activity of mitochondria and cytoskeleton, cellular structures directly involved in steroid hormone production [39]. In addition, in both in vivo mice of different ages and in in vitro Leydig cells, G15 treatment determined an increase in ERα and ERβ and aromatase mRNA expression. However, after GPER blockage, intratesticular androgen concentration significantly increased in immature mice, decreased in mature males and did not change in aged animals. These observed changes after G15 treatment reflected Leydig cell heterogeneity to estrogen regulation during male life.

Another study demonstrated that GPER activation, using both estradiol [E2] and selective agonist G1, decreased in a dose-dependent manner, testosterone production in rat Leydig primary cultures. The observation that E2 and G1 determined the same decrease in testosterone production also in adult human testis, suggested that GPER-dependent non genomic signaling represented an important mechanism regulating estradiol-dependent steroidogenesis in human testis [40].

Studies performed on GPER knockout mice revealed GPER involvement in the regulation of obesity, insulin resistance and glucose intolerance [41]. In particular, a relationship between GPER activity and lipid metabolism derived from observation that GPER knockout mice developed visceral obesity and showed an increased level of low density lipoproteins [41]. Milon and collegues

demonstrated that in mouse MA-10, tumor cells resembling the immature type of adult Leydig cell lineage [42], lipid homeostasis and metabolism were affected by estrogens [43]. This study demonstrated that G15 induced protein expression changes of steroidogenic [LHR and 3β-HSD] and lipid droplet [PLIN and LC3] markers. Specifically, LHR, 3β-HSD, PLIN, and LC3 expression decreased, while degenerating lipid droplets appeared, indicating lipophagosome formation [43]. These results suggested a GPER role in lipophagy inhibition that is a crucial event in maintaining lipid homeostasis [44] and testosterone biosynthesis.

In this context, the functional interaction among GPER and pathways activated by different receptors is an interesting aspect that was recently studied in Leydig cells. Gorowska–Wojtowicz and colleagues [45] for the first time have shown the importance of relationship between GPER-PPARα and PPARγ in maintaining morphological and functional state of Leydig cells. GPER is an important partner of PPARα and PPARγ in steroidogenic state regulation of Leydig cells through both direct and indirect control at different regulatory levels. In particular, GPER and PPARα action occurs through the PI3K/Akt pathways, while PPARγ prefers the Ras/Raf pathways. Moreover, modified GPER-PPAR crosstalk was found in human LCTs, being a possible cause of LCTs development. This last aspect will be explained in the paragraph on GPER role in testicular tumors. A very recent study by Kotula–Balak and colleagues [46] asserted that exists a GPER-ERRβ-PPARγ interaction in the immature wild boar testicle that affects Leydig cells function [46]. It also highlights the involvement of these receptors in cellular processes through cAMP activation and Raf/Ras/ERK pathways modulating cholesterol concentration and estradiol levels. These cellular and molecular regulations seem to be crucial for the proper development and functions of Leydig cells.

Another interesting aspect recently evaluated is the GPER involvement in miRNA-estrogen regulation [47]. Dysregulation of testicular steroidogenic function by BPA through its action on miRNA has been demonstrated in Leydig cells isolated from murine testis [48]. Recently, Pawlicki and colleagues, using G15, xenoestrogen BPA and its derivatives TBBPA and TCBPA, clarified the GPER involvement on epigenetic regulation in immature boar Leydig cells [49]. The authors suggested that both G15 and different xenoestrogens, except for BPA and G15 plus TCBPA, reduced the GPER protein expression. Furthermore, the use of the above mentioned chemical compounds, modulated the expression of some proteins that are important for miRNA biosynthesis in Leydig cells. In particular, the EXPO5 and DICER mRNA expressions were downregulated while the DROSHA and AGO2 mRNA expressions were significantly upregulated only by G15 plus BPA and TCBPA, respectively. These results confirmed that GPER-modulated expression exerted by G15 and BPA derivatives affected the levels of proteins controlling miRNA biogenesis and function.

2.2. GPER in Telocytes

Recent studies, confirmed the presence of telocytes in interstitium; these cells are a novel type of interstitial cell, named also interstitial Cajal-like cells that are involved in testicular homeostasis maintenance and spermatogenesis regulation [50]. Telocytes are easily distinguished from other interstitial tissue cells for the presence of telopodes [51], a long prolongation containing caveolae, mitochondria and endoplasmic reticulum. Recently, Pawlicki and colleagues confirmed telocytes presence in mouse testis and investigated the GPER role in this cell type [52]. Interestingly, the same authors, inactivating GPER trough G15, demonstrated protein expression changes of telocytes functional markers such as CD34, c-kit, PDGFRα and β, VEGF, and vimentin. Moreover, GPER inhibition caused an increase in telocytes number, ERRs mRNA expression and mouse testis relaxin concentration, a protein exclusively secreted by Leydig cells. These results suggested that telocytes number and the expression of important proteins regulating interstitial compartment physiology may be modulated by GPER activity.

Telocytes presence has been demonstrated in testicular interstitium of bank voles [53]. It is known that in these photoperiodic rodents, melatonin endogenously controls reproductive system function through interaction with the hypothalamic–pituitary–gonadal axis. Recently, it has been

demonstrated that in male bank voles bred under different light cycles [long day, LD; short day, SD], the photoperiod and melatonin signaling regulate telocytes distribution [53]. Surprisingly, melatonin concentration in these animals is regulated by GPER, decreasing in both LD and SD animals after G15 treatment. In addition, the same authors highlighted that GPER signaling regulated telocyte marker CD34 expression and it is implicated in lipid metabolism. In fact, in GPER-blocked testis, single telocytes were present in the interstitium of LD animals, while in that of SD animals they were absent. Concomitantly, in bank vole interstitial tissue, GPER inhibition induced a decrease in leptin and adiponectin expression and an increase in cholesterol content, suggesting a possible role in maintaining lipid balance and steroidogenic efficiency of interstitial tissue.

3. GPER Role in Testicular Tubular Compartment

Tubular compartment contains germ cells and two different types of somatic cells, the peritubular cells and Sertoli cells. Peritubular cells or myofibroblasts form concentric layers around the tubules separated by collagen layers. They produce several factors involved in cellular contractility such as panactin, desmin, gelsoline, myosin, and actin [54] and secrete extracellular matrix and typical connective tissue cell factors such as collagen, laminin vimentin, fibronectin, growth factors, and adhesion molecules [55,56]. Sertoli cells extend from the basal lamina to the lumen of tubules and envelop and support germ cells during spermatogenesis. This process includes mitotic divisions of spermatogonia that differentiate into spermatocytes and meiotic divisions of spermatocytes to produce spermatids that differentiate into spermatozoa [57]. Several studies investigated GPER role in regulating the several steps of spermatogenesis. In this section, we will summarize the results obtained in studies focused on GPER role in Sertoli and peritubular cells as well as in regulating germ cell maturation (Figure 1).

3.1. GPER in Sertoli Cells

Sertoli cells, being intimately associated with each other and germ cells through specific junctions and being primary targets of follicle stimulating hormone [FSH] and testosterone, represent the main mediators of both endocrine and paracrine spermatogenesis control [58]. Considering that each Sertoli cell supports a limited germ cell number, the proliferation of immature Sertoli cells represents an important phenomenon, which determines sperm production capacity. It has been reported that activation of various signaling pathways including cAMP/PKA, ERK1/2, PI3K/Akt, and mTORC1/p70SK6 as well as numerous hormonal factors such as FSH, the insulin family of growth factors, activin, cytokines, and estrogens, are involved in the proliferation of immature Sertoli cells [59]. Particularly, it has been reported that, in fetal and immature rats, Sertoli cells, which are the main source of estrogens [60–62], expressed a functional GPER [33] besides ERs [63]. It has been proposed that estrogens regulate Sertoli cell proliferation or Sertoli cell maturation depending on the ER activated. Lucas and colleagues demonstrated that estradiol binding ERα, through MAPK3/1 and PI3K/NFkB pathways, increased CD1 expression and promoted Sertoli cell proliferation, while binding ERβ, through PI3K/CREB signaling, determined an increase expression of CDKN1B cell cycle inhibitor and promoted cell differentiation [64]. Moreover, in immature rat Sertoli cells, estradiol or G1-dependent GPER stimulation, through EGFR transactivation, determined MAPK3/1 phosphorylation that was responsible for proapoptotic BAX decrease and antiapoptotic BCL2 increase in the gene expression [33,65]. Furthermore, E2 or G1 binding GPER upregulated BCL2 and BCL2L2 through the EGFR/MAPK3/1 and PIK3 pathways activation, while through EGFR/MAPK3/1/phospho-CREB signaling, E2 or G1 decreased BAX expression in cultured Sertoli cells from 15 d-old rats [66]. Proliferative effects were also observed in cultured immature boar Sertoli cells; in this cell type GPER triggered a Src/PI3K/Akt pathway activation that was involved in E2-induced cell proliferation via S-phase kinase-associated protein 2 (Skp2) mRNA and protein increase [67]. In another study, it has been demonstrated that proliferation of mouse immature Sertoli cells TM4 can be stimulated by nanomolar concentrations of BPA, through a mechanism involving GPER. Particularly,

the authors reported that the rapid activation of GPER/EGFR/ERK1/2 and ERα/β/ERK1/2 pathways was involved in BPA-induced cell growth stimulation. Low doses of BPA significantly increased BCL2 and PCNA expression, while decreased those of p21 and p53. Additionally, BPA up-regulated GPER mRNA and protein expression in a dose-dependent manner, thus contributing to increased stimulatory action of low BPA doses on immature Sertoli cell growth [68]. Taken together, these results suggest that GPER activation in Sertoli cells can modulate the molecular mechanism involved in the maintenance of Sertoli cell number, normal testis development and homeostasis.

3.2. GPER in Peritubular Cells

In primates, including humans, testicular peritubular cells are located in a space between the germinal epithelium and the interstitial compartment [69]. Main characteristic of these cells is that they differentiate during puberty by expressing different markers including those of smooth muscle [70]. Several data suggest that estrogens via GPER can regulate both the vascular tone [71] and vascular function [72]. Moreover, it has been demonstrated that human peritubular cells produce several factors such as the GDNF, necessary for spermatogonial stem cell niche [73] and others that play a fundamental role in the spermatogenesis paracrine regulation. Sandner and colleagues [74] demonstrated that GPER is expressed in testicular peritubular cells of human and non-human primates and it is involved in regulation of testicular function. Specifically, in rhesus monkeys these cells express GPER only at the beginning of puberty while in humans this expression is lost due to idiopathic infertility. In tissues deriving from newborn monkeys or until childhood, GPER was mainly expressed in vascular smooth muscle cells; while in those deriving from prepuberal animals, this receptor was only expressed in interstitial cells. In men, the onset of GPER expression in peritubular cells around puberty suggested a role related to fertility. Testicular biopsies from men with normal spermatogenesis showed normal peritubular GPER expression, while those with impaired spermatogenesis exhibited a decreased or deficient GPER immunostaining [74]. These results indicated that estrogenic signaling via GPER is involved in the regulation of smooth muscle-like phenotype of peritubular cells.

3.3. GPER in Germ Cells

It is now known that estrogens exert regulatory effects on spermatogenesis through interaction with classic estrogens receptors and also with alternative receptors such as GPER [3,35,75–80]. The first report indicating estrogens' proliferative effects on testicular germ stem cells is attributed to Cobellis and colleagues, who, using a frog model characterized by slow progression of spermatogenesis, demonstrated that estradiol induced nuclear c-Fos activity, leading to spermatogonia multiplication [81]. Other studies corroborated also that estrogens' proliferative effects on spermatogonia involved ERK1/2 rapid activation [82,83]. Our previous data confirmed GPER expression in mouse testis, supporting the hypothesis that this receptor represents the alternative receptor through which estrogens can sustain spermatogenesis in ERKO mice; in fact, these animals displayed a less severe testicular phenotype compared to that of ArKO mice [78]. Using as experimental model the GC-1, an immortalized cell line that displayed specific features common to type B spermatogonia, we confirmed GPER-dependent pathways involved in spermatogonia cell proliferation. Specifically, we demonstrated that estradiol, through a GPER/ERα cross talk, activated a rapid EGFR/ERK/c-fos signaling cascade, which in turn induced CD1 expression and then cell proliferation [84]. Sheng and colleagues demonstrated that in GC-1 cells low doses of BPA activated the GPER/EGFR/ERK and GPER/PKG pathways, which in turn phosphorylated the transcription factor CREB and the cell cycle regulator Rb. The latter proteins were the key factors involved in the modulation of GC-1 cell proliferation [85]. In another study, the same authors demonstrated that, through the GPER/EGFR/ERK, GPER/EGFR/ERK/ERα/c-Fos, and GPER/PKG pathways, BPA significantly induced GPER gene and protein expression in GC-1 cells. These molecular events contributed to increased cell proliferation via a regulatory loop [86].

The ability of estrogens to induce rapid signaling through GPER and ERs was demonstrated by our research group in primary cultures of pachytene spermatocytes isolated from adult rat testis. In this cell

type, physiological concentrations of estradiol as well as G1 and PPT were able to induce rapid ERK1/2 and c-Jun phosphorylation, effects that were abolished by AG1478, PD98059 and ICI182780 inhibitors. Additionally, treatments with E2 or G1 drastically reduced CA1 and B1 mRNA expression. The EGFR and MAPK inhibitors reversed this effect on both cyclins while ER antagonist was able to reverse E2- but not G1-inhibition, thus confirming the E2/GPER/ERK1/2/c-Jun pathway involvement in CA1 and CB1 mRNA expression changes. The inhibition of cyclins expression was associated with an increase of E2 and G1-dependent BAX mRNA expression, which was completely reversed in the presence of EGFR and MAPK inhibitors. Collectively our data indicated that E2, in pachytene spermatocytes, through both ERα and/or GPER, was able to trigger a rapid EGFR/ERK/c-Jun pathway involved in gene expression modulation of cell cycle and apoptosis regulators [31]. In another study, in order to clarify the effector pathways controlling spermatocytes apoptosis, we used the GC-2 [87], an immortalized mouse pachytene spermatocyte-derived cell line. These cells reproduced the same effects that we observed in spermatocytes primary cultures [31]. In fact, in GC-2 cells we demonstrated that ERα and GPER activation by E2, PPT and G1 caused a rapid and sustained ERK and c-Jun phosphorylation, as well as apoptosis. However, only concomitant ERα and GPER silencing abolished E2-dependent effects on cell proliferation. All these data confirmed that E2, by activating both ERα and GPER, was able to decrease cell proliferation through an ERK1/2, c-Jun and p38-dependent mitochondrial apoptotic pathway in GC-2 cells [32]. Using GC-2 cells, Wang and colleagues demonstrated that low doses of BPA, by activating GPER, determined a rapid ERK1/2 phosphorylation, an increase in c-Fos, and a decrease in CD1 gene expression. In addition, BPA-dependent GPER activation inhibited cell growth and induced apoptosis. Moreover, immunohistochemistry analysis, performed on testis of BPA-treated mice, showed that this compound induced spermatocytes apoptosis without affecting the morphological structure of seminiferous tubules [88]. GPER expression was demonstrated also in primary cultures of adult rat RS. In these cells, estradiol, through GPER, ERα and ERβ interaction, activated pathways involved in the regulation of genes controlling rat RS apoptosis and/or maturation. Specifically, E2, PPT, G1 and specific ERβ agonist DPN, caused a rapid ERK1⁄2 phosphorylation increase, through EGFR transactivation. The ability of specific EGFR, ERs and MAPK inhibitors to reverse this effect confirmed the involvement of GPER and ERs in ERK1/2 phosphorylation. Moreover, while E2, G1 and PPT downregulated CB1 and up-regulated BAX mRNA expression, DPN produced the opposite effects on the same genes. All above mentioned results confirmed that E2, through ERs and GPER, modulates rat RS apoptosis and differentiation [30]. Studies investigating the role of GPER in germ cells suggest an important role of this receptor in modulating two important aspects of spermatogenesis: the proliferation of spermatogonia and the physiological apoptosis regulating the number of spermatocytes and spermatids.

4. GPER Role in Epididymis

Spermatozoa acquire mobility and fertility during their transit through the epididymis [89]. Epididymal function is regulated by androgens and estrogens signaling. GPER expression was also demonstrated in the epididymis of several species including boar [90], rat [91–93], sheep [94] and bull [95], although its immunolocalization by region and cell type is not well known [93]. The highest expression of GPER has been identified in corpus and cauda in adult rats, suggesting a role for non-classical estrogen signaling in sperm maturation in the corpus, and sperm protection/storage in the cauda [93] (Figure 1). Menad and colleagues investigated GPER expression in epididymis of fat sand rats, highlighting how it varied between seasons, among the different segments and across cellular compartments [91]. The same authors also investigated the effects of castration alone or followed by testosterone treatment and efferent ducts ligation. Results evidenced that in castrated animals, GPER underwent a nuclear translocation, while after treatment with testosterone, GPER is mainly localized in the cytoplasm. Instead, in animals with ducts ligation, GPER was mainly localized at the cytoplasmic level in the principal cells of caput epididymis, but with lower intensity in the cauda epididymis [91].

Taken together, these results suggest how GPER can mediate estrogen cell signaling differently between the breeding and resting seasons and how androgens can be involved in regulating GPER expression.

Several studies are available regarding on the presence and actions of ERs in spermatozoa [96–100], but less information exists on GPER. GPER expression was found in the mid-piece, equatorial segment and acrosome of pig spermatozoa, while in humans it was exclusively identified in the sperm mid-piece [101]. This receptor was detected also in the neck, flagellum and head of the stallion spermatozoa [102,103]. In sperm cells isolated from the corpus and caput of the boar epididymis, GPER is less expressed in the acrosome and more expressed in the flagellum, while in epididymal sperm from the cauda, it is mainly localized in the acrosome [90]. This expression pattern suggested a GPER role during the epididymal maturation. It is well known that during this process, spermatozoa undergo several changes leading to their fertilizing ability. These changes include binding of the proteins secreted by epididymis to sperm plasma membrane or sperm proteins post-translational modifications [104]. It is conceivable that proteins expressed between caput and epididymal corpus [105] could bind sperm membrane receptors including GPER. These results suggest a potential involvement of estrogenic signaling in both spermatozoa and epididymis post-testicular maturation. Recently, GPER was revealed in bull ejaculated and capacitated spermatozoa [95], where it was detected in the post-acrosomal region and in the apical part of the acrosome, suggesting its role in rapid signaling such as calcium fluxes [106] and kinase activation [107], which are involved in sperm capacitation and acrosome reaction.

5. GPER Role in Testicular Tumors

Testicular tumors account for 1-1.5% of all male cancers [108]; they comprise two broad groups: germ neoplasms (TGCTs) representing 95% of all testicular cancers and the rarer non germ neoplasms which include Leydig cell tumors (LCTs), Sertoli cell tumors and gonadoblastoma.

TGCTs are classified into two sub-categories, based on their histological characteristics, seminoma and non-seminoma (embryonal carcinoma, teratoma, choriocarcinoma and yolk sac tumors), both aroused from a non-invasive form of disease named germ cell neoplasia in situ (CIS) [109]. TGCTs mainly occur in young men (18-35 years old) and their incidence shows geographical and ethnic differences [110]. TGCTs, particularly seminomas, display a good sensitivity to cisplatin-based chemotherapy and radiation; unfortunately, the non-seminoma histotype is more aggressive and has a poor prognosis, since it is less sensitive to chemotherapy and radiotherapy [111,112].

LCTs are a rare disease mainly characterized by interstitial steroids secretion [113] infertility, virilizing syndromes in prepubertal boys, testicular swelling, erectile dysfunction, loss of libido, and gynecomastia [114]. There are two peaks in the LCTs incidence: one during the prepubertal age between 3 and 9 years, the other in adulthood between 30 and 60 years [114]. LCTs are usually benign while an estimated 10–15% are malignant [115]. Mainly treatment of LCTs is the surgical resection for both benign and malignant pathological forms. However, therapeutic options are very limited and include the use of radiotherapy and chemotherapy often ineffective [116]. These therapeutic approaches are complicated by the elevated testicular susceptibility to their toxic effects [117]. Since the prognosis is poor with an average survival of approximately two years [115,116,118], it is necessary identify new therapeutic approaches for the treatment of malignant LCTs.

It has been shown that GPER is expressed in TGCTs. Specifically, it is overexpressed in seminoma and embryonal carcinoma [119], whereas ERα is missing. It suggests that in these tumors estrogens can exert proliferative effects through GPER (Figure 2).

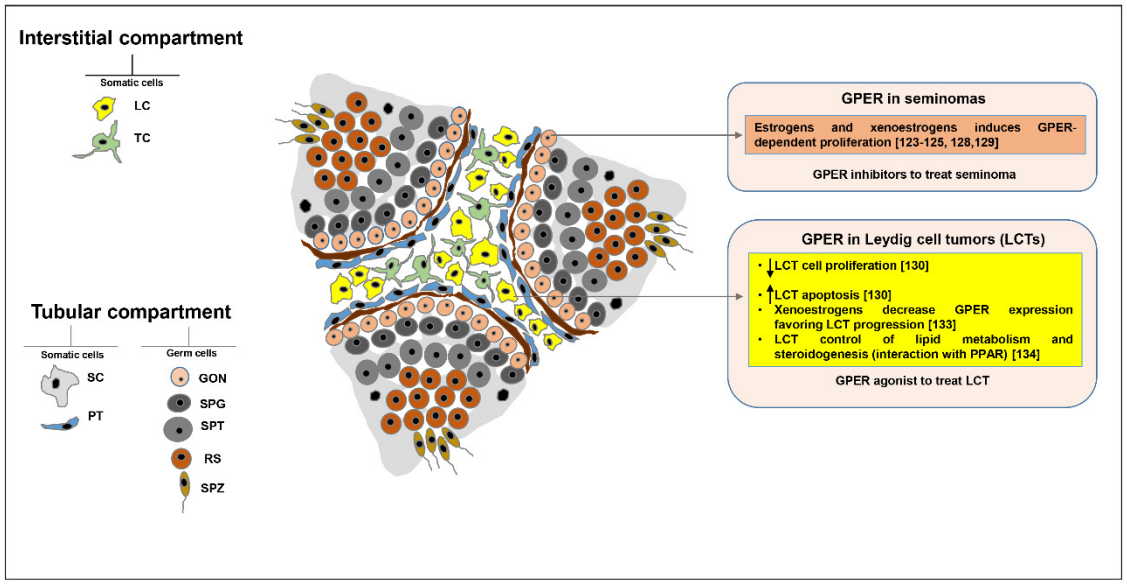

Figure 2. GPER role in testicular tumorigenesis. In this figure are summarized the knowledge ofGPER role in seminomas and Leydig cell tumors [LCTs]. LC: Leydig cells; TC: telocytes; SC: Sertoli cells; PT: peritubular cells; GON: gonocytes; SPG: spermatogonia; SPT: spermatocytes; RS: round spermatids; SPZ: spermatozoa.

Rago and colleagues demonstrated that seminomas and embryonal carcinomas had a positive ERβ1 and ERβ2 immunoreactivity, while ERα signal was undetectable [120]. Indeed, in a seminoma cell line which lacks ERα expression, ERβ activation has been shown to be associated with cell necrosis and autophagy [121]. Using the JKT-1, a cell line derived from a human testicular seminoma and expressing GPER, ERβ, but not ERα [122], it has been demonstrated that estradiol [123], BPA [124,125] and G1 through GPER activated a PKA/CREB signaling leading to cell proliferation increase. On the other hand, E2 through ERβ [126,127] or G15 through GPER/ERK pathway, decreased cell proliferation. In another study, it has been demonstrated that estradiol through a GPER-cAMP/PKA/CREB signaling induced ERα36 isoform expression in TCam-2 seminoma cell line, leading to cell proliferation increase [128]. Boscia and colleagues showed that GPER overexpression was associated with ERβ down regulation in both human testicular CIS and seminomas. In addition, ERβ reduced expression was due to the GPER/ERK/c-Fos estrogen activated pathway in TCam-2 seminoma cell line. The observation that high levels of GPER protein correlated with low levels of ERβ suggested a potential therapeutic role of GPER inhibitors for the treatment of CIS and seminomas [129] (Figure 2).

On the contrary, in Leydig cell tumors, where ERα is overexpressed, GPER activation is associated with a marked reduction of cell growth in vitro and in vivo [130] (Figure 2). Specifically, G1 treatment determined inhibitory effects consequent to the initiation of the mitochondria-dependent apoptotic pathway in R2C Leydig tumor cell line [130]. This pathway that required a sustained ERK1/2 activation, was confirmed by DNA fragmentation, a decrease in BCL2 and an increase in BAX expression, cytochrome c release, caspase 3, and PARP1 activation after G1 treatment. These effects have been demonstrated for other tumor cell types including those of the breast [131] and prostate [132]. In addition, in vivo administration of G1 to male CD1 mice, decreased the growth of R2C xenograft tumors without any alteration in testicular morphology [130]. All results suggested that GPER may represent a potential therapeutic option to preserve fertility for Leydig cell tumor treatment [130].

An innovative aspect in the study of GPER role in Leydig cell tumors is the functional interaction among GPER and other receptors. Recently, Gorowska-Wojtowicz and colleagues [133] examined mainly the relationship between GPER and PPARs expression and estrogen level after several xenoestrogens treatment. The authors demonstrated that in tissues from mice MA-10 xenograft models and in MA-10 cells treated with BPA and TCBPA, PPARα expression was increased while that of

GPER, PPARβ and PPARγ was decreased together with estradiol production. These results indicated that changes in GPER and PPARs expression after xenoestrogens exposure observed both in vivo and in vitro are involved in the alteration of cell tumor microenvironment. Recently, Kotula–Balak and colleagues highlighted that the functional interaction between GPER and PPAR controls lipid metabolism and steroidogenesis in LCTs. In fact, in these tumors, analysis of mRNA and proteins showed a greater expression of GPER and a reduction of PPARα, β and γ expression. Consequently, it was also observed that there are alterations in lipid- and cholesterol-associated proteins such as LHR, PKA, PLIN, HSL, StAR, TSPO, HMGCS, and HMGCR, together with the cGMP and PI3K-Akt-mTOR pathways. These changes of expression could be primary disturbances in healthy Leydig cell, and the study of these alterations could be useful to design a new therapeutic approach for Leydig cell tumors [134].

Another interesting aspect that could be investigated in the future for the treatment of testicular tumors, arises from the observation that GPER activation has combinatorial effects with immune checkpoint inhibitors. In fact, in a recent paper, Natale and colleagues demonstrated that GPER activation made tumors more responsive to immune checkpoint blockade increasing survival, with up to half of mice clearing their tumor [135]. Very recently, the same research group observed similar results on Pancreatic Ductal Adenocarcinoma [PDAC] [136]. In particular, G1 treatment inhibited PDAC proliferation, depleted the oncodriver and stem cell marker c-Myc, depleted PD-L1, and increased tumor cell immunogenicity. These observations on preclinical models are supported by the preliminary results obtained by clinical trial on patients with advanced solid and hematologic cancers treated with LNS8891, an highly specific GPER agonist [137].

Taken together, these results suggest GPER as a useful potential target for the development of new pharmacological tools against testicular tumors.

6. Conclusions

The discovery of the transmembrane estrogen-binding protein GPER has opened new perspectives to better understand molecular mechanisms mediating estrogen action in testicular physiology, as well as in testicular tumors (Table 1).

Table 1. Participation of GPER in testicular physiology in main cell types and changes in testicular tumors.

Cell Types	Testicular Physiology	Testicular Tumors
SPG	GPER activation induces proliferation [84–86]	GPER is overexpressed in seminoma and embryonal carcinoma [119], (whereas ERα is missing [120]) GPER mediates estrogen and xenoestrogen-dependent proliferation in seminomas [123–125,128,129]
SPT	GPER activation induces apoptosis [31,32,88]	
RS	GPER activation induces apoptosis [30]	
LC	GPER is involved in: LC morphology and function [38]	LCT [where ERα is overexpressed]: GPER activation decrease cell proliferation and induces apoptosis [130] Xenoestrogens decrease GPER expression favoring LCT progression [133] GPER is involved in LCT control of lipid metabolism and steroidogenesis (interaction with PPAR) [134]
	LC androgens production [40]	
	LC lipophagy inhibition [43]	
	LC miRNA biogenesis [49]	
	LC development and function [PPAR crosstalk] [46]	
SC	GPER activation induces proliferation in immature testis [65–68]	Sertoli cell tumors: GPER is expressed but the role has been not identified.

SPG: spermatogonia; SPT: spermatocytes; RS: round spermatids; SC: Sertoli cells; LC: Leydig cells; Leydig cell tumor [LCT].

In interstitial compartment, GPER appears to play an important role in regulating estrogen-dependent lipid homeostasis and testosterone biosynthesis that occur in Leydig cells. Furthermore, very recent results have also shown an important role of GPER in regulating the number and physiology of telocytes that contribute to maintain lipid balance and steroidogenic

efficiency of interstitial tissue. In tubular compartment, GPER can mediate estrogen action on both somatic as well as germ cells. The reduced GPER expression in peritubular cell seems to be associated to infertility, while the role of GPER in the maintenance of Sertoli cell number and consequently for normal testis development and homeostasis is well known. Studies investigating GPER action in germ cells suggest an important role of this receptor in modulating two important aspects of spermatogenesis: the proliferation of spermatogonia and the physiological apoptosis regulating spermatocytes and spermatids number. GPER seems to be also involved in mediating signaling regulating spermatozoa maturation in epididymis.

An interesting aspect discovered in the last years is the functional interaction among GPER and other receptors such as ERs, PPARs, and ERRs in interstitial and tubular compartments. This aspect has recently opened a new interesting perspective in understanding the lipid homeostasis and metabolism of testis. This last aspect is particularly important for the study of testicular tumorigenesis. In fact, in Leydig cell tumors, greater expression of GPER and a reduction of the PPARα, β and γ expression are correlated with the alterations in several lipid- and cholesterol-associated proteins, determining disturbances that could be related to tumorigenesis and cancer progression. Moreover, results indicating that GPER activation by selective ligands can allow for opposite outcomes in seminoma and LCTs (Figure 2) should open new perspectives to define the mechanisms behind estrogen-dependent testicular tumorigenesis. In this context, GPER appears to be a very interesting potential target together with other nuclear receptors for the development of new pharmacological tools against estrogen-dependent testicular cancer.

Author Contributions: A.C. and V.P. conceived the plan of the review, performed the searching, screened the articles and wrote the whole manuscript. A.D.L. brought their expertise in the searching, screening the articles and writing "GPER Role in Testicular Tumors". A.C. and V.P. did also the figures and table in collaboration with A.D.L., M.C.N., P.A., D.L.P. and L.Z. A.D.L., M.C.N., P.A., D.L.P. and L.Z. provided minor corrections. All authors have read and agreed to the published version of the manuscript.

Funding: This work was supported by ex 60% to Department of Pharmacy, Health and Nutritional Sciences, University of Calabria, Arcavacata di Rende (Cosenza), Italy.

Acknowledgments: Arianna De Luca was supported by a fellowship from PAC (Progetto Strategico Regionale Calabria Alta Formazione) Calabria 2014/2020–Asse Prioritario 12, Linea B, Azione 10.5.12; Paola Avena was supported by a fellowship from Fondazione Umberto Veronesi (FUV). Authors thank Prof. Domenico Sturino and Dr. Anna Internò for English proofreading.

Conflicts of Interest: The authors declare no conflict of interest.

Abbreviations

AC	adenylyl cyclase;
AGO2	argonaute 2;
Akt	protein kinase b [PKB];
ArKO	aromatase knockout;
BAX	BCL2 associated X protein;
BCL2	B-cell lymphoma 2;
BCL2L2	BCL2 like protein 2;
BPA	bisphenol a;
cAMP	cyclic adenosine monophosphate;
CDKN1B	cyclin dependent kinase inhibitor 1b;
CA1	cyclin A1;
CB1	cyclin B1;
CD1	cyclin D1;
cGMP	cyclic guanosine monophosphate;
CIS	germ cell neoplasia in situ;
CREB	cAMP response element-binding protein;
DICER	dicer 1, ribonuclease III;
DPN	2,3-bis[4-Hydroxyphenyl]-propionitrile;

DROSHA	drosha ribonuclease III;
E2	17beta-estradiol;
EGFR	epidermal growth factor receptor;
ERα	estrogen receptor α;
ERβ	estrogen receptor β;
ERs	estrogen receptors;
ERE	estrogen response element;
ERK	extracellular signal-regulated kinase;
ERKO	estrogen receptor knockout;
ERRβ	estrogen-related receptor β;
ERRs	estrogen-related receptors;
EXPO5	exportin-5;
FSH	follicle stimulatimg hormone;
G15	[3aS,4R,9bR]-4-[6-bromo-1,3-benzodioxol-5-yl]-3a,4,5,9b-tetrahydro-3H-cyclopenta[c]quinolone;
G1	[±]-1-[[3aR*,4S*,9bS*]-4-[6-Bromo-1,3-benzodioxol-5-yl]-3a,4,5,9b-tetrahydro-3H-cyclopenta[c] quinolin-8-yl]-ethanone;
GDNF	glial cell-derived neurotrophic factor;
GPCR	G protein-coupled receptor;
GPER	G protein-coupled estrogen receptor 1;
HMGCR	hydroxymethylglutaril-coa reductase;
HMGCS	hydroxymethylglutaril-coa synthase;
3β-HSD	3β-hydroxysteroid dehydrogenase;
HSL	hormone sensitive lipase;
LC3	microtubule-associated protein 1A/1B-light chain;
LCT	leydig cell tumor;
LHR	luteotropin receptor;
MAPK	mitogen-activated protein kinase;
mTOR	mammalian target of rapamycin;
mTORC1	mammalian target of rapamycin complex 1;
NFkB	nuclear factor kappa-light-chain-enhancer of activated B cells;
p70SK6	ribosomal protein s6 kinase beta-1;
PARP1	poly [ADP-ribose] polymerase 1;
PCNA	proliferating cell nuclear antigen;
PDAC	pancreatic ductal adenocarcinoma;
PDGFR	platelet-derived growth factor receptor;
PD-L1	programmed death ligand 1;
PI3K	phosphoinositide 3-kinase;
PKA	protein kinase a;
PKG	cGMP-dependent protein kinase;
PLC	phospholipase c;
PLIN	perilipin;
PPARα	peroxisome proliferator-activated receptor α;
PPARβ	peroxisome proliferator-activated receptor β;
PPARγ	peroxisome proliferator-activated receptor γ;
PPARs	peroxisome proliferator-activated receptors;
PPT	4,4′,4′′-[4-Propyl-[1H] -pyrazole-1,3,5-triyl] trisphenol;
Rb	retinoblastoma protein;
RS	round spermatids;
Skp2	s-phase kinase-associated protein 2;
Src	proto-oncogene tyrosine-protein kinase;
StAR	acute steroidogenic regulatory protein;
TBBPA	tetrabromobisphenol A;
TCBPA	tetrachlorobisphenol A;
TGTCs	testicular germ cell tumors;
TORC1	mammalian target of rapamycin complex 1;
TSPO	translocator protein;
VEGF	vascular endothelium growth factor;

References

1. Weinbauer, G.; Luetjens, C.M.; Simoni, M.; Nieschlag, E. *Physiology of Testicular Function. Andrology*; Springer Science and Business Media LLC: Berlin/Heidelberg, Germany, 2010; pp. 11–59. ISBN 978-3-540-78354-1. [CrossRef]
2. Liu, Y.; Liang, Y.; Wang, S.; Tarique, I.; Vistro, W.A.; Zhang, H.; Haseeb, A.; Gandahi, N.S.; Iqbal, A.; An, T.; et al. Identification and characterization of telocytes in rat testis. *Aging* **2019**, *11*, 5757–5768. [CrossRef] [PubMed]
3. Akingbemi, B.T. Estrogen regulation of testicular function. *Reprod. Biol. Endocrinol.* **2005**, *3*, 51. [CrossRef] [PubMed]
4. Carreau, S.; Hess, R.A. Oestrogens and spermatogenesis. *Philos. Trans. R. Soc. Lond. B Biol. Sci.* **2010**, *365*, 1517–1535. [CrossRef] [PubMed]
5. Carreau, S.; Bouraima-Lelong, H.; Delalande, C. Estrogen, a female hormone involved in spermatogenesis. *Adv. Med. Sci-Poland* **2012**, *57*, 31–36. [CrossRef]
6. Nilsson, S.; Makela, S.; Treuter, E.; Tujague, M.; Thomsen, J.; Andersson, G.; Enmark, E.; Pettersson, K.; Warner, M.; Gustafsson, J.A. Mechanisms of estrogen action. *Physiol. Rev.* **2001**, *81*, 1535–1565. [CrossRef]
7. McDonnell, D.P.; Norris, J.D. Connections and regulation of the human estrogen receptor. *Science* **2002**, *296*, 1642–1644. [CrossRef]
8. Hammes, S.R.; Levin, E.R. Extranuclear steroid receptors: Nature and actions. *Endocr. Rev.* **2007**, *28*, 726–741. [CrossRef]
9. Kelly, M.J.; Levin, E.R. Rapid actions of plasma membrane estrogen receptors. *Trends Endocrin. Met.* **2001**, *12*, 152–156. [CrossRef]
10. Levin, E.R. Cellular functions of plasma membrane estrogen receptors. *Steroids* **2002**, *67*, 471–475. [CrossRef]
11. Pedram, A.; Razandi, M.; Aitkenhead, M.; Hughes, C.C.W.; Levin, E.R. Integration of the non-genomic and genomic actions of estrogen-Membrane-initiated signaling by steroid to transcription and cell biology. *J. Biol. Chem.* **2002**, *277*, 50768–50775. [CrossRef] [PubMed]
12. Katzenellenbogen, B.S.; Katzenellenbogen, J.A. Estrogen receptor transcription and transactivation Estrogen receptor alpha and estrogen receptor beta: Regulation by selective estrogen receptor modulators and importance in breast cancer. *Breast Cancer Res.* **2000**, *2*, 335–344. [CrossRef] [PubMed]
13. Lazari, M.F.M.; Lucas, T.F.G.; Yasuhara, F.; Gomes, G.R.O.; Siu, E.R.; Royer, C.; Fernandes, S.A.F.; Porto, C.S. Estrogen receptors and function in the male reproductive system. *Arq. Bras. Endocrinol. Metab.* **2009**, *53*, 923–933. [CrossRef] [PubMed]
14. Wang, Z.Y.; Zhang, X.T.; Shen, P.; Loggie, B.W.; Chang, Y.C.; Deuel, T.F. Identification, cloning, and expression of human estrogen receptor-alpha 36, a novel variant of human estrogen receptor-alpha 66. *Biochem. Bioph. Res Commun.* **2005**, *336*, 1023–1027. [CrossRef] [PubMed]
15. Wang, Z.Y.; Zhang, X.T.; Shen, P.; Loggie, B.W.; Chang, Y.; Deuel, T.F. A variant of estrogen receptor-alpha, hER-alpha 36: Transduction of estrogen- and antiestrogen-dependent membrane-initiated mitogenic signaling. *Proc. Natl. Acad. Sci. USA* **2006**, *103*, 9063–9068. [CrossRef]
16. Li, L.; Haynes, M.P.; Bender, J.R. Plasma membrane localization and function of the estrogen receptor alpha variant (ER46) in human endothelial cells. *Proc. Natl. Acad. Sci. USA* **2003**, *100*, 4807–4812. [CrossRef]
17. Revankar, C.M.; Cimino, D.F.; Sklar, L.A.; Arterburn, J.B.; Prossnitz, E.R. A transmembrane intracellular estrogen receptor mediates rapid cell signaling. *Science* **2005**, *307*, 1625–1630. [CrossRef]
18. Levin, E.R. G protein-coupled receptor 30: Estrogen receptor or collaborator? *Endocrinology* **2009**, *150*, 1563–1565. [CrossRef]
19. Revankar, C.M.; Mitchell, H.D.; Field, A.S.; Burai, R.; Corona, C.; Ramesh, C.; Sklar, L.A.; Arterburn, J.B.; Prossnitz, E.R. Synthetic estrogen derivatives demonstrate the functionality of intracellular GPR30. *ACS Chem. Biol.* **2007**, *2*, 536–544. [CrossRef]
20. Thomas, P.; Dong, J. Binding and activation of the seven-transmembrane estrogen receptor GPR30 by environmental estrogens: A potential novel mechanism of endocrine disruption. *J. Steroid Biochem. Mol. Biol.* **2006**, *102*, 175–179. [CrossRef]
21. Bologa, C.G.; Revankar, C.M.; Young, S.M.; Edwards, B.S.; Arterburn, J.B.; Kiselyov, A.S.; Parker, M.A.; Tkachenko, S.E.; Savchuck, N.P.; Sklar, L.A.; et al. Virtual and biomolecular screening converge on a selective agonist for GPR30. *Nat. Chem. Biol.* **2006**, *2*, 207–212. [CrossRef]

22. Filardo, E.J.; Thomas, P. Minireview: G protein-coupled estrogen receptor-1, GPER-1: Its mechanism of action and role in female reproductive cancer, renal and vascular physiology. *Endocrinology* **2012**, *153*, 2953–2962. [CrossRef] [PubMed]
23. Filardo, E.J.; Quinn, J.A.; Bland, K.I.; Frackelton, A.R., Jr. Estrogen-induced activation of Erk-1 and Erk-2 requires the G protein-coupled receptor homolog, GPR30, and occurs via trans-activation of the epidermal growth factor receptor through release of HB-EGF. *Mol. Endocrinol.* **2000**, *14*, 1649–1660. [CrossRef] [PubMed]
24. Filardo, E.J. Epidermal growth factor receptor (EGFR) transactivation by estrogen via the G-protein-coupled receptor, GPR30: A novel signaling pathway with potential significance for breast cancer. *J. Steroid Biochem. Mol. Biol.* **2002**, *80*, 231–238. [CrossRef]
25. Prossnitz, E.R.; Barton, M. Signaling, physiological functions and clinical relevance of the G protein-coupled estrogen receptor GPER. *Prostag. Other Lipid Mediat.* **2009**, *89*, 89–97. [CrossRef] [PubMed]
26. Prossnitz, E.R.; Maggiolini, M. Mechanisms of estrogen signaling and gene expression via GPR30. *Mol. Cell. Endocrinol.* **2009**, *308*, 32–38. [CrossRef]
27. Prossnitz, E.R.; Barton, M. The G-protein-coupled estrogen receptor GPER in health and disease. *Nat. Rev. Endocrinol.* **2011**, *7*, 715–726. [CrossRef]
28. Prenzel, N.; Zwick, E.; Daub, H.; Leserer, M.; Abraham, R.; Wallasch, C.; Ullrich, A. EGF receptor transactivation by G-protein-coupled receptors requires metalloproteinase cleavage of proHB-EGF. *Nature* **1999**, *402*, 884–888. [CrossRef]
29. Filardo, E.J.; Quinn, J.A.; Frackelton, A.R., Jr.; Bland, K.I. Estrogen action via the G protein-coupled receptor, GPR30: Stimulation of adenylyl cyclase and cAMP-mediated attenuation of the epidermal growth factor receptor-to-MAPK signaling axis. *Mol. Endocrinol.* **2002**, *16*, 70–84. [CrossRef]
30. Chimento, A.; Sirianni, R.; Zolea, F.; Bois, C.; Delalande, C.; Ando, S.; Maggiolini, M.; Aquila, S.; Carreau, S.; Pezzi, V. Gper and ESRs are expressed in rat round spermatids and mediate oestrogen-dependent rapid pathways modulating expression of cyclin B1 and Bax. *Int. J. Androl.* **2011**, *34*, 420–429. [CrossRef]
31. Chimento, A.; Sirianni, R.; Delalande, C.; Silandre, D.; Bois, C.; Ando, S.; Maggiolini, M.; Carreau, S.; Pezzi, V. 17 beta-estradiol activates rapid signaling pathways involved in rat pachytene spermatocytes apoptosis through GPR30 and ER alpha. *Mol. Cell. Endocrinol.* **2010**, *320*, 136–144. [CrossRef]
32. Chimento, A.; Sirianni, R.; Casaburi, I.; Ruggiero, C.; Maggiolini, M.; Ando, S.; Pezzi, V. 17beta-Estradiol activates GPER- and ESR1-dependent pathways inducing apoptosis in GC-2 cells, a mouse spermatocyte-derived cell line. *Mol. Cell. Endocrinol.* **2012**, *355*, 49–59. [CrossRef] [PubMed]
33. Lucas, T.F.; Royer, C.; Siu, E.R.; Lazari, M.F.; Porto, C.S. Expression and signaling of G protein-coupled estrogen receptor 1 (GPER) in rat sertoli cells. *Biol. Reprod.* **2010**, *83*, 307–317. [CrossRef] [PubMed]
34. Qian, H.; Xuan, J.; Liu, Y.; Shi, G. Function of G-Protein-Coupled Estrogen Receptor-1 in Reproductive System Tumors. *J. Immunol. Res.* **2016**, *2016*, 7128702. [CrossRef]
35. Chimento, A.; Sirianni, R.; Casaburi, I.; Pezzi, V. GPER Signaling in Spermatogenesis and Testicular Tumors. *Front. Endocrinol.* **2014**, *5*, 30. [CrossRef]
36. Romano, S.N.; Gorelick, D.A. Crosstalk between nuclear and G protein-coupled estrogen receptors. *Gen. Comp. Endocrinol.* **2018**, *261*, 190–197. [CrossRef]
37. Skinner, M.K.; Norton, J.N.; Mullaney, B.P.; Rosselli, M.; Whaley, P.D.; Anthony, C.T. Cell-cell interactions and the regulation of testis function. *Ann. N. Y. Acad. Sci.* **1991**, *637*, 354–363. [CrossRef] [PubMed]
38. Kotula-Balak, M.; Pawlicki, P.; Milon, A.; Tworzydlo, W.; Sekula, M.; Pacwa, A.; Gorowska-Wojtowicz, E.; Bilinska, B.; Pawlicka, B.; Wiater, J.; et al. The role of G-protein-coupled membrane estrogen receptor in mouse Leydig cell function-in vivo and in vitro evaluation. *Cell Tissue Res.* **2018**, *374*, 389–412. [CrossRef] [PubMed]
39. Sewer, M.B.; Li, D. Regulation of steroid hormone biosynthesis by the cytoskeleton. *Lipids* **2008**, *43*, 1109–1115. [CrossRef]
40. Vaucher, L.; Funaro, M.G.; Mehta, A.; Mielnik, A.; Bolyakov, A.; Prossnitz, E.R.; Schlegel, P.N.; Paduch, D.A. Activation of GPER-1 estradiol receptor downregulates production of testosterone in isolated rat Leydig cells and adult human testis. *PLoS ONE* **2014**, *9*, e92425. [CrossRef]
41. Sharma, G.; Prossnitz, E.R. GPER/GPR30 Knockout Mice: Effects of GPER on Metabolism. *Methods Mol. Biol.* **2016**, *1366*, 489–502. [CrossRef]
42. Ascoli, M. Effects of hypocholesterolemia and chronic hormonal stimulation on sterol and steroid metabolism in a Leydig cell tumor. *J. Lipid Res.* **1981**, *22*, 1247–1253.

43. Milon, A.; Kaczmarczyk, M.; Pawlicki, P.; Bilinska, B.; Duliban, M.; Gorowska-Wojtowicz, E.; Tworzydlo, W.; Kotula-Balak, M. Do estrogens regulate lipid status in testicular steroidogenic Leydig cell? *Acta Histochem.* **2019**, *121*, 611–618. [CrossRef]
44. Yang, P.L.; Hsu, T.H.; Wang, C.W.; Chen, R.H. Lipid droplets maintain lipid homeostasis during anaphase for efficient cell separation in budding yeast. *Mol. Biol. Cell.* **2016**, *27*, 2368–2380. [CrossRef]
45. Gorowska-Wojtowicz, E.; Dutka, P.; Kudrycka, M.; Pawlicki, P.; Milon, A.; Plachno, B.J.; Tworzydlo, W.; Pardyak, L.; Kaminska, A.; Hejmej, A.; et al. Regulation of steroidogenic function of mouse Leydig cells: G-coupled membrane estrogen receptor and peroxisome proliferator-activated receptor partnership. *J. Physiol. Pharmacol.* **2018**, *69*. [CrossRef]
46. Kotula-Balak, M.; Duliban, M.; Pawlicki, P.; Tuz, R.; Bilinska, B.; Plachno, B.J.; Arent, Z.J.; Krakowska, I.; Tarasiuk, K. The meaning of non-classical estrogen receptors and peroxisome proliferator-activated receptor for boar Leydig cell of immature testis. *Acta Histochem.* **2020**, *122*, 151526. [CrossRef]
47. Vidal-Gomez, X.; Perez-Cremades, D.; Mompeon, A.; Dantas, A.P.; Novella, S.; Hermenegildo, C. MicroRNA as Crucial Regulators of Gene Expression in Estradiol-Treated Human Endothelial Cells. *Cell. Physiol. Biochem.* **2018**, *45*, 1878–1892. [CrossRef]
48. Gao, G.Z.; Zhao, Y.; Li, H.X.; Li, W. Bisphenol A-elicited miR-146a-5p impairs murine testicular steroidogenesis through negative regulation of Mta3 signaling. *Biochem. Biophys. Res. Commun.* **2018**, *501*, 478–485. [CrossRef]
49. Pawlicki, P.; Duliban, M.; Tuz, R.; Ptak, A.; Milon, A.; Gorowska-Wojtowicz, E.; Tworzydlo, W.; Plachno, B.J.; Bilinska, B.; Knapczyk-Stwora, K.; et al. Do G-protein coupled estrogen receptor and bisphenol A analogs influence on Leydig cell epigenetic regulation in immature boar testis ex vivo? *Anim. Reprod. Sci.* **2019**, *207*, 21–35. [CrossRef]
50. Hasirci, E.; Turunc, T.; Bal, N.; Goren, M.R.; Celik, H.; Kervancioglu, E.; Dirim, A.; Tekindal, M.A.; Ozkardes, H. Distribution and number of Cajal-like cells in testis tissue with azoospermia. *Kaohsiung J. Med. Sci.* **2017**, *33*, 181–186. [CrossRef]
51. Cretoiu, S.M.; Popescu, L.M. Telocytes revisited. *Biomol. Concepts* **2014**, *5*, 353–369. [CrossRef]
52. Pawlicki, P.; Hejmej, A.; Milon, A.; Lustofin, K.; Plachno, B.J.; Tworzydlo, W.; Gorowska-Wojtowicz, E.; Pawlicka, B.; Kotula-Balak, M.; Bilinska, B. Telocytes in the mouse testicular interstitium: Implications of G-protein-coupled estrogen receptor (GPER) and estrogen-related receptor (ERR) in the regulation of mouse testicular interstitial cells. *Protoplasma* **2019**, *256*, 393–408. [CrossRef] [PubMed]
53. Milon, A.; Pawlicki, P.; Rak, A.; Mlyczynska, E.; Plachno, B.J.; Tworzydlo, W.; Gorowska-Wojtowicz, E.; Bilinska, B.; Kotula-Balak, M. Telocytes are localized to testis of the bank vole (Myodes glareolus) and are affected by lighting conditions and G-coupled membrane estrogen receptor (GPER) signaling. *Gen. Comp. End.* **2019**, *271*, 39–48. [CrossRef] [PubMed]
54. Holstein, A.F.; Maekawa, M.; Nagano, T.; Davidoff, M.S. Myofibroblasts in the lamina propria of human semi-niferous tubules are dynamic structures of heterogeneous phenotype. *Arch. Histol. Cytol.* **1996**, *59*, 109–125. [CrossRef] [PubMed]
55. Albrecht, M.; Ramsch, R.; Kohn, F.M.; Schwarzer, J.U.; Mayerhofer, A. Isolation and cultivation of human testicular peritubular cells: A new model for the investigation of fibrotic processes in the human testis and male infertility. *J. Clin. Endocrinol. Metab.* **2006**, *91*, 1956–1960. [CrossRef]
56. Schell, C.; Albrecht, M.; Mayer, C.; Schwarzer, J.U.; Frungieri, M.B.; Mayerhofer, A. Exploring human testicular peritubular cells: Identification of secretory products and regulation by tumor necrosis factor-alpha. *Endocrinology* **2008**, *149*, 1678–1686. [CrossRef] [PubMed]
57. de Kretser, D.M.; Loveland, K.L.; Meinhardt, A.; Simorangkir, D.; Wreford, N. Spermatogenesis. *Hum. Reprod.* **1998**, *13* (Suppl. S1), 1–8. [CrossRef]
58. Jegou, B. The Sertoli-germ cell communication network in mammals. *Int. Rev. Cytol.* **1993**, *147*, 25–96.
59. Meroni, S.B.; Galardo, M.N.; Rindone, G.; Gorga, A.; Riera, M.F.; Cigorraga, S.B. Molecular Mechanisms and Signaling Pathways Involved in Sertoli Cell Proliferation. *Front. Endocrinol.* **2019**, *10*, 224. [CrossRef]
60. Papadopoulos, V.; Carreau, S.; Szerman-Joly, E.; Drosdowsky, M.A.; Dehennin, L.; Scholler, R. Rat testis 17 beta-estradiol: Identification by gas chromatography-mass spectrometry and age related cellular distribution. *J. Steroid. Biochem.* **1986**, *24*, 1211–1216. [CrossRef]
61. Levallet, J.; Bilinska, B.; Mittre, H.; Genissel, C.; Fresnel, J.; Carreau, S. Expression and immunolocalization of functional cytochrome P450 aromatase in mature rat testicular cells. *Biol. Reprod.* **1998**, *58*, 919–926. [CrossRef]

62. Bouraima-Lelong, H.; Vanneste, M.; Delalande, C.; Zanatta, L.; Wolczynski, S.; Carreau, S. Aromatase gene expression in immature rat Sertoli cells: Age-related changes in the FSH signalling pathway. *Reprod. Fert. Dev.* **2010**, *22*, 508–515. [CrossRef] [PubMed]
63. Lucas, T.F.; Siu, E.R.; Esteves, C.A.; Monteiro, H.P.; Oliveira, C.A.; Porto, C.S.; Lazari, M.F. 17beta-estradiol induces the translocation of the estrogen receptors ESR1 and ESR2 to the cell membrane, MAPK3/1 phosphorylation and proliferation of cultured immature rat Sertoli cells. *Biol. Reprod.* **2008**, *78*, 101–114. [CrossRef] [PubMed]
64. Lucas, T.F.G.; Lazari, M.F.M.; Porto, C.S. Differential role of the estrogen receptors ESR1 and ESR2 on the regulation of proteins involved with proliferation and differentiation of Sertoli cells from 15-day-old rats. *Mol. Cell. Endocrinol.* **2014**, *382*, 84–96. [CrossRef] [PubMed]
65. Lucas, T.F.; Pimenta, M.T.; Pisolato, R.; Lazari, M.F.; Porto, C.S. 17beta-estradiol signaling and regulation of Sertoli cell function. *Spermatogenesis* **2011**, *1*, 318–324. [CrossRef]
66. Royer, C.; Lucas, T.F.; Lazari, M.F.; Porto, C.S. 17Beta-estradiol signaling and regulation of proliferation and apoptosis of rat Sertoli cells. *Biol. Reprod.* **2012**, *86*, 108. [CrossRef]
67. Yang, W.R.; Zhu, F.W.; Zhang, J.J.; Wang, Y.; Zhang, J.H.; Lu, C.; Wang, X.Z. PI3K/Akt Activated by GPR30 and Src Regulates 17beta-Estradiol-Induced Cultured Immature Boar Sertoli Cells Proliferation. *Reprod. Sci.* **2017**, *24*, 57–66. [CrossRef]
68. Ge, L.C.; Chen, Z.J.; Liu, H.Y.; Zhang, K.S.; Liu, H.; Huang, H.B.; Zhang, G.; Wong, C.K.; Giesy, J.P.; Du, J.; et al. Involvement of activating ERK1/2 through G protein coupled receptor 30 and estrogen receptor alpha/beta in low doses of bisphenol A promoting growth of Sertoli TM4 cells. *Toxicol. Lett.* **2014**, *226*, 81–89. [CrossRef]
69. Maekawa, M.; Kamimura, K.; Nagano, T. Peritubular myoid cells in the testis: Their structure and function. *Arch. Histol. Cytol.* **1996**, *59*, 1–13. [CrossRef]
70. Schlatt, S.; Weinbauer, G.F.; Arslan, M.; Nieschlag, E. Appearance of alpha-smooth muscle actin in peritubular cells of monkey testes is induced by androgens, modulated by follicle-stimulating hormone, and maintained after hormonal withdrawal. *J. Androl.* **1993**, *14*, 340–350. [CrossRef]
71. Prabhushankar, R.; Krueger, C.; Manrique, C. Membrane estrogen receptors: Their role in blood pressure regulation and cardiovascular disease. *Curr. Hypertens. Rep.* **2014**, *16*, 408. [CrossRef]
72. Haas, E.; Bhattacharya, I.; Brailoiu, E.; Damjanovic, M.; Brailoiu, G.C.; Gao, X.; Mueller-Guerre, L.; Marjon, N.A.; Gut, A.; Minotti, R.; et al. Regulatory role of G protein-coupled estrogen receptor for vascular function and obesity. *Circ. Res.* **2009**, *104*, 288–291. [CrossRef]
73. Spinnler, K.; Kohn, F.M.; Schwarzer, U.; Mayerhofer, A. Glial cell line-derived neurotrophic factor is constitutively produced by human testicular peritubular cells and may contribute to the spermatogonial stem cell niche in man. *Hum. Reprod.* **2010**, *25*, 2181–2187. [CrossRef]
74. Sandner, F.; Welter, H.; Schwarzer, J.U.; Kohn, F.M.; Urbanski, H.F.; Mayerhofer, A. Expression of the oestrogen receptor GPER by testicular peritubular cells is linked to sexual maturation and male fertility. *Andrology* **2014**, *2*, 695–701. [CrossRef]
75. Hess, R.A.; Bunick, D.; Lee, K.H.; Bahr, J.; Taylor, J.A.; Korach, K.S.; Lubahn, D.B. A role for oestrogens in the male reproductive system. *Nature* **1997**, *390*, 509–512. [CrossRef]
76. Carreau, S.; Delalande, C.; Silandre, D.; Bourguiba, S.; Lambard, S. Aromatase and estrogen receptors in male reproduction. *Mol. Cell. Endocrinol.* **2006**, *246*, 65–68. [CrossRef]
77. Hewitt, S.C.; Harrell, J.C.; Korach, K.S. Lessons in estrogen biology from knockout and transgenic animals. *Annu Rev Physiol* **2005**, *67*, 285–308. [CrossRef]
78. Murata, Y.; Robertson, K.M.; Jones, M.E.; Simpson, E.R. Effect of estrogen deficiency in the male: The ArKO mouse model. *Mol. Cell. Endocrinol.* **2002**, *193*, 7–12. [CrossRef]
79. Honda, S.; Harada, N.; Ito, S.; Takagi, Y.; Maeda, S. Disruption of sexual behavior in male aromatase-deficient mice lacking exons 1 and 2 of the cyp19 gene. *Biochem. Biophys. Res. Commun.* **1998**, *252*, 445–449. [CrossRef]
80. Robertson, K.M.; O'Donnell, L.; Jones, M.E.; Meachem, S.J.; Boon, W.C.; Fisher, C.R.; Graves, K.H.; McLachlan, R.I.; Simpson, E.R. Impairment of spermatogenesis in mice lacking a functional aromatase (cyp 19) gene. *Proc. Natl. Acad. Sci. USA* **1999**, *96*, 7986–7991. [CrossRef]
81. Cobellis, G.; Pierantoni, R.; Minucci, S.; Pernas-Alonso, R.; Meccariello, R.; Fasano, S. c-fos activity in Rana esculenta testis: Seasonal and estradiol-induced changes. *Endocrinology* **1999**, *140*, 3238–3244. [CrossRef] [PubMed]

82. Chieffi, P.; Colucci-D'Amato, G.L.; Staibano, S.; Franco, R.; Tramontano, D. Estradiol-induced mitogen-activated protein kinase (extracellular signal-regulated kinase 1 and 2) activity in the frog (Rana esculenta) testis. *J. Endocrinol.* **2000**, *167*, 77–84. [CrossRef] [PubMed]
83. Chieffi, P.; Colucci D'Amato, L.; Guarino, F.; Salvatore, G.; Angelini, F. 17 beta-estradiol induces spermatogonial proliferation through mitogen-activated protein kinase (extracellular signal-regulated kinase 1/2) activity in the lizard (Podarcis s. sicula). *Mol. Reprod. Dev.* **2002**, *61*, 218–225. [CrossRef] [PubMed]
84. Sirianni, R.; Chimento, A.; Ruggiero, C.; De Luca, A.; Lappano, R.; Ando, S.; Maggiolini, M.; Pezzi, V. The novel estrogen receptor, G protein-coupled receptor 30, mediates the proliferative effects induced by 17beta-estradiol on mouse spermatogonial GC-1 cell line. *Endocrinology* **2008**, *149*, 5043–5051. [CrossRef]
85. Sheng, Z.G.; Zhu, B.Z. Low concentrations of bisphenol A induce mouse spermatogonial cell proliferation by G protein-coupled receptor 30 and estrogen receptor-alpha. *Environ. Heal. Perspect.* **2011**, *119*, 1775–1780. [CrossRef]
86. Sheng, Z.G.; Huang, W.; Liu, Y.X.; Zhu, B.Z. Bisphenol A at a low concentration boosts mouse spermatogonial cell proliferation by inducing the G protein-coupled receptor 30 expression. *Toxicol. Appl. Pharmacol.* **2013**, *267*, 88–94. [CrossRef] [PubMed]
87. Hofmann, M.C.; Hess, R.A.; Goldberg, E.; Millan, J.L. Immortalized germ cells undergo meiosis in vitro. *Proc. Natl. Acad. Sci. USA* **1994**, *91*, 5533–5537. [CrossRef]
88. Wang, C.; Zhang, J.; Li, Q.; Zhang, T.; Deng, Z.; Lian, J.; Jia, D.; Li, R.; Zheng, T.; Ding, X.; et al. Low concentration of BPA induces mice spermatocytes apoptosis via GPR30. *Oncotarget* **2017**, *8*, 49005–49015. [CrossRef]
89. Cooper, T.G. Epididymis and sperm function. *Andrology* **1996**, *28* (Suppl. S1), 57–59.
90. Krejcirova, R.; Manasova, M.; Sommerova, V.; Langhamerova, E.; Rajmon, R.; Manaskova-Postlerova, P. G protein-coupled estrogen receptor (GPER) in adult boar testes, epididymis and spermatozoa during epididymal maturation. *Int. J. Biol. Macromol.* **2018**, *116*, 113–119. [CrossRef]
91. Menad, R.; Fernini, M.; Smai, S.; Bonnet, X.; Gernigon-Spychalowicz, T.; Moudilou, E.; Khammar, F.; Exbrayat, J.M. GPER1 in sand rat epididymis: Effects of seasonal variations, castration and efferent ducts ligation. *Anim. Reprod. Sci.* **2017**, *183*, 9–20. [CrossRef]
92. Hess, R.A.; Fernandes, S.A.; Gomes, G.R.; Oliveira, C.A.; Lazari, M.F.; Porto, C.S. Estrogen and its receptors in efferent ductules and epididymis. *J. Androl.* **2011**, *32*, 600–613. [CrossRef] [PubMed]
93. Martinez-Traverso, G.B.; Pearl, C.A. Immunolocalization of G protein-coupled estrogen receptor in the rat epididymis. *Reprod. Biol. Edocrinol.* **2015**, *13*, 48. [CrossRef] [PubMed]
94. Ge, W.; Xiao, L.; Duan, H.; Jiang, Y.; Lv, J.; Ding, Z.; Hu, J.; Zhao, X.; Zhang, Y. Androgen receptor, aromatase, oestrogen receptor alpha/beta and G protein-coupled receptor 30 expression in the testes and epididymides of adult sheep. *Reprod. Domest. Anim.* **2020**, *55*, 460–468. [CrossRef]
95. Antalikova, J.; Secova, P.; Horovska, L.; Krejcirova, R.; Simonik, O.; Jankovicova, J.; Bartokova, M.; Tumova, L.; Manaskova-Postlerova, P. Missing Information from the Estrogen Receptor Puzzle: Where Are They Localized in Bull Reproductive Tissues and Spermatozoa? *Cells* **2020**, *9*. [CrossRef] [PubMed]
96. Kotula-Balak, M.; Hejmej, A.; Lydka, M.; Cierpich, A.; Bilinska, B. Detection of aromatase, androgen, and estrogen receptors in bank vole spermatozoa. *Theriogenology* **2012**, *78*, 385–392. [CrossRef]
97. Rago, V.; Siciliano, L.; Aquila, S.; Carpino, A. Detection of estrogen receptors ER-alpha and ER-beta in human ejaculated immature spermatozoa with excess residual cytoplasm. *Reprod. Biol. Endocrinol.* **2006**, *4*, 36. [CrossRef]
98. Gunawan, A.; Kaewmala, K.; Uddin, M.J.; Cinar, M.U.; Tesfaye, D.; Phatsara, C.; Tholen, E.; Looft, C.; Schellander, K. Association study and expression analysis of porcine ESR1 as a candidate gene for boar fertility and sperm quality. *Anim. Reprod. Science* **2011**, *128*, 11–21. [CrossRef] [PubMed]
99. Rago, V.; Aquila, S.; Panza, R.; Carpino, A. Cytochrome P450arom, androgen and estrogen receptors in pig sperm. *Reprod. Biol Endocrinol.* **2007**, *5*, 23. [CrossRef] [PubMed]
100. Luconi, M.; Francavilla, F.; Porazzi, I.; Macerola, B.; Forti, G.; Baldi, E. Human spermatozoa as a model for studying membrane receptors mediating rapid nongenomic effects of progesterone and estrogens. *Steroids* **2004**, *69*, 553–559. [CrossRef]
101. Rago, V.; Giordano, F.; Brunelli, E.; Zito, D.; Aquila, S.; Carpino, A. Identification of G protein-coupled estrogen receptor in human and pig spermatozoa. *J. Anat.* **2014**, *224*, 732–736. [CrossRef]

102. Gautier, C.; Barrier-Battut, I.; Guenon, I.; Goux, D.; Delalande, C.; Bouraima-Lelong, H. Implication of the estrogen receptors GPER, ESR1, ESR2 in post-testicular maturations of equine spermatozoa. *Gen. Comp. Endocrinol.* **2016**, *233*, 100–108. [CrossRef] [PubMed]
103. Arkoun, B.; Gautier, C.; Delalande, C.; Barrier-Battut, I.; Guenon, I.; Goux, D.; Bouraima-Lelong, H. Stallion spermatozoa: Putative target of estrogens; presence of the estrogen receptors ESR1, ESR2 and identification of the estrogen-membrane receptor GPER. *Gen. Comp. Endocrinol.* **2014**, *200*, 35–43. [CrossRef]
104. Cornwall, G.A. Role of posttranslational protein modifications in epididymal sperm maturation and extracellular quality control. *Adv. Exp. Med. Biol.* **2014**, *759*, 159–180. [CrossRef]
105. Dacheux, J.L.; Belleannee, C.; Guyonnet, B.; Labas, V.; Teixeira-Gomes, A.P.; Ecroyd, H.; Druart, X.; Gatti, J.L.; Dacheux, F. The contribution of proteomics to understanding epididymal maturation of mammalian spermatozoa. *Syst. Biol. Reprod. Med.* **2012**, *58*, 197–210. [CrossRef]
106. Prossnitz, E.R.; Oprea, T.I.; Sklar, L.A.; Arterburn, J.B. The ins and outs of GPR30: A transmembrane estrogen receptor. *J. Steroid Biochem. Mol. Biol.* **2008**, *109*, 350–353. [CrossRef] [PubMed]
107. Schwartz, N.; Verma, A.; Bivens, C.B.; Schwartz, Z.; Boyan, B.D. Rapid steroid hormone actions via membrane receptors. *Bioch. Biophys. Acta* **2016**, *1863*, 2289–2298. [CrossRef]
108. Boccellino, M.; Vanacore, D.; Zappavigna, S.; Cavaliere, C.; Rossetti, S.; D'Aniello, C.; Chieffi, P.; Amler, E.; Buonerba, C.; Di Lorenzo, G.; et al. Testicular cancer from diagnosis to epigenetic factors. *Oncotarget* **2017**, *8*, 104654–104663. [CrossRef]
109. Batool, A.; Karimi, N.; Wu, X.N.; Chen, S.R.; Liu, Y.X. Testicular germ cell tumor: A comprehensive review. *Cell. Mol. Life Sci.* **2019**, *76*, 1713–1727. [CrossRef]
110. Baroni, T.; Arato, I.; Mancuso, F.; Calafiore, R.; Luca, G. On the Origin of Testicular Germ Cell Tumors: From Gonocytes to Testicular Cancer. *Front. Endocrinol.* **2019**, *10*, 343. [CrossRef] [PubMed]
111. Albers, P.; Albrecht, W.; Algaba, F.; Bokemeyer, C.; Cohn-Cedermark, G.; Fizazi, K.; Horwich, A.; Laguna, M.P.; Nicolai, N.; Oldenburg, J. Guidelines on Testicular Cancer: 2015 Update. *Eur. Urol.* **2015**, *68*, 1054–1068. [CrossRef]
112. Facchini, G.; Rossetti, S.; Berretta, M.; Cavaliere, C.; D'Aniello, C.; Iovane, G.; Mollo, G.; Capasso, M.; Della Pepa, C.; Pesce, L.; et al. Prognostic and predictive factors in testicular cancer. *Eur. Rev. Med. Pharmaco. Sci.* **2019**, *23*, 3885–3891. [CrossRef]
113. Feldman, P.S.; Kovacs, K.; Horvath, E.; Adelson, G.L. Malignant Leydig cell tumor: Clinical, histologic and electron microscopic features. *Cancer* **1982**, *49*, 714–721. [CrossRef]
114. Muheilan, M.M.; Shomaf, M.; Tarawneh, E.; Murshidi, M.M.; Al-Sayyed, M.R.; Murshidi, M.M. Leydig cell tumor in grey zone: A case report. *Int. J. Surg. Case Rep.* **2017**, *35*, 12–16. [CrossRef]
115. Kim, I.; Young, R.H.; Scully, R.E. Leydig cell tumors of the testis. A clinicopathological analysis of 40 cases and review of the literature. *Am. J. Surg. Pathol.* **1985**, *9*, 177–192. [CrossRef] [PubMed]
116. Jou, P.; Maclennan, G.T. Leydig cell tumor of the testis. *J. Urol.* **2009**, *181*, 2299–2300. [CrossRef] [PubMed]
117. Sawhney, P.; Giammona, C.J.; Meistrich, M.L.; Richburg, J.H. Cisplatin-induced long-term failure of spermatogenesis in adult C57/Bl/6J mice. *J. Androl.* **2005**, *26*, 136–145.
118. Grem, J.L.; Robins, H.I.; Wilson, K.S.; Gilchrist, K.; Trump, D.L. Metastatic Leydig cell tumor of the testis. Report of three cases and review of the literature. *Cancer* **1986**, *58*, 2116–2119. [CrossRef]
119. Franco, R.; Boscia, F.; Gigantino, V.; Marra, L.; Esposito, F.; Ferrara, D.; Pariante, P.; Botti, G.; Caraglia, M.; Minucci, S.; et al. GPR30 is overexpressed in post-puberal testicular germ cell tumors. *Cancer Biol. Ther.* **2011**, *11*, 609–613. [CrossRef]
120. Rago, V.; Romeo, F.; Giordano, F.; Ferraro, A.; Ando, S.; Carpino, A. Identification of ERbeta1 and ERbeta2 in human seminoma, in embryonal carcinoma and in their adjacent intratubular germ cell neoplasia. *Reprod. Biol. Endocrinol.* **2009**, *7*, 56. [CrossRef] [PubMed]
121. Guido, C.; Panza, S.; Santoro, M.; Avena, P.; Panno, M.L.; Perrotta, I.; Giordano, F.; Casaburi, I.; Catalano, S.; De Amicis, F.; et al. Estrogen receptor beta (ERbeta) produces autophagy and necroptosis in human seminoma cell line through the binding of the Sp1 on the phosphatase and tensin homolog deleted from chromosome 10 (PTEN) promoter gene. *Cell Cycle* **2012**, *11*, 2911–2921. [CrossRef]
122. Kinugawa, K.; Hyodo, F.; Matsuki, T.; Jo, Y.; Furukawa, Y.; Ueki, A.; Tanaka, H. Establishment and characterization of a new human testicular seminoma cell line, JKT-1. *Int. J. Urol.* **1998**, *5*, 282–287. [CrossRef] [PubMed]

123. Bouskine, A.; Nebout, M.; Mograbi, B.; Brucker-Davis, F.; Roger, C.; Fenichel, P. Estrogens promote human testicular germ cell cancer through a membrane-mediated activation of extracellular regulated kinase and protein kinase A. *Endocrinology* **2008**, *149*, 565–573. [CrossRef] [PubMed]
124. Bouskine, A.; Nebout, M.; Brucker-Davis, F.; Benahmed, M.; Fenichel, P. Low doses of bisphenol A promote human seminoma cell proliferation by activating PKA and PKG via a membrane G-protein-coupled estrogen receptor. *Environ. Health Perspect.* **2009**, *117*, 1053–1058. [CrossRef] [PubMed]
125. Chevalier, N.; Bouskine, A.; Fenichel, P. Bisphenol A promotes testicular seminoma cell proliferation through GPER/GPR30. *Int. J. Cancer* **2012**, *130*, 241–242. [CrossRef]
126. Roger, C.; Lambard, S.; Bouskine, A.; Mograbi, B.; Chevallier, D.; Nebout, M.; Pointis, G.; Carreau, S.; Fenichel, P. Estrogen-induced growth inhibition of human seminoma cells expressing estrogen receptor beta and aromatase. *J. Mol. Endocrinol.* **2005**, *35*, 191–199. [CrossRef]
127. Chevalier, N.; Paul-Bellon, R.; Camparo, P.; Michiels, J.F.; Chevallier, D.; Fenichel, P. Genetic variants of GPER/GPR30, a novel estrogen-related G protein receptor, are associated with human seminoma. *Int. J. Mol. Sci.* **2014**, *15*, 1574–1589. [CrossRef]
128. Wallacides, A.; Chesnel, A.; Ajj, H.; Chillet, M.; Flament, S.; Dumond, H. Estrogens promote proliferation of the seminoma-like TCam-2 cell line through a GPER-dependent ERalpha36 induction. *Mol. Cell. Endocrinol.* **2012**, *350*, 61–71. [CrossRef]
129. Boscia, F.; Passaro, C.; Gigantino, V.; Perdona, S.; Franco, R.; Portella, G.; Chieffi, S.; Chieffi, P. High Levels of Gpr30 Protein in Human Testicular Carcinoma In Situ and Seminomas Correlate with Low Levels of Estrogen Receptor-Beta and Indicate a Switch in Estrogen Responsiveness. *J. Cell. Physiol.* **2015**, *230*, 1290–1297. [CrossRef]
130. Chimento, A.; Casaburi, I.; Bartucci, M.; Patrizii, M.; Dattilo, R.; Avena, P.; Ando, S.; Pezzi, V.; Sirianni, R. Selective GPER activation decreases proliferation and activates apoptosis in tumor Leydig cells. *Cell Death Dis.* **2013**, *4*, e747. [CrossRef]
131. Ariazi, E.A.; Brailoiu, E.; Yerrum, S.; Shupp, H.A.; Slifker, M.J.; Cunliffe, H.E.; Black, M.A.; Donato, A.L.; Arterburn, J.B.; Oprea, T.I.; et al. The G protein-coupled receptor GPR30 inhibits proliferation of estrogen receptor-positive breast cancer cells. *Cancer Res.* **2010**, *70*, 1184–1194. [CrossRef]
132. Chan, Q.K.; Lam, H.M.; Ng, C.F.; Lee, A.Y.; Chan, E.S.; Ng, H.K.; Ho, S.M.; Lau, K.M. Activation of GPR30 inhibits the growth of prostate cancer cells through sustained activation of Erk1/2, c-jun/c-fos-dependent upregulation of p21, and induction of G(2) cell-cycle arrest. *Cell Death Diff.* **2010**, *17*, 1511–1523. [CrossRef] [PubMed]
133. Gorowska-Wojtowicz, E.; Duliban, M.; Kudrycka, M.; Dutka, P.; Pawlicki, P.; Milon, A.; Zarzycka, M.; Placha, W.; Kotula-Balak, M.; Ptak, A.; et al. Leydig cell tumorigenesis–implication of G-protein coupled membrane estrogen receptor, peroxisome proliferator-activated receptor and xenoestrogen exposure. In vivo and in vitro appraisal. *Tissue Cell* **2019**, *61*, 51–60. [CrossRef] [PubMed]
134. Kotula-Balak, M.; Gorowska-Wojtowicz, E.; Milon, A.; Pawlicki, P.; Tworzydlo, W.; Plachno, B.J.; Krakowska, I.; Hejmej, A.; Wolski, J.K.; Bilinska, B. Towards understanding leydigioma: Do G protein-coupled estrogen receptor and peroxisome proliferator-activated receptor regulate lipid metabolism and steroidogenesis in Leydig cell tumors? *Protoplasma* **2020**. [CrossRef] [PubMed]
135. Natale, C.A.; Li, J.; Zhang, J.; Dahal, A.; Dentchev, T.; Stanger, B.Z.; Ridky, T.W. Activation of G protein-coupled estrogen receptor signaling inhibits melanoma and improves response to immune checkpoint blockade. *eLife* **2018**, *7*. [CrossRef]
136. Natale, C.A.; Li, J.; Pitarresi, J.R.; Norgard, R.J.; Dentchev, T.; Capell, B.C.; Seykora, J.T.; Stanger, B.Z.; Ridky, T.W. Pharmacologic Activation of the G Protein-Coupled Estrogen Receptor Inhibits Pancreatic Ductal Adenocarcinoma. *Cell. Mol. Gastroenter. Hepatol.* **2020**. [CrossRef]
137. Phase 1 Study to Determine the MTD, Safety, Tolerability, PK and Preliminary Anti-Tumor Effects of LNS8801alone and in Combination with Pembrolizumab. Available online: https://clinicaltrials.gov/ct2/show/NCT04130516 (accessed on 6 August 2020).

Received: 28 October 2020 | Revised: 8 January 2021 | Accepted: 11 January 2021

DOI: 10.1111/jcmm.16317

ORIGINAL ARTICLE

WILEY

SIRT1 is involved in adrenocortical cancer growth and motility

Adele Chimento | Arianna De Luca | Marta Claudia Nocito | Sara Sculco | Paola Avena | Davide La Padula | Lucia Zavaglia | Rosa Sirianni | Ivan Casaburi | Vincenzo Pezzi

Department of Pharmacy and Health and Nutritional Sciences, University of Calabria, Arcavacata di Rende, Cosenza, Italy

Correspondence
Adele Chimento and Rosa Sirianni, Department of Pharmacy and Health and Nutritional Sciences, University of Calabria, Via Pietro Bucci, Arcavacata di Rende, Cosenza 87036, Italy.
Emails: adele.chimento@unical.it; rosa.sirianni@unical.it

Funding information
Fondazione Umberto Veronesi (FUV).; MIUR (Ministero dell'Istruzione, dell'Università e della Ricerca); PAC (Progetto Strategico Regionale Calabria Alta Formazione) Calabria 2014/2020; Associazione Italiana per la Ricerca sul Cancro (AIRC)

Abstract

Adrenocortical cancer (ACC) is a rare tumour with unfavourable prognosis, lacking an effective treatment. This tumour is characterized by IGF-II (insulin-like growth factor II) overproduction, aromatase and ERα (oestrogen receptor alpha) up-regulation. Previous reports suggest that ERα expression can be regulated by sirt1 (sirtuin 1), a nicotinamide adenine dinucleotide (NAD+)-dependent class III histone deacetylases that modulates activity of several substrates involved in cellular stress, metabolism, proliferation, senescence, protein degradation and apoptosis. Nevertheless, sirt1 can act as a tumour suppressor or oncogenic protein. In this study, we found that in H295R and SW13 cell lines, sirt1 expression is inhibited by sirtinol, a potent inhibitor of sirt1 activity. In addition, sirtinol is able to decrease ACC cell proliferation, colony and spheroids formation and to activate the intrinsic apoptotic mechanism. Particularly, we observed that sirtinol interferes with E2/ERα and IGF1R (insulin growth factor 1 receptor) pathways by decreasing receptors expression. Sirt1 involvement was confirmed by using a specific sirt1 siRNA. More importantly, we observed that sirtinol can synergize with mitotane, a selective adrenolitic drug, in inhibiting adrenocortical cancer cell growth. Collectively, our data reveal an oncogenic role for sirt1 in ACC and its targeting could implement treatment options for this type of cancer.

KEYWORDS
adrenocortical cancer, ERα, IGF1R, sirt1, sirtinol

1 | INTRODUCTION

ACC is a rare tumour of the adrenal gland, extremely invasive and with relatively short life expectancies.[1] This tumour is characterized by considerable morphological, clinical and genetic heterogeneity limiting the availability of specific pharmacological treatments.[2] Molecular studies identified a correlation between ACC onset and genetic mutations, particularly involving TP53, CTNNB1 (β-catenin) and IGF-II genes.[3] Recently, genomic characterizations of ACC expanded the list of known mutations including also those on PRKAR1A (protein kinase cAMP-dependent regulatory type I alpha), RPL22 (ribosomal protein L22), TERF2 (telomere specific protein 2), CCNE1 (cyclin E1) and NF1 (neurofibromatosis type 1) genes [4] and revealed high heterogeneity and

Casaburi and Pezzi shared senior authorship.

histotype-specific genomic profiles.[5] The IGF-II overexpression is the most widespread molecular event that occurs in 90% of the ACC patients and causes an autocrine mitogenic effect through activation of different signalling pathways mediated by IGF1R.[6] In addition, this tumour has an increased aromatase and ERα expression[7] and a cross-talk between ERα and IGF1R pathways has been demonstrated.[8] In particular, in H295R cells, IGF-II-IGF1R signalling activation leads to an increased aromatase expression and, as a consequence, local oestrogens production, which in turn, through an autocrine mechanism, activates ERα and downstream molecular events that overlap with IGF1R signal.[8] Moreover, the use of hydroxytamoxifen, an active metabolite of the oestrogen antagonist tamoxifen, decreases IGF1R expression and counteract E2- and IGF-II-induced ACC cell growth, both in vitro and in vivo.[8] These results revealed the central role of the oestrogenic pathway and supported the possibility of using anti-oestrogens as treatment for ACC.

Currently, the main therapeutic approach against ACC is represented by surgery followed by adjuvant drug treatment with mitotane administered as monotherapy or in combination with doxorubicin, vincristine and etoposide in order to decrease recurrence risk.[2] However, these therapeutic approaches are ineffective for all forms of ACCs. Several clinical trials evaluated effectiveness of targeted therapy, however with discouraging results.[9,10] For this reason, the widening on knowledge regarding the molecular pathways involved in ACC progression represents a necessary step to develop new therapeutic strategies against this tumour.

It has been reported that ERα expression can be regulated by sirt1,[11] a mammalian NAD+-dependent deacetylase that belongs to HDACs (class III histone deacetylases).[12] Sirt1 targets specific histones such as histone H1 at lysine 26 (H1K26), H3K9 and H4K16, regulating chromatin silencing and heterochromatin formation, and several non-histone proteins including p53, FOXOs (class O forkhead box transcription factors), PPAR-γ (peroxisome proliferator-activated receptor-gamma), CREB (cyclic AMP-responsive element-binding protein), FXR (farnesoid X receptor), HIF-1α (hypoxia-inducible factor-1α), Myc, 5'-deoxyribose-5-phosphate lyase Ku70, E2F1, NF-kB (nuclear factor kappa-light-chain-enhancer of activated B cells), PGC-1α (peroxisome proliferator-activated receptor-g coactivator-1α), LXR (liver X receptor) and other, modulating their activity, subcellular localization or association with other proteins.[12]

Although sirt1 is typically localized in the nucleus, a nucleocytoplasmic shuttling has been reported clarifying its different distribution in various tissues and cells affecting its function.[13] In mammalian cells, sirt1 plays an important role in various biological process such as gene transcription, energy and lipid metabolism, insulin secretion and ageing.[14] Moreover, sirt1 is involved in neurodegenerative, immune/autoimmune, age- and heart-related disease [14] and in cancer.[15] Particularly, sirt1 has a role in cell proliferation, migration, invasion, genome stability, senescence and apoptosis exerting pro- and anti-tumour activity.[16] The involvement of sirt1 in genome stability, through chromatin regulation and DNA repair, explains its role as tumour suppressor.[17]

In contrast, other reports indicates that sirt1 promotes cell proliferation and metastasis in a variety of cancers including pancreatic,[18] hepatocellular,[19] prostate,[20] lung,[21] breast,[22] cervical,[23] endometrial[24] and ovarian[25] carcinoma.

In this effort, sirtinol (2-[(2-Hydroxynaphthalen-1-ylmethylene) amino]-N-(1-phenethyl) Benzamide), a potent inhibitor for sirt1[26] exhibited anti-proliferative effects in several human cancer cells[27] and was proposed as anti-tumour agent.[28]

Starting from these observations, aim of this study was to evaluate the role of sirt1 in ACC. To this purpose, we targeted sirt1 pharmacologically and by RNA-silencing to evaluate the effects on adrenocortical cancer cell proliferation and metastatic potential.

2 | MATERIALS AND METHODS

2.1 | Cell cultures

Adrenocortical tumour cells (H295R and SW13 cells) were purchased from the American Type Culture Collection (ATCC, Rockville, MD). H295R cells were maintained as previously described.[29] SW13 were maintained in high glucose DMEM (Dulbecco's modified Eagle's medium) (Thermo Fisher Scientific, Monza, Italy) supplemented with 10% foetal bovine serum, 1% glutamine and 1% penicillin-streptomycin (Sigma-Aldrich Srl., Milan, Italy). All cells were maintained at 37°C in a humidified atmosphere of 95% air and 5% CO2. Cell monolayers were subcultured into 6-well plate for protein and RNA extraction (1 x 10^6 cells/plate), into 12-multi-well for colony formation (2 x 10^3 cells/well) and wound healing assay (3 x 10^5 cells/well) and into 48-multi-well for MTT assay (2 x 10^4 cells/well). Doubling time for SW13 cells is about 24 hours and for H295R cells is 48-72-hours: this difference has been considered in cell experiments.[30] H295R and SW13 cells were maintained in complete medium for 48 and 24 hours, respectively, and then treated with sirtinol (Sigma-Aldrich) in complete medium.

2.2 | Reagents and antibodies

DMEM-F12 (Dulbecco's modified Eagle's medium-F12) was purchased from Sigma (Sigma-Aldrich). FBS (foetal bovine serum), ITS (insulin-transferrin-selenium), L-glutamine, DMSO (dimethyl sulfoxide), MTT (3-[4,5-dimethylthiazol-2-yl]-2,5-diphenyltetrazoliumbromide), penicillin, streptomycin and sirtinol were purchased from Sigma (Sigma-Aldrich). Antibodies against sirt1, ERα, IGF1R, CCND1 (cyclin D1), vimentin, N-cadherin, bax (bcl2 associated x), bcl-2 (B-cell lymphoma 2), parp-1 (poly(ADP-ribose) polymerase 1), cytochrome c, pCREB-1^{Ser133} (phospho cyclic AMP response element binding) and GAPDH (glyceraldehyde 3-phosphate dehydrogenase) were purchased from Santa Cruz (Santa Cruz Biotechnology, Inc, Heidelberg, Germany). Antibody against VDAC1 (voltage-dependent anion-selective channel protein 1)/

Gene	Forward primer	Reverse primer
SIRT1	CAGTGGCTGGAACAGTGAGA	AGCGCCATGGAAAATGTAAC
ESR1	CACCATTGATAAAAACAGGAGGAA	CTCCCTCCTCTTCGGTCTTTTC
CCND1	CACGCGCAGACCTTCCG	ATGGAGGGCGGATTGGAA
IGF1R	AAGGCTGTGACCCTCACCAT	CGATGCTGAAAGAACGTCCAA
18S	CGGCGACGACCCATTCGAAC	GAATCGAACCCTGATTCCCCGTC

TABLE 1 Primers oligonucleotide sequences. The indicated primers oligonucleotide sequences were used for the amplification of following genes: SIRT1: sirtuin 1; ESR1: oestrogen receptor alpha; CCND1: cyclin D1; IGF1R: insulin growth factor receptor 1; 18S: 18S ribosomal RNA

porin) was purchased from Abcam (Abcam, Cambridge, UK). HRP (Horseradish peroxidase)-conjugated secondary antibodies were purchased from Bethyl (Bethyl Laboratories, Montgomery, TX, USA) and ECL (Electrochemiluminescence) Western blotting detection system from Santa Cruz (Santa Cruz Biotechnology, Santa Cruz CA, USA). The TRIzol reagent, High Capacity cDNA Reverse Transcription Kit and PowerUp™ SYBR™ Green Master Mix were purchased from Thermo Fisher Scientific (Thermo Fisher Scientific).

2.3 | Cell viability assay

The effect of sirtinol on cell viability was measured using MTT assay as previously described.[29,31]

2.4 | RNA silencing

Cells were subcultured in 6-multi-well plates (2.5×10^5 cells/well) for Western blot analysis or in 24-multi-well plates (0.5×10^5 cells/well) for cell viability assay. The next day, as recommended by manufacturer, cells were transfected with control siRNA (siRNA scrambled) or sirt1 siRNA (Thermo Fisher Scientific) in complete medium using lipofectamine RNAiMAX transfection reagent (Thermo Fisher Scientific) for a total of 72 hours.

2.5 | Spheroids cultures

A single cell suspension was prepared using 1x Trypsin-EDTA (ethylenediaminetetraacetic acid) solution (Sigma-Aldrich) and manual disaggregation (21 gauge needle).[32] Cell were seeded in non-adherent conditions as described by De luca and collegues.[33]

2.6 | Colony Formation Assay

Two thousand cells were seeded in 12-well plates and allowed to grow out in the absence or presence of different sirtinol concentrations for 14 (H295R) or 7 (SW13) days. Colonies were stained with 0.05% Coomassie Blue in methanol/water/acetic acid (45:45:10, v/v). Colony number was assessed using Image J (NIH) and normalized to untreated cells.

2.7 | Wound healing assay

Cells were grown in 12-well plates until about 80-90% confluency was reached and then a 10-μL pipette tip was used to create a scratch/wound with clear edges across the width of a well. Wells were treated either with vehicle (DMSO) or 40 μmol/L sirtinol. Photographs were acquired with Olympus CKX53 microscope at 0 hours or 24 hours. All experiments were performed in triplicates.

2.8 | Transwell migration assay

The transwell inserts (8 μm pore size, 24-well plate, Corning Costar, Cambridge, MA) were used to evaluate cell migration ability. The cells (5×10^4/well) were seeded in the boyden insert and solvent or sirtinol were added in the well; the cells were allowed to migrate across the membrane for 24 hours. At the end of the experiment, migrated cells were stained with Coomassie Brilliant Blue solution for 10 minutes and counted under an inverted microscope (Olympus CKX53).

2.9 | RNA extraction, reverse transcription and qPCR

The RNA extraction was performed as previously described.[29] One (for H295R) or 2 (for SW13) micrograms of total RNA were reverse-transcribed in a final volume of 50 μL using the High Capacity cDNA Reverse Transcription Kit (Thermo Fisher Scientific); cDNA was diluted 1:2 in DNAse and RNAse free water. Primer sequences are shown in Table 1. PCR reactions were performed in the QuantStudio^{Tm} 3 Real Time PCR System (Thermo Fisher Scientific) using 0.3 (for H295R) or 0.6 (for SW13) μmol/L of each primer. PowerUp™ SYBR™ Green Master Mix (Thermo Fisher Scientific) with the dissociation protocol was used for gene amplification; negative controls contained water instead of first-strand cDNA. Each sample was normalized to its 18S rRNA (18S) content. Final results were expressed as n-fold differences relative to a calibrator and calculated using the ΔΔCt method.

2.10 | Western blot analysis

RIPA lysis buffer was used to lysate cells.[34] Western blot analysis was performed using equal quantity of protein. Protein concentration was determined by Bradford method (Sigma-Aldrich) and equal amounts

were subjected to Western blot analysis. All membranes were incubated for 12 hours at 4°C with antibodies against sirt1, ERα, IGF1R, CCND1, vimentin, N-cadherin, bax, bcl-2, parp1 and cytochrome c (all from Santa Cruz Biotechnology, Santa Cruz CA, USA). Membranes were incubated with HRP-conjugated secondary antibodies (Bethyl Laboratories, Montgomery, TX, USA), and immunoreactive bands were visualized with the ECL Western blotting detection system (Santa Cruz Biotechnology, Santa Cruz CA, USA). GAPDH (Santa Cruz Biotechnology, Santa Cruz CA, USA) or VDAC1/porin (Abcam, Cambridge, UK) antibodies were used as a loading control.

2.11 | Cytochrome c detection

Cytochrome c (cyt c) detection in mitochondrial and cytoplasmic fractions was performed as previously reported.[29]

2.12 | Terminal deoxynucleotidyl transferase dUTP nick-end labeling (TUNEL) assay

Cells seeded onto glass coverslips were treated with sirtinol for 48 hours, washed with PBS and then fixed in 4% paraformaldehyde for 15 minutes at room temperature. The cells were subsequently washed with PBS and then soaked for 20 minutes in PBS containing 0.25% of Triton X-100. After two washes with deionized water, slides were incubated with TdT (terminal deoxynucleotidyl transferase) enzyme and EdUTP (5-ethynyl-2'-deoxyuridine 5'-triphosphate) overnight at room temperature, using Click-iT TUNEL Alexa Fluor Imaging Assay (Thermo Fisher Scientific). The next day cells were incubated with a solution containing Alexa Fluor azide for 30 minutes at room temperature and then stained with DAPI (4',6-diamidino-2-phenylindole) solution in order to analyse the nuclear morphology. Cells were observed under a fluorescence microscope (Olympus BX41) with a 20X objective.

2.13 | Phase-contrast microscopy for morphological evaluation

H295R and SW13 cells were seeded into 48-well plates at a density of 2 x 10^4 cells/well, and then transfected with a specific sirt1 siRNA. Additionally, cells were treated with sirtinol (40 μmol/L) and mitotane (10 μmol/L) alone or in combination for 72 hours. Cells were observed under an inverted phase contrast microscope (Olympus CKX53) with a 10X objective.

2.14 | Statistics

Statistical analyses were performed as previously indicated.[29] Coefficient of drug interaction (CDI) was calculated as: CDI = AB/(A × B). AB represents the percentage of viable cells remaining after the treatment with the combined drugs, while A and B represent the percentage of viable cells remaining after single treatments. CDI < 1 indicates a synergistic effect, CDI = 1 indicates an additive effect, CDI > 1 indicates antagonism.

3 | RESULTS

3.1 | Sirt1 inhibition exerts anti-proliferative effects in human adrenocortical cancer cells

We first treated cells with increasing concentrations of sirtinol in order to evaluate effects on sirt1. Using Western blot analysis, we revealed that 40 μmol/L sirtinol for 24 hours significantly decreased sirt1 protein expression in H295R (Figure 1A) and SW13 cells (Figure 1B). The same doses were tested on time course experiments to evaluate effects on cell viability, highlighting a clear inhibitory effect on both H295R (Figure 1C) and SW13 (Figure 1D) cells. Sirt1 gene expression breakdown with a specific siRNA (siRNAsirt1) showed a significant reduction in protein content compared to the control (siRNA scrambled) cells (insert, Figure 1E and F) after 72 hours. Sirt1 silencing was able to inhibit H295R (Figure 1E) and SW13 (Figure 1F) cell proliferation by 50% and 40%, respectively. Additionally, sirtinol suppressed the colony-forming ability of both cell lines (Figure 1G and H).

3.2 | Sirt1 inhibition induces apoptosis in human adrenocortical cancer cells

In order to verify if the reduction in cell viability after sirt1 depletion was associated with an apoptotic mechanism, cells were exposed

FIGURE 1 Sirtinol or sirt1 gene silencing reduce H295R and SW13 cell growth. (A,B) H295R (A) or SW13 (B) cells were untreated (0) or treated with increasing doses (5; 10; 20, 40, 80 μmol/L) of sirtinol for 24 h. Total protein extracts were examined by Western blotting analysis for sirt1 expression; GAPDH was used to normalize protein expression. Blots are from one experiment representative of three with similar results. H295R (C) or SW13 (D) cells were untreated (0) or treated with increasing doses (5; 10; 20, 40, 80 μmol/L) of sirtinol for 24, 48 and 72 h. Cell viability was evaluated by MTT assay (*$P < .05$ vs 0). (E,F) MTT assay was performed on H295R (E) or SW13 (F) cells transfected for 72 h with control siRNA (siRNA scrambled) or with siRNA for sirt1 (siRNA sirt1). Results were expressed as mean ± SE of three separate experiments (*$P < .05$ vs siRNA scrambled). The insert in E or F illustrates a Western blot of proteins from H295R or SW13, respectively, assessing the expression of sirt1 in the presence of siRNA scrambled or siRNA sirt1. GAPDH was used to normalize protein expression. Below images represent the morphological changes of H295R (E) or SW13 (F) cells after sirt1 silencing. These were observed by an Inverted Optic Microscope (magnification X100) and are from a representative experiment. (G,H) Colony formation assay was performed on H295R (G) or SW13 (H) cells (2000 cells/well) plated in the absence (basal) or presence with sirtinol (40 μmol/L). Relative colony formation rate was evaluated 14 (for H295R) or 6 (for SW13) days later (*$P < .05$ vs basal). Upper images are from a representative experiment

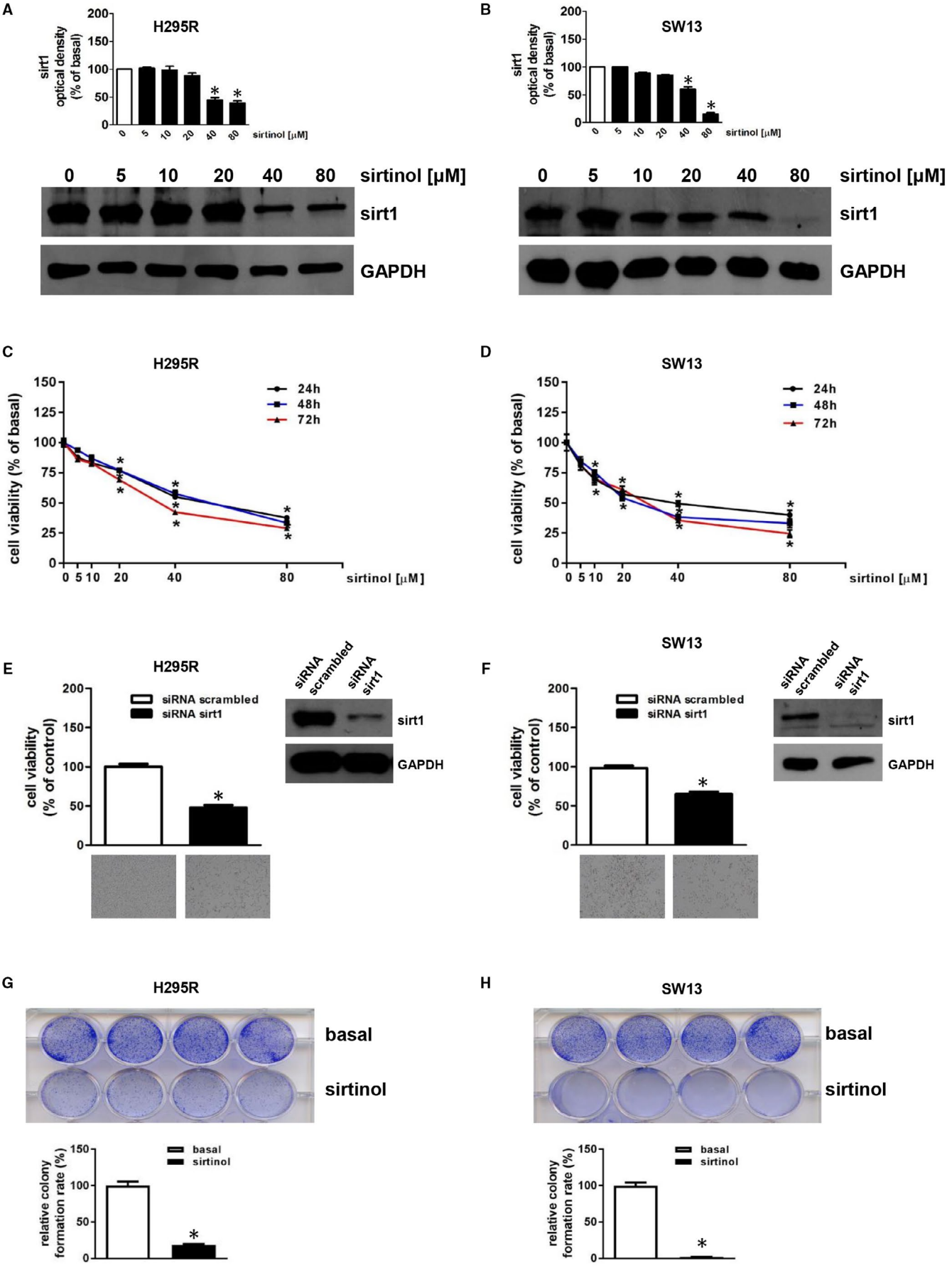
A
H295R
sirt1 optical density (% of basal)
sirtinol [μM]
0 5 10 20 40 80 sirtinol [μM]
sirt1
GAPDH
B
SW13
C
H295R
cell viability (% of basal)
24h
48h
72h
D
SW13
E
H295R
siRNA scrambled
siRNA sirt1
cell viability (% of control)
F
SW13
G
H295R
basal
sirtinol
relative colony formation rate (%)
H
SW13

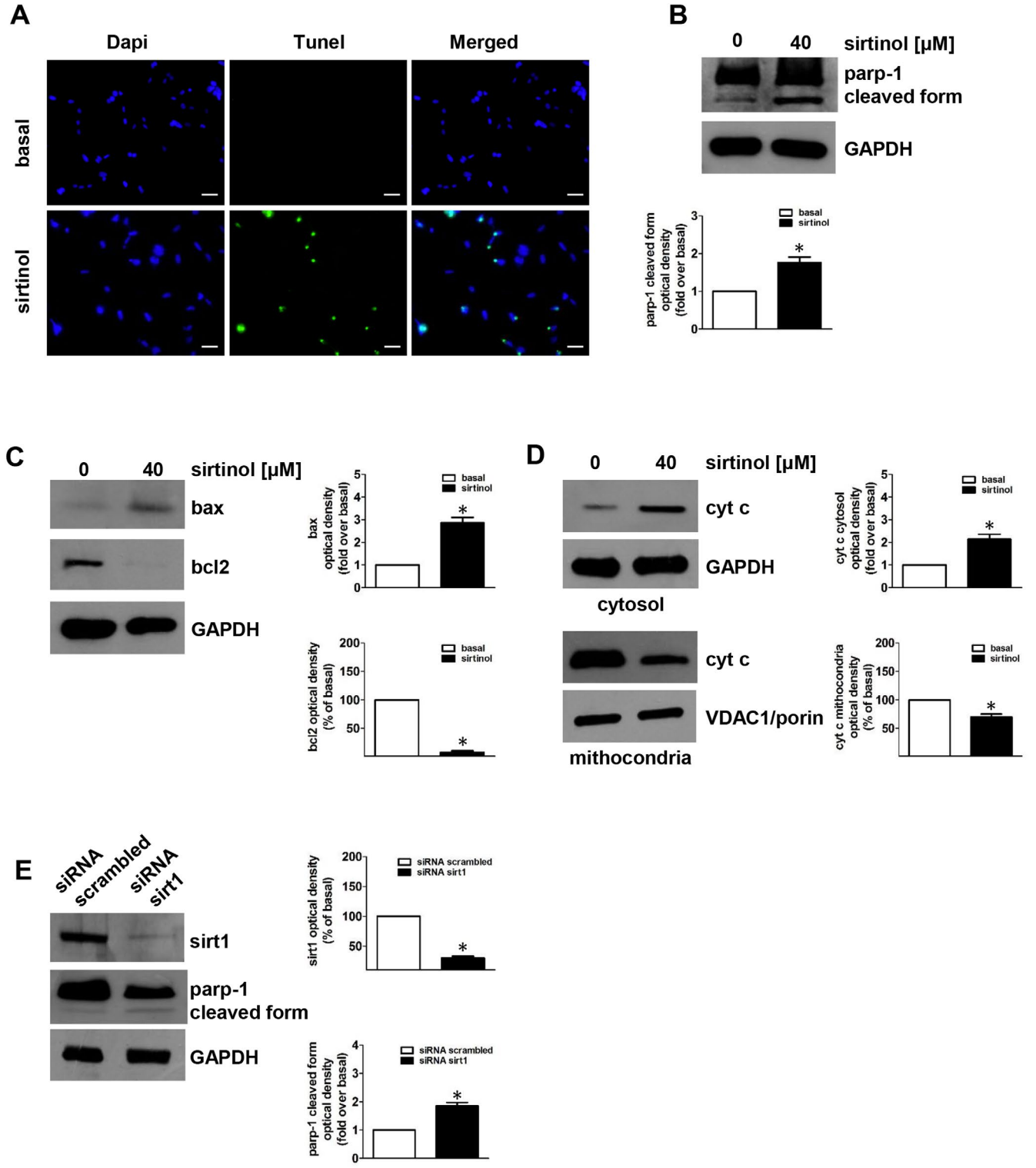

to sirtinol for 48 hours and subjected to TUNEL assay. Sirtinol induced apoptosis in H295R cells as showed by an increased number of TUNEL-positive cells (green) (Figure 2A). To specify the apoptotic mechanism activated by sirtinol, we measured the expression of different apoptototic-related proteins by Western blot analysis. Sirtinol significantly increased parp-1 cleavage (Figure 2B) and bax expression while decreased bcl-2 content (Figure 2C). It was suggested that cytosolic translocation of cytochrome c is a crucial event in the mitochondria-dependent apoptotic pathway. Consequently, we investigated if cytochrome c was released into the cytosol after sirtinol treatment. Cytosolic and mitochondrial protein extraction was performed and analysed by Western blot assay (Figure 2D). Cells treated with sirtinol showed increased cytochrome c levels in the cytosolic compartment while decreased in the mitochondrial fraction

FIGURE 2 Sirtinol or sirt1 gene silencing induce apoptosis in adrenocortical cancer cells. (A) TUNEL assay was performed on H295R cells, which were previously untreated (basal) or treated with sirtinol (40 μmol/L) for 48 h. Nuclei counterstaining was executed employing DAPI. Fluorescent signal was observed under a fluorescent microscope (magnification X200). Scale bar= 25μm. Images are from a representative experiment. (B-D) H295R cells were treated with sirtinol (40 μmol/L) for 24 h. Parp-1(B), bax and bcl-2 (C) were evaluated by Western blot. (B, below panel; C right panels) Graphs correspond to means of standardized optical densities from three experiments, bars correspond to SE (*$P < .05$ vs basal). Results are expressed as % of inhibition or fold induction versus basal. Western blot analyses of cytochrome c (cyt c) (D) were performed on cytosolic and mitochondrial protein fractions. Blots are from one experiment representative of three with similar results. GAPDH and VDAC1/porin were used as a loading control for cytosolic and mitochondrial proteins, respectively. (D, right panels) Graphs correspond to means of standardized optical densities from three experiments, bars correspond to SE (*$P < .05$ vs basal). Results are expressed as % inhibition or fold induction respect to basal. (E) H295R cells were transfected for 72 h with control siRNA (siRNA scrambled) or with siRNA for sirt1 (siRNA sirt1). Parp-1 and sirt1 were evaluated by Western blot. Blots are from one experiment representative of three with similar results. GAPDH was used to normalize protein expression. (E, right panels) Graphs correspond to means of standardized optical densities from three experiments, bars correspond to SE (*$P < .05$ vs basal). Results are expressed as % inhibition or fold induction respect to basal

(Figure 2D). Parp-1 activation was also observed in the presence of sirt1 siRNA (Figure 2E). Apoptosis was activated by sirtinol also in SW13 cells, as evidenced by parp-1 cleavage (Figure S1A), increase in bax and decrease in bcl-2 protein expression (Figure S1B) and mitochondrial cytochrome c release (Figure S1C). In addition, sirt1 silencing led to parp-1 cleavage (Figure S1D).

3.3 | Sirt1 inhibition reduces motility of human adrenocortical cancer cells

To examine the effects of sirtinol on migratory and invasive properties of H295R cells, transwell migration and wound healing assays were performed. Sirtinol inhibits H295R migratory ability (Figure 3A, 3B). To explain the inhibitory effect on cell migration, we evaluated the expression levels of key genes involved in the acquisition of mesenchymal phenotype. N-cadherin and vimentin were reduced by sirtinol (Figure 3C) and siRNA for sirt1 (Figure 3D). These results suggest that sirt1 has a role in regulating expression of genes involved in ACC cell motility

We also evaluated adrenocortical cancer cells ability to grow in anchorage-independent manner forming 3-dimensional spheres. This model system enriches spheres of cancer stem cells and progenitor cells and more closely mimics tumours in vivo.[33] When H295R cells were grown as spheroids in the presence of sirtinol, we observed a substantial decrease in spheres number (Figure 3E). Altogether, these data indicate that sirt1 functions as metastatic promoter in ACC.

3.4 | Sirt1 is part of the genomic and non-genomic ERα actions

In order to clarify how sirt1 regulates ACC growth, we investigated its role in E2/ERα and IGF1R signalling. Using a quantitative real-time PCR analysis, we observed that inhibition of sirt1 reduces mRNA levels of ERα and CCND1, a major ERα target gene involved in cell cycle regulation,[35] in H295R (Figure 4A) as well as in SW13 cells (Figure S2A). Similar effects were reproduced at the protein level by both sirtinol and sirt1 siRNA in H295R (Figure 4B,C) and SW13 (Figure S2B,C) cells, confirming a role for sirt1 in ERα genomic actions in ACC. Our previous data demonstrated that ERα, in a non-genomic fashion, is involved in CREB phosphorylation.[8] Our results showed that E2 caused a strong activation of CREB, confirming previous report [8]; this effect was abrogated by co-treatment with sirtinol in both H295R (Figure 4D) and SW13 cells (Figure S2D).

CREB is a transcription factor involved in IGF1R expression.[8] Our results indicated that sirtinol treatment decreases IGF1R mRNA and protein expression levels in both H295R (Figure 4E,F) and SW13 (Figure S2E,F) cells. Similar effects were observed by sirt1 gene silencing in H295R (Figure 4G) and SW13 cells (Figure S2G). These data suggest that sirt1 modulates E2/ERα and IGF1R pathways.

3.5 | Sirtinol potentiates mitotane effects in human adrenocortical cancer cell growth

We finally conducted experiments to establish if sirtinol is able to potentiate the effects of mitotane on cell growth. As evidenced in Figure 5, 10 μmol/L mitotane was able to reduce H295R cell viability by 20%, when combined with sirtinol 40 μmol/L inhibition increased to about 60% (Figure 5A). The coefficient of drug interaction (CDI) method[36] was then used to evaluate the effects of sirtinol and mitotane on H295R cell viability. Based on CDI value (0.95), at the tested doses, the two drugs exert a synergistic effect. Figure 5B shows H295R cell morphology after 72-hours exposure to sirtinol, mitotane and combination of the two drugs. Treatments decrease attachment to the plate, with the combination producing a more pronounced effect. It can be appreciated the presence of spherical dead cells, more abundant with sirtinol plus mitotane, confirming data derived from CDI (Figure 5B). Effects of combined mitotane and sirtinol treatment were also studied in SW13 cells. As showed in Figure 5C, sirtinol combined with the subtherapeutic 10 μmol/L dose of mitotane was able to potentiate its effects (CDI value: 0.80) (Figure 5C). Moreover, sirtinol 40 μmol/L has pronounced effects on cells viability compared to mitotane, but the combination of the two drugs has more profound effects on cell death and detachment from the plate (Figure 5D). Collectively these data, support the hypothesis of synergistic anti-proliferative effects of mitotane and sirtinol.

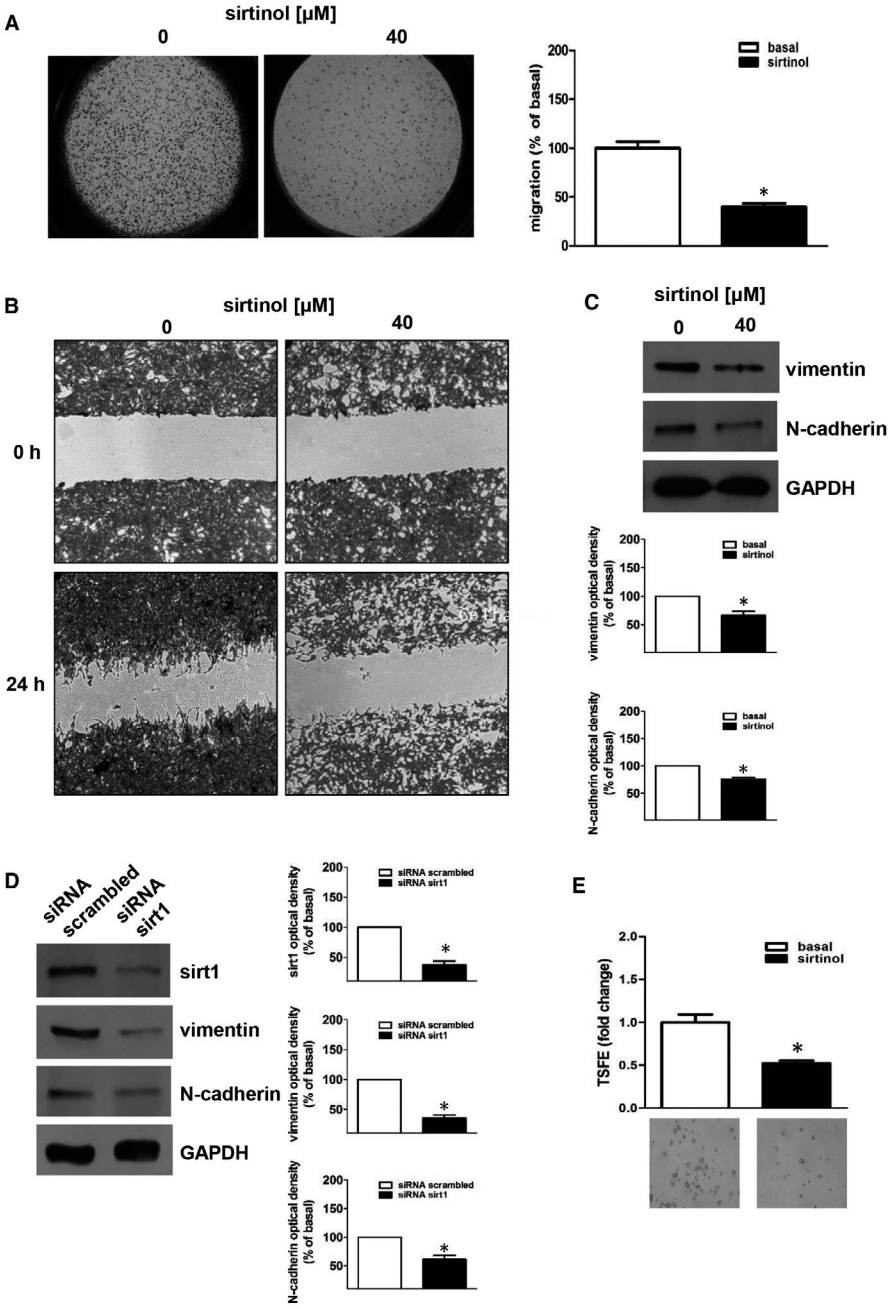

FIGURE 3 Sirtinol or sirt1 gene silencing inhibit H295R migration and invasion. (A, B) H295R cells were untreated (basal, 0) or treated with sirtinol (40 μmol/L) for 24 h. Transwell migration (A) and wound healing (B) assays were performed as described in 'Materials and Methods'. Images are from a representative experiment (A, magnification X20; B, magnification X100). (A) In the transwell migration assay, sirtinol was added in the lower compartment. After 24 h of incubation, migrated cells to the lower surfaces of the membranes were observed under a microscope and then counted. Right graph represents the mean ± SE of three independent experiments of migrated cells number expressed setting untreated cells as 100% (basal) (*$P \leq .05$ vs basal). (C,D) Western blot analyses of vimentin, N-cadherin and sirt1 were executed on H295R cells, which were previously untreated (0) or treated with sirtinol (40 μmol/L) for 24 h (C) or transfected for 72 h with control siRNA (siRNA scrambled) or with siRNA for sirt1 (siRNA sirt1) (D). Blots are from one experiment representative of three with similar results. GAPDH was used to normalize protein expression. (C, below panels; D, right panels) Graphs correspond to means of standardized optical densities from three experiments, bars correspond to SE (*$P < .05$ vs basal). Results are expressed as % inhibition respect to basal. (E) H295R cells were plated on low-attachment plates and then left untreated (basal) or treated with sirtinol (40 μmol/L). Tumour spheres formation efficiency (TSFE) was evaluated 5 d later (*$P < .05$ vs basal). Images below graphs are from a representative experiment (magnification X200)

4 | DISCUSSION

In this study, for the first time, we evidenced a role for sirt1 in ACC cell growth and EMT (epithelial/mesenchymal transition). Sirt1 functions in tumour have been widely discussed, indicating an effect as both a tumour suppressor and oncogenic factor, depending on the cell context. Literature data converged in asserting that sirt1 may modulate a delicate balance between suppression and promotion of tumorigenesis, depending on its level of activity, spatial and temporal distribution and the stage of tumorigenesis.[37]

In this study, we evaluated sirt1 expression and function in H295R and SW13 adrenocortical cancer cells. We demonstrated that pharmacological inhibition of sirt1 by sirtinol reduced H295R and SW13 cell viability in a time- and dose-dependent manner and decreased cell ability to form colonies. Similarly, gene silencing with a specific siRNA produces the same inhibitory effects on cell viability, confirming the oncogenic function of this protein. In support to its oncogenic role, it has been reported that sirt1 deacetylates and inactivates tumour suppressors promoting cell proliferation and angiogenesis and blocking apoptosis.[27,38] Data from a study in human breast cancer, MCF-7, and lung cancer, H1299, cells show that sirtinol induced senescence-like growth arrest characterized by induction of β-galactosidase activity and increased expression of plasminogen activator inhibitor.[27] In human colorectal carcinoma cells, sirt1 deficiency attenuated viability in vitro and tumorigenicity in vivo.[39] Additionally, another paper reported how in human epithelial cancer cells derived from colorectal, breast and cervical carcinomas, sirt1 silencing induces growth arrest and/or apoptosis.[40] Similarly, in cutaneous T-cell lymphoma sirt1 knockdown resulted in reduced cellular metabolism and proliferation, increased apoptosis and PARP-1 inactivation.[41]

To explore the mechanism responsible for sirtinol anti-cancer effects in adrenocortical cancer cells, we first confirmed its ability to activate apoptosis. Here, we demonstrated that sirt1 inhibition using sirtinol activates apoptosis, demonstrated by TUNEL assay, increased cytochrome c release into the cytoplasm, up-regulation of bax, down-regulation of bcl-2 and inactivation of parp-1. Sirtinol ability to produce such effects is in agreement with other previous reports in breast cancer cells. Sirt1 inhibition allows the increase of bax expression, cytochrome c release, decrease of bcl-2 and activation of apoptosis.[42,43] In this paper, we also confirmed a role for sirt1 in the EMT, a process in which the loss of non-mobile epithelial phenotype allows cells to dissolve their cellular junctions and transform into individual and mobile mesenchymal cells leading tumour metastasis.[44] We demonstrated that the lack of sirt1 interferes with H295R cell motility and migration reducing the expression of some EMT markers such as N-cadherin and vimentin. These results are in agreement with other reports demonstrating sirt1 involvement in EMT. In triple negative breast cancer, sirt1 induces tumour invasion by targeting EMT-related pathway.[45,46] Similarly, sirt1 was found to promote EMT in hepatocellular,[47] prostate[48] and oral squamous.[49] Although sirt1 inhibition modulates expression of EMT protein markers in H295R cells, this event was not observed in SW13 cells. Indeed, SW13 cells can exist in two subtypes, one expressesing vimentin (SW13+) and another lacking expression of this protein (SW13-)[50] and for our study we used this subtype. Of note, SW13 cells are a depot in the adrenal of a primary lung cancer, while H295R cells derive from a female affected by a primary adrenocortical carcinoma[30] and this observation can explain the different characteristics in terms of motility between the two cell lines. It can therefore be postulated that invasion and migration of SW13 relies on other mesenchymal markers such as βIII-tubulin that is expressed only in SW13 vimentin-deficient cells.[51] In fact, βIII-tubulin confers brain metastatic potential to breast cancer cells by regulating invasion[52] and Integrin-Src signalling.[53] β-tubulin depletion reduces metastasis via down-regulation of signalling molecules such as β3 Integrin, p-FAK and p-Src in MDA-MB231 cells.[53] Furthermore, pathological EMT also shows great complexity depending on the tissue context. In fact, the expression and function of different EMT inducers vary considerably between different types of cancer and therefore can function in a tumour-type-specific manner.[54] Induction of EMT characteristics can result in the expression of stem cell markers and increased ability to form spheres.[55,56] Starting from our previous results indicating that H295R cells grown in low-attachment plates undergo anchorage-independent growth, promoting the growth of 3-dimensional spheres with the properties of cancer stem cells and progenitor cells,[33] we demonstrated that sirt1 is able to modulate this mechanism. In fact, sirtinol reduced H295R spheres formation.

In the second part of our study, we wanted to investigate the specific molecular pathway responsible for sirtinol effects. Particularly, evaluating effects on key regulators of ACC, such as ERα and IGF1R in our experimental models. Previous studies demonstrated that aromatase and ERα are overexpressed in ACC,[7] local oestrogens bind and activate ERα, which through genomic and non-genomic mechanisms, regulates cell growth.[8] Here, we demonstrated that loss of sirt1 down-regulated ERα and its target gene CCND1.[35, 57] We found that sirtinol attenuated E2-dependent CCND1 expression (data not shown). Additionally, sirtinol prevented E2-dependent CREB activation, highlighting its ability to interfere with ERα non-genomic action.[8]

Importanly, we demonstrated a synergistic inhibitory action of sirtinol and mitotane on H295R and SW13 cell viability. Mitotane has been clinically used for decades as adjuvant therapy for adrenocortical carcinoma, despite its side effects. Patients achieving plasma mitotane levels above 14 mg/L show a good response rate and an improved survival, however, this concentration cannot be reached in all patients, because of the neurological and gastrointestinal adverse effects.[58] We evidenced that when used in combination with sirtinol, mitotane dose can be lowered to one-fifth of the therapeutic dose. In general, treatment strategies combining mitotane with other drugs could increase the response rate of patients, as compared with monotherapy. This can occur because the combination allows synergistic effects that potentially increase the in vivo antineoplastic action, or because the two drugs elicit different mechanisms that increase patients chances to get a clinical benefit from at least one of the two treatments. It was demonstrated that a combination of mitotane and chemotherapeutic drugs might be more

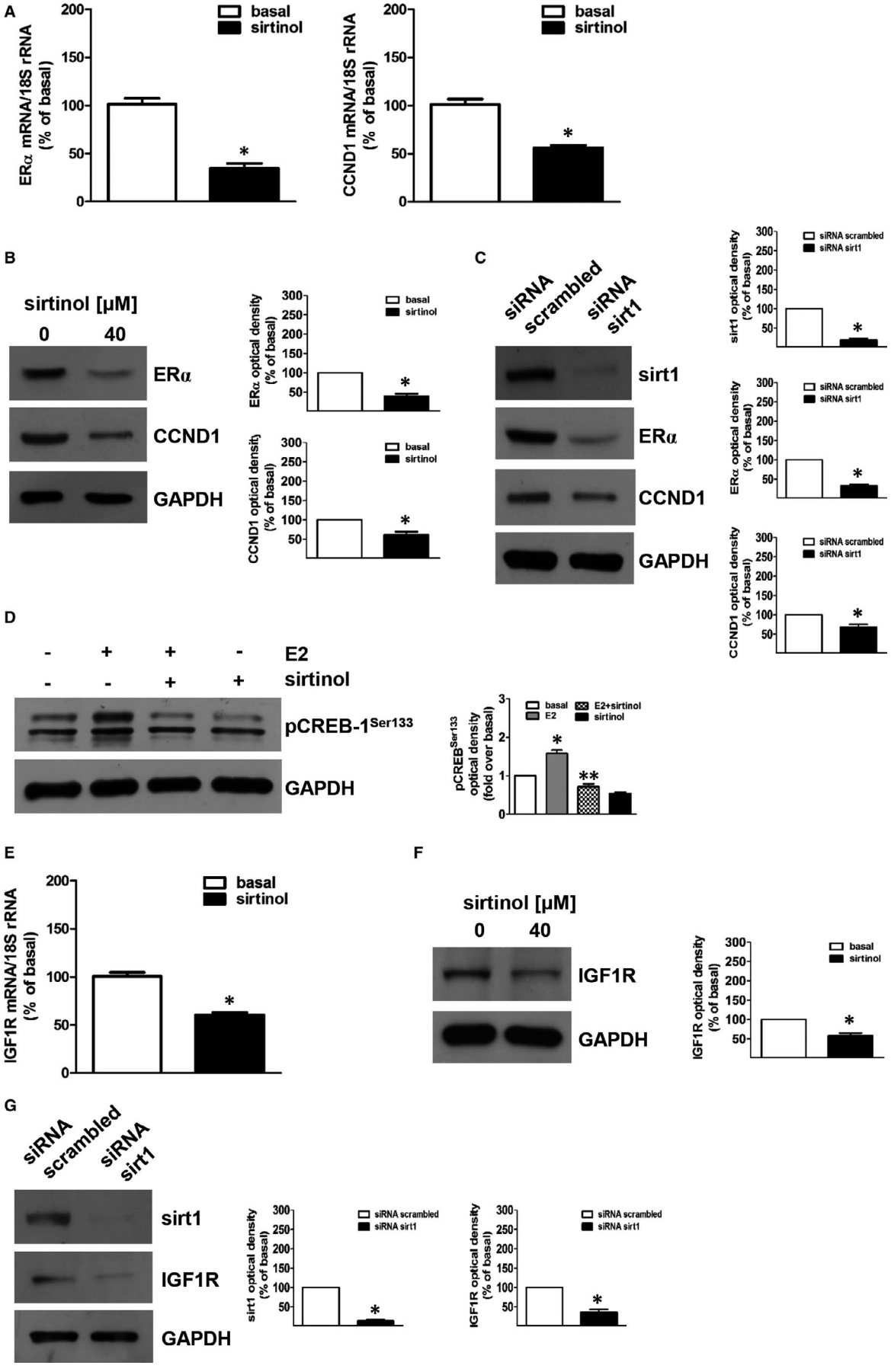
A
ERα mRNA/18S rRNA (% of basal)
CCND1 mRNA/18S rRNA (% of basal)
basal
sirtinol
B
sirtinol [μM]
0
40
ERα
CCND1
GAPDH
ERα optical density (% of basal)
CCND1 optical density (% of basal)
C
siRNA scrambled
siRNA sirt1
sirt1
ERα
CCND1
GAPDH
sirt1 optical density (% of basal)
ERα optical density (% of basal)
CCND1 optical density (% of basal)
D
E2
sirtinol
pCREB-1Ser133
GAPDH
pCREBSer133 optical density (fold over basal)
basal
E2
E2+sirtinol
sirtinol
E
IGF1R mRNA/18S rRNA (% of basal)
F
IGF1R
GAPDH
IGF1R optical density (% of basal)
G
sirt1
IGF1R
GAPDH

FIGURE 4 Sirtinol or sirt1 gene silencing inhibit ERα expression and oestrogen-dependent pathways. (A,E) H295R cells were untreated (basal, 0) or treated with sirtinol (40 μmol/L) for 24 h. The mRNA was extracted and analysed by real-time RT-PCR. Gene expression of ERα and cyclin D1 (CCND1) (A) or IGF1R (E) in every sample was standardized to 18S rRNA content. N-fold differences of gene expression compared to calibrator (untreated sample) were used to graph final results. Data correspond to mean ± SE of values from at least three separate RNA samples (*$P < .05$ vs calibrator). (B,F) H295R cells were untreated (basal, 0) or treated with sirtinol (40 μmol/L) for 24 h. Total protein extracts were analysed by Western blot analysis for the expression of ERα and CCND1 (B) or IGF1R (F); GAPDH was used to normalize protein expression. Blots are from one experiment representative of three with similar results. (B,F right panels) Graphs correspond to means of standardized optical densities from three experiments, bars correspond to SE (*$P < .05$ vs basal). Results are expressed as % inhibition respect to basal. (C,G) H295R cells were transfected for 72 h in the presence of control siRNA (siRNA scrambled) or siRNA for sirt1 (siRNA sirt1). Total protein extracts were analysed by Western blot analysis for the expression of sirt1, ERα and CCND1 (C) or sirt1 and IGF1R (G); GAPDH was used to normalize protein expression. Blots are from one experiment representative of three with similar results. (C,G right panels) Graphs correspond to means of standardized optical densities from three experiments, bars correspond to SE (*$P < .05$ vs basal). Results are expressed as % of inhibition versus basal. (D) H295R cells were untreated (–) or treated with sirtinol (40 μmol/L) for 24 h. Then, cells were treated with estradiol (E2) (100 nmol/L) for 1 h as indicated. Total protein extracts were analysed by Western blot analysis for the expression of pCREB-1^{Ser133}; GAPDH was used to normalize protein expression. Blots are from one experiment representative of three with similar results. (D, right panel). Graphs correspond to means of standardized optical densities from three experiments, bars correspond to SE (*$P < .05$ vs basal; **$P < .05$ vs E2). Folds induction versus basal or E2 were used to express results

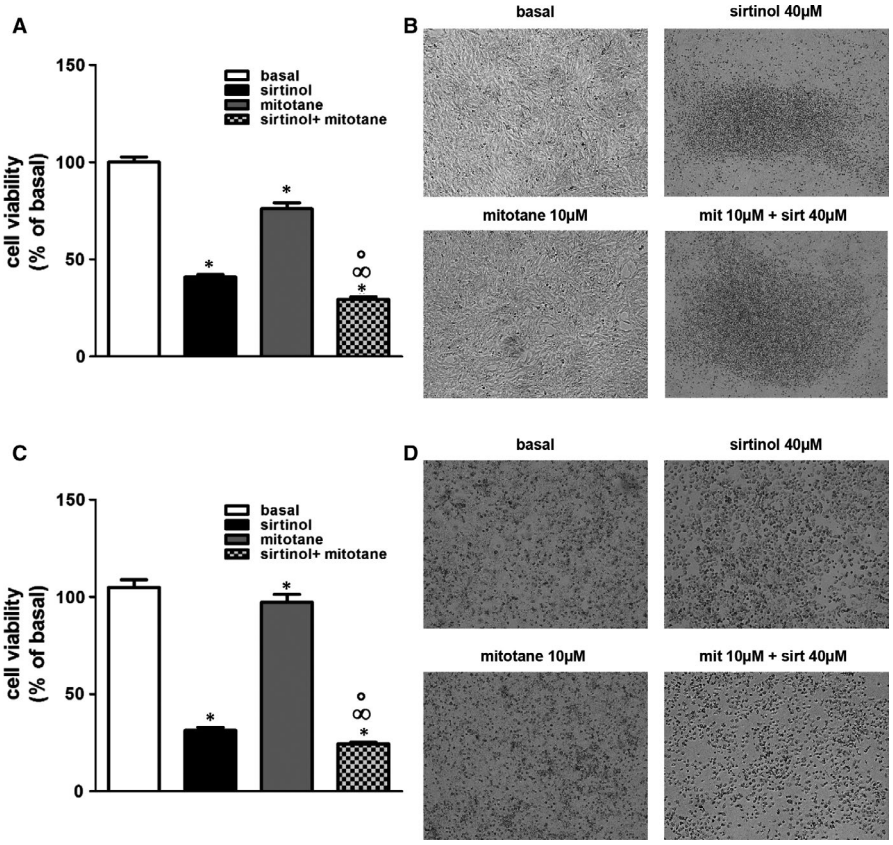

FIGURE 5 Sirtinol and mitotane display synergistic inhibitory effects on adrenocortical cancer cell growth. H295R (A) and SW13 (C) cells were left untreated (basal) or treated with sirtinol (40 μmol/L) and mitotane alone (10 μmol/L) or in combination for 72 h. Cell viability was evaluated by MTT assay (*$P < .05$ vs basal; °$P < .05$ vs sirtinol; ∞$P < .05$ vs mitotane). (B, D) Morphological changes of H295R (B) and SW13 (D) cells after treatments. Cell images were acquired using an Inverted Microscope (magnification X100)

effective in ACC treatment.[58] A recent study indicated that the use of nilotinib, a tyrosine kinase inhibitor, in combination with mitotane inhibited cell viability more significantly then mitotane alone.[59] In another work, addition of mTOR (mammalian target of rapamycin) inhibitor, sirolimus, to low concentrations of mitotane improved the anti-proliferative effects exerted by mitotane alone.[60]

Overall, our study proves that targeting sirt1 is sufficient to reduce activity of two major players in ACC: oestrogens and IGF-II. Additionally, sirtinol ability to synergize with mitotane provides a rationale for further investigating sirtinol effects in vivo on both tumour growth and metastases and opens new perspectives for a different therapeutic approach to targeting this tumour.

5 | CONCLUSIONS

In conclusion, in this study we provide evidences regarding the role of sirt1 as an oncogenic and anti-apoptotic factor in ACC. In particular, we revealed that both sirt1 pharmacological inhibition (sirtinol) and gene silencing reduce proliferation of H295R and SW13 adrenocortical

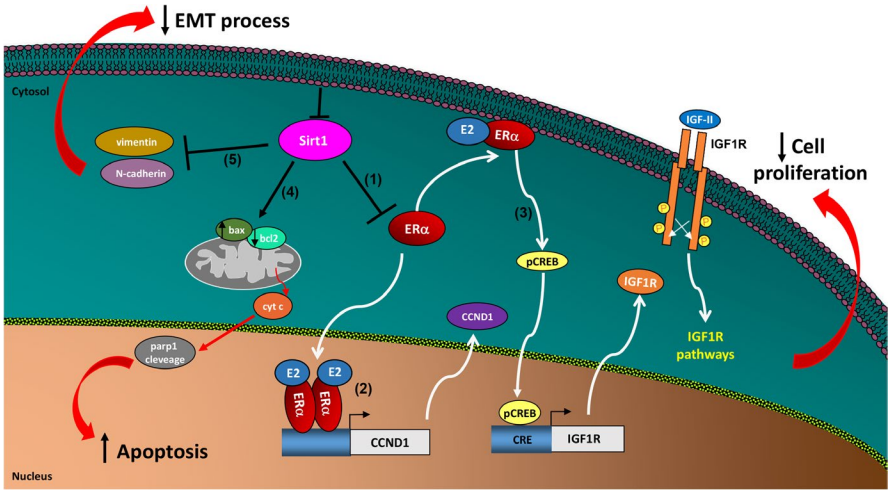

FIGURE 6 Schematic representation of molecular mechanisms induced by sirt1 inhibition in ACC cells. Sirt1 inhibition reduces ERα expression (1). Reduction of ERα genomic action decreases CCND1 expression (2) influencing ACC cell proliferation. Reduction of ERα non-genomic action decreases CREB phosphorylation and consequently IGF1R expression (3) influencing ACC cell proliferation. In addition, sirt1 inhibition causes ACC cell death by activating the intrinsic apoptotic pathway (4). Moreover sirt1 depletion reduces ACC cell motility regulating EMT process (5)

cancer cells by interfering with E2/ERα and IGF1R pathways through the inhibition of several proteins, such as ERα, CCND1 and IGF1R (Figure 6) and activating apoptosis. In addition, we confirmed a role for sirt1 in adrenocortical cancer cell motility and EMT process. The observation that a single drug such as sirtinol is able to block several targets involved in ACC growth and metastasis, together with the discovery that sirtinol can synergize with mitotane in inhibiting tumour growth, opens new perspectives for a different therapeutic approach of ACC. Finally, our results, confirming the oncogenic role of sirt1 in adrenocortical cancer cells, propose it as a useful molecular target against ACC.

ACKNOWLEDGEMENTS

This work was supported by MIUR (Ministero dell'Istruzione, dell'Università e della Ricerca), ex 60%-2018 to Department of Pharmacy and Health and Nutritional Sciences University of Calabria and by AIRC (Associazione Italiana per la Ricerca sul Cancro), projects n. IG20122. ADL was supported by a fellowship from PAC (Progetto Strategico Regionale Calabria Alta Formazione) Calabria 2014/2020—Asse Prioritario 12, Linea B, Azione 10.5.12; PA was supported by a post-doc fellowship 2020 from Fondazione Umberto Veronesi (FUV).

CONFLICT OF INTEREST

The authors declare that they have no conflict of interest.

AUTHOR CONTRIBUTIONS

Adele Chimento: Conceptualization (equal); Data curation (equal); Investigation (equal); Methodology (equal); Validation (equal); Writing-original draft (equal). **Arianna De Luca:** Investigation (equal); Methodology (equal); Validation (equal). **Marta Claudia Nocito:** Investigation (equal); Methodology (equal); Validation (equal). **Sara Sculco:** Investigation (equal); Methodology (equal); Validation (equal). **Paola Avena:** Investigation (equal); Methodology (equal); Validation (equal). **Davide La Padula:** Investigation (equal); Methodology (equal); Validation (equal). **Lucia Zavaglia:** Investigation (equal); Methodology (equal); Validation (equal). **Rosa Sirianni:** Data curation (equal); Investigation (equal); Methodology (equal); Validation (equal). **Ivan Casaburi:** Data curation (equal); Investigation (equal); Methodology (equal); Supervision (equal); Validation (equal). **Vincenzo Pezzi:** Conceptualization (equal); Data curation (equal); Investigation (equal); Methodology (equal); Supervision (equal); Validation (equal); Writing-original draft (equal).

ETHICAL APPROVAL

This article does not contain any studies with human participants or animals performed by any of the authors.

ORCID

Vincenzo Pezzi https://orcid.org/0000-0003-2311-2286

REFERENCES

1. Jouinot A, Bertherat J. Management of endocrine disease Adrenocortical carcinoma: differentiating the good from the poor prognosis tumors. *Eur J Endocrinol*. 2018;178(5):R215-R230.
2. Stigliano A, Cerquetti L, Lardo P, Petrangeli E, Toscano V. New insights and future perspectives in the therapeutic strategy of adrenocortical carcinoma (Review). *Oncol Rep*. 2017;37(3):1301-1311.
3. Barlaskar FM, Hammer GD. The molecular genetics of adrenocortical carcinoma. *Rev Endocr Metab Dis*. 2007;8(4):343-348.
4. Zheng SY, Cherniack AD, Dewal N, et al. Comprehensive pan-genomic characterization of adrenocortical carcinoma. *Cancer Cell*. 2016;29(5):723-736.
5. Vatrano S, Volante M, Duregon E, et al. Detailed genomic characterization identifies high heterogeneity and histotype-specific genomic profiles in adrenocortical carcinomas. *Modern Pathol*. 2018;31(8):1257-1269.
6. Almeida MQ, Fragoso MCBV, Lotfi CFP, et al. Expression of insulin-like growth factor-II and its receptor in pediatric and adult adrenocortical tumors. *J Clin Endocr Metab*. 2008;93(9):3524-3531.
7. Barzon L, Masi G, Pacenti M, et al. Expression of aromatase and estrogen receptors in human adrenocortical tumors. *Virchows Arch*. 2008;452(2):181-191.
8. Sirianni R, Zolea F, Chimento A, et al. Targeting estrogen receptor-alpha reduces adrenocortical cancer (ACC) cell growth in vitro and in vivo: potential therapeutic role of selective estrogen receptor modulators (SERMs) for ACC treatment. *J Clin Endocrinol Metabol*. 2012;97(12):E2238-E2250.

9. Naing A, Kurzrock R, Burger A, et al. Phase I Trial of Cixutumumab Combined with Temsirolimus in Patients with Advanced Cancer. *Clin Cancer Res*. 2011;17(18):6052-6060.
10. Lerario AM, Worden FP, Ramm CA, et al. The Combination of Insulin-Like Growth Factor Receptor 1 (IGF1R) Antibody Cixutumumab and Mitotane as a First-Line Therapy for Patients with Recurrent/Metastatic Adrenocortical Carcinoma: a Multi-institutional NCI-Sponsored Trial (vol 5, pg 232, 2014). *Horm Cancer-Us*. 2014;5(6):424-424.
11. Yao Y, Li HZ, Gu YS, Davidson NE, Zhou Q. Inhibition of SIRT1 deacetylase suppresses estrogen receptor signaling. *Carcinogenesis*. 2010;31(3):382-387.
12. Wang YJ, He J, Liao MY, et al. An overview of Sirtuins as potential therapeutic target: Structure, function and modulators. *Eur J Med Chem*. 2019;161:48-77.
13. Tanno M, Sakamoto J, Miura T, Shimamoto K, Horio Y. Nucleocytoplasmic shuttling of the NAD(+)-dependent histone deacrtylase SIRT1. *J Biol Chem*. 2007;282(9):6823-6832.
14. Rahman S, Islam R. Mammalian Sirt1: insights on its biological functions. *Cell Commun Signal*. 2011;9:11.
15. Liu T, Liu PY, Marshall GM. The critical role of the class III histone deacetylase SIRT1 in cancer. *Cancer Res*. 2009;69(5):1702-1705.
16. Song NY, Surh YJ. Janus-faced role of SIRT1 in tumorigenesis. *Ann N Y Acad Sci*. 2012;1271:10-19.
17. Wu X, Cao N, Fenech M, Wang X. Role of Sirtuins in Maintenance of Genomic Stability: Relevance to Cancer and Healthy Aging. *DNA Cell Biol*. 2016;35(10):542-575.
18. Jin J, Chu Z, Ma P, Meng Y, Yang Y. SIRT1 promotes the proliferation and metastasis of human pancreatic cancer cells. *Tumour Biol*. 2017;39(3):1010428317691180.
19. Portmann S, Fahrner R, Lechleiter A, et al. Antitumor effect of SIRT1 inhibition in human HCC tumor models in vitro and in vivo. *Mol Cancer Ther*. 2013;12(4):499-508.
20. Lovaas JD, Zhu L, Chiao CY, Byles V, Faller DV, Dai Y. SIRT1 enhances matrix metalloproteinase-2 expression and tumor cell invasion in prostate cancer cells. *Prostate*. 2013;73(5):522-530.
21. Chen G, Zhang B, Xu H, et al. Suppression of Sirt1 sensitizes lung cancer cells to WEE1 inhibitor MK-1775-induced DNA damage and apoptosis. *Oncogene*. 2017;36(50):6863-6872.
22. Elangovan S, Ramachandran S, Venkatesan N, et al. SIRT1 is essential for oncogenic signaling by estrogen/estrogen receptor alpha in breast cancer. *Cancer Res*. 2011;71(21):6654-6664.
23. Xia XY, Zhou XM. Knockdown of SIRT1 inhibits proliferation and promotes apoptosis of paclitaxel-resistant human cervical cancer cells. *Cell Mol Biol*. 2018;64(6):36-41.
24. Asaka R, Miyamoto T, Yamada Y, et al. Sirtuin 1 promotes the growth and cisplatin resistance of endometrial carcinoma cells: a novel therapeutic target. *Lab Invest*. 2015;95(12):1363-1373.
25. Mvunta DH, Miyamoto T, Asaka R, et al. SIRT1 Regulates the Chemoresistance and Invasiveness of Ovarian Carcinoma Cells. *Transl Oncol*. 2017;10(4):621-631.
26. Peck B, Chen CY, Ho KK, et al. SIRT Inhibitors Induce Cell Death and p53 Acetylation through Targeting Both SIRT1 and SIRT2. *Mol Cancer Ther*. 2010;9(4):844-855.
27. Ota H, Tokunaga E, Chang K, et al. Sirt1 inhibitor, Sirtinol, induces senescence-like growth arrest with attenuated Ras-MAPK signaling in human cancer cells. *Oncogene*. 2006;25(2):176-185.
28. Jiang YH, Liu JJ, Chen D, Yan LL, Zheng WP. Sirtuin Inhibition: Strategies, Inhibitors, and Therapeutic Potential. *Trends Pharmacol Sci*. 2017;38(5):459-472.
29. Chimento A, Sirianni R, Casaburi I, et al. GPER agonist G-1 decreases adrenocortical carcinoma (ACC) cell growth in vitro and in vivo. *Oncotarget*. 2015;6(22):19190-19203.
30. Wang T, Rainey WE. Human adrenocortical carcinoma cell lines. *Mol Cell Endocrinol*. 2012;351(1):58-65.
31. Chimento A, Casaburi I, Rosano C, et al. Oleuropein and hydroxytyrosol activate GPER/ GPR30-dependent pathways leading to apoptosis of ER-negative SKBR3 breast cancer cells. *Mol Nutr Food Res*. 2014;58(3):478-489.
32. Shaw FL, Harrison H, Spence K, et al. A Detailed Mammosphere Assay Protocol for the Quantification of Breast Stem Cell Activity. *J Mammary Gland Biol*. 2012;17(2):111-117.
33. De Luca A, Fiorillo M, Peiris-Pages M, et al. Mitochondrial biogenesis is required for the anchorage-independent survival and propagation of stem-like cancer cells. *Oncotarget*. 2015;6(17):14777-14795.
34. Sirianni R, Chimento A, Malivindi R, Mazzitelli I, Ando S, Pezzi V. Insulin-like growth factor-I, regulating aromatase expression through steroidogenic factor 1, supports estrogen-dependent tumor Leydig cell proliferation. *Can Res*. 2007;67(17):8368-8377.
35. Liu MM, Albanese C, Anderson CM, et al. Opposing action of estrogen receptors alpha and beta on cyclin D1 gene expression. *J Biol Chem*. 2002;277(27):24353-24360.
36. Wang Y, Chang J, Liu X, et al. Discovery of piperlongumine as a potential novel lead for the development of senolytic agents. *Aging*. 2016;8(11):2915-2926.
37. Bosch-Presegue L, Vaquero A. The dual role of sirtuins in cancer. *Genes Cancer*. 2011;2(6):648-662.
38. Huffman DM, Grizzle WE, Bamman MM, et al. SIRT1 is significantly elevated in mouse and human prostate cancer. *Can Res*. 2007;67(14):6612-6618.
39. Chen XJ, Sun K, Jiao SF, et al. High levels of SIRT1 expression enhance tumorigenesis and associate with a poor prognosis of colorectal carcinoma patients. *Scientific Rep*. 2014;4:7481.
40. Ford J, Jiang M, Milner J. Cancer-specific functions of SIRT1 enable human epithelial cancer cell growth and survival. *Can Res*. 2005;65(22):10457-10463.
41. Nihal M, Ahmad N, Wood GS. SIRT1 is upregulated in cutaneous T-cell lymphoma, and its inhibition induces growth arrest and apoptosis. *Cell Cycle*. 2014;13(4):632-640.
42. Wang J, Kim TH, Ahn MY, et al. Sirtinol, a class III HDAC inhibitor, induces apoptotic and autophagic cell death in MCF-7 human breast cancer cells. *Int J Oncol*. 2012;41(3):1101-1109.
43. Kuo SJ, Lin HY, Chien SY, Chen DR. SIRT1 suppresses breast cancer growth through downregulation of the Bcl-2 protein. *Oncol Rep*. 2013;30(1):125-130.
44. Voulgari A, Pintzas A. Epithelial-mesenchymal transition in cancer metastasis: Mechanisms, markers and strategies to overcome drug resistance in the clinic. *Bba-Rev Cancer*. 2009;1796(2):75-90.
45. Jin MS, Hyun CL, Park IA, et al. SIRT1 induces tumor invasion by targeting epithelial mesenchymal transition-related pathway and is a prognostic marker in triple negative breast cancer. *Tumor Biol*. 2016;37(4):4743-4753.
46. Chung SY, Jung YY, Park IA, et al. Oncogenic role of SIRT1 associated with tumor invasion, lymph node metastasis, and poor disease-free survival in triple negative breast cancer. *Clin Exp Metastas*. 2016;33(2):179-185.
47. Hao C, Zhu PX, Yang X, et al. Overexpression of SIRT1 promotes metastasis through epithelial-mesenchymal transition in hepatocellular carcinoma. *BMC Cancer*. 2014;14:978.
48. Byles V, Zhu L, Lovaas JD, et al. SIRT1 induces EMT by cooperating with EMT transcription factors and enhances prostate cancer cell migration and metastasis. *Oncogene*. 2012;31(43):4619-4629.
49. Chen IC, Chiang WF, Huang HH, Chen PF, Shen YY, Chiang HC. Role of SIRT1 in regulation of epithelial-to-mesenchymal transition in oral squamous cell carcinoma metastasis. *Mol Cancer*. 2014;13:254.
50. Sarria AJ, Lieber JG, Nordeen SK, Evans RM. The presence or absence of a vimentin-type intermediate filament network affects the shape of the nucleus in human SW-13 cells. *J Cell Sci*. 1994;107(Pt 6):1593-1607.
51. Butler R, Robertson J, Gallo JM. Mutually exclusive expression of beta(III)-tubulin and vimentin in adrenal cortex carcinoma SW13 cells. *Febs Lett*. 2000;470(2):198-202.

52. Liu YJ, Chang YJ, Kuo YT, Liang PH. Targeting beta-tubulin/CCT-beta complex induces apoptosis and suppresses migration and invasion of highly metastatic lung adenocarcinoma. *Carcinogenesis*. 2020;41(5):699-710.
53. Kanojia D, Morshed RA, Zhang L, et al. betaIII-Tubulin Regulates Breast Cancer Metastases to the Brain. *Mol Cancer Ther*. 2015;14(5):1152-1161.
54. Lu W, Kang Y. Epithelial-Mesenchymal Plasticity in Cancer Progression and Metastasis. *Dev Cell*. 2019;49(3):361-374.
55. Mani SA, Guo W, Liao MJ, et al. The epithelial-mesenchymal transition generates cells with properties of stem cells. *Cell*. 2008;133(4):704-715.
56. Karnoub AE, Dash AB, Vo AP, et al. Mesenchymal stem cells within tumour stroma promote breast cancer metastasis. *Nature*. 2007;449(7162):557-U4.
57. Sabbah M, Courilleau D, Mester J, Redeuilh G. Estrogen induction of the cyclin D1 promoter: involvement of a cAMP response-like element. *Proc Natl Acad Sci U S A*. 1999;96(20):11217-11222.
58. Fassnacht M, Dekkers OM, Else T, et al. European Society of Endocrinology Clinical Practice Guidelines on the management of adrenocortical carcinoma in adults, in collaboration with the European Network for the Study of Adrenal Tumors. *Eur J Endocrinol*. 2018;179(4):G1-G46.
59. Silveira E, Cavalcante IP, Kremer JL, de Mendonca POR, Lotfi CFP. The tyrosine kinase inhibitor nilotinib is more efficient than mitotane in decreasing cell viability in spheroids prepared from adrenocortical carcinoma cells. *Cancer Cell Int*. 2018;18:29.
60. De Martino MC, van Koetsveld PM, Feelders RA, et al. Effects of combination treatment with sirolimus and mitotane on growth of human adrenocortical carcinoma cells. *Endocrine*. 2016;52(3):664-667.

SUPPORTING INFORMATION

Additional supporting information may be found online in the Supporting Information section.

How to cite this article: Chimento A, De Luca A, Nocito MC, et al. SIRT1 is involved in adrenocortical cancer growth and motility. *J Cell Mol Med*. 2021;25:3856–3869. https://doi.org/10.1111/jcmm.16317

biomedicines

MDPI

Review

Antitumoral Activities of Curcumin and Recent Advances to ImProve Its Oral Bioavailability

Marta Claudia Nocito †, Arianna De Luca †, Francesca Prestia, Paola Avena, Davide La Padula, Lucia Zavaglia, Rosa Sirianni, Ivan Casaburi, Francesco Puoci, Adele Chimento *,‡ and Vincenzo Pezzi *,‡

Department of Pharmacy and Health and Nutritional Sciences, University of Calabria, Via Pietro Bucci, Arcavacata di Rende, 87036 Cosenza, Italy; nocitomarta90@tiscali.it (M.C.N.); ariannadl@hotmail.it (A.D.L.); francescaprestia908@gmail.com (F.P.); paola.avena@unical.it (P.A.); davidelapadula@live.it (D.L.P.); luciazavaglia@hotmail.it (L.Z.); rosa.sirianni@unical.it (R.S.); ivan.casaburi@unical.it (I.C.); francesco.puoci@unical.it (F.P.)

* Correspondence: adele.chimento@unical.it (A.C.); v.pezzi@unical.it (V.P.); Tel.: +39-0984-493184 (A.C.); +39-0984-493148 (V.P.)

† These authors contributed equally to this work.

‡ These authors shared senior authorship.

Abstract: Curcumin, a main bioactive component of the *Curcuma longa* L. rhizome, is a phenolic compound that exerts a wide range of beneficial effects, acting as an antimicrobial, antioxidant, anti-inflammatory and anticancer agent. This review summarizes recent data on curcumin's ability to interfere with the multiple cell signaling pathways involved in cell cycle regulation, apoptosis and the migration of several cancer cell types. However, although curcumin displays anticancer potential, its clinical application is limited by its low absorption, rapid metabolism and poor bioavailability. To overcome these limitations, several curcumin-based derivatives/analogues and different drug delivery approaches have been developed. Here, we also report the anticancer mechanisms and pharmacokinetic characteristics of some derivatives/analogues and the delivery systems used. These strategies, although encouraging, require additional in vivo studies to support curcumin clinical applications.

Keywords: curcumin; cancer cells; bioavailability; curcumin derivatives; curcumin analogues; curcumin delivery systems

Citation: Nocito, M.C.; De Luca, A.; Prestia, F.; Avena, P.; La Padula, D.; Zavaglia, L.; Sirianni, R.; Casaburi, I.; Puoci, F.; Chimento, A.; et al. Antitumoral Activities of Curcumin and Recent Advances to ImProve Its Oral Bioavailability. *Biomedicines* **2021**, *9*, 1476. https://doi.org/10.3390/biomedicines9101476

Academic Editor: Pavel B. Drašar

Received: 22 September 2021
Accepted: 7 October 2021
Published: 14 October 2021

1. Introduction

Curcuma is one of the largest genera in the Zingiberaceae family which comprises approximately 133 species [1]. It is widely distributed in the tropical regions spanning India to Southern China and Northern Australia [1]. The species of greatest interest is *Curcuma longa* L., which is cultivated particularly in India. It consists of an underground root (rhizome) from which, once dried and ground, a powder with a characteristic yellow-orange color is obtained. Curcumin extract is composed of three curcuminoids at different proportions such as curcumin (1, 7-bis (hydroxyl-3-methoxyphenyl)-1,6-heptadiene-3, 5-dione) (curcumin I) (~77%), demethoxy curcumin (curcumin II) (17–18%) and bis-demethoxycurcumin (curcumin III) (3–5%) (Figure 1) [2]. The volatile fraction is quantitatively important, which mainly contains several terpenic compounds including α-zingiberene, curlone and α-turmerone [3]. Among the curcuminoids, the polyphenol curcumin is the most active. It possesses a wide range of pharmacological proprieties [4,5], acting as an antimicrobial [6], antiviral [7], antifungal [8], antioxidant [9], antimalarial [10], anti-inflammatory [11], antiaging [12] and antitumoral [13] agent. In recent years, extensive research indicated that this polyphenol can prevent and suppress tumor initiation, promotion and progression and can be used to treat cancer by interfering with several signaling pathways [13,14]. At a molecular level, curcumin's anticarcinogenic effects are attributed

to its ability to modulate transcription factors, growth regulators, adhesion molecules, apoptotic genes, angiogenesis regulators, and more [14]. In vitro studies demonstrated that curcumin suppresses the proliferation of a wide variety of tumor cells; downregulates the expression of transcription factors (NF-kB, AP-1 and Egr-1), COX2, MMPs, TNF, chemokines, cell surface adhesion molecules and cyclins, growth factor receptors (such as EGFR and HER2); and inhibits tyrosine and serine/threonine kinases (i.e., JNK) activity [14]. By inhibiting STAT3, NF-kB and WNT/β-catenin signaling pathways, curcumin interferes with cancer development and progression [15–17]. In addition, the inhibition of Sp-1 and its regulated genes may serve as an important mechanism to prevent cancer formation, migration, and invasion [14]. Additionally, curcumin induces apoptosis through both mitochondria-dependent [18] as well as mitochondria-independent mechanisms [19], depending on the cell type.

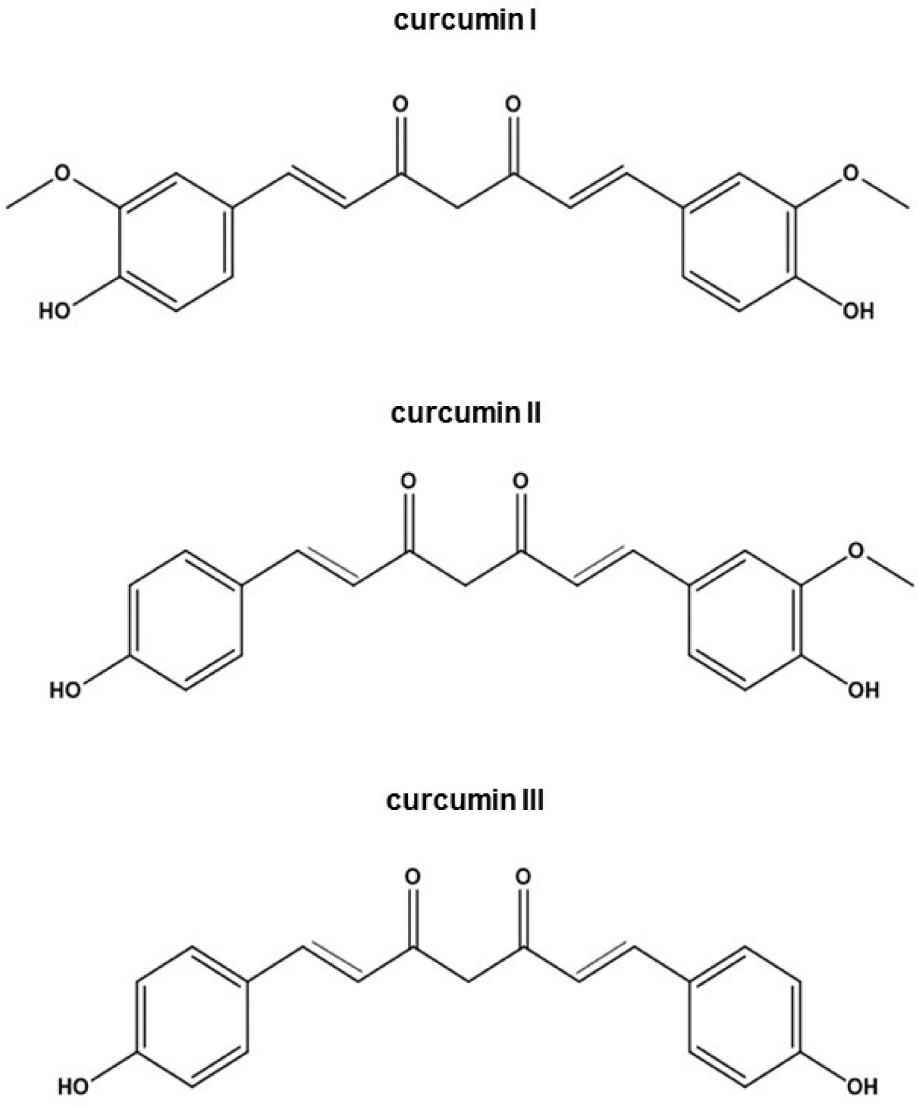

Figure 1. Chemical structures of curcumin I, II, III.

Despite curcumin's anticancer potential, its therapeutic application is limited by its poor bioavailability, due to the low or very low absorption after oral intake. After oral administration, curcumin is metabolized into curcumin glucuronide and curcumin sulfonate by the liver during phase II reactions. Glucuronidation and sulfation increase curcumin's water solubility, but decrease its effectiveness and accelerate its removal via urine [20]. Specifically, the different factors contributing to the low bioavailability include

the low plasma level, tissue distribution, poor absorption, high rate of metabolism, inactivity of metabolic products, rapid elimination and clearance from the body [21]. In order to improve curcumin pharmacokinetic characteristics and then biological activity, synthetic derivatives/analogues [22–24] and various drug delivery strategies have been developed [25–30].

In this review, we summarize the recent advances in molecular mechanisms activated by curcumin and the elicited inhibition of cancer cell growth and progression. Additionally, the improved pharmacokinetic proprieties of curcumin derivatives/analogues, and the attempted targeted and triggered drug delivery systems, are reviewed.

2. Antitumoral Activities of Curcumin

Dietary polyphenolic phytochemicals are able to block tumor initiation or progression [31]. Several studies indicated that curcumin can effectively prevent and treat cancer at the initiation, promotion and progression level [32]. This propriety is due to its ability to target critical processes primarily involved in cancer development, such as proliferation, apoptosis and metastasis.

2.1. Antiproliferative Effects of Curcumin

Some molecular alterations associated with carcinogenesis occur in signaling pathways regulating cell proliferation [31]. Accumulating data show that curcumin displays in vitro antiproliferative effects on several types of cancer such as breast, colorectal, bladder, brain and gastrointestinal through several mechanisms of action [33] (see Table 1 for a summary of the data). Generally, the antiproliferative effects of curcumin could be attributed to its ability to regulate cell cycle progression, protein kinases activity and transcription factor expression.

In breast cancer cell lines, curcumin inhibits proliferation by reducing cyclin D1 expression at mRNA and protein levels, consequently decreasing CDK4 activity [34,35]. In MCF-7 breast cancer cells, curcumin caused G1 cell cycle arrest, cyclin E proteosomal degradation, p53 upregulation and an increase in p21 and p27 CDK inhibitor levels [36]. In MCF-7 and MDA-MB-231 breast cancer cells, a G2/M cell cycle arrest by curcumin was also reported. Specifically, following GSK3β upregulation, a loss of nuclear β-catenin produced a downregulation of its downstream target, cyclin D1 [37]. Additionally, curcumin is a potent inhibitor of NF-kB [16], a critical regulator of cell proliferation and survival [38]. Liu et al. demonstrated that in MCF-7 cells, curcumin markedly decreased cell proliferation in a concentration- and time-dependent manner by regulating the NF-kB signaling, as shown by a decrease in p65 and an increase in IκB protein expression [16]. Moreover, Zhou et al. demonstrated that, in MCF-7 cells and MCF-7 xenografts, a combination of curcumin with the chemotherapeutic agent mitomycin C produced cell cycle arrest at the G1 phase as a consequence of decreased cyclin D1, cyclin E, cyclin A, CDK2, and CDK4 expression, along with the induction of the cell cycle inhibitor p21 and p27 [35]. The potent inhibitory effect produced by curcumin and mitomycin C combination on MCF-7 growth was also observed in MCF-7- and MDA-MB-231-derived cancer stem cells [39]. In addition, curcumin was proven to be effective to sensitize MDA-MB-231 and MCF-7 cells to commonly used chemotherapeutic agents paclitaxel, cisplatin and doxorubicin [39]. In a recent work, it has been shown that curcumin inhibited the growth of MDA-MB-231 and MDA-MB-468 triple-negative breast cancer cells by reducing the expression of histone methyl transferase EZH2 and reactivating that of DLC1 [40]. EZH2 is an oncogenic factor commonly upregulated in human cancers [41], while DLC1 is a downregulated tumor suppressor in many malignant tumors [42].

In vitro studies showed that curcumin significantly inhibited colon cancer cell growth modulating multiple molecular targets and distinct signaling pathways [43,44]. A study performed by Lim et al. demonstrated that in a HCT-116 human colon cancer cell line, curcumin downregulated CDK2 expression, causing G1 phase arrest [45]. Moreover, in the same cell line, curcumin enhanced ROS generation and downregulated the transcription

factor E2F4 and its target genes, including cyclin A, p21 and p27 [46]. Another study by Watson et al. investigated curcumin cytotoxicity in HCT-116 and HT29 cell lines, showing a time- and dose-dependent cell proliferation inhibition when p53 was upregulated [47]. Curcumin prevented cell proliferation by cell cycle arrest at the G2/M phase in both HCT116 p53+/+ and p53−/− cells in a concentration-dependent manner and induced senescence accompanied by autophagy [48]. Recently, Calibasi-Kocal et al. demonstrated antiproliferative, wound healing, anti-invasive and antimigratory effects of curcumin not only on HCT-116 cells, but also on the LoVo metastatic colorectal cancer cell line, confirming its anticancer activity [44].

The antitumoral effects of curcumin were also demonstrated in bladder cancer cells. Curcumin's inhibitory effects were observed in T24 [49,50], 5637 [50] and in RT4 [49] human bladder cancer cell lines. In T24 and RT4 cells, a decrease in Trop2, a cell surface receptor that transduces via calcium signals, is required for curcumin-mediated effects including inhibition of cell proliferation and migration, apoptosis and cell cycle arrest. A Trop2 decrease caused a reduction in the expression levels of its downstream target cyclin E1, and an increase in p27 levels [49].

Curcumin has been shown to decrease malignant characteristics of glioblastoma cells acting on several targets, including growth factor receptors, kinases, transcriptional factors and inflammatory cytokines [51]. In the U87 human glioma cell line, curcumin inhibited proliferation-suppressing cyclin D1 and induced p21 expression. In these cells, curcumin via ERK and JNK signaling induced expression of the transcription factor Egr-1 which, in turn, increased p21 gene expression [52]. In the same cells, curcumin induced G2/M cell cycle arrest and apoptosis by increasing FoxO1 expression [53]. In U251 and SNB19 human glioblastoma cells curcumin reduced the expression of Skp2 and upregulated p57 [54]. Skp2, a component of the ubiquitin proteasome system, is responsible for ubiquitin-mediated degradation of the cell cycle inhibitors p21, p27 and p57 [55]. Recently, Luo et al. demonstrated that curcumin decreased proliferation of U251 and LN229 human glioblastoma cells via inhibition of HDGF [56], an angiogenesis-promoting growth factor commonly upregulated in gliomas. In human glioma cell lines U251 and LN229, HDGF forms a complex with β-catenin promoting tumor growth and metastasis. Curcumin significantly reduced HDGF expression, and consequently its binding to β-catenin [56]. Moreover, several studies provided evidence that curcumin potentiated the effects of chemotherapy and radiation therapy while protecting normal tissue, selectively inducing cell death in glioblastoma cancer cells [57,58].

In gastrointestinal cancer cell lines, curcumin inhibited ODC and increased SMOX activity, two key enzymes in polyamine synthesis and catabolism, respectively. Importantly, elevated levels of polyamines have been associated with several cancers, and altered levels of the rate limiting enzymes in both biosynthesis and catabolism have been observed. The combination of curcumin with ODC inhibitor DFMO significantly potentiated ODC inhibition decreasing AGS gastric adenocarcinoma cell growth [59]. Evidence regarding curcumin's potential in gastric cancer prevention has been accumulating. Curcumin induced cell-cycle arrest at the G1 phase by downregulating cyclin D1 expression in BGC823, SGC7901, MKN1 and MGC803 gastric cancer cells by inhibiting EGF/PAK1/NF-kB pathway [60]. Moreover, curcumin exerted antiproliferative effects by inhibiting the Wnt/β-catenin signaling pathway. In SNU1, SNU-5 and AGS human gastric cancer cells, curcumin caused a reduction in Wnt3a, LRP6, phospho-LRP6, β-catenin, phospho-β-catenin, c-Myc and survivin [61]. The antiproliferative effects of curcumin were also demonstrated in SGC-7901 and BGC-823 gastric cancer cells by activating p53/p21 and inhibiting PI3K signaling pathways [62]. In another work, SGC7901 gastric cancer cell proliferation was reduced after curcumin treatment via c-Myc/long non-coding RNA (lncRNA) H19 downregulation and p53 upregulation [63]. Studies reported that H19, an oncogenic lncRNA [64], is abnormally upregulated in gastric cancer and contributes to cellular proliferation by directly inactivating p53 [65]. Furthermore, the oncogene c-Myc was shown to directly induce H19 expression by binding to the H19 promoter, and

thereby promoting proliferation of gastric cancer cells [66]. A recent investigation defined curcumin effects on microRNAs expression related to gastric cancer cell proliferation [67]. In SGC-7901 cells, curcumin inhibited cell cycle progression and induced apoptosis by upregulating miR-34a, which decreased CDK4 and cyclin D1 protein expression. The same effects were obtained by transfecting the cells with specific miR-34a agomir [67]. In BGC-823 and SGC7901 gastric cancer cells, curcumin inhibited cell proliferation and increased cell death by upregulating miR-33b which, in turn, decreased expression of the apoptosis inhibitor XIAP by targeting its 3′ UTR [68].

Mounting evidence indicates that curcumin affects several molecular pathways involved in melanoma pathogenesis, making it a promising therapeutic agent to be used against this type of cancer [69]. This phytochemical compound was able to arrest cell cycle at the G2/M phase by inhibiting NF-kB and iNOS activity in human melanoma A375 and MeWo cells [70]. Another study postulated that curcumin's effect on cell cycle arrest at the G2/M phase was dependent on PDE inhibition, an enzyme that catalyzed cAMP and/or cGMP hydrolysis. Specifically, curcumin decreased cell proliferation and cell cycle progression by inhibiting PDE1A, cyclin A, UHRF1 and DNMT1 expression while increasing that of p21 and p27 in B16F10 murine melanoma cells [71]. Another report showed that curcumin caused cell cycle arrest at the G2/M phase, and induced autophagy by downregulating Akt/mTOR axis in human melanoma A375 and C8161 cell lines [72]. Curcumin antiproliferative effects were also observed in other three melanoma cell lines (C32, G-361, and WM 266-4), all of which are characterized by B-Raf mutations. In these cells, curcumin antitumor effects were associated with the suppression of NF-kB and IKK activity but were independent from the inhibition of B-Raf/MEK/ERK and Akt pathways [73].

2.2. Pro-Apoptotic Effects of Curcumin

In addition to antiproliferative properties, curcumin shows extensive therapeutic potential as an apoptotic inducer through several mechanisms demonstrated in different cancer cell models (see Table 1 for a summary of the data). In MCF-7 breast cancer cells, a sub-cytotoxic dose of curcumin induced apoptotic cell death through an increase in histone H3 acetylation and glutathionylation which, in turn, promoted the transcriptional activation of different proapoptotic genes [74]. Several reports indicated that, in breast cancer cells, curcumin induced apoptosis via p53-dependent and -independent pathways [75,76]. Patel et al. demonstrated that, in MCF-7 cells, curcumin enhanced p53 expression and activated Parp-1-mediated apoptotic pathways [77]. The p53-independent effects of curcumin were observed in cancer cells lacking a functional p53 protein such as MDA-MB-231. In these cells, curcumin induced ROS generation which altered mitochondrial membrane permeability, reduced intracellular GSH levels, increased Bax/Bcl-2 ratio and cleaved-caspase 3 expression [78]. In MDA-MB-231 cells, curcumin inhibited NF-kB p65, triggering apoptosis [79]. Moreover, in the same cell line, curcumin was able to mediate apoptotic cell death through FAS inhibition [80].

The apoptotic effects of curcumin were evident in melanoma. In A375 cells, curcumin promoted tumor cell apoptosis by inhibiting the JAK-2/STAT-3 signaling pathway and downregulating Bcl-2 [81]. Moreover, the ability of curcumin to induce apoptosis was demonstrated in four human melanoma cell lines (PMWK, Sk-mel-2, Sk-mel-28, and Mewo) with mutant p53 through the activation of FAS/caspase 8 pathway [82]. Curcumin-dependent apoptosis was also observed in HEY ovarian cancer cells where p53 knockdown or p53 inhibition did not prevent curcumin's inhibitory effect. In these cells, apoptosis occurred through the activation of p38 MAPK, the inhibition of pro-survival Akt signaling, along with a decreased expression of Bcl-2 and survivin [83]. Additionally, in the multiple myeloma RPMI 8226 cell line, curcumin upregulated p53 and Bax protein levels and downregulated MDM2, a known p53 inhibitor [84].

In colorectal cancer cells, curcumin triggered the apoptotic process via the subsequent modulation of various target molecules [43]. In HT-29 colon cancer cells, curcumin-induced

apoptosis was related to a decreased COX2 expression and AKT phosphorylation along with an increased activation of AMPK signaling [85]. Moreover, this polyphenol promoted apoptosis in HCT116, HT29, and SW620 colorectal cancer cell lines by suppressing constitutive and inducible NF-kB activity and NF-kB-regulated gene products such as Bcl-2, Bcl-xL, IAP-2, COX2 and cyclin D1 [86]. Additionally, Narayan et al. showed that curcumin inhibited the Wnt/β-catenin pathway by inducing the caspase 3-mediated cleavage of beta-catenin, E-cadherin and APC, leading to loss of cell–cell adhesion and apoptosis in HCT-116 colon cancer cells [87]. It has been reported that curcumin can activate extrinsic apoptotic pathway, upregulating DR5 protein in HCT-116 and HT-29 colon cancer cells [88]. Furthermore, curcumin triggered Fas-mediated caspase 8 activation in HT-29 cells [89]. In these cells, treatment with curcumin caused a mithocondrial [Ca^{2+}] increase, cytochrome c release from mitochondria to cytosol, mithocondrial membrane potential reduction, Bax increase and Bcl-2 as well as caspase 3 and 7 activation [89]. Curcumin-induced Bcl-2 downregulation and Bax upregulation in both HCT-116 [90] and COLO-205 colon cancer cells [91].

Caspase 3/7 activity was investigated by Shi et al. in bladder cancer cells. The authors demonstrated the ability of curcumin to induce apoptosis through a caspase-dependent mechanism in two human urinary bladder carcinoma cells [50]. The same apoptotic mechanism was also observed in other cancer types such as glioblastoma [92]. A similar feature also occurs in human osteosarcoma (HOS) cells, where curcumin caused cell cycle arrest determining apoptosis, as demonstrated by caspase 3 and PARP-1 cleavage [93]. Recently, it was observed that curcumin inhibited ODC activity and polyamine biosynthesis in AGS gastric adenocarcinoma cells. In this type of cell, curcumin caused an increase in ROS levels responsible for DNA damage and, thus, apoptosis [59].

The pro-apoptotic effects of curcumin are also mediated by the modulation of miRNAs in several cancer cells. Curcumin reduced Bcl-2 expression by upregulating miR-15a and miR-16 in MCF-7 cells [94] and promoted apoptosis through the miR-186 signaling pathway in human lung adenocarcinoma cells [95]. Recently, in RT4 schwannoma cells, Sohn et al. demonstrated that curcumin enhanced the expression of apoptotic protein Bax and decreased Bcl-2, as well as determined caspase 3/9 activation. All of these events were related to curcumin-mediated miRNA 344a-3p upregulation [96].

2.3. Antimetastatic Effects of Curcumin

In addition to the antiproliferative and apoptotic effects, curcumin acts as an antimetastatic agent (see Table 1 for a summary of the data) [15,44]. The metastatic cascade starts with the loss of cell-to-cell and cell-to-substrate adhesion, a feature of the EMT process, which allows the acquisition of a mobile phenotype, the dissociation of cells from primary tumor and the spread to distant tissues and organs [97].

The effects of curcumin on genes involved in EMT was evaluated in breast cancer cells. It was demonstrated that curcumin decreased the gene transcription and protein expression of Axl, Slug, CD24 and RhoA, which regulate EMT and, consequently, migration and invasion of MCF-10F and MDA-MB-231 breast cancer cells. Curcumin elicited these effects through the upregulation of miR-34a, which acts as a tumor suppressor gene in both cell lines [98]. The antimetastatic effects of curcumin occur through the modulation of several signaling pathways, including NF-kB. NF-kB/p65 transcriptionally regulates TWIST1, SLUG and SIP1 which, in turn, repress E-cadherin while activating the mesenchymal markers N-cadherin and MMP11, resulting in EMT progression [99]. In MCF-7 cells, curcumin was able to inhibit uPA production by preventing NF-kB activation [100]. Through the same mechanism, curcumin downregulated CXCL1 and 2, two inflammatory cytokines involved in MDA-MB-231 breast cancer cells migration [101]. A critical event in tumor cell invasion and metastasis is the degradation of the extracellular matrix by MMPs, enzymes that degrade a range of extracellular matrix proteins, allowing cancer cells to migrate and invade [102]. Curcumin was able to inhibit LPA-activated invasion by attenuating the RhoA/ROCK/MMPs pathway in MCF-7 cells [103]. Similarly, in SO-Rb50 and Y79 human

retinoblastoma cell lines, curcumin reduced migration and invasion by decreasing MMP2, RhoA, ROCK1 and vimentin expression. The authors provided evidence that, in these cells, curcumin's antitumor activity requires miR-99a upregulation and JAK/STAT3 pathway inhibition [104]. MMP's decrease after curcumin treatment was also observed in T24 and 5637 human bladder cancer cell lines [50]. Additionally, in T24 and RT4 bladder cancer cells, curcumin's antimetastatic mechanism included a Trop2 decrease [49], a gene also involved in tumor aggressiveness and metastasis formation [105]. In prostate cancer cells, curcumin treatment suppressed EGF, heregulin-stimulated PC-3 and androgen-induced LNCaP cell invasion. Particularly, curcumin significantly reduced MMP9 activity and downregulated cellular matriptase, a membrane-anchored serine protease involved in tumor formation and invasion [106]. Recently, in an HCT-116 human colorectal carcinoma cell line, it has been demonstrated that the expression of proteins related to cell migration, including MMP9 and claudin-3, was downregulated by increasing doses of curcumin [107]. These data were confirmed by an independent group using the same cell line in addition to LoVo human metastatic colon cancer cells, establishing curcumin anti-invasive and antimigratory properties [44]. Furthermore, in human melanoma A375 cells, curcumin decreased MMP2 and MMP9 expression while increasing TIMP-2, a tissue inhibitor of metalloproteinases [81]. Activation of melanoma cell migration and invasion by OPN was also counteracted by curcumin. Specifically, curcumin was able to downregulate pro-MMP2 activation by preventing OPN-mediated NF-kB nuclear translocation [108]. The ability of curcumin to interfere with NFk-B pathway was also evident in Hela cervical cancer cells, where it was also demonstrated an effect on Wnt/β-catenin signaling, two pathways involved in proliferation and invasion of cervical cancer [17]. It has been shown that STAT3 activation is associated with metastasis formation in several tumors [109]. In SCLC cells curcumin inhibited cell migration, invasion and angiogenesis by inhibiting JAK/STAT3 signaling activated in response to IL-6. As a consequence, curcumin downregulated the expression of ICAM, VEGF, MMP2 and MMP7 STAT3-regulated genes involved in tumor invasion [110]. Curcumin inhibited the JAK/STAT3 signaling pathway also in SKOV3 human ovarian cancer cells, causing a decrease in fascin, an actin-binding protein involved in cell adhesion, migration, and invasion [15]. Curcumin is able to prevent invasion by inhibiting AKT, mTOR and P70S6K phosphorylation, as demonstrated in human melanoma A375 and C8161 cells [72] and TC1889 human thymic carcinoma cells [111]. Additionally, it has been demonstrated that curcumin reduced cell invasion and migration in NSCLC A549 cells by increasing miR-206, which further suppressed PI3K/AKT/mTOR pathway activation [112]. The observation that curcumin inhibited NEDD4-mediated signaling in SNB19 and A1207 glioma cells, thus interfering with cell motility, is very interesting [113]. NEDD4 is a E3-ubiquitin ligase involved in the degradation of CNrasGEFs, guanine nucleotide exchange factors (GEFs), that serve as RAS activators, thus, promoting glioma cell migration and invasion [114].

Table 1. Antitumoral activities of curcumin.

Biological Effects	Mechanisms of Action	Cancer Type	References
Antiproliferative			
	CDK2 decrease	Breast	[35]
	CDK4 decrease		[34,35]
	Cell cycle arrest at G1 phase		[16,35,36]
	Cell cycle arrest at G2/M phase		[37]
	Cell viability decrease		[39]
	Cyclin A decrease		[35]
	Cyclin D1 decrease		[34,35,37]
	Cyclin E decrease		[35,36]
	DLC1 increase		[40]
	EZH2 decrease		[40]
	GSK3β increase		[37]
	Increased sensibility to chemotherapeutic agents		[39]
	IκB increase		[16]

Table 1. *Cont.*

Biological Effects	Mechanisms of Action	Cancer Type	References
Antiproliferative			
	NF-kB p65 decrease		[16]
	p21 and p27 increase		[35,36]
	p53 increase		[36]
	β-catenin decrease		[37]
	CDK2 decrease	Colon	[45]
	Cell cycle arrest at G1 phase		[45]
	Cell cycle arrest at G2/M phase		[47,48]
	Cell viability decrease		[44]
	Cyclin A decrease		[46]
	E2F4, decrease		[46]
	p21 and p27 increase		[46]
	p53 increase		[47]
	ROS increase		[46]
	Cell cycle arrest at G2/M phase	Bladder	[49]
	Cell viability decrease		[49,50]
	Cyclin E1 decrease		[49]
	p27 increase		[49]
	Trop2 decrease		[49]
	Cell cycle arrest at G2/M phase	Glioma	[53]
	Cyclin D1 decrease		[52]
	Egr-1 increase		[52]
	FoxO1 increase		[53]
	p21 increase		[52]
	Cell cycle arrest at G2/M phase	Glioblastoma	[54]
	HDGF / β-catenin complex inhibition		[56]
	p57 increase		[54]
	Skp2 decrease		[54]
	CDK4 decrease	Gastric	[67]
	Cell cycle arrest at G1 phase		[60]
	Cell cycle arrest at G0/G1-S phase		[67]
	c-myc decrease		[61]
	c-myc/(lncRNA) H19 pathway downregulation		[63]
	Cyclin D1 decrease		[67]
	EGF/PAK1/NF-kB/cyclin D1 pathway inhibition		[60]
	LRP6 ans phospho-LRP6 decrease		[61]
	miR-33b increase		[68]
	miR-34a increase		[67]
	ODC activity decrease		[59]
	p21 increase		[62]
	p53 increase		[62,63]
	PI3K signaling inhibition		[62]
	SMOX mRNA and activity increase		[59]
	Wnt3a decrease		[61]
	XIAP decrease		[68]
	β-catenin and phospho β-catenin decrease		[61]
	Akt/mTOR pathway downregulation	Melanoma	[72]
	Cell cycle arrest at G2/M phase		[70–72]
	Cyclin A decrease		[71]
	DNMT1 decrease		[71]
	IKK inhibition		[73]
	iNOS inhibition		[70]
	NF-kB inhibition		[70,73]
	p21 and p27 increase		[71]
	PDE decrease		[71]
	UHRF1 decrease		[71]

Table 1. *Cont.*

Biological Effects	Mechanisms of Action	Cancer Type	References
Pro-apoptotic			
	Bad increase	Breast	[77]
	Bax increase		[79]
	Bax/Bcl-2 ratio increase		[78]
	Bcl-2 decrease		[79,94]
	Cleaved caspase 3 increase		[78]
	Cleaved Parp-1 increase		[77]
	FAS inhibition		[80]
	GSH decrease		[78]
	Histone H3 acetylation and glutathionylation increase		[74]
	miR-15a and miR-16 increase		[94]
	NF-kBp65 decrease		[79]
	p53 increase		[77]
	ROS increase		[78]
	Bcl-2 decrease	Melanoma	[81]
	JAK-2/STAT-3 signaling inhibition		[81]
	p53-independent Fas/caspase 8 pathway activation		[82]
	Akt signaling inhibition	Ovarian	[83]
	Bcl-2 and survivin decrease		[83]
	p38 MAPK activation		[83]
	Bax and p53 increase	Myeloma	[84]
	MDM2 decrease		[84]
	AMPK increase	Colon	[85]
	APC decrease		[87]
	Bax increase		[89–91]
	Bcl-2 decrease		[86,89–91]
	Bcl-xL decrease		[86]
	Caspase 3 activation		[87,89]
	Caspase 7 activation		[89]
	COX2 decrease		[86]
	Cyclin D1 decrease		[86]
	DR5 upregulation		[88]
	E-cadherin decrease		[87]
	Fas-mediated caspase 8 activation		[89]
	IAP-2 decrease		[86]
	Mithocondrial [Ca^{2+}] increase		[89]
	Mithocondrial cytochrome c release		[89]
	Mithocondrial membrane potential reduction		[89]
	pAKT decrease		[85]
	β-catenin decrease		[87]
	Caspase 3/7 activation	Bladder	[50]
	Caspase 3/7 activation	Glioblastoma	[92]
	Bax increase		[92]
	Bcl-2 decrease		[92]
	Caspase 3 activation	Hosteosarcoma	[93]
	Parp-1 cleavage		[93]
	DNA damage	Gastric	[59]
	ODC activity decrease		[59]
	ROS production		[59]
	miR-186 pathway activation	Lung	[95]
	Bax and cleaved caspase 3/9 increase	Bladder	[96]
	Bcl2 decrease		[96]
	miRNA 344a-3p increase		[96]

Table 1. *Cont.*

Biological Effects	Mechanisms of Action	Cancer Type	References
Antimetastatic			
	Axl decrease	Breast	[98]
	CD24 decrease		[98]
	CXCL1 and 2 decrease		[101]
	miR-34a increase		[98]
	NF-kB inhibition		[100,101]
	Rho-A decrease		[98]
	RhoA/ROCK/MMPs/Vimentin pathway inhibition		[103]
	Slug decrease		[98]
	uPA decrease		[100]
	JAK/STAT3 pathway inhibition	Retinoblastoma	[104]
	miR-99a increase		[104]
	MMP2 decrease		[104]
	RhoA decrease		[104]
	ROCK1 decrease		[104]
	Vimentin decrease		[104]
	MMPs signaling pathways inhibition	Bladder	[50]
	Trop2 decrease		[49]
	Cellular matriptase downregulation	Prostate	[106]
	MMP9 decrease		[106]
	Angiogenesis inhibition	Colon	[44]
	Claudin-3 decrease		[107]
	Metastasis inhibition		[44]
	MMP9 decrease		[107]
	MMP2 decrease	Melanoma	[81,108]
	MMP9 decrease		[81]
	NF-kB signaling pathways inhibition		[108]
	TIMP-2 increase		[81]
	NF-kB and Wnt/βcatenin pathways inhibition	Cervical	[17]
	ICAM decrease	SCLC	[110]
	VEGF decrease		[110]
	MMP2 and MMP7 decrease		[110]
	STAT3 decrease		[110]
	IL-6-inducible JAK/STAT3 phosphorylation reduction		[110]
	Fascin decrease	Ovarian	[15]
	JAK/STAT3 signaling pathway inhibition		[15]
	pAkt, pmTOR, pP70S6K downregulation	Melanoma	[72]
	miR-27a decrease	Thymic	[111]
	mTOR and Notch-1 pathways inhibition		[111]
	miR-206 increase	NSCLC	[112]
	PI3K/AKT/mTOR pathway inhibition		[112]
	NEDD4 signaling pathways inhibition	Glioma	[113]

3. Bioavailability of Curcumin and Therapeutic Promises

Although the beneficial effects of curcumin are known, it has not yet been approved as a therapeutic agent due to its low bioavailability [21]. Among factors contributing to this limit, the following can be included: low water solubility, poor absorption, low tissue distribution, high rate of metabolism, inactivity of metabolic products and/or rapid elimination and clearance from the body [115]. Curcumin undergoes extensive phase I and II biotransformation [116]. The primary site of metabolism for curcumin is the liver, together with the intestine and gut microbiota; curcumin double bonds are reduced in enterocytes

and hepatocytes by a reductase to produce dihydrocurcumin, tetrahydrocurcumin, hexahydrocurcumin and octahydrocurcumin. Phase II metabolism that occurs in the intestinal and hepatic cytosol is quite active on both curcumin and its phase I metabolites, especially through conjugation reaction with glucuronic acid and sulfate at the phenolic site catalyzed by UGTs and SULTs enzymes, respectively [116].

Over the years, in order to improve curcumin pharmacokinetic profile and cellular uptake, several strategies have been developed. These include curcumin structural derivatives, analogues preparation and novel drug delivery systems that could enhance its solubility and extend its plasma residence time.

3.1. Curcumin Structural Derivatives and Analogues

Structural modifications on the curcumin chemical backbone led to curcumin derivatives and analogues [22–24,117,118]. The derivatives category includes all those compounds that maintain the basic structure of pharmacophore and, specifically, the two phenolic rings and the α, β-unsaturated dichetonic bridge which are the portions responsible for the molecule pharmacological activities (Figure 2) [119]. Curcumin derivatives are generally synthesized by modification of the hydroxyl group of the phenol ring, which can be acylated, alkylated, glycosylated and aminoacylated (Figure 2A). Studies on the kinetic stability of synthetic curcumin derivatives showed that glycosylation of the pharmacophore aromatic ring improves the water solubility of the compound, which increases its kinetic stability and leads to a better therapeutic response. In the II phase of curcumin metabolism, conjugation reactions take place on the hydroxyl groups (4-OH) attached to the phenyl rings of curcumin [116]. Thus, curcumin stability can be increased by masking the 4-OH groups, thereby extending the active molecule retention time in the body. Benzyl rings are also crucial for inhibiting tumor growth; their modification with hydrophobic substituents such as CH3 groups have been linked with an enhancement of the curcumin derivatives antitumor activity [120]. O-methoxy substitution was found to be more effective in suppressing the NF-kB activity, although this modification simultaneously affected curcumin lipophilicity [2]. Methoxy groups could be demethylated to hydroxyl groups. The reactive chain methylene group, responsible for conformational flexibility, is important for its antitumor/anticancer activity but not for redox regulatory or apoptotic activities. This group could be acylated, alkylated or substituted with an arylidene group (Ar-CH), thereby introducing substituents on the C7 chain [121]. The hydrogenation reaction of double bonds and carbonyl groups on the C7 chain allows the simplest derivatives to be obtained (Figure 2B), such as DHC, THC, HHC and OHC [119]. A comparative study on curcumin and its derivatives demonstrated greater antioxidant activity for several hydrogenated curcumin derivatives compared to the original compound [122]. Tetrahydrocurcumin, a non-electrophilic curcumin derivative, showed greater antioxidant activity than DHC and unmodified curcumin, although it failed to suppress STAT3 signaling pathway and to induce apoptosis [123]. This is evidence that the electrophilic nature of curcumin is essential for STAT3 signaling pathway inhibition. Other curcumin derivatives also include those obtained by exploiting the reactivity of the central β-diketone with hydrazine (Figure 2C). Such heterocyclizations reactions lead to a masking and stiffening of the central 1,3-diketone 1,3-ketoenol system [124] and, after evaluation of the antioxidant activity of these compounds, it is possible to assert that several of these azoles are better antioxidants than curcumin [125]. Oxidation and cleavage are further possible modifications to the β-diketone functional group, all suitably operated to improve the characteristics of the original pharmacophore (Figure 2C). Additionally, it is possible to adopt another approach which may help to increase the curcumin bioavailability, such as the formation of metal complexes, or coordination compounds, which are adducts formed by the reaction of Lewis acids and bases [126]. Metal complexes are generally obtained by reacting curcumin, which exploits the chelating capacity of the β-diketone group with a metal salt. The metals most used for this purpose are Boron, Copper, Iron, Gallium, Manganese, Palladium, Vanadium, Zinc and Magnesium. By complexing curcumin with metal ions, such as Zn^{2+}, Cu^{2+}, Mg^{2+}, an increase in water/glycerol solubility (1:1) and fair stability to light and heat were observed [22,126].

Numerous curcumin analogues have been synthesized and tested to study their interaction with known biological targets and improve the pharmacological profile of this natural product [24,127]. Some curcumin analogues are not obtained starting from the original molecule, but they are synthesized following a condensation reaction between aryl-aldehydes and acetylacetone; through this biosynthetic route, many curcumin analogues have been obtained. The use of acetylacetone derivatives, bearing substituents on the central carbon, leads to analogues with alkyl substituents on the central carbon of the C7 chain [128]. Another strategy concerns the modification of the carbon atom number that makes up the central C7 chain [128]. A greater antitumor activity than curcumin has been observed with the use of a variety of newly synthesized DAP curcumin analogues. These compounds, which possess two aromatic rings (aryl groups) joined by five carbon atoms, were able to suppress cancer growth through modulation of several factors such as NF-kB, MAPK, STAT, AKT-PTEN [127]. DAPs anticancer effects in different cancer cell lines were summarized by Paulraj and co-workers [127].

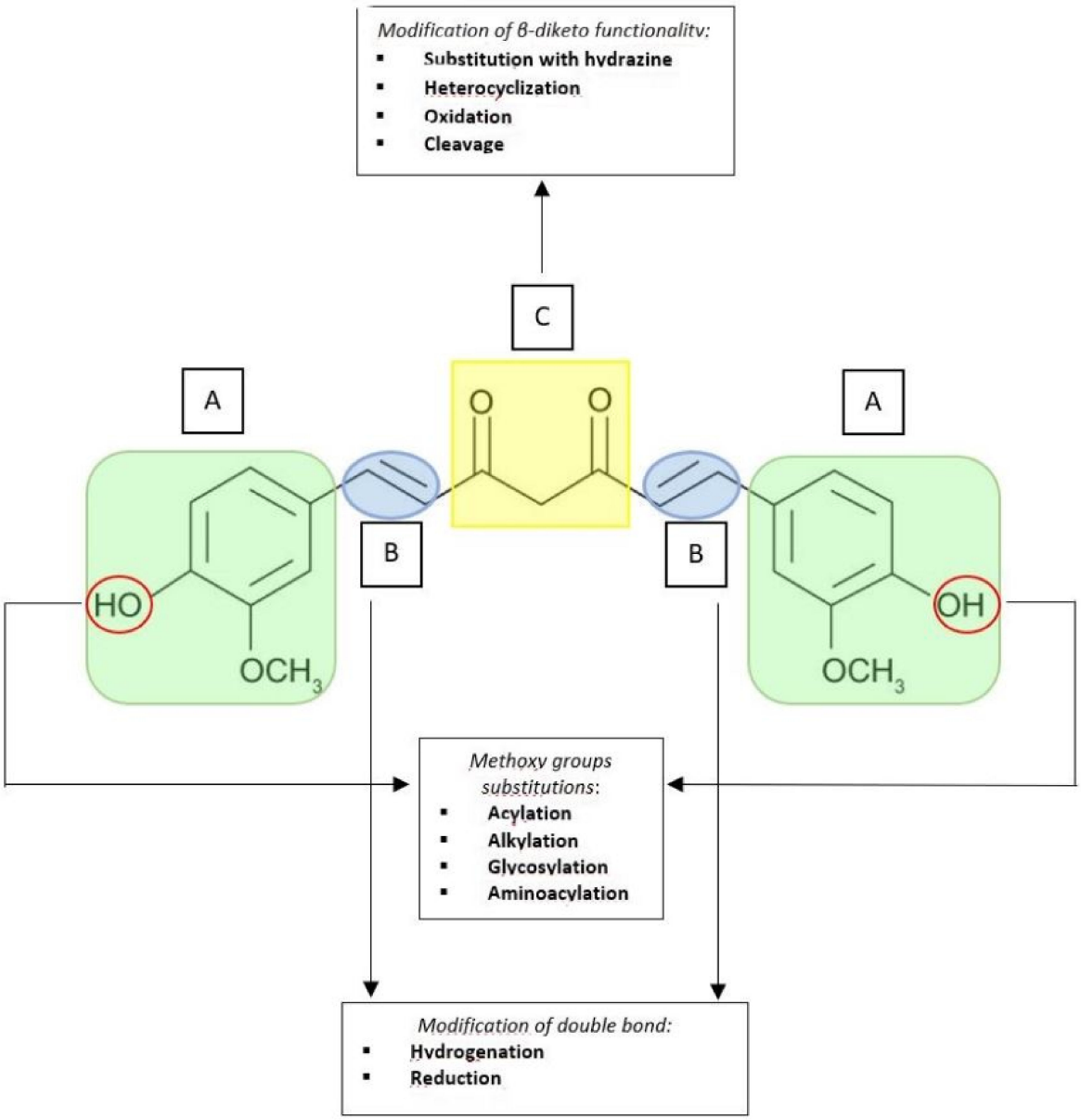

Figure 2. General chemical structure of curcumin derivatives. Curcumin chemical structure include two aromatic rings (**A**) linked to a β-dichetonic group (**C**) through a double bond (**B**).

A particular scientific interest has been shown towards the EF24 analogue, which displayed a better antitumor activity, a lower toxicity in normal cells, a marked increase in bioavailability and a lower metabolic rate compared to the natural compound [23,24]. In vivo studies have shown that, while dietary curcumin is poorly absorbed through the intestinal tract and therefore does not have a therapeutic effect at low doses, on the contrary, EF24 has greater oral bioavailability in mice [129], explaining, to some extent, its improved in vivo activity compared to curcumin. Several studies indicated that EF24 reduces cancer cell growth by inducing cell cycle arrest followed by caspase-mediated apoptosis [130,131]. These actions occur by modulating multiple pathways that determining the inhibition of NF-kB [132] and HIF-1α activity [133] and regulating reactive oxygen species (ROS) [131,134]. NF-kB signaling suppression has been found to be a fundamental aspect for its anticancer activity, since NF-kB is a transcription factor involved in the regulation of genes that monitor cell proliferation, differentiation, cell cycle control and metastasis [135]. According to a discovery by Yin et al. [136], EF24 is able to inhibit the catalytic activity of the IKK protein complex, which blocks the phosphorylation of IkB and causes its degradation while preventing the nuclear translocation of the p65 subunit. EF24 conferred radiation-induced cell death mainly by inhibiting radiation-induced NF-kB signaling in MCF-7 cells [137]. Similar effects were also observed in human neuroblastoma cells [138]. EF24 also regulates HIF-1α expression, which is closely associated with the outcome of chemotherapy in cancer treatment. EF24 overcomes sorafenib resistance through VHL tumor suppressor-dependent HIF-1α degradation and NF-kB inactivation in hepatocellular carcinoma cells [139]. Another notable EF24 antitumor mechanism is ROS production regulation. Tan et al. showed that EF24 inhibited ROS generation and activated ARE-dependent gene transcription in platinum-sensitive (IGROV1) and platinum-resistant (SK-OV-3) human ovarian cancer cells [134]. On the contrary, the ability of EF24 to increase ROS production and then induce apoptosis in cancer cells via a redox-dependent mechanism was found in breast MDA-MB-231, prostate DU-145 [140], gastric SGC-7901 and BGC-823 [141], and colon HCT-116 and SW-620 human cancer cells [131], suggesting that the EF24 role in ROS induction may be cell type dependent. EF24 ability to interfere with the targeted inhibition of antiapoptotic proteins belonging to the Bcl-2 family is being exploited in clinical settings for the treatment of age-related diseases. Although this mechanism has not been fully elucidated, the function of EF24 and other curcumin analogues as senolytic agents is well demonstrated, as they are able to selectively kill the senescent cells (cells that are no longer able to replicate) that accumulate in various organs and tissues as a result of the progress of the damage that occurs with aging. EF24 exerts its senolytic effect by inducing apoptotic death in target cells via proteasome-mediated downregulation from Bcl-2 family proteins, which represents a protection factor for senescent cells, as they are resistant to the induction of apoptosis as a result of the expression of these proteins [23].

Selvendiran et al. [142] demonstrated the ability of curcumin analog HO-3867 to reduce in vitro and in vivo ovarian cancer growth. In particular, this compound enhanced the therapeutic potential of cisplatin in A2780R drug-resistant ovarian cancer cells. The results confirmed that the co-administration of HO-3867 with cisplatin resulted in greater inhibitory effects than cisplatin alone, with cell cycle arrest and apoptotic mechanism being significantly induced by targeting the STAT3 pathway in both in vitro cells and in vivo xenograft tumors [142].

A recent study investigated the antitumor properties of MS13, another diarylpentanoid curcumin analog, on primary (SW480) and metastatic (SW620) human colon cancer cells [143]. MS13 was more cytotoxic in a dose-dependent manner and had a higher growth inhibitory effect towards SW480 and SW620 cells compared to curcumin. Several factors may explain its increased cytotoxicity activity; these include removal of β-diketone, the reduction in the electron donation capacity of OH at position 4′ [144] or the 3′,4′-dimethoxy or 3′-methoxy-4′-hydroxy substituents on the phenyl rings [145].

Recently, Shen et al. [146] tested the efficacy of the B14 analog in MCF-7 and MDA-MB-2310 breast cancer cells. The results indicated that B14 was more potent than curcumin in inhibiting cell viability, colony formation, migration and invasion. Particularly, this analog,

functioning simultaneously in multiple pathways, displayed a selective antitumor activity on MCF-7 and MDA-MB-231 cells, but not on MCF-10A breast epithelial cells. Furthermore, in tumor-bearing mice, analog B14 significantly reduced tumor growth and inhibited cell proliferation and angiogenesis. Additionally, pharmacokinetic tests revealed that B14 was more stable and bioavailable than curcumin in vivo [146].

3.2. Curcumin Delivery Systems

As already stated, despite curcumin's remarkable beneficial biological effects, it showed low water solubility in acid and neutral conditions, chemical instability in neutral and alkaline environments, and rapid enzymatic metabolism, which limit its bioavailability. Curcumin bioavailability can be enhanced by:

(a). Delaying metabolism through its entrapment within the hydrophobic phases that isolate it from aqueous phase or cell membranes enzymes;

(b). Improving its bioaccessibility through an increase in the quantity that is solubilized inside the mixed micelles present in the small intestine; this can be achieved by inserting surfactants, phospholipids, fatty acids or monoglycerides into the curcumin-loaded carrier particles;

(c). Promoting its absorption by loading curcumin into particles carrier that contain substances able to increase epithelium cell membranes permeability or block efflux transporters [147]. Therefore, in order to ameliorate curcumin's pharmacokinetic characteristics, various methodological approaches have been attempted, such as polymeric approaches, magnetic approaches, solid lipid nanoparticles, liposomes, phytosomes, micelles, β-cyclodextrins and solid dispersions [21,25–30,148–150] (Figure 3) [151–154]. In addition to these approaches, curcumin conjugation with substances, such as piperine, which is able to inhibit its metabolism [27,155], has emerged as a prominent solution to increase curcumin serum concentration.

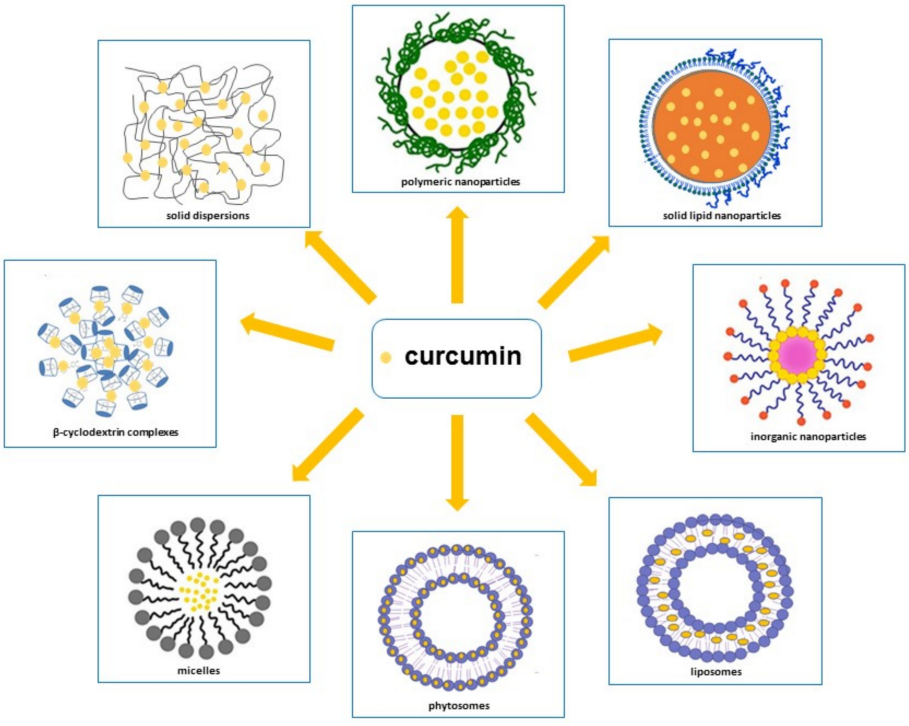

Figure 3. Principal delivery systems to enhance curcumin oral bioavailability. In the figure the polymeric nanoparticles, inorganic nanoparticles and micelles images were adapted from Praditya et al. [151], the phytosomes and liposomes images were adapted from Yang et al. [152], the solid lipid na-noparticles image was adapted from Li et al. [153] and the β cyclodextrin complexes image was adapted from Yallapu et al. [154].

3.2.1. Nanoparticles

Nanotechnology is a fast-developing field that is attracting an increasing amount of attention in the fields of drug delivery and cancer therapy, which provides an important route to develop the aqueous formulations of hydrophobic drugs [156]. Nanoparticles, which are 1000 times smaller than the human cell average, possess unique physical, chemical and biological properties that can be useful for both controlled and targeted drug delivery, and for improving the pharmacokinetics and solubility of drugs [156]. It is important to note that the particle sizes of the neosynthesized carriers may influence the therapeutic effects and drug biocompatibility, as well as the chemical-physical characteristics of the devices used [156]. Various types of nanoparticle, such as polymeric, solid lipid and inorganic nanoparticles [156], are widely used to enhance the therapeutic applications of curcumin. Using nanoparticle formulations, it is possible to increase the curcumin water solubility, ensure its intracellular delivery [157], improve the efficacy and limit the toxicity in the settings of cancer therapy, as well as inducing the chemo and radio sensitization of cancer cells [158].

Polymeric Nanoparticles

Polymeric nanoparticles (NPs), which possess the advantage of being small and biocompatible, are prepared using either natural or synthetic biodegradable polymers such as silk fibroin, chitosan, PEG, PLA), PGA, PCL and PLGA [156,157,159] (see Table 2 for a summary of the data).

Formulations of nanoparticles based on polymer PLGA have been shown to be effective for enhancing curcumin's therapeutic effects against cervical cancer [160]. Specifically, the results provided show that nano-curcumin effectively inhibited the growth of Caski and SiHa cervical cancer cells, arrested the cell cycle in the G1-S transition phase and induced apoptosis. Both cell lines revealed a significantly more evident inhibitory effect of curcumin/nano-curcumin on cell proliferation at higher concentrations (20 and 25 μM) and nano-curcumin was found to be more effective than free curcumin at reducing the clonogenic capacity of cervical cancer cells. Furthermore, treatment with nano-curcumin caused a marked decrease in miRNA-21 levels, an onco-miRNA associated with chemoresistance, in vitro and in vivo models, and improved expression of miRNA-214 tumor suppressor [160]. In another study, the anticancer potential of curcumin-encapsulated PLGA nano-formulation was investigated [161]. This formulation showed a superior cell uptake, retention and release in A2780CP highly metastatic ovarian and MDA-MB-231 breast cancer cells [161]. Additionally, it has a greater antiproliferative effect than free curcumin, as demonstrated by the IC50 values; the IC50 of nano-curcumin is 13.9 μM and 9.1 μM in A2780CP and MDA-MB-231 tumor cells, respectively, while the free curcumin showed higher IC50 values (15.2 μM in A2780CP and 16.4 μM in MDA-MB-231 cells compared to nano-curcumin in metastatic tumor cells [161]. The curcumin PLGA nanoparticles effect on cellular viability have been evaluated in LNCaP, PC3 and DU145 cancer and PWR1E non-tumorigenic prostate cell lines [162]. The results showed that the IC50 of this formulation ranged from 20 μM to 22.5 μM, while that of free curcumin ranged from 32 μM to 34 μM across all tumor cell lines, representing an almost 35% reduction in the IC50 value with curcumin-loaded nanoparticles. The evaluation of molecular mechanism of curcumin PLGA nanoparticles displayed that they were able to arrest cell cycle and induce apopotosis by interfering with the NF-kB activity [162]. To increase the anticancer efficiency of curcumin, Bisht et al. designed curcumin polymeric nanoparticles using the micellar aggregates of cross-linked and random copolymers of NIPAAM, with VP and PEG-A [163]. The authors revealed that these NPs were heavily absorbed and were able to block the clonogenicity of the MiaPaca pancreatic cancer cell lines compared to untreated cells or cells exposed to empty polymeric nanoparticles [163]. The superior anticancer effects of curcumin-loaded nanoparticles prepared with amphilic methoxy poly(ethylene glycol)-polycaprolactone (mPEG–PCL) block copolymers compared to free curcumin was confirmed in a human lung adenocarcinoma A549 transplanted mice model [164]. More-

over, curcumin NPs showed little toxicity to normal tissues including bone marrow, liver and kidney at a therapeutic dose. Curcumin silk fibroin nanoparticles (CUR-SF NPs) provided a more stable release and generated much more emphasized anticancer effects than the results obtained with the curcumin free in HCT116 colon cancer cells [165]. In this study, the methods underlying how the controlled release of CUR-SF NPs is able to improve the curcumin cellular uptake in tumor cells were elucidated. Interestingly, the anticancer effect of CUR-SF NPs that involved cell-cycle arrest in the G0/G1 and G2/M phases and apoptosis induction in cancer cells, was improved, while the side effect on normal human colon mucosal epithelial cells was reduced [165]. In another work, curcumin- and piperine-loaded zein-chitosan nanoparticles were characterized by investigating their shapes, morphologies, particle sizes and cell cytotoxicity [166]. The results showed that zein-chitosan nanoparticles loaded with curcumin and piperine have an average size of about 500 nm and high encapsulation efficiencies for curcumin (89%) and piperine (87%). Furthermore, this formulation showed good cytotoxic effects on SH-SY5Y neuroblastoma cell line [166]. A recent study confirmed the enhanced solubility and bioavailability of curcumin within chitosan nanoparticles [167]. This formulation exhibited a sustained release of drug from NPs and a four-fold higher cytotoxic activity on HeLa cervical cancer cells; in fact, DNA damage, cell cycle blockage and elevated ROS levels confirmed the anticancer activity following apoptotic pathways caused by this formulation.

Solid Lipid Nanoparticles

Solid lipid nanoparticles (SLNs) are colloidal lipid carriers of size between 50 and 1000 nm and composed by biodegradable physiological lipids [168]. Unlike liposomes, they are rigid particles used both for hydrophobic drugs loading and for their controlled and targeted delivery to the reticuloendothelial system. SLNs possess the advantages of high drug load capacity, good stability, excellent biocompatibility and increased bioavailability [169]. In SLN preparation, lipids are used with a low melting point and solids at room or body temperature and surfactants through various methods including HPH [170]. Among the solid lipids used in SLN preparation there are monostearin, glyceryl monostearate, precyrene ATO 5 (mono, di, triglycerides of C16-C18 fatty acids), compritol ATO 888, stearic acid and glyceryl trioleate which can improve the curcumin chemical stability [168]. Surfactants such as poloxamer 188, Tween 80 and DDAB, are able to reduce interfacial tension between lipid hydrophobic surface and aqueous environment by acting as surface stabilizers [168]. Several studies have evaluated not only curcumin SLNs physico-chemical properties, stability, bioenhancement, bioavailability, but also cellular uptake in vitro and antitumor efficacy in vitro and in vivo [171–174] (see Table 2 for a summary of the data). Curcumin SLNs using tristearin and PEGylated surfactants have recently been prepared [174]. The study showed that SLN-loaded curcumin with long PEGylates showed increased absorption and long-term stability after oral administration in rats. Furthermore, the bioavailability of curcumin was also 12 times higher in SLNs formulated with long PEGylates than in those formulated with shorter PEGylates [174]. In another study, it has been demonstrated that the presence of sodium caseinate (NaCas) and sodium caseinate-lactose (NaCas-Lac) conjugates as bioemulsifiers to stabilize curcumin SLNs provided a steric hindrance, allowing dispersibility and greater curcumin stability at pH acid. In addition, this formulation displayed a better antioxidant activity compared to that of free curcumin [175]. However, the SLNs use as oral delivery system is limited by drug burst release from SLNs in acid environment. In order to inhibit curcumin rapid release in acid conditions and improve curcumin bioavailability, Baek et al. prepared curcumin SLNs coated with N-carboxymethyl chitosan [171]. The results showed that this formulation showed a prolonged release in simulated intestinal fluid and greater absorption and oral bioavailability compared to free curcumin. Furthermore, curcumin exhibited a strong cytotoxicity compared to curcumin solution in MCF-7 breast cancer cells [171]. Using glyceryl monostearate and poloxamer 188 surfactant were developed curcumin SLNs and evaluated its efficiency in MDA-MB-231 breast cancer cells [176]. The results

confirmed that curcumin was stably encapsulated in the lipid matrix and its solubility and release were improved compared to the free curcumin solution. Moreover, curcumin SLNs exhibited higher cellular uptake and higher cytotoxicity by apoptosis induction compared to the free drug [176]. Guorgui et al. demonstrated that plasma levels of curcumin encapsulated in SLNs and in d-α-Tocopheryl polyethylene glycol 1000 succinate-stabilized curcumin (TPGS-CUR) increased when administrated in mice [172]. Additionally, these formulations reduced growth of Hodgkin's lymphoma xenograft models by 50.5% and 43.0%, respectively, compared to free curcumin [172]. Similarly, inhibitory effects were observed in Hodgkin lymphoma L-540 cells, as proven by curcumin SLNs ability to reduce the expression of XIAP and Mcl-1, proteins involved in cell proliferation and apoptosis, and of cytokines IL-6 and TNF-α as well as to enhance the growth inhibitory effect of bleomycin, doxorubicin and vinblastine chemotherapeutic drugs [172].

Inorganic Nanoparticles

Recently, inorganic nanoparticles have received considerable attention, particularly in the oncology field for diagnostic and therapeutic applications [177,178]. They have specific physical size-dependent properties, such as the contrasting effect and magnetism as well as good microbial resistance and excellent storage capacity [179].

The in vitro and in vivo therapeutic efficacy of curcumin-loaded magnetic nanoparticles (MNPs) was evaluated in several tumors including pancreatic cancer [180] (see Table 2 for a summary of the data). Specifically, HPAF-II and Panc-1 human pancreatic cancer cells exhibited efficient internalization of this formulation in a dose-dependent manner. Moreover, they inhibited both in vitro HPAF-II and Panc-1 cell proliferation and in vivo tumor growth in an HPAF-II xenograft mouse model. The growth-inhibitory effect of MNPs-CUR formulation correlated with the suppression of PCNA, Bcl-xL, induced Mcl-1, MUC1, collagen I, and enhanced membrane β-catenin expression. Interestingly, MNPs-CUR formulation improved serum bioavailability of curcumin in mice up to 2.5-fold as compared with free curcumin [180]. Folic-acid-tagged aminated-starch-/ZnO-coated iron oxide nanoparticles were prepared for the targeted delivery of curcumin. Particularly, the authors provided evidence that ZnO-incorporated aminated-starch-coated iron oxide nanoparticles showed a significant controlled release of curcumin in vitro and reduced HepG2 liver and MCF-7 breast cancer cell viability without toxic effects on human lymphocytes [181]. In addition, folic acid taging to the nanoparticles led to both an increase in cellular uptake and in ROS generation [181]. The curcumin pluronic stabilized Fe3O4 magnetic nanoparticles (CUR-PSMNPs) showed aqueous colloidal stability, biocompatibility as well high loading affinity for curcumin and better curcumin release in acidic conditions [182]. Additionally, cell viability studies confirmed that curcumin and CUR–PSMNPs significantly reduced MCF-7 cell proliferation with IC50 values of 25.1 and 18.4 μM, respectively. The higher toxicity of CUR–PSMNPs were due to its significant greater cellular uptake respect to pure drug [182]. PEGylated curcumin was used as the surface modification of magnetic nanoparticles (MNP@PEG-CUR) in order to simultaneously ameliorate magnetic targeting characteristic of nanoparticles and PEG conjugated drug. The results indicated that MNP@PEG-CUR showed higher drug release in acidic conditions, biocompatibility and low cytotoxicity at physiological pH [183]. Gangwar et al. prepared curcumin conjugated silica coated nanoparticles and observed good stability in aqueous medium, sustained drug release and greater anticancer properties. Particularly, cytotoxicity analysis revealed that conjugate was more toxic on HeLa cervical cancer cells compared to normal fibroblasts [184]. In another work, Manju et al. reported the synthesis of water-soluble HA-CUR@AuNPs attached to curcumin and explored their targeted delivery onto cancer cells (C6 glyoma, HeLa cervical and Caco-2 colon cancer cells). The results indicated that this formulation displayed good aqueous solubility, superior cellular uptake and anticancer effects respect to free curcumin. The authors highlighted how the greater targeting efficacy via hyaluronic acid- and folate receptor-mediated endocytosis could increase the overall intracellular accumulation of HA-CUR@AuNPs [185].

3.2.2. Liposomes

Liposomes are self-assembled spherical vesicles of different sizes ranging from 20 nm to several microns in diameter and composed of one or more bilayers surrounding aqueous unit [186]. Liposomes that can carry both hydrophilic and hydrophobic molecules are excellent drug delivery systems characterized by high biocompatibility and biodegradability, high stability, low toxicity, better solubility, targeting for specific cells, controlled distribution, flexibility and ease of preparation [186]. However, in some cases, they can undergo rapid elimination from the bloodstream, physical and chemical instability, aggregation, fusion, degradation, hydrolysis and phospholipid oxidation [187]. The liposomal systems are designed with the aim of allowing curcumin to be distributed over aqueous medium and increasing its bioavailability and therapeutic effect [188] (see Table 2 for a summary of the data). The preparation method used affects the nature of the formed liposomes, as well as curcumin-carrying capacity. One study compared the characteristics of curcumin-loaded liposomes prepared using three different methods such as thin film, ethanol injection and pH-based methods [189]. The results indicated that both liposomes initial diameters and encapsulation efficiency decreased with the following trend, respectively: thin film (453 nm; 78%)> pH-driven (217 nm; 66%)> injection of ethanol (115 nm; 39%). Furthermore, it has also been shown that the source of phospholipids can also affect the physicochemical characteristics of curcumin-loaded liposomes. Liposomes produced from milk fat globule membranes (MFGMs) offered better protection than those of soy lecithin [190]. However, the instability of conventional liposomes under the physiological conditions found in the gastrointestinal tract hindered clinical applications. Indeed, coated liposomes with thiolated chitosan or other agents are made in order to improve liposome stability and then curcumin bioavailability [187,191]. It has been observed that liposome formulations improved curcumin aqueous solubility and bioavailability by 700-fold and to 8–20-fold, respectively, in tumor-bearing mice [192]. Moreover, antiproliferative activity of DMPC liposomal curcumin was evaluated in LNCaP and C4-2B prostate cancer cell lines [193]. The results showed that liposomal curcumin caused a greater inhibition of cell proliferation than free curcumin and even at doses 10 times lower [193]. Dhule et al. showed that the 2-hydroxypropyl-γ-cyclodextrin/curcumin-liposome complex was able to inhibit KHOS osteosarcoma cancer cell proliferation by inducing apoptosis in vitro as well as reduce the growth of a xenograft osteosarcoma model in vivo [194]. Furthermore, liposomes encapsulating doxorubicin and curcumin, reduced C26 colon cancer cell proliferation to a greater extent than those loaded with doxorubicin alone [195]. A liposomal curcumin formulation also resulted in the dose-dependent inhibition of the proliferation and motility and apoptosis induction in Ishikawa and HEC-1 endometrial cancer cells. These inhibitory effects occurred probably through negative regulation of the NF-kB pathway [196]. Moreover, a recent study demonstrated that small curcumin molecules encapsulated in liposome nanocarriers significantly increased the blue-light-emitting diode (BLED)-induced photodynamic therapy (BLED-PDT) effect, by increasing intracellular ROS levels and apoptosis in human lung A549 cancer cells [197].

3.2.3. Phytosomes

Curcumin is also often complexed with different types of phospholipids such as phosphatidylcholine, or other lipid carriers, in order to create phytosomal formulations. The use of phosphatidylcholine in the molecule complexation is useful in allowing the efficient transport across cell membranes and then absorption. In the phytosome, it is possible to observe an interaction between the active substance (i.e., curcumin) and the polar head of the phospholipid; this bond permits curcumin to become an integral part of the membrane [198]. Phytosomes application for the curcumin delivery has the advantage of improved its absorption and bioavailability as well as enhanced its therapeutic benefits [199–201] (see Table 2 for a summary of the data). The relative absorption of standardized curcuminoid mixture (curcumin, demethoxycurcumin, and bisdemethoxycurcumin) and its corresponding lecithin formulation (Meriva) was investigated in a randomized,

double-blind, crossover human study. The results indicated that total curcuminoid absorption was about 29-fold higher for Meriva compared to unformulated curcuminoid mixture. Therefore, the improved curcuminoids absorption could explain the Meriva clinical efficacy at significantly lower doses than unformulated curcuminoids [202]. A recent study, which a CPC was prepared and solidified with Soluplus [polyvinyl caprolactam-polyvinyl acetate polyethylene glycol graft copolymer] carrier, demonstrated that solydifing process enhanced CPC flowability and dissolution rate as well as curcumin oral bioavailabilty in rats [203].

3.2.4. Micelles

Micelles consist of self-assembled aggregates of surfactants or block copolymers ranging in size from 10 to 100 nm [204]; they can be formed by dissolution, dialysis, emulsion, solvent evaporation and lyophilization [204]. Micelles, given their small molecular size that ensure an effective macromolecules transport across cell membrane, are prepared to solubilize curcumin [205]. Micelles, are systems capable to improve the gastro-intestinal absorption of curcumin, increasing plasma levels and decreasing the kinetics of elimination, with a consequent enhancement in bioavailability and a hepato-protective effect likened to free curcumin [205] (see Table 2 for a summary of the data). In addition, an increase in water solubility facilitates the development of a stable and homogenous solution for intravenous applications. Additionally, the nanoscale of micelles and presentation of the hydrophilic stabilizing interface can prolong their circulation time in vivo and enhance the cellular uptake [205]. Letchford et al. formulated curcumin micelles that contained copolymers of deblock MePEG-b-PCL that achieved an approximately 13×10^5-fold increase in water solubility [206]. Similarly, a previous study confirmed a 60-fold increase in the biological half-life of curcumin polymeric micellar compared to the free form when administered orally in rat models [207]. Schiborr et al. also observed that the use of curcumin micelles in volunteers determined a significant increase in drug plasma concentration formulated in micelles compared to that of native curcuminoids [208]. The uptake and transepithelial transport of native curcumin and micellar formulation (Sol-CUR) have been evaluated using a Caco-2 cell model [209]. The results showed that Sol-CUR caused a 185-fold increase in AUC compared to native curcumin. This curcumin oral bioavailability improvement was dependent on Sol-CUR's higher intestinal absorption and distribution [209]. Recently, pharmacokinetic studies confirmed a significant enhancement of aqueous solubility, as well as stability, dissolution, and permeability of curcumin formulated in micelles compared to free drug [210]. A study by Chen et al. focused on the synthesis, physico-chemical characterization and in vitro evaluation of curcumin loaded in the super hydrophilic zwitterionic polymers PSBMA micelles. The results demonstrated that this innovative formulation exhibited greater stability, cellular uptake and tumor cytotoxicity compared to native curcumin [211]. Interestingly, various studies using curcumin polymer micelles may provide an indication of very promising therapeutic potential in cancer treatment. Curcumin delivery from nano-sized polymer micelles formulated with MPEG-P [CL-co-PDO] were evaluated in PC-3 human prostate cancer cell line. The results indicated that mixed micelle copolymers possessed a higher encapsulation efficiency (>95%), a prolonged drug release profile, and a dose-dependent cytotoxicity effect on tumor cells in contrast to that of free curcumin [212]. Patil et al. prepared CUR-MM of Pluronic F-127 (PF127) and Gelucire® 44/14 (GL44) in order to enhance its oral bioavailability and cytotoxicity in A549 human lung cancer cell line [213]. The in vitro dissolution profile of CUR-MMs revealed a controlled curcumin release. Furthermore, this formulation showed a significant improvement in in vitro cytotoxic activity and in vivo oral bioavailability of curcumin by approximately 3 and 55 times, respectively, compared to curcumin alone. These effects could be attributed to solubilization of hydrophobic curcumin into micelle core as well as to the ability of PF127 and GL44 to inhibit P-gp mediated efflux. In another work, it has been demonstrated that CUR-MPP-TPGS-MMs showed small size, high drug-loading and sustained release profile.

Furthermore, they improved the intestinal absorption of curcumin after oral administration and then oral bioavailability in rats [214].

3.2.5. Curcumin/β-Cyclodextrin and Solid Dispersions Formulations

Among various strategies performed to improve oral curcumin solubility there are cyclodextrin (CD) inclusion complexes and solid dispersions (SDs) [215] (see Table 2 for a summary of the data). Cyclodextrins are bucket-shaped oligosaccharides, consisting of six (a-), seven (b-) or eight (g-) units of D-glucopyranose linked through an a-1,4-glycosidic bond to form macrocycles and are widely known as solubilizing and stabilizing agents [216]. β-CD, with its hydrophilic outer surface and hydrophobic inner cavity, has become a benchmark for nanotechnology research due to its modern lumen size, high drug load, low cost of production, best stability of the lipophilic drug, easy modification by molecules and good biocompatibility characteristics [217]. Mangolim et al. demonstrated that curcumin-β-CD complex exhibited a sunlight stability 18% higher and a 31-fold increased solubility compared to the pure drug [218]. Liquid-type β-cyclodextrins curcumin delivery carrier is one of the most widely used types in the food industry [219]. Particularly, the delivery carrier of hydroxypropyl β-CD curcumin prepared by saturated aqueous solution increased curcumin solubility in water by 276 times [220] and oral bioavailability by 3 times [221]. In addition, the solid granule-based β-cyclodextrins curcumin delivery vector had very good storage stability and increased its bioavailability significantly [222]. The formulations of CD combined with curcumin (CUR-CD) have been shown to have enhanced the antiproliferative, anti-inflammatory and anticancer effects of the nutraceutical agent [22]. The therapeutic effect of CUR-CD encapsulated into positively charged biodegradable chitosan (CUR-CD-CS) nanoparticles was investigated on the SCC25 skin cancer cell line. The study demonstrated that CD presence not only increased curcumin solubility and cellular absorption, but also promoted cell cytotoxicity [223]. Yallapu et al. showed that β-CD-curcumin inclusion complex (CD30) possessed an improved uptake and a greater potent therapeutic efficacy in DU145 prostate cancer cells compared to the free drug [154]. Similarly, the formulation of β-cyclodextrin-curcumin complex (CD15) enhanced curcumin delivery and improved its therapeutic efficacy compared to free curcumin in in vitro A549, NCI-H446 and NCI-H520 human lung carcinoma cell lines and in vivo mouse hepatoma H22 xenograft models. Particularly, through regulation of MAPK/NF-kB pathway, CD15 upregulated p53/p21 pathway, downregulated Cyclin E-CDK2 combination and increased Bax/caspase 3 expression to induce cellar apoptosis and G1-phase arrest [224]. A study demonstrated that in HeLa cervical cancer cells, curcumin encapsulated in crosslinked β-CD nanoparticles acted extremely rapidly on cell metabolism resulting in a significant cancer cell growth inhibition [225]. Recently, a nano-drug system namely FA-CUR-NPs consisting of FA, β-CD, εCL and curcumin was performed to improve curcumin delivery in cervical cancer tissues which overexpress FRs and to achieve controllable release in vitro and in vivo. In this system, FA binding to FRs was used as a targeting molecule, β-CD modified by ε-CL as delivery carrier and for controlling drug release and curcumin as a model drug to limit multidrug resistance after administration [226]. The study demonstrated that in vitro curcumin release rate from FA-CUR-NPs under tumor microenvironment conditions (pH 6.4), was three times faster than that under systemic circulation conditions (pH 7.4). Additionally, in vitro cytotoxicity was proportional to cellular uptake efficiency and the in vivo marked accumulation in tumor site was responsible of greater antitumor activity. These findings indicated FA-CUR-NPs could represent a promising approach for improving cancer therapy through active targeting and controllable release [226]. Moreover, in another work the use of hydroxypropyl-β-CD as a carrier-solubilizer improved solubility of the curcumin–piperine system, its permeability through biological membranes (gastrointestinal tract, blood–brain barrier), the antioxidant and antimicrobial activities and as well as the enzymatic inhibition against acetylcholinesterase and butyrylcholinesterase [227].

The SDs technology transforms crystalline materials into amorphous materials: an active substance is incorporated into a carrier, which is generally selected from suitable

polymers [228]. The active ingredient, originally crystalline, is usually transformed into amorphous form in the dispersion and it is for these reasons that SD is a consolidated method applied to improve the solubility and bioavailability of drugs with poor water solubility such as curcumin [228]. The major outcomes of this technique include prolonged survival, antitumor and antimetastasis, anti-inflammatory, antibacterial activity, enhanced stability and bioavailability [229,230]. Seo et al. prepared solid dispersions of curcumin with Solutol® HS15 SD showing greater solubility and bioavailability compared to free curcumin [231]. Similarly, curcumin SDs with cellulose acetate and mannitol showed a better solubility in water and an improvement in oral bioavailability of about seven times compared to curcumin [232]. In another work, Texeira et al. demonstrated how solid dispersions of Gelucire®50/13-Aerosil curcumin possess stability over time up to 9 months and an improvement in water solubility and in dissolution rate of about 3600- and 7.3-fold, respectively. Furthermore, the major curcumin gastrointestinal absorption resulted in a systemic bioavailability increase and greater anti-inflammatory activity in rats [229]. Antioxidant and antigenotoxic effects of curcumin formulated in SDs compared to unmodified drug were evaluated in Wistar rats. The results showed that curcumin SDs, even if they did not alter the antigenotoxic effects observed with free curcumin, displayed a better water solubility, with a maximum of absorption in the gastrointestinal tract [233]. Recently, curcumin SDs were obtained using Poloxamer 407 as the encapsulant agent and their cytotoxic effects were evaluated against tumoral (breast, lung, cervical and hepatocellular carcinoma) and PLP2 non-tumoral cells. These formulations that were readily dispersible in water had cytotoxicity against all the tested tumor cell lines without toxic effects for non-tumor cells [234].

3.2.6. Curcumin Conjugates Formulations

Combinations of curcumin with other compounds increase its solubility and cellular absorption, extend the residence in plasma improving the pharmacokinetic profile and then oral bioavailability (see Table 2 for a summary of the data). Curcumin conjugation by covalent bond with piperine, an alkaloid of black pepper and known as an inhibitor of hepatic and intestinal glucuronidation [235], enhanced curcumin serum level and a significantly reduced elimination half-life and clearance, producing 154% and 2000% increase in bioavailability in rats and humans, respectively [236]. Another study also showed that piperine (20 mg/kg orally) when administrated with curcumin (2 g/kg orally) increased the bioavailability of the latter up to 20 times more in epileptic rats [237]. Similarly, both intestinal absorption and curcumin bioavailability has been found to be improved following concomitantly oral intake with piperine in rats [238]. In a clinical study, the curcumin-lecithin-piperine formulation, namely BCM-95CG (Biocurcumax®), administrated to healthy subjects aged 28–50 years significantly improved curcumin bioavailability and showed a better pharmacokinetic profile than pure curcumin [239]. An in vitro study conducted by Sing et al. demonstrated that conjugates of curcumin, piperic acid and glycine, prepared by esterifying the sites of metabolic conjugation 4 and 4′ phenolic hydroxyls, triggered a mitochondrion-dependent apoptosis in MCF-7 and MDA-MB-231 breast cancer cell lines; however, the authors highlighted that the conjugation did not affect the efficacy of parent molecule, while these compounds could work in vivo as prodrugs with improved pharmacokinetic profile. This suggested other in vivo studies were needed to elucidate the therapeutic potential of curcumin conjugates in breast cancer [240].

Table 2. Strategies to enhance bioavailability and/or antitumoral effects of curcumin.

Composition	Outcomes	References
Polymeric Nanoparticles (NPs)		
PLGA + CUR	Superior anticancer effects respect to free curcumin in cervical cancer cells	[160]
PLGA + CUR	Superior cellular uptake and anticancer effects respect to free curcumin in ovarian and breast cancer cells	[161]
PLGA + CUR	Superior cellular uptake and anticancer effects respect to free curcumin in prostate cancer cells	[162]
NIPAAM+ VP + PEG-A + CUR	Superior cellular absorbition and anticancer effects respect to free curcumin in pancreatic cancer cells	[163]
mPEG-PCL + CUR	Superior anticancer effects respect to free curcumin in human lung adenocarcinoma cancer cells	[164]
silk fibroin + CUR	Superior cellular uptake and anticancer effects respect to free curcumin in colon cancer cells	[165]
zein-chitosan +CUR	High encapsulation efficiencies for curcumin. Superior anticancer effects respect to free curcumin in neuroblastoma cell line	[166]
chitosan +CUR	Enhanced curcumin solubility and bioavailability. Sustained drug release from NPs and anticancer effects with respect to free curcumin in cervical cancer cells	[167]
Solid Lipid Nanoparticles (SLNs)		
SLNs + N-carboxymethyl chitosan+ CUR	Prolonged release in simulated intestinal fluid, greater absorption and oral bioavailability compared to free curcumin. Superior anticancer effects respect to free curcumin in breast cancer cells	[171]
SLNs + CUR, d-α-Tocopheryl polyethylene glycol 1000 succinate-stabilized curcumin (TPGS) + CUR	Superior curcumin plasma levels in mice. Superior anticancer effects respect to free curcumin in Hodgkin lymphoma cells and in Hodgkin's lymphoma xenograft models	[172]
SLNs + tristearin + PEGylated + CUR	Superior bioavailability, absorption and long-term stability after oral administration in the rats	[174]
SLNs + NaCas + NaCas-Lac + CUR	Superior stability at pH acid and antioxidant activity with respect to free curcumin	[175]
SLNs + glyceryl monostearate + poloxamer 188 + CUR	Superior stability, solubility, cellular uptake, release and anticancer effects respect to free curcumin in breast cancer cells	[176]
Inorganic Nanoparticles		
MNPs + CUR	Superior cellular uptake in vitro. Superior bioavailability in vivo. Superior in vitro and in vivo therapeutic efficacy respect to free curcumin in pancreatic cancer cells and in pancreatic cancer xenografts model	[180]
Folic-acid-tagged aminated-starch-/ZnO-coated iron oxide nanoparticles + CUR	Significant controlled release of curcumin and reduced hepatic and breast cancer cells viability in vitro. Cellular uptake increase in vitro	[181]
PSMNPs + CUR	Aqueous colloidal stability, biocompatibility, high loading affinity for curcumin and better curcumin release in acidic conditions. Superior cellular uptake and anticancer effects respect to free curcumin in breast cancer cells	[182]

Table 2. *Cont.*

Composition	Outcomes	References
Inorganic Nanoparticles		
MNP@PEG + CUR	Higher drug release in acidic conditions, biocompatibility and low cytotoxicity at physiological pH	[183]
Silica + CUR	Good stability in aqueous medium, sustained drug release and greater anticancer properties in cervical cancer cells compared to normal fibroblasts	[184]
HA-CUR@AuNPs	Good aqueous solubility, superior cellular uptake and anticancer effects respect to free curcumin in cervical, glioma and colon cancer cells	[185]
Liposomes		
Liposome + CUR	Improved curcumin aqueous solubility and bioavailability in tumor-bearing mice	[192]
DMPC + CUR	Superior anticancer effects respect to free curcumin in prostate cancer cells	[193]
2-hydroxypropyl-γ-cyclodextrin/ liposome + CUR	Superior in vitro and in vivo anticancer effects respect to free curcumin in osteosarcoma cancer cells	[194]
Liposome + doxorubicin + CUR	Superior anticancer effects respect to those loaded with doxorubicin alone in colon cancer cells	[195]
Liposome + CUR	Superior anticancer effects respect to free curcumin in endometrial cancer cells	[196]
Liposome + CUR + BLED-PDT therapy	Enhancement of BLED-PDT therapy effect by curcumin liposome in lung cancer cells	[197]
Phytosomes		
Curcuminoids + lecithin (Meriva ®)	Improved absorption and clinical efficacy respect to unformulated curcuminoid mixtures	[198]
Soluplus® [polyvinyl caprolactam-polyvinyl acetate polyethylene glycol graft copolymer] + CPC	Improved flowability, dissolution rate and oral bioavailability in rats	[203]
Micelles		
MePEG-b-PCL + CUR	Improved water solubility	[206]
MePEG-b-PCL + CUR	Improved biological half-life with respect to the free curcumin in rat models	[207]
Tween-80 micelles + CUR	Improved drug plasma concentration with respect to free curcumin in volunteers	[208]
Micellar formulation + CUR (Sol-CUR)	Superior uptake, transepithelial transport, distribution and bioavailability in colon cancer cell model	[209]
Micelles + CUR	Enhancement of aqueous solubility, stability, dissolution and permeability of curcumin formulated in micelles compared to free drug	[210]
PSBMA + CUR	Greater stability, cellular uptake and tumor cytotoxicity compared to free curcumin	[211]
MPEG-P [CL-co-PDO] + CUR	Superior encapsulation efficiency, prolonged drug release profile and antitumor effects respect to free curcumin in prostate cancer cells	[212]
Pluronic F-127 + Gelucire® 44/14 micelles + CUR	Controlled curcumin release, superior oral bioavailability in vivo and in vitro antitumor effects in lung cancer cells respect to free curcumin	[213]
CUR-MPP-TPGS-MMs	Small size, high drug-loading and sustained release. Improved intestinal absorption and oral bioavailabil-ity in rats	[214]

Table 2. *Cont.*

Composition	Outcomes	References
Curcumin/β-Cyclodextrin (β-CD) and Solid Dispersions (SDs)		
β-CD + CUR	Superior sunlight stability and solubility respect to pure colourant	[218]
Liquid-type β-CD + CUR	Improved solubility in water and bioavailability	[220,221]
Solid type β-CD + CUR	Improved storage stability and biovailability	[222]
CUR-CD-CS	Superior solubility, cellular absorption and antitumor effects compared to free curcumin in skin cancer cells	[223]
β-CD + CUR	Improved uptake and therapeutic efficacy in prostate cancer cells	[154]
β-CD + CUR	Improved delivery and therapeutic efficacy compared to free curcumin in both in vitro lung carcinoma cell lines and in vivo mouse hepatoma xenograft models	[224]
β-CD + CUR	Superior anticancer effects respect to free curcumin in cervical cancer cells	[225]
FA-CUR-NPs	Improved drug release rate, cellular uptake efficiency and in vitro and in vivo antitumor activity respect to free curcumin in cervical cancer cells	[226]
Hydroxypropyl-β-CD+ CUR+piperine	Improved solubility of the curcumin–piperine system, its permeability through biological membranes, antioxidant and antimicrobial activities and enzymatic inhibition	[227]
SDs (with Gelucire®50/13-Aerosil) + CUR	Improved stability, water solubility, dissolution rate, bioavailability and anti-inflammatory activity in rats	[229]
Solutol® HS15 SDs + CUR	Improved solubility and bioavailability compared to free curcumin	[231]
SDs (with cellulose acetate and mannitol) + CUR	Improved water solubility and oral bioavailability compared to free curcumin	[232]
SDs + CUR	Superior water solubility and gastrointestinal absorption in rats	[233]
SDs (with Poloxamer 407) + CUR	Improved water dispersibility and cytotoxic effects against breast, lung, cervical and hepatocellular cancer cells	[234]
Curcumin Conjugates Formulations		
Piperine + CUR	Curcumin enhanced serum levels, reduced elimination half-life and clearance, increased bioavailability in rats and humans	[236]
Piperine + CUR	Curcumin increased bioavailability in epileptic rats	[237]
Piperine + CUR	Curcumin enhanced intestinal absorption and bioavailability in rats	[238]
BCM-95CG (Biocurcumax®): piperine + lecithin + CUR	Curcumin improved bioavailability and pharmacokinetic profile respect to free drug in healthy subjects	[239]

4. In Situ Implant Systems

Unlike blood circulation nanosystems that are injected directly into blood vessels, nanoimplant systems have been used as large containers of drugs that must be released directly and exclusively at the application site for the treatment of topical diseases. When loaded into a membrane made with biodegradable nanofibers, curcumin may be helpful in preventing post-operative relapse of solid tumor. Different researchers have attempted to charge curcumin into nanofiber membranes by electrospinning and, by adjusting the curcumin dosage, they have found that it is possible to control the drug's loading capacity [241]. Curcumin-loaded nanofiber membrane showed a good local delivery of hydrophobic drug, sustained release, biocompatibility and biodegradability and strong cytotoxicity against rat glioma 9L cells [242]. Therefore, this formulation could represent an ideal candidate for the prevention of postoperative tumor relapse after excision [243]. Further to the application of nanocrystallized curcumin in cancer therapy, tissue engineering is another biomedical

field where curcumin could also have a particular impact on bone formation. The choice of hydrogels as the base material could be appropriate due to their porosity and practical operation in clinical application. The hybrid hydrogel-micelle system was used to control malignant pleural effusion, which reduced the number of pleural tumor foci and prolonged survival time to malignant pleural effusion of carrier mice [244]. Angiogenesis is also effectively inhibited using this approach, and the micelle-hydrogel hybrid has been shown to be an exceptional transport system.

5. Clinical Trials with Curcumin

In recent decades, several clinical studies have been performed to evaluate the effect of curcumin in cancer patients. Depending on the tumor type, curcumin can act by causing a decrease in the patients symptoms or, in other cases, it can lead to an improvement in tumor markers and vital parameters [245]. Currently, 71 clinical studies reported in cancer patients treated with curcumin alone or in combination with other compounds were listed in the United States National Library of Medicine (clinicaltrials.gov). Pharmacologically, curcumin is shown to be well-tolerated and relatively safe to use in patients. The clinical trials conducted, thus far, have reported relatively no toxicity [246]. Phase I clinical trial conducted by Cheng et al. showed that oral administration of 8 g/day of curcumin for 3 months is non-toxic to patients with high-risk or pre-malignant lesions [247].

A phase II trial of curcumin conducted in twenty-five patients with advanced pancreatic cancer showed that oral curcumin was tolerated without toxicity at doses of 8 g/d for up to 18 months [248]. Particularly, it has been observed that two of them showed clinical biological activity; one patient reported having a stable disease for up to 18 months and another had a marked tumor regression along with an increase in the serum levels of cytokines (IL-6, IL-8, IL-10, and IL-1 receptor antagonists) [248]. Additionally, curcumin downregulated expression of the NF-kB, COX-2, and phosphorylated signal transducer and activator of transcription 3 in peripheral blood mononuclear cells from patients [248]. In another phase II pilot study, a combination of docetaxel, prednisone and curcumin was well-tolerated in patients with castration-resistant prostate cancer [249]. Dützmann et al. investigated the intratumoral concentrations and clinical tolerance of micellar curcuminoids composed by 57.4 mg curcumin, 11.2 mg demethoxycurcumin, and 1.4 mg bis-demethoxycurcumin administrated three times day for 4 days in glioblastoma patients [250]. The results revealed that oral administration of this formulation generated quantifiable concentrations of total curcuminoids in glioblastomas with likely effects on intratumoral energy metabolism [250]. Furthermore, in patients with orbital pseudotumors, head and neck squamous carcinoma, breast, lung and prostate cancers, curcumin application demonstrated beneficial effects with reductions in tumors volume and tumor markers [245]. Another study carried out on 11 volunteer patients with osteosarcoma aimed to quantitatively evaluate curcumin levels in the bloodstream following the intake of SLNs; this study highlighted an improvement in the bioavailability of this polyphenol, when compared with the results obtained on subjects who received unformulated curcuminoids extract [173]. However, further studies are needed to evaluate both the long-term tolerability after chronic administration and the relationship between plasma curcumin levels and disease markers. In a phase I clinical trial, an oral formulation of curcumin was evaluated in fifteen patients with advanced colorectal cancer refractory to standard chemotherapies. The results showed an absence of toxicity with curcumin, while 2 of the 15 patients showed stable disease after 2 months of curcumin treatment [251]. Carroll et al., in a phase II clinical study conducted on patients with colon cancer lesions, demonstrated that curcumin administration for 30 days determined a significant 40% reduction in aberrant crypt foci (ACF) [252]. These data suggested curcumin use as a cancer prevention agent. However, although curcumin in cancer patients has often improved life quality and reduced tumor markers, it is also true that curcumin has sometimes shown limited effect in some patients with disease advanced stage. Preclinical studies conducted so far confirmed the important role of curcumin and, in particular, the benefits that its synthetic derivatives or nanoformulations could bring to human health.

New efforts are needed to confirm the efficacy of curcumin-based products for the treatment of human diseases and to ensure that the products are non-toxic once introduced into the body. Several ongoing clinical trials should provide a deeper understanding of curcumin-based formulation efficacy and mechanism of action against human diseases.

6. Conclusions

Curcumin is one of the most promising clinical compounds of the last few decades. Its therapeutic benefits have been demonstrated in various chronic diseases and, above all, in various cancers. Precisely in the antitumor field, curcumin is able to modulate the action of growth factors, cytokines, transcription factors and genes that regulate cell proliferation, apoptosis and the metastatic process. Some of curcumin's multiple pharmacological activities have been used experimentally and clinically in both humans and animals. Notable among these are the antioxidant, anti-inflammatory and anticarcinogenic properties, which all seem related. It is encouraging that curcumin is of low toxicity. Most of the data supporting the antitumour activity of curcumin was obtained in vitro. Unfortunately, the challenges of low solubility and rapid elimination and then poor bioavailability, have delayed its adoption as a therapeutic agent. These efforts have led to the development of several curcumin formulations that have been systematically prepared to improve the absorption, water solubility, distribution and, hence, the bioavailability of curcumin. These methods have been promising with respect to preclinical and clinical efficacy and involve the use of both synthetic derivatives and analogues of curcumin as well as formulations of nanoparticles, liposomes, phytosomes, micelles and natural adjuvants such as piperine. All of these approaches generated a significant improvement in the bioavailability, absorption and retention time of curcumin, along with increased delivery to target tissues, as widely reported. However, further investigations are needed to fulfil the significant promise they currently hold and reveal new perspectives for the further enhancement of the therapeutic capacity of this interesting natural molecule. In particular, more epidemiological and clinical trials involving large numbers of subjects should be conducted to support to the obtained in vivo and in vitro results and to confirm curcumin's usefulness in cancer treatment and/or prevention.

Author Contributions: Conceptualization, original draft preparation, writing, search and identification of articles, A.C. and V.P.; screening articles, writing, M.C.N., A.D.L., F.P. (Francesca Prestia); figures preparation, M.C.N., F.P. (Francesca Prestia), F.P. (Francesco Puoci); tables preparation, M.C.N., A.D.L., F.P. (Francesca Prestia) and A.C.; writing and editing, R.S., I.C., F.P. (Francesco Puoci); editing, P.A., D.L.P., L.Z., A.D.L. and A.C.; supervision, A.C. and V.P. All authors have read and agreed to the published version of the manuscript.

Funding: This work was supported by a special award (Department of Excellence, Italian Law 232/2016) from the Italian Ministry of Research and University (MIUR) to the Department of Pharmacy, Health and Nutritional Sciences of the University of Calabria (Italy), and by MIUR ex 60% (VP, AC) and by AIRC (Associazione Italiana per la Ricerca sul Cancro), projects n. IG20122. A.D.L. was supported by a fellowship from PAC (Progetto Strategico Regionale Calabria Alta Formazione) Calabria 2014/2020—Asse Prioritario 12, Linea B, Azione 10.5.12; P.A. was supported by a post-doc fellowship 2021 from Fondazione Umberto Veronesi (FUV).

Data Availability Statement: Not applicable.

Conflicts of Interest: The authors declare no conflict of interest.

Abbreviations

AKT	protein kinase B
AMPK	adenosine monophosphate (AMP)-activated protein kinase
AP-1	activator protein1
APC	adenomatous polyposis coli

ARE	antioxidant response element
AUC	area under curve
AuNPs	gold nanoparticles
Bcl-2	B-cell lymphoma 2
Bcl-xL	B-cell lymphoma-extra large
cAMP	cyclic adenosine monophosphate
CDK2	cyclin-dependent kinase 2
CDK4	cyclin-dependent kinase 4
CD	cyclodextrin
cGMP	cyclic guanosin monophosphate
CNrasGEFs	cyclic nucleotide-ras guanine nucleotide exchange factors
COX2	cyclooxygenase-2
CPC	curcumin phospholipid complex
CUR	curcumin
CUR-CD-CS	curcumin-loaded cyclodextrin chitosan
CUR-MMs	curcumin mixed micelles
CUR-MPP-TPGS-MMs	curcumin-loaded methoxy poly(ethylene glycol)-poly(lactide) (mPEG-PLA)/D-α-tocopherol polyethylene glycol 1000 succinate (TPGS) mixed micelles
CUR-PSMNPs	curcumin pluronic stabilized Fe3O4 magnetic nanoparticles
CUR-SF NPs	curcumin silk fibroin nanoparticles
DAPs	diarylpentanoids
DDAB	dimethyl dioctadecyl ammonium bromide
DFMO	difluoro-methylornithine
DHC	dihydrocurcumin
DMPC	dimyristoyl phosphatidylcholine
DNMT1	DNA methyltransferase 1
E2F4	E2F trascription factor 4
EGFR	epidermal growth factor receptor
Egr-1	early growth response 1
EMT	epithelial mesenchymal transition
ERK	extracellulare signal-regulated kinase
EZH2	enhancer of zeste homolog 2
FA	folic acid
FA-CUR-NPs	folate receptor-targeted β-cyclodextrin nanoparticles
Fas	fas-associated protein with death domain
FAS	fatty acid synthase
FRs	folic receptors
GSH	glutathione
GSK3β	glycogen synthase kinase 3 beta
HA-CUR@AuNPs	hyaluronic acid curcumin gold nanoparticles
HDGF	hepatoma-derived growth factor
HER2	human epidermal growth factor receptor 2
HHC	hexahydrocurcumin
HIF-1α	hypoxia-inducible factor 1-alpha
HPH	high pressure homogenization
IAP-2	inhibitor of apoptosis protein-2
ICAM1	intercellular adhesion molecule 1
IC50	half-maximal inhibitory concentration
IFN-g	interferon gamma
IkB	inhibitor of KB
IKK	IκB kinase
IL-6	interleukin-6
JAK2	janus kinase 2
JNK	c-jun-N-terminal kinase
LPA	lysophosphatidic acid
LRP6	LDL (low density lipoprotein) receptor related protein 6

MAPK	mitogen-activated protein kinase
Mcl-1	myeloid cell leukemia 1
MDM2	mouse double minute 2 homolog
MePEG-b-PCL	methoxy poly (ethylene glycol) -block-polycaprolactone
miRNA	microRNA
MMPs	matrix metalloproteinases
MNPs	magnetic nanoparticles
MPEG-P [CL-co-PDO]	methoxy poly (ethylene glycol) -b-poly (ε-caprolactone-co-dioxanone)
mPEG–PCL	methoxy poly(ethylene glycol)–polycaprolactone
mTOR	mechanistic target of rapamycin
MUC1	mucin 1
NaCas	sodium caseinate
NaCas-Lac	sodium caseinate-lactose
NF-κB	nuclear factor-κB
NIPAAM	N-isopropylacrylamide
NPs	nanoparticles
NSCLC	non-small cell lung cancer
NVP	N-vinyl-2-pyrrolidone
ODC	ornithine decarboxylase
OHC	octahydrocurcumin
OPN	osteopontin
PAK1	p21 (RAC1) activated kinase 1
PARP-1	poly (ADP-ribose) polymerase 1
PCL	poly-(ε-caprolactone)
PCNA	proliferating cell nuclear antigen
PDE	cyclic nucleotide phosphodiesterase
PDE1A	phosphodiesterase 1A
PEG	polyethylene glycol
PEG-A	poly(ethylene glycol) monoacrylate
PGA	polyglycolide acid
P-gp	p-glycoprotein 1
PI3K	phosphoinositide 3-kinase
PLA	polylactide
PLGA	polylactic-co-glycolic acid
PSMNPs	pluronic stabilized Fe3O4 magnetic nanoparticles
PSBMA	poly (sulphobetaine methacrylate)
RhoA	ras homolog family member A
ROCK1	rho associated coiled-coil containing protein kinase 1
ROS	reactive oxygen species
SCLC	small cell lung cancer
SDs	solid dispersions
SIP1	smad interacting protein 1
SLNs	solid lipid nanoparticles
SMOX	spermine oxidase
STAT3	signal transducer and activator of transcription 3
SULT	sulfotransferase
THC	tetrahydrocurcumin
TNF-α	tumor necrosis factor-a
TPGS	d-α-Tocopheryl polyethylene glycol 1000 succinate
UGT	UDP-glucurosyltransferase
UHRF1	ubiquitin like with PHD and ring finger domain 1
u-PA	urokinase-type plasminogen activator
VEGF	vascular endothelial growth factor
VHL	Von Hippel-Lindau tumor suppressor
VP	N-vinyl-2-pyrrolidone
XIAP	X-linked inhibitor of apoptosis protein
β-CD	β- cyclodextrins
εCL	ε-caprolactone

References

1. Prasad, S.; Aggarwal, B.B. Turmeric, the golden spice: From traditional medicine to modern medicine. In *Herbal Medicine: Biomolecular and Clinical Aspects*; Benzie, I.F.F., Wachtel-Galor, S., Eds.; CRC Press: Boca Raton, FL, USA, 2011.
2. Sandur, S.K.; Pandey, M.K.; Sung, B.; Ahn, K.S.; Murakami, A.; Sethi, G.; Limtrakul, P.; Badmaev, V.; Aggarwal, B.B. Curcumin, demethoxycurcumin, bisdemethoxycurcumin, tetrahydrocurcumin and turmerones differentially regulate anti-inflammatory and anti-proliferative responses through a ROS-independent mechanism. *Carcinogenesis* **2007**, *28*, 1765–1773. [CrossRef]
3. Dosoky, N.S.; Satyal, P.; Setzer, W.N. Variations in the volatile compositions of Curcuma species. *Foods* **2019**, *8*, 53. [CrossRef] [PubMed]
4. Kunnumakkara, A.B.; Bordoloi, D.; Padmavathi, G.; Monisha, J.; Roy, N.K.; Prasad, S.; Aggarwal, B.B. Curcumin, the golden nutraceutical: Multitargeting for multiple chronic diseases. *Br. J. Pharm.* **2017**, *174*, 1325–1348. [CrossRef] [PubMed]
5. Patel, S.S.; Acharya, A.; Ray, R.S.; Agrawal, R.; Raghuwanshi, R.; Jain, P. Cellular and molecular mechanisms of curcumin in prevention and treatment of disease. *Crit. Rev. Food Sci. Nutr.* **2020**, *60*, 887–939. [CrossRef] [PubMed]
6. Adamczak, A.; Ozarowski, M.; Karpinski, T.M. Curcumin, a natural antimicrobial agent with strain-specific activity. *Pharmaceuticals* **2020**, *13*, 153. [CrossRef]
7. Jennings, M.R.; Parks, R.J. Curcumin as an antiviral agent. *Viruses* **2020**, *12*, 1242. [CrossRef]
8. Chen, C.; Long, L.; Zhang, F.; Chen, Q.; Chen, C.; Yu, X.; Liu, Q.; Bao, J.; Long, Z. Antifungal activity, main active components and mechanism of Curcuma longa extract against *Fusarium graminearum*. *PLoS ONE* **2018**, *13*, e0194284. [CrossRef]
9. Jagetia, G.C. Antioxidant activity of curcumin protects against the radiation-induced micronuclei formation in cultured human peripheral blood lymphocytes exposed to various doses of gamma-Radiation. *Int. J. Radiat. Biol.* **2021**, *97*, 485–493. [CrossRef]
10. Busari, Z.A.; Dauda, K.A.; Morenikeji, O.A.; Afolayan, F.; Oyeyemi, O.T.; Meena, J.; Sahu, D.; Panda, A.K. Antiplasmodial activity and toxicological assessment of curcumin PLGA-encapsulated nanoparticles. *Front. Pharm.* **2017**, *8*, 622. [CrossRef]
11. Fadus, M.C.; Lau, C.; Bikhchandani, J.; Lynch, H.T. Curcumin: An age-old anti-inflammatory and anti-neoplastic agent. *J. Tradit. Complement. Med.* **2017**, *7*, 339–346. [CrossRef]
12. Zia, A.; Farkhondeh, T.; Pourbagher-Shahri, A.M.; Samarghandian, S. The role of curcumin in aging and senescence: Molecular mechanisms. *Biomed. Pharmacother. Biomed. Pharmacother.* **2021**, *134*, 111119. [CrossRef]
13. Wang, H.; Zhang, K.; Liu, J.; Yang, J.; Tian, Y.; Yang, C.; Li, Y.; Shao, M.; Su, W.; Song, N. Curcumin regulates cancer progression: Focus on ncRNAs and molecular signaling pathways. *Front. Oncol.* **2021**, *11*, 660712. [CrossRef] [PubMed]
14. Kunnumakkara, A.B.; Bordoloi, D.; Harsha, C.; Banik, K.; Gupta, S.C.; Aggarwal, B.B. Curcumin mediates anticancer effects by modulating multiple cell signaling pathways. *Clin. Sci.* **2017**, *131*, 1781–1799. [CrossRef] [PubMed]
15. Kim, M.J.; Park, K.S.; Kim, K.T.; Gil, E.Y. The inhibitory effect of curcumin via fascin suppression through JAK/STAT3 pathway on metastasis and recurrence of ovary cancer cells. *BMC Women's Health* **2020**, *20*, 256. [CrossRef]
16. Liu, J.L.; Pan, Y.Y.; Chen, O.; Luan, Y.; Xue, X.; Zhao, J.J.; Liu, L.; Jia, H.Y. Curcumin inhibits MCF-7 cells by modulating the NF-kappaB signaling pathway. *Oncol. Lett.* **2017**, *14*, 5581–5584. [CrossRef] [PubMed]
17. Ghasemi, F.; Shafiee, M.; Banikazemi, Z.; Pourhanifeh, M.H.; Khanbabaei, H.; Shamshirian, A.; Amiri Moghadam, S.; ArefNezhad, R.; Sahebkar, A.; Avan, A.; et al. Curcumin inhibits NF-kB and Wnt/beta-catenin pathways in cervical cancer cells. *Pathol. Res. Pract.* **2019**, *215*, 152556. [CrossRef] [PubMed]
18. Kuttikrishnan, S.; Siveen, K.S.; Prabhu, K.S.; Khan, A.Q.; Ahmed, E.I.; Akhtar, S.; Ali, T.A.; Merhi, M.; Dermime, S.; Steinhoff, M.; et al. Curcumin induces apoptotic cell death via inhibition of PI3-kinase/AKT pathway in B-precursor acute lymphoblastic leukemia. *Front. Oncol.* **2019**, *9*, 484. [CrossRef]
19. Mortezaee, K.; Salehi, E.; Mirtavoos-Mahyari, H.; Motevaseli, E.; Najafi, M.; Farhood, B.; Rosengren, R.J.; Sahebkar, A. Mechanisms of apoptosis modulation by curcumin: Implications for cancer therapy. *J. Cell. Physiol.* **2019**, *234*, 12537–12550. [CrossRef]
20. Wahlstrom, B.; Blennow, G. A study on the fate of curcumin in the rat. *Acta Pharmacol. Toxicol.* **1978**, *43*, 86–92. [CrossRef]
21. Anand, P.; Kunnumakkara, A.B.; Newman, R.A.; Aggarwal, B.B. Bioavailability of curcumin: Problems and promises. *Mol. Pharm.* **2007**, *4*, 807–818. [CrossRef]
22. Tomeh, M.A.; Hadianamrei, R.; Zhao, X. A review of curcumin and its derivatives as anticancer agents. *Int. J. Mol. Sci.* **2019**, *20*, 1033. [CrossRef] [PubMed]
23. Li, W.; He, Y.; Zhang, R.; Zheng, G.; Zhou, D. The curcumin analog EF24 is a novel senolytic agent. *Aging* **2019**, *11*, 771–782. [CrossRef] [PubMed]
24. He, Y.; Li, W.; Hu, G.; Sun, H.; Kong, Q. Bioactivities of EF24, a novel curcumin analog: A review. *Front. Oncol.* **2018**, *8*, 614. [CrossRef] [PubMed]
25. Jamwal, R. Bioavailable curcumin formulations: A review of pharmacokinetic studies in healthy volunteers. *J. Integr. Med.* **2018**, *16*, 367–374. [CrossRef] [PubMed]
26. Adiwidjaja, J.; McLachlan, A.J.; Boddy, A.V. Curcumin as a clinically-promising anti-cancer agent: Pharmacokinetics and drug interactions. *Expert Opin. Drug Metab. Toxicol.* **2017**, *13*, 953–972. [CrossRef] [PubMed]
27. Olotu, F.; Agoni, C.; Soremekun, O.; Soliman, M.E.S. An update on the pharmacological usage of curcumin: Has it failed in the drug discovery pipeline? *Cell Biochem. Biophys.* **2020**, *78*, 267–289. [CrossRef]
28. Yallapu, M.M.; Nagesh, P.K.; Jaggi, M.; Chauhan, S.C. Therapeutic applications of curcumin nanoformulations. *AAPS J.* **2015**, *17*, 1341–1356. [CrossRef]

29. Karthikeyan, A.; Senthil, N.; Min, T. Nanocurcumin: A promising candidate for therapeutic applications. *Front. Pharmacol.* **2020**, *11*, 487. [CrossRef]
30. Ma, Z.; Wang, N.; He, H.; Tang, X. Pharmaceutical strategies of improving oral systemic bioavailability of curcumin for clinical application. *J. Control. Release Off. J. Control. Release Soc.* **2019**, *316*, 359–380. [CrossRef]
31. Kotecha, R.; Takami, A.; Espinoza, J.L. Dietary phytochemicals and cancer chemoprevention: A review of the clinical evidence. *Oncotarget* **2016**, *7*, 52517–52529. [CrossRef]
32. Rahmani, A.H.; Al Zohairy, M.A.; Aly, S.M.; Khan, M.A. Curcumin: A potential candidate in prevention of cancer via modulation of molecular pathways. *BioMed Res. Int.* **2014**, *2014*, 761608. [CrossRef] [PubMed]
33. Song, X.; Zhang, M.; Dai, E.; Luo, Y. Molecular targets of curcumin in breast cancer (Review). *Mol. Med. Rep.* **2019**, *19*, 23–29. [CrossRef] [PubMed]
34. Mukhopadhyay, A.; Banerjee, S.; Stafford, L.J.; Xia, C.; Liu, M.; Aggarwal, B.B. Curcumin-induced suppression of cell proliferation correlates with down-regulation of cyclin D1 expression and CDK4-mediated retinoblastoma protein phosphorylation. *Oncogene* **2002**, *21*, 8852–8861. [CrossRef] [PubMed]
35. Zhou, Q.M.; Wang, X.F.; Liu, X.J.; Zhang, H.; Lu, Y.Y.; Su, S.B. Curcumin enhanced antiproliferative effect of mitomycin C in human breast cancer MCF-7 cells in vitro and in vivo. *Acta Pharmacol. Sin.* **2011**, *32*, 1402–1410. [CrossRef]
36. Aggarwal, B.B.; Banerjee, S.; Bharadwaj, U.; Sung, B.; Shishodia, S.; Sethi, G. Curcumin induces the degradation of cyclin E expression through ubiquitin-dependent pathway and up-regulates cyclin-dependent kinase inhibitors p21 and p27 in multiple human tumor cell lines. *Biochem. Pharmacol.* **2007**, *73*, 1024–1032. [CrossRef]
37. Prasad, C.P.; Rath, G.; Mathur, S.; Bhatnagar, D.; Ralhan, R. Potent growth suppressive activity of curcumin in human breast cancer cells: Modulation of Wnt/beta-catenin signaling. *Chem. Biol. Interact.* **2009**, *181*, 263–271. [CrossRef]
38. Colomer, C.; Marruecos, L.; Vert, A.; Bigas, A.; Espinosa, L. NF-kappaB members left home: NF-kappaB-independent roles in cancer. *Biomedicines* **2017**, *5*, 26. [CrossRef]
39. Zhou, Q.; Ye, M.; Lu, Y.; Zhang, H.; Chen, Q.; Huang, S.; Su, S. Curcumin improves the tumoricidal effect of mitomycin C by suppressing ABCG2 expression in stem cell-like breast cancer cells. *PLoS ONE* **2015**, *10*, e0136694. [CrossRef]
40. Zhou, X.; Jiao, D.; Dou, M.; Zhang, W.; Lv, L.; Chen, J.; Li, L.; Wang, L.; Han, X. Curcumin inhibits the growth of triple-negative breast cancer cells by silencing EZH2 and restoring DLC1 expression. *J. Cell. Mol. Med.* **2020**, *24*, 10648–10662. [CrossRef]
41. Chase, A.; Cross, N.C. Aberrations of EZH2 in cancer. *Clin. Cancer Res.* **2011**, *17*, 2613–2618. [CrossRef] [PubMed]
42. Ren, G.; Li, G. Tumor suppressor gene DLC1: Its modifications, interactive molecules, and potential prospects for clinical cancer application. *Int. J. Biol. Macromol.* **2021**, *182*, 264–275. [CrossRef] [PubMed]
43. Pricci, M.; Girardi, B.; Giorgio, F.; Losurdo, G.; Ierardi, E.; Di Leo, A. Curcumin and colorectal cancer: From basic to clinical evidences. *Int. J. Mol. Sci.* **2020**, *21*, 2364. [CrossRef]
44. Calibasi-Kocal, G.; Pakdemirli, A.; Bayrak, S.; Ozupek, N.M.; Sever, T.; Basbinar, Y.; Ellidokuz, H.; Yigitbasi, T. Curcumin effects on cell proliferation, angiogenesis and metastasis in colorectal cancer. *J. BUON Off. J. Balk. Union Oncol.* **2019**, *24*, 1482–1487.
45. Lim, T.G.; Lee, S.Y.; Huang, Z.; Lim, D.Y.; Chen, H.; Jung, S.K.; Bode, A.M.; Lee, K.W.; Dong, Z. Curcumin suppresses proliferation of colon cancer cells by targeting CDK2. *Cancer Prev. Res.* **2014**, *7*, 466–474. [CrossRef]
46. Kim, K.C.; Lee, C. Curcumin induces downregulation of E2F4 expression and apoptotic cell death in HCT116 human colon cancer cells; Involvement of reactive oxygen species. *Korean J. Physiol. Pharmacol. Off. J. Korean Physiol. Soc. Korean Soc. Pharmacol.* **2010**, *14*, 391–397. [CrossRef]
47. Watson, J.L.; Hill, R.; Yaffe, P.B.; Greenshields, A.; Walsh, M.; Lee, P.W.; Giacomantonio, C.A.; Hoskin, D.W. Curcumin causes superoxide anion production and p53-independent apoptosis in human colon cancer cells. *Cancer Lett.* **2010**, *297*, 1–8. [CrossRef] [PubMed]
48. Mosieniak, G.; Adamowicz, M.; Alster, O.; Jaskowiak, H.; Szczepankiewicz, A.A.; Wilczynski, G.M.; Ciechomska, I.A.; Sikora, E. Curcumin induces permanent growth arrest of human colon cancer cells: Link between senescence and autophagy. *Mech. Ageing Dev.* **2012**, *133*, 444–455. [CrossRef] [PubMed]
49. Zhang, L.; Yang, G.; Zhang, R.; Dong, L.; Chen, H.; Bo, J.; Xue, W.; Huang, Y. Curcumin inhibits cell proliferation and motility via suppression of TROP2 in bladder cancer cells. *Int. J. Oncol.* **2018**, *53*, 515–526. [CrossRef]
50. Shi, J.; Zhang, X.; Shi, T.; Li, H. Antitumor effects of curcumin in human bladder cancer in vitro. *Oncol. Lett.* **2017**, *14*, 1157–1161. [CrossRef] [PubMed]
51. Walker, B.C.; Mittal, S. Antitumor activity of curcumin in glioblastoma. *Int. J. Mol. Sci.* **2020**, *21*, 9435. [CrossRef]
52. Choi, B.H.; Kim, C.G.; Bae, Y.S.; Lim, Y.; Lee, Y.H.; Shin, S.Y. P21(Waf1/Cip1) expression by curcumin in U-87MG human glioma cells: Role of early growth response-1 expression. *Cancer Res.* **2008**, *68*, 1369–1377. [CrossRef] [PubMed]
53. Cheng, C.; Jiao, J.T.; Qian, Y.; Guo, X.Y.; Huang, J.; Dai, M.C.; Zhang, L.; Ding, X.P.; Zong, D.; Shao, J.F. Curcumin induces G2/M arrest and triggers apoptosis via FoxO1 signaling in U87 human glioma cells. *Mol. Med. Rep.* **2016**, *13*, 3763–3770. [CrossRef] [PubMed]
54. Wang, L.; Ye, X.; Cai, X.; Su, J.; Ma, R.; Yin, X.; Zhou, X.; Li, H.; Wang, Z. Curcumin suppresses cell growth and invasion and induces apoptosis by down-regulation of Skp2 pathway in glioma cells. *Oncotarget* **2015**, *6*, 18027–18037. [CrossRef] [PubMed]
55. Wu, J.; Su, H.K.; Yu, Z.H.; Xi, S.Y.; Guo, C.C.; Hu, Z.Y.; Qu, Y.; Cai, H.P.; Zhao, Y.Y.; Zhao, H.F.; et al. Skp2 modulates proliferation, senescence and tumorigenesis of glioma. *Cancer Cell Int.* **2020**, *20*, 71. [CrossRef]

56. Luo, Q.; Luo, H.; Fu, H.; Huang, H.; Huang, H.; Luo, K.; Li, C.; Hu, R.; Zheng, C.; Lan, C.; et al. Curcumin suppresses invasiveness and migration of human glioma cells in vitro by inhibiting HDGF/beta-catenin complex. *Nan Fang Yi Ke Da Xue Xue Bao J. South. Med. Univ.* **2019**, *39*, 911–916. [CrossRef]
57. Fratantonio, D.; Molonia, M.S.; Bashllari, R.; Muscara, C.; Ferlazzo, G.; Costa, G.; Saija, A.; Cimino, F.; Speciale, A. Curcumin potentiates the antitumor activity of Paclitaxel in rat glioma C6 cells. *Phytomed. Int. J. Phytother. Phytopharm.* **2019**, *55*, 23–30. [CrossRef]
58. Seyithanoglu, M.H.; Abdallah, A.; Kitis, S.; Guler, E.M.; Kocyigit, A.; Dundar, T.T.; Gundag Papaker, M. Investigation of cytotoxic, genotoxic, and apoptotic effects of curcumin on glioma cells. *Cell. Mol. Biol.* **2019**, *65*, 101–108. [CrossRef]
59. Murray-Stewart, T.; Dunworth, M.; Lui, Y.; Giardiello, F.M.; Woster, P.M.; Casero, R.A., Jr. Curcumin mediates polyamine metabolism and sensitizes gastrointestinal cancer cells to antitumor polyamine-targeted therapies. *PLoS ONE* **2018**, *13*, e0202677. [CrossRef]
60. Cai, X.Z.; Wang, J.; Li, X.D.; Wang, G.L.; Liu, F.N.; Cheng, M.S.; Li, F. Curcumin suppresses proliferation and invasion in human gastric cancer cells by downregulation of PAK1 activity and cyclin D1 expression. *Cancer Biol. Ther.* **2009**, *8*, 1360–1368. [CrossRef]
61. Zheng, R.; Deng, Q.; Liu, Y.; Zhao, P. Curcumin inhibits gastric carcinoma cell growth and induces apoptosis by suppressing the Wnt/beta-catenin signaling pathway. *Med. Sci. Monit. Int. Med. J. Exp. Clin. Res.* **2017**, *23*, 163–171. [CrossRef]
62. Fu, H.; Wang, C.; Yang, D.; Wei, Z.; Xu, J.; Hu, Z.; Zhang, Y.; Wang, W.; Yan, R.; Cai, Q. Curcumin regulates proliferation, autophagy, and apoptosis in gastric cancer cells by affecting PI3K and P53 signaling. *J. Cell. Physiol.* **2018**, *233*, 4634–4642. [CrossRef]
63. Liu, G.; Xiang, T.; Wu, Q.F.; Wang, W.X. Curcumin suppresses the proliferation of gastric cancer cells by downregulating H19. *Oncol. Lett.* **2016**, *12*, 5156–5162. [CrossRef]
64. Ghafouri-Fard, S.; Esmaeili, M.; Taheri, M. H19 lncRNA: Roles in tumorigenesis. *Biomed. Pharmacother.* **2020**, *123*, 109774. [CrossRef]
65. Yang, F.; Bi, J.; Xue, X.; Zheng, L.; Zhi, K.; Hua, J.; Fang, G. Up-regulated long non-coding RNA H19 contributes to proliferation of gastric cancer cells. *FEBS J.* **2012**, *279*, 3159–3165. [CrossRef]
66. Yoshimura, H.; Matsuda, Y.; Yamamoto, M.; Kamiya, S.; Ishiwata, T. Expression and role of long non-coding RNA H19 in carcinogenesis. *Front. Biosci.* **2018**, *23*, 614–625. [CrossRef]
67. Sun, C.; Zhang, S.; Liu, C.; Liu, X. Curcumin promoted miR-34a expression and suppressed proliferation of gastric cancer cells. *Cancer Biother. Radiopharm.* **2019**, *34*, 634–641. [CrossRef]
68. Sun, Q.; Zhang, W.; Guo, Y.; Li, Z.; Chen, X.; Wang, Y.; Du, Y.; Zang, W.; Zhao, G. Curcumin inhibits cell growth and induces cell apoptosis through upregulation of miR-33b in gastric cancer. *Tumor Biol. J. Int. Soc. Oncodev. Biol. Med.* **2016**, *37*, 13177–13184. [CrossRef] [PubMed]
69. Nabavi, S.M.; Russo, G.L.; Tedesco, I.; Daglia, M.; Orhan, I.E.; Nabavi, S.F.; Bishayee, A.; Nagulapalli Venkata, K.C.; Abdollahi, M.; Hajheydari, Z. Curcumin and melanoma: From chemistry to medicine. *Nutr. Cancer* **2018**, *70*, 164–175. [CrossRef] [PubMed]
70. Zheng, M.; Ekmekcioglu, S.; Walch, E.T.; Tang, C.H.; Grimm, E.A. Inhibition of nuclear factor-kappaB and nitric oxide by curcumin induces G2/M cell cycle arrest and apoptosis in human melanoma cells. *Melanoma Res.* **2004**, *14*, 165–171. [CrossRef] [PubMed]
71. Abusnina, A.; Keravis, T.; Yougbare, I.; Bronner, C.; Lugnier, C. Anti-proliferative effect of curcumin on melanoma cells is mediated by PDE1A inhibition that regulates the epigenetic integrator UHRF1. *Mol. Nutr. Food Res.* **2011**, *55*, 1677–1689. [CrossRef]
72. Zhao, G.; Han, X.; Zheng, S.; Li, Z.; Sha, Y.; Ni, J.; Sun, Z.; Qiao, S.; Song, Z. Curcumin induces autophagy, inhibits proliferation and invasion by downregulating AKT/mTOR signaling pathway in human melanoma cells. *Oncol. Rep.* **2016**, *35*, 1065–1074. [CrossRef] [PubMed]
73. Siwak, D.R.; Shishodia, S.; Aggarwal, B.B.; Kurzrock, R. Curcumin-induced antiproliferative and proapoptotic effects in melanoma cells are associated with suppression of I kappa B kinase and nuclear factor KB activity and are independent of the B-Raf/mitogen-activated/extracellular signal-regulated protein kinase pathway and the Akt pathway. *Cancer* **2005**, *104*, 879–890. [CrossRef] [PubMed]
74. Cianfruglia, L.; Minnelli, C.; Laudadio, E.; Scire, A.; Armeni, T. Side effects of curcumin: Epigenetic and antiproliferative implications for normal dermal fibroblast and breast cancer cells. *Antioxidants* **2019**, *8*, 382. [CrossRef] [PubMed]
75. Talib, W.H.; Al-Hadid, S.A.; Ali, M.B.W.; Al-Yasari, I.H.; Ali, M.R.A. Role of curcumin in regulating p53 in breast cancer: An overview of the mechanism of action. *Breast Cancer* **2018**, *10*, 207–217. [CrossRef]
76. Bae, Y.H.; Ryu, J.H.; Park, H.J.; Kim, K.R.; Wee, H.J.; Lee, O.H.; Jang, H.O.; Bae, M.K.; Kim, K.W.; Bae, S.K. Mutant p53-Notch1 signaling axis is involved in curcumin-induced apoptosis of breast cancer cells. *Korean J. Physiol. Pharmacol. Off. J. Korean Physiol. Soc. Korean Soc. Pharmacol.* **2013**, *17*, 291–297. [CrossRef]
77. Patel, P.B.; Thakkar, V.R.; Patel, J.S. Cellular effect of curcumin and citral combination on breast cancer cells: Induction of apoptosis and cell cycle arrest. *J. Breast Cancer* **2015**, *18*, 225–234. [CrossRef]
78. Moghtaderi, H.; Sepehri, H.; Attari, F. Combination of arabinogalactan and curcumin induces apoptosis in breast cancer cells in vitro and inhibits tumor growth via overexpression of p53 level in vivo. *Biomed. Pharmacother.* **2017**, *88*, 582–594. [CrossRef]
79. Chiu, T.L.; Su, C.C. Curcumin inhibits proliferation and migration by increasing the Bax to Bcl-2 ratio and decreasing NF-kappaBp65 expression in breast cancer MDA-MB-231 cells. *Int. J. Mol. Med.* **2009**, *23*, 469–475. [CrossRef]

80. Fan, H.; Liang, Y.; Jiang, B.; Li, X.; Xun, H.; Sun, J.; He, W.; Lau, H.T.; Ma, X. Curcumin inhibits intracellular fatty acid synthase and induces apoptosis in human breast cancer MDA-MB-231 cells. *Oncol. Rep.* **2016**, *35*, 2651–2656. [CrossRef]
81. Zhang, Y.P.; Li, Y.Q.; Lv, Y.T.; Wang, J.M. Effect of curcumin on the proliferation, apoptosis, migration, and invasion of human melanoma A375 cells. *Genet. Mol. Res.* **2015**, *14*, 1056–1067. [CrossRef]
82. Bush, J.A.; Cheung, K.J., Jr.; Li, G. Curcumin induces apoptosis in human melanoma cells through a Fas receptor/caspase-8 pathway independent of p53. *Exp. Cell Res.* **2001**, *271*, 305–314. [CrossRef] [PubMed]
83. Watson, J.L.; Greenshields, A.; Hill, R.; Hilchie, A.; Lee, P.W.; Giacomantonio, C.A.; Hoskin, D.W. Curcumin-induced apoptosis in ovarian carcinoma cells is p53-independent and involves p38 mitogen-activated protein kinase activation and downregulation of Bcl-2 and survivin expression and Akt signaling. *Mol. Carcinog.* **2010**, *49*, 13–24. [CrossRef] [PubMed]
84. Li, W.; Wang, Y.; Song, Y.; Xu, L.; Zhao, J.; Fang, B. A preliminary study of the effect of curcumin on the expression of p53 protein in a human multiple myeloma cell line. *Oncol. Lett.* **2015**, *9*, 1719–1724. [CrossRef] [PubMed]
85. Lee, Y.K.; Park, S.Y.; Kim, Y.M.; Park, O.J. Regulatory effect of the AMPK-COX-2 signaling pathway in curcumin-induced apoptosis in HT-29 colon cancer cells. *Ann. N. Y. Acad. Sci.* **2009**, *1171*, 489–494. [CrossRef]
86. Sandur, S.K.; Deorukhkar, A.; Pandey, M.K.; Pabon, A.M.; Shentu, S.; Guha, S.; Aggarwal, B.B.; Krishnan, S. Curcumin modulates the radiosensitivity of colorectal cancer cells by suppressing constitutive and inducible NF-kappaB activity. *Int. J. Radiat. Oncol. Biol. Phys.* **2009**, *75*, 534–542. [CrossRef]
87. Narayan, S. Curcumin, a multi-functional chemopreventive agent, blocks growth of colon cancer cells by targeting beta-catenin-mediated transactivation and cell-cell adhesion pathways. *J. Mol. Histol.* **2004**, *35*, 301–307. [CrossRef]
88. Jung, E.M.; Lim, J.H.; Lee, T.J.; Park, J.W.; Choi, K.S.; Kwon, T.K. Curcumin sensitizes tumor necrosis factor-related apoptosis-inducing ligand (TRAIL)-induced apoptosis through reactive oxygen species-mediated upregulation of death receptor 5 (DR5). *Carcinogenesis* **2005**, *26*, 1905–1913. [CrossRef]
89. Cao, A.; Li, Q.; Yin, P.; Dong, Y.; Shi, H.; Wang, L.; Ji, G.; Xie, J.; Wu, D. Curcumin induces apoptosis in human gastric carcinoma AGS cells and colon carcinoma HT-29 cells through mitochondrial dysfunction and endoplasmic reticulum stress. *Apoptosis* **2013**, *18*, 1391–1402. [CrossRef]
90. Moragoda, L.; Jaszewski, R.; Majumdar, A.P. Curcumin induced modulation of cell cycle and apoptosis in gastric and colon cancer cells. *Anticancer Res.* **2001**, *21*, 873–878.
91. Su, C.C.; Lin, J.G.; Li, T.M.; Chung, J.G.; Yang, J.S.; Ip, S.W.; Lin, W.C.; Chen, G.W. Curcumin-induced apoptosis of human colon cancer colo 205 cells through the production of ROS, Ca^{2+} and the activation of caspase-3. *Anticancer Res.* **2006**, *26*, 4379–4389.
92. Klinger, N.V.; Mittal, S. Therapeutic potential of curcumin for the treatment of brain tumors. *Oxidative Med. Cell. Longev.* **2016**, *2016*, 9324085. [CrossRef]
93. Lee, D.S.; Lee, M.K.; Kim, J.H. Curcumin induces cell cycle arrest and apoptosis in human osteosarcoma (HOS) cells. *Anticancer Res.* **2009**, *29*, 5039–5044. [PubMed]
94. Yang, J.; Cao, Y.; Sun, J.; Zhang, Y. Curcumin reduces the expression of Bcl-2 by upregulating miR-15a and miR-16 in MCF-7 cells. *Med. Oncol.* **2010**, *27*, 1114–1118. [CrossRef]
95. Zhang, J.; Du, Y.; Wu, C.; Ren, X.; Ti, X.; Shi, J.; Zhao, F.; Yin, H. Curcumin promotes apoptosis in human lung adenocarcinoma cells through miR-186* signaling pathway. *Oncol. Rep.* **2010**, *24*, 1217–1223. [CrossRef]
96. Sohn, E.J.; Bak, K.M.; Nam, Y.K.; Park, H.T. Upregulation of microRNA 344a-3p is involved in curcumin induced apoptosis in RT4 schwannoma cells. *Cancer Cell Int.* **2018**, *18*, 199. [CrossRef]
97. Gao, D.; Mittal, V.; Ban, Y.; Lourenco, A.R.; Yomtoubian, S.; Lee, S. Metastatic tumor cells—Genotypes and phenotypes. *Front. Biol.* **2018**, *13*, 277–286. [CrossRef] [PubMed]
98. Gallardo, M.; Kemmerling, U.; Aguayo, F.; Bleak, T.C.; Munoz, J.P.; Calaf, G.M. Curcumin rescues breast cells from epithelialmesenchymal transition and invasion induced by antimiR34a. *Int. J. Oncol.* **2020**, *56*, 480–493. [CrossRef] [PubMed]
99. Pires, B.R.; Mencalha, A.L.; Ferreira, G.M.; de Souza, W.F.; Morgado-Diaz, J.A.; Maia, A.M.; Correa, S.; Abdelhay, E.S. NF-kappaB is involved in the regulation of EMT genes in breast cancer cells. *PLoS ONE* **2017**, *12*, e0169622. [CrossRef] [PubMed]
100. Zong, H.; Wang, F.; Fan, Q.X.; Wang, L.X. Curcumin inhibits metastatic progression of breast cancer cell through suppression of urokinase-type plasminogen activator by NF-kappa B signaling pathways. *Mol. Biol. Rep.* **2012**, *39*, 4803–4808. [CrossRef]
101. Bachmeier, B.E.; Mohrenz, I.V.; Mirisola, V.; Schleicher, E.; Romeo, F.; Hohneke, C.; Jochum, M.; Nerlich, A.G.; Pfeffer, U. Curcumin downregulates the inflammatory cytokines CXCL1 and -2 in breast cancer cells via NFkappaB. *Carcinogenesis* **2008**, *29*, 779–789. [CrossRef]
102. Irani, S. Emerging insights into the biology of metastasis: A review article. *Iran. J. Basic Med. Sci.* **2019**, *22*, 833–847. [CrossRef] [PubMed]
103. Sun, K.; Duan, X.; Cai, H.; Liu, X.; Yang, Y.; Li, M.; Zhang, X.; Wang, J. Curcumin inhibits LPA-induced invasion by attenuating RhoA/ROCK/MMPs pathway in MCF7 breast cancer cells. *Clin. Exp. Med.* **2016**, *16*, 37–47. [CrossRef] [PubMed]
104. Li, Y.; Sun, W.; Han, N.; Zou, Y.; Yin, D. Curcumin inhibits proliferation, migration, invasion and promotes apoptosis of retinoblastoma cell lines through modulation of miR-99a and JAK/STAT pathway. *BMC Cancer* **2018**, *18*, 1230. [CrossRef]
105. Zaman, S.; Jadid, H.; Denson, A.C.; Gray, J.E. Targeting Trop-2 in solid tumors: Future prospects. *Onco Targets Ther.* **2019**, *12*, 1781–1790. [CrossRef] [PubMed]

106. Cheng, T.S.; Chen, W.C.; Lin, Y.Y.; Tsai, C.H.; Liao, C.I.; Shyu, H.Y.; Ko, C.J.; Tzeng, S.F.; Huang, C.Y.; Yang, P.C.; et al. Curcumin-targeting pericellular serine protease matriptase role in suppression of prostate cancer cell invasion, tumor growth, and metastasis. *Cancer Prev. Res.* **2013**, *6*, 495–505. [CrossRef] [PubMed]
107. Xiang, L.; He, B.; Liu, Q.; Hu, D.; Liao, W.; Li, R.; Peng, X.; Wang, Q.; Zhao, G. Antitumor effects of curcumin on the proliferation, migration and apoptosis of human colorectal carcinoma HCT116 cells. *Oncol. Rep.* **2020**, *44*, 1997–2008. [CrossRef]
108. Philip, S.; Kundu, G.C. Osteopontin induces nuclear factor kappa B-mediated promatrix metalloproteinase-2 activation through I kappa B alpha /IKK signaling pathways, and curcumin (diferulolylmethane) down-regulates these pathways. *J. Biol. Chem.* **2003**, *278*, 14487–14497. [CrossRef]
109. Jin, W. Role of JAK/STAT3 signaling in the regulation of metastasis, the transition of cancer stem cells, and chemoresistance of cancer by epithelial-mesenchymal transition. *Cells* **2020**, *9*, 217. [CrossRef]
110. Yang, C.L.; Liu, Y.Y.; Ma, Y.G.; Xue, Y.X.; Liu, D.G.; Ren, Y.; Liu, X.B.; Li, Y.; Li, Z. Curcumin blocks small cell lung cancer cells migration, invasion, angiogenesis, cell cycle and neoplasia through Janus kinase-STAT3 signalling pathway. *PLoS ONE* **2012**, *7*, e37960. [CrossRef]
111. Han, Z.; Zhang, J.; Zhang, K.; Zhao, Y. Curcumin inhibits cell viability, migration, and invasion of thymic carcinoma cells via downregulation of microRNA-27a. *Phytother. Res. PTR* **2020**, *34*, 1629–1637. [CrossRef]
112. Wang, N.; Feng, T.; Liu, X.; Liu, Q. Curcumin inhibits migration and invasion of non-small cell lung cancer cells through up-regulation of miR-206 and suppression of PI3K/AKT/mTOR signaling pathway. *Acta Pharm.* **2020**, *70*, 399–409. [CrossRef] [PubMed]
113. Wang, X.; Deng, J.; Yuan, J.; Tang, X.; Wang, Y.; Chen, H.; Liu, Y.; Zhou, L. Curcumin exerts its tumor suppressive function via inhibition of NEDD4 oncoprotein in glioma cancer cells. *Int. J. Oncol.* **2017**, *51*, 467–477. [CrossRef]
114. Zhang, H.; Nie, W.; Zhang, X.; Zhang, G.; Li, Z.; Wu, H.; Shi, Q.; Chen, Y.; Ding, Z.; Zhou, X.; et al. NEDD4-1 regulates migration and invasion of glioma cells through CNrasGEF ubiquitination in vitro. *PLoS ONE* **2013**, *8*, e82789. [CrossRef]
115. Ravindranath, V.; Chandrasekhara, N. Absorption and tissue distribution of curcumin in rats. *Toxicology* **1980**, *16*, 259–265. [CrossRef]
116. Pan, M.H.; Huang, T.M.; Lin, J.K. Biotransformation of curcumin through reduction and glucuronidation in mice. *Drug Metab. Dispos.* **1999**, *27*, 486–494.
117. Basile, V.; Ferrari, E.; Lazzari, S.; Belluti, S.; Pignedoli, F.; Imbriano, C. Curcumin derivatives: Molecular basis of their anti-cancer activity. *Biochem. Pharmacol.* **2009**, *78*, 1305–1315. [CrossRef]
118. Sribalan, R.; Kirubavathi, M.; Banuppriya, G.; Padmini, V. Synthesis and biological evaluation of new symmetric curcumin derivatives. *Bioorg. Med. Chem. Lett.* **2015**, *25*, 4282–4286. [CrossRef]
119. Bayomi, S.M.; El-Kashef, H.A.; El-Ashmawy, M.B.; Nasr, M.N.A.; El-Sherbeny, M.A.; Badria, F.A.; Abou-Zeid, L.A.; Ghaly, M.A.; Abdel-Aziz, N.I. Synthesis and biological evaluation of new curcumin derivatives as antioxidant and antitumor agents. *Med. Chem. Res.* **2013**, *22*, 1147–1162. [CrossRef]
120. Xu, G.; Chu, Y.; Jiang, N.; Yang, J.; Li, F. The three dimensional quantitative structure activity relationships (3D-QSAR) and docking studies of curcumin derivatives as androgen receptor antagonists. *Int. J. Mol. Sci.* **2012**, *13*, 6138–6155. [CrossRef] [PubMed]
121. Zhao, C.; Liu, Z.; Liang, G. Promising curcumin-based drug design: Mono-carbonyl analogues of curcumin (MACs). *Curr. Pharm. Des.* **2013**, *19*, 2114–2135. [PubMed]
122. Somparn, P.; Phisalaphong, C.; Nakornchai, S.; Unchern, S.; Morales, N.P. Comparative antioxidant activities of curcumin and its demethoxy and hydrogenated derivatives. *Biol. Pharm. Bull.* **2007**, *30*, 74–78. [CrossRef] [PubMed]
123. Anand, P.; Thomas, S.G.; Kunnumakkara, A.B.; Sundaram, C.; Harikumar, K.B.; Sung, B.; Tharakan, S.T.; Misra, K.; Priyadarsini, I.K.; Rajasekharan, K.N.; et al. Biological activities of curcumin and its analogues (Congeners) made by man and Mother Nature. *Biochem. Pharmacol.* **2008**, *76*, 1590–1611. [CrossRef] [PubMed]
124. Reddy, A.R.; Dinesh, P.; Prabhakar, A.S.; Umasankar, K.; Shireesha, B.; Raju, M.B. A comprehensive review on SAR of curcumin. *Mini Rev. Med. Chem.* **2013**, *13*, 1769–1777. [CrossRef] [PubMed]
125. Sherin, D.R.; Rajasekharan, K.N. Mechanochemical synthesis and antioxidant activity of curcumin-templated azoles. *Arch. Pharm.* **2015**, *348*, 908–914. [CrossRef]
126. Wanninger, S.; Lorenz, V.; Subhan, A.; Edelmann, F.T. Metal complexes of curcumin–synthetic strategies, structures and medicinal applications. *Chem. Soc. Rev.* **2015**, *44*, 4986–5002. [CrossRef]
127. Paulraj, F.; Abas, F.; Lajis, N.H.; Othman, I.; Naidu, R. Molecular pathways modulated by curcumin analogue, diarylpentanoids in cancer. *Biomolecules* **2019**, *9*, 270. [CrossRef]
128. Yerdelen, K.O.; Gul, H.I.; Sakagami, H.; Umemura, N.; Sukuroglu, M. Synthesis and cytotoxic activities of a curcumin analogue and its bis-mannich derivatives. *Lett. Drug Des. Discov.* **2015**, *12*, 643–649. [CrossRef]
129. Reid, J.M.; Buhrow, S.A.; Gilbert, J.A.; Jia, L.; Shoji, M.; Snyder, J.P.; Ames, M.M. Mouse pharmacokinetics and metabolism of the curcumin analog, 4-piperidinone,3,5-bis[(2-fluorophenyl)methylene]-acetate(3E,5E) (EF-24; NSC 716993). *Cancer Chemother. Pharmacol.* **2014**, *73*, 1137–1146. [CrossRef]
130. Selvendiran, K.; Tong, L.; Vishwanath, S.; Bratasz, A.; Trigg, N.J.; Kutala, V.K.; Hideg, K.; Kuppusamy, P. EF24 induces G2/M arrest and apoptosis in cisplatin-resistant human ovarian cancer cells by increasing PTEN expression. *J. Biol. Chem.* **2007**, *282*, 28609–28618. [CrossRef]

131. He, G.; Feng, C.; Vinothkumar, R.; Chen, W.; Dai, X.; Chen, X.; Ye, Q.; Qiu, C.; Zhou, H.; Wang, Y.; et al. Curcumin analog EF24 induces apoptosis via ROS-dependent mitochondrial dysfunction in human colorectal cancer cells. *Cancer Chemother. Pharmacol.* **2016**, *78*, 1151–1161. [CrossRef]
132. Kasinski, A.L.; Du, Y.; Thomas, S.L.; Zhao, J.; Sun, S.Y.; Khuri, F.R.; Wang, C.Y.; Shoji, M.; Sun, A.; Snyder, J.P.; et al. Inhibition of IkappaB kinase-nuclear factor-kappaB signaling pathway by 3,5-bis(2-flurobenzylidene)piperidin-4-one (EF24), a novel monoketone analog of curcumin. *Mol. Pharmacol.* **2008**, *74*, 654–661. [CrossRef]
133. Thomas, S.L.; Zhong, D.; Zhou, W.; Malik, S.; Liotta, D.; Snyder, J.P.; Hamel, E.; Giannakakou, P. EF24, a novel curcumin analog, disrupts the microtubule cytoskeleton and inhibits HIF-1. *Cell Cycle* **2008**, *7*, 2409–2417. [CrossRef]
134. Tan, X.; Sidell, N.; Mancini, A.; Huang, R.P.; Shenming, W.; Horowitz, I.R.; Liotta, D.C.; Taylor, R.N.; Wieser, F. Multiple anticancer activities of EF24, a novel curcumin analog, on human ovarian carcinoma cells. *Reprod. Sci.* **2010**, *17*, 931–940. [CrossRef]
135. Yu, H.; Lin, L.; Zhang, Z.; Zhang, H.; Hu, H. Targeting NF-kappaB pathway for the therapy of diseases: Mechanism and clinical study. *Signal Transduct. Target. Ther.* **2020**, *5*, 209. [CrossRef] [PubMed]
136. Yin, D.L.; Liang, Y.J.; Zheng, T.S.; Song, R.P.; Wang, J.B.; Sun, B.S.; Pan, S.H.; Qu, L.D.; Liu, J.R.; Jiang, H.C.; et al. EF24 inhibits tumor growth and metastasis via suppressing NF-kappaB dependent pathways in human cholangiocarcinoma. *Sci. Rep.* **2016**, *6*, 32167. [CrossRef] [PubMed]
137. Aravindan, S.; Natarajan, M.; Herman, T.S.; Awasthi, V.; Aravindan, N. Molecular basis of 'hypoxic' breast cancer cell radiosensitization: Phytochemicals converge on radiation induced Rel signaling. *Radiat. Oncol* **2013**, *8*, 46. [CrossRef] [PubMed]
138. Aravindan, S.; Natarajan, M.; Awasthi, V.; Herman, T.S.; Aravindan, N. Novel synthetic monoketone transmute radiation-triggered NFkappaB-dependent TNFalpha cross-signaling feedback maintained NFkappaB and favors neuroblastoma regression. *PLoS ONE* **2013**, *8*, e72464. [CrossRef]
139. Liang, Y.; Zheng, T.; Song, R.; Wang, J.; Yin, D.; Wang, L.; Liu, H.; Tian, L.; Fang, X.; Meng, X.; et al. Hypoxia-mediated sorafenib resistance can be overcome by EF24 through Von Hippel-Lindau tumor suppressor-dependent HIF-1alpha inhibition in hepatocellular carcinoma. *Hepatology* **2013**, *57*, 1847–1857. [CrossRef] [PubMed]
140. Adams, B.K.; Cai, J.; Armstrong, J.; Herold, M.; Lu, Y.J.; Sun, A.; Snyder, J.P.; Liotta, D.C.; Jones, D.P.; Shoji, M. EF24, a novel synthetic curcumin analog, induces apoptosis in cancer cells via a redox-dependent mechanism. *Anti-Cancer Drugs* **2005**, *16*, 263–275. [CrossRef] [PubMed]
141. Zou, P.; Xia, Y.; Chen, W.; Chen, X.; Ying, S.; Feng, Z.; Chen, T.; Ye, Q.; Wang, Z.; Qiu, C.; et al. EF24 induces ROS-mediated apoptosis via targeting thioredoxin reductase 1 in gastric cancer cells. *Oncotarget* **2016**, *7*, 18050–18064. [CrossRef] [PubMed]
142. Selvendiran, K.; Ahmed, S.; Dayton, A.; Kuppusamy, M.L.; Rivera, B.K.; Kalai, T.; Hideg, K.; Kuppusamy, P. HO-3867, a curcumin analog, sensitizes cisplatin-resistant ovarian carcinoma, leading to therapeutic synergy through STAT3 inhibition. *Cancer Biol. Ther.* **2011**, *12*, 837–845. [CrossRef]
143. Ismail, N.I.; Othman, I.; Abas, F.; Lajis, N.H.; Naidu, R. The curcumin analogue, MS13 (1,5-Bis(4-hydroxy-3- methoxyphenyl)-1,4-pentadiene-3-one), inhibits cell proliferation and induces apoptosis in primary and metastatic human colon cancer cells. *Molecules* **2020**, *25*, 3798. [CrossRef] [PubMed]
144. Liang, G.; Shao, L.; Wang, Y.; Zhao, C.; Chu, Y.; Xiao, J.; Zhao, Y.; Li, X.; Yang, S. Exploration and synthesis of curcumin analogues with improved structural stability both in vitro and in vivo as cytotoxic agents. *Bioorg. Med. Chem.* **2009**, *17*, 2623–2631. [CrossRef]
145. Lin, L.; Shi, Q.; Nyarko, A.K.; Bastow, K.F.; Wu, C.C.; Su, C.Y.; Shih, C.C.; Lee, K.H. Antitumor agents. 250. Design and synthesis of new curcumin analogues as potential anti-prostate cancer agents. *J. Med. Chem.* **2006**, *49*, 3963–3972. [CrossRef] [PubMed]
146. Shen, H.; Shen, J.; Pan, H.; Xu, L.; Sheng, H.; Liu, B.; Yao, M. Curcumin analog B14 has high bioavailability and enhances the effect of anti-breast cancer cells in vitro and in vivo. *Cancer Sci.* **2021**, *112*, 815–827. [CrossRef] [PubMed]
147. Zheng, B.; McClements, D.J. Formulation of more efficacious curcumin delivery systems using colloid science: Enhanced solubility, stability, and bioavailability. *Molecules* **2020**, *25*, 2791. [CrossRef]
148. Bansal, S.S.; Goel, M.; Aqil, F.; Vadhanam, M.V.; Gupta, R.C. Advanced drug delivery systems of curcumin for cancer chemoprevention. *Cancer Prev. Res.* **2011**, *4*, 1158–1171. [CrossRef] [PubMed]
149. Munjal, B.; Pawar, Y.B.; Patel, S.B.; Bansal, A.K. Comparative oral bioavailability advantage from curcumin formulations. *Drug Deliv. Transl. Res.* **2011**, *1*, 322–331. [CrossRef]
150. Sun, M.; Su, X.; Ding, B.; He, X.; Liu, X.; Yu, A.; Lou, H.; Zhai, G. Advances in nanotechnology-based delivery systems for curcumin. *Nanomedicine* **2012**, *7*, 1085–1100. [CrossRef]
151. Praditya, D.; Kirchhoff, L.; Bruning, J.; Rachmawati, H.; Steinmann, J.; Steinmann, E. Anti-infective Properties of the Golden Spice Curcumin. *Front. Microbiol.* **2019**, *10*, 912. [CrossRef]
152. Yang, S.; Liu, L.; Han, J.; Tang, Y. Encapsulating plant ingredients for dermocosmetic application: An updated review of delivery systems and characterization techniques. *Int. J. Cosmet. Sci.* **2020**, *42*, 16–28. [CrossRef] [PubMed]
153. Li, R.; Lim, S.J.; Choi, H.G.; Lee, M.K. Solid lipid nanoparticles as drug delivery system for water-insoluble drugs. *J. Pharm. Investig.* **2010**, *40*, 63–73. [CrossRef]
154. Yallapu, M.M.; Jaggi, M.; Chauhan, S.C. beta-Cyclodextrin-curcumin self-assembly enhances curcumin delivery in prostate cancer cells. *Colloids Surf. B Biointerfaces* **2010**, *79*, 113–125. [CrossRef] [PubMed]
155. Hewlings, S.J.; Kalman, D.S. Curcumin: A review of its effects on human health. *Foods* **2017**, *6*, 92. [CrossRef] [PubMed]
156. Mitchell, M.J.; Billingsley, M.M.; Haley, R.M.; Wechsler, M.E.; Peppas, N.A.; Langer, R. Engineering precision nanoparticles for drug delivery. *Nat. Rev. Drug Discov.* **2021**, *20*, 101–124. [CrossRef] [PubMed]

157. Umerska, A.; Gaucher, C.; Oyarzun-Ampuero, F.; Fries-Raeth, I.; Colin, F.; Villamizar-Sarmiento, M.G.; Maincent, P.; Sapin-Minet, A. Polymeric nanoparticles for increasing oral bioavailability of curcumin. *Antioxidants* **2018**, *7*, 46. [CrossRef]
158. Ferrari, R.; Sponchioni, M.; Morbidelli, M.; Moscatelli, D. Polymer nanoparticles for the intravenous delivery of anticancer drugs: The checkpoints on the road from the synthesis to clinical translation. *Nanoscale* **2018**, *10*, 22701–22719. [CrossRef] [PubMed]
159. Li, Z.; Shi, M.; Li, N.; Xu, R. Application of functional biocompatible nanomaterials to improve curcumin bioavailability. *Front. Chem.* **2020**, *8*, 589957. [CrossRef]
160. Zaman, M.S.; Chauhan, N.; Yallapu, M.M.; Gara, R.K.; Maher, D.M.; Kumari, S.; Sikander, M.; Khan, S.; Zafar, N.; Jaggi, M.; et al. Curcumin nanoformulation for cervical cancer treatment. *Sci. Rep.* **2016**, *6*, 20051. [CrossRef]
161. Yallapu, M.M.; Gupta, B.K.; Jaggi, M.; Chauhan, S.C. Fabrication of curcumin encapsulated PLGA nanoparticles for improved therapeutic effects in metastatic cancer cells. *J. Colloid Interface Sci.* **2010**, *351*, 19–29. [CrossRef]
162. Mukerjee, A.; Vishwanatha, J.K. Formulation, characterization and evaluation of curcumin-loaded PLGA nanospheres for cancer therapy. *Anticancer Res.* **2009**, *29*, 3867–3875.
163. Bisht, S.; Feldmann, G.; Soni, S.; Ravi, R.; Karikar, C.; Maitra, A.; Maitra, A. Polymeric nanoparticle-encapsulated curcumin ("nanocurcumin"): A novel strategy for human cancer therapy. *J. Nanobiotechnol.* **2007**, *5*, 3. [CrossRef] [PubMed]
164. Yin, H.T.; Zhang, D.G.; Wu, X.L.; Huang, X.E.; Chen, G. In vivo evaluation of curcumin-loaded nanoparticles in a A549 xenograft mice model. *Asian Pac. J. Cancer Prev. APJCP* **2013**, *14*, 409–412. [CrossRef] [PubMed]
165. Xie, M.; Fan, D.; Li, Y.; He, X.; Chen, X.; Chen, Y.; Zhu, J.; Xu, G.; Wu, X.; Lan, P. Supercritical carbon dioxide-developed silk fibroin nanoplatform for smart colon cancer therapy. *Int. J. Nanomed.* **2017**, *12*, 7751–7761. [CrossRef] [PubMed]
166. Baspinar, Y.; Ustundas, M.; Bayraktar, O.; Sezgin, C. Curcumin and piperine loaded zein-chitosan nanoparticles: Development and in-vitro characterisation. *Saudi Pharm. J. SPJ Off. Publ. Saudi Pharm. Soc.* **2018**, *26*, 323–334. [CrossRef] [PubMed]
167. Yadav, P.; Bandyopadhyay, A.; Chakraborty, A.; Sarkar, K. Enhancement of anticancer activity and drug delivery of chitosan-curcumin nanoparticle via molecular docking and simulation analysis. *Carbohydr. Polym.* **2018**, *182*, 188–198. [CrossRef] [PubMed]
168. Manjunath, K.; Reddy, J.S.; Venkateswarlu, V. Solid lipid nanoparticles as drug delivery systems. *Methods Find. Exp. Clin. Pharmacol.* **2005**, *27*, 127–144. [CrossRef]
169. Mukherjee, S.; Ray, S.; Thakur, R.S. Solid lipid nanoparticles: A modern formulation approach in drug delivery system. *Indian J. Pharm. Sci.* **2009**, *71*, 349–358. [CrossRef]
170. Jenning, V.; Lippacher, A.; Gohla, S.H. Medium scale production of solid lipid nanoparticles (SLN) by high pressure homogenization. *J. Microencapsul.* **2002**, *19*, 1–10. [CrossRef]
171. Baek, J.S.; Cho, C.W. Surface modification of solid lipid nanoparticles for oral delivery of curcumin: Improvement of bioavailability through enhanced cellular uptake, and lymphatic uptake. *Eur. J. Pharm. Biopharm.* **2017**, *117*, 132–140. [CrossRef]
172. Guorgui, J.; Wang, R.; Mattheolabakis, G.; Mackenzie, G.G. Curcumin formulated in solid lipid nanoparticles has enhanced efficacy in Hodgkin's lymphoma in mice. *Arch. Biochem. Biophys.* **2018**, *648*, 12–19. [CrossRef] [PubMed]
173. Gota, V.S.; Maru, G.B.; Soni, T.G.; Gandhi, T.R.; Kochar, N.; Agarwal, M.G. Safety and pharmacokinetics of a solid lipid curcumin particle formulation in osteosarcoma patients and healthy volunteers. *J. Agric. Food Chem.* **2010**, *58*, 2095–2099. [CrossRef]
174. Ban, C.; Jo, M.; Park, Y.H.; Kim, J.H.; Han, J.Y.; Lee, K.W.; Kweon, D.H.; Choi, Y.J. Enhancing the oral bioavailability of curcumin using solid lipid nanoparticles. *Food Chem.* **2020**, *302*, 125328. [CrossRef]
175. Huang, S.; He, J.; Cao, L.; Lin, H.; Zhang, W.; Zhong, Q. Improved physicochemical properties of curcumin-loaded solid lipid nanoparticles stabilized by sodium caseinate-lactose Maillard conjugate. *J. Agric. Food Chem.* **2020**, *68*, 7072–7081. [CrossRef]
176. Bhatt, H.; Rompicharla, S.V.K.; Komanduri, N.; Aashma, S.; Paradkar, S.; Ghosh, B.; Biswas, S. Development of curcumin-loaded solid lipid nanoparticles utilizing glyceryl monostearate as single lipid using QbD approach: Characterization and evaluation of anticancer activity against human breast cancer cell line. *Curr. Drug Deliv.* **2018**, *15*, 1271–1283. [CrossRef]
177. Wang, F.; Li, C.; Cheng, J.; Yuan, Z. Recent advances on inorganic nanoparticle-based cancer therapeutic agents. *Int. J. Environ. Res. Public Health* **2016**, *13*, 1182. [CrossRef]
178. Huynh, K.H.; Pham, X.H.; Kim, J.; Lee, S.H.; Chang, H.; Rho, W.Y.; Jun, B.H. Synthesis, properties, and biological applications of metallic alloy nanoparticles. *Int. J. Mol. Sci.* **2020**, *21*, 5174. [CrossRef]
179. Kouhpanji, M.R.Z.; Stadler, B.J.H. A guideline for effectively synthesizing and characterizing magnetic nanoparticles for advancing nanobiotechnology: A review. *Sensors* **2020**, *20*, 2554. [CrossRef] [PubMed]
180. Yallapu, M.M.; Ebeling, M.C.; Khan, S.; Sundram, V.; Chauhan, N.; Gupta, B.K.; Puumala, S.E.; Jaggi, M.; Chauhan, S.C. Novel curcumin-loaded magnetic nanoparticles for pancreatic cancer treatment. *Mol. Cancer Ther.* **2013**, *12*, 1471–1480. [CrossRef] [PubMed]
181. Saikia, C.; Das, M.K.; Ramteke, A.; Maji, T.K. Evaluation of folic acid tagged aminated starch/ZnO coated iron oxide nanoparticles as targeted curcumin delivery system. *Carbohydr. Polym.* **2017**, *157*, 391–399. [CrossRef] [PubMed]
182. Barick, K.C.; Ekta; Gawali, S.L.; Sarkar, A.; Kunwar, A.; Priyadarsinicd, K.I.; Hassan, P.A. Pluronic stabilized Fe3O4 magnetic nanoparticles for intracellular delivery of curcumin. *RSC Adv.* **2016**, *6*, 98674–98681. [CrossRef]
183. Ayubi, M.; Karimi, M.; Abdpour, S.; Rostamizadeh, K.; Parsa, M.; Zamani, M.; Saedi, A. Magnetic nanoparticles decorated with PEGylated curcumin as dual targeted drug delivery: Synthesis, toxicity and biocompatibility study. *Mater. Sci. Eng. C Mater. Biol. Appl.* **2019**, *104*, 109810. [CrossRef] [PubMed]

184. Gangwar, R.K.; Tomar, G.B.; Dhumale, V.A.; Zinjarde, S.; Sharma, R.B.; Datar, S. Curcumin conjugated silica nanoparticles for improving bioavailability and its anticancer applications. *J. Agric. Food Chem.* **2013**, *61*, 9632–9637. [CrossRef]
185. Manju, S.; Sreenivasan, K. Gold nanoparticles generated and stabilized by water soluble curcumin-polymer conjugate: Blood compatibility evaluation and targeted drug delivery onto cancer cells. *J. Colloid Interface Sci.* **2012**, *368*, 144–151. [CrossRef]
186. Sercombe, L.; Veerati, T.; Moheimani, F.; Wu, S.Y.; Sood, A.K.; Hua, S. Advances and challenges of liposome assisted drug delivery. *Front. Pharm.* **2015**, *6*, 286. [CrossRef]
187. Li, R.; Deng, L.; Cai, Z.; Zhang, S.; Wang, K.; Li, L.; Ding, S.; Zhou, C. Liposomes coated with thiolated chitosan as drug carriers of curcumin. *Mater. Sci. Eng. C Mater. Biol. Appl.* **2017**, *80*, 156–164. [CrossRef]
188. Huang, M.G.; Liang, C.P.; Tan, C.; Huang, S.; Ying, R.F.; Wang, Y.S.; Wang, Z.J.; Zhang, Y.F. Liposome co-encapsulation as a strategy for the delivery of curcumin and resveratrol. *Food Funct.* **2019**, *10*, 6447–6458. [CrossRef]
189. Cheng, C.; Peng, S.; Li, Z.; Zou, L.; Liu, W.; Liu, C. Improved bioavailability of curcumin in liposomes prepared using a pH-driven, organic solvent-free, easily scalable process. *RSC Adv.* **2017**, *7*, 25978–25986. [CrossRef]
190. Jin, H.H.; Lu, Q.; Jiang, J.G. Curcumin liposomes prepared with milk fat globule membrane phospholipids and soybean lecithin. *J. Dairy Sci.* **2016**, *99*, 1780–1790. [CrossRef] [PubMed]
191. Cuomo, F.; Cofelice, M.; Venditti, F.; Ceglie, A.; Miguel, M.; Lindman, B.; Lopez, F. In-vitro digestion of curcumin loaded chitosan-coated liposomes. *Colloids Surf. B Biointerfaces* **2018**, *168*, 29–34. [CrossRef] [PubMed]
192. Hamano, N.; Bottger, R.; Lee, S.E.; Yang, Y.; Kulkarni, J.A.; Ip, S.; Cullis, P.R.; Li, S.D. Robust microfluidic technology and new lipid composition for fabrication of curcumin-loaded liposomes: Effect on the anticancer activity and safety of cisplatin. *Mol. Pharm.* **2019**, *16*, 3957–3967. [CrossRef]
193. Thangapazham, R.L.; Puri, A.; Tele, S.; Blumenthal, R.; Maheshwari, R.K. Evaluation of a nanotechnology-based carrier for delivery of curcumin in prostate cancer cells. *Int. J. Oncol.* **2008**, *32*, 1119–1123. [CrossRef]
194. Dhule, S.S.; Penfornis, P.; Frazier, T.; Walker, R.; Feldman, J.; Tan, G.; He, J.; Alb, A.; John, V.; Pochampally, R. Curcumin-loaded gamma-cyclodextrin liposomal nanoparticles as delivery vehicles for osteosarcoma. *Nanomed. Nanotechnol. Biol. Med.* **2012**, *8*, 440–451. [CrossRef]
195. Tefas, L.R.; Sylvester, B.; Tomuta, I.; Sesarman, A.; Licarete, E.; Banciu, M.; Porfire, A. Development of antiproliferative long-circulating liposomes co-encapsulating doxorubicin and curcumin, through the use of a quality-by-design approach. *Drug Des. Dev. Ther.* **2017**, *11*, 1605–1621. [CrossRef]
196. Xu, H.; Gong, Z.; Zhou, S.; Yang, S.; Wang, D.; Chen, X.; Wu, J.; Liu, L.; Zhong, S.; Zhao, J.; et al. Liposomal curcumin targeting endometrial cancer through the NF-kappaB pathway. *Cell. Physiol. Biochem.* **2018**, *48*, 569–582. [CrossRef]
197. Swami Vetha, B.S.; Oh, P.S.; Kim, S.H.; Jeong, H.J. Curcuminoids encapsulated liposome nanoparticles as a blue light emitting diode induced photodynamic therapeutic system for cancer treatment. *J. Photochem. Photobiol. B: Biol.* **2020**, *205*, 111840. [CrossRef] [PubMed]
198. Lu, M.; Qiu, Q.; Luo, X.; Liu, X.; Sun, J.; Wang, C.; Lin, X.; Deng, Y.; Song, Y. Phyto-phospholipid complexes (phytosomes): A novel strategy to improve the bioavailability of active constituents. *Asian J. Pharm. Sci.* **2019**, *14*, 265–274. [CrossRef] [PubMed]
199. Marczylo, T.H.; Verschoyle, R.D.; Cooke, D.N.; Morazzoni, P.; Steward, W.P.; Gescher, A.J. Comparison of systemic availability of curcumin with that of curcumin formulated with phosphatidylcholine. *Cancer Chemother. Pharmacol.* **2007**, *60*, 171–177. [CrossRef] [PubMed]
200. Maiti, K.; Mukherjee, K.; Gantait, A.; Saha, B.P.; Mukherjee, P.K. Curcumin-phospholipid complex: Preparation, therapeutic evaluation and pharmacokinetic study in rats. *Int. J. Pharm.* **2007**, *330*, 155–163. [CrossRef]
201. Stohs, S.J.; Ji, J.; Bucci, L.R.; Preuss, H.G. A comparative pharmacokinetic assessment of a novel highly bioavailable curcumin formulation with 95% curcumin: A randomized, double-blind, crossover study. *J. Am. Coll. Nutr.* **2018**, *37*, 51–59. [CrossRef]
202. Cuomo, J.; Appendino, G.; Dern, A.S.; Schneider, E.; McKinnon, T.P.; Brown, M.J.; Togni, S.; Dixon, B.M. Comparative absorption of a standardized curcuminoid mixture and its lecithin formulation. *J. Nat. Prod.* **2011**, *74*, 664–669. [CrossRef]
203. Wang, J.; Wang, L.; Zhang, L.; He, D.; Ju, J.; Li, W. Studies on the curcumin phospholipid complex solidified with Soluplus®. *J. Pharm. Pharm.* **2018**, *70*, 242–249. [CrossRef] [PubMed]
204. Ghezzi, M.; Pescina, S.; Padula, C.; Santi, P.; Del Favero, E.; Cantu, L.; Nicoli, S. Polymeric micelles in drug delivery: An insight of the techniques for their characterization and assessment in biorelevant conditions. *J. Control Release* **2021**, *332*, 312–336. [CrossRef] [PubMed]
205. Kheiri Manjili, H.; Ghasemi, P.; Malvandi, H.; Mousavi, M.S.; Attari, E.; Danafar, H. Pharmacokinetics and in vivo delivery of curcumin by copolymeric mPEG-PCL micelles. *Eur. J. Pharm. Biopharm.* **2017**, *116*, 17–30. [CrossRef]
206. Letchford, K.; Liggins, R.; Burt, H. Solubilization of hydrophobic drugs by methoxy poly(ethylene glycol)-block-polycaprolactone diblock copolymer micelles: Theoretical and experimental data and correlations. *J. Pharm. Sci.* **2008**, *97*, 1179–1190. [CrossRef] [PubMed]
207. Ma, Z.; Shayeganpour, A.; Brocks, D.R.; Lavasanifar, A.; Samuel, J. High-performance liquid chromatography analysis of curcumin in rat plasma: Application to pharmacokinetics of polymeric micellar formulation of curcumin. *Biomed. Chromatogr. BMC* **2007**, *21*, 546–552. [CrossRef]
208. Schiborr, C.; Kocher, A.; Behnam, D.; Jandasek, J.; Toelstede, S.; Frank, J. The oral bioavailability of curcumin from micronized powder and liquid micelles is significantly increased in healthy humans and differs between sexes. *Mol. Nutr. Food Res.* **2014**, *58*, 516–527. [CrossRef]

209. Frank, J.; Schiborr, C.; Kocher, A.; Meins, J.; Behnam, D.; Schubert-Zsilavecz, M.; Abdel-Tawab, M. Transepithelial transport of curcumin in Caco-2 cells is significantly enhanced by micellar solubilisation. *Plant Foods Hum. Nutr.* **2017**, *72*, 48–53. [CrossRef]
210. Parikh, A.; Kathawala, K.; Song, Y.; Zhou, X.F.; Garg, S. Curcumin-loaded self-nanomicellizing solid dispersion system: Part I: Development, optimization, characterization, and oral bioavailability. *Drug Deliv. Transl. Res.* **2018**, *8*, 1389–1405. [CrossRef]
211. Chen, S.; Li, Q.; Li, H.; Yang, L.; Yi, J.Z.; Xie, M.; Zhang, L.M. Long-circulating zein-polysulfobetaine conjugate-based nanocarriers for enhancing the stability and pharmacokinetics of curcumin. *Mater. Sci. Eng. C Mater. Biol. Appl.* **2020**, *109*, 110636. [CrossRef]
212. Song, L.; Shen, Y.Y.; Hou, J.W.; Lei, L.; Guo, S.R.; Qian, C.Y. Polymeric micelles for parenteral delivery of curcumin: Preparation, characterization and in vitro evaluation. *Colloid Surf. A* **2011**, *390*, 25–32. [CrossRef]
213. Patil, S.; Choudhary, B.; Rathore, A.; Roy, K.; Mahadik, K. Enhanced oral bioavailability and anticancer activity of novel curcumin loaded mixed micelles in human lung cancer cells. *Phytomed. Int. J. Phytother. Phytopharm.* **2015**, *22*, 1103–1111. [CrossRef]
214. Duan, Y.; Zhang, B.; Chu, L.; Tong, H.H.; Liu, W.; Zhai, G. Evaluation in vitro and in vivo of curcumin-loaded mPEG-PLA/TPGS mixed micelles for oral administration. *Colloids Surf. B Biointerfaces* **2016**, *141*, 345–354. [CrossRef] [PubMed]
215. Hani, U.; Shivakumar, H.G. Solubility enhancement and delivery systems of curcumin a herbal medicine: A review. *Curr. Drug Deliv.* **2014**, *11*, 792–804. [CrossRef]
216. Szejtli, J. Introduction and general overview of cyclodextrin chemistry. *Chem. Rev.* **1998**, *98*, 1743–1754. [CrossRef]
217. Bakshi, P.R.; Londhe, V.Y. Widespread applications of host-guest interactive cyclodextrin functionalized polymer nanocomposites: Its meta-analysis and review. *Carbohydr. Polym.* **2020**, *242*, 116430. [CrossRef]
218. Mangolim, C.S.; Moriwaki, C.; Nogueira, A.C.; Sato, F.; Baesso, M.L.; Neto, A.M.; Matioli, G. Curcumin-beta-cyclodextrin inclusion complex: Stability, solubility, characterisation by FT-IR, FT-Raman, X-ray diffraction and photoacoustic spectroscopy, and food application. *Food Chem.* **2014**, *153*, 361–370. [CrossRef] [PubMed]
219. Guo, S. Encapsulation of curcumin into β-cyclodextrins inclusion: A review. *E3S Web Conf.* **2019**, *131*, 01100. [CrossRef]
220. Jantarat, C.; Sirathanarun, P.; Ratanapongsai, S.; Watcharakan, P.; Sunyapong, S.; Wadu, A. Curcumin-hydroxypropyl-β-cyclodextrin inclusion complex preparation methods: Effect of common solvent evaporation, freeze drying, and pH shift on solubility and stability of curcumin. *Trop. J. Pharm. Res.* **2014**, *13*, 1215–1223. [CrossRef]
221. Li, N.; Wang, N.; Wu, T.; Qiu, C.; Wang, X.; Jiang, S.; Zhang, Z.; Liu, T.; Wei, C.; Wang, T. Preparation of curcumin-hydroxypropyl-beta-cyclodextrin inclusion complex by cosolvency-lyophilization procedure to enhance oral bioavailability of the drug. *Drug Dev. Ind. Pharm.* **2018**, *44*, 1966–1974. [CrossRef]
222. Ghanghoria, R.; Kesharwani, P.; Agashe, H.B.; Jain, N.K. Transdermal delivery of cyclodextrin-solubilized curcumin. *Drug Deliv. Transl. Res.* **2013**, *3*, 272–285. [CrossRef] [PubMed]
223. Popat, A.; Karmakar, S.; Jambhrunkar, S.; Xu, C.; Yu, C. Curcumin-cyclodextrin encapsulated chitosan nanoconjugates with enhanced solubility and cell cytotoxicity. *Colloids Surf. B Biointerfaces* **2014**, *117*, 520–527. [CrossRef] [PubMed]
224. Zhang, L.; Man, S.; Qiu, H.; Liu, Z.; Zhang, M.; Ma, L.; Gao, W. Curcumin-cyclodextrin complexes enhanced the anti-cancer effects of curcumin. *Environ. Toxicol. Pharmacol.* **2016**, *48*, 31–38. [CrossRef] [PubMed]
225. Moller, K.; Macaulay, B.; Bein, T. Curcumin encapsulated in crosslinked cyclodextrin nanoparticles enables immediate inhibition of cell growth and efficient killing of cancer cells. *Nanomaterials* **2021**, *11*, 489. [CrossRef] [PubMed]
226. Hong, W.; Guo, F.; Yu, N.; Ying, S.; Lou, B.; Wu, J.; Gao, Y.; Ji, X.; Wang, H.; Li, A.; et al. A novel folic acid receptor-targeted drug delivery system based on curcumin-loaded beta-cyclodextrin nanoparticles for cancer treatment. *Drug Des. Dev. Ther.* **2021**, *15*, 2843–2855. [CrossRef]
227. Stasilowicz, A.; Tykarska, E.; Lewandowska, K.; Kozak, M.; Miklaszewski, A.; Kobus-Cisowska, J.; Szymanowska, D.; Plech, T.; Jenczyk, J.; Cielecka-Piontek, J. Hydroxypropyl-beta-cyclodextrin as an effective carrier of curcumin–piperine nutraceutical system with improved enzyme inhibition properties. *J. Enzym. Inhib. Med. Chem.* **2020**, *35*, 1811–1821. [CrossRef]
228. Tran, P.H.L.; Tran, T.T.D. Developmental strategies of curcumin solid dispersions for enhancing bioavailability. *Anti-Cancer Agents Med. Chem.* **2020**, *20*, 1874–1882. [CrossRef]
229. Teixeira, C.C.; Mendonca, L.M.; Bergamaschi, M.M.; Queiroz, R.H.; Souza, G.E.; Antunes, L.M.; Freitas, L.A. Microparticles containing curcumin solid dispersion: Stability, bioavailability and anti-inflammatory activity. *AAPS PharmSciTech* **2016**, *17*, 252–261. [CrossRef]
230. Basniwal, R.K.; Khosla, R.; Jain, N. Improving the anticancer activity of curcumin using nanocurcumin dispersion in water. *Nutr. Cancer* **2014**, *66*, 1015–1022. [CrossRef]
231. Seo, S.W.; Han, H.K.; Chun, M.K.; Choi, H.K. Preparation and pharmacokinetic evaluation of curcumin solid dispersion using Solutol® HS15 as a carrier. *Int. J. Pharm.* **2012**, *424*, 18–25. [CrossRef] [PubMed]
232. Wan, S.; Sun, Y.; Qi, X.; Tan, F. Improved bioavailability of poorly water-soluble drug curcumin in cellulose acetate solid dispersion. *AAPS PharmSciTech* **2012**, *13*, 159–166. [CrossRef]
233. Mendonca, L.M.; Machado Cda, S.; Teixeira, C.C.; Freitas, L.A.; Bianchi, M.L.; Antunes, L.M. Comparative study of curcumin and curcumin formulated in a solid dispersion: Evaluation of their antigenotoxic effects. *Genet. Mol. Biol.* **2015**, *38*, 490–498. [CrossRef]
234. Silva de Sa, I.; Peron, A.P.; Leimann, F.V.; Bressan, G.N.; Krum, B.N.; Fachinetto, R.; Pinela, J.; Calhelha, R.C.; Barreiro, M.F.; Ferreira, I.; et al. In vitro and in vivo evaluation of enzymatic and antioxidant activity, cytotoxicity and genotoxicity of curcumin-loaded solid dispersions. *Food Chem. Toxicol.* **2019**, *125*, 29–37. [CrossRef]

235. Han, H.K. The effects of black pepper on the intestinal absorption and hepatic metabolism of drugs. *Expert Opin. Drug Metab. Toxicol.* **2011**, *7*, 721–729. [CrossRef]
236. Shoba, G.; Joy, D.; Joseph, T.; Majeed, M.; Rajendran, R.; Srinivas, P.S. Influence of piperine on the pharmacokinetics of curcumin in animals and human volunteers. *Planta Med.* **1998**, *64*, 353–356. [CrossRef] [PubMed]
237. Sharma, V.; Nehru, B.; Munshi, A.; Jyothy, A. Antioxidant potential of curcumin against oxidative insult induced by pentylenetetrazol in epileptic rats. *Methods Find. Exp. Clin. Pharmacol.* **2010**, *32*, 227–232. [CrossRef]
238. Suresh, D.; Srinivasan, K. Tissue distribution & elimination of capsaicin, piperine & curcumin following oral intake in rats. *Indian J. Med. Res.* **2010**, *131*, 682–691.
239. Antony, B.; Merina, B.; Iyer, V.S.; Judy, N.; Lennertz, K.; Joyal, S. A pilot cross-over study to evaluate human oral bioavailability of BCM-95®CG (Biocurcumax™), a novel bioenhanced preparation of curcumin. *Indian J. Pharm. Sci.* **2008**, *70*, 445–449. [CrossRef] [PubMed]
240. Singh, D.V.; Agarwal, S.; Singh, P.; Godbole, M.M.; Misra, K. Curcumin conjugates induce apoptosis via a mitochondrion dependent pathway in MCF-7 and MDA-MB-231 cell lines. *Asian Pac. J. Cancer Prev. APJCP* **2013**, *14*, 5797–5804. [CrossRef] [PubMed]
241. Peng, J.R.; Qian, Z.Y. Drug delivery systems for overcoming the bioavailability of curcumin: Not only the nanoparticle matters. *Nanomed. Nanotechnol. Biol. Med.* **2014**, *9*, 747–750. [CrossRef]
242. Guo, G.; Fu, S.; Zhou, L.; Liang, H.; Fan, M.; Luo, F.; Qian, Z.; Wei, Y. Preparation of curcumin loaded poly(epsilon-caprolactone)-poly(ethylene glycol)-poly(epsilon-caprolactone) nanofibers and their in vitro antitumor activity against Glioma 9L cells. *Nanoscale* **2011**, *3*, 3825–3832. [CrossRef]
243. Wang, C.; Ma, C.; Wu, Z.K.; Liang, H.; Yan, P.; Song, J.; Ma, N.; Zhao, Q.H. Enhanced bioavailability and anticancer effect of curcumin-loaded electrospun nanofiber: In vitro and in vivo study. *Nanoscale Res. Lett.* **2015**, *10*, 439. [CrossRef] [PubMed]
244. Qin, X.; Xu, Y.; Zhou, X.; Gong, T.; Zhang, Z.R.; Fu, Y. An injectable micelle-hydrogel hybrid for localized and prolonged drug delivery in the management of renal fibrosis. *Acta Pharm. Sin. B* **2021**, *11*, 835–847. [CrossRef] [PubMed]
245. Salehi, B.; Stojanovic-Radic, Z.; Matejic, J.; Sharifi-Rad, M.; Anil Kumar, N.V.; Martins, N.; Sharifi-Rad, J. The therapeutic potential of curcumin: A review of clinical trials. *Eur. J. Med. Chem.* **2019**, *163*, 527–545. [CrossRef] [PubMed]
246. Gupta, S.C.; Patchva, S.; Aggarwal, B.B. Therapeutic roles of curcumin: Lessons learned from clinical trials. *AAPS J.* **2013**, *15*, 195–218. [CrossRef]
247. Cheng, A.L.; Hsu, C.H.; Lin, J.K.; Hsu, M.M.; Ho, Y.F.; Shen, T.S.; Ko, J.Y.; Lin, J.T.; Lin, B.R.; Ming-Shiang, W.; et al. Phase I clinical trial of curcumin, a chemopreventive agent, in patients with high-risk or pre-malignant lesions. *Anticancer Res.* **2001**, *21*, 2895–2900.
248. Dhillon, N.; Aggarwal, B.B.; Newman, R.A.; Wolff, R.A.; Kunnumakkara, A.B.; Abbruzzese, J.L.; Ng, C.S.; Badmaev, V.; Kurzrock, R. Phase II trial of curcumin in patients with advanced pancreatic cancer. *Clin. Cancer Res.* **2008**, *14*, 4491–4499. [CrossRef]
249. Mahammedi, H.; Planchat, E.; Pouget, M.; Durando, X.; Cure, H.; Guy, L.; Van-Praagh, I.; Savareux, L.; Atger, M.; Bayet-Robert, M.; et al. The new combination docetaxel, prednisone and curcumin in patients with castration-resistant prostate cancer: A pilot phase II study. *Oncology* **2016**, *90*, 69–78. [CrossRef]
250. Dutzmann, S.; Schiborr, C.; Kocher, A.; Pilatus, U.; Hattingen, E.; Weissenberger, J.; Gessler, F.; Quick-Weller, J.; Franz, K.; Seifert, V.; et al. Intratumoral concentrations and effects of orally administered micellar curcuminoids in glioblastoma patients. *Nutr. Cancer* **2016**, *68*, 943–948. [CrossRef]
251. Sharma, R.A.; Euden, S.A.; Platton, S.L.; Cooke, D.N.; Shafayat, A.; Hewitt, H.R.; Marczylo, T.H.; Morgan, B.; Hemingway, D.; Plummer, S.M.; et al. Phase I clinical trial of oral curcumin: Biomarkers of systemic activity and compliance. *Clin. Cancer Res. Off. J. Am. Assoc. Cancer Res.* **2004**, *10*, 6847–6854. [CrossRef]
252. Carroll, R.E.; Benya, R.V.; Turgeon, D.K.; Vareed, S.; Neuman, M.; Rodriguez, L.; Kakarala, M.; Carpenter, P.M.; McLaren, C.; Meyskens, F.L., Jr.; et al. Phase IIa clinical trial of curcumin for the prevention of colorectal neoplasia. *Cancer Prev. Res.* **2011**, *4*, 354–364. [CrossRef] [PubMed]

cancers

MDPI

Article

Hydroxycholesterol Binds GPER and Induces Progression of Estrogen Receptor-Negative Breast Cancer

Paola Avena [1,†], Ivan Casaburi [1,†], Lucia Zavaglia [1], Marta C. Nocito [1], Davide La Padula [1], Vittoria Rago [1], Jing Dong [2], Peter Thomas [2], Chieko Mineo [3], Rosa Sirianni [1,*,‡] and Philip W. Shaul [3,*,‡]

1 Department of Pharmacy, Health and Nutritional Sciences, University of Calabria, Arcavacata di Rende, 87036 Cosenza, Italy; paola.avena@unical.it (P.A.); ivan.casaburi@unical.it (I.C.); luciazavaglia@hotmail.it (L.Z.); nocitomarta90@tiscali.it (M.C.N.); davidelapadula@live.it (D.L.P.); vittoria.rago@unical.it (V.R.)
2 Marine Science Institute, University of Texas at Austin, Port Aransas, TX 78373, USA; jingdong@mail.utexas.edu (J.D.); peter.thomas@utexas.edu (P.T.)
3 Center for Pulmonary and Vascular Biology, Department of Pediatrics, University of Texas Southwestern Medical Center, Dallas, TX 75390, USA; chieko.mineo@utsouthwestern.edu
* Correspondence: rosa.sirianni@unical.it (R.S.); philip.shaul@utsouthwestern.edu (P.W.S.); Tel.: +39-0984-493182 (R.S.); +1-214-648-2015 (P.W.S.)
† These authors contributed equally to this work.
‡ Co-last authors, These authors contributed equally to this work.

Simple Summary: Breast cancer is the most common cancer in women, and there is a known link between high cholesterol levels and breast cancer. However, how cholesterol impacts breast cancer is poorly understood, particularly in the case of an aggressive form of cancer known as estrogen receptor negative breast cancer. Using cells in culture and models of breast tumors in mice, we have determined that an abundant metabolite of cholesterol known as 27-hydroxycholesterol stimulates estrogen receptor negative breast cancer growth. We have also determined how 27-hydroxycholesterol stimulates the growth, identifying a new mechanism of action of 27-hydroxycholesterol. These new findings may explain the link between high cholesterol and estrogen receptor negative breast cancer, and they may lead to the development of new therapies for a type of breast cancer that presently lacks specific treatments.

Abstract: Cholesterol affects the proliferation of breast cancer (BC) and in particular of estrogen receptor-negative (ER−) BC. Cholesterol is converted to 27-hydroxycholesterol (27HC), which promotes the growth of ER+ BC. Potentially, 27HC can be involved in cholesterol-dependent ER− BC proliferation. Stable MDA-MB-231 silenced clones for CYP7B1 (27HC metabolizing enzyme) show an increased basal proliferation rate, which is not observed in the presence of lipoprotein-deprived serum. Furthermore, the treatment of SKBR3, MDA-MB-231 and MDA-MB-468 with 27HC increased cell proliferation that was prevented by G15, a selective G Protein-Coupled Estrogen Receptor (GPER) inhibitor, suggested this receptor to be a potential 27HC target. Binding experiments demonstrate that 27HC is a new ligand for GPER. We show that ERK1/2 and NFκB are part of the 27HC/GPER pathway. The stable silencing of GPER prevents NFκB activation and reduces basal and 27HC-dependent tumor growth. Additionally, conditioned medium from ER− BC cells treated with 27HC promotes tube formation, which does not occur in GPER silenced cells. Collectively, these data demonstrate that cholesterol conversion into 27HC promotes ER− BC growth and progression, and the expression of GPER is required for its effects.

Keywords: GPER; breast cancer; 27-hydroxycholesterol; angiogenesis

Citation: Avena, P.; Casaburi, I.; Zavaglia, L.; Nocito, M.C.; La Padula, D.; Rago, V.; Dong, J.; Thomas, P.; Mineo, C.; Sirianni, R.; et al. Hydroxycholesterol Binds GPER and Induces Progression of Estrogen Receptor-Negative Breast Cancer. *Cancers* **2022**, *14*, 1521. https://doi.org/10.3390/cancers14061521

Academic Editor: John R. Hawse

Received: 18 February 2022
Accepted: 9 March 2022
Published: 16 March 2022

1. Introduction

Breast cancer (BC) is the most common cancer among women, and despite improvements in early diagnosis and treatment, is the second-highest cause of cancer death. Clas-

sification of BC has commonly been related to the expression of estrogen receptor (ER), progesterone receptor (PR), and human epidermal growth factor receptor 2 (HER2). Recently, gene expression profiling by DNA microarray analysis has led to the classification of breast tumors into five or six subtypes [1–3]. These classifications can guide treatment and predict responses to therapy. Tumors that are ER− and do not express the PR or HER2 (triple negative, TNBC) are the most difficult to treat and have the worst prognosis [2,3]. Lacking a well-defined receptor and pathway signature, chemotherapy remains the treatment of choice, but the recurrence rate is still high. Among the potential factors associated with breast cancer, cholesterol has recently received considerable attention. Epidemiologic studies have provided inconclusive results, indicating that there may be a relationship between abnormal plasma cholesterol levels and breast cancer risk. However, more compelling evidence has been obtained in laboratory studies, and these studies indicate that cholesterol is able to regulate proliferation, migration, and signaling pathways in breast cancer. Many groups were able to show that lipoproteins stimulated the growth of breast cancer cells in vitro [4–7]. The pro-proliferative effect of LDL appears to be dependent on the ER status since only ER− breast cancer cell lines display increased proliferation in the presence of LDL [6].

Cholesterol can be metabolized to oxysterols, which control the feedback regulation of cholesterol biosynthesis. Among them, 27-hydroxycholesterol (27HC) has been associated with the growth and metastases of several cancers [8]. The oxysterol, 27HC, exerts its effects by binding to liver X receptors (LXR), alpha and beta [9,10] and estrogen receptor-α (ERα) [11,12]. Since its identification as a SERM, 27HC has been implicated in several diseases, including atherosclerosis, osteoporosis, cancer, and Alzheimer's disease [13]. In the context of ER+ breast tumors, the binding of 27HC to ERα increases cancer growth [14,15], while the activation of LXRα is involved in pro-metastatic effects [15]. In the context of ER− BC, it has been shown that monocytes present at the primary site are responsible for the production of 27HC [16], which can be utilized by ER− BC cells to increase migratory ability [17]. Importantly, CYP27A1, the enzyme responsible for 27HC synthesis, is heterogeneously expressed among primary tumors, with a high expression significantly associated with a high tumor grade, ER negativity, and basal-like subtypes [18]. On the contrary, tumor cells from patients with TNBC display a low immunoreactivity for CYP7B1, the enzyme responsible for the degradation of 27HC [19]. Furthermore, in ER− BC, 27HC induces reactive oxygen species (ROS) production and Stat-3 activation to promote VEGF production and angiogenesis [20], a necessary event in the metastatic processes. The two known receptors binding 27HC are unlikely to mediate its effects since, by definition, these tumors are ER negative and the activation of LXRα represses ER− BC proliferation [21]. Despite the role of 27HC in ER− BC, the receptor mediating its effects in this context is still unknown.

GPR30, a G-protein-coupled receptor encoded by the GPER (G-protein estrogen receptor) gene, has been linked to estrogen effects in several physiological and pathological settings [22]. Different from nuclear ER knockout mice, GPER KO mice did not manifest an infertile phenotype. However, GPER was implicated in obesity, insulin resistance, cardiovascular dysfunction, and breast cancer progression [22]. GPER is prevalent in TNBC and presumed to be involved in the growth of this tumor, becoming a potential candidate as a therapeutic target [23–28]. In two TNBC cell lines, MDA-MB-435 and HCC1806, GPER activation by its agonists, estradiol, and tamoxifen increased proliferation, and GPER silencing completely prevented this effect [24]. Additionally, GPER was strongly expressed in the TNBC cell lines, MDA-MB-468 and MDA-MB-436, and its agonists led to the rapid activation of the ERK1/2 pathway, which is responsible for increased cell growth, survival, migration, and invasion through upregulating the expression of genes associated with cell cycle, anti-apoptotic and proliferative mechanisms [26]. In vitro experimental results were supported by clinical data from TNBC patients, indicating a strong association between positivity for GPER and pERK1/2 and large tumor size and advanced stage [24]. Additionally, in ER negative BC cells, GPER increases VEGF production to support angiogenesis [29].

Altogether, these observations highlight an overlap between GPER- and 27HC-dependent effects. Therefore, in this study, we asked if 27HC could bind and activate GPER to increase the metastatic potential of ER− BC.

2. Materials and Methods

2.1. Cell Culture and Clones Selection

The human breast cancer cell lines, SKBR3 and MDA-MB-231, were obtained from the American Type Culture Collection (ATCC, Manassas, VA, USA). MDA-MB-468 cells were a gift from Prof. Richard Pestell (Department of Cancer Biology, Thomas Jefferson University, Philadelphia, PA, USA). SKBR3 human breast cancer cells were maintained in phenol red-free RPMI 1640 containing 10% fetal bovine serum (FBS) and antibiotics (Pen/Strep), and the TNBC cell lines, MDA-MB-231 and MDA-MB-468, were maintained in DMEM/F- 12 containing 10% FBS and 1 mg/mL penicillin-streptomycin. Cells were maintained in phenol red-free media containing 5% FBS-DCC (fetal bovine serum, dextran-coated charcoal-treated) for three days before being plated for specific experiments using phenol red-free media with 0.5% FBS-DCC. During experimental treatments, the cells were grown in phenol red-free media containing 5% FBS-DCC. Additionally, specific experiments were performed on cells grown in a medium containing lipoprotein-free serum (LPF-FBS) (Sigma-Aldrich, Inc. St. Louis, MO, USA).

Stable MDA-MB-231 and MDA-MB-468 cell lines were created, harboring control shRNA or shRNA-targeting GPER. These cell lines were generated by transfecting MDA-MB-231 cells with short hairpin RNA (shRNA) plasmids (pGFP-V-RS HuSH vector; Origene, Rockville, MD, USA). Stable clones were selected using 10 µg/mL puromycin and maintained in growth medium containing 1µg/mL of puromycin (Millipore Sigma, St. Louis, MO, USA). GPER mRNA levels were determined by real-time PCR using the following primers: Forward, 5′-CGCTCTTCCTGCAGGTCAA-3′, and reverse, 5′-ATGTAGCGGTCGAAGCTCATC-3′; they were normalized to 18S ribosomal RNA. GPER protein levels in each clone were determined by Western blotting using an anti-GPER antibody (MBL International Corporation, Woburn, MA, USA).

Stable MDA-MB-231 cell lines were created, harboring control shRNA or shRNA-targeting CYP27A1 or CYP7B1. These cell lines were generated by infecting MDA-MB-231 cells with lentiviral particles containing three to five expression constructs, each encoding target-specific 19–25 nt (plus hairpin) shRNA designed to knock down gene expression (Santa Cruz Biotechnology Inc., Dallas, TX, USA). Stable clones were selected using 10 µg/mL puromycin and maintained in a growth medium containing 1µg/mL of puromycin (Sigma-Aldrich, Inc. St. Louis, MO, USA). CYP27A1 and CYP7B1mRNA levels were determined by real-time PCR using the following primers: CYP27A1- Forward, 5′-TGCGCCAGGCTCTGAACCAG-3′, and Reverse, 5′-TCCACTTGGGGAGGAAGGTG-3′; CYP7B1 Forward, 5′-GGCCCTCTGCTTGCTTGTC-3′, and Reverse, 5′-GAAGCCAACCTTTTATCAATGGA-3′; they were normalized to 18S ribosomal RNA.

The human embryonic kidney HEK293 cell line was obtained from ATCC. For use in GPER competitive binding assays, human HEK293 cells were stably transfected with GPER [30], cells expressing GPER were selectively maintained with 500 µg/mL geneticin, and the cells were cultured in DMEM/Ham's F-12 medium without phenol red supplemented with 5% fetal bovine serum (FBS) and 100 µg/mL of gentamicin in 150 mm diameter plates. The medium was replaced every 1–2 days, and the cells reached 80% confluence after 3 days in culture, at which time the medium was replaced with medium-lacking FBS, and the cells were cultured for another day before binding experiments were performed.

2.2. Proliferation and Viability Quantitation

SKBR3, MDA-MD-231, and MDA-MD-468 cell proliferation was assessed by quantifying [^{3}H]thymidine incorporation (Perkin-Elmer Life Sciences, Boston, MA, USA) as previously described [14]. Cell viability was measured using 3-[4,5-dimethylthiazol-2-yl]-2,5-diphenyltetrazolium bromide (MTT) assay as previously described. Fresh MTT

(Sigma-Aldrich, Inc. St. Louis, MO, USA), resuspended in PBS, was then added to each well (final concentration 0.33 mg/mL). After 2 h incubation, cells were lysed with 200 µL of DMSO, and optical density was measured at 570 nm in a multi-plate reader.

2.3. Western Blot Analysis

Following cell treatment, total protein extraction was performed using RIPA buffer as previously described [31]. Proteins were separated by 10% SDS-PAGE and immunoblotted overnight with specific antibodies against pERK1/2 (Cell Signaling Technology, Danvers, MA, USA) or total ERK1/2 (Cell Signaling Technology). In studies of NF-kB activation, following treatment, cytoplasmic and nuclear extracts were prepared from cultured cells [32], and immunoblotting was performed using antibodies against NF-κB p65 (Abcam, Cambridge, UK), glyceraldehyde 3-phosphate dehydrogenase (GAPDH), or Lamin B (Santa Cruz Biotechnology, Dallas, TX, USA). Membranes were incubated with horseradish peroxidase (HRP)-conjugated secondary antibodies (Santa Cruz Biotechnology, Dallas, TX, USA), and immunoreactive bands were visualized with the ECL Western blotting detection system (Santa Cruz Biotechnology, Dallas, TX, USA).

2.4. RNA Extraction, Reverse Transcription and Real-Time PCR

Following total RNA extraction, 1 µg of total RNA was reverse transcribed and then used for PCR reactions, performed in the QuantStudio 3 Real-Time PCR System (Applied Biosystem, Waltham, MA, USA). Final results were expressed as n-fold differences in gene expression relative to 18S and calibrator and calculated using the ΔΔCt method as previously shown [31]. Primers sequence are indicated in Table 1.

Table 1. QPCR primers sequence.

Gene	Forward Primer (5′-3′)	Reverse Primer (5′-3′)
ZEB1	GCACCTGAAGAGGACCAGAG	TGCATCTGGTGTTCCATTTT
VIMENTIN	CCTTGAACGCAAAGTGGAATC	GACATGCTGTTCCTGAATCTGAG
TWIST	CGGGAGTCCGCAGTCTTA	TGAATCTTGCTCAGCTTGTC
SNAI2	CATGCCTGTCATACCACAAC	GGTGTCAGATGGAGGAGGG
VEGF	TGCAGATTATGCGGATCAAACC	TGCATTCACATTTGTTGTGCTGTAG
CCND1	CACGCGCAGACCTTCGT	ATGGAGGGCGGATTGGAA
18S	CGGCGACGACCCATTCGAAC	GAATCGAACCCTGATTCCCCGTC

2.5. GPER Competitive Binding Assay

[^{3}H]E2 binding to plasma membranes of HEK293 cells transfected with GPER was evaluated as previously reported [30]. Specific E2 binding was calculated from the binding of 4 nM [2,4,6,7-^{3}H]E2 ([^{3}H]E2, ~89 Ci/mmol) alone (total binding) and in the presence of 100-fold excess (400 nM) nonradioactive E2 (nonspecific binding). Competitive binding assays were run in triplicate with 4 nM [^{3}H]E2, and competitor was added over a concentration range of 1 nM to 10 µM (dissolved in 1 µL ethanol). After a 30 min incubation at 4 °C with the plasma membrane fractions, the reaction was stopped by filtration (Whatman GF/B filters), filters were washed, and bound radioactivity was measured by scintillation counting. The displacement of [^{3}H]E2 binding by the competitor was expressed as a percentage of the maximum specific binding of E2. The competition curves and IC50 values (competitor concentrations that cause 50% displacement of [^{3}H]-E2) were calculated from the mean values from three separate competitive binding assays.

2.6. Mammosphere Formation Assay

A single-cell suspension was prepared using enzymatic (Trypsin-EDTA, Millipore Sigma, #T3924) and manual disaggregation (25-gauge needle). Cells were plated in 6-well

tissue culture plates covered with poly-2-hydroxyethyl-methacrylate (poly-HEMA, Millipore Sigma, #P3932) to prevent cell attachment, at a density of 0.5×10^3 cells/mL in mammosphere medium (DMEM-F12/B27/EGF (20 ng/mL)/Pen-Strep/Glu) [33]. Cells were grown for 5 days and maintained at 37 °C in a humidified atmosphere containing 5% CO_2 in the absence or presence of treatments. After 5 days of culture, spheres > 50 µm were counted using an eyepiece graticule. The percentage of plated cells that generated spheres was calculated to yield the percentage mammosphere formation, and values are expressed relative to those for basal conditions equaling one (1 = 100% MFE, mammosphere forming efficiency).

2.7. Orthotopic Breast Tumor Xenograft Model

Non-manipulated MDA-MB-231, or stable MDA-MB-231 cell lines harboring control shRNA or shRNA-targeting GPER (1.5×10^6 cells) were implanted unilaterally into the mammary fat pad of 6-week-old female SCID mice (Harlen Envigo). Tumor volume was then measured intermittently with calipers. In studies of 27HC, when non-manipulated MDA-MB-231 cell tumors reached an average volume of 100 mm^3, treatment was initiated with vehicle or 100 µg 27HC injected subcutaneously every other day [14]. At 28 d, the tumors were harvested and weighed. All animal procedures were approved by the University of Texas Southwestern Medical Center Institutional Animal Care and Use Committee.

2.8. Histopathological Analysis and Staining

At tumor harvest, formalin-fixed, paraffin-embedded tissues were sectioned at 5 µm, mounted on slides precoated with polylysine, and stained with hematoxylin and eosin. Sections were deparaffinized and dehydrated. Slides were permeabilized with 0.2% Triton X-100, followed by blocking with serum (30 min, room temperature), and incubated with anti- Ki67 (Abcam), Endomucin (BioRad, Hercules, CA, USA), CD31 (Biolegend, San Diego, CA, USA), Vimentin (Dako, Copenhagen, Danmark) antibody, and diaminobenzidine-conjugated secondary antibody (1:200, 30 min, room temperature). Secondary antibody alone was used as a negative control. Slides were observed and photographed with an OLYMPUS BX51 microscope.

2.9. Conditioned Medium

Breast cancer cells were seeded at 250,000 cells/well in a 6-well plate in a medium containing 5% FBS-DCC for 3 days, cells were washed and incubated for additional 12 h with medium without serum, before treatment for 24 h with 27HC resuspended in DMSO in medium containing 1% FBS-DCC. Thereafter, the supernatants were collected, centrifuged at 3500 rpm for 5 min to remove cell debris, and used as a conditioned medium for EA.hy926. Stably silenced breast cancer clones were seeded at 250,000 cells/well in a 6-well plate in a medium containing 5% FBS-DCC for 3 days, supernatants were collected, centrifuged at 3500 rpm for 5 min to remove cell debris, and used as conditioned medium for EA.hy926.

2.10. Tube Formation Assay

The day before the experiment, confluent EA.hy926 were starved overnight at 37 °C in serum-free medium. Growth factor-reduced Matrigel® (R&D Systems Inc. Minneapolis, MN, USA) was thawed overnight at 4 °C, plated on the bottom of prechilled 96-well plates and left at 37 °C for 1 h for gelification. Starved EA.hy926 were collected by enzymatic detachment (0.25% trypsin-EDTA solution, Life Technologies, Carlsbad, CA, USA), counted and resuspended in conditioned medium from breast cancer cells. Then, 10,000 cells/well were seeded on Matrigel and incubated at 37 °C. Tube formation was observed starting from 4 h after cell seeding and quantified using the software NIH ImageJ (National Institutes of Health (NIH), Bethesda, MD, USA).

2.11. Statistical Analysis

All cell culture and xenograft experiments were performed on at least three separate occasions. Data are expressed as mean ± standard error of the mean (SEM), and statistical analysis was performed using GraphPad Prism 5.0 software (GraphPad Software, version 7.0 La Jolla, CA, USA). Comparisons between two groups were conducted using Student's *t*-test, and comparisons between 3 or more groups were conducted by analysis of variance (ANOVA) with Newman–Keuls Multiple Comparison post hoc testing. Xenografts growth curve analysis was conducted using Two-way ANOVA followed by Bonferroni post hoc testing. Significance was defined as $p < 0.05$.

3. Results

3.1. TNBC Cells Convert Cholesterol to 27HC to Increase Tumor Growth

LDL-cholesterol increases the growth of TNBC [4,34]. We evaluated the growth of BC cells in medium containing regular FBS or lipoprotein-free FBS (LPF-FBS). After 96 h in culture, a significant decrease in the proliferation rate of the three tested ER− cell lines was observed (Figure 1A).

To define the role of 27HC in the cholesterol-dependent effect on TNBC growth, the CYP27A1 gene, encoding for the 27HC synthesizing enzyme (shCYP27A1, sh27A1), and the CYP7B1 gene, encoding for 27HC metabolizing enzyme (shCYP7B1, sh7B1), were stably silenced in MDA-MD231 cells (Figure 1B,C). These two cell lines have proliferation rates that differ from control cells (shcontrol, shC). ShCYP27A1 cells grow slower, with a 30% decrease in the proliferation rate, while shCYP7B1 cells grow faster and manifest a 20% increase compared to shC cells (Figure 1D). Importantly, the increased proliferation rate observed for shCYP7B1 cells requires cholesterol (Figure 1E). Cyclin D1 and E expression is increased in shCYP7B1 versus shC cells when cholesterol is available (FBS) (Figure S1A–C). This difference cannot be appreciated in the absence of cholesterol (LPF-FBS) (Figure S1D–F). Collectively, these data demonstrate that, in TNBC, cholesterol is converted to 27HC and increases tumor growth.

Treatment with exogenous 27HC increased the proliferation of the three cell lines (Figure 1F–H). Additionally, 27HC favored breast cancer growth as mammospheres (Figure 1G and Figure S2A,B). The in vitro data were confirmed in vivo and MDA-MB-231 were grafted in the mammary fat pad of mice treated for 4 weeks with either a vehicle or 27HC, which was able to increase both tumor volume and weight (Figure 1H,I).

Similar in vivo data were obtained by treating mice grafted with MDA-MB-468 with 27HC (Figure S2C,D).

3.2. 27HC Binds to GPR30 and Mediates ERK1/2 and NFκB Activation to Increase Tumor Proliferation

The observed 27HC effects are unlikely to be related to the known 27HC receptors: LXR and ERα. Our models are ER− and previous reports indicated that LXRα activation decreases the proliferation of MDA-MB-231 and SKBR3 [21] and MDA-MB-468 [35]. Accordingly, LXR synthetic agonist, T1317, reduced the proliferation of all three cell lines. We considered the possibility of 27HC binding to GPER since the activation of this receptor has been reported to increase the growth of ER− BC cells [36]. We confirmed that all three cell lines used in the study express the GPER protein (GPR30) (Figure 2A). Binding studies demonstrated that 27HC competes for [^{3}H]E2 binding to GPER with an IC50 of 0.50–0.80 μM (Figure 2B). The addition of G15, a selective GPER inhibitor, was able to prevent 27HC-stimulated cell growth in all three cell lines (Figure 2C and Figure S3A,B). Collectively, these data demonstrate that 27HC binds to GPER to induce the growth of ER− BC cells.

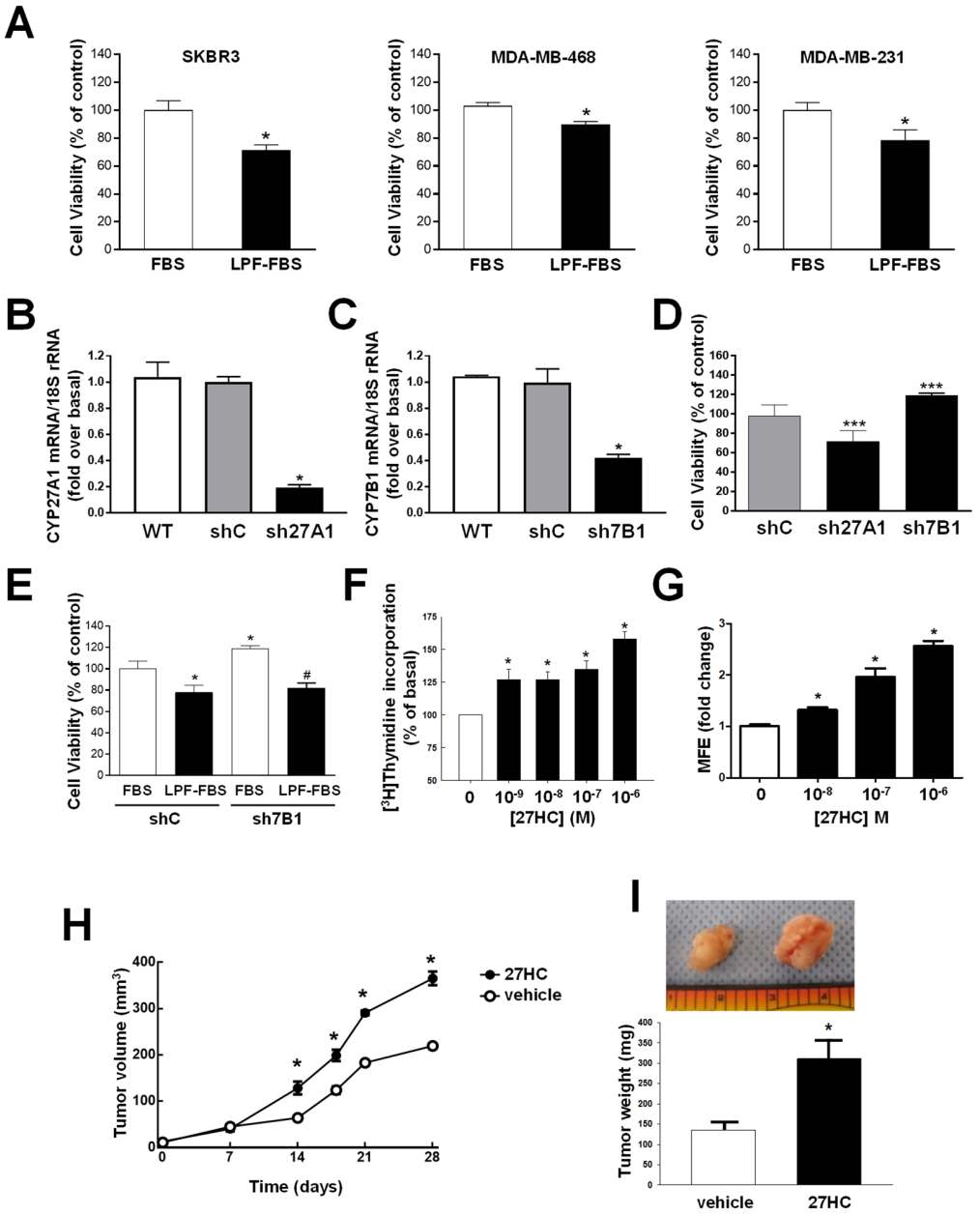

Figure 1. Cholesterol metabolism to 27HC increases ER− BC growth. (**A**) SKBR3, MDA-MB-468 and MDA-MB-231 were grown for 96 h in the presence of 5% FBS or lipoprotein-free FBS (LPF-FBS) (SIGMA), and cell viability was evaluated by MTT assay. * $p < 0.05$ vs. FBS. (**B**,**C**). MDA-MB-231 were stably silenced by CYP27A1 (sh27A1) (**B**) and CYP7B1 (sh7B1) (**C**) using gene-specific shRNA. (**D**) Cell viability of sh27A1 and sh7B1 cells was evaluated by MTT assay in comparison to shcontrol (shC) cells at 96 h. *** $p < 0.001$ vs. shC. (**E**) ShC and sh7B1 cells were grown for 96 h in the presence of 5% FBS or 5% LPF-FBS. * $p < 0.05$ vs. shC-FBS; # $p < 0.05$ vs. sh7B1-FBS. (**F**) Proliferation was evaluated by ^{3}H-thymidine incorporation in MDA-MB-231 cells treated for 48 h with increasing concentrations of 27HC, * $p < 0.05$ vs. 0 μM 27HC. (**G**) MDA-MB-231 cells were cultured under non-adherent conditions and grown in the presence of vehicle (0 M) or 27HC (10^{-8}, 10^{-7}, 10^{-6} M) for 5 days, and spheres > 50 μm were quantified. Findings are expressed relative to mammosphere formation efficiency (MFE) under basal conditions (0 M). Values are mean±SEM, n = 9, * $p < 0.05$ vs. vehicle. (**H**,**I**). Xenografts were initiated using MDA-MB-231 cells, and the mice were administered vehicle versus 27HC for 28 days. (**H**) Growth curves of tumors measured by caliper. * $p < 0.05$ vs. 0 μM 27HC. (**I**) Representative tumors and final tumor weights. Values are mean ± SEM, n = 7, * $p = 0.009$ vs. vehicle.

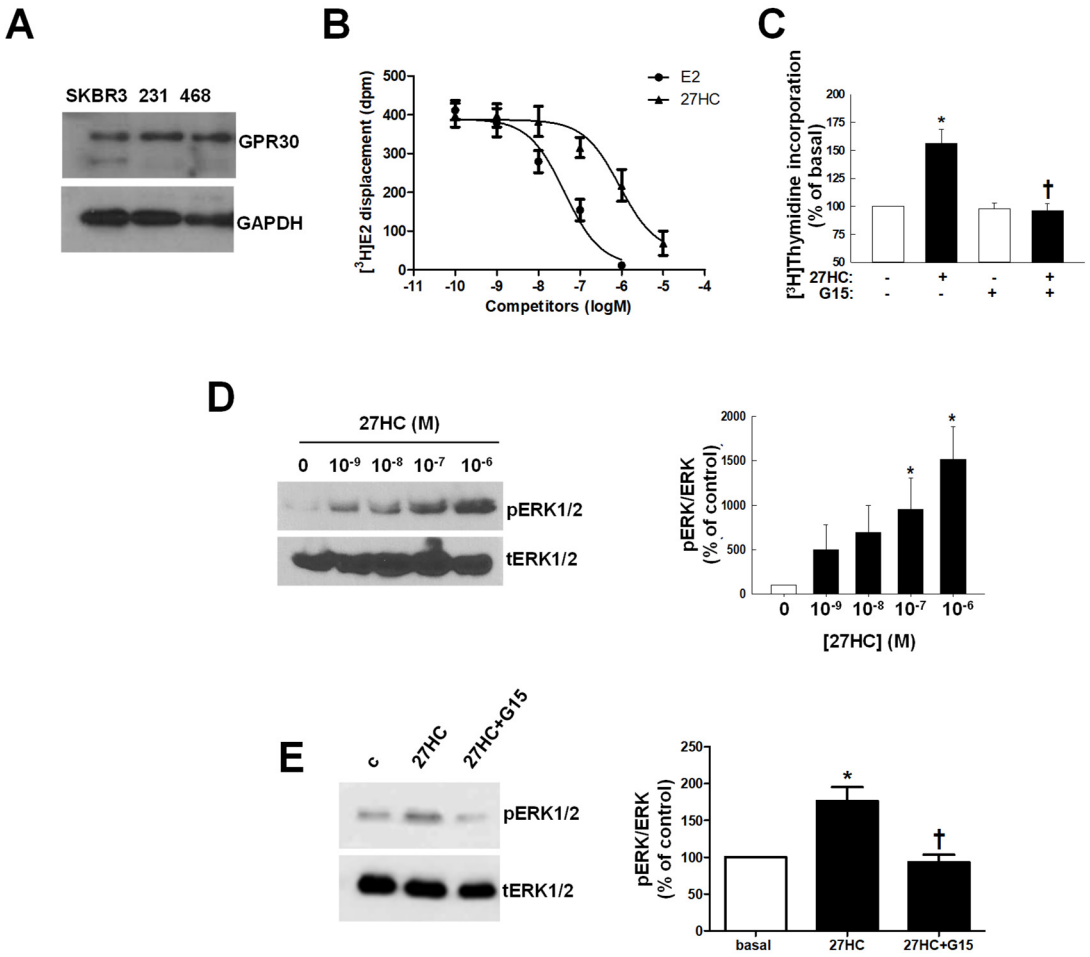

Figure 2. 27HC binds to GPR30 and activates ERK1/2. (**A**). GPR30 expression was evaluated in whole-cell lysates from SKBR3, MDA-MB-231 (231) and MDA-MB-468 (468) cells. (**B**) Estradiol (E2) and 27HC competitive binding to GPR30 was evaluated using plasma membranes isolated from GPR30-expressing HEK293 cells. [^{3}H]E2 displacement is shown in the presence of increasing concentrations of E2 or 27HC. Values are mean ± SEM, n = 3. (**C**). Cells were treated for 48 h with 27HC 10^{-6} M with or without G15 (10^{-6} M), * $p < 0.05$ vs. basal (untreated cells); † $p < 0.05$ vs. 27HC. (**D**,**E**) Western blot analysis was performed to detect posphorylated ERK1/2 (pERK1/2) or total ERK1/2 (tERK1/2) on whole-cell lysates from MDA-MB-231 cells treated for 15 min with 0 to 10^{-6} M 27HC (**D**) or with 27HC 10^{-6} M and G15 10^{-6} M alone or in combination (**E**). Left panels display representative Western blots, and right panels provide summary data. Values are mean ± SEM, n = 3.

ERK1/2 are part of the GPR30 downstream pathway [37]. In response to 27HC we observed a dose-dependent increase in ERK1/2 phosphorylation (Figure 2D and Figure S3C,D), which was prevented by G15 (Figure 2E and Figure S3E,F).

Furthermore, the nuclear factor κB (NFκB), a regulator of cell cycle [38], is also part of the GPER pathway [39] and we wanted to investigate its activation in the response to 27HC in our cell models. Cells were treated for increasing times (0.5 to 6 h) with the oxysterol to evaluate changes in nuclear localization of p65, an NFκB component (Figure 3A and Figure S4A,B). In a time-dependent manner, 27HC can increase p65 nuclear translocation, influencing the expression of cyclin D1 (CCND1), a known NFκB target gene [40] (Figure 3B and Figure S4C,D). Importantly, the presence of parthenolide (PTL), an NFκB inhibitor, prevented 27HC-dependent CCND1 upregulation (Figure 3C and Figure S4E,F) and, consequently, cell growth (Figure 3D and Figure S4G,H).

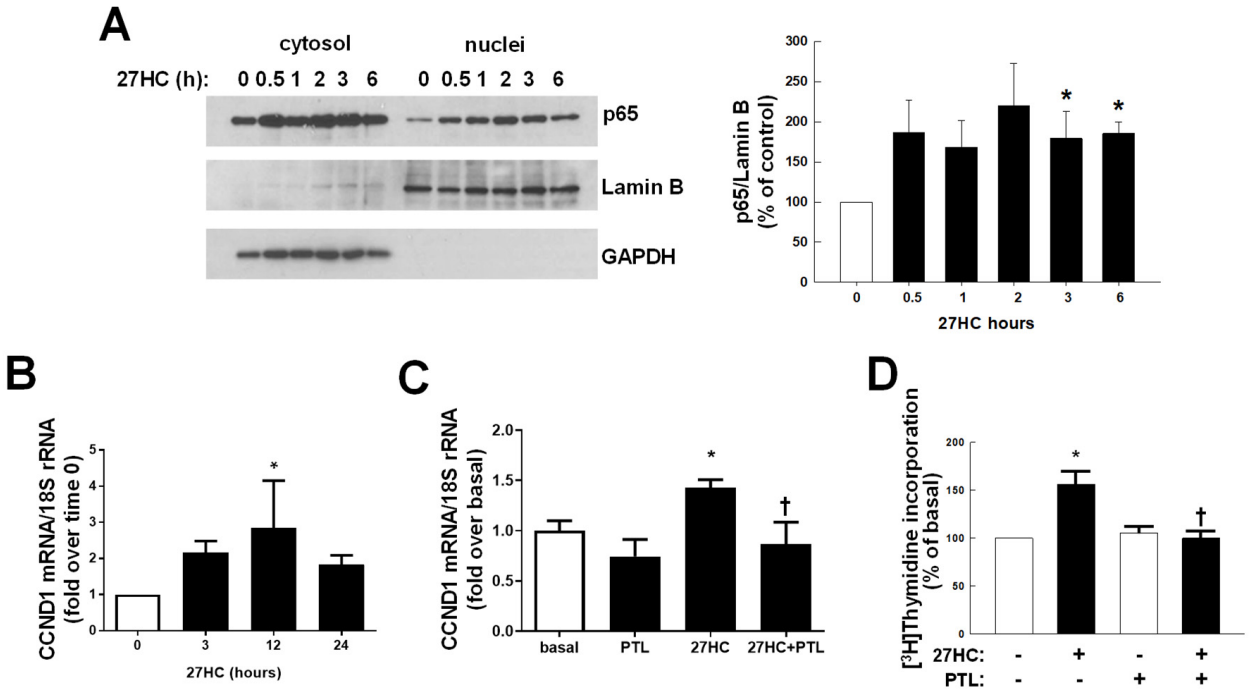

Figure 3. NFκB is part of 27HC-activated pathway and is required for cyclin D1 transcription. (**A**). MDA-MB-231 cells were treated with 27HC (10^{-6} M) for 0–6 h, cytosolic and nuclear fractions were obtained, and Western blotting was performed for p65, Lamin B and GAPDH. Left panels display representative Western blots, and right panels provide summary data. Values are mean ± SEM, n = 5, * $p < 0.05$ vs. control (0 h). (**B**,**C**) QPCR analysis of cyclin D1 in MDA-MB-231 cells treated for increasing times with 27HC (10^{-6}M) alone (**B**) or combined with parthenolide (PTL) (5×10^{-6} M) (**C**). (**D**) Cells were treated for 48h with 27HC (10^{-6} M) and PTL (5×10^{-6} M) alone and combined, proliferation was evaluated by ^{3}H-thymidine incorporation over 6 h. * $p < 0.05$ vs. basal (untreated cells); † $p < 0.05$ vs. 27HC treated cells.

To further prove that GPR30 mediates 27HC-stimulated cell growth, GPER was stably silenced in MDA-MB-231 cells (shGPER) (Figure 4A). In these cells, 27HC no longer increased cell proliferation (Figure 4B). GPER-silenced MDA-MB-468 cells behaved similarly (Figure S5A,B). In shC cells, 27HC still has the ability to induce p65 nuclear translocation in a time-dependent manner, this effect is lost in shGPER cells (Figure 4C–E). Shcontrol and shGPER cells were grafted in immune-deficient mice, and while 27HC increased tumor volume and the mass of shcontrol tumors, it did not affect shGPER growth. Importantly, the growth rate of shGPER cells in vivo was slower than the shcontrol counterpart (Figure 4F,G). Staining for Ki67 confirmed that the proliferative index increased in response to 27HC in shcontrol cells but not in silenced cells. Additionally, vehicle-treated shGPER tumors showed less Ki67 stain than vehicle-treated shcontrol (Figure 4H).

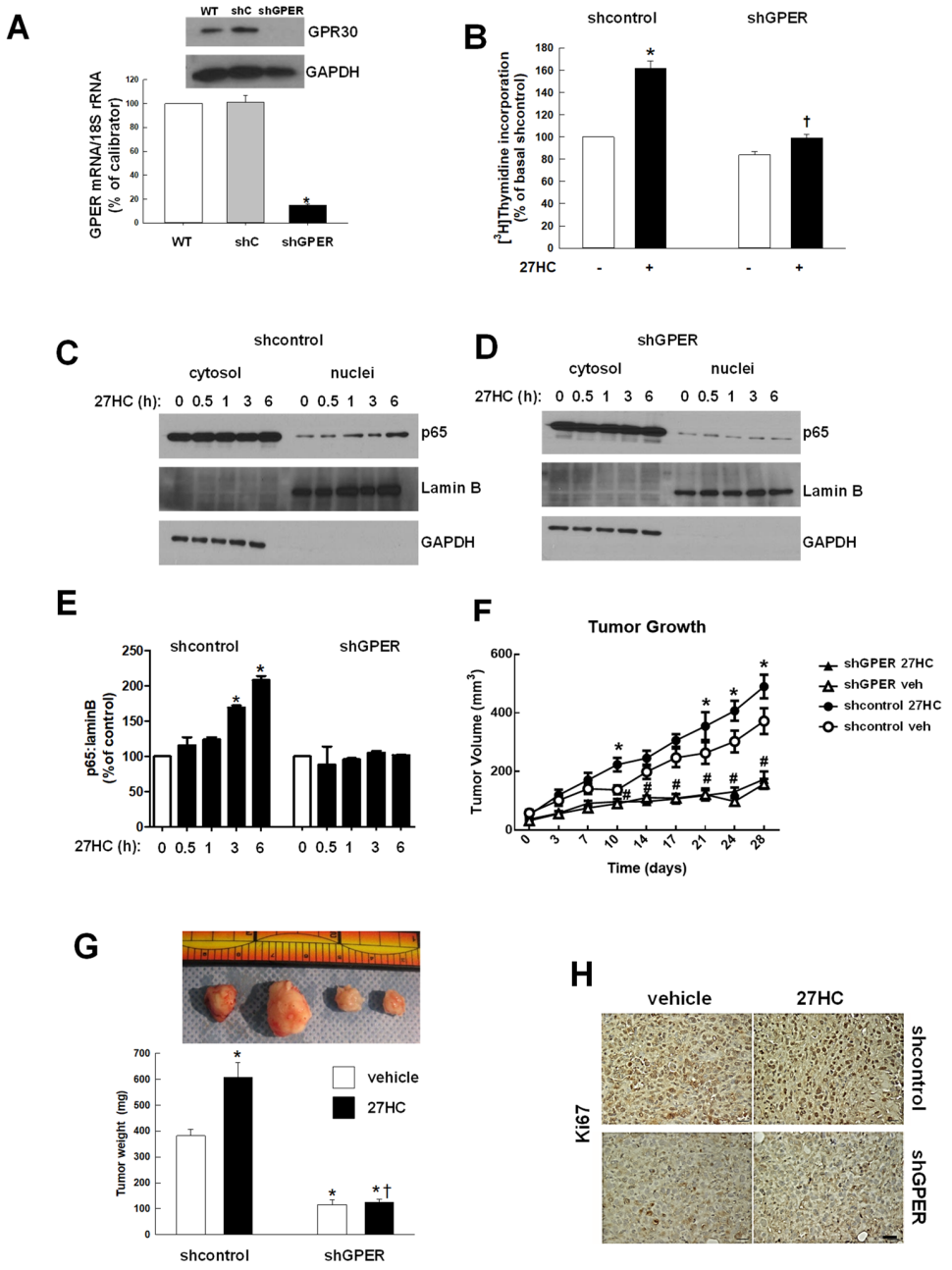

Figure 4. GPR30 mediates 27HC effects in ER− breast cancer cells. (**A**). GPER expression in parental (WT), shcontrol (shC) and stably GPER-silenced (shGPER) MDA-MB-231 cells were evaluated by Western blot analysis on whole-cell lysates (upper inset) and by real-time QPCR (lower graph). (**B**). Cells were left untreated (−) or treated (+) for 48h with 27HC (10^{-6} M) and proliferation was evaluated by ^{3}H-thymidine incorporation. (**C**–**E**) ShC and shGPER MDA-MB-231 cells were treated with 27HC (10^{-6} M) for 0–6 h, cytosolic and nuclear fractions were obtained, and Western blotting was performed for p65, Lamin B and GAPDH. Representative immunoblots are shown in (**C**,**D**), and quantitative summary data are shown in (**E**). Values are mean ± SEM, n = 5, * $p < 0.05$ vs. control (0)**.** (**F**,**G**) Xenografts were initiated by implanting either shcontrol or shGPER MDA-MB-231 cells into the mammary fat pads of SCID mice. (**F**)**.** Growth curves of tumors were measured by caliper. * $p < 0.05$ vs. shcontrol vehicle, # $p < 0.05$ vs. shcontrol 27HC. (**G**) Representative tumors and final tumor weights. Values are mean ± SEM, n = 7, * $p < 0.05$ vs. shcontrol vehicle, † $p < 0.05$ vs. shcontrol 27HC. (**H**) Ki67 abundance was evaluated in tumors by immunostaining. Primary images were obtained with a 20× objective, scale bar 25 µm.

3.3. 27HC Increases Cell Migration

We evaluated the effects of 27HC on cell migration and observed an increased motility in response to the oxysterol (Figure 5A and Figure S6A,B). Accordingly, shCYP7B1 cells displayed a more aggressive phenotype as evidenced by an increased migratory ability that was counteracted by the use of G15 (Figure 5B). By contrast, GPER gene silencing negatively impacted cell motility (Figure 5C and Figure S6C). Migration increases following the activation of epithelial-to-mesenchymal transition (EMT) genes, and we showed that 27HC modulates EMT markers in all three cell lines (Figure 5D and Figure S6D–H). Indeed, vimentin expression was increased in shCYP7B1 cells and decreased in shGPER cells (Figure 5E,F). Importantly, 27HC increased vimentin expression in xenograft tumors, as evidenced by a stronger IHC staining, which was not observed in samples from 27HC-treated shGPER xenografts (Figure 5G).

3.4. 27HC Requires GPER to Induce Tumor Angiogenesis

GPER activation was linked to angiogenesis in BC cells [29]. Particularly, GPER signaling mediates VEGF gene transcription. The treatment of BC cells with 27HC evidenced a time-dependent increase in VEGF mRNA levels (Figure 6A and Figure S7A,B). The conditioned medium (CM) collected from 27HC-treated cells (Figure 6B) caused an increase in tube formation and branching (Figure 6C and Figure S7C,D). ShCYP7B1 and shGPER cells were used to further confirm that 27HC production by ER− BC cells activates GPER to support VEGF production and angiogenesis. VEGF expression is increased in shCYP7B1 compared to shcontrol cells, and endothelial cells exposed to CM from shCYP7B1 cells displayed more organized tube-like structures (Figure 6D). On the other hand, VEGF production is decreased in shGPER cells, and their CM was less effective in inducing tube formation in EA.hy926 cells (Figure 6E).

To establish the ability of 27HC to promote angiogenesis in vivo, xenografts from experiments indicated in Figure 1H,I and Figure 4F,G were evaluated by IHC for known markers of endothelial cells: CD31 and endomucin [41]. The expression of these markers increased in the presence of 27HC in xenografts from parental (Figure 6F) and shcontrol (Figure 6G) MDA-MD-231 cells but not in those from shGPER cells (Figure 6G). Vascular density was also decreased in shGPER compared to shcontrol xenografts (Figure 6G).

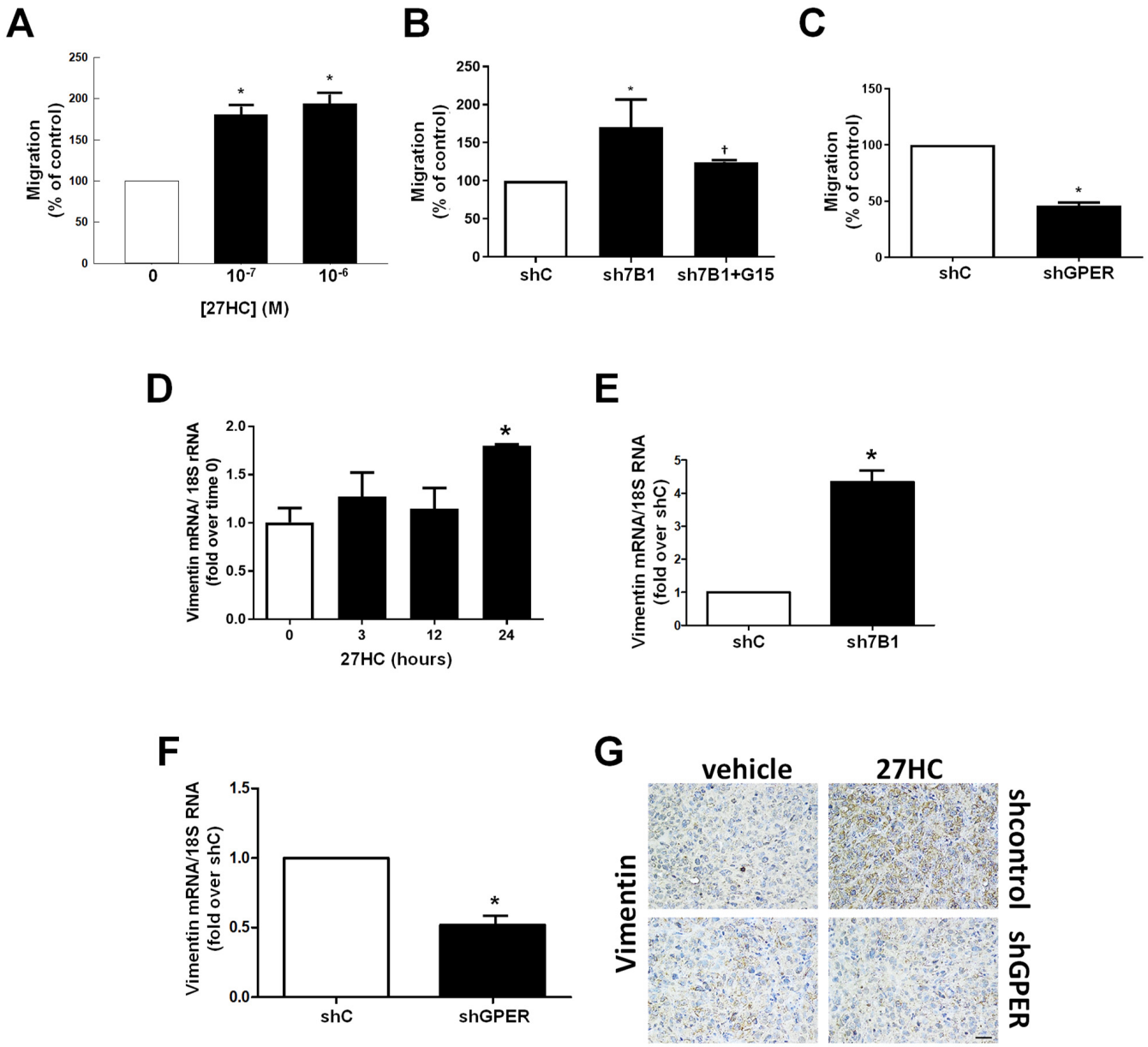

Figure 5. 27HC via GPR30 induces EMT to sustain ER− BC cell migration. (**A**,**C**) Counts of MDA-MB-231 (**A**), shcontrol (shC) and shCYP7B1 (sh7B1) cells +/− G15 (10^{-6} M), (**B**) shC and shGPER cells (**C**) migrated through Boyden chambers. (**D**–**F**). QPCR analysis of vimentin in MDA-MB-231 cells treated for the indicated times with 27HC (10^{-6} M) (**D**), shC and sh7B1 (**E**) shC and shGPER (**F**). (**G**) Vimentin abundance was evaluated by immunostaining in xenografts tumors of shcontrol or shGPER MDA-MB-231 cells. Images were obtained with a 20× objective, scale bar 25 μm. * $p < 0.05$ vs. basal (untreated cells) or shC cells; † $p < 0.05$ vs. sh7B1 cells.

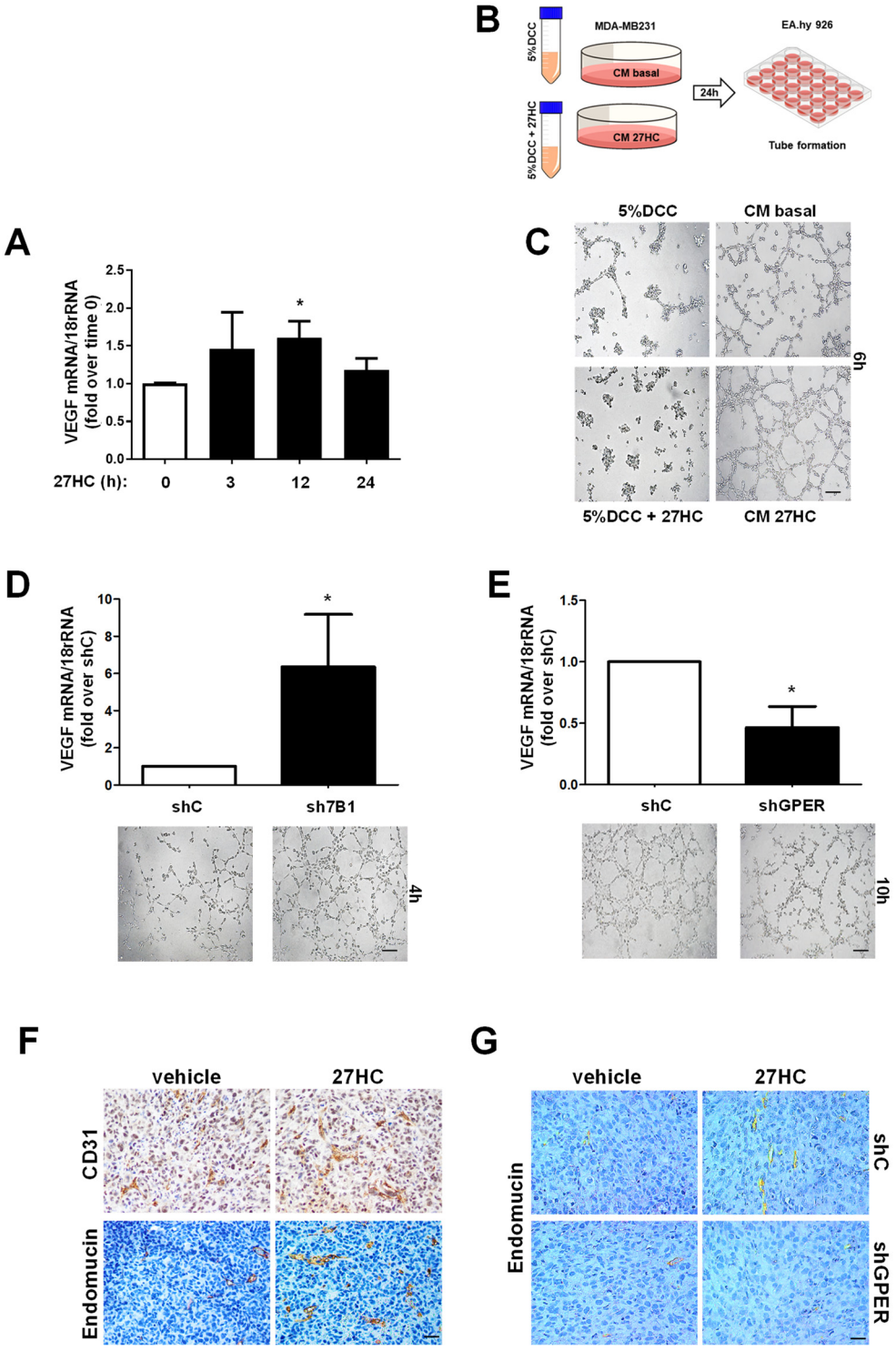

Figure 6. GPR30 is required to promote 27HC-induced angiogenesis in ER− BC cells. (**A**)**.** QPCR analysis of VEGF in MDA-MB-231 cells treated for the indicated times with 27HC (10^{-6} M) * $p < 0.05$ vs. basal (untreated) cells. (**B**) Graphical protocol used for the preparation of MDA-MB-231 conditioned medium (CM). (**C**–**E**) Tube formation in EA.hy926 exposed to conditioned media collected from MDA-MB-231 without (basal) and with 27HC (10^{-6} M) (**C**) and from shC, sh7B1 (**D**) and shGPER (**E**) * $p < 0.05$ vs. shC cells. Images were obtained with a 10× objective, scale bar 50 µm. (**F**). Abundance of CD31 and endomucin was evaluated by immunostaining in xenografts tumors of parental (**F**) or shC and shGPER (**F**) MDA-MB-231 cells. Images were obtained with a 20× objective, scale bar 25 µm.

4. Discussion

Dysregulation of cholesterol homeostasis was associated with multiple types of cancer. Numerous studies showed increased levels of cholesterol in tumors as compared to normal tissues [42,43]. This is related to increased import via the low-density lipoprotein receptor (LDL receptor) and scavenger receptor class B type I (SR-B1, HDL receptor); inhibition of its export by the ABC transporters, ABCA1 and ABCG1; or deregulated cholesterol biosynthesis through the activation of sterol regulatory element-binding protein (SREBP); and the consequent upregulation of 3-hydroxy-3-methyl-glutaryl-coenzyme A reductase (HMGCR). Cholesterol increases the proliferation and motility of ER− BC cells [44,45]. Statins, which inhibit HMGCR, are more effective for preventing the growth of ER− than ER+ breast cancer cell lines [46,47]; additionally, they reduce TNBC cell metastases [48]. A recent study demonstrated that the moderate/strong expression of HMGCR is associated with prognostically adverse tumor characteristics such as higher histological grade, high Ki67, and ER negativity [49].

In recent years, increasing research interests have focused on the role of cholesterol metabolites oxysterols in tumorigenesis and cancer progression, with special attention toward 27HC, the most abundant circulating oxysterol in humans [8]. Since CYP7B1 is less expressed in TNBC tissues [19], in this study, we asked if cholesterol-related effects could depend on its conversion into 27HC. We proved this hypothesis by showing that: 1. TNBC cells silenced for CYP7B1 expression, manifest an increased proliferation when compared to control cells; 2. this increase is not observed when cells are grown in serum-deprived of lipoproteins. The impact of impaired 27HC catabolism on cell proliferation was previously shown for ER+ cells [14]. However, while 27HC acts through ERα in ER+ cells; here, we show that in ER− cells, the 27HC effect is related to GPER as demonstrated by [^{3}H]E2 competition ligand-binding assay.

The finding of 27HC as a GPER ligand is not only relevant to breast cancer. Indeed, the role of GPER as a membrane-based estrogen receptor is still controversial, and conflicting results regarding the GPER-mediated signaling events in response to estrogens continue to emerge [50]. The binding of 27HC to GPER could help find an explanation for many of these controversies. A dual ligand ability has already been demonstrated for other GPCRs, such as sphingosine 1-phosphate receptor 2 (S1PR2), binding both Sphingosine 1-phosphate (S1P) and conjugated bile acids [51]; cannabinoid receptor 1 (CB1), binding both anandamide and 2-arachidonoylglycerol; and GPR119, binding lysophosphatidylcholine, oleoylethanolamide and 2-oleoylglycerol, among others.

We excluded the possibility that LXRs mediate the proliferative effects of 27HC since LXR activation inhibits ER− tumor cell proliferation [21,35]. This inhibition seems related to a decrease in cholesterol content as a consequence of the increased transcription of cholesterol efflux genes (ABCA1 and ABCG1), decreased LDLR expression (cholesterol uptake), and the accelerated degradation of HMGCR (cholesterol synthesis). The treatment of TNBC cells with 27HC instead causes an increase in proliferation, both in vitro and in animal models. Most importantly, this effect is not observed if GPER is stably silenced, further confirming the involvement of this receptor in 27HC-dependent proliferative effects. A study that evaluated the impact of a high-cholesterol diet (HCD) and 27HC on ER− breast tumor, using Met1 cells, a mouse ER− BC cell line, did not show any effect on the growth but found only a significant increase in metastasis formation [52]. However, a previous study, using MDA-MD-231 grafted in SCID mice fed an HCD, showed a significant increase in growth compared to xenografts grown in mice fed a control diet. Importantly, ezetimibe, a cholesterol-lowering drug, was able to prevent the effects of HCD [53]. Another study evaluated the effects of HCD on the xenografts growth of MDA-MD-231 cells in SCID mice. The authors not only demonstrated an increase in tumor size in mice fed for 10 weeks HCD, but also an increase in Ki67 positive cells [45]. 27HC levels parallel cholesterol, then, an increase in serum cholesterol is associated with increased 27HC, making the oxysterol a plausible effector for HCD. Additionally, the observation that 27HC does not increase Ki67 staining in xenografts from shGPER cells further supports the hypothesis of GPER

involvement in mediating its action. The oncogenic role of GPER in TNBC is supported by the observation that Ki67 staining is clearly reduced in shGPER vehicle-treated xenografts, making this receptor a plausible target for BC therapy.

After binding to GPER, 27HC activates NFκB, which plays a prominent role in malignant proliferation, the prevention of apoptosis, resistance to chemotherapy, metastasis, and angiogenesis [54]. Studies from gene expression profiling analysis revealed that the NFκB pathway may be a key regulator of TNBC [55–58]. In our study, we show that 27HC increases p65 nuclear translocation in a GPER-dependent manner, up-regulating the transcription of its target gene, cyclin D1, a key proliferative gene.

The gene 27HC was also shown to be involved in the activation of EMT in MDA-MB-231, where it promoted STAT-3 phosphorylation, increased vimentin and MMP9 transcription, favoring a more aggressive phenotype [17]. Our data support these previous findings and define GPR30 as the receptor mediating 27HC-induced EMT and migration in ER− BC. The relevance of such an interaction is further proved by the behavior of stably silenced cells, where the higher 27HC levels (shCYP7B1) promote EMT and migration, while the absence of GPER (shGPER) causes a significant decrease in vimentin expression and, consequently, cell motility.

In both ER− and ER+ BC cells, 27HC is also involved in angiogenesis. Its angiogenetic effects occur following ROS production, STAT-3 phosphorylation, and HIF-1α transcription, and, ultimately, via VEGF synthesis [20]. Additionally, it was previously shown that, in SKBR3 cells, GPR30 activation by its synthetic ligand promotes the synthesis of factor(s) involved in angiogenesis. G1-treated SKBR3 cells promote tube formation in vitro and neoangiogenesis in vivo [29]. Our data link these independent observations, demonstrating that 27HC needs GPR30 to induce VEGF production and angiogenesis. This becomes clear from in vivo experiments comparing xenografts from MDA-MB-231 shcontrol and shGPER cells: 27HC increases endomucin staining only in control cells; the vehicle-treated group of shGPER xenografts shows less endomucin expression than the shcontrol counterpart. Collectively, our study demonstrates that 27HC is a new ligand for GPR30, and their signaling axis is involved in ER− BC progression. Interfering with the 27HC mechanism of action could represent a new targeted therapy for ER− BC, particularly for triple negative breast tumors, a type of cancer that still lacks specific interventions.

Supplementary Materials: The following supporting information can be downloaded at: https://www.mdpi.com/article/10.3390/cancers14061521/s1, Figure S1. 27HC increases ER− BC growth. Figure S2. 27HC activates proliferation of SKBR3 and MDA-MB-468 cells. Figure S3. GPR30 mediates 27HC effects in SKBR3 and MDA-MB-468 cells. Figure S4. NFκB/Cyclin D1 pathway is activated by 27HC in SKBR3 and MDA-MB-468 cells. Figure S5. GPR30 mediates 27HC-dependent proliferation in MDA-MB468 cells. Figure S6. Effects of 27HC on migration and EMT markers in SKBR3 and MDA-MB-468 cells. Figure S7. 27HC induces angiogenesis in ER− breast cancer cells.

Author Contributions: Conceptualization, C.M., P.T., R.S., I.C. and P.W.S.; Data curation, P.A., I.C., L.Z., M.C.N., D.L.P., V.R. and J.D.; Writing—original draft preparation, P.W.S., R.S. and I.C.; Writing—review and editing, P.W.S., R.S. and I.C.; Supervision, C.M., P.W.S. and R.S.; Funding acquisition, P.W.S., R.S. and P.T. All authors have read and agreed to the published version of the manuscript.

Funding: Pfizer Inc. Investigator Initiated Research Grant WS1909436 to PWS; National Institutes of Health grant R01HL087564 to PWS; Fondazione AIRC per la Ricerca sul Cancro grant IG15230 to RS; H.E.B. Endowed Chair in Marine Science to PT.

Institutional Review Board Statement: Experiments on mice were approved by the Institutional Animal Care and Use Committee at UT Southwestern.

Informed Consent Statement: Not applicable.

Data Availability Statement: Data are available upon reasonable request.

Acknowledgments: The authors thank Ivan Yuhanna (UT Southwestern) for technical assistance.

Conflicts of Interest: The authors declare no conflict of interest. The funders had no role in the design of the study; in the collection, analyses, or interpretation of data; in the writing of the manuscript; or in the decision to publish the results.

References

1. Sørlie, T.; Perou, C.M.; Tibshirani, R.; Aas, T.; Geisler, S.; Johnsen, H.; Hastie, T.; Eisen, M.B.; Van De Rijn, M.; Jeffrey, S.S.; et al. Gene expression patterns of breast carcinomas distinguish tumor subclasses with clinical implications. *Proc. Natl. Acad. Sci. USA* **2001**, *98*, 10869–10874. [CrossRef]
2. Bernard, P.S.; Parker, J.S.; Mullins, M.; Cheung, M.C.U.; Leung, S.; Voduc, D.; Vickery, T.; Davies, S.; Fauron, C.; He, X.; et al. Supervised risk predictor of breast cancer based on intrinsic subtypes. *J. Clin. Oncol.* **2009**, *27*, 1160–1167. [CrossRef]
3. Perou, C.M.; Sørile, T.; Eisen, M.B.; Van De Rijn, M.; Jeffrey, S.S.; Ress, C.A.; Pollack, J.R.; Ross, D.T.; Johnsen, H.; Akslen, L.A.; et al. Molecular portraits of human breast tumours. *Nature* **2000**, *406*, 747–752. [CrossRef] [PubMed]
4. Rotheneder, M.; Kostner, G.M. Effects of low- and high-density lipoproteins on the proliferation of human breast cancer cells In vitro: Differences between hormone-dependent and hormone-independent cell lines. *Int. J. Cancer* **1989**, *43*, 875–879. [CrossRef] [PubMed]
5. Pussinen, P.J.; Karten, B.; Wintersperger, A.; Reicher, H.; McLean, M.; Malle, E.; Sattler, W. The human breast carcinoma cell line HBL-100 acquires exogenous cholesterol from high-density lipoprotein via CLA-1 (CD-36 and LIMPII analogous 1)-mediated selective cholesteryl ester uptake. *Biochem. J.* **2000**, *349*, 559–566. [CrossRef]
6. Antalis, C.J.; Arnold, T.; Rasool, T.; Lee, B.; Buhman, K.K.; Siddiqui, R.A. High ACAT1 expression in estrogen receptor negative basal-like breast cancer cells is associated with LDL-induced proliferation. *Breast Cancer Res. Treat.* **2010**, *122*, 661–670. [CrossRef] [PubMed]
7. Gospodarowicz, D.; Lui, G.M.; Gonzalez, R. High-Density Lipoproteins and the Proliferation of Human Tumor Cells Maintained on Extracellular Matrix-coated Dishes and Exposed to Defined Medium. *Cancer Res.* **1982**, *42*, 3704–3713. [CrossRef]
8. Chimento, A.; Casaburi, I.; Avena, P.; Trotta, F.; De Luca, A.; Rago, V.; Pezzi, V.; Sirianni, R. Cholesterol and Its Metabolites in Tumor Growth: Therapeutic Potential of Statins in Cancer Treatment. *Front. Endocrinol.* **2019**, *9*, 807. [CrossRef] [PubMed]
9. Janowski, B.A.; Willy, P.J.; Devi, T.R.; Falck, J.R.; Mangelsdorf, D.J. An oxysterol signalling pathway mediated by the nuclear receptor LXRα. *Nature* **1996**, *383*, 728–731. [CrossRef] [PubMed]
10. Janowski, B.A.; Grogan, M.J.; Jones, S.A.; Wisely, G.B.; Kliewer, S.A.; Corey, E.J.; Mangelsdorf, D.J. Structural requirements of ligands for the oxysterol liver X receptors LXRa and LXRβ. *Proc. Natl. Acad. Sci. USA* **1999**, *96*, 266–271. [CrossRef]
11. DuSell, C.D.; Nelson, E.R.; Wang, X.; Abdo, J.; Mödder, U.I.; Umetani, M.; Gesty-Palmer, D.; Javitt, N.B.; Khosla, S.; McDonnell, D.P. The endogenous selective estrogen receptor modulator 27-hydroxycholesterol is a negative regulator of bone homeostasis. *Endocrinology* **2010**, *151*, 3675–3685. [CrossRef] [PubMed]
12. Umetani, M.; Domoto, H.; Gormley, A.K.; Yuhanna, I.S.; Cummins, C.L.; Javitt, N.B.; Korach, K.S.; Shaul, P.W.; Mangelsdorf, D.J. 27-Hydroxycholesterol is an endogenous SERM that inhibits the cardiovascular effects of estrogen. *Nat. Med.* **2007**, *13*, 1185–1192. [CrossRef] [PubMed]
13. He, S.; Nelson, E.R. 27-Hydroxycholesterol, an endogenous selective estrogen receptor modulator. *Maturitas* **2017**, *104*, 29–35. [CrossRef]
14. Wu, Q.; Ishikawa, T.; Sirianni, R.; Tang, H.; McDonald, J.G.; Yuhanna, I.S.; Thompson, B.; Girard, L.; Mineo, C.; Brekken, R.A.; et al. 27-Hydroxycholesterol promotes cell-autonomous, ER-positive breast cancer growth. *Cell Rep.* **2013**, *5*, 637–645. [CrossRef]
15. Nelson, E.R.; Wardell, S.E.; Jasper, J.S.; Park, S.; Suchindran, S.; Howe, M.K.; Carver, N.J.; Pillai, R.V.; Sullivan, P.M.; Sondhi, V.; et al. 27-Hydroxycholesterol links hypercholesterolemia and breast cancer pathophysiology. *Science* **2013**, *342*, 1094–1098. [CrossRef]
16. Shi, S.-Z.; Lee, E.-J.; Lin, Y.-J.; Chen, L.; Zheng, H.-Y.; He, X.-Q.; Peng, J.-Y.; Noonepalle, S.K.; Shull, A.Y.; Pei, F.C.; et al. Recruitment of monocytes and epigenetic silencing of intratumoral CYP7B1 primarily contribute to the accumulation of 27-hydroxycholesterol in breast cancer. *Am. J. Cancer Res.* **2019**, *9*, 2194–2208.
17. Shen, Z.; Zhu, D.; Liu, J.; Chen, J.; Liu, Y.; Hu, C.; Li, Z.; Li, Y. 27-Hydroxycholesterol induces invasion and migration of breast cancer cells by increasing MMP9 and generating EMT through activation of STAT-3. *Environ. Toxicol. Pharmacol.* **2017**, *51*, 1–8. [CrossRef]
18. Kimbung, S.; Chang, C.Y.; Bendahl, P.O.; Dubois, L.; Thompson, J.W.; McDonnell, D.P.; Borgquist, S. Impact of 27-hydroxylase (CYP27A1) and 27-hydroxycholesterol in breast cancer. *Endocr. Relat. Cancer* **2017**, *24*, 339–349. [CrossRef]
19. Torres-Luquis, O.; Madden, K.; N'dri, N.M.R.; Berg, R.; Olopade, O.F.; Ngwa, W.; Abuidris, D.; Mittal, S.; Lyn-Cook, B.; Mohammed, S.I. LXR/RXR pathway signaling associated with triple-negative breast cancer in African American women. *Breast Cancer Targets Ther.* **2019**, *11*, 1–12. [CrossRef]
20. Zhu, D.; Shen, Z.; Liu, J.; Chen, J.; Liu, Y.; Hu, C.; Li, Z.; Li, Y. The ROS-mediated activation of STAT-3/VEGF signaling is involved in the 27-hydroxycholesterol-induced angiogenesis in human breast cancer cells. *Toxicol. Lett.* **2016**, *264*, 79–86. [CrossRef]
21. Vedin, L.L.; Lewandowski, S.A.; Parini, P.; Gustafsson, J.Å.; Steffensen, K.R. The oxysterol receptor LXR inhibits proliferation of human breast cancer cells. *Carcinogenesis* **2009**, *30*, 575–579. [CrossRef] [PubMed]
22. Prossnitz, E.R.; Barton, M. The G-protein-coupled estrogen receptor GPER in health and disease. *Nat. Rev. Endocrinol.* **2011**, *7*, 715–726. [CrossRef] [PubMed]

23. Lappano, R.; Rosano, C.; De Marco, P.; De Francesco, E.M.; Pezzi, V.; Maggiolini, M. Estriol acts as a GPR30 antagonist in estrogen receptor-negative breast cancer cells. *Mol. Cell. Endocrinol.* **2010**, *320*, 162–170. [CrossRef] [PubMed]
24. Girgert, R.; Emons, G.; Gründker, C. Inactivation of GPR30 reduces growth of triple-negative breast cancer cells: Possible application in targeted therapy. *Breast Cancer Res. Treat.* **2012**, *134*, 199–205. [CrossRef] [PubMed]
25. Steiman, J.; Peralta, E.A.; Louis, S.; Kamel, O. Biology of the estrogen receptor, GPR30, in triple negative breast cancer. *Am. J. Surg.* **2013**, *206*, 698–703. [CrossRef] [PubMed]
26. Yu, T.; Liu, M.; Luo, H.; Wu, C.; Tang, X.; Tang, S.; Hu, P.; Yan, Y.; Wang, Z.; Tu, G. GPER mediates enhanced cell viability and motility via non-genomic signaling induced by 17β-estradiol in triple-negative breast cancer cells. *J. Steroid Biochem. Mol. Biol.* **2014**, *143*, 392–403. [CrossRef]
27. Zhou, K.; Sun, P.; Zhang, Y.; You, X.; Li, P.; Wang, T. Estrogen stimulated migration and invasion of estrogen receptor-negative breast cancer cells involves an ezrin-dependent crosstalk between G protein-coupled receptor 30 and estrogen receptor beta signaling. *Steroids* **2016**, *111*, 113–120. [CrossRef]
28. Albanito, L.; Sisci, D.; Aquila, S.; Brunelli, E.; Vivacqua, A.; Madeo, A.; Lappano, R.; Pandey, D.P.; Picard, D.; Mauro, L.; et al. Epidermal growth factor induces G protein-coupled receptor 30 expression in estrogen receptor-negative breast cancer cells. *Endocrinology* **2008**, *149*, 3799–3808. [CrossRef]
29. De Francesco, E.M.; Pellegrino, M.; Santolla, M.F.; Lappano, R.; Ricchio, E.; Abonante, S.; Maggiolini, M. GPER mediates activation of HIF1α/VEGF signaling by estrogens. *Cancer Res.* **2014**, *74*, 4053–4064. [CrossRef]
30. Thomas, P.; Pang, Y.; Filardo, E.J.; Dong, J. Identity of an estrogen membrane receptor coupled to a G protein in human breast cancer cells. *Endocrinology* **2005**, *146*, 624–632. [CrossRef]
31. Trotta, F.; Avena, P.; Chimento, A.; Rago, V.; De Luca, A.; Sculco, S.; Nocito, M.C.; Malivindi, R.; Fallo, F.; Pezzani, R.; et al. Statins Reduce Intratumor Cholesterol Affecting Adrenocortical Cancer Growth. *Mol. Cancer Ther.* **2020**, *19*, 1909–1921. [CrossRef]
32. Andrews, N.C.; Faller, D.V. A rapid micrqpreparation technique for extraction of DNA-binding proteins from limiting numbers of mammalian cells. *Nucleic Acids Res.* **1991**, *19*, 2499. [CrossRef] [PubMed]
33. De Luca, A.; Fiorillo, M.; Peiris-Pagès, M.; Ozsvari, B.; Smith, D.L.; Sanchez-Alvarez, R.; Martinez-Outschoorn, U.E.; Cappello, A.R.; Pezzi, V.; Lisanti, M.P.; et al. Mitochondrial biogenesis is required for the anchorage-independent survival and propagation of stem-like cancer cells. *Oncotarget* **2015**, *6*, 14777. [CrossRef]
34. Chajès, V.; Mahon, M.; Kostner, G.M. Influence of LDL oxidation on the proliferation of human breast cancer cells. *Free Radic. Biol. Med.* **1996**, *20*, 113–120. [CrossRef]
35. Hutchinson, S.A.; Lianto, P.; Roberg-Larsen, H.; Battaglia, S.; Hughes, T.A.; Thorne, J.L. ER-Negative Breast Cancer Is Highly Responsive to Cholesterol Metabolite Signalling. *Nutrients* **2019**, *11*, 2618. [CrossRef] [PubMed]
36. Xu, F.; Wang, X.; Wu, N.; He, S.; Yi, W.; Xiang, S.; Zhang, P.; Xie, X.; Ying, C. Bisphenol A induces proliferative effects on both breast cancer cells and vascular endothelial cells through a shared GPER-dependent pathway in hypoxia. *Environ. Pollut.* **2017**, *231*, 1609–1620. [CrossRef] [PubMed]
37. Filardo, E.J.; Quinn, J.A.; Bland, K.I.; Frackelton, J. Estrogen-induced activation of Erk-1 and Erk-2 requires the G protein-coupled receptor homolog, GPR30, and occurs via trans-activation of the epidermal growth factor receptor through release of HB-EGF. *Mol. Endocrinol.* **2000**, *14*, 1649–1660. [CrossRef] [PubMed]
38. Ledoux, A.C.; Perkins, N.D. NF-κB and the cell cycle. *Biochem. Soc. Trans.* **2014**, *42*, 76–81. [CrossRef]
39. Zhu, P.; Liao, L.Y.; Zhao, T.T.; Mo, X.M.; Chen, G.G.; Liu, Z.M. GPER/ERK&AKT/NF-κB pathway is involved in cadmium-induced proliferation, invasion and migration of GPER-positive thyroid cancer cells. *Mol. Cell. Endocrinol.* **2017**, *442*, 68–80. [CrossRef]
40. Hinz, M.; Krappmann, D.; Eichten, A.; Heder, A.; Scheidereit, C.; Strauss, M. NF-κB Function in Growth Control: Regulation of Cyclin D1 Expression and G0/G1-to-S-Phase Transition. *Mol. Cell. Biol.* **1999**, *19*, 2690–2698. [CrossRef]
41. Wang, D.; Stockard, C.; Harkins, L.; Lott, P.; Salih, C.; Yuan, K.; Buchsbaum, D.; Hashim, A.; Zayzafoon, M.; Hardy, R.; et al. Immunohistochemistry in the evaluation of neovascularization in tumor xenografts. *Biotech. Histochem.* **2008**, *83*, 179–189. [CrossRef] [PubMed]
42. Dessì, S.; Batetta, B.; Anchisi, C.; Costelli, P.; Tessitore, L.; Baccino, F.M. Cholesterol metabolism during the growth of a rat ascites hepatoma (Yoshida ah-130). *Br. J. Cancer* **1992**, *66*, 779–808. [CrossRef] [PubMed]
43. Schaffner, C.P. Prostatic cholesterol metabolism: Regulation and alteration. *Prog. Clin. Biol. Res.* **1981**, *75 A*, 279–324.
44. Antalis, C.J.; Uchida, A.; Buhman, K.K.; Siddiqui, R.A. Migration of MDA-MB-231 breast cancer cells depends on the availability of exogenous lipids and cholesterol esterification. *Clin. Exp. Metastasis* **2011**, *28*, 733–741. [CrossRef] [PubMed]
45. Rodrigues Dos Santos, C.; Domingues, G.; Matias, I.; Matos, J.; Fonseca, I.; De Almeida, J.M.; Dias, S. LDL-cholesterol signaling induces breast cancer proliferation and invasion. *Lipids Health Dis.* **2014**, *13*, 16. [CrossRef] [PubMed]
46. Kumar, A.S.; Benz, C.C.; Shim, V.; Minami, C.A.; Moore, D.H.; Esserman, L.J. Estrogen receptor-negative breast cancer is less likely to arise among lipophilic statin users. *Cancer Epidemiol. Biomarkers Prev.* **2008**, *17*, 1028–1033. [CrossRef] [PubMed]
47. Borgquist, S.; Jögi, A.; Pontén, F.; Rydén, L.; Brennan, D.J.; Jirström, K. Prognostic impact of tumour-specific HMG-CoA reductase expression in primary breast cancer. *Breast Cancer Res.* **2008**, *10*, R79. [CrossRef] [PubMed]
48. Wolfe, A.R.; Debeb, B.G.; Lacerda, L.; Larson, R.; Bambhroliya, A.; Huang, X.; Bertucci, F.; Finetti, P.; Birnbaum, D.; Van Laere, S.; et al. Simvastatin prevents triple-negative breast cancer metastasis in pre-clinical models through regulation of FOXO3a. *Breast Cancer Res. Treat.* **2015**, *154*, 495–508. [CrossRef]

49. Bjarnadottir, O.; Feldt, M.; Inasu, M.; Bendahl, P.O.; Elebro, K.; Kimbung, S.; Borgquist, S. Statin use, HMGCR expression, and breast cancer survival—The Malmö Diet and Cancer Study. *Sci. Rep.* **2020**, *10*, 558. [CrossRef]
50. Luo, J.; Liu, D. Does GPER Really Function as a G Protein-Coupled Estrogen Receptor in vivo? *Front. Endocrinol.* **2020**, *11*, 148. [CrossRef]
51. Nagahashi, M.; Yuza, K.; Hirose, Y.; Nakajima, M.; Ramanathan, R.; Hait, N.C.; Hylemon, P.B.; Zhou, H.; Takabe, K.; Wakai, T. The roles of bile acids and sphingosine-1-phosphate signaling in the hepatobiliary diseases. *J. Lipid Res.* **2016**, *57*, 1636–1643. [CrossRef] [PubMed]
52. Baek, A.E.; Yu, Y.R.A.; He, S.; Wardell, S.E.; Chang, C.Y.; Kwon, S.; Pillai, R.V.; McDowell, H.B.; Thompson, J.W.; Dubois, L.G.; et al. The cholesterol metabolite 27 hydroxycholesterol facilitates breast cancer metastasis through its actions on immune cells. *Nat. Commun.* **2017**, *8*, 864. [CrossRef] [PubMed]
53. Pelton, K.; Coticchia, C.M.; Curatolo, A.S.; Schaffner, C.P.; Zurakowski, D.; Solomon, K.R.; Moses, M.A. Hypercholesterolemia induces angiogenesis and accelerates growth of breast tumors in vivo. *Am. J. Pathol.* **2014**, *184*, 2099–2110. [CrossRef] [PubMed]
54. Naugler, W.E.; Karin, M. NF-κB and cancer—Identifying targets and mechanisms. *Curr. Opin. Genet. Dev.* **2008**, *18*, 19–26. [CrossRef] [PubMed]
55. Ossovskaya, V.; Wang, Y.; Budoff, A.; Xu, Q.; Lituev, A.; Potapova, O.; Vansant, G.; Monforte, J.; Daraselia, N. Exploring Molecular Pathways of Triple-Negative Breast Cancer. *Genes Cancer* **2011**, *2*, 870–879. [CrossRef]
56. Nedeljković, M.; Damjanović, A. Mechanisms of Chemotherapy Resistance in Triple-Negative Breast Cancer-How We Can Rise to the Challenge. *Cells* **2019**, *8*, 957. [CrossRef] [PubMed]
57. Li, M.X.; Jin, L.T.; Wang, T.J.; Feng, Y.J.; Pan, C.P.; Zhao, D.M.; Shao, J. Identification of potential core genes in triple negative breast cancer using bioinformatics analysis. *Onco. Targets Ther.* **2018**, *11*, 4105–4112. [CrossRef]
58. Narrandes, S.; Huang, S.; Murphy, L.; Xu, W. The exploration of contrasting pathways in Triple Negative Breast Cancer (TNBC). *BMC Cancer* **2018**, *18*, 22. [CrossRef]